

# Aero- dynamics

---

1

N. F. Krasnov

Fundamentals of Theory.  
Aerodynamics of an  
Airfoil and a Wing

Translated from the Russian by  
G. Leib



Mir Publishers Moscow

---

First published 1985  
Revised from the 1980 Russian edition

*На английском языке*

© Издательство «Высшая школа», 1980  
© English translation, Mir Publishers, 1985

Aero-  
dynamics  
1

Н. Ф. Краснов

# Аэродинамика

Часть I

Основы теории

Аэродинамика профиля и крыла

Издательство

«Высшая школа»

Москва

## Preface

Aerodynamics is the theoretical foundation of aeronautical, rocket, space, and artillery engineering and the cornerstone of the aerodynamic design of modern craft. The fundamentals of aerodynamics are used in studying the external flow over various bodies or the motion of air (a gas) inside various objects. Engineering success in the fields of aviation, artillery, rocketry, space flight, motor vehicle transport, and so on, i.e. fields that pertain to the flow of air or a gas in some form or other, depends on a firm knowledge of aerodynamics.

The present textbook, in addition to the general laws of flow of a fluid, treats the application of aerodynamics, chiefly in rocketry and modern high-speed aviation. The book consists of two parts, each forming a separate volume. The first of them concerns the fundamental concepts and definitions of aerodynamics and the theory of flow over an airfoil and a wing, including an unsteady flow (Chapters 1-9), while the second describes the aerodynamic design of craft and their individual parts (Chapters 10-15). The two parts are designed for use in a two-semester course of aerodynamics, although the first part can be used independently by those interested in individual problems of theoretical aerodynamics.

A sound theoretical background is important to the study of any subject because creative solutions of practical problems, scientific research, and discoveries are impossible without it. Students should therefore devote special attention to the first five chapters, which deal with the fundamental concepts and definitions of aerodynamics, the kinematics of a fluid, the fundamentals of fluid dynamics, the theory of shocks, and the method of characteristics used widely in investigating supersonic flows. Chapters 6 and 7, which relate to the flow over airfoils, are also important to a fundamental understanding of the subject. These chapters contain a fairly complete discussion of the general theory of flow of a gas in two-dimensional space (the theory of two-dimensional flow). The information on the supersonic steady flow over a wing in Chapter 8 relates directly to these materials. The aerodynamic design of most modern craft is based on studies of such flow.

One of the most topical areas of modern aerodynamic research is the study of optimal aerodynamic configurations of craft and their separate (isolated) parts (the fuselage, wing, empennage). Therefore, a small section (6.5) that defines a finite-span wing with the most advantageous planform in an incompressible flow has been included here. This section presents important practical and methodological information on the conversion of the aerodynamic coefficients of a wing from one aspect ratio to another.

The study of non-stationary gas flows is a rather well developed field of modern theoretical and practical aerodynamics. The results of this study are widely used in calculating the effect of aerodynamic forces and moments on

craft whose motion is generally characterized by non-uniformity, and the non-stationary aerodynamic characteristics thus calculated are used in the dynamics of craft when studying their flight stability. Chapter 9 concerns the general relations of the aerodynamic coefficients in unsteady flow. Aerodynamic derivatives (stability derivatives) are analysed, as is the concept of dynamic stability. Unsteady flow over a wing is also considered. The most important section of this chapter is devoted to numerical methods of calculating the stability derivatives of a lifting surface of arbitrary planform, generally with a curved leading edge (i.e. with variable sweep along the span). Both exact and approximate methods of determining the non-stationary aerodynamic characteristics of a wing are given.

A special place in the book is devoted to the most important theoretical and applied problems of high-speed aerodynamics, including the thermodynamic and kinetic parameters of dissociating gases, the equations of motion and energy, and the theory of shocks and its relation to the physicochemical properties of gases at high temperatures. Considerable attention is given to shock waves (shocks), which are a manifestation of the specific properties of supersonic flows. The concept of the thickness of a shock is discussed, and the book includes graphs of the functions characterizing changes in the parameters of a gas as it passes through a shock.

Naturally, a textbook cannot reflect the entire diversity of problems facing the science of aerodynamics. I have tried to provide the scientific information for specialists in the field of aeronautic and rocket engineering. This information, if mastered in its entirety, should be sufficient for young specialists to cope independently with other practical aerodynamic problems that may appear. Among these problems, not reflected in the book, are magnetogasdynamics investigations, the application of the method of characteristics to three-dimensional gas flows, and experimental aerodynamics. I will be happy if study of this textbook leads students to a more comprehensive, independent investigation of modern aerodynamics.

The book is the result of my experience teaching courses in aerodynamics at the N.E. Bauman Higher Engineering College in Moscow, USSR. Intended for college and junior-college students, it will also be a useful aid to specialists in research institutions, design departments, and industrial enterprises.

All physical quantities are given according to the International System of Units (SI).

In preparing the third Russian edition of the book, which the present English edition has been translated from, I took account of readers' remarks and of the valuable suggestions made by the reviewer, professor A.M. Mkhiteryan, to whom I express my profound gratitude.

*Nikolai F. Krasnov*

## Contents

Preface	5
Introduction	13
Chapter 1	25
<b>Basic Information from Aerodynamics</b>	
1.1. Forces Acting on a Moving Body	25
Surface Force	25
Property of Pressures in an Ideal Fluid	26
Influence of Viscosity on the Flow of a Fluid	28
1.2. Resultant Force Action	36
Components of Aerodynamic Forces and Moments	36
Conversion of Aerodynamic Forces and Moments from One Coordinate System to Another	40
1.3. Determination of Aerodynamic Forces and Moments According to the Known Distribution of the Pressure and Shear Stress. Aerodynamic Coefficients	41
Aerodynamic Forces and Moments and Their Coefficients	41
1.4. Static Equilibrium and Static Stability	52
Concept of Equilibrium and Stability	52
Static Longitudinal Stability	53
Static Lateral Stability	57
1.5. Features of Gas Flow at High Speeds	58
Compressibility of a Gas	58
Heating of a Gas	59
State of Air at High Temperatures	65
Chapter 2	
<b>Kinematics of a Fluid</b>	
2.1. Approaches to the Kinematic Investigation of a Fluid	71
Lagrangian Approach	71
Eulerian Approach	72
Streamlines and Pathlines	73
2.2. Analysis of Fluid Particle Motion	74
2.3. Vortex-Free Motion of a Fluid	79

**Chapter 3**  
**Fundamentals**  
**of Fluid Dynamics**

2.4.	Continuity Equation	80
	General Form of the Equation	80
	Cartesian Coordinate System	81
	Curvilinear Coordinate System	82
	Continuity Equation of Gas Flow along a Curved Surface	86
	Flow Rate Equation	88
2.5.	Stream Function	89
2.6.	Vortex Lines	90
2.7.	Velocity Circulation	91
	Concept	91
	Stokes Theorem	92
	Vortex-Induced Velocities	94
2.8.	Complex Potential	96
2.9.	Kinds of Fluid Flows	97
	Parallel Flow	98
	Two-Dimensional Point Source and Sink	98
	Three-Dimensional Source and Sink	100
	Doublet	100
	Circulation Flow (Vortex)	103

**Chapter 4**  
**Shock Wave Theory**

3.1.	Equations of Motion of a Viscous Fluid	106
	Cartesian Coordinates	106
	Vector Form of the Equations of Motion	113
	Curvilinear Coordinates	114
	Cylindrical Coordinates	116
	Spherical Coordinates	118
	Equations of Two-Dimensional Flow of a Gas Near a Curved Surface	120
3.2.	Equations of Energy and Diffusion of a Gas	121
	Diffusion Equation	121
	Energy Equation	124
3.3.	System of Equations of Gas Dynamics. Initial and Boundary Conditions	129
3.4.	Integrals of Motion for an Ideal Fluid	134
3.5.	Aerodynamic Similarity	138
	Concept of Similarity	138
	Similarity Criteria Taking Account of the Viscosity and Heat Conduction	141
3.6.	Isentropic Gas Flows	149
	Configuration of Gas Jet	149
	Flow Velocity	150
	Pressure, Density, and Temperature	152
	Flow of a Gas from a Reservoir	154
4.1.	Physical Nature of Shock Wave Formation	159
4.2.	General Equations for a Shock	162
	Oblique Shock	163
	Normal Shock	168
4.3.	Shock in the Flow of a Gas with	

**Chapter 5**  
**Method  
of Characteristics**

**Chapter 6**  
**Airfoil and  
Finite-Span Wing  
in an Incompressible  
Flow**

**Chapter 7**  
**An Airfoil in a  
Compressible Flow**

Constant Specific Heats	169
System of Equations	169
Formulas for Calculating the Parameters of a Gas Behind a Shock	170
Oblique Shock Angle	176
4.4. Hodograph	179
4.5. A Normal Shock in the Flow of a Gas with Constant Specific Heats	184
4.6. A Shock at Hypersonic Velocities and Constant Specific Heats of a Gas	186
4.7. A Shock in a Flow of a Gas with Varying Specific Heats and with Dissociation and Ionization	188
4.8. Relaxation Phenomena	193
Non-Equilibrium Flows	193
Equilibrium Processes	195
Relaxation Effects in Shock Waves	196
5.1. Equations for the Velocity Potential and Stream Function	200
5.2. The Cauchy Problem	205
5.3. Characteristics	209
Compatibility Conditions	209
Determination of Characteristics	209
Orthogonality of Characteristics	213
Transformation of the Equations for Characteristics in a Hodograph	214
Equations for Characteristics in a Hodograph for Particular Cases of Gas Flow	219
5.4. Outline of Solution of Gas-Dynamic Problems According to the Method of Characteristics	222
5.5. Application of the Method of Characteristics to the Solution of the Problem on Shaping the Nozzles of Supersonic Wind Tunnels	230
6.1. Thin Airfoil in an Incompressible Flow	234
6.2. Transverse Flow over a Thin Plate	240
6.3. Thin Plate at an Angle of Attack	243
6.4. Finite-Span Wing in an Incompressible Flow	249
6.5. Wing with Optimal Planform Conversion of Coefficients $c_y$ and $c_{x,t}$ from One Wing Aspect Ratio to Another	258
7.1. Subsonic Flow over a Thin Airfoil Linearization of the Equation for the Velocity Potential Relation Between the Parameters of a Compressible and Incompressible Fluid Flow over a Thin Airfoil	264
7.2. Khristianovich Method Content of the Method	269

---

Conversion of the Pressure Coefficient for an Incompressible Fluid to the Number $M_\infty > 0$	271
Conversion of the Pressure Coefficient from $M_{\infty 1} > 0$ to $M_{\infty 2} > 0$	272
Determination of the Critical Num- ber $M$	273
Aerodynamic Coefficients	274
<b>7.3.</b> Flow at Supercritical Velocity over an Airfoil ( $M_\infty > M_{\infty,cr}$ )	274
<b>7.4.</b> Supersonic Flow of a Gas with Con- stant Specific Heats over a Thin Plate	278
<b>7.5.</b> Parameters of a Supersonic Flow over an Airfoil with an Arbitrary Con- figuration	285
Use of the Method of Characteristics	285
Hypersonic Flow over a Thin Airfoil	291
Nearly Uniform Flow over a Thin Airfoil	293
Aerodynamic Forces and Their Coefficients	293
<b>7.6.</b> Sideslipping Wing Airfoil	294
Definition of a Sideslipping Wing	299
Aerodynamic Characteristics of a Sideslipping Wing Airfoil	301
Suction Force	305
 <b>Chapter 8</b>	
<b>A Wing in</b>	
<b>a Supersonic Flow</b>	
<b>8.1.</b> Linearized Theory of Supersonic Flow over a Finite-Span Wing	308
Linearization of the Equation for the Potential Function	308
Boundary Conditions	310
Components of the Total Values of the Velocity Potentials and Aero- dynamic Coefficients	313
Features of Supersonic Flow over Wings	315
<b>8.2.</b> Method of Sources	317
<b>8.3.</b> Wing with a Symmetric Airfoil and Triangular Planform ( $\alpha = 0, c_{y_a} = 0$ )	321
Flow over a Wing Panel with a Sub- sonic Leading Edge	321
Triangular Wing Symmetric about the $x$ -Axis with Subsonic Leading Edges	326
Semi-Infinite Wing with a Supersonic Edge	328
Triangular Wing Symmetric about the $x$ -Axis with Supersonic Leading Edges	330
<b>8.4.</b> Flow over a Tetragonal Symmetric Airfoil Wing with Subsonic Edges at a Zero Angle of Attack	331
<b>8.5.</b> Flow over a Tetragonal Symmetric Airfoil Wing with Edges of Different Kinds (Subsonic and Supersonic)	343

**Chapter 9**  
**Aerodynamic**  
**Characteristics**  
**of Craft in**  
**Unsteady Motion**

Leading and Middle Edges are Subsonic, Trailing Edge is Supersonic	343
Leading Edge is Subsonic, Middle and Trailing Edges are Supersonic	345
Wing with All Supersonic Edges	346
General Relation for Calculating the Drag	350
8.6. Field of Application of the Source Method	351
8.7. Doublet Distribution Method	353
8.8. Flow over a Triangular Wing with Subsonic Leading Edges	355
8.9. Flow over a Hexagonal Wing with Subsonic Leading and Supersonic Trailing Edges	366
8.10. Flow over a Hexagonal Wing with Supersonic Leading and Trailing Edges	372
8.11. Drag of Wings with Subsonic Leading Edges	381
8.12. Aerodynamic Characteristics of a Rectangular Wing	385
8.13. Reverse-Flow Method	391
 9.1. General Relations for the Aerodynamic Coefficients	395
9.2. Analysis of Stability Derivatives and Aerodynamic Coefficients	398
9.3. Conversion of Stability Derivatives upon a Change in the Position of the Force Reduction Centre	404
9.4. Particular Cases of Motion	406
Longitudinal and Lateral Motions	406
Motion of the Centre of Mass and Rotation about It	407
Pitching Motion	408
9.5. Dynamic Stability	410
Definition	410
Stability Characteristics	413
9.6. Basic Relations for Unsteady Flow	416
Aerodynamic Coefficients	416
Cauchy-Lagrange Integral	420
Wave Equation	423
9.7. Basic Methods of Solving Non-Stationary Problems	425
Method of Sources	425
Vortex Theory	428
9.8. Numerical Method of Calculating the Stability Derivatives for a Wing in an Incompressible Flow	431
Velocity Field of an Oblique Horse-shoe Vortex	431
Vortex Model of a Wing	436
Calculation of Circulatory Flow	439
Aerodynamic Characteristics	446
Deformation of a Wing Surface	451

Influence of Compressibility (the Number $M_\infty$ ) on Non-Stationary Flow	452
9.9. Unsteady Supersonic Flow over a Wing	456
9.10. Properties of Aerodynamic Derivatives	478
9.11. Approximate Methods for Determining the Non-Stationary Aerodynamic Characteristics	488
Hypotheses of Harmonicity and Stationarity	488
Tangent-Wedge Method	489
<b>References</b>	493
<b>Supplementary Reading</b>	494
<b>Name Index</b>	495
<b>Subject Index</b>	497

## Introduction

**Aerodynamics** is a complex word originating from the Greek words  $\alpha\eta\rho$  (air) and  $\delta\theta\nu\alpha\mu\tau$  (power). This name has been given to a science that, being a part of mechanics—the science of the motion of bodies in general—studies the laws of motion of air depending on the acting forces and on their basis establishes special laws of the interaction between air and a solid body moving in it.

The practical problems confronting mankind in connection with flights in heavier-than-air craft provided an impetus to the development of aerodynamics as a science. These problems were associated with the determination of the forces and moments (what we call the aerodynamic forces and moments) acting on moving bodies. The main task in investigating the action of forces was calculation of the buoyancy, or lift, force.

At the beginning of its development, aerodynamics dealt with the investigation of the motion of air at quite low speeds because aircraft at that time had a low flight speed. It is quite natural that aerodynamics was founded theoretically on **hydrodynamics**—the science dealing with the motion of a dropping (incompressible) liquid. The cornerstones of this science were laid in the 18th century by L. Euler (1707-1783) and D. Bernoulli (1700-1782), members of the Russian Academy of Sciences. In his scientific treatise "The General Principles of Motion of Fluids" (in Russian—1755), Euler for the first time derived the fundamental differential equations of motion of ideal (non-viscous) fluids. The fundamental equation of hydrodynamics establishing the relation between the pressure and speed in a flow of an incompressible fluid was discovered by Bernoulli. He published this equation in 1738 in his works "Fluid Mechanics" (in Russian).

At low flight speeds, the influence on the nature of motion of air of such its important property as compressibility is negligibly small. But the development of artillery—rifle and rocket—and high-speed aircraft moved to the forefront the task of studying the laws



of motion of air or in general of a gas at high speeds. It was found that if the forces acting on a body moving at a high speed are calculated on the basis of the laws of motion of air at low speeds, they may differ greatly from the actual forces. It became necessary to seek the explanation of this phenomenon in the nature itself of the motion of air at high speeds. It consists in a change in its density depending on the pressure, which may be quite considerable at such speeds. It is exactly this change that underlies the property of compressibility of a gas.

Compressibility causes a change in the internal energy of a gas, which must be considered when calculating the parameters determining the motion of the fluid. The change in the internal energy associated with the parameters of state and the work that a compressed gas can do upon expansion is determined by the first law of thermodynamics. Hence, thermodynamic relations were used in the aerodynamics of a compressible gas.

A liquid and air (a gas) differ from each other in their physical properties owing to their molecular structure being different. Digressing from these features, we can take into account only the basic difference between a liquid and a gas associated with the degree of their compressibility. Accordingly, in **aerohydromechanics**, which deals with the motion of liquids and gases, it is customary to use the term **fluid** to designate both a liquid and a gas, distinguishing between an incompressible and a compressible fluid when necessary.

Aerohydromechanics treats laws of motion common to both liquids and gases, which made it expedient and possible to combine the studying of these laws within the bounds of a single science of aerodynamics (or aeromechanics). In addition to the general laws characterizing the motion of fluids, there are laws obeyed only by a gas or only by a liquid.

Fluid mechanics studies the motion of fluids at a low speed at which a gas behaves practically like an incompressible liquid. In these conditions, the enthalpy of a gas is large in comparison with its kinetic energy, and one does not have to take account of the change in the enthalpy with a change in the speed of the flow, i.e. with a change in the kinetic energy of the fluid. This is why there is no need to use thermodynamic concepts and relations in low-speed aerodynamics (hydrodynamics). The mechanics of a gas differs from that of a liquid when the gas has a high speed. At such speeds, a gas flowing over a craft experiences not only a change in its density, but also an increase in its temperature that may result in various physicochemical transformations in it. A substantial part of the kinetic energy associated with the speed of a flight is converted into heat and chemical energy.

All these features of motion of a gas resulted in the appearance of **high-speed aerodynamics** or **gas dynamics**—a special branch of

aerodynamics studying the laws of motion of air (a gas) at high subsonic and supersonic speeds, and also the laws of interaction between a gas and a body travelling in it at such speeds.

One of the founders of gas dynamics was academician S. Chaplygin (1869-1942), who in 1902 published an outstanding scientific work "On Gas Jets" (in Russian). Equations are derived in this work that form the theoretical foundation of modern gas dynamics and entered the world's science under the name of the Chaplygin equations.

The development of theoretical aerodynamics was attended by the creation of **experimental aerodynamics** devoted to the experimental investigation of the interaction between a body and a gas flow past it with the aid of various technical means such as a wind tunnel that imitate the flow of aircraft.

Under the guidance of professor N. Zhukovsky (1847-1921), the first aerodynamic laboratories in Russia were erected (at the Moscow State University, the Moscow Higher Technical College, and at Kuchino, near Moscow). In 1918, the Central Aerohydrodynamic Institute (TsAGI) was organized by Zhukovsky's initiative with the direct aid of V. Lenin. At present it is one of the major world centres for the science of aerodynamics bearing the name of N. Zhukovsky.

The development of aviation, artillery, and rocketry, and the maturing of the theoretical fundamentals of aerodynamics changed the nature of aerodynamic installations, from the first, comparatively small and low-speed wind tunnels up to the giant high-speed tunnels of TsAGI (1940) and modern hypersonic installations, and also special facilities in which a supersonic flow of a heated gas is artificially created (what we call high-temperature tunnels, shock tunnels, plasma installations, etc.).

The nature of the interaction between a gas and a body moving in it may vary. At low speeds, the interaction is mainly of a force nature. With a growth in the speed, the force interaction is attended by heating of the surface owing to heat transfer from the gas to the body: this gives rise to **thermal interaction**. At very high speeds, aerodynamic heating is so great that it may lead to failure of the material of a craft wall because of its fusion or sublimation and, as a result, to the entrainment of the destroyed material (ablation) and to a change in the nature of heating of the wall. Aerodynamic heating may also cause **chemical interaction** between a solid wall and the gas flowing over it, as a result of which the same effect of ablation appears. High flight speeds may also cause ablation as a result of **mechanical interaction** between the gas and a moving body consisting in erosion of the material of a wall and damage to its structure.

The investigation of all kinds of interaction between a gas and a craft allows one to perform aerodynamic calculations associated with the evaluation of the quantitative criteria of this interaction,

namely, with determination of the aerodynamic forces and moments, heat transfer, and ablation. As posed at present, this problem consists not only in determining the overall aerodynamic quantities (the total lift force or drag, the total heat flux from the gas to a surface, etc.), but also in evaluating the distribution of the aerodynamic properties—dynamic and thermal—over a surface of an aircraft moving through a gas (the pressure and shearing stress of friction, local heat fluxes, local ablation).

The solution of such a problem requires a deeper investigation of the flow of a gas than is needed to determine the overall aerodynamic action. It consists in determining the properties of the gas characterizing its flow at each point of the space it occupies and at each instant.

The modern methods of studying the flow of a gas are based on a number of principles and hypotheses established in aerodynamics. One of them is the **continuum hypothesis**—the assumption of the continuity of a gas flow according to which we may disregard the intermolecular distances and molecular movements and consider the continuous changes of the basic properties of a gas in space and in time. This hypothesis follows from the condition consisting in that the free path of molecules and the amplitude of their vibrational motion are sufficiently small in comparison with the linear dimensions characterizing flow around a body, for example the wing span and the diameter or length of the fuselage (or body).

The introduced continuum hypothesis should not contradict the concept of the compressibility of a gas, although the latter should seem to be incompressible in the absence of intermolecular distances. The reality of a compressible continuum follows from the circumstance that the existence of intermolecular distances may be disregarded in many investigations, but at the same time one may assume the possibility of the concentration (density) varying as a result of a change in the magnitude of these distances.

In aerodynamic investigations, the interaction between a gas and a body moving in it is based on the **principle of inverted flow** according to which a system consisting of a gas (air) at rest and a moving body is replaced with a system consisting of a moving gas and a body at rest. When one system is replaced with the other, the condition must be satisfied that the free-stream speed of the gas relative to the body at rest equals the speed of this body in the gas at rest. The principle of inverted motion follows from the general principle of relativity of classical mechanics according to which forces do not depend on which of two interacting bodies (in our case the gas or craft) is at rest and which is performing uniform rectilinear motion.

The system of differential equations underlying the solution of problems of flow over objects is customarily treated separately in

modern aerodynamics for two basic kinds of motion: free (inviscid) flow and flow in a thin layer of the gas adjacent to a wall or boundary—in the boundary layer, where motion is considered with account taken of viscosity. This division of a flow is based on the **hypothesis of the absence of the reverse influence of the boundary layer on the free flow**. According to this hypothesis, the parameters of inviscid flow, i.e. on the outer surface of the boundary layer, are the same as on a wall in the absence of this layer.

The finding of the aerodynamic parameters of craft in unsteady motion characterized by a change in the kinematic parameters with time is usually a very intricate task. Simplified ways of solving this problem are used for practical purposes. Such simplification is possible when the change occurs sufficiently slowly. This is characteristic of many craft. When determining their aerodynamic characteristics, we can proceed from the **hypothesis of steadiness** in accordance with which these characteristics in unsteady motion are assumed to be the same as in steady motion, and are determined by the kinematic parameters of this motion at a given instant.

When performing aerodynamic experiments and calculations, account must be taken of various circumstances associated with the physical similitude of the flow phenomena being studied. Aerodynamic calculations of full-scale craft (rockets, airplanes) are based on preliminary widespread investigations (theoretical and experimental) of flow over models. The conditions that must be observed in such investigations on models are found in the theory of dynamic similitude, and typical and convenient parameters determining the basic conditions of the processes being studied are established. They are called **dimensionless numbers or similarity criteria**. The modern problems of similarity and also the theory of dimensions widely used in aerodynamics are set out in a fundamental work of academician L. Sedov titled "Similarity and Dimensional Methods in Mechanics" [1].

Aerodynamics, figuratively speaking, is a multibranch science. In accordance with the needs of the rapidly developing aviation, rocket, and cosmic engineering, more or less clearly expressed basic scientific trends have taken shape in aerodynamics. They are associated with the aerodynamic investigations of craft as a whole and their individual structural elements, and also of the most characteristic kinds of gas flows and processes attending the flow over a body. It is quite natural that any classification of aerodynamics is conditional to a certain extent because all these trends or part of them are interrelated. Nevertheless, such a "branch" specialization of the aerodynamic science is of a practical interest.

The two main paths along which modern aerodynamics is developing can be determined. The first of them is what is called **force aerodynamics** occupied in solving problems connected with the

force action of a fluid, i.e. in finding the distribution of the pressure and shearing stress over the surface of a craft, and also with the distribution of the resultant aerodynamic forces and moments. The data obtained are used for strength analysis of a craft as a whole and of individual elements thereof, and also for determining its flight characteristics. The second path includes problems of **aero-thermodynamics** and **aerodynamic heating**—a science combining aerodynamics, thermodynamics, and heat transfer and studying flow over bodies in connection with thermal interaction. As a result of these investigations, we find the heat fluxes from a gas to a wall and determine its temperature. These data are needed in analysing the strength and designing the cooling of craft. At the same time, the taking into account of the changes in the properties of a gas flowing over a body under the influence of high temperatures allows us to determine more precisely the quantitative criteria of force interaction of both the external flow and of the boundary layer.

All these problems are of a paramount importance for very high air speeds at which the thermal processes are very intensive. Even greater complications are introduced into the solution of such problems, however, because it is associated with the need to take into consideration the chemical processes occurring in the gas, and also the influence of chemical interaction between the gas and the material of the wall.

If we have in view the range of air speeds from low subsonic to very high supersonic ones, then, as already indicated, we can separate the following basic regions in the science of investigating flow: aerodynamics of an incompressible fluid, or fluid mechanics (the Mach number of the flow is  $M = 0$ ), and high-speed aerodynamics. The latter, in turn, is divided into **subsonic** ( $M < 1$ ), **transonic** ( $M \approx 1$ ), **supersonic** ( $M > 1$ ) and **hypersonic** ( $M \gg 1$ ) **aerodynamics**. It must be noted that each of these branches studies flow processes that are characterized by certain specific features of flows with the indicated Mach numbers. This is why the investigation of such flows can be based on a different mathematical foundation.

We have already indicated that aerodynamic investigations are based on a division of the flow near bodies into two kinds: free (external) inviscid flow and the boundary layer. An independent section of aerodynamics is devoted to each of them.

**Aerodynamics of an ideal fluid** studies a free flow and investigates the distribution of the parameters in inviscid flow over a body that are treated as parameters on the boundary layer edge and, consequently, are the boundary conditions for solving the differential equations of this layer. The inviscid parameters include the pressure. If we know its distribution, we can find the relevant resultant forces and moments. Aerodynamics of an ideal fluid is based on Euler's fundamental equations.

**Aerodynamics of a boundary layer** is one of the broadest and most developed sections of the science of a fluid in motion. It studies viscous gas flow in a boundary layer. The solution of the problem of flow in a boundary layer makes it possible to find the distribution of the shearing stresses and, consequently, of the resultant aerodynamic forces and moments caused by friction. It also makes it possible to calculate the transfer of heat from the gas flowing over a body to a boundary. The conclusions of the boundary layer theory can also be used for correcting the solution on inviscid flow, particularly for finding the correction to the pressure distribution due to the influence of the boundary layer.

The modern theory of the boundary layer is based on fundamental investigations of A. Navier, G. Stokes, O. Reynolds, L. Prandtl, and T. von Kármán. A substantial contribution to the development of the boundary layer theory was made by the Soviet scientists A. Dorodnitsyn, L. Loitsyansky, A. Melnikov, N. Kochin, G. Petrov, V. Streminsky, and others. They created a harmonious theory of the boundary layer in a compressible gas, worked out methods of calculating the flow of a viscous fluid over various bodies (two- and three-dimensional), investigated problems of the transition of a laminar boundary layer into a turbulent one, and studied the complicated problems of turbulent motion.

In aerodynamic investigations involving low airspeeds, the thermal processes in the boundary layer do not have to be taken into account because of their low intensity. When high speeds are involved, however, account must be taken of heat transfer and of the influence of the high boundary layer temperatures on friction. It is quite natural that abundant attention is being given to the solution of such problems, especially recently. In the Soviet Union, professors L. Kalikhman, I. Kibel, V. Iyevlev and others are developing the gas-dynamic theory of heat transfer, studying the viscous flow over various bodies at high temperatures of the boundary layer. Similar problems are also being solved by a number of foreign scientists.

At hypersonic flow speeds, the problems of aerodynamic heating are not the only ones. That ionization occurs at such speeds because of the high temperatures and the gas begins to conduct electricity causes new problems associated with control of the plasma flow with the aid of a magnetic field. When describing the processes of interaction of a moving body with plasma, the relevant aerodynamic calculations must take into account electromagnetic forces in addition to gas-dynamic ones. These problems are studied in **magnetogasdynamics**.

The motion of fluids in accordance with the continuum hypothesis set out above is considered in a special branch of aerodynamics—**continuum aerodynamics**. Many theoretical problems of this branch

of aerodynamics are treated in a fundamental work of L. Sedov: "Continuum Mechanics" (in Russian—a textbook for universities) [2]. It must be noted that the continuum hypothesis holds only for conditions of flight at low altitudes, i.e. in sufficiently dense layers of the atmosphere where the mean free path of the air molecules is small. At high altitudes in conditions of a greatly rarefied atmosphere, the free path of molecules becomes quite significant, and the air can no longer be considered as a continuum. This is why the conclusions of continuum aerodynamics are not valid for such conditions.

The interaction of a rarefied gas with a body moving in it is studied in a special branch of aerodynamics—**aerodynamics of rarefied gases**. The rapid development of this science during recent years is due to the progress in space exploration with the aid of artificial satellites of the Earth and rocket-propelled vehicles, as well as in various types of rocket systems (ballistic, intercontinental, global missiles, etc.) performing flights near the earth at very high altitudes.

The conditions of flow over craft and, consequently, their aerodynamic characteristics vary depending on how the parameters of the gas change at fixed points on a surface. A broad class of flow problems of a practical significance can be solved, as already noted, in steady-state aerodynamics, presuming that the parameters are independent of the time at these points. When studying flight stability, however, account must be taken of the unsteady nature of flow due to the non-uniform airspeed, and of vibrations or rotation of the craft, because in these conditions the flow over a body is characterized by a local change in its parameters with time. The investigation of this kind of flow relates to **unsteady aerodynamics**.

We have considered a classification of modern aerodynamics by the kinds of gas flows. It is obvious that within the confines of each of these branches of aerodynamics, flow is studied as applied to various configurations of craft or their parts. In addition to such a classification, of interest are the branches of modern aerodynamics for which the configuration of a craft or its individual elements is the determining factor.

As regards its aerodynamic scheme, a modern aircraft in the generalized form is a combination of a hull (fuselage), wings, a tail unit (empennage), elevators, and rudders. When performing aerodynamic calculations of such combinations, one must take into account the effects of **aerodynamic interference**—the aerodynamic interaction between all these elements of an aircraft. Accordingly, in particular, the overall aerodynamic characteristics such as the lift force, drag, or moment must be evaluated as the sum of similar characteristics of the isolated hull, wings, tail unit, elevators, and rudders with corrections made for this interaction.

Hence, this scheme of aerodynamic calculations presumes a knowl-

edge of the aerodynamic characteristics of the separate constituent parts of an aircraft.

Aerodynamic calculations of the lifting planes of wings is the subject of a special branch of the aerodynamic science—**wing aerodynamics**. The outstanding Russian scientists and mechanics N. Zhukovsky (Joukowski) and S. Chaplygin are by right considered to be the founders of the aerodynamic theory of a wing.

The beginning of the 20th century was noted by the remarkable discovery by Zhukovsky of the nature of the lift force of a wing; he derived a formula for calculating this force that bears his name. His work on the bound vortices that are a hydrodynamic model of a wing was far ahead of his time. The series of wing profiles (Zhukovsky wing profiles) he developed were widely used in designing airplanes.

Academician S. Chaplygin is the author of many prominent works on wing aerodynamics. In 1910 in his work “On the Pressure of a Parallel Flow on Obstacles” (in Russian), he laid the foundations of the theory of an infinite-span wing. In 1922, he published the scientific work “The Theory of a Monoplane Wing” (in Russian) that sets out the theory of a number of wing profiles (Chaplygin wing profiles) and also develops the theory of stability of a monoplane wing. Chaplygin is the founder of the theory of a finite-span wing.

The fundamental ideas of Zhukovsky and Chaplygin were developed in the works of Soviet scientists specializing in aerodynamics. Associate member of the USSR Academy of Sciences V. Golubev (1884-1954) investigated the flow past short-span wings and various kinds of high-lift devices. Important results in the potential wing theory were obtained by academician M. Keldysh (1911-1978), and also by academicians M. Lavrentyev and L. Sedov. Academician A. Dorodnitsyn summarized the theory of the lifting (loaded) line for a side-slipping wing.

Considerable achievements in the theory of subsonic gas flows belong to M. Keldysh and F. Frankl, who strictly formulated the problem of a compressible flow past a wing and generalized the Kutta-Zhukovsky theorem for this case.

Academician S. Khristianovich in his work “The Flow of a Gas Past a Body at High Subsonic Speeds” (in Russian) [3] developed an original and very effective method for taking into account the influence of compressibility on the flow over airfoils of an arbitrary configuration.

The foreign scientists L. Prandtl (Germany) and H. Glauert (Great Britain) studied the problem of the influence of compressibility on flow past wings. They created an approximate theory of a thin wing in a subsonic flow at a small angle of attack. The results they obtained can be considered as particular cases of the general theory of flow developed by Khristianovich.

A great contribution to the aerodynamics of a wing was made by academician A. Nekrasov (1883-1954), who developed a harmonious theory of a lifting plane in an unsteady flow. Keldysh and Lavrentyev solved the important problem on the flow over a vibrating airfoil by generalizing Chaplygin's method for a wing with varying circulation. Academician Sedov established general formulas for unsteady aerodynamic forces and moments acting on an arbitrarily moving wing.

Professors F. Frankl, E. Krasilshchikova, and S. Falkovich developed the theory of steady and unsteady supersonic flow over thin wings of various configurations.

Important results in studying unsteady aerodynamics of a wing were obtained by professor S. Belotserkovsky, who widely used numerical methods and computers.

The results of aerodynamic investigations of wings can be applied to the calculation of the aerodynamic characteristics of the tail unit, and also of elevators and rudders shaped like a wing. The specific features of flow over separate kinds of aerodynamic elevators and rudders and the presence of other kinds of controls resulted in the appearance of a special branch of modern aerodynamics—the **aerodynamics of controls**.

Modern rocket-type craft often have the configuration of bodies of revolution or are close to them. Combined rocket systems of the type "hull-wing-tail unit" have a hull (body of revolution) as the main component of the aerodynamic system. This explains why the **aerodynamics of hulls (bodies of revolution)**, which has become one of the important branches of today's aerodynamic science, has seen intensive development in recent years.

A major contribution to the development of aerodynamics of bodies of revolution was made by professors F. Frankl and E. Karpovich, who published an interesting scientific work "The Gas Dynamics of Slender Bodies" (in Russian).

The Soviet scientists I. Kibel and F. Frankl, who specialized in aerodynamics, developed the method of characteristics that made it possible to perform effective calculations of axisymmetric supersonic flow past pointed bodies of revolution of an arbitrary thickness.

A group of scientific workers of the Institute of Mathematics of the USSR Academy of Sciences (K. Babenko, G. Voskresensky, and others) developed a method for the numerical calculation of three-dimensional supersonic flow over slender bodies in the general case when chemical reactions in the flow are taken into account. The important problem on the supersonic flow over a slender cone was solved by the foreign specialists in aerodynamics G. Taylor (Great Britain) and Z. Copal (USA).

The intensive development of modern mathematics and computers and the improvement on this basis of the methods of aerodynamic

investigations lead to greater and greater success in solving many complicated problems of aerodynamics including the determination of the overall aerodynamic characteristics of a craft. Among them are the aerodynamic derivatives at subsonic speeds, the finding of which a work of S. Belotserkovsky and B. Skripach [4] is devoted to. In addition, approximate methods came into use for appraising the effect of aerodynamic interference and calculating the relevant corrections to aerodynamic characteristics when the latter were obtained in the form of an additive sum of the relevant characteristics of the individual (isolated) elements of a craft. The solution of such problems is the subject of a special branch of the aerodynamic science—**interference aerodynamics**.

At low supersonic speeds, aerodynamic heating is comparatively small and cannot lead to destruction of a craft member. The main problem solved in the given case is associated with the choice of the cooling for maintaining the required boundary temperature. More involved problems appear for very high airspeeds when a moving body has a tremendous store of kinetic energy. For example, if a craft has an orbital or escape speed, it is sufficient to convert only 25-30% of this energy into heat for the entire material of a structural member to evaporate. The main problem that appears, particularly, in organizing the safe re-entry of a craft into the dense layers of the atmosphere consists in dissipating this energy so that a minimum part of it will be absorbed in the form of heat by the body. It was found that blunt-nosed bodies have such a property. This is exactly what resulted in the development of aerodynamic studies of such bodies.

An important contribution to investigating the problems of **aerodynamics of blunt-nosed bodies** was made by Soviet scientists—academicians A. Dorodnitsyn, G. Cherny, O. Belotserkovsky, and others. Similar investigations were performed by M. Lighthill (Great Britain), P. Garabedian (USA), and other foreign scientists.

Blunting of the front surface must be considered in a certain sense as a way of thermal protection of a craft. The blunted nose experiences the most intensive thermal action, therefore it requires thermal protection to even a greater extent than the peripheral part of the craft. The most effective protection is associated with the use of various coatings whose material at the relevant temperatures is gradually destroyed and ablated. Here a considerable part of the energy supplied by the heated air to the craft is absorbed. The development of the theory and practical methods of calculating ablation relates to a modern branch of the aerodynamic science—**aerodynamics of ablating surfaces**.

A broad range of aerodynamic problems is associated with the determination of the interaction of a fluid with a craft having an arbitrary preset shape in the general case. The shapes of craft sur-

faces can also be chosen for special purposes ensuring a definite aerodynamic effect. The shape of blunt bodies ensures a minimum transfer of heat to the entire body. Consequently, a blunt surface can be considered optimal from the viewpoint of heat transfer. In designing craft, the problem appears of choosing a shape with the minimum force action. One of these problems is associated, particularly, with determination of the shape of a craft head ensuring the smallest drag at a given airspeed. Problems of this kind are treated in a branch of aerodynamics called aerodynamics of optimal shapes.

## **Basic Information from Aerodynamics**

### **1.1. Forces Acting on a Moving Body**

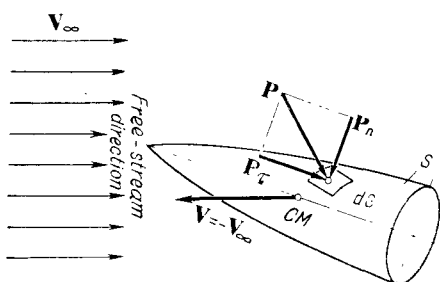
#### **Surface Force**

Let us consider the forces exerted by a gaseous viscous continuum on a moving body. This action consists in the uniform distribution over the body's surface of the forces  $P_n$  produced by the normal and the forces  $P_\tau$  produced by the shear stresses (Fig. 1.1.1). The surface element  $dS$  being considered is acted upon by a resultant force called a surface one. This force  $P$  is determined according to the rule of addition of two vectors:  $P_n$  and  $P_\tau$ . The force  $P_n$  in addition to the force produced by the pressure, which does not depend on the viscosity, includes a component due to friction (Maxwell's hypothesis).

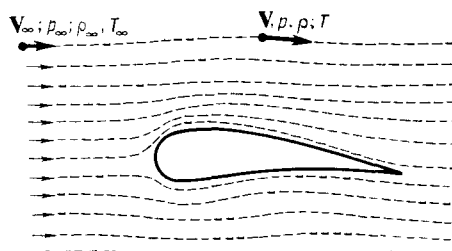
In an ideal fluid in which viscosity is assumed to be absent, the action of a force on an area consists only in that of the forces produced by the normal stress (pressure). This is obvious, because if the force deviated from a normal to the area, its projection onto this area would appear, i.e. a shear stress would exist. The latter, however, is absent in an ideal fluid.

In accordance with the principle of inverted flow, the effect of the forces will be the same if we consider a body at rest and a uniform flow over it having a velocity at infinity equal to the speed of the body before inversion. We shall call this velocity the **velocity at infinity** or the **free-stream velocity** (the velocity of the undisturbed flow) and shall designate it by  $-V_\infty$ , in contrast to  $V$  (the velocity of the body relative to the undisturbed flow), i.e.  $|V| = |V_\infty|$ .

A free stream is characterized by the undisturbed parameters—the pressure  $p_\infty$ , density  $\rho_\infty$ , and temperature  $T_\infty$  differing from their counterparts  $p$ ,  $\rho$ , and  $T$  of the flow disturbed by the body (Fig. 1.1.2). The physical properties of a gas (air) are also characterized by the following kinetic parameters: the dynamic viscosity  $\mu$  and the coefficient of heat conductivity  $\lambda$  (the undisturbed parameters are  $\mu_\infty$  and  $\lambda_\infty$ , respectively), as well as by thermodynamic para-

**Fig. 1.1.1**

Forces acting on a surface element of a moving body

**Fig. 1.1.2**

Designation of parameters of disturbed and undisturbed flows

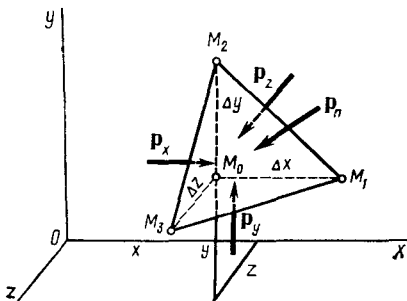
meters: the specific heats at constant pressure  $c_p$  ( $c_{p\infty}$ ) and constant volume  $c_v$  ( $c_{v\infty}$ ) and their ratio (the adiabatic exponent)  $k = c_p/c_v$ , ( $k_\infty = c_{p\infty}/c_{v\infty}$ ).

#### Property of Pressures In an Ideal Fluid

To determine the property of pressures in an ideal fluid, let us take an elementary particle of the fluid having the shape of a tetrahedron  $M_0M_1M_2M_3$  with edge dimensions of  $\Delta x$ ,  $\Delta y$ , and  $\Delta z$  (Fig. 1.1.3) and compile equations of motion for the particle by equating the product of the mass of this element and its acceleration to the sum of the forces acting on it. We shall write these equations in projections onto the coordinate axes. We shall limit ourselves to the equations of motion of the tetrahedron in the projection onto the  $x$ -axis, taking into account that the other two have a similar form. The product of the mass of an element and its acceleration in the direction of the  $x$ -axis is  $\rho_{av} \Delta W dV_x/dt$ , where  $\rho_{av}$  is the average density of the fluid contained in the elementary volume  $\Delta W$ , and  $dV_x/dt$  is the projection of the particle's acceleration onto the  $x$ -axis.

The forces acting on our particle are determined as follows. As we have already established, these forces include what we called the surface force. Here it is determined by the action of the pressure on the faces of our particle, and its projection onto the  $x$ -axis is

$$p_x \Delta S_x - p_n \Delta S_n \cos(\hat{n}, x).$$

**Fig. 1.1.3**

Normal stresses acting on a face of an elementary fluid particle having the shape of a tetrahedron

Another force acting on the isolated fluid volume is the **mass (body) force** proportional to the mass of the particle in this volume. Mass forces include gravitational ones, and in particular the force of gravity. Another example of these forces is the mass force of an electromagnetic origin, known as a **ponderomotive force**, that appears in a gas if it is an electric conductor (ionized) and is in an electromagnetic field. Here we shall not consider the motion of a gas under the action of such forces (see a special course in magnetogasdynamics).

In the case being considered, we shall write the projection of the mass force onto the  $x$ -axis in the form of  $X\rho_{av}\Delta W$ , denoting by  $X$  the projection of the mass force related to a unit of mass. With account taken of these values for the projections of the surface and mass forces, we obtain an equation of motion

$$\rho_{av} \Delta W \frac{dV_x}{dt} = X\rho_{av} \Delta W + p_x \Delta S_x - p_n \Delta S_n \cos(\vec{n}, \vec{x})$$

where  $\Delta S_x$  and  $\Delta S_n$  are the areas of faces  $M_0M_2M_3$  and  $M_1M_2M_3$ , respectively,  $\cos(\vec{n}, \vec{x})$  is the cosine of the angle between a normal  $n$  to face  $M_1M_2M_3$  and the  $x$ -axis, and  $p_x$  and  $p_n$  are the pressures acting on faces  $M_0M_2M_3$  and  $M_1M_2M_3$ , respectively.

Dividing the equation obtained by  $\Delta S_x$  and having in view that  $\Delta S_x = \Delta S_n \cos(\vec{n}, \vec{x})$ , let us pass over to the limit with  $\Delta x$ ,  $\Delta y$ , and  $\Delta z$  tending to zero. Consequently, the terms containing  $\Delta W/\Delta S_x$  will also tend to zero because  $\Delta W$  is a small quantity of the third order, while  $\Delta S_x$  is a small quantity of the second order in comparison with the linear dimensions of the surface element. As a result, we have  $p_x = p_n = 0$ , and, therefore,  $p_x = p_n$ .

When considering the equations of motion in projections onto the  $y$ - and  $z$ -axes, we find that  $p_y = p_n$  and  $p_z = p_n$ .

Since our surface element with the normal  $n$  is oriented arbitrarily, we can arrive at the following conclusion from the results obtained. The pressure at any point of a flow of an ideal fluid is identical on

all surface elements passing through this point, i.e. it does not depend on the orientation of these elements. Consequently, the pressure can be treated as a scalar quantity depending only on the coordinates of a point and the time.

### Influence of Viscosity on the Flow of a Fluid

**Laminar and Turbulent Flow.** Two modes of flow are characteristic of a viscous fluid. The first of them is **laminar** flow distinguished by the orderly arrangement of the individual filaments that do not mix with one another. Momentum, heat, and matter are transferred in a laminar flow at the expense of molecular processes of friction, heat conduction, and diffusion. Such a flow usually appears and remains stable at moderate speeds of a fluid.

If in given conditions of flow over a surface the speed of the flow exceeds a certain limiting (critical) value of it, a laminar flow stops being stable and transforms into a new kind of motion characterized by lateral mixing of the fluid and, as a result, by the vanishing of the ordered, laminar flow. Such a flow is called **turbulent**. In a turbulent flow, the mixing of macroscopic particles having velocity components perpendicular to the direction of longitudinal motion is imposed on the molecular chaotic motion characteristic of a laminar flow. This is the basic distinction of a turbulent flow from a laminar one. Another distinction is that if a laminar flow may be either steady or unsteady, a turbulent flow in its essence has an unsteady nature when the velocity and other parameters at a given point depend on the time. According to the notions of the kinetic theory of gases, random (disordered, chaotic) motion is characteristic of the particles of a fluid, as of molecules.

When studying a turbulent flow, it is convenient to deal not with the instantaneous (actual) velocity, but with its **average** (mean statistical) value during a certain time interval  $t_2$ . For example, the component of the average velocity along the  $x$ -axis is  $\bar{V}_x =$

$$= [1/(t_2 - t_1)] \int_{t_1}^{t_2} V_x dt, \text{ where } V_x \text{ is the component of the actual velocity at the given point that is a function of the time } t. \text{ The components } \bar{V}_y \text{ and } \bar{V}_z \text{ along the } y\text{- and } z\text{-axes are expressed similarly. Using the concept of the average velocity, we can represent the actual velocity as the sum } V_x = \bar{V}_x + V'_x \text{ in which } V'_x \text{ is a variable additional component known as the fluctuation velocity component (or the velocity fluctuation). The fluctuation components of the velocity along the } y\text{- and } z\text{-axes are denoted by } V'_y \text{ and } V'_z, \text{ respectively.}$$

By placing a measuring instrument with a low **inertia** (for example, a hot-wire anemometer) at the required point of a flow, we can record

or measure the fluctuation speed. In a turbulent flow, the instrument registers the deviation of the speed from the mean value—the fluctuation speed.

The kinetic energy of a turbulent flow is determined by the sum of the kinetic energies calculated according to the mean and fluctuation speeds. For a point in question, the kinetic energy of a fluctuation flow can be determined as a quantity proportional to the mean value of the mean square fluctuation velocities. If we resolve the fluctuation flow along the axes of a coordinate system, the kinetic energy of each of the components of such a flow will be proportional to the relevant mean square components of the fluctuation velocities, designated by  $\overline{V_x'^2}$ ,  $\overline{V_y'^2}$ , and  $\overline{V_z'^2}$  and determined from the expression

$$\overline{V_{x(y,z)}'^2} = \frac{1}{t_2 - t_1} \int_{t_1}^{t_2} V_{x(y,z)}'^2 dt$$

The concepts of average and fluctuating quantities can be extended to the pressure and other physical parameters. The existence of fluctuation velocities leads to additional normal and shear stresses and to the more intensive transfer of heat and mass. All this has to be taken into account when running experiments in aerodynamic tunnels. The turbulence in the atmosphere was found to be relatively small and, consequently, it should be just as small in the working part of a tunnel. An increased turbulence affects the results of an experiment adversely. The nature of this influence depends on the **turbulence level** (or the **initial turbulence**), determined from the expression

$$\varepsilon = \frac{1}{\bar{V}} \sqrt{(\overline{V_x'^2} + \overline{V_y'^2} + \overline{V_z'^2})/3} \quad (1.1.1)$$

where  $\bar{V}$  is the overall average speed of the turbulent flow at the point being considered.

In modern low-turbulence aerodynamic tunnels, it is possible in practice to reach an initial turbulence close to what is observed in the atmosphere ( $\varepsilon \approx 0.01-0.02$ ).

The important characteristics of turbulence include the root mean square (rms) fluctuations  $\sqrt{\overline{V_x'^2}}$ ,  $\sqrt{\overline{V_y'^2}}$ , and  $\sqrt{\overline{V_z'^2}}$ . These quantities, related to the overall average speed, are known as the **turbulence intensities** in the corresponding directions and are denoted as

$$\varepsilon_x = \sqrt{\overline{V_x'^2}/\bar{V}}, \quad \varepsilon_y = \sqrt{\overline{V_y'^2}/\bar{V}}, \quad \varepsilon_z = \sqrt{\overline{V_z'^2}/\bar{V}} \quad (1.1.2)$$

Using these characteristics, the initial turbulence (1.1.1) can be expressed as follows:

$$\varepsilon = \sqrt{(\varepsilon_x^2 + \varepsilon_y^2 + \varepsilon_z^2)/3} \quad (1.1.1')$$

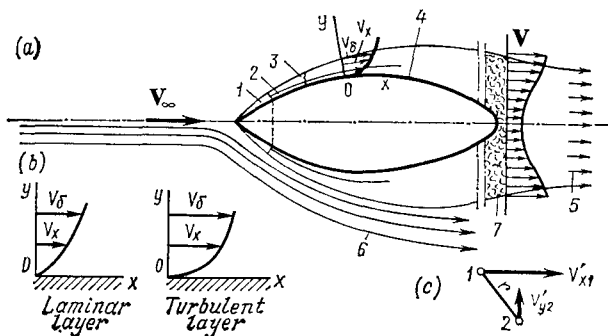


Fig. 1.1.4

Flow of a viscous fluid over a body:

*a*—schematic view of flow; *l*—laminar boundary layer;  
*2*—viscous sublayer; *3*—turbulent boundary layer; *4*—surface in the flow; *5*—wake; *6*—free flow;  
*7*—wake vortex; *b*—velocity profile in the boundary layer; *c*—diagram defining the  
 concept of a two-point correlation coefficient;  $V_\delta$  is the velocity component at the outer edge  
 of the boundary layer

Turbulence is of a vortex nature, i.e. mass, momentum, and energy are transferred by fluid particles of a vortex origin. Hence it follows that fluctuations are characterized by a statistical association. The **correlation coefficient** between fluctuations at points of the region of a disturbed flow being studied is a quantitative measure of this association. In the general form, this coefficient between two random fluctuating quantities  $\varphi$  and  $\psi$  is written as (see [5])

$$R = \overline{\varphi\psi}/(\overline{V\varphi^2}\overline{V\psi^2}) \quad (1.1.3)$$

If there is no statistical association between the quantities  $\varphi$  and  $\psi$ , then  $R = 0$ ; if, conversely, these quantities are regularly associated, the correlation coefficient  $R = 1$ . This characteristic of turbulence is called a **two-point correlation coefficient**. Its expression can be written (Fig. 1.1.4*c*) for two points *1* and *2* of a fluid volume with the relevant fluctuations  $V'_{x1}$  and  $V'_{y2}$  in the form

$$R = \overline{V'_{x1}V'_{y2}}/(\sqrt{\overline{V'^2_{x1}}}\sqrt{\overline{V'^2_{y2}}}) \quad (1.1.3')$$

When studying a three-dimensional turbulent flow, one usually considers a large number of such coefficients. The concept of the **turbulence scale** is introduced to characterize this flow. It is determined by the expression

$$L = \int_0^\infty R dr \quad (1.1.4)$$

The turbulence scale is a linear dimension characterizing the length of the section of a flow on which fluid particles move "in

association", i.e. have statistically associated fluctuations. By moving together the points being considered in a turbulent flow, in the limit at  $r \rightarrow 0$  we can obtain a **one-point correlation coefficient**. With this condition, (1.1.3') acquires the form

$$R = \overline{V'_x V'_y} / (\overline{V'^2} \overline{V'^2}) \quad (1.1.5)$$

This coefficient characterizes the statistical association between fluctuations at a point and, as will be shown below, directly determines the shear stress in a turbulent flow.

Turbulence will be **homogeneous** if its averaged characteristics found for a point (the level and intensity of turbulence, the one-point correlation coefficient) are the same for the entire flow (invariance of the characteristics of turbulence in transfers). Homogeneous turbulence is **isotropic** if its characteristics do not depend on the direction for which they are calculated (invariance of the characteristics of turbulence in rotation and reflection). Particularly, the following condition is satisfied for an isotropic flow:

$$\overline{V'^2} = \overline{V'^2} = \overline{V'^2}$$

If this condition is satisfied for all points, the turbulence is **homogeneous** and **isotropic**. For such turbulence, the constancy of the two-point correlation coefficient is retained with various directions of the line connecting the two points in the fluid volume being considered.

For an isotropic flow, the correlation coefficient (1.1.5) can be expressed in terms of the turbulence level  $\epsilon = \sqrt{\overline{V'^2}} - \bar{V}$ :

$$R = \overline{V'_x V'_y} / \overline{V'^2} = \overline{V'_x V'_y} / (\bar{V}^2 \epsilon^2) \quad (1.1.6)$$

The introduction of the concept of averaged parameters or properties appreciably facilitates the investigation of turbulent flows. Indeed, for practical purposes, there is no need to know the instantaneous values of the velocities, pressures, or shear stresses, and we can limit ourselves to their time-averaged values. The use of averaged parameters simplifies the relevant equations of motion (the Reynolds equations).

Such equations, although they are simpler, include the partial derivatives with respect to time of the averaged velocity components  $\bar{V}_x$ ,  $\bar{V}_y$ , and  $\bar{V}_z$  because in the general case, the turbulent motion is unsteady. In practical cases, however, averaging is performed for a sufficiently long interval of time, and now investigation of an unsteady flow can be reduced to the investigation of steady flow (quasi-steady turbulent flow).

**Shear Stress.** Let us consider the formula for the shear stress in a laminar flow. Here friction appears because of diffusion of the

molecules attended by transfer of the momentum from one layer to another. This leads to a change in the flow velocity, i.e. to the appearance of the relative motion of the fluid particles in the layers. In accordance with a hypothesis first advanced by I. Newton, the shear stress for given conditions is proportional to the velocity of this motion per unit distance between layers with particles moving relative to one another. If the distance between the layers is  $\Delta n$ , and the relative speed of the particles is  $\Delta v$ , the ratio  $\Delta v/\Delta n$  at the limit when  $\Delta n \rightarrow 0$ , i.e. when the layers are in contact, equals the derivative  $\partial v/\partial n$  known as the **normal velocity gradient**. On the basis of this hypothesis, we can write Newton's friction law:

$$\tau = \mu \frac{\partial v}{\partial n} \quad (1.1.7)$$

where  $\mu$  is a proportionality factor depending on the properties of a fluid, its temperature and pressure; it is better known as the **dynamic viscosity**.

The magnitude of  $\mu$  for a gas in accordance with the formula of the kinetic theory is

$$\mu = 0.499 \rho \bar{c} l \quad (1.1.8)$$

At a given density  $\rho$ , it depends on kinetic characteristics of a gas such as the mean free path  $l$  and the mean speed  $\bar{c}$  of its molecules.

Let us consider friction in a turbulent flow. We shall proceed from the simplified scheme of the appearance of additional friction forces in turbulent flow proposed by L. Prandtl for an incompressible fluid, and from the semi-empirical nature of the relations introduced for these forces. Let us take two layers in a one-dimensional flow characterized by a change in the averaged velocity only in one direction. With this in view, we shall assume that the velocity in one of the layers is such that  $\bar{V}_x \neq 0$ ,  $\bar{V}_y = \bar{V}_z = 0$ . For the adjacent layer at a distance of  $\Delta y = l'$  from the first one, the averaged velocity is  $\bar{V}_x + (d\bar{V}_x/dy) l'$ . According to Prandtl's hypothesis, a particle moving from the first layer into the second one retains its velocity  $\bar{V}_x$  and, consequently, at the instant when this particle appears in the second layer, the fluctuation velocity  $V'_x = (d\bar{V}_x/dy) l'$  is observed.

The momentum transferred by the fluid mass  $\rho V'_y dS$  through the area element  $dS$  is  $\rho V'_y (\bar{V}_x + V'_x) dS$ . This momentum determines the additional force produced by the stress originating from the fluctuation velocities. Accordingly, the shear (friction) stress (in magnitude) in the turbulent flow due to fluctuations is

$$|\tau_t| = \rho V'_y (\bar{V}_x + V'_x)$$

Averaging this expression, we obtain

$$|\bar{\tau}_t| = \frac{\rho \bar{V}_x}{t_2 - t_1} \int_{t_1}^{t_2} V'_y dt + \frac{\rho}{t_2 - t_1} \int_{t_1}^{t_2} V'_y V'_x dt = \rho \bar{V}_x \bar{V}'_y + \rho \bar{V}'_x \bar{V}'_y$$

where  $\bar{V}'_x \bar{V}'_y$  is the averaged value of the product of the fluctuation velocities, and  $\bar{V}'_y$  is the averaged value of the fluctuation velocity.

We shall show that this value of the velocity equals zero. Integrating the equality  $V_y = \bar{V}_y + V'_y$  termwise with respect to  $t$  within the limits from  $t_1$  to  $t_2$  and then dividing it by  $t_2 - t_1$ , we find

$$\begin{aligned} \frac{1}{t_2 - t_1} \int_{t_1}^{t_2} V_y dt &= \frac{1}{t_2 - t_1} \int_{t_1}^{t_2} \bar{V}_y dt + \frac{1}{t_2 - t_1} \int_{t_1}^{t_2} V'_y dt \\ &= \bar{V}_y + \frac{1}{t_2 - t_1} \int_{t_1}^{t_2} V'_y dt \end{aligned}$$

But since, by definition,  $\bar{V}_y = \frac{1}{t_2 - t_1} \int_{t_1}^{t_2} V_y dt$ , it is obvious that

$\bar{V}'_y = \frac{1}{t_2 - t_1} \int_{t_1}^{t_2} V'_y dt = 0$ . Hence, the averaged value of the shear stress due to fluctuations can be expressed by the relation  $|\bar{\tau}_t| = \rho \bar{V}'_x \bar{V}'_y$  that is the generalized Reynolds formula. Its form does not depend on any specific assumptions on the structure of the turbulence.

The shear stress determined by this formula can be expressed directly in terms of the correlation coefficient. In accordance with (1.1.5), we have

$$|\tau_t| = \rho R \sqrt{\bar{V}'_x^2} \sqrt{\bar{V}'_y^2} \quad (1.1.9)$$

or for an isotropic flow for which we have  $\sqrt{\bar{V}'_x^2} = \sqrt{\bar{V}'_y^2}$ ,

$$|\tau_t| = \rho R \bar{V}'_x^2 = \rho R e^2 \bar{V}^2 \quad (1.1.9')$$

According to this expression, an additional shear stress due to fluctuations does not necessarily appear in any flow characterized by a certain turbulence level. Its magnitude depends on the measure of the statistical mutual association of the fluctuations determined by the correlation coefficient  $R$ .

The generalized Reynolds formula for the shear stress in accordance with Prandtl's hypothesis on the proportionality of the fluctuation velocities [ $V'_y = a V'_x = a l' (d\bar{V}_x/dy)$ , where  $a$  is a coefficient]

can be transformed as follows:

$$|\bar{\tau}_t| = \rho \bar{V}'_x \bar{V}'_y = \frac{\rho}{t_2 - t_1} \left( \frac{d\bar{V}_x}{dy} \right)^2 \int_{t_1}^{t_2} l'^2 a \, dt = \rho l^2 \left( \frac{d\bar{V}_x}{dy} \right)^2 \quad (1.1.10)$$

Here the proportionality coefficient  $a$  has been included in the averaged value of  $l'$ , designated by  $l$ .

The quantity  $l$  is called the **mixing length** and is, as it were, an analogue of the mean free path of molecules in the kinetic theory of gases. The sign of the shear stress is determined by that of the velocity gradient. Consequently,

$$\tau_t = \rho l^2 | d\bar{V}_x/dy | d\bar{V}_x/dy \quad (1.1.10')$$

The total value of the shear stress is obtained if to the value  $\tau_t$  due to the expenditure of energy by particles on their collisions and chaotic mixing we add the shear stress occurring directly because of the viscosity and due to mixing of the molecules characteristic of a laminar flow, i.e. the value  $\tau_l = \mu d\bar{V}_x/dy$ . Hence,

$$\tau = \tau_l + \tau_t = \mu d\bar{V}_x/dy + \rho l^2 | d\bar{V}_x/dy | d\bar{V}_x/dy \quad (1.1.11)$$

Prandtl's investigations show that the mixing length  $l = \kappa y$ , where  $\kappa$  is a constant. Accordingly, at a wall of the body in the flow, we have

$$\tau_{y=0} = \tau_l = |\mu d\bar{V}_x/dy|_{y=0} \quad (1.1.12)$$

It follows from experimental data that in a turbulent flow in direct proximity to a wall, where the intensity of mixing is very low, the shear stress remains the same as in laminar flow, and relation (1.1.12) holds for it. Beyond the limits of this flow, the stress  $\tau_l$  will be very small, and we may consider that the shear stress is determined by the quantity (1.1.10').

**Boundary Layer.** It follows from relations (1.1.7) and (1.1.10) that for the same fluid flowing over a body, the shear stress at different sections of the flow is not the same and is determined by the magnitude of the local velocity gradient.

Investigations show that the velocity gradient is the largest near a wall because a viscous fluid experiences a retarding action owing to its adhering to the surface of the body in the fluid. The velocity of the flow is zero at the wall (see Fig. 1.1.4) and gradually increases with the distance from the surface. The shear stress changes accordingly—at the wall it is considerably greater than far from it. The thin layer of fluid adjacent to the surface of the body in a flow that is characterized by large velocity gradients along a normal to it and, consequently, by considerable shear stresses is called a **boundary layer**. In this layer, the viscous forces have a magnitude of the

same order as all the other forces (for example, the forces of inertia and pressure) governing motion and, therefore, taken into account in the equations of motion.

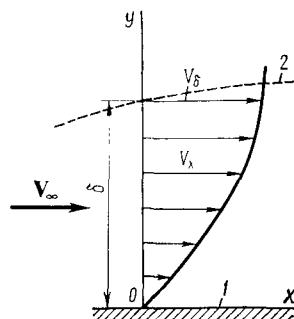
A physical notion of the boundary layer can be obtained if we imagine the surface in the flow to be coated with a pigment soluble in the fluid. It is obvious that the pigment diffuses into the fluid and is simultaneously carried downstream. Consequently, the coloured zone is a layer gradually thickening downstream. The coloured region of the fluid approximately coincides with the boundary layer. This region leaves the surface in the form of a coloured **wake** (see Fig. 1.1.4a).

As shown by observations, for a turbulent flow, the difference of the coloured region from the boundary layer is comparatively small, whereas in a laminar flow this difference may be very significant. According to theoretical and experimental investigations, with an increase, in the velocity, the thickness of the layer diminishes, and the wake becomes narrower.

The nature of the velocity distribution over the cross section of a boundary layer depends on whether it is laminar or turbulent. Owing to lateral mixing of the particles and also to their collisions, this distribution of the velocity, more exactly of its time-averaged value, will be appreciably more uniform in a turbulent flow than in a laminar one (see Fig. 1.1.4). The distribution of the velocities near the surface of a body in a flow also allows us to make the conclusion on the higher shear stress in a turbulent boundary layer determined by the increased value of the velocity gradient.

Beyond the limits of the boundary layer, there is a part of the flow where the velocity gradients and, consequently, the forces of friction are small. This part of the flow is known as the **external free flow**. In investigation of an external flow, the influence of the viscous forces is disregarded. Therefore, such a flow is also considered to be **inviscid**. The velocity in the boundary layer grows with an increasing distance from the wall and asymptotically approaches a theoretical value corresponding to the flow over the body of an inviscid fluid, i.e. to the value of the velocity in the external flow at the boundary of the layer.

We have already noted that in direct proximity to it a wall hinders mixing, and, consequently, we may assume that the part of the boundary layer adjacent to the wall is in conditions close to laminar ones. This thin section of a quasilaminar boundary layer is called a **viscous sublayer** (it is also sometimes called a **laminar sublayer**). Later investigations show that fluctuations are observed in the viscous sublayer that penetrate into it from a turbulent core, but there is no correlation between them (the correlation coefficient  $R = 0$ ). Therefore, according to formula (1.1.9), no additional shear stresses appear.

**Fig. 1.1.5**

Boundary layer:

- 1—wall of a body in the flow;  
2—outer edge of the layer.

The main part of the boundary layer outside of the viscous sublayer is called the **turbulent core**. The studying of the motion in a boundary layer is associated with the simultaneous investigation of the flow of a fluid in a turbulent core and a viscous sublayer.

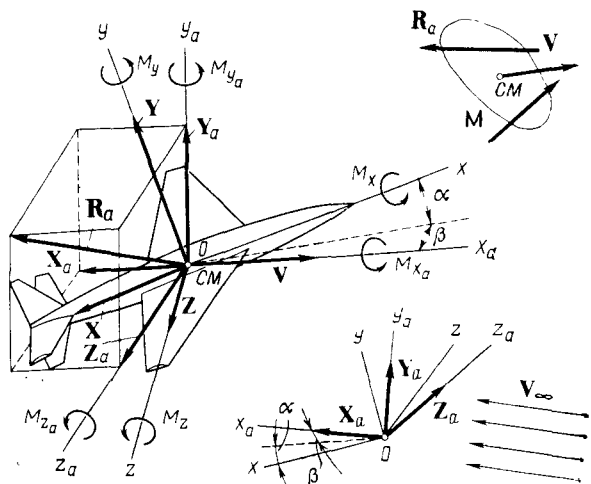
The change in the velocity over the cross section of the boundary layer is characterized by its gradually growing with the distance from the wall and asymptotically approaching the value of the velocity in the external flow. For practical purposes, however, it is convenient to take the part of the boundary layer in which this change occurs sufficiently rapidly, and the velocity at the boundary of this layer differs only slightly from its value in the external flow. The distance from the wall to this boundary is what is conventionally called the **thickness of the boundary layer**  $\delta$  (Fig. 1.1.5). This thickness is usually defined as the distance from the contour of a body to a point in the boundary layer at which the velocity differs from its value in the external layer by not over one per cent.

The introduction of the concept of a boundary layer made possible effective research of the friction and heat transfer processes because owing to the smallness of its thickness in comparison with the dimensions of a body in a flow, it became possible to simplify the differential equations describing the motion of a gas in this region of a flow, which makes their integration easier.

## 1.2. Resultant Force Action

### Components of Aerodynamic Forces and Moments

The forces produced by the normal and shear stresses continuously distributed over the surface of a body in a flow can be reduced to a single resultant vector  $R_a$  of the aerodynamic forces and a resultant vector  $M$  of the moment of these forces (Fig. 1.2.1) relative to a reference point called the **centre of moments**. Any point of the body

**Fig. 1.2.1**

Aerodynamic forces and moments acting on a craft in the flight path ( $x_a$ ,  $y_a$ , and  $z_a$ ) and body axis ( $x$ ,  $y$ , and  $z$ ) coordinate systems

can be this centre. Particularly, when testing craft in wind tunnels, the moment is found about one of the points of mounting of the model that may coincide with the nose of the body, the leading edge of a wing, etc. When studying real cases of the motion of such craft in the atmosphere, one can determine the aerodynamic moment about their centre of mass or some other point that is a centre of rotation.

In engineering practice, instead of considering the vectors  $R_a$  and  $M$ , their projections onto the axes of a coordinate system are usually dealt with. Let us consider the **flight path** and **fixed or body axis** orthogonal coordinate systems (Fig. 1.2.1) encountered most often in aerodynamics. In the flight path system, the aerodynamic forces and moments are usually given because the investigation of many problems of flight dynamics is connected with the use of coordinate axes of exactly such a system. Particularly, it is convenient to write the equations of motion of a craft's centre of mass in projections onto these axes. The **flight path** axis  $Ox_a$  of a velocity system is always directed along the velocity vector of a craft's centre of mass. The axis  $Oy_a$  of the flight path system (the **lift axis**) is in the plane of symmetry and is directed upward (its positive direction). The axis  $Oz_a$  (the **lateral axis**) is directed along the span of the right (starboard) wing (a right-handed coordinate system). In inverted flow, the flight path axis  $Ox_a$  coincides with the direction of the flow velocity, while the axis  $Oz_a$  is directed along

the span of the left (port) wing so as to retain a right-handed coordinate system. The latter is called a **wind coordinate system**.

Aerodynamic calculations can be performed in a fixed or body axis coordinate system. In addition, rotation of a craft is usually investigated in this system because the relevant equations are written in body axes. In this system, rigidly fixed to a craft, the **longitudinal body axis**  $Ox$  is directed along the principal axis of inertia. The **normal axis**  $Oy$  is in the plane of symmetry and is oriented toward the upper part of the craft. The **lateral body axis**  $Oz$  is directed along the span of the right wing and forms a right-handed coordinate system. The positive direction of the  $Ox$  axis from the tail to the nose corresponds to non-inverted flow (Fig. 1.2.1). The origins of both coordinate systems—the flight path (wind) and the body axis systems—are at a craft's centre of mass.

The projections of the vector  $\mathbf{R}_a$  onto the axes of a flight path coordinate system are called the **drag force**  $X_a$ , and **lift force**  $Y_a$ , and the **side force**  $Z_a$ , respectively. The corresponding projections of the same vector onto the axes of a body coordinate system are called the **longitudinal**  $X$ , the **normal**  $Y$ , and the **lateral**  $Z$  forces.

The projections of the vector  $\mathbf{M}$  onto the axes in the two coordinate systems have the same name: the components relative to the longitudinal axis are called the **rolling moment** (the relevant symbols are  $M_{x_a}$  in a flight path system and  $M_x$  in a body one), the components relative to the vertical axis are called the **yawing moment** ( $M_{y_a}$  or  $M_y$ ), and those relative to the lateral axis are called the **pitching moment** ( $M_{z_a}$  or  $M_z$ ).

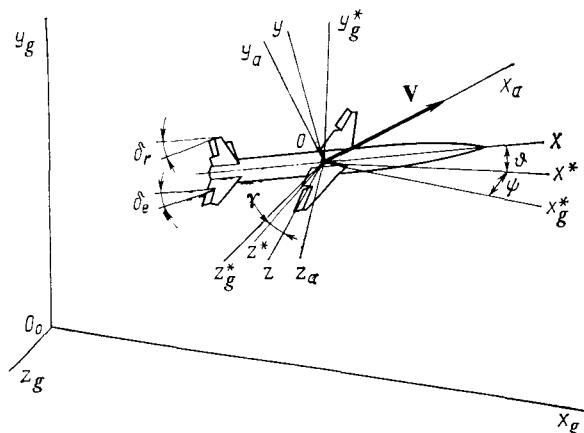
In accordance with the above, the vectors of the aerodynamic forces and moment in the flight path and body axis coordinate systems are:

$$\mathbf{R}_a = \mathbf{X}_a + \mathbf{Y}_a + \mathbf{Z}_a = \mathbf{X} + \mathbf{Y} + \mathbf{Z} \quad (1.2.1)$$

$$\mathbf{M} = M_{x_a} + M_{y_a} + M_{z_a} = M_x + M_y + M_z \quad (1.2.2)$$

We shall consider a moment about an axis to be positive if it tends to turn the craft counterclockwise (when watching the motion from the tip of the moment vector). In accordance with the adopted arrangement of the coordinate axes, a positive moment in Fig. 1.2.1 increases the angle of attack, and a negative moment reduces it.

The magnitude and direction of the forces and moments at a given airspeed and altitude depend on the orientation of the body relative to the velocity vector  $\mathbf{V}$  (or if inverted flow is being considered, relative to the direction of the free-stream velocity  $\mathbf{V}_\infty$ ). This orientation, in turn, underlies the relevant mutual arrangement of the coordinate systems associated with the flow and the body. This arrangement is determined by the **angle of attack**  $\alpha$  and the **sideslip angle**  $\beta$  (Fig. 1.2.1). The first of them is the angle between

**Fig. 1.2.2**

Determining the position of a craft in space

the axis  $Ox$  and the projection of the vector  $\mathbf{V}$  onto the plane  $xOy$ , and the second is the angle between the vector  $\mathbf{V}$  and the plane  $xOy$ .

The angle of attack is considered to be positive if the projection of the air velocity onto the normal axis is negative. The sideslip angle is positive if this projection onto the lateral axis is positive.

When studying a flight, a **normal earth-fixed coordinate system** is used relative to which the position of a body moving in space is determined. The origin of coordinates of this system (Fig. 1.2.2) coincides with a point on the Earth's surface, for example with the launching point. The axis  $O_0y_g$  is directed upward along a local vertical, while the axes  $O_0x_g$  and  $O_0z_g$  coincide with a horizontal plane. The axis  $O_0x_g$  is usually oriented in the direction of flight, while the direction of the axis  $O_0z_g$  corresponds to a right-handed coordinate system.

If the origin of an earth-fixed system of coordinates is made to coincide with the centre of mass of a craft, we obtain a normal earth-fixed coordinate system also known as a local geographical coordinate system  $Ox^*_gy^*_gz^*$  (Fig. 1.2.2). The position of a craft relative to this coordinate system is determined by three angles: the yawing (course) angle  $\psi$ , the pitching angle  $\vartheta$ , and the rolling (banking) angle  $\gamma$ .

The angle  $\psi$  is formed by the projection of the longitudinal body axis  $Ox$  onto the horizontal plane  $x^*_gOy^*_g(Ox^*)$  and the axis  $Ox^*_g$ ; this angle is positive if the axis  $Ox^*_g$  coincides with the projection of  $Ox^*$  by clockwise rotation about the axis  $Oy^*$ .

The angle  $\vartheta$  is that between the axis  $Ox$  and the horizontal plane  $x^*_gOz^*_g$  and will be positive if this plane is below the longitudinal

body axis. The angle  $\gamma$  is formed upon the rotation (rolling) of a craft about the longitudinal axis  $Ox$  and is measured in magnitude as the angle between the lateral body axis and the axis  $Oz_g$  displaced to a position corresponding to a zero yawing angle (or as the angle between the axis  $Oz$  and its projection onto a horizontal plane—the axis  $Oz_g^*$ ). If displacement of the axis  $Oz_g^*$  with respect to the lateral axis occurs clockwise, the angle  $\gamma$  is positive.

The pitching angle determines the inclination of a craft to the horizon, and the yawing angle—the deviation of the direction of its flight from the initial one (for an aircraft this is the deviation from its course, for a projectile or rocket this is the deviation from the plane of launching).

**Conversion of Aerodynamic Forces  
and Moments from One Coordinate System  
to Another**

Knowing the angles  $\alpha$  and  $\beta$ , we can convert the components of the force and moment in one coordinate system to components in another system in accordance with the rules of analytical geometry. Particularly, the components of the aerodynamic force and moment in a body axis system are converted to the drag force and the rolling moment, respectively, in a flight path system of coordinates by the formulas

$$X_a = X \cos(\widehat{xx}_a) + Y \cos(\widehat{yx}_a) + Z \cos(\widehat{zx}_a) \quad (1.2.3)$$

$$M_{x_a} = M_x \cos(\widehat{xx}_a) + M_y \cos(\widehat{yx}_a) + M_z \cos(\widehat{zx}_a) \quad (1.2.3')$$

where  $\cos(\widehat{xx}_a)$ ,  $\cos(\widehat{yx}_a)$ ,  $\cos(\widehat{zx}_a)$  are the cosines of the angles between the axis  $Ox_a$  and the axes  $Ox$ ,  $Oy$ , and  $Oz$ , respectively.

The expressions for the other components of the force vector, and also for the components of the moment vector, are written in a similar way. The values of the direction cosines used for converting forces and moments from one coordinate system to another are given in Table 1.2.1.

*Table 1.2.1*

Body axis system	Flight path system		
	$Ox_a$	$Oy_a$	$Oz_a$
$Ox$	$\cos \alpha \cos \beta$	$\sin \alpha$	$-\cos \alpha \sin \beta$
$Oy$	$-\sin \alpha \cos \beta$	$\cos \alpha$	$\sin \alpha \sin \beta$
$Oz$	$\sin \beta$	0	$\cos \beta$

In accordance with the data of Table 1.2.1, Eqs. (1.2.3) and (1.2.3') acquire the following form:

$$X_a = X \cos \alpha \cos \beta - Y \sin \alpha \cos \beta + Z \sin \beta \quad (1.2.4)$$

$$M_{x_a} = M_x \cos \alpha \cos \beta - M_y \sin \alpha \cos \beta + M_z \sin \beta \quad (1.2.4')$$

For example, for the motion of the aircraft shown in Fig. 1.2.1, Eq. (1.2.4) yields, with the relevant signs:

$$-X_a = -X \cos \alpha \cos \beta - Y \sin \alpha \cos \beta + Z \sin \beta$$

The force and moment components\* are converted in a similar way from a flight path to a body axis coordinate system. For example, by using the data of Table 1.2.1, we obtain the following conversion formulas for the longitudinal force and the rolling moment:

$$X = X_a \cos \alpha \cos \beta + Y_a \sin \alpha - Z_a \cos \alpha \sin \beta \quad (1.2.5)$$

$$M_x = M_{x_a} \cos \alpha \cos \beta + M_{y_a} \sin \alpha - M_{z_a} \cos \alpha \sin \beta \quad (1.2.5')$$

We can go over from a local geographical coordinate system (a normal system) to a body axis or flight path one, or vice versa, if we know the cosines of the angles between the corresponding axes. Their values can be determined from Fig. 1.2.2 that shows the mutual arrangement of the axes of these coordinate systems.

### 1.3. Determination of Aerodynamic Forces and Moments According to the Known Distribution of the Pressure and Shear Stress. Aerodynamic Coefficients

#### Aerodynamic Forces and Moments and Their Coefficients

Assume that for a certain angle of attack and sideslip angle, and also for given parameters of the free stream (the speed  $V_\infty$ , static pressure  $p_\infty$ , density  $\rho_\infty$ , and temperature  $T_\infty$ ), we know the distribution of the pressure  $p$  and shear stress  $\tau$  over the surface of the body in the flow. We want to determine the resultant values of the aerodynamic forces and moments.

The isolated surface element  $dS$  of the body experiences a normal force produced by the excess pressure  $(p - p_\infty) dS$  and the tangential

\* We shall omit the word "components" below for brevity, but shall mean it and use formulas for scalar quantities.

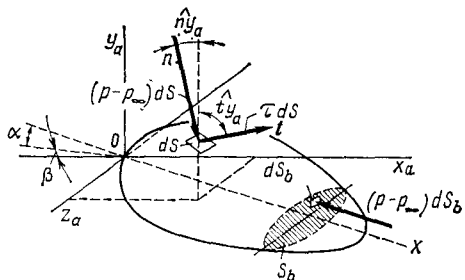


Fig. 1.3.1

Action of pressure and friction (shear) forces on an elementary area

force  $\tau dS$ . The sum of the projections of these forces onto the  $x$ -axis of a wind (flight path) coordinate system is (Fig. 1.3.1)

$$[(p - p_\infty) \cos(\hat{n}, x_a) + \tau \cos(\hat{t}, x_a)] dS \quad (1.3.1)$$

where  $n$  and  $t$  are a normal and a tangent to the element of area, respectively.

The other two projections onto the axes  $y_a$  and  $z_a$  are obtained by a similar formula with the corresponding cosines. To find the resultant forces, we have to integrate expression (1.3.1) over the entire surface  $S$ . Introducing into these equations the **pressure coefficient**  $\bar{p} = (p - p_\infty)/q_\infty$  and the **local friction factor**  $c_{f,x} = \tau/q_\infty$ , where  $q_\infty = \rho_\infty V_\infty^2/2$  is the velocity head, we obtain formulas for the drag force, the lift force, and the side force, respectively:

$$X_a = q_\infty S_r \int \limits_{(S)} [\bar{p} \cos(\hat{n}, x_a) + c_{f,x} \cos(\hat{t}, x_a)] dS / S_r \quad (1.3.2)$$

$$Y_a = q_\infty S_r \int \limits_{(S)} [-\bar{p} \cos(\hat{n}, y_a) + c_{f,x} \cos(\hat{t}, y_a)] dS / S_r \quad (1.3.3)$$

$$Z_a = -q_\infty S_r \int \limits_{(S)} [\bar{p} \cos(\hat{n}, z_a) + c_{f,x} \cos(\hat{t}, z_a)] dS / S_r \quad (1.3.4)$$

We can choose a random surface area such as that of a wing in plan view or the area of the largest cross section (the mid-section) of the fuselage as the characteristic area  $S_r$  in these formulas. The integrals in formulas (1.3.2)-(1.3.4) are dimensionless quantities taking into account how the aerodynamic forces are affected by the nature of the flow over a body of a given geometric configuration and by the distribution of the dimensionless coefficients of pressure and friction due to this flow.

In formulas (1.3.2) for the force  $X_a$ , the dimensionless quantity is usually designated by  $c_x$  and is known as the **drag coefficient**.

In the other two formulas, the corresponding symbols  $c_{y_a}$  and  $c_{z_a}$  are introduced. The relevant quantities are known as the **aerodynamic lift coefficient** and the **aerodynamic side-force coefficient**. With a view to the above, we have

$$X_a = c_{x_a} q_\infty S_r, \quad Y_a = c_{y_a} q_\infty S_r, \quad Z_a = c_{z_a} q_\infty S_r \quad (1.3.5)$$

We can obtain general relations for the moments in the same way as formulas (1.3.2)–(1.3.4) for the forces. Let us consider as an example such a relation for the pitching moment  $M_{z_a}$ . It is evident that the elementary value of this moment  $dM_{z_a}$  is determined by the sum of the moments about the axis  $z_a$  of the forces acting on an area  $dS$  in a plane at right angles to the axis  $z_a$ . If the coordinates of the area  $dS$  are  $y_a$  and  $x_a$ , the elementary value of the moment is

$$\begin{aligned} dM_{z_a} = q_\infty S_r & \{ [\bar{p} \cos(\hat{n}, \hat{y}_a) - c_{f,x} \cos(\hat{t}, \hat{y}_a)] x_a \\ & - [\bar{p} \cos(\hat{n}, \hat{x}_a) + c_{f,x} \cos(\hat{t}, \hat{x}_a)] y_a \} dS / S_r \end{aligned}$$

Integrating this expression over the surface  $S$  and introducing the dimensionless parameter

$$\begin{aligned} m_{z_a} = \frac{M_{z_a}}{q_\infty S_r L} = \int_{(S)} & \{ [\bar{p} \cos(\hat{n}, \hat{y}_a) - c_{f,x} \cos(\hat{t}, \hat{y}_a)] x_a \\ & - [\bar{p} \cos(\hat{n}, \hat{x}_a) + c_{f,x} \cos(\hat{t}, \hat{x}_a)] y_a \} \frac{dS}{S_r L} \quad (1.3.6) \end{aligned}$$

in which  $L$  is a characteristic geometric length, we obtain a formula for the pitching moment:

$$M_{z_a} = m_{z_a} q_\infty S_r L \quad (1.3.7)$$

The parameter  $m_{z_a}$  is called the **aerodynamic pitching-moment coefficient**. The formulas for the other components of the moment are written similarly:

$$M_{x_a} = m_{x_a} q_\infty S_r L \quad \text{and} \quad M_{y_a} = m_{y_a} q_\infty S_r L \quad (1.3.8)$$

The dimensionless parameters  $m_{x_a}$  and  $m_{y_a}$  are called the **aerodynamic rolling-moment** and **yawing-moment coefficients**, respectively.

The relevant coefficients of the aerodynamic forces and moments can also be introduced in a body axis coordinate system. The use of these coefficients allows the forces and moments to be written as follows:

$$\begin{aligned} X &= c_x q_\infty S_r, \quad M_x = m_x q_\infty S_r L \\ Y &= c_y q_\infty S_r, \quad M_y = m_y q_\infty S_r L \\ Z &= c_z q_\infty S_r, \quad M_z = m_z q_\infty S_r L \end{aligned} \quad (1.3.9)$$

The quantities  $c_x$ ,  $c_y$ , and  $c_z$  are called the **aerodynamic longitudinal-force**, **normal-force**, and **lateral-force coefficients**, and the parameters  $m_x$ ,  $m_y$ , and  $m_z$ —the **aerodynamic body axis rolling-moment**, **yawing-moment**, and **pitching-moment coefficients**, respectively.

An analysis of the expressions for the aerodynamic forces (1.3.2)–(1.3.4) allows us to arrive at the conclusion that each of these forces can be resolved into a component due to the pressure and a component associated with the shear stresses appearing upon the motion of a viscous fluid. For example, the drag  $X_a = X_{a,p} + X_{a,f}$ , where  $X_{a,p}$  is the **pressure drag** and  $X_{a,f}$  is the **friction drag**. Accordingly, the overall coefficient of drag equals the sum of the coefficients of pressure and friction drags:  $c_{x_a} = c_{x_{a,p}} + c_{x_{a,f}}$ .

Similarly, the aerodynamic lift- and side-force coefficients, and also the moments, can be represented as the sum of two components. The forces, moments, and their coefficients are written in the same way in a body axes. For example, the longitudinal-force coefficient  $c_x = c_{x,p} + c_{x,f}$ , where  $c_{x,p}$  and  $c_{x,f}$  are the coefficients of the longitudinal forces due to pressure and friction, respectively.

The components of the aerodynamic forces and moments depending on friction are not always the same as those depending on the pressure as regards their order of magnitude. Investigations show that the influence of friction is more appreciable for flow over long and thin bodies. In practice, it is good to take this influence into account mainly when determining the drag or longitudinal force.

When a surface in a flow has a plane area at its tail part (a bottom cut of the fuselage or a blunt trailing edge of a wing), the pressure drag is usually divided into two more components, namely, the pressure drag on a side surface (the **nose drag**), and the drag due to the pressure on the base cut or section (the **base drag**). Hence, the overall drag and the relevant aerodynamic coefficient are

$$X_a = X_{a,n} + X_{a,b} + X_{a,f} \quad \text{and} \quad c_{x_a} = c_{x_{a,n}} + c_{x_{a,b}} + c_{x_{a,f}}$$

When determining the longitudinal force and its coefficient, we obtain

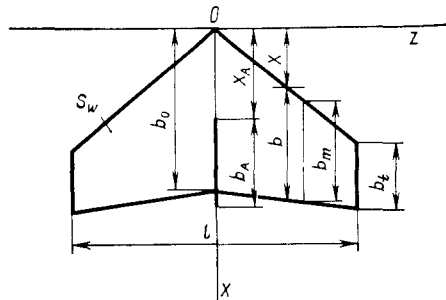
$$X = X_n + X_b + X_f \quad \text{and} \quad c_x = c_{x,n} + c_{x,b} + c_{x,f}$$

In accordance with Fig. 1.3.1, we have

$$X_b = -q_\infty \int_{S_b} \bar{p}_b dS_b \quad \text{and} \quad c_{x,b} = \frac{X_b}{q_\infty S_r}$$

where  $\bar{p}_b = (p_b - p_\infty)/q_\infty$  (this quantity is negative because a rarefaction appears after a bottom cut, i.e.  $p_b < p_\infty$ ).

**Characteristic Geometric Dimensions.** The absolute value of an aerodynamic coefficient, which is arbitrary to a certain extent,

**Fig. 1.3.2**

Schematic view of a wing:  
 $b_0$ —centre chord,  $b_t$ —tip chord,  
and  $b$ —local chord

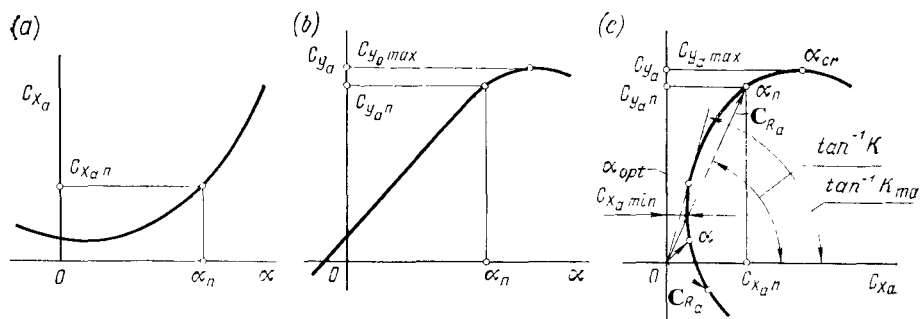
depends on the choice of the characteristic geometric dimensions  $S_r$  and  $L$ . To facilitate practical calculations, however, a characteristic geometric quantity is chosen beforehand. In aerospace technology, the area of the mid-section (the largest cross section) of the body  $S_r = S_{\text{mid}}$  is usually chosen as the characteristic area, and the length of the rocket is taken as the characteristic linear dimension  $L$ .

In aerodynamic calculations of aircraft, the wing plan area  $S_r = S_w$ , the wing span  $l$  (the distance between the wing tips) or the wing chord  $b$  are adopted as the characteristic dimensions. By the **chord of a wing** is meant a length equal to the distance between the farthest points of an airfoil (section). For a wing with a rectangular planform, the chord equals the width of the wing. In practice, a wing usually has a chord varying along its span. Either the **mean geometric chord**  $b = b_m$  equal to  $b_m = S_w/l$  or the **mean aerodynamic chord**  $b = b_A$  is taken as the characteristic dimension for such a wing. The mean aerodynamic chord is determined as the chord of the airfoil of an equivalent rectangular wing for which with an identical wing plan area the moment aerodynamic characteristics are approximately the same as of the given wing.

The length of the mean aerodynamic chord and the coordinate of its leading edge are determined as follows (Fig. 1.3.2):

$$b_A = \frac{2}{S_w} \int_0^{l/2} b^2 dz, \quad x_A = \frac{2}{S_w} \int_0^{l/2} bx dz$$

When calculating forces and moments according to known aerodynamic coefficients, the geometric dimensions must be used for which these coefficients were evaluated. Should such calculations have to be performed for other geometric dimensions, the aerodynamic coefficients must be preliminarily converted to the relevant geometric dimension. For this purpose, one must use the relations  $c_1 S_1 = c_2 S_2$  (for the force coefficients), and  $m_1 S_1 L_1 = m_2 S_2 L_2$  (for the moment coefficients) obtained from the conditions of the constancy

**Fig. 1.3.3**

Constructing a polar of the first kind of a craft:

$c_{x_a}$  vs.  $\alpha$ ;  $b$ — $c_{y_a}$  vs.  $\alpha$ ;  $c$ —polar of first kind

of the forces and moments acting on the same craft. These relations are used to find the coefficients  $c_2$  and  $m_2$ , respectively, converted to the new characteristic dimensions  $S_2$  and  $L_2$ :

$$c_2 = c_1 (S_1/S_2), \quad m_2 = m_1 (S_1 L_1 / S_2 L_2)$$

where the previous dimensions  $S_1$ ,  $L_1$  and aerodynamic coefficients  $c_1$ ,  $m_1$ , as well as the new dimensions  $S_2$ ,  $L_2$  are known.

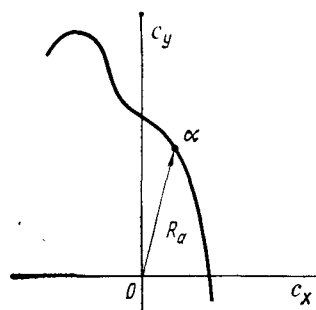
**Polar of a Craft.** A very important aerodynamic characteristic that has found widespread use is what is known as the **polar** of a craft. It establishes a relation between the lift and drag forces or, which is the same, between the lift and drag coefficients in a flight path coordinate system. This curve, called a **polar of the first kind** (Fig. 1.3.3c) is the locus of the tips of the resultant aerodynamic force vectors  $R_a$  acting on a craft at various angles of attack [or of the vectors of the coefficient  $c_{R_a}$  of this force determined in accordance with the relation  $c_{R_a} = R_a/(S_r q_\infty)$ ].

A polar of the first kind is constructed with the aid of graphs of  $c_{x_a}$  versus  $\alpha$  and  $c_{y_a}$  versus  $\alpha$  so that the values of  $c_{x_a}$  and  $c_{y_a}$  are laid off along the axes of abscissas and ordinates, respectively. The relevant angle of attack  $\alpha$ , which is a parameter of the polar in the given case, is written at each point of the curve.

A polar of the first kind is convenient for practical use because it allows one to readily find for any angle of attack such a very important aerodynamic characteristic of a craft as its lift-to-drag ratio

$$K = c_{y_a}/c_{x_a} = Y_a/X_a \quad (1.3.10)$$

If the scales of  $c_{y_a}$  (or  $Y_a$ ) and  $c_{x_a}$  (or  $X_a$ ) are the same, the quantity  $K$  equals the slope of a vector drawn from the origin of coordi-

**Fig. 1.3.4**

Drag polar of the second kind

nates (the pole) to the point of the polar diagram corresponding to the chosen angle of attack.

We can use a polar to determine the **optimal angle of attack**  $\alpha_{\text{opt}}$  corresponding to the **maximum lift-to-drag ratio**:

$$K_{\max} = \tan \alpha_{\text{opt}} \quad (1.3.10')$$

if we draw a tangent to the polar from the origin of coordinates.

The characteristic points of a polar include the point  $c_{y_a \max}$  corresponding to the **maximum lift force** that is achieved at the critical angle of attack  $\alpha_{cr}$ . We can mark a point on the curve determining the minimum drag coefficient  $c_{x_a \min}$  and the corresponding values of the angle of attack and the lift coefficient.

A polar is symmetric about the axis of abscissas if a craft has horizontal symmetry. For such a craft, the value of  $c_{x_a \min}$  corresponds to a zero lift force,  $c_{y_a} = 0$ .

In addition to a polar of the first kind, a **polar of the second kind** is sometimes used. It differs in that it is plotted in a body axis coordinate system along whose axis of abscissas the values of the longitudinal-force coefficient  $c_x$  are laid off, and along the axis of ordinates—the normal-force coefficients  $c_y$  (Fig. 1.3.4). This curve is used, particularly, in the strength analysis of craft.

Theoretical and experimental investigations show that in the most general case, the aerodynamic coefficients depend for a given body configuration and angle of attack on dimensionless variables such as the Mach number  $M_\infty = V_\infty/a_\infty$  and the Reynolds number  $Re_\infty = V_\infty L \rho_\infty / \mu_\infty$ . In these expressions,  $a_\infty$  is the speed of sound in the oncoming flow,  $\rho_\infty$  and  $\mu_\infty$  are the density and dynamic viscosity of the gas, respectively, and  $L$  is the length of the body. Hence, a multitude of polar curves exists for each given craft. For example, for a definite number  $Re_\infty$ , we can construct a family of such curves each of which corresponds to a definite value of the

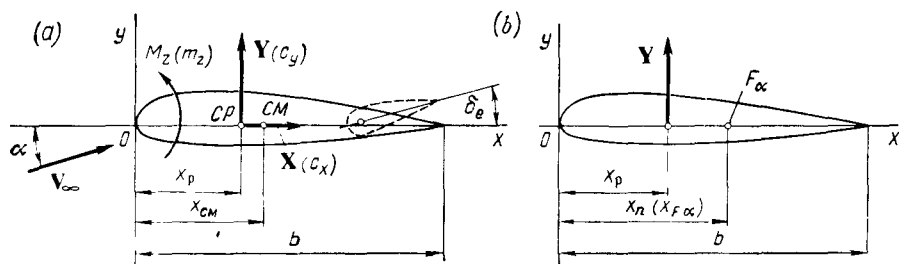


Fig. 1.3.5

Determination of the centre of pressure (a) and aerodynamic centre (b)

velocity  $M_\infty$ . The curves in Figs. 1.3.3 and 1.3.4 correspond to a fixed value of  $Re_\infty$  and determine the relation between  $c_{y_a}$  and  $c_{x_a}$  for low-speed flights (of the order of 100 m/s) when the aerodynamic coefficients do not depend on  $M_\infty$ .

**Centre of Pressure and Aerodynamic Centre.** The **centre of pressure (CP)** of a craft is the point through which the resultant of the aerodynamic forces passes. The centre of pressure is a conditional point because actually the action of fluid results not in a concentrated force, but in forces distributed over the surface of the moving body. It is customarily assumed that for symmetric bodies or ones close to them this conditional point is on one of the following axes—the longitudinal axis of the craft passing through the centre of mass, the axis of symmetry of a body of revolution, or on the chord of an airfoil.

Accordingly, the longitudinal force  $X$  is arranged along this axis, while the centre of pressure when motion occurs in the pitching plane is considered as the point of application of the normal force  $Y$ . The position of this centre of pressure is usually determined by the coordinate  $x_p$  measured from the front point on the contour of the body in a flow. If the pitching moment  $M_z$  about this point and the normal force  $Y$  are known (Fig. 1.3.5a), the coordinate of the centre of pressure

$$x_p = -M_z/Y \quad (1.3.11)$$

A moment  $M_z$  tending to reduce the angle of attack is considered to be negative (Fig. 1.3.5a); hence the coordinate  $x_p$  is positive. Taking into account that

$$M_z = m_z q_\infty S_r b \quad \text{and} \quad Y = c_y q_\infty S_r$$

we obtain

$$x_p = -m_z b / c_y$$

whence

$$x_p/b = c_p = -m_z/c_y \quad (1.3.11')$$

The dimensionless quantity  $c_p$  defined as the ratio between the distance to the centre of pressure and the characteristic length of a body (in the given case the wing chord  $b$ ) is called the **centre-of-pressure coefficient**. With small angles of attack, when the lift and normal-force coefficients are approximately equal ( $c_{y_a} \approx c_y$ ), we have

$$c_p = -m_{z_a}/c_{y_a} \quad (1.3.12)$$

In the case being considered of a two-dimensional flow past a body, the pitching-moment coefficients in wind (flight path) and body axis coordinate systems are the same, i.e.  $m_{z_a} = m_z$ .

For a symmetric airfoil when at  $\alpha \rightarrow 0$  the quantities  $c_y$  and  $m_z$  simultaneously take on zero values in accordance with the expressions

$$c_y = (\partial c_y / \partial \alpha) \alpha, \quad m_z = (\partial m_z / \partial \alpha) \alpha$$

holding at small angles of attack (here the derivatives  $\partial c_y / \partial \alpha$  and  $\partial m_z / \partial \alpha$  are constant quantities that can be determined for an angle of attack of  $\alpha \approx 0$ ), the coefficient  $c_p$  equals a constant value not depending on the angle of attack:

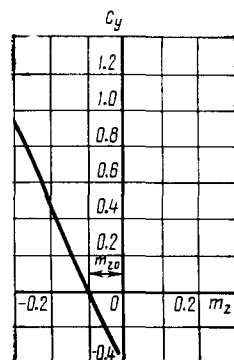
$$c_p = -\partial m_z / \partial c_y \quad (1.3.13)$$

The value of the coefficient  $c_p$  and of the dimensionless coordinate of the centre of mass  $\bar{x}_{CM} = x_{CM} b$  can be used to determine the pitching-moment coefficients about this centre:

$$m_z' = c_y (\bar{x}_{CM} - c_p) \quad (1.3.14)$$

Investigations show that in real conditions of flow, an appreciable displacement of the centre of pressure can be observed in craft even upon a slight change in the angles of attack. This is especially noticeable in craft with an asymmetric configuration or upon deflection of an elevator, which disturbs the existing symmetry. In these conditions, the centre of pressure is not convenient for use as a characteristic point in estimating the position of the resultant of the aerodynamic forces and the appearing pitching moment about the centre of mass. In these conditions, it is more convenient to assess the flight properties of a craft according to the **aerodynamic centre location**. To reveal the meaning of this concept, let us consider an asymmetric airfoil and evaluate the moment  $M_{zn}$  about an arbitrary point  $F_n$  with the coordinate  $x_n$  on the chord of the airfoil. It follows from Fig. 1.3.5b that

$$M_{zn} = Y (x_n - x_p)$$

**Fig. 1.3.6**

Relation between the moment coefficient  $m_z$  and normal-force coefficient  $c_y$  for an asymmetric aircraft

or, since  $-Yx_p = M_z$  is the moment about the front point  $O$ , we have

$$M_{zn} = Yx_n + M_z$$

Going over to aerodynamic coefficients, we obtain

$$m_{zn} = c_y (x_n/b) + m_z \quad (1.3.15)$$

For small angles of attack when there is a linear dependence of  $m_z$  on  $c_y$  of the form

$$m_z = m_{z0} + (\partial m_z / \partial c_y) c_y \quad (1.3.16)$$

we obtain

$$m_{zn} = c_y (x_n/b) + m_{z0} + (\partial m_z / \partial c_y) c_y$$

or

$$m_{zn} = m_{z0} + c_y (\partial m_z / \partial c_y + x_n/b) \quad (1.3.17)$$

where  $m_{z0}$  is the coefficient of the moment about a point on the leading edge at  $c_y = 0$  (Fig. 1.3.6).

The second term in (1.3.17) determines the increment of the moment associated with a change in the normal-force coefficient. If we choose the point  $F_\alpha$  on a chord whose coordinate  $x_n = x_{F_\alpha}$  is determined by the condition (see Fig. 1.3.5b)

$$x_n/b = x_{F_\alpha}/b = \bar{x}_{F_\alpha} = -\partial m_z / \partial c_y \quad (1.3.18)$$

the coefficient of the moment about this point will not depend on  $c_y$ , and at all (small) angles of attack it will be a constant quantity. This point is called the **aerodynamic centre** (AC) of the given body. The aerodynamic centre is evidently the point of application of the additional normal force produced by the angle of attack [the coefficient of this force is  $(\partial c_y / \partial \alpha) \alpha = c_y^\alpha \alpha$ ]. The pitching moment about an axis passing through this point does not depend on the

angle of attack. Such a point is called the **angle-of-attack aerodynamic centre of a craft**. The centre of pressure and the aerodynamic centre are related by the expression

$$c_p = -\frac{m_z}{c_y} = -\frac{m_{z0} + (\partial m_z / \partial c_y) c_y}{c_y} = c_{p0} + \bar{x}_{F_\alpha} \quad (1.3.19)$$

where  $c_{p0} = -m_{z0}/c_y$ . For a symmetric configuration,  $m_{z0} = 0$ , and, consequently, the centre of pressure coincides with the aerodynamic centre.

Expression (1.3.19) holds, however, for a symmetric configuration provided with an elevator deflected through a certain angle  $\delta_e$  (see Figs. 1.2.2 and 1.3.5). In this case, the moment coefficient is

$$m_z = m_z^\alpha \alpha + m_z^{\delta_e} \delta_e \quad (1.3.20)$$

and the normal-force coefficient is

$$c_y = c_y^\alpha \alpha + c_y^{\delta_e} \delta_e \quad (1.3.21)$$

where  $m_z^\alpha = \partial m_z / \partial \alpha$ ,  $c_y^\alpha = \partial c_y / \partial \alpha$ ,  $m_z^{\delta_e} = \partial m_z / \partial \delta_e$ , and  $c_y^{\delta_e} = \partial c_y / \partial \delta_e$ .

If a configuration is not symmetric, then

$$m_z = m_{z0} + m_z^\alpha \alpha + m_z^{\delta_e} \delta_e \quad (1.3.22)$$

$$c_y = c_{y0} + c_y^\alpha \alpha + c_y^{\delta_e} \delta_e \quad (1.3.23)$$

The point of application of the normal force due to the elevator deflection angle and proportional to this angle is known as the **elevator-deflection aerodynamic centre**. The moment of the forces about a lateral axis passing through this centre is evidently independent of the angle  $\delta_e$ . In the general case for an asymmetric configuration, its centre of pressure coincides with none of the aerodynamic centres (based on  $\alpha$  or  $\delta_e$ ). In a particular case, in a symmetric craft at  $\alpha = 0$ , the centre of pressure coincides with the aerodynamic centre based on  $\delta_e$ .

Using the definition of the aerodynamic centres based on the angle of attack and the elevator deflection angle and introducing the corresponding coordinates  $x_{F_\alpha}$  and  $x_{F_\delta}$ , we find the coefficient of the moment about the centre of mass. This coefficient is evaluated by formula (1.3.22), in which

$$m_z^\alpha = c_y^\alpha (\bar{x}_{CM} - \bar{x}_{F_\alpha}), \quad m_z^{\delta_e} = c_y^{\delta_e} (\bar{x}_{CM} - \bar{x}_{F_\delta}) \quad (1.3.24)$$

where  $\bar{x}_{F_\alpha} = x_{F_\alpha}/b$  and  $\bar{x}_{F_\delta} = x_{F_\delta}/b$  are the relative coordinates of the aerodynamic centres.

## 1.4. Static Equilibrium and Static Stability

### Concept of Equilibrium and Stability

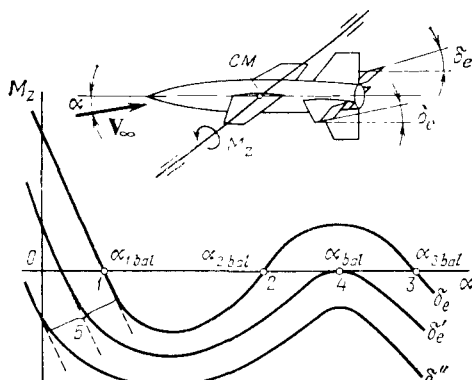
The state of static equilibrium is determined by the flight conditions and the corresponding force action at which the overall aerodynamic moment about the centre of mass in the absence of rotation and with the angle of attack and the sideslip angle remaining constant is zero ( $M = 0$ ). Such equilibrium corresponds to conditions of steady rectilinear motion of a craft, when the parameters of this motion do not depend on the time.

It is evident that for axisymmetric configurations over which the fluid flows in a longitudinal direction, the equality  $M = 0$  is achieved with undeflected elevators and rudders and with zero angles of attack and sideslip. Hence, in this case, equilibrium, called the **trim equilibrium of a craft**, sets in at the **balance angle of attack** and **sideslip angle** ( $\alpha_{\text{bal}}$ ,  $\beta_{\text{bal}}$ ) equal to zero. The need to balance flight at other angles ( $\alpha \neq \alpha_{\text{bal}}$  and  $\beta \neq \beta_{\text{bal}}$ ) requires the corresponding turning of the elevators.

Equilibrium of a craft (particularly, with the elevators fixed in place) may be stable or unstable. Equilibrium of a craft is considered to be **stable** if after the introduction of a random short-time disturbance it returns to its initial position. If these disturbances cause it to deflect still more from the initial position, equilibrium is said to be **unstable**.

The nature of the equilibrium of a craft is determined by its **static stability or instability**. To reveal the essence of static stability, we can consider the flow of air in a wind tunnel past a craft fixed at its centre of mass and capable of turning about it (Fig. 1.4.1). For a given elevator angle  $\delta_e$ , a definite value of the aerodynamic moment  $M_z$  corresponds to each value of the angle of deflection of the craft  $\alpha$  (the angle of attack). A possible relation between  $\alpha$  and  $M_z$  for a certain angle  $\delta_e$  is shown in Fig. 1.4.1, where points 1, 2, and 3 determining the balance angles  $\alpha_{1\text{bal}}$ ,  $\alpha_{2\text{bal}}$ , and  $\alpha_{3\text{bal}}$  at which the aerodynamic moment equals zero correspond to the equilibrium positions. The figure also shows two other moment curves for the elevator angles  $\delta'_e$  and  $\delta''_e$ .

Let us consider equilibrium at point 1. If the craft is deviated through an angle smaller or larger than  $\alpha_{1\text{bal}}$ , the induced moments, positive or negative, respectively, will result in an increase (reduction) of this angle to its previous value  $\alpha_{1\text{bal}}$ , i.e. these moments are **stabilizing ones**. Consequently, the position of equilibrium at point 1 is stable (the craft is statically stable). It can be shown similarly that such a position of stable equilibrium also corresponds to point 3.

**Fig. 1.4.1**

Dependence of the aerodynamic moment  $M_z$  on the angle of attack  $\alpha$  of a craft and the deflection of the elevators  $\delta_e$ :

1, 2, 3, 4—points of intersection of the moment curve with the  $\alpha$ -axis that determine the balance angles of attack; 5—region of a linear change in the pitching moment with the angle of attack and the elevator angle

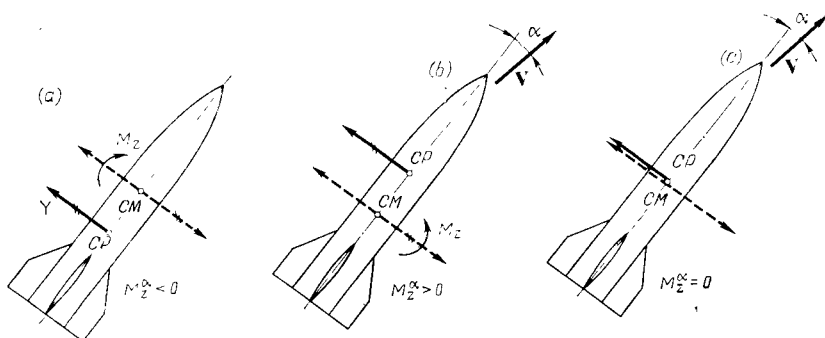
In the first case, free rotation of the craft continues until it occupies the equilibrium position at point 1, and in the second case—at point 3.

At point 2 ( $\alpha_{2\text{bal}}$ ) the equilibrium is unstable. Indeed, examination of Fig. 1.4.1 reveals that at values of the angle  $\alpha$  larger or smaller than  $\alpha_{2\text{bal}}$ , moments are induced, positive or negative, respectively, that tend to increase (or reduce)  $\alpha$ . Hence, these moments are destabilizing, and the craft will be statically unstable.

Static stability is schematically divided into longitudinal and lateral stability. For static longitudinal stability, it is assumed that all the disturbing forces and moments act in the longitudinal plane of the body axes  $xOy$ . Hence, only such movements of a craft are investigated that occur in its plane of symmetry in the absence of roll and slip. When analysing static lateral stability, the disturbed movements of a craft are considered that are associated with a change in the rolling and sideslip angles at a constant angle of attack. Such movements are always mutually related. Deflection of the ailerons causes not only roll, but also slip. At the same time, turning of the rudders also leads to rolling. Therefore investigation of lateral stability is associated with an analysis of both rolling and yawing moments.

#### Static Longitudinal Stability

When such stability exists, an induced longitudinal moment about the centre of mass will be stabilizing. In this case, the direction of the change in the moment  $M_z$  (and accordingly of the coefficient  $m_z$ ) is opposite to the change in the angle  $\alpha$ . Consequently, the condition of static longitudinal stability can be expressed in accordance with one of the curves shown in Fig. 1.4.1 by the inequalities  $\partial M_z / \partial \alpha < 0$  or  $\partial m_z / \partial \alpha = m_z' < 0$  (the derivatives are evaluated for the balance angle of attack  $\alpha = \alpha_{\text{bal}}$ ).

**Fig. 1.4.2**

Action of a force and moment in analysing the static stability of a craft:  
 a—static stability; b—static instability; c—neutrality relative to static stability

With **static longitudinal instability**, a destabilizing (tilting) moment appears that tends to increase the angle of attack in comparison with its balance value. Consequently, the inequalities  $\partial M_z / \partial \alpha > 0$  or  $m_z^\alpha > 0$  are the condition for static longitudinal instability.

A craft will be **neutral** relative to static longitudinal stability if upon a small deflection from the balance angle of attack neither a stabilizing nor a destabilizing moment is induced. This angle of attack  $\alpha = \alpha_{\text{bal}}$  in Fig. 1.4.1 corresponds to point 4 at which the moment curve is tangent to the horizontal axis. It is obvious that here the coefficient of the restoring moment  $\Delta m_z = m_{z\alpha_{\text{bal}}}^\alpha \Delta \alpha = 0$ .

**Criteria of Static Stability.** The derivative  $m_z^\alpha$  on which the magnitude of the stabilizing or destabilizing moment depends is called the **coefficient (degree) of static longitudinal stability**. This stability criterion relates to configurations both with and without axial symmetry.

For axisymmetric craft, we can assume that the criterion of static stability equals the difference between the distances from the nose of a craft to its centre of mass and centre of pressure, i.e. the quantity  $Y = x_{\text{CM}} - x_p$ , or in the dimensionless form

$$\bar{Y} = x_{\text{CM}}/b - x_p/b = \bar{x}_{\text{CM}} - c_p$$

If the coefficient of the centre of pressure  $c_p$  is larger than the relative coordinate of the centre of mass  $\bar{x}_{\text{CM}}$ , i.e. if the centre of pressure is behind the centre of mass, the craft is statically stable; when the centre of pressure is in front (the difference  $\bar{x}_{\text{CM}} - c_p$  is positive), the craft is statically unstable; when both centres coincide, the craft is neutral.

The action of the relevant pitching moments about a lateral axis passing through the centre of mass is shown in Fig. 1.4.2.

The criterion  $\bar{Y} = \bar{x}_{CM} - c_p$  determines the **margin of static stability**. It may be negative (static stability), positive (static instability), and zero (neutrality relative to longitudinal stability).

The quantity  $\bar{Y}$  is determined by the formula  $\bar{Y} = m_z/c_y$  in which the pitching moment coefficient is evaluated about the centre of mass. For small values of  $\alpha$ , the coefficients  $m_z$  and  $c_y$  can be written in the form  $m_z = m_z^{\alpha}\alpha$ , and  $c_y = c_y^{\alpha}\alpha$ . With this taken into account, we have

$$Y = m_z^{\alpha}/c_y^{\alpha} = \partial m_z/\partial c_y = \bar{x}_{CM} - c_p \quad (1.4.1)$$

Hence it follows that the derivative  $\partial m_z/\partial c_y = m_z^{cy}$  may be considered as a criterion determining the qualitative and quantitative characteristics of longitudinal stability. If  $m_z^{cy} < 0$ , we have static longitudinal stability, if  $m_z^{cy} > 0$ , we have instability, and if  $m_z^{cy} = 0$ , we have neutrality. The parameter  $m_z^{cy}$  is also called the **coefficient (degree) of static longitudinal stability**.

To appraise the static stability of asymmetric craft or of symmetric craft with deflected elevators, the concept of the aerodynamic centre is used. The dimensionless coordinate of this point with respect to the angle of attack is determined by the formula  $\bar{x}_{F_{\alpha}} = -m_z^y$ . Taking this into account and assuming in (1.3.17) that the quantity  $x_n$  equals the coordinate  $x_{CM}$  of the centre of mass, we obtain

$$m_z = m_{z0} - c_y (\bar{x}_{F_{\alpha}} - \bar{x}_{CM})$$

Differentiation of this expression with respect to  $c_y$  yields

$$m_z^{cy} = -(\bar{x}_{F_{\alpha}} - \bar{x}_{CM}) \quad (1.4.2)$$

Accordingly, the longitudinal stability is determined by the mutual arrangement of the aerodynamic centre and centre of mass of a craft. When the aerodynamic centre is behind the centre of mass (the difference  $\bar{x}_{F_{\alpha}} - \bar{x}_{CM}$  is positive), the relevant craft is statically stable, and when it is in front of the centre of mass (the difference  $\bar{x}_{F_{\alpha}} - \bar{x}_{CM}$  is negative), the craft is unstable.

By correspondingly choosing the centre of mass (or by centering), we can ensure the required margin of static stability. Centering (trimming) is **central** if the centre of mass coincides with the aerodynamic centre of the craft.

When the centering is changed, the degree of longitudinal stability is

$$m_z^{cy} = (m_z^{cy})' + \bar{x}_{CM} - \bar{x}_{CM}' \quad (1.4.2')$$

where the primed parameters correspond to the previous centering of the craft.

**Influence of Elevator Deflection.** Investigations show (see Fig. 1.4.1) that when the moment curve  $M_z = f(\alpha)$  is not linear, its slope at the points of intersection with the horizontal axis is not the same for different elevator angles. This indicates a difference in the value of the coefficients of static longitudinal stability. A glance at Fig. 1.4.1, for example, shows that upon a certain deflection of the elevator ( $\delta_e$ ), stability at low angles of attack ( $\alpha \approx \alpha_{1\text{bal}}$ ) may change to instability at larger values of them ( $\alpha \approx \alpha_{2\text{bal}}$ ) and may be restored at still larger angles ( $\alpha \approx \alpha_{3\text{bal}}$ ). To avoid this phenomenon, it is necessary to limit the range of the angles of attack to low values at which a linear dependence of the pitching moment coefficient on the angle of attack and elevator angle is retained. In this case, the degree of stability does not change because at all possible (small) elevator angles the inclination of the moment curve to the axis of abscissas is the same.

The condition of a linear nature of the moment characteristic makes it possible to use concepts such as the aerodynamic centre or neutral centering ( $x_{F_\alpha} = x_{CM}$ ) when studying the flying properties of craft. These concepts lose their sense when the linear nature is violated.

**Longitudinal Balancing.** Let us consider a flight at a uniform speed in a longitudinal plane along a curvilinear trajectory with a constant radius of curvature. Such a flight is characterized by a constant angular velocity  $\Omega_z$  about a lateral axis passing through the centre of mass. This velocity can exist provided that the inclination of the trajectory changes insignificantly.

The constancy of the angular velocity is due to the equilibrium of the pitching moments about the lateral axis, i.e. to longitudinal balancing of the craft at which the equality  $M_z = 0$  holds, i.e.

$$m_{z0} + m_z^\alpha \alpha_{\text{bal}} + m_z^{\Omega z} \Omega_z = 0$$

This equation allows us to find the elevator angle needed to ensure balanced flight at the given values of  $\alpha_{\text{bal}}$  and  $\Omega_z$ :

$$\delta_{e.\text{bal}} = -(1/m_z^{\delta e}) (m_{z0} + m_z^\alpha \alpha_{\text{bal}} + m_z^{\Omega z} \Omega_z) \quad (1.4.3)$$

For conditions of a high static stability, we have  $m_z^{\Omega z} \Omega_z \ll m_z^\alpha \alpha_{\text{bal}}$ ; consequently

$$\delta_{e.\text{bal}} = (-1/m_z^{\delta e}) (m_{z0} + m_z^\alpha \alpha_{\text{bal}}) \quad (1.4.3')$$

For a craft with an axisymmetric configuration,  $m_{z0} = 0$ , therefore

$$\delta_{e.\text{bal}} = -(m_z^\alpha / m_z^{\delta e}) \alpha_{\text{bal}} \quad (1.4.4)$$

The normal (lift) force coefficient corresponds to the balance angle of attack and elevator angle, namely,

$$c_{y.\text{bal}} = c_{y0} + (c_y^\alpha + c_y^{\delta e} \delta_{e.\text{bal}} / \alpha_{\text{bal}}) \alpha_{\text{bal}} \quad (1.4.5)$$

The values of  $c_{y_0}$  are usually very small even for asymmetric configurations (at low  $\delta_e$  and  $\alpha$ ) and equal zero exactly for craft with axial symmetry. Hence, with a sufficient degree of accuracy, we can write

$$c_{y.\text{bal}} = (c_y^\alpha + c_y^{\delta_e} \delta_{e.\text{bal}}/\alpha_{\text{bal}}) \alpha_{\text{bal}} \quad (1.4.6)$$

### Static Lateral Stability

To analyse the lateral stability of a craft, one must consider jointly the nature of the change in the rolling and sideslip angles upon the simultaneous action of the perturbing rolling  $M_x$  and yawing  $M_y$  moments. If after the stopping of such action these angles diminish, tending to their initial values, we have static lateral stability. Hence, when investigating lateral stability, one must consider simultaneously the change in the aerodynamic coefficients  $m_x$  and  $m_y$ . In most practical cases, however, lateral stability can be divided into two simpler kinds—rolling stability and directional stability—and can be studied separately by considering the change in the relevant moment coefficients  $m_x(\gamma)$  and  $m_y(\beta)$ .

Let us consider **static rolling stability**. Assume that in steady motion at the angle of attack  $\alpha_d$  the craft is turned about the axis  $Ox$  through a certain rolling angle  $\gamma$ . This turn with a constant orientation of the axis  $Ox$  relative to the velocity vector  $\mathbf{V}$  causes the appearance of the angle of attack  $\alpha \approx \alpha_d \cos \gamma$  and the sideslip angle  $\beta \approx \alpha_d \sin \gamma$ . The slip, in turn, causes a rolling moment to appear whose coefficient  $m_x = m_x^\beta \beta \approx m_x^\beta \alpha_d \sin \gamma$ . Differentiating with respect to  $\gamma$ , we obtain  $m_x^\gamma = m_x^\beta \alpha$ .

The derivative  $m_x^\gamma$  is a measure of the static rolling stability. If  $m_x^\gamma < 0$  (the moment tends to eliminate rolling), the craft has static rolling stability; at  $m_x^\gamma > 0$ , a disturbing moment is formed, and **static rolling instability** sets in; when  $m_x^\gamma = 0$ , the craft is neutral with respect to rolling stability.

Since a flight usually occurs at positive angles of attack, the signs of the derivatives  $m_x^\gamma$  and  $m_x^\beta$  coincide. Hence, in analysing rolling motion, we can use the derivative  $m_x^\beta$  known as the coefficient (degree) of static rolling stability.

**Static directional stability** is characterized by a coefficient (degree) determined by the derivative  $\partial M_y / \partial \beta$  (or  $\partial m_y / \partial \beta = m_y^\beta$ ). If the quantity  $m_y^\beta < 0$ , the craft has static directional stability; at  $m_y^\beta > 0$ , it has static instability, and when  $m_y^\beta = 0$ , neutrality.

The concept of directional stability is associated with the property of a craft to eliminate an appearing sideslip angle  $\beta$ . At the same time, a craft does not maintain the stability of its own flight direction because after changing its direction of motion under the action of various disturbances, it does not return to its previous

direction, but like a weathercock, turns with its nose part in the direction of the new velocity vector  $\mathbf{V}$ .

Similar to the aerodynamic centre based on the angle of attack, we can introduce the concept of the **aerodynamic centre based on the sideslip angle** whose coordinate we shall designate by  $x_{F_\beta}$ . Using this concept, we can represent the degree of static directional stability in the form

$$m_y^c z = -(\bar{x}_{F_\beta} - \bar{x}_{CM}) \quad (1.4.7)$$

where  $\bar{x}_{F_\beta} = x_{F_\beta}/l$  and  $\bar{x}_{CM} = x_{CM}/l$  ( $l$  is a characteristic geometric dimension that can determine the wing span, fuselage length, etc.).

Hence, the static directional stability or instability depends on the mutual position of the centre of mass and the aerodynamic centre. A rear arrangement of the aerodynamic centre ( $\bar{x}_{F_\beta} > \bar{x}_{CM}$ ) determines static directional stability ( $m_y^c z < 0$ ), while its front arrangement ( $\bar{x}_{F_\beta} < \bar{x}_{CM}$ ) determines static instability ( $m_y^c z > 0$ ). When the two centres coincide ( $\bar{x}_{F_\beta} = \bar{x}_{CM}$ ), the craft is neutral as regards static directional stability ( $m_y^c z = 0$ ).

A particular case of motion of a craft in the plane of the angle of attack can be characterized by a constant angular velocity ( $\Omega_y = \text{const}$ ) and stabilization with respect to rolling with the aid of an automatic pilot ( $\Omega_x \approx 0$ ). The condition for such steady motion is **lateral trim** of the craft when the yawing moment vanishes, i.e.

$$m_y = m_{y0} + m_y^\beta \beta + m_y^{\delta_r} \delta_r + m_y^{\Omega_y} \Omega_y = 0$$

All craft customarily have longitudinal symmetry, therefore  $m_{y0} = 0$ . When this condition holds, the equation obtained allows us to determine the balance rudder angle  $\delta_r = \delta_{r,bal}$  corresponding to the given values of the balance sideslip angle  $\beta_{bal}$  and the angular velocity  $\Omega_y$ . Most craft have a sufficiently high degree of static directional stability at which the term  $m_y^{\Omega_y} \Omega_y$  is negligible. Therefore

$$\delta_{r,bal} = (-m_y^\beta / m_y^{\delta_r}) \beta_{bal} \quad (1.4.8)$$

This relation, like (1.4.4), will be accurate for conditions of rectilinear motion.

## 1.5. Features of Gas Flow at High Speeds

### Compressibility of a Gas

One of the important properties of a gas is its compressibility—its ability to change its density under the action of a pressure. All the processes associated with the flow of a gas are characterized by

a change in the pressure and, consequently, by the influence of compressibility on these processes to some extent. Investigations show that as long as the speeds are low, the change in the density owing to insignificant changes in the pressure is not large, and the effect of compressibility may be ignored. To study low-speed flow over bodies, one may use the equations of hydrodynamics that studies the laws of motion of an incompressible fluid.

In practice, the influence of compressibility may be ignored in the range of air speeds from a few metres per second to 100-150 m/s. In real conditions, this corresponds to Mach numbers from  $M_\infty = V_\infty/a_\infty = 0$  to  $M_\infty = 0.3\text{-}0.45$  (here  $a_\infty$  is the speed of sound in an undisturbed flow). Idealization of the process consists in assuming the Mach number to equal zero within this region of speeds because small disturbances (sound oscillations) propagate in an incompressible fluid at an infinitely high speed and, consequently, the ratio of the flight speed to that of sound tends to zero.

Modern craft have high airspeeds at which flow over them is attended by a considerable change in the pressure and, consequently, by a substantial change in the density and temperature. In the conditions of a flight at high speeds, one must take into account the influence of compressibility, which may be very significant, on the effects of interaction of the fluid and a body. This is one of the most important features of high-speed aerodynamics.

### Heating of a Gas

The appreciable increase in the speeds of craft made it necessary to take into account the features of gas streams due to the change in the physicochemical properties of the air in aerodynamic investigations. In "conventional" supersonic aerodynamics, the compressibility was taken into consideration as the most important manifestation of a feature of flow at high speeds, while the influence of the temperature on the thermodynamic parameters and kinetic coefficients of air, and also on the physicochemical processes that may proceed in it was disregarded. For very high (hypersonic) speeds, however, the features associated with the influence of high temperatures come to the forefront.

High temperatures appear owing to deceleration of the gas stream when the kinetic energy of ordered motion of the particles transforms into the internal energy of the gas.

At a temperature of the order of 1500 K, **excitation of the vibrational levels** of the internal energy of the oxygen and nitrogen molecules in the air becomes noticeable. At a temperature of about 3000 K and a pressure of  $10^5$  Pa, the vibrational degrees of freedom of the oxygen molecules are completely excited, and further elevation of the temperature allows the atoms to surmount the action

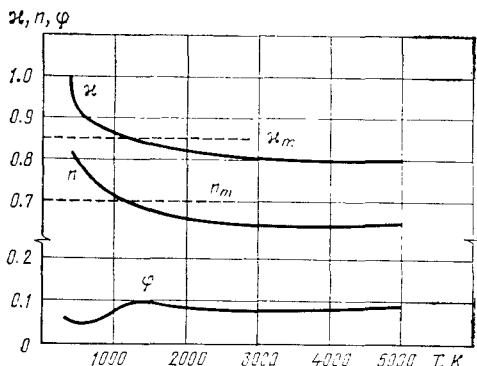
of the intramolecular forces. As a result, for example, a diatomic molecule breaks up into two individual atoms. This process is known as **dissociation**. The latter is attended by **recombination**—the formation of a new molecule when two atoms collide ( $O_2 \rightleftharpoons 2O$ ). This heat-producing reaction is accompanied by the collision of two atoms with a third particle that carries off part of the released energy and thus ensures the creation of a stable molecule. In addition, chemical reactions occur in the air that result in the appearance of a certain amount of nitrogen monoxide NO. The latter also dissociates upon further heating with the formation of atomic nitrogen and oxygen by the equations



At a temperature of 5000-6000 K and a pressure of  $10^5$  Pa, the oxygen molecules dissociate almost completely. In addition, at such a temperature, the major part of the nitrogen molecules dissociate with simultaneous recombination of the atoms into molecules. This process follows the equation  $N_2 \rightleftharpoons 2N$ . The intensity of dissociation is determined by the **degree of dissociation**. It equals the ratio of the number of air particles broken up in dissociation to the total number of atoms and molecules. The degree of dissociation depends on the temperature and pressure.

Elevation of the temperature is attended by an increase in the degree of dissociation because the speed and energy of the moving molecules grow, and this increases the probability of their collision and decomposition. The intensity of dissociation grows with lowering of the pressure (density) because of the lesser probability of triple collisions of the particles that lead to the formation of molecules from atoms. For example, oxygen begins to dissociate already at  $T = 2000$  K if the pressure is  $10^2$  Pa, whereas at standard atmospheric pressure (approximately  $10^5$  Pa)  $O_2$  begins to dissociate at  $T = 3000$  K. The temperature at which nitrogen begins to dissociate lowers from 6000 K at a pressure of  $10^5$  Pa to 4000 K at 10 Pa.

At 5000-6000 K, still another process begins to develop. It consists in that because of the large influx of energy, first the electron degrees of freedom are excited, and then electrons break away from the nitrogen and oxygen atoms and also from the nitrogen monoxide molecules. This process is called **ionization**. It occurs mainly because of collision of the air particles in their thermal motion, which explains why it is also called **thermal ionization**. Ionization is more intensive with elevation of the temperature and is attended by a growth in the concentration of the free electrons. The intensity of this process is characterized by the **degree of ionization**. It equals the ratio of the number of ionized atoms (molecules) to their total number. Investigations show that nitrogen, for example, is fully ionized

**Fig. 1.5.1**

Change in the exponents  $\varphi$ ,  $n$ , and  $k$  in the relevant formulas for determining the specific heat, dynamic viscosity, and thermal conductivity

thermally (the degree of ionization is unity) at a temperature of 17 000 K and a pressure of  $10^5$  Pa.

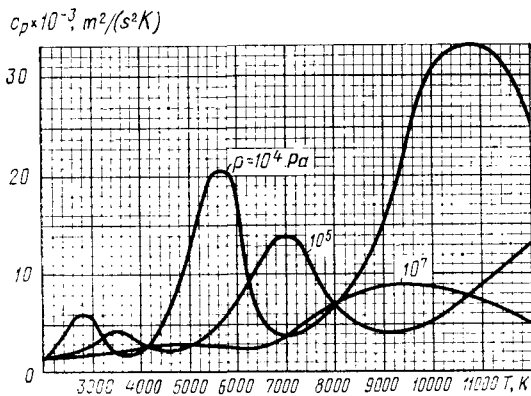
**Change in Specific Heats.** When air is heated, the heat supplied goes not only to increase the energy of the translational and rotational motion of the molecules, but also to increase the energy of vibration of the atoms in a molecule, to do the work needed to overcome the forces of interaction between atoms upon the dissociation of a molecule, and also to detach the electrons from atoms in ionization. The result is an increase in the specific heats.

Before dissociation begins, the change in the specific heat of air is determined only by the temperature. The influence of the temperature on the specific heat at a constant pressure can be estimated by the formula

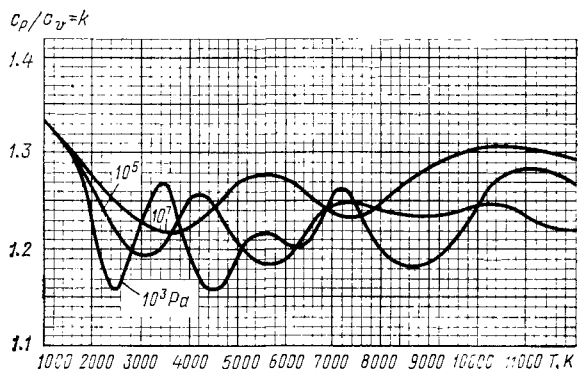
$$c_p/c_{p\infty} = (T/T_\infty)^\varphi \quad (1.5.1)$$

where the exponent  $\varphi$ , in turn, depends on the temperature (Fig. 1.5.1). For  $T > 4000$  K, this exponent can be assumed to be constant and equal to 0.1. For  $T_\infty = 288$  K, the specific heat  $c_{p\infty} = 1000 \text{ J/(kg}\cdot\text{K)}$  [or  $1000 \text{ m}^2/(\text{s}^2\cdot\text{K})$ ]. Formula (1.5.1) may be used for values of  $T$  up to 2200–2500 K, at which the vibrational degrees of freedom are close to the state of complete excitation.

When dissociation sets in, the specific heat depends not only on the temperature, but also on the pressure. The specific heats and the adiabatic exponents  $k = c_p/c_r$  were calculated for conditions of thermodynamic equilibrium at high temperatures on computers by a group of Soviet scientists headed by Associate member of the USSR Academy of Sciences A. Predvoditelev [6, 7]. These calculations were performed for temperatures from 1000 to 6000 K without account being taken of ionization because its influence in this temperature interval is negligible. For higher temperatures, the influence of equilibrium single ionization was taken into account. It was con-

**Fig. 1.5.2**

Change in the specific heat  $c_p$  of air at high temperatures

**Fig. 1.5.3**

Change in the ratio of the specific heats  $k = c_p/c_v$  for air at high temperatures

sidered to be completed at  $T = 12\,000$  K and  $p = 10^2$  Pa. Curves plotted according to the data in [6, 7] and characterizing the change in  $c_p$  and  $k$  at high temperatures are given in Figs. 1.5.2. and 1.5.3 (see [8]). The data obtained indicate that at a temperature up to 2000 K and a pressure of  $10^5$  Pa and above, the values of  $c_p$  and  $k = c_p/c_v$  are determined by the temperature and do not virtually depend on the pressure.

The general trend observed upon a change in the specific heats and their ratio is such that when the pressure drops and the degrees of dissociation and ionization, consequently, grow, the value of  $c_p$  increases, and that of the ratio  $k = c_p/c_v$  diminishes, although not monotonically.

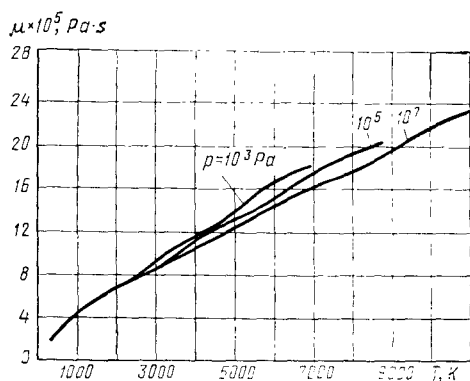


**Fig. 1.5.4**  
Change in the dynamic viscosity of air at high temperatures

**Kinetic Coefficients.** The processes of friction and heat transfer occurring in a viscous heat-conducting gas depend on kinetic parameters of the gas such as the dynamic viscosity  $\mu$  and the thermal conductivity  $\lambda$ . It was established that in the absence of dissociation, the coefficient  $\mu$  depends only on the temperature and is determined by the formula

$$\mu/\mu_\infty = (T/T_\infty)^n \quad (1.5.2)$$

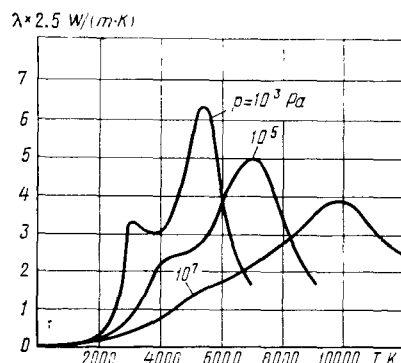
in which the exponent  $n$  depends on the temperature (see Fig. 1.5.1). In approximate calculations, the mean value  $n_m \approx 0.7$  may be used for a sufficiently large temperature interval; here the initial value of  $\mu$  may be taken equal to  $\mu_\infty = 1.79 \times 10^{-5}$  Pa·s, which corresponds to  $T_\infty = 288$  K. Formula (1.5.2) is used for temperatures up to 2000–2500 K. With elevation of the temperature, this formula gives appreciable errors. Investigations show that for high temperatures up to 9000 K the dynamic viscosity of air in conditions of equilibrium dissociation can be determined with an accuracy up to 10% by Sutherland's formula

$$\mu/\mu_\infty = (T/T_\infty)^{1/2} (1 + 111/T_\infty)/(1 + 111/T) \quad (1.5.3)$$

This formula yields better results for temperatures under 1500 K than (1.5.2). It has been established by accurate calculations that the dynamic viscosity at high temperatures also depends on the pressure. Figure 1.5.4 presents a graph (see [8]) characterizing the change in the coefficient  $\mu$  at temperatures up to 12 000 K within the pressure interval from  $10^3$  to  $10^7$  Pa.

Like the viscosity, the thermal conductivity at temperatures up to about 2000 K is independent of the pressure and is determined by the power formula

$$\lambda/\lambda_\infty = (T/T_\infty)^\alpha \quad (1.5.4)$$

**Fig. 1.5.5**

Change in the thermal conductivity of air at high temperatures

in which the exponent  $\alpha$  depends, as can be seen from Fig. 1.5.1, on the temperature. For approximate calculations, one may take the mean value  $\alpha_m$  equal to 0.85, and the value of  $\lambda_\infty$  corresponding to  $T_\infty = 261$  K equal to  $23.2 \text{ W}/(\text{m}\cdot\text{K})$ . Dissociating air is characterized by a dependence of the thermal conductivity on the temperature and pressure. The corresponding plot is shown in Fig. 1.5.5.

The origin of viscous forces and the appearance of the process of thermal conduction in a gas are associated with the molecular structure of a substance. Gas molecules upon their proper motion transfer mass, energy, and momentum from one place to another. A result of the change in the momentum is the appearance of viscous forces, while the transfer of energy gives rise to the property of thermal conduction. Therefore, elevation of the temperature is attended by an increase in the thermal conductivity and the dynamic viscosity in a gas. When dissociation sets in, the nature of the change in  $\lambda$  and  $\mu$  is quite involved. At a low degree of dissociation, the values of  $\lambda$  drop, which is caused by the expenditure of internal energy on breaking of the molecular bonds and, as a consequence, by lowering of the temperature of the gas. When the degree of dissociation grows, the more intensive breaking up of the molecules into atoms leads to a growth in the number of particles participating in the transport processes, which results in an increase in the coefficient  $\lambda$ .

When a gas is heated strongly, the expenditure of its internal energy on ionization substantially grows, which lowers the thermal conduction. The dynamic viscosity in a gas grows monotonically with the temperature because with the onset of dissociation and ionization more and more particles are formed that participate in the transport of momentum, and this gives rise to an increase in the viscous (friction) forces.

### State of Air at High Temperatures

**Equation of State.** Investigation of the flow of air over bodies shows that the relations of conventional aerodynamics based on the constancy of the thermodynamic characteristics and of the physico-chemical structure are sufficiently reliable as long as the air remains comparatively "cold", its specific heats change insignificantly, and, consequently, we may apply the thermal equation of state of a perfect gas

$$p = R\rho T \text{ or } p = R_0\rho T/(\mu_m)_0 \quad (1.5.5)$$

where  $R$  and  $R_0$  are the individual and universal (molar) gas constants, respectively [ $R_0 = 8.314 \times 10^3 \text{ J/(kmol}\cdot\text{K)}$ ],  $\rho$  is the density,  $T$  is the temperature, and  $(\mu_m)_0$  is the mean molar mass of air having a constant composition.

A gas satisfying Eq. (1.5.5) is said to be **thermally perfect**. The caloric equation of state  $i = pc_p/(\rho R)$ , which determines a relation for the enthalpy, corresponds to Eq. (1.5.5). If we take into account that  $c_p/R = k/(k - 1)$ , we have

$$i = [k/(k - 1)] p/\rho \quad (1.5.6)$$

A gas whose state is determined by Eq. (1.5.6) corresponding to the condition at which  $c_p$  and  $c_v$  are constant and independent of the temperature is said to be **calorically perfect**.

It must be taken into account that the need to consider the change in the specific heats with the temperature sets in before the need to use an equation of state differing from that for a perfect gas. For example, calculations show that the change in the specific heats with the temperature when passing through a normal shock wave begins from free-stream Mach numbers of  $M_\infty = 3\text{-}4$ . At  $M_\infty = 6\text{-}7$ , the equation of state for a perfect gas retains its significance, as does the equation for the speed of sound

$$a^2 = kRT \quad (1.5.7)$$

because the composition of the gas heated behind the shock wave does not change.

Hence, in this case a gas is not calorically perfect, but does have the properties of a thermally perfect gas.

For a gas with a varying heat capacity, the caloric equation of state (1.5.6) gives a large error. The actual relation between the enthalpy and temperature is determined by the function  $f_1(T)$  that is more complicated than (1.5.6).

The following equation holds for dissociating air, for which the specific heats and molar mass are functions of its state:

$$p = (R_0/\mu_m) \rho T \quad (1.5.8)$$

in which  $\mu_m = f_2(p, T)$ .

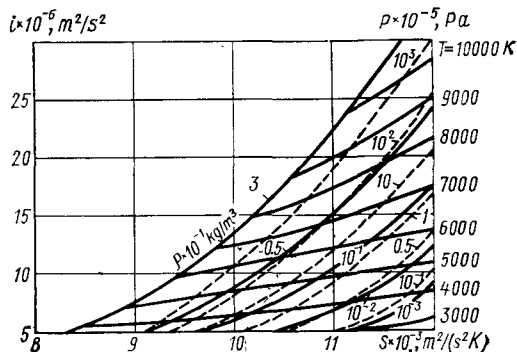


**Fig. 1.5.6**  
An  $i$ - $S$  diagram for dissociating air

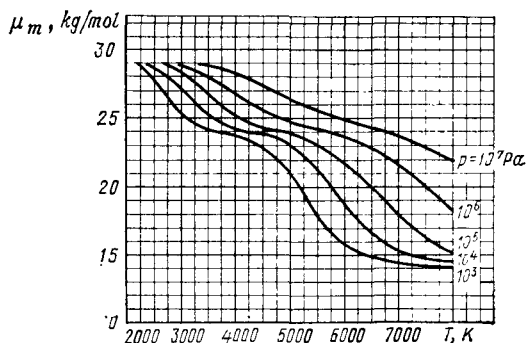


**Fig. 1.5.7**  
Change in the mean molar mass of air at high temperatures

The caloric equation of a dissociating gaseous medium also acquires a more complicated nature, and in the general form it can be written as  $i = f_3(p, T)$ . Such a fluid no longer has the properties of a perfect gas for which the enthalpy depends only on the temperature.

The thermal and caloric equations of state of a dissociating (real) gas are still more complicated because they additionally take account of the forces of interaction between the molecules, and also the proper volume of the latter. These equations are solved by numerical methods with the aid of computers and are usually presented in the form of tables or phase diagrams.

The results of calculating the parameters of state of air in conditions of thermodynamic equilibrium for elevated temperatures at pressure intervals from  $10^2$  to  $10^7$  Pa are given in [6, 7]. These results

of calculations were used to compile an atlas of phase diagrams [8]. The most widespread use for thermal calculations in aerodynamics has been found by the *i-S* diagram (enthalpy-entropy diagram) of dissociating air shown in Fig. 1.5.6. This diagram, which presents the caloric equation of state in a graphic form, contains curves of  $p = \text{const}$  (isobars),  $T = \text{const}$  (isotherms), and  $\rho = \text{const}$  (isochors—dashed lines).

Sometimes the caloric phase diagram depicting  $i$  against  $p$  with curves of  $T = \text{const}$ ,  $\rho = \text{const}$ , and  $S = \text{const}$  may be more convenient for calculations. Such a diagram constructed according to the data of an *i-S* one is given in [8]. It graphically depicts the thermal equation of state in different variants.

Graphs allowing one to determine the mean molar mass  $\mu_m$  of dissociated and ionized air (Fig. 1.5.7) and also the speed of sound (Fig. 1.5.8) as a function of  $p$  and  $T$  [7] or of  $i$  and  $S$  [8] are important for practical calculations. Examination of these graphs reveals that the speed of sound changes noticeably with the temperature and to a smaller extent depends on the pressure, which is explained by the insignificant influence of the structure of air on the nature of propagation of small disturbances. At the same time, the change in the structure of air upon its dissociation appreciably affects the molar mass, which is expressed in the strong influence of the pressure on the value of  $\mu_m$ . Three characteristic sections on which  $\mu_m$  diminishes with increasing temperature can be noted in Fig. 1.5.7. The first of them is due to dissociation of oxygen, the second—of nitrogen, and the third—to ionization of the components of the air. The general trend of a decrease in the mean molar mass of a gas that dissociates and becomes ionized is due to the breaking up of the molecules into atoms, and also to the detachment of electrons. An increase in the pressure leads to more intensive recombinations. This results in a certain growth in  $\mu_m$ .

**Diatomie Model of Air.** A model of the air is sometimes used in aerodynamic investigations that is a diatomic gas consisting of a mixture of oxygen and nitrogen in accordance with their mass composition. Such a mixture is treated as a single perfect gas if the mixture components are inert and no reactions occur between them.

At elevated temperatures, the mixture of gases *reacts chemically* because the diatomic gas dissociates and the atoms formed participate in recombination. The dissociation is assumed to be in equilibrium. This means that in the chemical reaction determined for the *pure* dissociating diatomic gas by the simplest equation of a binary process



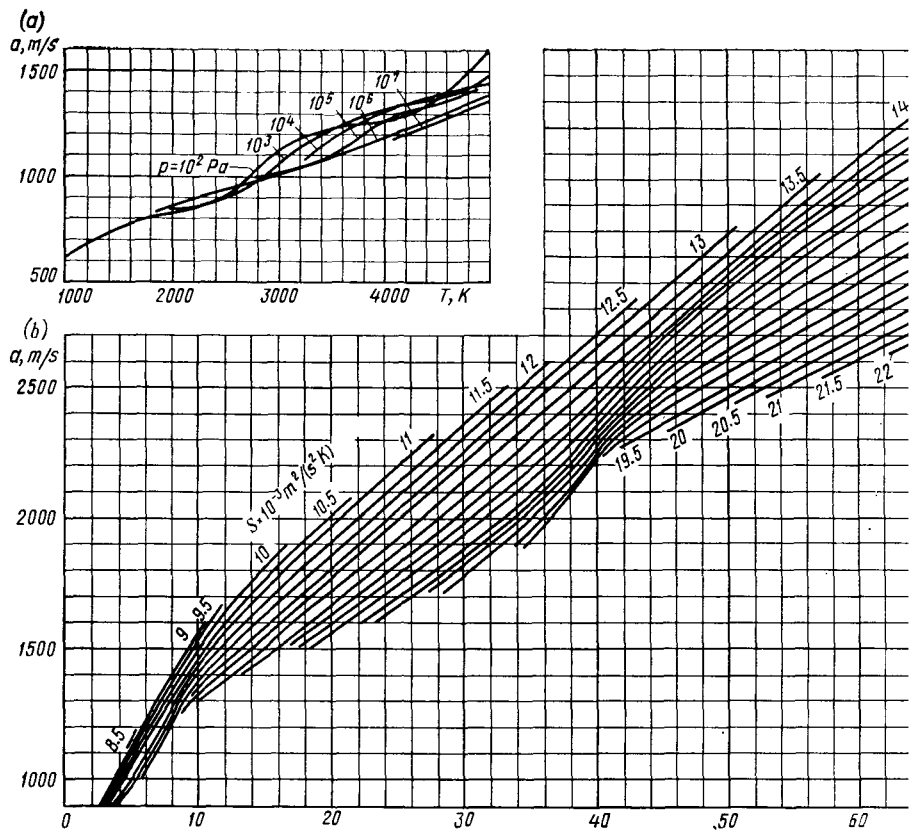


**Fig. 1.5.8**

Speed of sound in air at high temperatures:

a—against the temperature and pressure; b—against the enthalpy and entropy

the rates of the direct reaction  $r_D$  and of the reverse one  $r_R$  (the rates of dissociation and recombination respectively) are identical.

Investigations of a dissociating flow are connected with the determination of the degree of equilibrium dissociation  $\alpha$ . Its value for the diatomic model of the air being considered is given in chemical thermodynamics by the expression

$$\alpha^2/(1 - \alpha) = (\rho_d/\rho) \exp(-T_d/T) \quad (1.5.10)$$

where

$$\alpha = n_A/(n_A + 2n_{A_2}) \quad (1.5.11)$$

$\rho_d$  and  $T_d$  are the characteristic density and temperature for dissociation, respectively,  $n_A$  is the number of atoms of the element A in a certain volume, and  $n_{A_2}$  is the number of molecules of the gas  $A_2$  in the same volume.

The characteristic temperature  $T_d = D/k$ , where  $D$  is the dissociation energy of one molecule of  $A_2$  and  $k$  is a gas constant related to one molecule (the Boltzmann constant). Investigations show that for the temperature interval from 1000 to 7000 K, the values of  $T_d$  and  $\rho_d$  can be assumed to be approximately constant and equal to  $T_d = 50\,000$  K,  $\rho_d = 150$  g/cm<sup>3</sup> for oxygen, and to  $T_d = 113\,000$  K,  $\rho_d = 130$  g/cm<sup>3</sup> for nitrogen.

To obtain an equation of state for the gas mixture appearing as a result of dissociation of diatomic molecules, we must use the expressions for determining the pressure  $p$  and molar gas constant  $R$  for the mixture of gases and the partial pressure  $p_i$  of a component:

$$\left. \begin{aligned} p &= \sum_i p_i, & R &= \sum_i c_i R_i; \\ p_i &= \rho_i T R_i = \rho_i T (k/m_i) = (x_i/V) T (k/m_i) \end{aligned} \right\} \quad (1.5.12)$$

where  $\rho_i$  is the density of a component,  $m_i$  is the mass of an atom or molecule,  $R_i$  is the gas constant for a component, and  $V$  is the volume of the gas mixture.

Equations (1.5.12) are known under the general name of **Dalton's law**.

We shall use the subscript A to designate an atomic component ( $i = 1$ ) and the subscript M—a molecular one ( $i = 2$ ). Since the concentration of a component is  $c_i = \rho_i/\rho$ , where  $\rho$  is the density of the mixture, then  $c_1 = c_A = \alpha = \rho_A/\rho$  and  $c_2 = c_M = \rho_M/\rho = 1 - \alpha$ .

If  $m_M = 2m_A$ , and the relation between the masses  $x_i$  of the components  $\rho_i$  and the quantities  $\rho$  and  $\alpha$  is established from the expressions  $\rho_A = \rho\alpha = x_A/V$ , and  $\rho_M = \rho(1 - \alpha) = x_M/V$ , from (1.5.12) we obtain an equation of state in the following form:

$$p = \rho T k [\rho_A/(\rho m_A) + \rho_M/(\rho m_A)] = [k/(2m_A)] \rho T (1 + \alpha) \quad (1.5.13)$$

where  $k/(2m_A)$  is the gas constant for 1 g of the component  $A_2$  in the mixture; when multiplied by  $1 + \alpha$ , it yields the gas constant  $R$  (the individual gas constant) for 1 g of a mixture of the components  $A$  and  $A_2$  whose masses are in the ratio  $\alpha/(1 - \alpha)$ .

It is known from thermodynamics that the mean molar mass of a mixture of gases is

$$\mu_m = \left( \sum_i c_i / \mu_i \right)^{-1} \quad (1.5.14)$$

where  $c_i$  is the mass concentration of a component,  $\mu_i$  is its molar mass, and the symbol  $\sum$  determines the number of moles in the mixture.

For a diatomic gas, we have  $\sum_i c_i = c_1 + c_2 = c_A + c_M = 1$ . Since  $c_A = \alpha$ ,  $c_M = 1 - \alpha$ , and  $2\mu_A = \mu_M = (\mu_m)_0$ , then

$$\mu_m = (c_A/\mu_A + c_M/\mu_M)^{-1} = (\mu_m)_0/(1 + \alpha) \quad (1.5.15)$$

This expression may be used for the transformation of the equation of state (1.5.8) for a dissociating gas of an arbitrary composition:

$$p = [R_0/(\mu_m)_0] \rho T (1 + \alpha) \quad (1.5.16)$$

## **Kinematics of a Fluid**

### **2.1. Approaches to the Kinematic Investigation of a Fluid**

Determination of the force interaction and heat transfer between a fluid and a body about which it flows is the main task of aerodynamic investigations. The solution of this problem is associated with studying of the motion of a fluid near a body. As a result, properties are found at each point of a flow that determine this motion. Among them are the velocity, pressure, density, and temperature. With definite prerequisites, this investigation can be reduced to determination of the **velocity field**, which is a set of velocities of the fluid particles, i.e. to solution of a kinematic problem. Next the known velocity distribution is used to determine the other properties, and also the resultant forces, moments, and heat fluxes.

There are two approaches to the kinematic investigation of a fluid, known as the Lagrangian and the Eulerian approaches.

#### **Lagrangian Approach**

This approach considers the motion of individual fluid particles and for each of them determines its pathline, i.e. the coordinates of the particles as a function of time. But since there is an infinite number of particles, to set a pathline one must identify the particles which this pathline relates to. The coordinates  $a$ ,  $b$ , and  $c$  at a certain instant  $t = t_0$  are selected as the characteristic of a particle. This means that from among an infinite set of pathlines, the one passing through the point whose coordinates are  $a$ ,  $b$ , and  $c$  will belong to the given particle. Accordingly, we shall write the equation of the pathline in the parametric form:

$$x = f_1(a, b, c, t); \quad y = f_2(a, b, c, t); \quad z = f_3(a, b, c, t) \quad (2.1.1)$$

where  $a$ ,  $b$ ,  $c$ , and  $t$  are the Lagrangian variables. The quantities  $a$ ,  $b$ , and  $c$  are variables determining the pathline.

---

The components of the velocity vector at each point of the pathline equal the partial derivatives  $V_x = \partial x / \partial t$ ,  $V_y = \partial y / \partial t$ , and  $V_z = \partial z / \partial t$ , while the components of the acceleration vector equal the relevant second partial derivatives  $W_x = \partial^2 x / \partial t^2$ ,  $W_y = \partial^2 y / \partial t^2$ , and  $W_z = \partial^2 z / \partial t^2$ .

### Eulerian Approach

The Eulerian approach is in greater favour in aerodynamic investigations. Unlike the Lagrangian approach, it fixes not a particle of a fluid, but a point of space with the coordinates  $x$ ,  $y$ , and  $z$  and studies the change in the velocity at this point with time. Hence, the Eulerian approach consists in expressing the velocities of particles as a function of the time  $t$  and the coordinates  $x$ ,  $y$ , and  $z$  of points in space, i.e. in setting the field of velocities determined by the vector  $\mathbf{V} = V_x \mathbf{i} + V_y \mathbf{j} + V_z \mathbf{k}$ , where  $\mathbf{i}$ ,  $\mathbf{j}$ , and  $\mathbf{k}$  are unit vectors along the coordinate axes, while  $V_x = dx/dt$ ,  $V_y = dy/dt$ , and  $V_z = dz/dt$  are the velocity vector components given in the form of the equations

$$V_x = f_1(x, y, z, t); \quad V_y = f_2(x, y, z, t); \quad V_z = f_3(x, y, z, t) \quad (2.1.2)$$

The quantities  $x$ ,  $y$ ,  $z$ , and  $t$  are called the **Eulerian variables**. By solving the simultaneous differential equations

$$\frac{dx}{dt} = f_1(x, y, z, t); \quad \frac{dy}{dt} = f_2(x, y, z, t); \quad \frac{dz}{dt} = f_3(x, y, z, t) \quad (2.1.3)$$

we can obtain equations of a family of pathlines in the parametric form coinciding with Eqs. (2.1.1) in which  $a$ ,  $b$ , and  $c$  are integration constants.

Hence, in the Eulerian approach, we can go over from a description of the kinematics to representation of a flow by the Lagrangian approach. The reverse problem associated with the transition from the Lagrangian approach [Eq. (2.1.1)] to the Eulerian one [Eq. (2.1.3)] consists in differentiation of Eqs. (2.1.1) with respect to time and the following exclusion of the constants  $a$ ,  $b$ , and  $c$  by means of Eqs. (2.1.1).

By calculating the total derivative of the velocity vector with respect to time, we obtain the acceleration vector

$$\mathbf{W} = \frac{d\mathbf{V}}{dt} = \frac{\partial \mathbf{V}}{\partial t} + V_x \frac{\partial \mathbf{V}}{\partial x} + V_y \frac{\partial \mathbf{V}}{\partial y} + V_z \frac{\partial \mathbf{V}}{\partial z} \quad (2.1.4)$$

Projection of the vector  $\mathbf{W}$  onto the axes of coordinates yields the components of the resultant acceleration. In the expanded form,

these components are as follows:

$$\left. \begin{aligned} W_x &= \frac{\partial V_x}{\partial t} + V_x \frac{\partial V_x}{\partial x} + V_y \frac{\partial V_x}{\partial y} + V_z \frac{\partial V_x}{\partial z} \\ W_y &= \frac{\partial V_y}{\partial t} + V_x \frac{\partial V_y}{\partial x} + V_y \frac{\partial V_y}{\partial y} + V_z \frac{\partial V_y}{\partial z} \\ W_z &= \frac{\partial V_z}{\partial t} + V_x \frac{\partial V_z}{\partial x} + V_y \frac{\partial V_z}{\partial y} + V_z \frac{\partial V_z}{\partial z} \end{aligned} \right\} \quad (2.1.5)$$

Relations (2.1.5) for the accelerations correspond to a flow characterized by a change in the velocity at a given point with time and, consequently, by the inequality  $\partial \mathbf{V}/\partial t \neq 0$ . Such a flow of a fluid is called **unsteady**. A flow of a fluid in which the velocity and other properties at a given point are independent of the time ( $\partial \mathbf{V}/\partial t = 0$ ) is called **steady**.

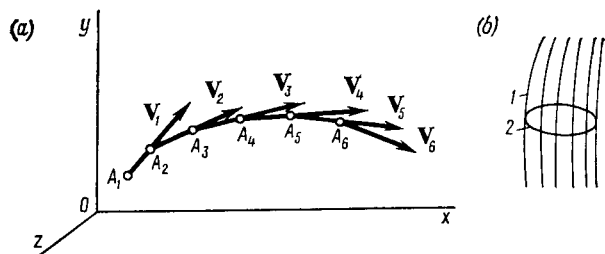
### Streamlines and Pathlines

At any instant, we can imagine a curve in a flow having the property that every particle of the fluid on it has a velocity tangent to the curve. Such a curve is called a **streamline**.

To obtain a streamline, one must proceed as follows. Take a point  $A_1$  (Fig. 2.1.1a) in the flow at the instant  $t = t_0$  and express the velocity of the particle at this point by the vector  $\mathbf{V}_1$ . Next take a point  $A_2$  adjacent to  $A_1$  on the vector  $\mathbf{V}_1$ . Assume that at the instant  $t = t_0$ , the velocity vector at this point is  $\mathbf{V}_2$ . Next consider a point  $A_3$  on the vector  $\mathbf{V}_2$ , the velocity at which is determined at the same instant by the vector  $\mathbf{V}_3$ , and so on. Such a construction yields a broken line consisting of segments of velocity vectors. By shrinking the size of these segments to zero and simultaneously increasing their number to infinity, at the limit we obtain a curve enveloping the entire family of velocity vectors. This is exactly a streamline. It is obvious that a definite streamline corresponds to each instant.

To obtain an equation of a streamline, let us take advantage of a property according to which at each point of this line the directions of the velocity vector  $\mathbf{V}$  and of the vector  $ds = \mathbf{i} dx + \mathbf{j} dy + \mathbf{k} dz$ , where  $dx$ ,  $dy$ , and  $dz$  are the projections of the streamline arc element  $ds$ , must coincide. Consequently, the cross product  $ds \times \mathbf{V} = 0$ , i.e.

$$\begin{vmatrix} \mathbf{i} & \mathbf{j} & \mathbf{k} \\ dx & dy & dz \\ V_x & V_y & V_z \end{vmatrix} = \mathbf{i}(V_z dy - V_y dz) - \mathbf{j}(V_z dx - V_x dz) + \mathbf{k}(V_y dx - V_x dy) = 0$$

**Fig. 2.1.1**

Construction of a streamline (a) and a stream tube (b):

1—streamlines; 2—contour

Hence since, for example,  $V_z dy - V_y dz = 0$ , and so on, we obtain a system of differential equations

$$dx/V_x = dy/V_y = dz/V_z \quad (2.1.6)$$

The solution of the problem on determining streamlines thus consists in integration of the system of equations (2.1.6). Each of the integrals of these equations  $F_1(x, y, z, C_1) = 0$  and  $F_2(x, y, z, C_2) = 0$  is a family of surfaces depending on one of the parameters,  $C_1$  or  $C_2$ , while the intersection of these surfaces forms a **family of streamlines**.

Unlike streamlines, which are constructed at a fixed instant, the concept of a pathline is associated with a certain time interval during which a particle covers a definite distance. It thus follows that a streamline and a **pathline** (or **trajectory**), which is the trace of motion of a single particle, coincide in a steady flow. If the flow is unsteady, a streamline and pathline in it do not coincide.

The concepts of a stream tube and a stream filament are considered in aerodynamics. If we draw streamlines through the points of an elementary closed contour (Fig. 2.1.1b), they form a surface called the surface of a stream tube. The part of the fluid confined within this surface is called a **stream tube**. If we draw pathlines through the points of an elementary closed contour, they form a surface confining a part of the fluid called a **stream filament**. A stream tube and a stream filament drawn through the points of the same closed contour in a steady flow coincide.

## 2.2. Analysis of Fluid Particle Motion

Unlike a solid body whose motion is determined by its translational motion together with its centre of mass and by rotation about an instantaneous axis passing through the centre, the motion of a

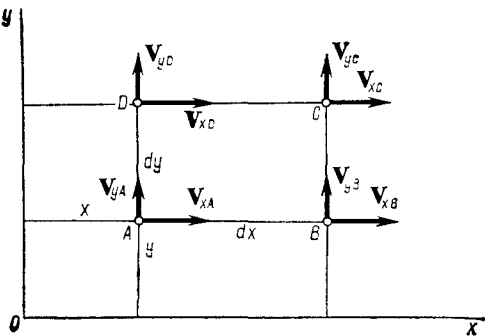


**Fig. 2.2.1**  
Motion of a fluid particle

fluid particle is characterized, in addition, by the presence of **strain** changing the shape of the particle.

Let us consider a fluid particle in the form of an elementary parallelepiped with edges of  $dx$ ,  $dy$ , and  $dz$ , and analyse the motion of face  $ABCD$  (Fig. 2.2.1). Since the coordinates of the vertices of the face are different, the velocities determined at a certain instant  $t = t_0$  are also different:

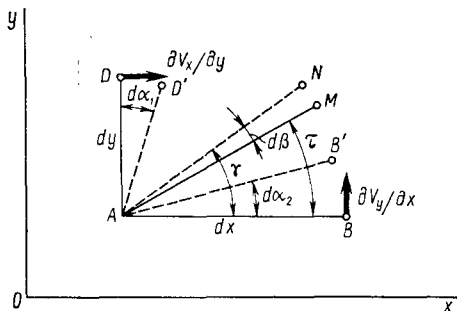
$$\left. \begin{aligned} V_{xA} &= V_x(x, y), & V_{xB} &= V_x(x + dx, y) \\ V_{yA} &= V_y(x, y), & V_{yB} &= V_y(x + dx, y) \\ V_{xC} &= V_x(x + dx, y + dy), & V_{xD} &= V_x(x, y + dy) \\ V_{yC} &= V_y(x + dx, y + dy), & V_{yD} &= V_y(x, y + dy) \end{aligned} \right\} \quad (2.2.1)$$

where  $x$  and  $y$  are the coordinates of point  $A$ .

Let us expand the expressions for the velocities into a Taylor series, leaving only small quantities of the first order in them, i.e. terms containing  $dx$ ,  $dy$ , and  $dz$  to a power not higher than the first one. Assuming that at point  $A$  the velocity  $V_{xA} = V_x$  and  $V_{yA} = V_y$ , we obtain

$$\left. \begin{aligned} V_{xB} &= V_x + (\partial V_x / \partial x) dx + \dots, & V_{xD} &= V_x + (\partial V_x / \partial y) dy + \dots \\ V_{yB} &= V_y + (\partial V_y / \partial x) dx + \dots, & V_{yD} &= V_y + (\partial V_y / \partial y) dy + \dots \\ V_{xC} &= V_x + (\partial V_x / \partial x) dx + (\partial V_x / \partial y) dy + \dots \\ V_{yC} &= V_y + (\partial V_y / \partial x) dx + (\partial V_y / \partial y) dy + \dots \end{aligned} \right\} \quad (2.2.2)$$

Examination of these expressions reveals that, for example, at point  $B$  the velocity component along the  $x$ -axis differs from the value of the velocity at point  $A$  by the quantity  $(\partial V_x / \partial x) dx$ . This signifies that point  $B$ , while participating in translational motion at the velocity  $V_x$  in the direction of the  $x$ -axis together with point  $A$ , simultaneously moves relative to it in the same direction at the

**Fig. 2.2.2**

Angular strain of a fluid particle

velocity  $(\partial V_x / \partial x) dx$ . The result is a linear strain of segment  $AB$ . The rate of this strain is  $\theta_x = \partial V_x / \partial x$ .

Point  $B$  moves in the direction of the  $y$ -axis at the velocity  $V_y$  together with point  $A$  and simultaneously moves relative to this point at the linear velocity  $(\partial V_y / \partial x) dx$  determined by the angular velocity of segment  $AB$ .

Considering point  $D$ , we can by analogy with point  $B$  determine that the relative linear velocity of this point in the direction of the  $y$ -axis is  $(\partial V_y / \partial y) dy$  and, consequently, the rate of linear strain of segment  $AD$  will be  $\theta_y = \partial V_y / \partial y$ . The angular velocity of the segment about point  $A$  is  $-\partial V_x / \partial y$  (the minus sign takes into account that point  $D$  rotates about point  $A$  in a direction opposite to that of rotation of point  $B$ ). Rotation of segments  $AD$  and  $AB$  causes distortion of the angle  $DAB$  (Fig. 2.2.2), i.e. angular strain of the particle is produced. Simultaneously, bisector  $AM$  of angle  $DAB$  may turn, the result being the appearance of an angle  $d\beta$  between it and bisector  $AN$  of the distorted angle  $D'AB'$ . Hence, the particle rotates additionally.

The angle of rotation of the bisector (Fig. 2.2.2) is

$$d\beta = \gamma - \tau$$

where  $\gamma = 0.5 [\pi/2 - (d\alpha_2 + d\alpha_1)]$  and  $\tau = \pi/4 - d\alpha_2$ .

The angles  $d\alpha_2$  and  $d\alpha_1$  shown in Fig. 2.2.2 equal  $(\partial V_y / \partial x) dt$  and  $(\partial V_x / \partial y) dt$ , respectively. Consequently

$$d\beta = 0.5 (d\alpha_2 - d\alpha_1) = 0.5 (\partial V_y / \partial x - \partial V_x / \partial y) dt$$

Hence we can find the angular velocity  $d\beta/dt$  of a fluid particle about the  $z$ -axis. Denoting it by  $\omega_z$ , we have

$$\omega_z = d\beta/dt = 0.5 (\partial V_y / \partial x - \partial V_x / \partial y) \quad (2.2.3)$$

If we consider the motion of edge  $AD$  relative to segment  $AB$ , the angular velocity of this edge will evidently be

$$2\epsilon_z = \partial V_y / \partial x + \partial V_x / \partial y \quad (2.2.4)$$

The quantity

$$\varepsilon_z = 0.5 (\partial V_y / \partial x + \partial V_x / \partial y) \quad (2.2.4')$$

is called the **semi-rate of downwash** of the right angle *DAB*.

Let us apply this reasoning to three-dimensional flow and consider point *C* belonging to a particle in the form of an elementary parallelepiped with edge lengths of  $dx$ ,  $dy$ , and  $dz$ . The velocity at this point at the instant  $t = t_0$  is a function of the coordinates  $x + dx$ ,  $y + dy$ , and  $z + dz$ . Writing the velocity components in the form of a Taylor series in which only small terms of the first order are retained, we have

$$\left. \begin{aligned} V_{xC} &= V_x + (\partial V_x / \partial x) dx + (\partial V_x / \partial y) dy + (\partial V_x / \partial z) dz \\ V_{yC} &= V_y + (\partial V_y / \partial x) dx + (\partial V_y / \partial y) dy + (\partial V_y / \partial z) dz \\ V_{zC} &= V_z + (\partial V_z / \partial x) dx + (\partial V_z / \partial y) dy + (\partial V_z / \partial z) dz \end{aligned} \right\} \quad (2.2.5)$$

Let us introduce a notation similar to that adopted when analysing the motion of a two-dimensional particle. We shall assume that  $\theta_z = \partial V_z / \partial z$ . This quantity determines the rate of linear strain of a three-dimensional particle in the direction of the *z*-axis. Let us also introduce the notation

$$\omega_x = 0.5 (\partial V_z / \partial y - \partial V_y / \partial z), \quad \omega_y = 0.5 (\partial V_x / \partial z - \partial V_z / \partial x) \quad (2.2.6)$$

The quantities  $\omega_x$  and  $\omega_y$  are the components of the angular velocity of a particle along the *x*- and *y*-axes, respectively. The components of the angular velocity of a particle  $\omega_x$ ,  $\omega_y$ , and  $\omega_z$  are considered to be positive upon rotation from the *x*-axis to the *y*-axis, from the *y*-axis to the *z*-axis, and from the *z*-axis to the *x*-axis, respectively. Accordingly, the signs of the derivatives  $\partial V_y / \partial x$ ,  $\partial V_z / \partial y$ , and  $\partial V_x / \partial z$  coincide with those of the angular velocity, while the signs of the derivatives  $\partial V_x / \partial y$ ,  $\partial V_y / \partial z$ , and  $\partial V_z / \partial x$  are opposite to those of the angular velocity.

By analogy with (2.2.4'), we have the values

$$\varepsilon_x = 0.5 (\partial V_z / \partial y + \partial V_y / \partial z), \quad \varepsilon_y = 0.5 (\partial V_x / \partial z + \partial V_z / \partial x) \quad (2.2.7)$$

that equal the semi-rate of downwash of the two right angles of the parallelepiped in planes *yOz* and *xOz*, respectively.

By performing simple transformations, we can see that

$$\begin{aligned} \partial V_z / \partial y &= \varepsilon_x + \omega_x; \quad \partial V_x / \partial z = \varepsilon_y + \omega_y; \quad \partial V_y / \partial x = \varepsilon_z + \omega_z \\ \partial V_y / \partial z &= \varepsilon_x - \omega_x; \quad \partial V_z / \partial x = \varepsilon_y - \omega_y; \quad \partial V_x / \partial y = \varepsilon_z - \omega_z \end{aligned}$$

With account taken of these expressions, the velocity components at point *C* can be represented in the following form:

$$\left. \begin{aligned} V_{xC} &= V_x + \theta_x dx + \varepsilon_y dz + \varepsilon_z dy + \omega_y dz - \omega_z dy \\ V_{yC} &= V_y + \theta_y dy + \varepsilon_z dx + \varepsilon_x dz + \omega_z dx - \omega_x dz \\ V_{zC} &= V_z + \theta_z dz + \varepsilon_x dy + \varepsilon_y dx + \omega_x dy - \omega_y dx \end{aligned} \right\} \quad (2.2.8)$$

Hence, the motion of point  $C$  can be considered as the result of addition of three kinds of motion: translational along a pathline together with point  $A$  at a velocity of  $\mathbf{V}(V_x, V_y, V_z)$ , rotation about it at the angular velocity

$$\boldsymbol{\omega} = \omega_x \mathbf{i} + \omega_y \mathbf{j} + \omega_z \mathbf{k} \quad (2.2.9)$$

and pure strain. This conclusion forms the content of the **Helmholtz theorem**. Strain, in turn, consists of linear strain characterized by the coefficients  $\theta_x$ ,  $\theta_y$ , and  $\theta_z$ , and of the angular strain determined by the quantities  $\varepsilon_x$ ,  $\varepsilon_y$ , and  $\varepsilon_z$ .

The linear strain of the element's edges causes a change in its volume  $\tau = dx dy dz$ , which is determined by the difference

$$d\tau = dx_1 dy_1 dz_1 - dx dy dz$$

where  $dx_1$ ,  $dy_1$ , and  $dz_1$  are the lengths of the edges at the instant  $t + dt$ .

Introducing the values of the lengths, we find

$$d\tau = (dx + \theta_x dx dt) (dy + \theta_y dy dt) (dz + \theta_z dz dt) - dx dy dz$$

Disregarding in this expression infinitesimal terms higher than the fourth order, we obtain

$$d\tau = (\theta_x + \theta_y + \theta_z) dx dy dz dt$$

Hence we can determine the rate of change of the relative volume, or the rate of the specific volume strain  $\theta = (1/\tau)d\tau/dt$ , which at each point of a flow equals the sum of the rates of linear strain along any three mutually perpendicular directions:

$$\theta = \theta_x + \theta_y + \theta_z \quad (2.2.10)$$

The quantity  $\theta$  is also known as the **divergence of the velocity vector** at a given point:

$$\operatorname{div} \mathbf{V} = \theta = \theta_x + \theta_y + \theta_z \quad (2.2.11)$$

Hence, the motion of a fluid particle has been shown to have a complicated nature and to be the result of summation of three kinds of motion: translational and rotational motion and strain.

A flow in which the particles experience rotation is called a **vortex** one, and the angular velocity components  $\omega_x$ ,  $\omega_y$ , and  $\omega_z$ —the **vortex components**. To characterize rotation, the concept of the velocity curl is introduced. It is expressed in the form  $\operatorname{curl} \mathbf{V} = 2\boldsymbol{\omega}$ . The **velocity curl** is a vector

$$\operatorname{curl} \mathbf{V} = (\operatorname{curl} \mathbf{V})_x \mathbf{i} + (\operatorname{curl} \mathbf{V})_y \mathbf{j} + (\operatorname{curl} \mathbf{V})_z \mathbf{k} \quad (2.2.12)$$

whose components equal the corresponding double values of a vortex component:

$$(\operatorname{curl} \mathbf{V})_x = 2\omega_x, (\operatorname{curl} \mathbf{V})_y = 2\omega_y, \text{ and } (\operatorname{curl} \mathbf{V})_z = 2\omega_z$$

### 2.3. Vortex-Free Motion of a Fluid

When investigating the motion of a fluid, we may often take no account of rotation because of the negligibly small angular velocities of the particles. Such motion is called **vortex-free** (or **irrotational**).

For a vortex-free flow,  $\omega = 0$  (or  $\text{curl } \mathbf{V} = 0$ ), and, consequently, the vortex components  $\omega_x$ ,  $\omega_y$ , and  $\omega_z$  equal zero. Accordingly, from formulas (2.2.3) and (2.2.6) we obtain

$$\partial V_x / \partial y = \partial V_y / \partial x, \quad \partial V_z / \partial y = \partial V_y / \partial z, \quad \partial V_x / \partial z = \partial V_z / \partial x \quad (2.3.1)$$

These equations are a necessary and sufficient condition for the differential trinomial  $V_x dx + V_y dy + V_z dz$  to be a total differential of a function characterizing the flow of a fluid in the same way as the velocity components  $V_x$ ,  $V_y$ , and  $V_z$ .

Designating this function in the form  $\varphi(x, y, z, t)$  and considering the time  $t$  as a parameter, we can write the expression

$$d\varphi = V_x dx + V_y dy + V_z dz$$

On the other hand, the same differential is

$$d\varphi = (\partial\varphi/\partial x) dx + (\partial\varphi/\partial y) dy + (\partial\varphi/\partial z) dz$$

Comparing the last two expressions, we find

$$V_x = \partial\varphi/\partial x, \quad V_y = \partial\varphi/\partial y, \quad V_z = \partial\varphi/\partial z \quad (2.3.2)$$

The function  $\varphi$  is called a **velocity potential** or a **potential function**, and the vortex-free flow characterized by this function is called a **potential flow**. Examination of relations (2.3.2) reveals that the partial derivative of the potential  $\varphi$  with respect to a coordinate equals the projection of the velocity onto the relevant coordinate axis. This property of the potential function also holds for an arbitrary direction. Particularly, the tangential component of the velocity at a point on an arbitrary curve  $s$  equals the partial derivative  $V_s = \partial\varphi/\partial s$ , while the normal component  $V_n = \partial\varphi/\partial n$ , where  $n$  is a normal to the arc  $s$  at the point being considered. For the polar coordinates  $r$  and  $\theta$ , the projections of the velocity vector  $\mathbf{V}$  of a point onto the direction of a polar position vector and onto a direction perpendicular to this vector equal, respectively, the partial derivatives

$$V_r = \partial\varphi/\partial r \text{ and } V_s = \partial\varphi/\partial s = (1/r) \partial\varphi/\partial\theta$$

It can be seen that the magnitude of the velocity in a certain direction is determined by the rapidity of the change in the potential  $\varphi$  in the same direction. If we consider the direction  $s$ , the rapidity of the change in the potential equals the partial derivative with

respect to this direction  $\partial\varphi/\partial s$ . The quantity  $\partial\varphi/\partial s$  can be considered as the projection onto the direction  $s$  of a vector known as the **gradient of the function**  $\varphi$  and coinciding with the direction of the most rapid increase in this function. It is evident that this vector equals the velocity vector  $\mathbf{V}$ . Denoting the gradient of a function in the form  $\text{grad } \varphi$ , we have

$$\mathbf{V} = \text{grad } \varphi \quad (2.3.3)$$

or

$$\mathbf{V} = \text{grad } \varphi = (\text{grad } \varphi)_x \mathbf{i} + (\text{grad } \varphi)_y \mathbf{j} + (\text{grad } \varphi)_z \mathbf{k} \quad (2.3.4)$$

where the coefficients in parentheses on the right-hand side are the projections of the vector of the velocity gradient onto the coordinate axes:

$$\begin{aligned} (\text{grad } \varphi)_x &= V_x = \partial\varphi/\partial x, & (\text{grad } \varphi)_y &= V_y = \partial\varphi/\partial y, \\ (\text{grad } \varphi)_z &= V_z = \partial\varphi/\partial z \end{aligned} \quad (2.3.5)$$

The use of the potential function appreciably simplifies the investigation of a fluid's motion because instead of determining three unknowns, the velocity components  $V_x$ ,  $V_y$ , and  $V_z$ , it is sufficient to find one unknown function  $\varphi$ , which makes it possible to completely calculate the velocity field.

## 2.4. Continuity Equation

### General Form of the Equation

The equation of continuity of motion in the mathematical form is the law of mass conservation—one of the most general laws of physics. This equation is one of the fundamental equations of aerodynamics used to find the parameters determining the motion of a gas.

To obtain the continuity equation, let us consider a moving volume of a fluid. This volume, varying with time, consists of the same particles. The mass  $m$  of this volume in accordance with the law of mass conservation remains constant, therefore  $\rho_m \tau = \text{const}$ , where  $\rho_m$  is the mean density within the limits of the volume  $\tau$ . Consequently, the derivative  $d(\rho_m \tau)/dt = 0$ , or, with a view to the density and volume being variables, we have

$$(1/\rho_m) d\rho_m/dt + (1/\tau) d\tau/dt = 0$$

This volume relates to an arbitrary finite volume. To obtain a relation characterizing the motion of a fluid at each point, let us go over to the limit with  $\tau \rightarrow 0$  in the last equation, which signifies contraction of this volume to an internal point. If the condition is observed that the moving fluid completely fills the space being stud-

ied and, consequently, no voids or discontinuities are formed, the density at a given point is a quite determinate quantity  $\rho$ , and we obtain the equation

$$(1/\rho) d\rho/dt + \operatorname{div} \mathbf{V} = 0 \quad (2.4.1)$$

in which the value of  $\lim_{\tau \rightarrow 0} [(1/\tau) d\tau/dt]$  has been replaced according to (2.2.10) and (2.2.11) with the divergence of the velocity.

Relation (2.4.1) is a **continuity equation**. It has been obtained in a general form and can therefore be used for any chosen coordinate system.

#### Cartesian Coordinate System

Let us consider the continuity equation in the Cartesian coordinate system. For this purpose, we calculate the derivative  $d\rho(x, y, z, t)/dt$  in (2.4.1) in accordance with (2.2.11). As a result, we obtain the continuity equation

$$\partial\rho/\partial t + \partial(\rho V_x)/\partial x + \partial(\rho V_y)/\partial y + \partial(\rho V_z)/\partial z = 0 \quad (2.4.2)$$

Introducing the concept of the divergence of the vector  $\rho \mathbf{V}$

$$\operatorname{div}(\rho \mathbf{V}) = \partial(\rho V_x)/\partial x + \partial(\rho V_y)/\partial y + \partial(\rho V_z)/\partial z$$

we obtain

$$\partial\rho/\partial t + \operatorname{div}(\rho \mathbf{V}) = 0 \quad (2.4.3)$$

instead of (2.4.2).

Continuity equation (2.4.2) describes an unsteady flow. For a steady flow,  $\partial\rho/\partial t = 0$  and, consequently,

$$\partial(\rho V_x)/\partial x + \partial(\rho V_y)/\partial y + \partial(\rho V_z)/\partial z = 0 \quad (2.4.4)$$

or

$$\operatorname{div}(\rho \mathbf{V}) = 0 \quad (2.4.4')$$

For a two-dimensional flow, the continuity equation is

$$\partial(\rho V_x)/\partial x + \partial(\rho V_y)/\partial y = 0 \quad (2.4.5)$$

For an incompressible flow,  $\rho = \text{const}$ , hence

$$\partial V_x/\partial x + \partial V_y/\partial y + \partial V_z/\partial z = 0 \quad (2.4.6)$$

or

$$\operatorname{div} \mathbf{V} = 0 \quad (2.4.7)$$

For potential motion, the continuity equation is transformed with account taken of (2.3.2) to the following form:

$$(1/\rho) d\rho/dt + \partial^2\varphi/\partial x^2 + \partial^2\varphi/\partial y^2 + \partial^2\varphi/\partial z^2 = 0 \quad (2.4.8)$$

For an incompressible fluid,  $\rho = \text{const}$ . therefore

$$\partial^2\varphi/\partial x^2 + \partial^2\varphi/\partial y^2 + \partial^2\varphi/\partial z^2 = 0 \quad (2.4.8')$$

The expression obtained is called the **Laplace equation**. The solution of this equation is known to be a harmonic function. Consequently, the velocity potential of an incompressible flow  $\varphi$  is such a harmonic function.

### Curvilinear Coordinate System

**Conversion Formulas.** It is more convenient to solve some problems in aerodynamics by using a curvilinear orthogonal coordinate system. Such systems include, particularly, the cylindrical and spherical coordinate systems.

In a cylindrical coordinate system, the position of a point  $P$  in space (Fig. 2.4.1) is determined by the angle  $\gamma$  made by the coordinate plane and a plane passing through point  $P$  and the coordinate axis  $Ox$ , and by the rectangular coordinates  $x$  and  $r$  in this plane. The formulas for transition from a Cartesian coordinate system to a cylindrical one have the following form:

$$x = x, \quad y = r \cos \gamma, \quad z = r \sin \gamma \quad (2.4.9)$$

In a spherical coordinate system, the position of point  $P$  (Figure 2.4.2) is determined by the angular coordinates  $\theta$  (the polar angle) and  $\psi$  (the longitude), as well as by the polar radius  $r$ . The relation between rectangular and spherical coordinates is determined as follows:

$$x = r \cos \theta, \quad y = r \sin \theta \cos \psi, \quad z = r \sin \theta \sin \psi \quad (2.4.10)$$

The relevant transformations of the equations of aerodynamics obtained in Cartesian coordinates to a curvilinear orthogonal system can be performed in two ways: either by direct substitution of (2.4.9) and (2.4.10) into these equations or by employing a more general approach based on the concept of generalized coordinate curves (see [9]). Let us consider this approach.

We shall represent the elementary lengths of arcs of the coordinate curves in the vicinity of point  $P$  in the general form:

$$ds_1 = h_1 dq_1, \quad ds_2 = h_2 dq_2, \quad ds_3 = h_3 dq_3 \quad (2.4.11)$$

where  $q_n$  ( $n = 1, 2, 3$ ) are the curvilinear coordinates, and  $h_i$  are coefficients known as **Lamé's coefficients**.

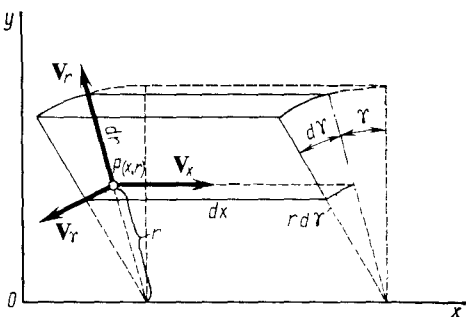
For cylindrical and spherical coordinates, respectively, we have

$$q_1 = x, \quad q_2 = r, \quad q_3 = \gamma \quad (2.4.12)$$

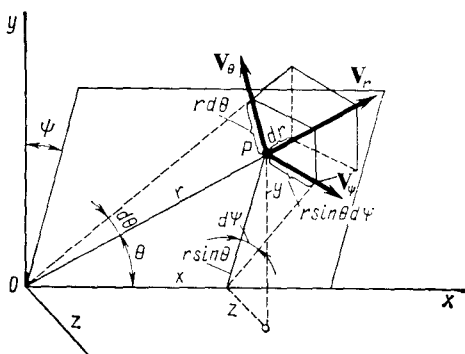
$$q_1 = r, \quad q_2 = \theta, \quad q_3 = \psi \quad (2.4.13)$$

It follows directly from Fig. 2.4.1 that for cylindrical coordinates

$$ds_1 = dx, \quad ds_2 = dr, \quad ds_3 = r d\gamma \quad (2.4.14)$$

**Fig. 2.4.1**

An elementary fluid particle in a cylindrical coordinate system

**Fig. 2.4.2**

An elementary fluid particle in a spherical coordinate system

Figure 2.4.2 allows us to determine the length of the arcs of the relevant coordinate lines in a spherical system:

$$ds_1 = dr, \quad ds_2 = r d\theta, \quad ds_3 = r \sin \theta d\psi \quad (2.4.15)$$

Consequently, for cylindrical coordinates, Lamé's coefficients have the form

$$h_1 = 1, \quad h_2 = 1, \quad h_3 = r \quad (2.4.16)$$

and for spherical ones

$$h_1 = 1, \quad h_2 = r, \quad h_3 = r \sin \theta \quad (2.4.17)$$

Let us consider some expressions for vector and scalar quantities in curvilinear coordinates that are needed to transform the continuity equation to these coordinates. The gradient of a scalar function  $\Phi$  is

$$\text{grad } \Phi = (\partial \Phi / \partial s_1) \mathbf{i}_1 + (\partial \Phi / \partial s_2) \mathbf{i}_2 + (\partial \Phi / \partial s_3) \mathbf{i}_3$$

where  $\mathbf{i}_1$ ,  $\mathbf{i}_2$ , and  $\mathbf{i}_3$  are unit vectors along the relevant coordinate lines.

Having in view formulas (2.4.11), we obtain

$$\text{grad } \Phi = \frac{1}{h_1} \cdot \frac{\partial \Phi}{\partial q_1} \mathbf{i}_1 + \frac{1}{h_2} \cdot \frac{\partial \Phi}{\partial q_2} \mathbf{i}_2 + \frac{1}{h_3} \cdot \frac{\partial \Phi}{\partial q_3} \mathbf{i}_3 \quad (2.4.18)$$

For further transformations, we shall use information from the course of mathematics dealing with vector analysis. Let us find the divergence of the velocity vector, writing it as the sum of the components along the coordinate lines:

$$\mathbf{V} = V_1 \mathbf{i}_1 + V_2 \mathbf{i}_2 + V_3 \mathbf{i}_3 = \sum_{n=1}^3 V_n \mathbf{i}_n \quad (2.4.19)$$

Performing the divergence operation for both sides of this equation, we obtain

$$\text{div } \mathbf{V} = \sum_{n=1}^3 (V_n \text{div } \mathbf{i}_n + \mathbf{i}_n \text{grad } V_n) \quad (2.4.20)$$

To determine  $\text{div } \mathbf{i}_n$ , we shall use a known relation of vector analysis

$$\text{div } \mathbf{i}_n = \text{div} [\mathbf{i}_m \times \mathbf{i}_j] = \mathbf{i}_j \text{curl } \mathbf{i}_m - \mathbf{i}_m \text{curl } \mathbf{i}_j \quad (2.4.21)$$

where  $n$  takes on consecutively the values of  $n = 1, 2, 3$  which the values of  $m = 2, 3, 1$  and  $j = 3, 1, 2$  correspond to. This relation includes the vectors  $\text{curl } \mathbf{i}_m$  or  $\text{curl } \mathbf{i}_j$  to be determined, for which we shall introduce the common symbol  $\text{curl } \mathbf{i}_n$ . Using (2.4.18) and the general methods of transforming vector quantities, we find

$$\text{curl } \mathbf{i}_n = \frac{1}{h_n} \left( \frac{1}{h_j} \cdot \frac{\partial h_n}{\partial q_j} \mathbf{i}_m - \frac{1}{h_m} \cdot \frac{\partial h_n}{\partial q_m} \mathbf{i}_j \right) \quad (2.4.22)$$

Let us introduce (2.4.22) into (2.4.21). For this purpose we shall first replace the subscript  $n$  in  $\text{curl } \mathbf{i}_n$  with  $m$  and  $j$ , and also correspondingly arrange the subscripts on the right-hand side of (2.4.22). As a result, we have

$$\text{div } \mathbf{i}_n = \frac{1}{h_n} \left( \frac{1}{h_m} \cdot \frac{\partial h_m}{\partial q_n} + \frac{1}{h_j} \cdot \frac{\partial h_j}{\partial q_n} \right) \quad (2.4.23)$$

Let us introduce these values into (2.4.20). Having in view that in this formula, in accordance with (2.4.18), we have

$$\mathbf{i}_n \cdot \text{grad } V_n = (1/h_n) \partial V_n / \partial q_n$$

we find the following expression for the divergence:

$$\text{div } \mathbf{V} = \frac{1}{h_1 h_2 h_3} \cdot \left[ \frac{\partial (V_1 h_2 h_3)}{\partial q_1} + \frac{\partial (V_2 h_3 h_1)}{\partial q_2} + \frac{\partial (V_3 h_1 h_2)}{\partial q_3} \right] \quad (2.4.24)$$

Having this expression, we can transform the continuity equation (2.4.1) to various forms of curvilinear orthogonal coordinates.

**Cylindrical Coordinates.** In cylindrical coordinates, Lamé's coefficients are given by expressions (2.4.16), and the values of  $q_n$  ( $n = 1, 2, 3$ ) by relations (2.4.12). The velocity components along the axes of cylindrical coordinates are

$$V_1 = V_x = dx/dt, \quad V_2 = V_r = dr/dt, \quad V_3 = V_\gamma = r d\gamma/dt \quad (2.4.25)$$

Taking this into account, the divergence of the velocity (2.4.24) becomes

$$\operatorname{div} \mathbf{V} = \frac{\partial V_x}{\partial x} + \frac{\partial V_r}{\partial r} + \frac{1}{r} \cdot \frac{\partial V_\gamma}{\partial \gamma} + \frac{V_r}{r} \quad (2.4.26)$$

To transform the derivative  $d\rho/dt$  in the continuity equation (2.4.1) to cylindrical coordinates, we use the transformation formula

$$\frac{df}{dt} = \frac{\partial f}{\partial t} + \frac{\partial f}{\partial q_1} \cdot \frac{dq_1}{dt} + \frac{\partial f}{\partial q_2} \cdot \frac{dq_2}{dt} + \frac{\partial f}{\partial q_3} \cdot \frac{dq_3}{dt} \quad (2.4.27)$$

in which  $f(x, y, z, t)$  is a function of Cartesian coordinates and time. We obtain

$$\begin{aligned} \frac{d\rho}{dt} &= \frac{\partial \rho}{\partial t} + \frac{dx}{dt} \cdot \frac{\partial \rho}{\partial x} + \frac{dr}{dt} \cdot \frac{\partial \rho}{\partial r} + \frac{d\gamma}{dt} \cdot \frac{\partial \rho}{\partial \gamma} \\ &= \frac{\partial \rho}{\partial t} + V_x \frac{\partial \rho}{\partial x} + V_r \frac{\partial \rho}{\partial r} + \frac{V_\gamma}{r} \cdot \frac{\partial \rho}{\partial \gamma}. \end{aligned} \quad (2.4.28)$$

Substituting their values for  $\operatorname{div} \mathbf{V}$  and  $d\rho/dt$  in Eq. (2.4.1), we find

$$\frac{\partial \rho}{\partial t} + \frac{\partial (\rho V_x)}{\partial x} + \frac{\partial (\rho V_r)}{\partial r} + \frac{1}{r} \cdot \frac{\partial (\rho V_\gamma)}{\partial \gamma} + \frac{\rho V_r}{r} = 0 \quad (2.4.29)$$

Let us write this equation in a somewhat different form:

$$r \frac{\partial \rho}{\partial t} + \frac{\partial (\rho r V_x)}{\partial x} + \frac{\partial (\rho r V_r)}{\partial r} + \frac{1}{r} \cdot \frac{\partial (\rho r V_\gamma)}{\partial \gamma} = 0 \quad (2.4.30)$$

For the particular case of steady motion

$$\frac{\partial (\rho r V_x)}{\partial x} + \frac{\partial (\rho r V_r)}{\partial r} + \frac{1}{r} \cdot \frac{\partial (\rho r V_\gamma)}{\partial \gamma} = 0 \quad (2.4.31)$$

For potential motion, substitutions may be made in the continuity equation:

$$V_x = \partial \varphi / \partial x, \quad V_r = \partial \varphi / \partial r, \quad V_\gamma = (1/r) (\partial \varphi / \partial \gamma) \quad (2.4.25')$$

If the motion of a gas is simultaneously axisymmetric as, for example, if it flows about a body of revolution at a zero angle of attack, the flow parameters do not depend on the angular coordinate  $\gamma$ , and the continuity equation has a simpler form:

$$\partial (\rho r V_x) / \partial x + \partial (\rho r V_r) / \partial r = 0 \quad (2.4.32)$$

**Spherical Coordinates.** Using relation (2.4.24), having in view formulas (2.4.13) for spherical coordinates, and also relations (2.4.17) for Lamé's coefficients and the expressions for the velocity components

$$V_1 = V_r = \frac{dr}{dt}, \quad V_2 = V_\theta = \frac{1}{r} \frac{d\theta}{dt}, \\ V_3 = V_\psi = r \sin \theta \frac{d\psi}{dt} \quad (2.4.33)$$

we obtain the following expression for the divergence of the velocity:

$$\operatorname{div} \mathbf{V} = \frac{1}{r^2} \cdot \frac{\partial (V_r r^2)}{\partial r} + \frac{1}{r \sin \theta} \cdot \frac{\partial (V_\theta \sin \theta)}{\partial \theta} + \frac{1}{r \sin \theta} \cdot \frac{\partial V_\psi}{\partial \psi} \quad (2.4.34)$$

We shall write the total derivative for the density  $d\rho/dt$  in accordance with (2.4.27) in the following form:

$$\begin{aligned} \frac{d\rho}{dt} &= \frac{\partial \rho}{\partial t} + \frac{dr}{dt} \cdot \frac{\partial \rho}{\partial r} + \frac{d\theta}{dt} \cdot \frac{\partial \rho}{\partial \theta} + \frac{d\psi}{dt} \cdot \frac{\partial \rho}{\partial \psi} \\ &= \frac{\partial \rho}{\partial t} + V_r \frac{\partial \rho}{\partial r} + \frac{V_\theta}{r} \cdot \frac{\partial \rho}{\partial \theta} + \frac{V_\psi}{r \sin \theta} \cdot \frac{\partial \rho}{\partial \psi} \end{aligned} \quad (2.4.35)$$

Introducing the values of  $\operatorname{div} \mathbf{V}$  from (2.4.34) and the derivative  $d\rho/dt$  from (2.4.35) into (2.4.1) and grouping terms, we have

$$\frac{\partial \rho}{\partial t} + \frac{1}{r^2} \cdot \frac{\partial (\rho V_r r^2)}{\partial r} + \frac{1}{r \sin \theta} \cdot \frac{\partial (\rho V_\theta \sin \theta)}{\partial \theta} + \frac{1}{r \sin \theta} \cdot \frac{\partial (\rho V_\psi)}{\partial \psi} = 0 \quad (2.4.36)$$

For steady motion, the partial derivative  $\partial \rho / \partial t = 0$ , hence

$$\frac{1}{r} \cdot \frac{\partial (\rho V_r r^2)}{\partial r} + \frac{1}{\sin \theta} \cdot \frac{\partial (\rho V_\theta \sin \theta)}{\partial \theta} + \frac{1}{\sin \theta} \cdot \frac{\partial (\rho V_\psi)}{\partial \psi} = 0 \quad (2.4.37)$$

In the particular case of an incompressible fluid ( $\rho = \text{const}$ )

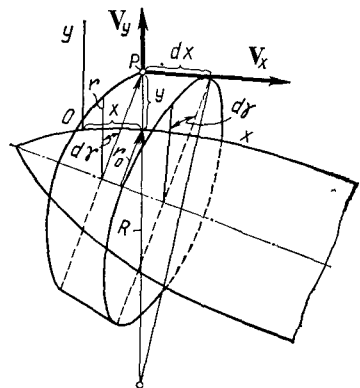
$$\frac{1}{r} \cdot \frac{\partial (V_r r^2)}{\partial r} + \frac{1}{\sin \theta} \cdot \frac{\partial (V_\theta \sin \theta)}{\partial \theta} + \frac{1}{\sin \theta} \cdot \frac{\partial V_\psi}{\partial \psi} = 0 \quad (2.4.38)$$

The following substitutions must be performed to transform the continuity equation for potential motion:

$$V_r = \frac{\partial \varphi}{\partial r}, \quad V_\theta = \frac{1}{r} \cdot \frac{\partial \varphi}{\partial \theta}, \quad V_\psi = \frac{1}{r \sin \theta} \cdot \frac{\partial \varphi}{\partial \psi} \quad (2.4.39)$$

#### Continuity Equation of Gas Flow along a Curved Surface

Let us consider a particular form of the continuity equation in curvilinear orthogonal coordinates that is used in studying flow over a curved wall. The  $x$ -axis in this system of coordinates coincides with the contour of the wall, and the  $y$ -axis with a normal to this wall at

**Fig. 2.4.3**

To the derivation of the continuity equation in curvilinear coordinates

the point being considered. The coordinates of point  $P$  on the plane (Fig. 2.4.3) equal the length  $x$  measured along the wall and the distance  $y$  measured along a normal to it, respectively. Assume that the wall is a surface of revolution in an axisymmetric flow of a gas. The curvilinear coordinates of point  $P$  are:

$$q_1 = x, \quad q_2 = y, \quad q_3 = \gamma \quad (2.4.40)$$

The elementary lengths of the coordinate line arcs are

$$ds_1 = (1 + y/R) dx, \quad ds_2 = dy, \quad ds_3 = r d\gamma \quad (2.4.41)$$

where  $r$  is the radial coordinate of point  $P$  measured along a normal to the axis of the surface of revolution, and  $R$  is the radius of curvature of the surface in the section being considered.

Consequently, Lamé's coefficients are

$$h_1 = 1 + y/R, \quad h_2 = 1, \quad h_3 = r \quad (2.4.42)$$

Let us use formula (2.4.24) for  $\operatorname{div} \mathbf{V}$  in which the velocity components are

$$\mathbf{V}_1 = V_x = ds_1/dt = (1 + y/R) dx/dt, \quad V_2 = V_y = dy/dt, \quad V_3 = 0 \quad (2.4.43)$$

Substitution yields

$$\operatorname{div} \mathbf{V} = \frac{1}{(1+y/R) r} \left\{ \frac{\partial (V_x r)}{\partial x} + \frac{\partial [V_y r (1+y/R)]}{\partial y} \right\} \quad (2.4.44)$$

Let us calculate the total derivative for the density:

$$\begin{aligned} \frac{d\rho}{dt} &= \frac{\partial \rho}{\partial t} + \frac{dx}{dt} \cdot \frac{\partial \rho}{\partial x} + \frac{dy}{dt} \cdot \frac{\partial \rho}{\partial y} \\ &= \frac{\partial \rho}{\partial t} + \frac{V_x}{1+y/R} \cdot \frac{\partial \rho}{\partial x} + V_y \frac{\partial \rho}{\partial y} \end{aligned} \quad (2.4.45)$$

Introducing expressions (2.4.44) and (2.4.45) into (2.4.1), after simple transformations we obtain the continuity equation

$$\frac{\partial \rho}{\partial t} r (1 + y/R) + \frac{\partial (\rho r V_x)}{\partial x} + \frac{\partial [\rho r (1 + y/R) V_y]}{\partial y} = 0 \quad (2.4.46)$$

When studying the motion of a gas near a wall with a small curvature or in a thin layer adjacent to a surface (for example, in a boundary layer), the coordinate  $y \ll R$ . Consequently

$$(\partial \rho / \partial t) r + \partial (\rho r V_x) / \partial x + \partial (\rho r V_y) / \partial y = 0 \quad (2.4.47)$$

The form of the obtained equation is the same as for a surface with a straight generatrix. For steady flow

$$\partial (\rho r V_x) / \partial x + \partial (\rho r V_y) / \partial y = 0 \quad (2.4.48)$$

For two-dimensional flow near a curved wall (a cylindrical surface), the continuity equation has the form

$$\frac{\partial \rho}{\partial t} (1 + y/R) + \frac{\partial (\rho V_x)}{\partial x} + \frac{\partial [\rho V_y (1 + y/R)]}{\partial y} = 0 \quad (2.4.49)$$

For  $y \ll R$ , we approximately have

$$\partial \rho / \partial t + \partial (\rho V_x) / \partial x + \partial (\rho V_y) / \partial y = 0 \quad (2.4.50)$$

Hence, for flow near a wall, the continuity equation in curvilinear coordinates has the same form as in Cartesian coordinates.

For steady flow,  $\partial \rho / \partial t = 0$ ; in this case the continuity equation is

$$\partial (\rho V_x) / \partial x + \partial (\rho V_y) / \partial y = 0 \quad (2.4.50')$$

Equations (2.4.48) and (2.4.50') can be combined into a single one:

$$\partial / (\rho V_x r^\epsilon) / \partial x + \partial / (\rho V_y r^\epsilon) / \partial y = 0 \quad (2.4.48')$$

where  $\epsilon = 0$  for a two-dimensional plane flow and  $\epsilon = 1$  for a three-dimensional axisymmetric flow.

### Flow Rate Equation

Let us consider a particular form of the continuity equation for a steady fluid flow having the shape of a stream filament. The mass of the fluid in a fixed volume confined within the surface of the filament and the end plane cross sections does not change in time because the condition that  $\partial \rho / \partial t = 0$  is observed at every point. Hence the mass of the fluid entering the volume in unit time via the end cross section with an area of  $S_1$  and equal to  $\rho_1 V_1 S_1$  is the same as the mass of the fluid  $\rho_2 V_2 S_2$  leaving through the opposite cross section with an area of  $S_2$  ( $\rho_1$  and  $\rho_2$  are the densities,  $V_1$  and  $V_2$  are the speeds in the first and second cross sections of the filament, respectively).

ly). We thus have  $\rho_1 V_1 S_1 = \rho_2 V_2 S_2$ . Since this equation can be related to any cross section, in the general form we have

$$\rho VS = \text{const} \quad (2.4.51)$$

This is the **flow rate equation**.

## 2.5. Stream Function

The studying of a vortex-free gas flow is simplified because it can be reduced to the finding of one unknown potential function completely determining the flow. We shall show that for certain kinds of a vortex flow there is also a function determining its kinematic characteristics.

Let us consider a two-dimensional (plane or spatial axisymmetric) steady vortex flow of a fluid. It can be established from continuity equation (2.4.32') that there is a function  $\psi$  of the coordinates  $x$  and  $y$  determined by the relations

$$\partial\psi/\partial x = -\rho y^\epsilon V_y; \quad \partial\psi/\partial y = \rho y^\epsilon V_x \quad (2.5.1)$$

Indeed, introducing these relations into (2.4.32'), we obtain  $\partial^2\psi/(\partial y \partial x) = \partial^2\psi/(\partial x \partial y)$ , i.e. an identity. Substituting (2.5.1) into the equation of streamlines  $V_y/\partial y = V_x/\partial x$  written in the form

$$\rho y^\epsilon V_y dx - \rho y^\epsilon V_x dy = 0 \quad (2.5.2)$$

we obtain the expression

$$(\partial\psi/\partial x) dx + (\partial\psi/\partial y) dy = 0$$

from which it follows that (2.5.2) is a differential of the function  $\psi$  and, consequently,

$$d\psi = 0 \quad (2.5.3)$$

Integrating (2.5.3), we find an equation of streamlines in the form

$$\psi(x, y) = \text{const} \quad (2.5.4)$$

The function  $\psi$ , called the **stream function**, completely determines the velocity of a vortex flow in accordance with the relations

$$V_x = (1/\rho y^\epsilon) \partial\psi/\partial y, \quad V_y = -(1/\rho y^\epsilon) \partial\psi/\partial x \quad (2.5.5)$$

We remind our reader that for a two-dimensional flow, we have to assume in these expressions that  $\epsilon = 0$ , while for a three-dimensional axisymmetric flow  $\epsilon = 1$  and  $y = r$ .

A family of streamlines of a potential flow can also be characterized by the function  $\psi = \text{const}$  that is associated with the velocity potential by the relations

$$\partial\varphi/\partial x = (1/\rho y^\epsilon) \partial\psi/\partial y, \quad \partial\varphi/\partial y = -(1/\rho y^\epsilon) \partial\psi/\partial x \quad (2.5.6)$$

Assuming in (2.5.5) and (2.5.6) that  $\rho = \text{const}$ , we obtain the relevant expressions for an incompressible flow:

$$V_x = (1/y^\epsilon) \partial\psi/\partial y, \quad V_y = -(1/y^\epsilon) \partial\psi/\partial x \quad (2.5.7)$$

$$\partial\varphi/\partial x = (1/y^\epsilon) \partial\psi/\partial y, \quad \partial\varphi/\partial y = -(1/y^\epsilon) \partial\psi/\partial x \quad (2.5.8)$$

Assuming in Eqs. (2.5.8) that  $\epsilon = 0$ , we obtain the following equations for an incompressible two-dimensional flow:

$$\partial\varphi/\partial x = \partial\psi/\partial y, \quad \partial\varphi/\partial y = -\partial\psi/\partial x \quad (2.5.9)$$

Knowing the velocity potential, we can use these equations to determine the stream function with an accuracy to within an arbitrary constant, and vice versa.

In addition to streamlines, we can construct a family of equipotential curves (on a plane) or of equipotential surfaces (in an axisymmetric flow) in a potential flow that is determined by the equation  $\varphi = \text{const}$ .

Let us consider the vectors

$$\text{grad } \varphi = (\partial\varphi/\partial x) \mathbf{i} + (\partial\varphi/\partial y) \mathbf{j} \text{ and } \text{grad } \psi = (\partial\psi/\partial x) \mathbf{i} + (\partial\psi/\partial y) \mathbf{j}$$

whose directions coincide with those of normals to the curves  $\varphi = \text{const}$  and  $\psi = \text{const}$ , respectively. The scalar (dot) product of these vectors is

$$\text{grad } \varphi \cdot \text{grad } \psi = (\partial\varphi/\partial x) \partial\psi/\partial x + (\partial\varphi/\partial y) \partial\psi/\partial y$$

With a view to formulas (2.3.2) and (2.5.5), we can establish that this product equals zero. Hence it follows that streamlines are orthogonal to equipotential lines (on a plane) or to equipotential surfaces (in an axisymmetric flow).

## 2.6. Vortex Lines

A **vortex line** is defined to be a curve  $s$  constructed at a definite instant in a fluid flow and having the property that at each point of it the angular velocity vector  $\omega$  coincides with the direction of a tangent.

A vortex line is constructed similarly to a streamline (see Fig. 2.1.1). The only difference is that the angular velocities of rotation of the particles  $\omega$  ( $\omega_1$ ,  $\omega_2$ , etc.) are taken instead of the linear velocities. In accordance with this definition, the cross product  $\omega \times d\mathbf{S} = 0$ , i.e.

$$\begin{vmatrix} \mathbf{i} & \mathbf{j} & \mathbf{k} \\ \omega_x & \omega_y & \omega_z \\ dx & dy & dz \end{vmatrix} = \mathbf{i}(\omega_y dz - \omega_z dy) - \mathbf{j}(\omega_x dz - \omega_z dx) + \mathbf{k}(\omega_x dy - \omega_y dx) = 0$$

Hence, taking into account that, for example,  $\omega_y dz - \omega_z dy = 0$ , and so on, we obtain an equation of a vortex line:

$$dx/\omega_x = dy/\omega_y = dz/\omega_z \quad (2.6.1)$$

By constructing vortex lines through the points of an elementary contour with a cross-sectional area of  $\sigma$ , we obtain a **vortex tube**. The product  $\omega\sigma$  is called the **intensity or strength of a vortex tube**, or simply the **vorticity**.

We shall prove that the vorticity is constant for all the sections of a vortex tube. For this purpose, we shall use the analogy with the flow of an incompressible fluid for which  $\operatorname{div} \mathbf{V} = 0$ . A corollary is the flow rate equation for a stream filament  $V_1 S_1 = V_2 S_2 = \dots = VS = \text{const}$ .

Let us consider vortex motion and the expression for the divergence of the angular velocity

$$\operatorname{div} \boldsymbol{\omega} = \partial \omega_x / \partial x + \partial \omega_y / \partial y + \partial \omega_z / \partial z$$

Substituting for the components of  $\boldsymbol{\omega}$  their values from (2.2.3) and (2.2.6), we obtain, provided that the second derivatives of  $V_x$ ,  $V_y$ , and  $V_z$  are continuous, the expression  $\operatorname{div} \boldsymbol{\omega} = 0$ . Using the analogy with the flow rate equation  $VS = \text{const}$ , we obtain an equation for the flow of the vector  $\boldsymbol{\omega}$  along a vortex tube in the form

$$\omega_1 \sigma_1 = \omega_2 \sigma_2 = \dots = \omega \sigma = \text{const} \quad (2.6.2)$$

This equation expresses the Helmholtz theorem on the constancy of the vorticity along a vortex tube. The property of a vortex tube consisting in that *it cannot break off suddenly or terminate in a sharp point* follows from this theorem. The termination in a sharp point is impossible because at a cross-sectional area of the tube of  $\sigma \rightarrow 0$ , the angular velocity  $\omega$  would tend to infinity according to the Helmholtz theorem, and this is not real physically.

## 2.7. Velocity Circulation

### Concept

Velocity circulation is of major significance in aerodynamics. This concept is used when studying the flow over craft and, particularly, when determining the lift force acting on a wing.

Let us consider in a fluid flow a fixed closed contour  $K$  at each point of which the velocity  $\mathbf{V}$  is known, and evaluate the integral over this contour:

$$\Gamma = \oint_K \mathbf{V} \cdot d\mathbf{s} \quad (2.7.1)$$

where  $\mathbf{V} \cdot d\mathbf{s}$  is the dot product of the vectors  $\mathbf{V}$  and  $d\mathbf{s}$ . The quantity  $\Gamma$  determined in this way is known as the **circulation of the velocity** around a closed contour. Since

$$\mathbf{V} = V_x \mathbf{i} + V_y \mathbf{j} + V_z \mathbf{k} \text{ and } d\mathbf{s} = dx \mathbf{i} + dy \mathbf{j} + dz \mathbf{k}$$

we have

$$\Gamma = \int_{(K)} V_x dx + V_y dy + V_z dz \quad (2.7.2)$$

Taking also into account that the dot product  $\mathbf{V} \cdot d\mathbf{s} = V \cos(\widehat{\mathbf{V} \cdot d\mathbf{s}}) ds = V_s ds$ , where  $V_s$  is the projection of the velocity onto a tangent, we obtain

$$\Gamma = \int_{(K)} V_s ds \quad (2.7.3)$$

If the contour coincides with a streamline in the form of a circle of radius  $r$  at each point of which the velocity  $V_s$  is identical in magnitude and direction, we have

$$\Gamma = 2\pi r V_s \quad (2.7.4)$$

The circulation of the velocity in a vortex-free flow can be expressed in terms of the velocity potential. Assuming that  $V_x dx + V_y dy + V_z dz = d\varphi$ , we obtain for an open contour

$$\Gamma = \int_{(L)} d\varphi = \varphi_A - \varphi_B \quad (2.7.5)$$

where  $\varphi_A$  and  $\varphi_B$  are the values of the potential function at the ends of the contour. For a closed contour,  $\varphi_A$  and  $\varphi_B$  are the values of the velocity potential at points  $A$  and  $B$  of the contour coinciding with each other. If the potential function is unambiguous, then  $\varphi_A = \varphi_B$ , and the velocity circulation around the closed contour is zero; ambiguity of the velocity potential ( $\varphi_A \neq \varphi_B$ ) determines a non-zero value of the circulation.

### Stokes Theorem

Let us consider elementary contour  $ABCD$  (see Fig. 2.2.1) and evaluate the circulation around this contour. We shall assume that the velocities are constant along each edge and are equal to the following values:

$$V_x (AB), \quad V_y + \frac{\partial V_y}{\partial x} dx (BC), \quad V_x + \frac{\partial V_x}{\partial y} dy (CD), \quad V_y (AD)$$

Considering the counterclockwise direction of circumventing the contour (from the  $x$ -axis toward the  $y$ -axis) to be positive, we obtain

for the circulation

$$d\Gamma_z = V_x dx + \left( V_y + \frac{\partial V_y}{\partial x} dx \right) dy - \left( V_x + \frac{\partial V_x}{\partial y} dy \right) dx - V_y dy$$

or

$$d\Gamma_z = (\partial V_y / \partial x - \partial V_x / \partial y) dx dy$$

According to (2.2.3), the quantity in parentheses equals the double value of the angular velocity component  $2\omega_z$ . Consequently,

$$d\Gamma_z = 2\omega_z dx dy \quad (2.7.6)$$

We can prove similarly that

$$d\Gamma_x = 2\omega_x dy dz \text{ and } d\Gamma_y = 2\omega_y dx dz$$

In these expressions, the products of the differentials are the areas confined by the relevant elementary contours. With a view to the results obtained, for the area element  $d\sigma$  oriented in space arbitrarily and confined within an elementary contour, the circulation is

$$d\Gamma_n = 2\omega_n d\sigma \quad (2.7.7)$$

where  $\omega_n$  is the component of the angular velocity along the direction of the normal  $n$  to the surface element  $d\sigma$ . In accordance with (2.7.7), the velocity circulation around an elementary closed contour equals the double strength of a vortex inside the contour.

Relation (2.7.7) can be used for a contour  $L$  of finite dimensions confining a surface  $S$  at each point of which the value of  $\omega_n$  is known. Here the velocity circulation around the contour is

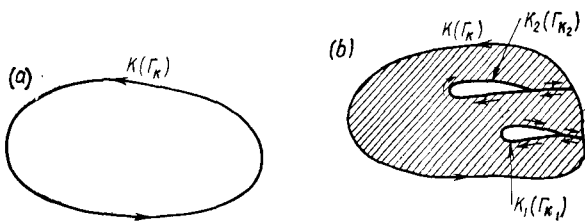
$$\Gamma = 2 \iint_{(S)} \omega_n d\sigma \quad (2.7.8)$$

Formula (2.7.8) expresses the Stokes theorem: the velocity circulation around the closed contour  $L$  equals the double integral of the strength of the vortices passing through the surface confined by the contour. The quantity determined by this formula is the vorticity (vortex strength) and is designated by

$$\kappa = 2 \iint_{(S)} \omega_n d\sigma \quad (2.7.8')$$

Combining formulas (2.7.3) and (2.7.8) for  $\Gamma$ , we obtain a relation expressing the integral over the contour  $K$  in terms of the integral over the surface  $S$  confined within this contour  $K$ :

$$\iint_{(K)} V_s ds = 2 \iint_{(S)} \omega_n d\sigma \quad (2.7.8'')$$

**Fig. 2.7.1**

Simply and triply connected regions on a plane:

a—simply connected region ( $\Gamma_K$  = circulation over the contour  $K$ ); b—triply connected region ( $\Gamma_K$  = circulation of the external contour,  $\Gamma_{K_1}$  and  $\Gamma_{K_2}$  = circulations over the internal contours  $K_1$  and  $K_2$ , respectively)

The above expressions relate to a simply connected contour (the region being considered is confined within a single contour, Fig. 2.7.1a). But the Stokes theorem can also be extended to multiply connected contours (a region confined by one external and several internal contours). Equation (2.7.8'') is used provided that the external contour is connected to the internal ones by auxiliary lines (cuts) so as to obtain a simply connected region. Now the double integral in (2.7.8'') is used for the hatched region (Fig. 2.7.1b), while the contour integral is taken for the obtained simply connected region, i.e. around the external contour, along all the cuts, and also around all the internal contours. In accordance with this, by formula (2.7.8''), and also with a view to Fig. 2.7.1b showing a triply connected region, we obtain

$$\Gamma_K - \Gamma_{K_1} - \Gamma_{K_2} = 2 \iint_S \omega_n d\sigma$$

whence the circulation over the contour  $K$  of the region being considered is

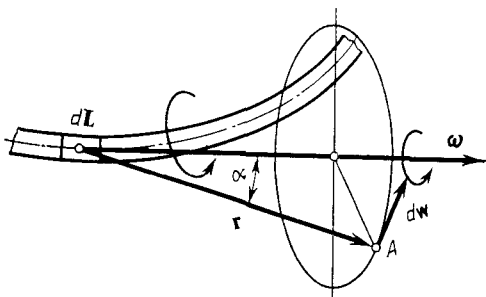
$$\Gamma_K = \Gamma_{K_1} + \Gamma_{K_2} + 2 \iint_S \omega_n d\sigma$$

Using this formula when we have  $n$  internal contours, we find

$$\Gamma_K = \sum_i^{i=n} \Gamma_{K_i} + 2 \iint_S \omega_n d\sigma$$

### Vortex-Induced Velocities

Appearing vortices produce additional velocities in the fluid-filled space surrounding them. This effect is similar to the electromagnetic influence of a conductor carrying an electric current. In

**Fig. 2.7.2**

Influence of a vortex

accordance with this analogy, the velocities produced by a vortex are said to be **induced**.

This electromagnetic analogy is expressed in that to determine the vortex-induced velocity, a **Biot-Savart relation** is used similar to the one expressing the known law of electromagnetic induction.

Let us consider a curvilinear vortex of an arbitrary shape (Fig. 2.7.2). The velocity vector  $dw$  induced by the vortex element  $dL$  at point  $A$  whose location is determined by the position vector  $r$  coincides in direction with the cross product  $r \times dL$ , i.e. the vector  $dw$  is perpendicular to the plane containing the vectors  $r$  and  $dL$ . The value of  $dw$  is determined with the aid of the Biot-Savart formula, which in the vector form is as follows:

$$dw = (\Gamma/4\pi) r \times dL r^3 \quad (2.7.9)$$

where  $\Gamma$  is the velocity circulation. The derivation of formula (2.7.9) is given in [10].

Since the magnitude of the cross product  $|r \times dL| = r \sin \alpha dL$ , where  $\alpha$  is the angle between the direction of a vortex element and the position vector  $r$ , the magnitude of the velocity induced at point  $A$  is

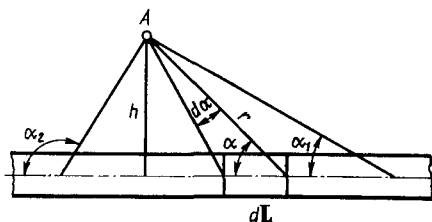
$$dw = (\Gamma/4\pi) \sin \alpha dL/r^2 \quad (2.7.10)$$

Let us use the Biot-Savart relation to calculate the velocity induced by a section of a line vortex (Fig. 2.7.3). Since  $r = h/\sin \alpha$ ,  $dL = r d\alpha/\sin \alpha = h d\alpha/\sin^2 \alpha$ , then

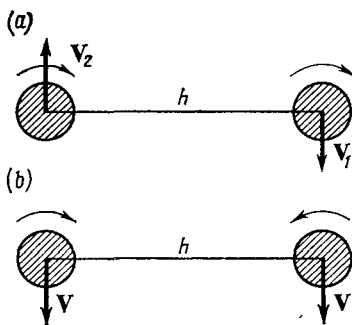
$$\omega = \frac{\Gamma}{4\pi h} \int_{\alpha_1}^{\alpha_2} \sin \alpha d\alpha = \frac{\Gamma}{4\pi h} (\cos \alpha_1 - \cos \alpha_2) \quad (2.7.11)$$

For a vortex both of whose ends extend to infinity (an infinite vortex),  $\alpha_1 = 0$ ,  $\alpha_2 = \pi$ , and, therefore,

$$w = \Gamma/(2\pi h) \quad (2.7.12)$$

**Fig. 2.7.3**

Influence of a line vortex on a fluid particle at point A

**Fig. 2.7.4**

Interaction of vortices:

*a*—vortices with an identical direction of rotation; *b*—vortices with opposite directions of motion

For a vortex, one end of which extends to infinity, and the other has its origin at point *A* (a semi-infinite vortex), we have  $\alpha_1 = 0$  and  $\alpha_2 = \pi/2$ . Consequently

$$w = \Gamma/(4\pi h) \quad (2.7.13)$$

If a fluid accommodates two or more vortices, they interact with one another, and as a result the vortex system is in motion. The velocity of this motion is determined with the aid of the Biot-Savart relation. Let us take as an example two infinite vortices with the same strength and direction of rotation (Fig. 2.7.4a). These vortices impart to each other the velocities  $V_2 = -\Gamma/(2\pi h)$  and  $V_1 = \Gamma/(2\pi h)$  that are equal in magnitude and opposite in direction. As a result, both vortices rotate about an axis passing through the middle of the distance between them. If of two vortices one has a strength of the opposite sign (Fig. 2.7.4b), the induced velocities are of the same direction and, consequently, the system of vortices moves translationally at the velocity  $V = \Gamma/(2\pi h)$  in a direction perpendicular to the straight line connecting the vortices.

## 2.8. Complex Potential

The motion of a vortex-free incompressible flow can be determined completely if we know the potential function  $\varphi$  or the stream function  $\psi$ , the relation between which is given by Eqs. (2.5.9), which

in the theory of the functions of a complex variable are known as the Cauchy-Riemann equations. They express the necessary and sufficient conditions needed for a combination of the two functions  $\varphi + i\psi$  to be an analytical function of the complex variable  $\sigma = x + iy$ , i.e. to be differentiable at all points of a certain region.

Let us introduce a symbol for this function:

$$W(\sigma) = \varphi + i\psi \quad (2.8.1)$$

The function  $W(\sigma)$  that is determined if the function of two real variables  $\varphi = \varphi(x, y)$  and  $\psi = \psi(x, y)$  satisfies differential equations (2.5.9) is called a **complex potential**. If we recall that the values of the functions  $\varphi(x, y)$  or  $\psi(x, y)$  allow one to determine the velocity field in a moving fluid unambiguously, then, consequently, any two-dimensional flow can be set by a complex potential. Hence, the problem on calculating such a flow can be reduced to finding the function  $W(\sigma)$ . Let us calculate the derivative of the function  $W(\sigma)$  with respect to the complex variable  $\sigma$ :

$$dW/d\sigma = \partial\varphi/\partial x + i\partial\psi/\partial x \quad (2.8.2)$$

Since  $\partial\varphi/\partial x = V_x$ ,  $\partial\psi/\partial x = -V_y$ , then

$$dW/d\sigma = V_x - iV_y \quad (2.8.3)$$

This expression is called the **complex velocity**. Its magnitude gives the value of the velocity itself,  $|dW/d\sigma| = \sqrt{V_x^2 + V_y^2} = V$ . It is evident that the real velocity vector  $\mathbf{V} = V_x + iV_y$  is the mirror image relative to the  $x$ -axis of the vector of the complex velocity. Let us denote by  $\theta$  the angle between the vector  $dW/d\sigma$  and the  $x$ -axis and determine the velocities  $V_x = V \cos \theta$  and  $V_y = V \sin \theta$ . Using the Euler formula

$$\cos \theta - i \sin \theta = e^{-i\theta}$$

we obtain

$$dW/d\sigma = Ve^{-i\theta} \quad (2.8.4)$$

## 2.9. Kinds of Fluid Flows

Let us consider the characteristic kinds of flows of an incompressible fluid, their geometric configuration (aerodynamic spectrum), expressions for the complex potentials, and also the relevant potential functions and stream functions.

**Parallel Flow**

Assume that the flow of a fluid is given by the complex potential

$$W(\sigma) = V(\cos \theta - i \sin \theta) \sigma \quad (2.9.1)$$

where  $V$  and  $\theta$  are constants for the given conditions.

According to (2.8.1)

$$\varphi + i\psi = V(\cos \theta - i \sin \theta)(x + iy)$$

whence we find the velocity potential and the stream function:

$$\varphi = V(x \cos \theta + y \sin \theta) \quad (2.9.2)$$

$$\psi = V(y \cos \theta - x \sin \theta) \quad (2.9.3)$$

Examination of the expressions for  $\varphi$  or  $\psi$  reveals that the flow being considered is plane and steady because they do not contain the time explicitly. In such a flow, the streamlines and pathlines coincide.

From (2.9.2), we can find the components of the flow velocity:

$$\partial\varphi/\partial x = V_x = V \cos \theta, \quad \partial\varphi/\partial y = V_y = V \sin \theta, \quad \partial\varphi/\partial z = V_z = 0 \quad (2.9.4)$$

Here  $V$  is the resultant velocity of the flow, and  $\theta$  is the angle between its direction and the  $x$ -axis. Assuming the stream function  $\psi$  in (2.9.3) to be constant and including  $V$  in it, we obtain the equation

$$y \cos \theta - x \sin \theta = \text{const} \quad (2.9.5)$$

A glance at this equation shows that the streamlines are parallel straight lines inclined to the  $x$ -axis at the angle  $\theta$  (Fig. 2.9.1). Since the velocity components  $V_x$  and  $V_y$  are positive, the flow will be directed as shown in Fig. 2.9.1. This flow is called a **forward plane-parallel one**.

In the particular case when the flow is parallel to the  $x$ -axis ( $\theta = 0$ ,  $V_x = V$ ,  $V_y = 0$ ), the complex potential is

$$W(\sigma) = V\sigma \quad (2.9.6)$$

**Two-Dimensional Point Source and Sink**

Let us consider the complex potential

$$W(\sigma) = (q/2\pi) \ln \sigma \quad (2.9.7)$$

where  $q$  is a constant. We can write this equation in the form

$$\varphi + i\psi = (q/2\pi) \ln (re^{i\theta}) = (q/2\pi) (\ln r + i\theta)$$

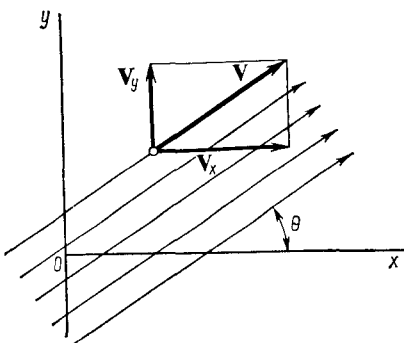


**Fig. 2.9.1**  
General view of a forward plane-parallel flow

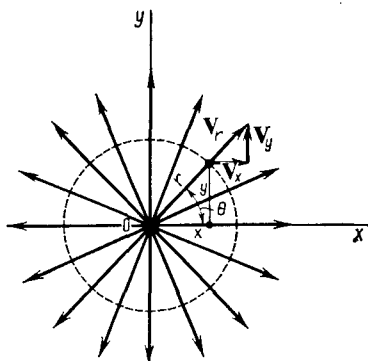


**Fig. 2.9.2**  
A two-dimensional point source

where  $r$  is the distance to a point with the coordinates  $x$  and  $y$  (the polar radius), and  $\theta$  is the polar angle.

It follows from the obtained equation that

$$\varphi = (q/2\pi) \ln r = (q/2\pi) \ln \sqrt{x^2 + y^2} \quad (2.9.8)$$

$$\psi = (q/2\pi) \theta \quad (2.9.9)$$

We find from (2.9.8) that the radial velocity component (in the direction of the radius  $r$ ) is

$$\frac{\partial \varphi}{\partial r} = V_r = q/(2\pi r) \quad (2.9.10)$$

and the component along a normal to this radius is  $V_s = 0$ .

We thus obtain a flow whose streamlines (pathlines) are a family of straight lines passing through the origin of coordinates (this also follows from the equation of a streamline  $\psi = \text{const}$ ). Such a radial flow issuing from the origin of coordinates is called a **two-dimensional point source** (Fig. 2.9.2).

The rate of flow of a fluid through a contour of radius  $r$  is  $2\pi r V_r = Q$ . Introducing into this equation the value of  $V_r$  from (2.9.10),

we find  $Q = q$ . The constant  $q$  is thus determined by the rate of flow of the fluid from the source. This quantity  $q$  is known as the **intensity or strength of the source**.

In addition to a source, there is a kind of motion of a fluid called a **two-dimensional point sink**. The complex potential of a sink is

$$W(\sigma) = -(q/2\pi) \ln \sigma \quad (2.9.11)$$

The minus sign indicates that unlike a source, motion occurs toward the centre. A sink, like a source, is characterized by its intensity, or strength,  $q$  (the rate of flow).

### Three-Dimensional Source and Sink

In addition to two-dimensional ones, there also exist **three-dimensional point sources (sinks)**. The flux from them is set by the following conditions:

$$V_x = \frac{q}{4\pi} \cdot \frac{\pm x}{R^3}; \quad V_y = \frac{q}{4\pi} \cdot \frac{\pm y}{R^3}; \quad V_z = \frac{q}{4\pi} \cdot \frac{\pm z}{R^3} \quad (2.9.12)$$

where  $R = \sqrt{x^2 + y^2 + z^2}$  and  $q$  is the strength of the source (plus sign) or sink (minus sign). The strength of a source (sink) equals the quantity  $q$  defined as the flow rate (per second) through the surface of a sphere of radius  $R$ . The resultant velocity is

$$V = \sqrt{V_x^2 + V_y^2 + V_z^2} = \pm q/(4\pi R^2) \quad (2.9.13)$$

and coincides with the direction of the position vector  $\mathbf{R}$ . Consequently, the velocity potential depends only on  $R$  and, therefore,

$$\partial\phi/\partial R = \pm q/(4\pi R^2)$$

Integration yields

$$\phi = \mp q/(4\pi R) \quad (2.9.14)$$

where the minus sign relates to a source, and the plus sign to a sink.

### Doublet

Let us consider a flow whose complex potential is

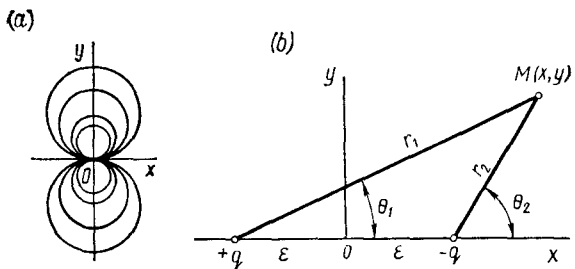
$$W(\sigma) = (M/2\pi) (1/\sigma) \quad (2.9.15)$$

where  $M$  is a constant. In accordance with this equation, we have

$$\varphi + i\psi = (M/2\pi) (1/re^{i\theta})$$

Let us transform the right-hand side of this equation. Taking into account that

$$\frac{1}{re^{i\theta}} = \frac{1}{r(\cos\theta + i\sin\theta)} = \frac{1}{r} (\cos\theta - i\sin\theta)$$

**Fig. 2.9.3**

To the definition of a doublet:

a—doublet streamlines; b—formation of a doublet

we obtain

$$\varphi + i\psi = (M/2\pi r) (\cos \theta - i \sin \theta)$$

Hence

$$\varphi = (M/2\pi) \cos \theta/r \quad (2.9.16)$$

$$\psi = -(M/2\pi) \sin \theta/r \quad (2.9.17)$$

Assuming that  $\psi = \text{const}$  and having in view that  $r = \sqrt{x^2 + y^2}$  and  $\sin \theta = y/r = y/\sqrt{x^2 + y^2}$ , we obtain an equation for a family of streamlines of the flow being considered:

$$y(x^2 + y^2) = \text{const} \quad (2.9.18)$$

The family of streamlines is an infinite set of circles passing through the origin of coordinates and having centres on the  $y$ -axis (Fig. 2.9.3a).

To comprehend the physical essence of this flow, let us consider the flow that is obtained by summation of the flows produced by a source and a sink of the same strength located on the  $x$ -axis at a small distance  $\epsilon$  from the origin of coordinates (Fig. 2.9.3b). For point  $M(x, y)$ , the velocity potential due to a source at the distance of  $r_1$  is  $\varphi_s = (q/2\pi) \ln r_1$  and due to a sink at a distance of  $r_2$  from this point is  $\varphi_{sk} = (-q/2\pi) \ln r_2$ .

To determine the resultant flow produced by the source and the sink, let us use the method of superposition of incompressible flows. According to this method, the velocity potential of the resultant flow is  $\varphi = \varphi_s + \varphi_{sk}$ . Indeed, owing to the continuity equation (the Laplace equation) obtained from (2.4.8'), we have

$$\frac{\partial^2 \varphi}{\partial x^2} + \frac{\partial^2 \varphi}{\partial y^2} = \frac{\partial^2 (\varphi_s + \varphi_{sk})}{\partial x^2} + \frac{\partial^2 (\varphi_s + \varphi_{sk})}{\partial y^2} = 0$$

Since the functions  $\varphi_s$  and  $\varphi_{sk}$  satisfy the equations

$$\partial^2 \varphi_s / \partial x^2 + \partial^2 \varphi_s / \partial y^2 = 0 \text{ and } \partial^2 \varphi_{sk} / \partial x^2 + \partial^2 \varphi_{sk} / \partial y^2 = 0$$

then  $\partial^2\varphi/\partial x^2 + \partial^2\varphi/\partial y^2$  identically equals zero. Consequently, the resultant function  $\varphi$  satisfies the continuity equation. The resultant potential from the source and the sink is

$$\varphi = (q/2\pi) \ln (r_1/r_2)$$

Since  $r_1 = \sqrt{(x+\varepsilon)^2 + y^2}$ ,  $r_2 = \sqrt{(x-\varepsilon)^2 + y^2}$ , then

$$\ln \frac{r_1}{r_2} = \frac{1}{2} \ln \frac{(x+\varepsilon)^2 + y^2}{(x-\varepsilon)^2 + y^2}, \text{ or } \ln \frac{r_1}{r_2} = \frac{1}{2} \ln \left[ 1 + \frac{4x\varepsilon}{(x-\varepsilon)^2 + y^2} \right].$$

The value of  $\varepsilon$  can be chosen so that the second term in the brackets will be small in comparison with unity. Using the formula for expansion of a logarithm into a series and disregarding the small terms of the second and higher orders, we obtain

$$\varphi = \frac{q}{\pi} \cdot \frac{x\varepsilon}{(x-\varepsilon)^2 + y^2} \quad (2.9.19)$$

Assume that the source and sink approach each other ( $\varepsilon \rightarrow 0$ ) and simultaneously their strengths increase so that the product  $q\varepsilon$  at the limit upon coincidence of the source and sink tends to a finite value  $M$ . The complicated flow formed is called a **doublet**, the quantity  $M$  characterizing this flow is called the **moment of the doublet** and the  $x$ -axis—the **axis of the doublet**. Going over to the limit in (2.9.19) for  $\varphi$  at  $\varepsilon \rightarrow 0$  and  $2q\varepsilon \rightarrow M$ , we obtain the following expression for a doublet

$$\varphi = \frac{M}{2\pi} \cdot \frac{x}{x^2 + y^2} = \frac{M}{2\pi} \cdot \frac{\cos \theta}{r}$$

It coincides with (2.9.16).

Hence, the flow being considered, characterized by the complex potential (2.9.15), is a doublet. This can also be shown if we consider the stream function of such a combined flow that will coincide with (2.9.17).

Differentiation of (2.9.16) yields the doublet velocity components:

$$\frac{\partial \varphi}{\partial r} = V_r = -\frac{M}{2\pi} \cdot \frac{\cos \theta}{r^2}, \quad \frac{1}{r} \cdot \frac{\partial \varphi}{\partial \theta} = V_s = -\frac{M}{2\pi} \cdot \frac{\sin \theta}{r^2} \quad (2.9.20)$$

Let us consider the three-dimensional case. For a flow produced by a source and a sink of the identical strength  $q$  located along the axis  $Ox$  at a small distance  $\varepsilon$  from the origin of coordinates, the potential function in accordance with (2.9.14) is

$$\varphi = \frac{q}{4\pi} \left( \frac{1}{R_2} - \frac{1}{R_1} \right) = \frac{q}{4\pi} \left[ \frac{1}{\sqrt{(x-\varepsilon)^2 + r^2}} - \frac{1}{\sqrt{(x+\varepsilon)^2 + r^2}} \right] \quad (2.9.20')$$

where  $r^2 = y^2 + z^2$ .

For small values of  $\varepsilon$ , we have

$$\varphi = (q/4\pi) 2x\varepsilon/(x^2 + r^2)^{3/2}$$

Hence in a limit process with  $\varepsilon \rightarrow 0$ , considering that the product  $q2\varepsilon$  tends to the finite limit  $M$ , we obtain for the flow produced by a doublet with the moment  $M$  the velocity potential

$$\varphi = (M/4\pi) x/(x^2 + r^2)^{3/2} \quad (2.9.21)$$

or

$$\varphi = -\frac{M}{4\pi} \cdot \frac{\partial}{\partial r} \left( \frac{1}{R} \right) \quad (2.9.21')$$

where  $R = (x^2 + r^2)^{1/2}$ .

### Circulation Flow (Vortex)

Let us consider a flow set by the complex potential

$$W(\sigma) = -ai \ln \sigma \quad (2.9.22)$$

where  $a$  is a constant. We can write this equation in the form

$$\varphi + i\psi = -ai \ln (re^{i\theta}) = a(\theta - i \ln r)$$

Hence

$$\varphi = a\theta \quad (2.9.23)$$

$$\psi = -a \ln r \quad (2.9.24)$$

It follows from (2.9.23) that the radial velocity component  $V_r = \partial\varphi/\partial r = 0$ , while the component  $V_s$  normal to the radius equals the derivative of  $\varphi$  with respect to the arc  $s$  of a streamline, i.e.

$$\partial\varphi/\partial s = (1/r) \partial\varphi/\partial\theta = V_s = a/r \quad (2.9.25)$$

We obtain the equation of streamlines (pathlines) from the condition  $\psi = \text{const}$ , from which in accordance with (2.9.24) we find the equation  $r = \text{const}$ . This equation represents a family of streamlines in the form of concentric circles. Flow along them is positive if it occurs counterclockwise (from the  $x$ -axis to the  $y$ -axis); in this case the coefficient  $a$  in (2.9.25) has the sign plus.

A flow in which the particles move (circulate) along concentric circles is said to be a **circulation flow** (Fig. 2.9.4).

The circulation of the velocity in the flow being considered is  $\Gamma = 2\pi r \partial\varphi/\partial s$ . Since  $\partial\varphi/\partial s = a/r$ , we have  $\Gamma = 2\pi a$ , whence  $a = \Gamma/(2\pi)$ . Hence, the physical meaning of the constant  $a$  is that its value is determined by the circulation of the flow which, as we have already established, equals the vorticity in turn. The flow produced by a vortex located at the origin of coordinates where  $V_s = a/r \rightarrow \infty$  is also called a **two-dimensional vortex source** or a **vortex**.

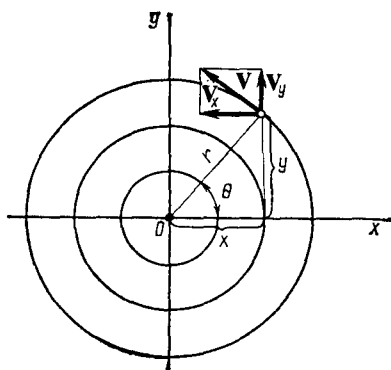


**Fig. 2.9.4**  
A circulation flow (point vortex)

We have treated the simplest cases of flow for which we have exactly determined the velocity potentials and stream functions. By combining these flows, we can, in definite conditions, obtain more complicated potential flows equivalent to the ones that appear over bodies of a given configuration.

Let us take as an example a flow formed by the superposition of a plane-parallel flow moving in the direction of the  $x$ -axis onto the flow due to a doublet. The complex potential of the resultant two-dimensional incompressible flow is obviously

$$W(\sigma) = W_1(\sigma) + W_2(\sigma) = V\sigma + (M/2\pi)(1/\sigma) \quad (2.9.26)$$

In accordance with this expression

$$\varphi + i\psi = V(x + iy) + (M/2\pi)/(x + iy) \quad (2.9.27)$$

whence

$$\begin{aligned} \varphi &= Vx + (M/2\pi)x/(x^2 + y^2), \\ \psi &= Vy - (M/2\pi)y/(x^2 + y^2) \end{aligned} \quad (2.9.28)$$

To find the family of streamlines, we equate the stream function to a constant:

$$C = Vy - (M/2\pi)y/(x^2 + y^2) \quad (2.9.29)$$

According to this equation, the streamlines are cubic curves. A value of the constant of  $C = 0$  corresponds to one of the streamlines. By Eq. (2.9.29), we obtain two equations for such a zero streamline:

$$y = 0, \quad x^2 + y^2 = M/(2\pi V) \quad (2.9.30)$$

Hence, the obtained streamline is either a horizontal axis or a circle of radius  $r_0 = [M/(2\pi V)]^{1/2}$  with its centre at the origin of coordinates. Assuming that the velocity  $V = 1$ , and the doublet moment  $M = 2\pi$ , we obtain a streamline in the form of a circle

with a unit radius. If we assume that this circle is a solid boundary surface, we can consider an incompressible flow near this surface as one flowing in a lateral direction over a cylinder of infinite length with a unit radius. The velocity potential of such an incompressible disturbed flow is determined by the first of Eqs. (2.9.28) having the form

$$\varphi = x [1 + 1/(x^2 + y^2)] \quad (2.9.31)$$

Introducing the polar coordinates  $\theta$  and  $r = x/\cos \theta = (x^2 + y^2)^{1/2}$ , we obtain

$$\varphi = r (1 + 1/r^2) \cos \theta \quad (2.9.31')$$

Differentiation yields the components of the velocity at a point on an arbitrary streamline along the directions of the radius  $r$  and of a normal  $s$  to it:

$$\begin{aligned} V_r &= \partial\varphi/\partial r = (1 - 1/r^2) \cos \theta, \\ V_s &= (1/r) \partial\varphi/\partial\theta = -(1 + 1/r^2) \sin \theta \end{aligned} \quad (2.9.32)$$

On a cylindrical surface in a flow (a zero streamline) for which  $r = 1$ , we find  $V_r = 0$  and  $V_s = -2 \sin \theta$ . The above example illustrates the application of the principle of flow superposition and the concept of a complex potential to the solution of a very simple problem on the flow of an incompressible fluid over a body.

## Fundamentals of Fluid Dynamics

### 3.1. Equations of Motion of a Viscous Fluid

The fundamental equations of aerodynamics include equations of motion forming its theoretical foundation. They relate quantities determining motion such as the velocity, normal, and shear stresses. The solution of the equations of motion allows one to determine these unknown quantities.

Let us consider the various kinds of equations of motion used in studying gas flows.

#### Cartesian Coordinates

We shall treat the motion of a fluid particle having the shape of an elementary parallelepiped with the dimensions  $dx$ ,  $dy$ , and  $dz$  constructed near point  $A$  with the coordinates  $x$ ,  $y$ , and  $z$ . Let the velocity components at this point be  $V_x$ ,  $V_y$ , and  $V_z$ . A fluid particle of mass  $\rho\tau$  (here  $\tau = dx dy dz$  is the elementary volume) moves under the action of the mass (body) and surface forces. We shall denote the projections of the mass force by  $X\rho\tau$ ,  $Y\rho\tau$ , and  $Z\rho\tau$ , and those of the surface force by  $P_x\tau$ ,  $P_y\tau$ , and  $P_z\tau$ . The quantities  $P_x$ ,  $P_y$ , and  $P_z$  are the projections of the surface force vector related to unit volume.

The equation of particle motion in the projection onto the  $x$ -axis has the form

$$\rho\tau dV_x/dt = X\rho\tau + P_x\tau$$

whence

$$dV_x/dt = X + (1/\rho) P_x \quad (3.1.1)$$

where  $dV_x/dt$  is the total acceleration in the direction of the  $x$ -axis.

We obtain similar equations in projections onto the  $y$ - and  $z$ -axes:

$$dV_y/dt = Y + (1/\rho) P_y \quad (3.1.2)$$

$$dV_z/dt = Z + (1/\rho) P_z \quad (3.1.3)$$

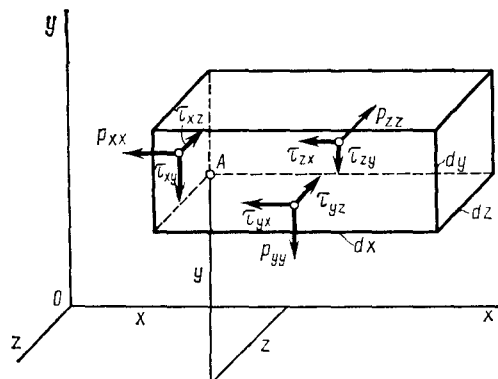


**Fig. 3.1.1**  
Surface forces acting on a fluid particle

The surface force can be expressed in terms of the stresses acting on the faces of an elementary parallelepiped. The difference in the surface forces in comparison with an ideal (inviscid) flow consists in that not only normal, but also shear stresses act on the faces of a particle.

Every surface force acting on a face has three projections onto the coordinate axes (Fig. 3.1.1). A unit of surface area of the left-hand face experiences a surface force whose projections will be designated by  $p_{xx}$ ,  $\tau_{xz}$ , and  $\tau_{xy}$ . The quantity  $p_{xx}$  is the normal stress, while  $\tau_{xz}$  and  $\tau_{xy}$  are the shear stresses. It can be seen that the first subscript indicates the axis perpendicular to the face being considered, and the second one indicates the axis onto which the given stress is projected. The rear face perpendicular to the  $z$ -axis experiences the stress components  $p_{zz}$ ,  $\tau_{zx}$ , and  $\tau_{zy}$ ; the bottom face perpendicular to the  $y$ -axis experiences the components  $p_{yy}$ ,  $\tau_{yx}$ , and  $\tau_{yz}$ .

We shall consider normal stresses to be positive if they are directed out of the element being studied and, consequently, subject it to omnidirectional tension as shown in Fig. 3.1.1. Positive shear stresses are present if for the three faces intersecting at initial point  $A$  these stresses are oriented along directions opposite to the positive directions of the coordinate axes, and for the other three faces—in the positive direction of these axes. With this in view, let us consider the projections of the surface forces onto the  $x$ -axis. The left-hand face experiences the force due to the normal stress  $-p_{xx} dy dz$ , and the right-hand one—the force  $[p_{xx} + (\partial p_{xx}/\partial x) dx] dy dz$ . The resultant of these forces is therefore  $(\partial p_{xx}/\partial x) dx dy dz$ . The components of the forces produced by the shear stresses acting on these faces are zero.

Account must be taken, however, of the shear stresses  $\tau_{zx}$  and  $\tau_{yx}$ . The rear face experiences the force  $-\tau_{zx} dx dy$ , and the front one—the force  $[\tau_{zx} + (\partial \tau_{zx}/\partial z) dz] dx dy$ . The resultant of these forces is  $(\partial \tau_{zx}/\partial z) dx dy dz$ . In a similar way, we find the resultant of the forces acting on the bottom and top faces. It is  $(\partial \tau_{yx}/\partial y) dx dy dz$ .

Hence, the projection onto the  $x$ -axis of the surface force related to unit volume is

$$P_x = \partial p_{xx}/\partial x + \partial \tau_{yx}/\partial y + \partial \tau_{zx}/\partial z \quad (3.1.4)$$

Similarly, the projections onto the other coordinate axes of the surface force related to unit volume are

$$\left. \begin{aligned} P_y &= \partial \tau_{xy}/\partial x + \partial p_{yy}/\partial y + \partial \tau_{zy}/\partial z \\ P_z &= \partial \tau_{xz}/\partial x + \partial \tau_{yz}/\partial y + \partial p_{zz}/\partial z \end{aligned} \right\} \quad (3.1.4')$$

According to the property of reciprocity of shear stresses, the values of these stresses acting along orthogonal faces equal each other, i. e.  $\tau_{zx} = \tau_{xz}$ ,  $\tau_{zy} = \tau_{yz}$ , and  $\tau_{yx} = \tau_{xy}$ .

Hence, of six shear stresses, three are independent.

To determine the values of the shear stresses, we shall use the hypothesis that stresses are proportional to the strains they produce. The application of this hypothesis is illustrated by Newton's formula for the shear stress appearing in the motion of a viscous fluid relative to a solid wall. By this formula,  $\tau_{yx} = \mu (\partial V_y/\partial x)$ , i.e. the stress is proportional to the half-speed  $\varepsilon_z = 0.5 (\partial V_y/\partial x)$  of angle distortion in the direction of the  $z$ -axis, whence  $\tau_{yx} = 2\mu \varepsilon_z$  (here  $\mu$  is the dynamic viscosity). This relation covers the general case of three-dimensional motion when the angular deformation in the direction of the  $z$ -axis is determined by the half-speed of distortion  $\varepsilon_z = 0.5 (\partial V_y/\partial x + \partial V_x/\partial y)$ . We shall write the other two values of the shear stress in the form  $\tau_{yz} = 2\mu \varepsilon_x$  and  $\tau_{zx} = 2\mu \varepsilon_y$ .

Consequently,

$$\left. \begin{aligned} \tau_{yx} &= 2\mu \varepsilon_z = \mu (\partial V_y/\partial x + \partial V_x/\partial y) \\ \tau_{yz} &= 2\mu \varepsilon_x = \mu (\partial V_y/\partial z + \partial V_z/\partial y) \\ \tau_{zx} &= 2\mu \varepsilon_y = \mu (\partial V_z/\partial x + \partial V_x/\partial z) \end{aligned} \right\} \quad (3.1.5)$$

We shall use the above-mentioned proportionality hypothesis to establish relations for the normal stresses  $p_{xx}$ ,  $p_{yy}$ , and  $p_{zz}$ . Under the action of the stress  $p_{xx}$ , a fluid particle experiences linear strain or deformation in the direction of the  $x$ -axis. If the relative linear deformation is  $\bar{\theta}'_x$ , then  $p_{xx} = E \bar{\theta}'_x$ , where  $E$  is a proportionality factor or the **modulus of longitudinal elasticity of the fluid**. The normal stresses  $p_{yy}$  and  $p_{zz}$  cause the particle to deform also in the directions of the  $y$ - and  $z$ -axes, which diminishes the deformation in the direction of the  $x$ -axis.

It is known from the course in the strength of materials that the decrease in the relative magnitude  $\Delta\bar{\theta}_x$  of this deformation for elastic bodies is proportional to the sum of the relative deformations in the directions of  $y$  and  $z$  under the action of the indicated stresses. Accordingly,

$$\Delta\bar{\theta}_x = -(1/m) (p_{yy}/E + p_{zz}/E)$$

where  $m$  is a constant known as the **coefficient of lateral linear deformation**.

The total relative deformation in the direction of the  $x$ -axis is

$$\bar{\theta}_x = \bar{\theta}'_x + \Delta\bar{\theta}_x = p_{xx}/E - (1/m) (p_{yy}/E + p_{zz}/E) \quad (3.1.6)$$

We can calculate the relative deformations  $\bar{\theta}_y$  and  $\bar{\theta}_z$  along the  $y$ - and  $z$ -axes in a similar way. The obtained expressions give us the normal stresses:

$$\left. \begin{aligned} p_{xx} &= E\bar{\theta}_x + (p_{yy} + p_{zz})/m \\ p_{yy} &= E\bar{\theta}_y + (p_{zz} + p_{xx})/m \\ p_{zz} &= E\bar{\theta}_z + (p_{xx} + p_{yy})/m \end{aligned} \right\} \quad (3.1.7)$$

The relative linear deformations of a particle along the directions of the coordinate axes determine its relative volume deformation. Designating the magnitude of this deformation by  $\bar{\theta}$ , we obtain

$$\bar{\theta} = \bar{\theta}_x + \bar{\theta}_y + \bar{\theta}_z \quad (3.1.8)$$

Summating Eqs. (3.1.7) and taking into account the expression for  $\bar{\theta}$ , we have

$$p_{xx} + p_{yy} + p_{zz} = mE\bar{\theta}/(m - 2) \quad (3.1.9)$$

Determining the sum  $p_{yy} + p_{zz}$  from this expression and introducing it into (3.1.6), we find

$$p_{xx} = \frac{m}{m+1} E\bar{\theta}_x + \frac{m}{m+1} \cdot \frac{E}{m-2} \bar{\theta} \quad (3.1.10)$$

For our following transformations, we shall use the known relation between the shear modulus  $G$ , the modulus of longitudinal elasticity  $E$ , and the coefficient of lateral deformation  $m$  that is valid for elastic media including a compressible fluid:

$$G = mE/[2(m + 1)] \quad (3.1.11)$$

Substituting this relation into (3.1.10), we obtain

$$p_{xx} = 2G\bar{\theta}_x + \frac{2G}{m-2} \bar{\theta} \quad (3.1.12)$$

Let us introduce the symbol

$$\bar{\sigma} = (p_{xx} + p_{yy} + p_{zz})/3 \quad (3.1.13)$$

Adding and subtracting  $\bar{\sigma}$  on the right-hand side of (3.1.12), we have

$$p_{xx} = \bar{\sigma} + 2G\bar{\theta}_x + \frac{2G}{m-2}\bar{\theta} - (p_{xx} + p_{yy} + p_{zz})/3$$

Transformations involving Eqs. (3.1.9) and (3.1.11) yield

$$p_{xx} = \bar{\sigma} + G(2\bar{\theta}_x - 2\bar{\theta}/3) \quad (3.1.14)$$

Similarly,

$$p_{yy} = \bar{\sigma} + G(2\bar{\theta}_y - 2\bar{\theta}/3); \quad p_{zz} = \bar{\sigma} + G(2\bar{\theta}_z - 2\bar{\theta}/3) \quad (3.1.14')$$

It has been established for an inviscid fluid that the pressure  $p$  at any point of the flow is identical for all the areas including this point, i.e. with a view to the adopted notation, in the case being considered we have  $p_{xx} = p_{yy} = p_{zz} = -p$ ; consequently,  $p = -(p_{xx} + p_{yy} + p_{zz})/3$ .

Hence, when studying the motion of a viscous fluid, the pressure can be determined as the arithmetical mean, taken with the minus sign, of the three normal stresses corresponding to three mutually perpendicular areas. Accordingly,  $\bar{\sigma} = -p$ .

The theory of elasticity establishes the following relations for the shear stresses acting in a solid body:

$$\tau_{yx} = G\gamma_{yx}, \quad \tau_{yz} = G\gamma_{yz}, \quad \tau_{zx} = G\gamma_{zx} \quad (3.1.15)$$

where  $\gamma_{yx}$ ,  $\gamma_{yz}$ , and  $\gamma_{zx}$  are the angles of shear in the directions of the axes  $z$ ,  $x$ , and  $y$ , respectively.

A comparison of formulas (3.1.15) with the corresponding relations (3.1.5) for a viscous fluid reveals that these formulas can be obtained from one another if the shear modulus  $G$  is replaced by the dynamic viscosity  $\mu$ , and the angles of shear  $\gamma$  by the relevant values of the speeds of distortion  $\varepsilon$  of the angles. In accordance with this analogy, when substituting  $\mu$  for  $G$  in formulas (3.1.14) and (3.1.14'), the strains (relative elongations)  $\bar{\theta}_x$ ,  $\bar{\theta}_y$ , and  $\bar{\theta}_z$  have to be replaced with the relevant values of the rates of strain  $\theta_x = \partial V_x / \partial x$ ,  $\theta_y = \partial V_y / \partial y$ ,  $\theta_z = \partial V_z / \partial z$ , and the volume strain  $\bar{\theta}$  by the rate of the volume strain  $\theta = \partial V_x / \partial x + \partial V_y / \partial y + \partial V_z / \partial z = \operatorname{div} \mathbf{V}$ .

The relevant substitutions in (3.1.14) and (3.1.14') yield:

$$\left. \begin{aligned} p_{xx} &= -p + \mu \left( 2 \frac{\partial V_x}{\partial x} - \frac{2}{3} \operatorname{div} \mathbf{V} \right) \\ p_{yy} &= -p + \mu \left( 2 \frac{\partial V_y}{\partial y} - \frac{2}{3} \operatorname{div} \mathbf{V} \right) \\ p_{zz} &= -p + \mu \left( 2 \frac{\partial V_z}{\partial z} - \frac{2}{3} \operatorname{div} \mathbf{V} \right) \end{aligned} \right\} \quad (3.1.16)$$

The second terms on the right-hand sides of expressions (3.1.16) determine the additional stresses due to viscosity.

By using relations (3.1.4), (3.1.4'), (3.1.5), and (3.1.16), we can evaluate the quantities  $P_x$ ,  $P_y$ , and  $P_z$ . For example, for  $P_x$  from (3.1.4) we obtain

$$\begin{aligned} P_x = & -\frac{\partial p}{\partial x} + \frac{\partial}{\partial x} \left[ \mu \left( 2 \frac{\partial V_x}{\partial x} - \frac{2}{3} \operatorname{div} \mathbf{V} \right) \right] + \frac{\partial}{\partial y} \left[ \mu \left( \frac{\partial V_y}{\partial x} + \frac{\partial V_x}{\partial y} \right) \right] \\ & + \frac{\partial}{\partial z} \left[ \mu \left( \frac{\partial V_z}{\partial x} + \frac{\partial V_x}{\partial z} \right) \right] = -\frac{\partial p}{\partial x} + \mu \Delta V_x + \frac{\mu}{3} \frac{\partial}{\partial x} \operatorname{div} \mathbf{V} \\ & + \frac{\partial \mu}{\partial x} \left( 2 \frac{\partial V_x}{\partial x} - \frac{2}{3} \operatorname{div} \mathbf{V} \right) + \frac{\partial \mu}{\partial y} \left( \frac{\partial V_x}{\partial y} + \frac{\partial V_y}{\partial x} \right) + \frac{\partial \mu}{\partial z} \left( \frac{\partial V_x}{\partial z} + \frac{\partial V_z}{\partial x} \right) \end{aligned}$$

where  $\Delta$  is the Laplacian operator:

$$\Delta = \partial^2/\partial x^2 + \partial^2/\partial y^2 + \partial^2/\partial z^2$$

Particularly,

$$\Delta V_x = \partial^2 V_x / \partial x^2 + \partial^2 V_x / \partial y^2 + \partial^2 V_x / \partial z^2$$

In a similar way, we can find the expressions for  $P_y$  and  $P_z$ .

The relations for the stresses due to the surface forces in a fluid have been obtained here by generalizing the laws relating stresses and strains in solids for a fluid having the property of elasticity and viscosity. We shall obtain the same relations proceeding from a number of hypothetic notions on the molecular forces acting in a fluid (see [9, 11]).

By compiling projections of the total acceleration in an expanded form according to the rule of calculating the derivative of a composite function  $f(x, y, z, t)$  in which, in turn,  $x$ ,  $y$ , and  $z$  are functions of the time  $t$ , and taking into consideration the expressions found for  $P_x$ ,  $P_y$ , and  $P_z$ , we can obtain the equations of motion (3.1.1)-(3.1.3) in the following form:

$$\left. \begin{aligned} \frac{\partial V_x}{\partial t} + V_x \frac{\partial V_x}{\partial x} + V_y \frac{\partial V_x}{\partial y} + V_z \frac{\partial V_x}{\partial z} &= X - \frac{1}{\rho} \cdot \frac{\partial p}{\partial x} \\ + v \Delta V_x + \frac{v}{3} \cdot \frac{\partial}{\partial x} \operatorname{div} \mathbf{V} + \frac{1}{\rho} \left[ \frac{\partial \mu}{\partial x} \left( 2 \frac{\partial V_x}{\partial x} - \frac{2}{3} \operatorname{div} \mathbf{V} \right) \right. \\ \left. + \frac{\partial \mu}{\partial y} \left( \frac{\partial V_x}{\partial y} + \frac{\partial V_y}{\partial x} \right) + \frac{\partial \mu}{\partial z} \left( \frac{\partial V_x}{\partial z} + \frac{\partial V_z}{\partial x} \right) \right] \\ \frac{\partial V_y}{\partial t} + V_x \frac{\partial V_y}{\partial x} + V_y \frac{\partial V_y}{\partial y} + V_z \frac{\partial V_y}{\partial z} &= Y - \frac{1}{\rho} \cdot \frac{\partial p}{\partial y} \\ + v \Delta V_y + \frac{v}{3} \cdot \frac{\partial}{\partial y} \operatorname{div} \mathbf{V} + \frac{1}{\rho} \left[ \frac{\partial \mu}{\partial y} \left( 2 \frac{\partial V_y}{\partial y} - \frac{2}{3} \operatorname{div} \mathbf{V} \right) \right. \\ \left. + \frac{\partial \mu}{\partial z} \left( \frac{\partial V_y}{\partial z} + \frac{\partial V_z}{\partial y} \right) + \frac{\partial \mu}{\partial x} \left( \frac{\partial V_y}{\partial x} + \frac{\partial V_x}{\partial y} \right) \right] \end{aligned} \right\} \quad (3.1.17)$$

$$\left. \begin{aligned} \frac{\partial V_z}{\partial t} + V_x \frac{\partial V_z}{\partial x} + V_y \frac{\partial V_z}{\partial y} + V_z \frac{\partial V_z}{\partial z} &= Z - \frac{1}{\rho} \cdot \frac{\partial p}{\partial z} \\ + v \Delta V_z + \frac{v}{3} \cdot \frac{\partial}{\partial z} \operatorname{div} \mathbf{V} + \frac{1}{\rho} \left[ \frac{\partial \mu}{\partial z} \left( 2 \frac{\partial V_z}{\partial z} - \frac{2}{3} \operatorname{div} \mathbf{V} \right) \right. \\ \left. + \frac{\partial \mu}{\partial x} \left( \frac{\partial V_z}{\partial x} + \frac{\partial V_x}{\partial z} \right) + \frac{\partial \mu}{\partial y} \left( \frac{\partial V_z}{\partial y} + \frac{\partial V_y}{\partial z} \right) \right] \end{aligned} \right\}$$

where  $v = \mu/\rho$  is the kinematic viscosity.

The differential equations (3.1.17) form the theoretical foundation of the gas dynamics of a viscous compressible fluid and are known as the **Navier-Stokes equations**. It is assumed in the equations that the dynamic viscosity  $\mu$  is a function of the coordinates  $x$ ,  $y$ , and  $z$ , i.e.  $\mu = f(x, y, z)$ . Presuming that  $\mu = \text{const}$ , the Navier-Stokes equations acquire the following form:

$$\left. \begin{aligned} \frac{dV_x}{dt} &= X - \frac{1}{\rho} \cdot \frac{\partial p}{\partial x} + v \Delta V_x + \frac{v}{3} \cdot \frac{\partial}{\partial x} \operatorname{div} \mathbf{V} \\ \frac{dV_y}{dt} &= Y - \frac{1}{\rho} \cdot \frac{\partial p}{\partial y} + v \Delta V_y + \frac{v}{3} \cdot \frac{\partial}{\partial y} \operatorname{div} \mathbf{V} \\ \frac{dV_z}{dt} &= Z - \frac{1}{\rho} \cdot \frac{\partial p}{\partial z} + v \Delta V_z + \frac{v}{3} \cdot \frac{\partial}{\partial z} \operatorname{div} \mathbf{V} \end{aligned} \right\} \quad (3.1.18)$$

When studying gas flows, the mass forces may be left out of account, and, therefore, we assume that  $X = Y = Z = 0$ . In this case, we have

$$\left. \begin{aligned} \frac{dV_x}{dt} &= - \frac{1}{\rho} \cdot \frac{\partial p}{\partial x} + v \Delta V_x + \frac{v}{3} \cdot \frac{\partial}{\partial x} \operatorname{div} \mathbf{V} \\ \frac{dV_y}{dt} &= - \frac{1}{\rho} \cdot \frac{\partial p}{\partial y} + v \Delta V_y + \frac{v}{3} \cdot \frac{\partial}{\partial y} \operatorname{div} \mathbf{V} \\ \frac{dV_z}{dt} &= - \frac{1}{\rho} \cdot \frac{\partial p}{\partial z} + v \Delta V_z + \frac{v}{3} \cdot \frac{\partial}{\partial z} \operatorname{div} \mathbf{V} \end{aligned} \right\} \quad (3.1.19)$$

For two-dimensional plane motion characterized by a varying dynamic viscosity  $\mu \neq \text{const}$ , equations are obtained from (3.1.17) as a result of simple transformations:

$$\left. \begin{aligned} \frac{\partial V_x}{\partial t} &= - \frac{1}{\rho} \cdot \frac{\partial p}{\partial x} + \frac{1}{\rho} \cdot \frac{\partial}{\partial x} \left[ \mu \left( 2 \frac{\partial V_x}{\partial x} - \frac{2}{3} \operatorname{div} \mathbf{V} \right) \right] \\ &\quad + \frac{2}{\rho} \cdot \frac{\partial}{\partial y} (\mu \epsilon_z) \\ \frac{\partial V_y}{\partial t} &= - \frac{1}{\rho} \cdot \frac{\partial p}{\partial y} + \frac{1}{\rho} \cdot \frac{\partial}{\partial y} \left[ \mu \left( 2 \frac{\partial V_y}{\partial y} - \frac{2}{3} \operatorname{div} \mathbf{V} \right) \right] \\ &\quad + \frac{2}{\rho} \cdot \frac{\partial}{\partial x} (\mu \epsilon_z) \end{aligned} \right\} \quad (3.1.20)$$

When  $\operatorname{div} \mathbf{V} = 0$ , and  $\mu = \text{const}$ , these equations are reduced to equations of motion of a viscous incompressible fluid.

Let us consider the equation of motion of an ideal (inviscid) compressible fluid. Assuming the coefficients  $\mu$  and  $\nu$  in (3.1.17) to be zero, we obtain:

$$\left. \begin{aligned} \frac{\partial V_x}{\partial t} + V_x \frac{\partial V_x}{\partial x} + V_y \frac{\partial V_x}{\partial y} + V_z \frac{\partial V_x}{\partial z} &= X - \frac{1}{\rho} \cdot \frac{\partial p}{\partial x} \\ \frac{\partial V_y}{\partial t} + V_x \frac{\partial V_y}{\partial x} + V_y \frac{\partial V_y}{\partial y} + V_z \frac{\partial V_y}{\partial z} &= Y - \frac{1}{\rho} \cdot \frac{\partial p}{\partial y} \\ \frac{\partial V_z}{\partial t} + V_x \frac{\partial V_z}{\partial x} + V_y \frac{\partial V_z}{\partial y} + V_z \frac{\partial V_z}{\partial z} &= Z - \frac{1}{\rho} \cdot \frac{\partial p}{\partial z} \end{aligned} \right\} \quad (3.1.17')$$

These equations were first obtained by Leonard Euler, which is why they are called **Euler equations**. They are the theoretical cornerstone of the science dealing with the motion of an ideal gas whose hypothetic properties are determined by the absence or negligibly small influence of viscosity.

#### Vector Form of the Equations of Motion

By multiplying Eqs. (3.1.18) by the unit vectors  $\mathbf{i}$ ,  $\mathbf{j}$ , and  $\mathbf{k}$ , respectively, and then summing them, we obtain an equation of motion in the vector form:

$$d\mathbf{V}/dt = \mathbf{G} - (1/\rho) \operatorname{grad} p + \nu \Delta \mathbf{V} + (\nu/3) \operatorname{grad} \operatorname{div} \mathbf{V} \quad (3.1.21)$$

where the vector of the mass forces in Cartesian coordinates is

$$\mathbf{G} = X\mathbf{i} + Y\mathbf{j} + Z\mathbf{k}$$

the pressure gradient is

$$\operatorname{grad} p = (\partial p / \partial x) \mathbf{i} + (\partial p / \partial y) \mathbf{j} + (\partial p / \partial z) \mathbf{k}$$

the vectors

$$\Delta \mathbf{V} = \Delta V_x \mathbf{i} + \Delta V_y \mathbf{j} + \Delta V_z \mathbf{k}$$

$$\operatorname{grad} \operatorname{div} \mathbf{V} = (\partial \operatorname{div} \mathbf{V} / \partial x) \mathbf{i} + (\partial \operatorname{div} \mathbf{V} / \partial y) \mathbf{j} + (\partial \operatorname{div} \mathbf{V} / \partial z) \mathbf{k}$$

If a fluid is incompressible,  $\operatorname{div} \mathbf{V} = 0$ , and, consequently,

$$d\mathbf{V}/dt = \mathbf{G} - (1/\rho) \operatorname{grad} p + \nu \Delta \mathbf{V} \quad (3.1.21')$$

In the absence of mass forces,  $\mathbf{G} = 0$ , therefore

$$d\mathbf{V}/dt = - (1/\rho) \operatorname{grad} p + \nu \Delta \mathbf{V} + (\nu/3) \operatorname{grad} \operatorname{div} \mathbf{V} \quad (3.1.21'')$$

The vector of the total acceleration can also be expressed as

$$d\mathbf{V}/dt = \partial \mathbf{V} / \partial t + \operatorname{grad} (V^2/2) + \operatorname{curl} \mathbf{V} \times \mathbf{V} \quad (3.1.22)$$

With account taken of (3.1.21") and (3.1.22), we can write the equation of motion as

$$\frac{\partial \mathbf{V}}{\partial t} + \text{grad} \frac{V^2}{2} + \text{curl } \mathbf{V} \times \mathbf{V} = -\frac{1}{\rho} \text{grad } p + v \Delta \mathbf{V} + \frac{v}{3} \text{grad div } \mathbf{V} \quad (3.1.22')$$

For an inviscid compressible fluid, the equation of motion is

$$\frac{\partial \mathbf{V}}{\partial t} + \text{grad} \frac{V^2}{2} + \text{curl } \mathbf{V} \times \mathbf{V} = -\frac{1}{\rho} \text{grad } p \quad (3.1.22'')$$

### Curvilinear Coordinates

Let us transform Eq. (3.1.22') using the concept of generalized curvilinear coordinates  $q_n$ . This allows us to go over comparatively simply to equations of motion containing a specific form of curvilinear orthogonal coordinates, as was done with respect to the continuity equation.

Let us consider the transformation of separate terms in (3.1.22'). For the second term on the left-hand side, and also for the first and third terms on the right-hand sides, with a view to (2.4.18), we have the following expressions:

$$\text{grad} \frac{V^2}{2} = \sum_{n=1}^3 \left( \text{grad} \frac{V^2}{2} \right)_n \mathbf{i}_n = \sum_{n=1}^3 \frac{1}{h_n} \cdot \frac{\partial (V^2/2)}{\partial q_n} \mathbf{i}_n \quad (3.1.23)$$

$$\text{grad } p = \sum_{n=1}^3 (\text{grad } p)_n \mathbf{i}_n = \sum_{n=1}^3 \frac{1}{h_n} \cdot \frac{\partial p}{\partial q_n} \mathbf{i}_n \quad (3.1.24)$$

$$\text{grad div } \mathbf{V} = \sum_{n=1}^3 (\text{grad div } \mathbf{V})_n \mathbf{i}_n = \sum_{n=1}^3 \frac{1}{h_n} \cdot \frac{\partial \text{div } \mathbf{V}}{\partial q_n} \mathbf{i}_n \quad (3.1.25)$$

For transformation of the vector product  $\text{curl } \mathbf{V} \times \mathbf{V}$ , it is necessary to find the form of the expression of the vector  $\text{curl } \mathbf{V}$  in generalized coordinates. For this purpose, let us calculate the curl of both sides of Eq. (2.4.19):

$$\text{curl } \mathbf{V} = \sum_{n=1}^3 (V_n \text{curl } \mathbf{i}_n + \text{grad } V_n \times \mathbf{i}_n) \quad (3.1.26)$$

where

$$\text{grad } V_n \times \mathbf{i}_n = (\text{grad } V_n)_j \mathbf{i}_m - (\text{grad } V_n)_m \mathbf{i}_j \quad (3.1.27)$$

Here the projections of the vector  $\text{grad } V_n$  onto the relevant coordinate directions are determined from expression (2.4.18) with  $V_n$  substituted for  $\Phi$ . Introducing (3.1.27), and also the expressions for  $\text{curl } \mathbf{i}_n$  from (2.4.22) into (3.1.26), we obtain the following expres-

sion for the curl of the velocity:

$$\text{curl } \mathbf{V} = \frac{1}{h_2 h_3} \left[ \frac{\partial (h_3 V_3)}{\partial q_2} - \frac{\partial (h_2 V_2)}{\partial q_3} \right] \mathbf{i}_1 + \frac{1}{h_3 h_1} \\ \times \left[ \frac{\partial (h_1 V_1)}{\partial q_3} - \frac{\partial (h_3 V_3)}{\partial q_1} \right] \mathbf{i}_2 + \frac{1}{h_1 h_2} \left[ \frac{\partial (h_2 V_2)}{\partial q_1} - \frac{\partial (h_1 V_1)}{\partial q_2} \right] \mathbf{i}_3 \quad (3.1.28)$$

Consequently, the cross product

$$\text{curl } \mathbf{V} \times \mathbf{V} = \sum_{n=1}^3 (\text{curl } \mathbf{V} \times \mathbf{V})_n \mathbf{i}_n \quad (3.1.29)$$

where the projection of this vector onto a tangent to the corresponding coordinate curve is

$$(\text{curl } \mathbf{V} \times \mathbf{V})_n = \frac{V_j}{h_j h_n} \left[ \frac{\partial (h_n V_n)}{\partial q_j} - \frac{\partial (h_j V_j)}{\partial q_n} \right] \\ - \frac{V_m}{h_n h_m} \left[ \frac{\partial (h_m V_m)}{\partial q_n} - \frac{\partial (h_n V_n)}{\partial q_m} \right] \quad (3.1.30)$$

Recall that the relation between the subscripts  $m$ ,  $j$ , and  $n$  is as follows:

$$\begin{array}{cccc} n & \dots & 1 & 2 & 3 \\ m & \dots & 2 & 3 & 1 \\ j & \dots & 3 & 1 & 2 \end{array}$$

The left-hand side of Eq. (3.1.22) is the vector of the total acceleration  $\mathbf{W} = d\mathbf{V}/dt$  that has the form

$$\mathbf{W} = \sum_{n=1}^3 W_n \mathbf{i}_n \quad (3.1.31)$$

where  $W_n$  is the projection of the acceleration vector onto the direction of a tangent to the coordinate line  $q_n$ .

Each quantity  $W_n$  can be considered as the sum of the relevant projections of the vectors  $\partial \mathbf{V} / \partial t$ , and also of the vectors (3.1.23) and (3.1.29) onto the indicated directions. Accordingly,

$$W_n = \frac{\partial V_n}{\partial t} + \frac{V_n}{h_n} \cdot \frac{\partial V_n}{\partial q_n} + \frac{V_m}{h_n h_m} \cdot \frac{\partial (h_n V_n)}{\partial q_m} \\ + \frac{V_j}{h_j h_n} \cdot \frac{\partial (h_n V_n)}{\partial q_j} - \frac{V_m^2}{h_n h_m} \cdot \frac{\partial h_m}{\partial q_n} - \frac{V_j^2}{h_j h_n} \cdot \frac{\partial h_j}{\partial q_n} \quad (3.1.32)$$

Let us apply the Laplacian operator to the vector  $\mathbf{V}$ , and use the expression

$$\Delta \mathbf{V} = \sum_{n=1}^3 \Delta V_n \mathbf{i}_n = \text{grad div } \mathbf{V} - \text{curl curl } \mathbf{V} \quad (3.1.33)$$

where  $\Delta V_n$  are the projections of the vector along the coordinate lines  $q_n$ .

The first vector on the right-hand side of (3.1.33) has been determined in the form of (3.1.25), while for calculating the second one Eq. (3.1.28) should be used. Taking the curl of both sides of this equation, we obtain

$$\begin{aligned}\operatorname{curl} \operatorname{curl} \mathbf{V} &= \sum_{n=1}^3 (\operatorname{curl} \operatorname{curl} \mathbf{V})_n \mathbf{i}_n \\ &= \sum_{n=1}^3 \frac{1}{h_m h_j} \left\{ \frac{\partial [h_j (\operatorname{curl} \mathbf{V})_j]}{\partial q_m} - \frac{\partial [h_m (\operatorname{curl} \mathbf{V})_m]}{\partial q_j} \right\} \mathbf{i}_n \quad (3.1.34)\end{aligned}$$

where the corresponding projections of the vector  $\operatorname{curl} \mathbf{V}$  are found from (3.1.28).

Having these data at hand, we can consider the transformation of the equations of motion as applied to specific forms of curvilinear orthogonal coordinates.

### Cylindrical Coordinates

In accordance with (2.4.12), (2.4.16), and (2.4.25), we have

$$\begin{aligned}q_1 &= x, \quad q_2 = r, \quad q_3 = \gamma, \quad h_1 = 1, \quad h_2 = 1, \quad h_3 = r, \\ V_1 &= V_x, \quad V_2 = V_r, \quad V_3 = V_\gamma\end{aligned}$$

Consequently,

$$W_1 = \frac{\partial V_x}{\partial t} + V_x \frac{\partial V_x}{\partial x} + V_r \frac{\partial V_x}{\partial r} + \frac{V_\gamma}{r} \cdot \frac{\partial V_x}{\partial \gamma}; \quad (\operatorname{grad} p)_1 = \partial p / \partial x$$

Next we find

$$(\operatorname{grad} \operatorname{div} \mathbf{V})_1 = \partial \operatorname{div} \mathbf{V} / \partial x$$

Since  $\operatorname{div} \mathbf{V}$  is determined by formula (2.4.26), we have

$$\frac{\partial \operatorname{div} \mathbf{V}}{\partial x} = \frac{\partial}{\partial x} \left( \frac{\partial V_x}{\partial x} + \frac{\partial V_r}{\partial r} + \frac{1}{r} \cdot \frac{\partial V_\gamma}{\partial \gamma} + \frac{V_r}{r} \right)$$

From (3.1.28), we have

$$(\operatorname{curl} \mathbf{V})_3 = \frac{\partial V_r}{\partial x} - \frac{\partial V_x}{\partial r} \quad (\operatorname{curl} \mathbf{V})_2 = \frac{1}{r} \left( \frac{\partial V_x}{\partial \gamma} - r \frac{\partial V_\gamma}{\partial x} \right)$$

Introducing these expressions into (3.1.34), we obtain

$$\begin{aligned}(\operatorname{curl} \operatorname{curl} \mathbf{V})_1 &= \frac{1}{r} \left\{ \frac{\partial}{\partial r} \left[ r \left( \frac{\partial V_r}{\partial x} - \frac{\partial V_x}{\partial r} \right) \right] - \frac{\partial}{\partial \gamma} \left[ \frac{1}{r} \left( \frac{\partial V_x}{\partial \gamma} - r \frac{\partial V_\gamma}{\partial x} \right) \right] \right\} \\ &= \frac{\partial^2 V_r}{\partial x \partial r} - \frac{\partial^2 V_x}{\partial r^2} + \frac{1}{r} \left( \frac{\partial V_r}{\partial x} - \frac{\partial V_x}{\partial r} \right) - \frac{1}{r^2} \left( \frac{\partial^2 V_x}{\partial \gamma^2} - r \frac{\partial^2 V_\gamma}{\partial x \partial \gamma} \right)\end{aligned}$$

Since  $(\text{grad div } \mathbf{V})_x = \partial \text{div } \mathbf{V} / \partial x$ , in accordance with (3.1.33) we have

$$\begin{aligned} (\Delta \mathbf{V})_x &= (\text{grad div } \mathbf{V})_x - (\text{curl curl } \mathbf{V})_x \\ &= \frac{\partial^2 V_x}{\partial x^2} + \frac{\partial^2 V_x}{\partial r^2} + \frac{1}{r^2} \cdot \frac{\partial^2 V_x}{\partial \gamma^2} + \frac{1}{r} \cdot \frac{\partial V_x}{\partial r} \end{aligned}$$

We thus compile an equation of motion in a projection onto the  $x$ -axis of a cylindrical coordinate system:

$$\begin{aligned} \frac{\partial V_x}{\partial t} + V_x \frac{\partial V_x}{\partial x} + V_r \frac{\partial V_x}{\partial r} + \frac{V_\gamma}{r} \cdot \frac{\partial V_x}{\partial \gamma} &= - \frac{1}{\rho} \cdot \frac{\partial p}{\partial x} \\ + v \Delta V_x + \frac{v}{3} \cdot \frac{\partial \text{div } \mathbf{V}}{\partial x} \end{aligned} \quad (3.1.35)$$

We obtain the other two equations in projections onto the coordinate lines  $r$  and  $\gamma$  in a similar way:

$$\left. \begin{aligned} \frac{\partial V_r}{\partial t} + V_x \frac{\partial V_r}{\partial x} + V_r \frac{\partial V_r}{\partial r} + \frac{V_\gamma}{r} \cdot \frac{\partial V_r}{\partial \gamma} - \frac{V_\gamma^2}{r} \\ = - \frac{1}{\rho} \cdot \frac{\partial p}{\partial r} + v \left( \Delta V_r - \frac{2}{r^2} \cdot \frac{\partial V_\gamma}{\partial \gamma} - \frac{V_r}{r^2} \right) + \frac{v}{3} \cdot \frac{\partial \text{div } \mathbf{V}}{\partial r} \\ \frac{\partial V_\gamma}{\partial t} + V_x \frac{\partial V_\gamma}{\partial x} + V_r \frac{\partial V_\gamma}{\partial r} + \frac{V_\gamma}{r} \cdot \frac{\partial V_\gamma}{\partial \gamma} + \frac{V_r V_\gamma}{r} \\ = - \frac{1}{\rho r} \cdot \frac{\partial p}{\partial \gamma} + v \left( \Delta V_\gamma + \frac{2}{r^2} \cdot \frac{\partial V_r}{\partial \gamma} - \frac{V_\gamma}{r^2} \right) + \frac{v}{3r} \cdot \frac{\partial \text{div } \mathbf{V}}{\partial \gamma} \end{aligned} \right\} \quad (3.1.35')$$

In these equations, we have introduced a symbol for the Laplacian operator in cylindrical coordinates:

$$\Delta = \frac{\partial^2}{\partial x^2} + \frac{\partial^2}{\partial r^2} + \frac{1}{r^2} \cdot \frac{\partial^2}{\partial \gamma^2} + \frac{1}{r} \cdot \frac{\partial}{\partial r}$$

We determine the divergence of the velocity by formula (2.4.26). For an axisymmetric flow, the equations of motion are simplified:

$$\left. \begin{aligned} \frac{\partial V_x}{\partial t} + V_x \frac{\partial V_x}{\partial x} + V_r \frac{\partial V_x}{\partial r} &= - \frac{1}{\rho} \cdot \frac{\partial p}{\partial x} + v \Delta V_x \\ + \frac{v}{3} \cdot \frac{\partial \text{div } \mathbf{V}}{\partial x} \\ \frac{\partial V_r}{\partial t} + V_x \frac{\partial V_r}{\partial x} + V_r \frac{\partial V_r}{\partial r} &= - \frac{1}{\rho} \cdot \frac{\partial p}{\partial r} + v \Delta V_r \\ + \frac{v}{3} \cdot \frac{\partial \text{div } \mathbf{V}}{\partial r} \end{aligned} \right\} \quad (3.1.36)$$

where  $\text{div } \mathbf{V} = \partial V_x / \partial x + \partial V_r / \partial r + V_r / r$ ;  $\Delta = \partial^2 / \partial x^2 + \partial^2 / \partial r^2 + (1/r) \partial / \partial r$ .

For a steady flow, one must assume in the equations that

$$\partial V_x / \partial t = \partial V_r / \partial t = \partial V_\gamma / \partial t = 0$$

### Spherical Coordinates

The spherical coordinates, Lamé coefficients, and the projections of the velocity vector onto the directions of the coordinate lines are related by formulas (2.4.13), (2.4.17), and (2.4.33):

$$q_1 = r, q_2 = \theta, q_3 = \psi, h_1 = 1, h_2 = r, h_3 = r \sin \theta,$$

$$V_1 = V_r, V_2 = V_\theta, V_3 = V_\psi$$

According to these data, from (3.1.32) we find the projection of the acceleration onto the direction of the coordinate line  $r$ :

$$W_1 = \frac{\partial V_r}{\partial t} + V_r \frac{\partial V_r}{\partial r} + \frac{V_\theta}{r} \cdot \frac{\partial V_r}{\partial \theta} + \frac{V_\psi}{r \sin \theta} \cdot \frac{\partial V_r}{\partial \psi} - \frac{V_\theta^2 + V_\psi^2}{r} \quad (3.1.37)$$

The projection of the pressure gradient is

$$(\text{grad } p)_1 = \frac{\partial p}{\partial r} \quad (3.1.38)$$

With a view to the expression for  $\text{div } \mathbf{V}$  (2.4.34), we find the relation

$$(\text{grad div } \mathbf{V})_1 = \frac{\partial \text{div } \mathbf{V}}{\partial r}$$

$$= \frac{\partial}{\partial r} \left[ \frac{1}{r^2} \cdot \frac{\partial (V_r r^2)}{\partial r} + \frac{1}{r \sin \theta} \cdot \frac{\partial (V_\theta \sin \theta)}{\partial \theta} + \frac{1}{r \sin \theta} \cdot \frac{\partial V_\psi}{\partial \psi} \right] \quad (3.1.39)$$

We shall use this relation for determining the projections  $(\Delta V)_1$  of the vector  $\Delta \mathbf{V}$ . To do this, we shall calculate the value of  $(\text{curl curl } \mathbf{V})_1$  in (3.1.33). From (3.1.28), we have

$$(\text{curl } \mathbf{V})_3 = \frac{1}{r} \left[ \frac{\partial (V_\theta r)}{\partial r} - \frac{\partial V_r}{\partial \theta} \right], \quad (\text{curl } \mathbf{V})_2 = \frac{1}{r \sin \theta} \left[ \frac{\partial V_r}{\partial \psi} - \frac{\partial (V_\psi r \sin \theta)}{\partial r} \right]$$

Introducing these relations into (3.1.34), we obtain

$$(\text{curl curl } \mathbf{V})_1 = \frac{1}{r^2 \sin \theta} \left\{ \frac{\partial \left\{ \sin \theta \left[ \frac{\partial (V_\theta r)}{\partial r} - \frac{\partial V_r}{\partial \theta} \right] \right\}}{\partial \theta} - \frac{\partial \left\{ \frac{1}{\sin \theta} \left[ \frac{\partial V_r}{\partial \psi} - \frac{\partial (V_\psi r \sin \theta)}{\partial r} \right] \right\}}{\partial \psi} \right\} \quad (3.1.40)$$

With a view to expressions (3.1.39) and (3.1.40), we find

$$\begin{aligned} (\Delta V)_1 &= (\text{grad div } \mathbf{V})_1 - (\text{curl curl } \mathbf{V})_1 = \Delta V_r - \frac{2V_r}{r^2} \\ &\quad - \frac{2}{r^2} \cdot \frac{\partial V_\theta}{\partial \theta} - \frac{2V_\theta \cot \theta}{r^2} - \frac{2}{r^2 \sin \theta} \cdot \frac{\partial V_\psi}{\partial \psi} \end{aligned} \quad (3.1.41)$$

where

$$\begin{aligned} \Delta V_r &= \frac{1}{r^2} \cdot \frac{\partial}{\partial r} \left( r^2 \frac{\partial V_r}{\partial r} \right) + \frac{1}{r^2 \sin \theta} \cdot \frac{\partial}{\partial \theta} \left( \sin \theta \frac{\partial V_r}{\partial \theta} \right) \\ &\quad + \frac{1}{r^2 \sin^2 \theta} \cdot \frac{\partial^2 V_r}{\partial \psi^2} \end{aligned} \quad (3.1.42)$$

Taking into account (3.1.37)-(3.1.39) and (3.1.41), we find the equation of motion in a projection onto the coordinate line  $r$ :

$$\begin{aligned} \frac{\partial V_r}{\partial t} + V_r \frac{\partial V_r}{\partial r} + \frac{V_\theta}{r} \cdot \frac{\partial V_r}{\partial \theta} + \frac{V_\psi}{r \sin \theta} \cdot \frac{\partial V_r}{\partial \psi} \\ - \frac{V_\theta^2 + V_\psi^2}{r} = - \frac{1}{\rho} \cdot \frac{\partial p}{\partial r} + v \left( \Delta V_r - \frac{2}{r^2} \cdot \frac{\partial V_\theta}{\partial \theta} \right. \\ \left. - \frac{2}{r^2 \sin \theta} \cdot \frac{\partial V_\psi}{\partial \psi} - \frac{2V_r}{r^2} - \frac{2V_\theta \cot \theta}{r^2} \right) + \frac{v}{3} \cdot \frac{\partial \operatorname{div} \mathbf{V}}{\partial r} \end{aligned} \quad (3.1.43)$$

We obtain the other two equations in a similar way:

$$\left. \begin{aligned} \frac{\partial V_\theta}{\partial t} + V_r \frac{\partial V_\theta}{\partial r} + \frac{V_\theta}{r} \cdot \frac{\partial V_\theta}{\partial \theta} + \frac{V_\psi}{r \sin \theta} \cdot \frac{\partial V_\theta}{\partial \psi} \\ \frac{V_r V_\theta - V_\psi^2 \cot \theta}{r} = - \frac{1}{r \rho} \cdot \frac{\partial p}{\partial \theta} + v \left( \Delta V_\theta + \frac{2}{r^2} \cdot \frac{\partial V_r}{\partial \theta} \right. \\ \left. - \frac{V_\theta}{r^2 \sin^2 \theta} - \frac{2 \cos \theta}{r^2 \sin^2 \theta} \cdot \frac{\partial V_\psi}{\partial \psi} \right) + \frac{v}{3} \cdot \frac{1}{r} \cdot \frac{\partial \operatorname{div} \mathbf{V}}{\partial \theta} \\ \frac{\partial V_\psi}{\partial t} + V_r \frac{\partial V_\psi}{\partial r} + \frac{V_\theta}{r} \cdot \frac{\partial V_\psi}{\partial \theta} + \frac{V_\psi}{r \sin \theta} \cdot \frac{\partial V_\psi}{\partial \psi} \\ + \frac{V_\psi (V_r + V_\theta \cot \theta)}{r} = - \frac{1}{\rho r \sin \theta} \cdot \frac{\partial p}{\partial \psi} \\ + v \left( \Delta V_\psi - \frac{V_\psi}{r^2 \sin^2 \theta} + \frac{2}{r^2 \sin \theta} \cdot \frac{\partial V_r}{\partial \psi} + \frac{2 \cos \theta}{r^2 \sin^2 \theta} \cdot \frac{\partial V_\theta}{\partial \psi} \right) \\ + \frac{v}{3r \sin \theta} \cdot \frac{\partial \operatorname{div} \mathbf{V}}{\partial \psi} \end{aligned} \right\} \quad (3.1.43')$$

where the Laplacian operator in spherical coordinates is

$$\Delta = \frac{1}{r^2} \cdot \frac{\partial}{\partial r} \left( r^2 \frac{\partial}{\partial r} \right) + \frac{1}{r^2 \sin \theta} \cdot \frac{\partial}{\partial \theta} \left( \sin \theta \frac{\partial}{\partial \theta} \right) + \frac{1}{r^2 \sin^2 \theta} \cdot \frac{\partial^2}{\partial \psi^2} \quad (3.1.44)$$

For two-dimensional spatial gas flows characterized by a change in the parameters (velocity, pressure, density, etc.) in the direction of only two coordinate lines, let us write the equation of motion in a simpler form:

$$\left. \begin{aligned} \frac{\partial V_r}{\partial t} + V_r \frac{\partial V_r}{\partial r} + \frac{V_\theta}{r} \cdot \frac{\partial V_r}{\partial \theta} - \frac{V_\theta^2}{r} = - \frac{1}{\rho} \cdot \frac{\partial p}{\partial r} \\ + v \left( \Delta V_r - \frac{2}{r^2} \cdot \frac{\partial V_\theta}{\partial \theta} - \frac{2V_r}{r^2} - \frac{2V_\theta \cot \theta}{r^2} \right) + \frac{v}{3} \cdot \frac{\partial \operatorname{div} \mathbf{V}}{\partial r} \\ \times \frac{\partial V_\theta}{\partial t} + V_r \frac{\partial V_\theta}{\partial r} + \frac{V_\theta}{r} \cdot \frac{\partial V_\theta}{\partial \theta} + \frac{V_r V_\theta}{r} = - \frac{1}{r \rho} \cdot \frac{\partial p}{\partial \theta} \\ + v \left( \Delta V_\theta + \frac{2}{r^2} \cdot \frac{\partial V_r}{\partial \theta} - \frac{V_\theta}{r^2 \sin^2 \theta} \right) + \frac{v}{3r} \cdot \frac{\partial \operatorname{div} \mathbf{V}}{\partial \theta} \end{aligned} \right\} \quad (3.1.45)$$

where

$$\Delta = \frac{1}{r^2} \cdot \frac{\partial}{\partial r} \left( r^2 \frac{\partial}{\partial r} \right) + \frac{1}{r^2 \sin \theta} \cdot \frac{\partial}{\partial \theta} \left( \sin \theta \frac{\partial}{\partial \theta} \right) \quad (3.1.46)$$

$$\operatorname{div} \mathbf{V} = \frac{1}{r^2} \cdot \frac{\partial (V_r r^2)}{\partial r} + \frac{1}{r \sin \theta} \cdot \frac{\partial (V_\theta \sin \theta)}{\partial \theta} \quad (3.1.47)$$

### Equations of Two-Dimensional Flow of a Gas Near a Curved Surface

For the case being considered, the curvilinear coordinates, Lamé coefficients, and velocity components are determined by formulas (2.4.40), (2.4.42), and (2.4.43), respectively. We shall adopt the further condition that motion occurs near a wall, and, consequently,  $y \ll R$ . Accordingly,

$$q_1 = x, q_2 = y, q_3 = \gamma, h_1 = 1, h_2 = 1, h_3 = r$$

$$V_1 = dx/dt = V_x, V_2 = V_y, V_3 = 0$$

With a view to these data, the acceleration component is

$$W_1 = \partial V_x / \partial t + V_x \partial V_x / \partial x + V_y \partial V_x / \partial y \quad (3.1.48)$$

and the projection of the pressure gradient is

$$(\operatorname{grad} p)_1 = \partial p / \partial x \quad (3.1.49)$$

In addition,

$$(\operatorname{grad} \operatorname{div} \mathbf{V})_1 = \partial \operatorname{div} \mathbf{V} / \partial x \quad (3.1.50)$$

where the divergence of the velocity has been determined by relation (2.4.44).

Consequently,

$$(\operatorname{grad} \operatorname{div} \mathbf{V})_1 = \frac{\partial}{\partial x} \left\{ \frac{1}{r} \left[ \frac{\partial (V_x r)}{\partial x} + \frac{\partial (V_y r)}{\partial y} \right] \right\} \quad (3.1.51)$$

We use (3.1.28) to calculate the projections of the velocity curl vector:

$$(\operatorname{curl} \mathbf{V})_3 = \partial V_y / \partial x - \partial V_x / \partial y, (\operatorname{curl} \mathbf{V})_2 = 0 \quad (3.1.52)$$

Introducing these expressions into (3.1.34), we obtain

$$(\operatorname{curl} \operatorname{curl} \mathbf{V})_1 = \frac{1}{r} \cdot \frac{\partial}{\partial y} \left[ r \left( \frac{\partial V_y}{\partial x} - \frac{\partial V_x}{\partial y} \right) \right] \quad (3.1.53)$$

With a view to relations (3.1.51) and (3.1.53), we have

$$\begin{aligned} (\Delta V)_1 &= (\operatorname{grad} \operatorname{div} \mathbf{V})_1 - (\operatorname{curl} \operatorname{curl} \mathbf{V})_1 = \frac{\partial}{\partial x} \left\{ \frac{1}{r} \left[ \frac{\partial (V_x r)}{\partial x} \right. \right. \\ &\quad \left. \left. + \frac{\partial (V_y r)}{\partial y} \right] \right\} - \frac{1}{r} \cdot \frac{\partial}{\partial y} \left[ r \left( \frac{\partial V_y}{\partial x} - \frac{\partial V_x}{\partial y} \right) \right] \end{aligned} \quad (3.1.54)$$

Similarly, when considering the coordinate line  $q_2$ , we have

$$W_2 = \partial V_y / \partial t + V_x \partial V_y / \partial x + V_y \partial V_y / \partial y \quad (3.1.55)$$

$$(\text{grad } p)_2 = \partial p / \partial y \quad (3.1.56)$$

$$(\text{grad div } \mathbf{V})_2 = \partial \text{div } \mathbf{V} / \partial y \quad (3.1.57)$$

$$(\Delta V)_2 = (\text{grad div } \mathbf{V})_2 - (\text{curl curl } \mathbf{V})_2$$

$$= -\frac{\partial}{\partial y} \left\{ \frac{1}{r} \left[ \frac{\partial (V_x r)}{\partial x} + \frac{\partial (V_y r)}{\partial y} \right] \right\} - \frac{1}{r} \cdot \frac{\partial}{\partial x} \left[ r \left( \frac{\partial V_y}{\partial x} - \frac{\partial V_x}{\partial y} \right) \right] \quad (3.1.58)$$

Using the obtained relations, we have:

$$\left. \begin{aligned} \frac{\partial V_x}{\partial t} + V_x \frac{\partial V_x}{\partial x} + V_y \frac{\partial V_x}{\partial y} &= -\frac{1}{\rho} \cdot \frac{\partial p}{\partial x} + v (\Delta V)_1 \\ &\quad + \frac{v}{3} \cdot \frac{\partial \text{div } \mathbf{V}}{\partial x} \\ \frac{\partial V_y}{\partial t} + V_x \frac{\partial V_y}{\partial x} + V_y \frac{\partial V_y}{\partial y} &= -\frac{1}{\rho} \cdot \frac{\partial p}{\partial y} + v (\Delta V)_2 \\ &\quad + \frac{v}{3} \cdot \frac{\partial \text{d } v \mathbf{V}}{\partial y} \end{aligned} \right\} \quad (3.1.59)$$

where  $(\Delta V)_1$  and  $(\Delta V)_2$  are determined by formulas (3.1.54) and (3.1.58), respectively.

We have thus obtained various forms of the equations of motion for a viscous liquid. Experience shows that this is needed because in some cases, when studying the laws of interaction of gas flows with bodies in them, it is convenient to use one form of the equation, and in others, a different form.

### 3.2. Equations of Energy and Diffusion of a Gas

#### Diffusion Equation

The motion of a dissociating viscous fluid can be investigated with account taken of the influence of gas diffusion on this motion. This is expressed, particularly, in that diffusion is taken into consideration when deriving the equation of energy—one of the fundamental equations of gas dynamics.

By **diffusion** is meant the levelling out of the concentration because of the molecular transfer of a substance. This is a thermodynamically irreversible process, and it is one of the reasons why a gas in motion loses mechanical energy.

The diffusion equation is an equation of the transfer of the  $i$ -th component in a gas mixture (it is a continuity equation for the same component).

To simplify our investigation, we can assume that the intensity of thermal and pressure diffusion is negligibly small and determine the diffusion flux of the  $i$ -th component in a direction  $n$  by the equation

$$Q_{i,d,n} = -\rho D_i \partial c_i / \partial n \quad (3.2.1)$$

where  $c_i$  is the concentration of the  $i$ -th component, and  $D_i$  is the diffusivity that determines the diffusion flux when a concentration gradient is present.

For a mixture of gas components, we must take into consideration the binary diffusivities corresponding to each pair of components, for example, to oxygen atoms and molecules, or to nitrogen atoms and molecules in the air. In approximate calculations, we can proceed from a certain value of the binary diffusivity  $\bar{D}$  that is the same for all the pairs of components. Taking this into account, we have  $Q_{i,d,n} = -\rho \bar{D} \partial c_i / \partial n$ . Considering the directions  $x$ ,  $y$ , and  $z$  along which diffusion occurs, we have

$$Q_{i,d,x} = -\rho \bar{D} \partial c_i / \partial x, \quad Q_{i,d,y} = -\rho \bar{D} \partial c_i / \partial y, \quad Q_{i,d,z} = -\rho \bar{D} \partial c_i / \partial z \quad (3.2.2)$$

or in the vector form

$$\mathbf{Q}_{i,d} = -\rho \bar{D} \operatorname{grad} c_i \quad (3.2.3)$$

The diffusion of a substance is directed into a region with a reduced concentration, therefore  $\partial c_i / \partial n$  has a negative sign. Since the right-hand side of (3.2.3) contains a minus sign, the quantity  $\mathbf{Q}_{i,d}$  is positive.

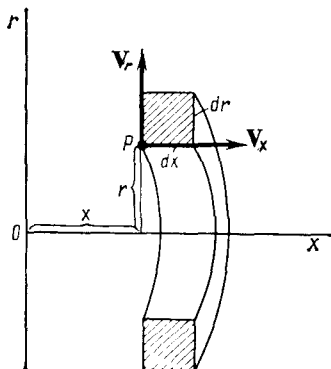
Let us consider the derivation of the diffusion equation in a cylindrical coordinate system assuming the motion to be steady. We shall assume the flow to be three-dimensional and symmetric about the  $x$ -axis, i.e. such in which the velocity component  $V_y = 0$ . Let us separate an elementary volume of the gas in the form of a ring with dimensions of  $dr$  and  $dx$  (Fig. 3.2.1) constructed near point  $P$  whose coordinates are  $x$  and  $r$  and whose velocity components are  $V_x$  and  $V_r$ . We shall assume that the substance diffuses only in a radial direction. Consequently, the flux of the  $i$ -th component through the internal surface of the element is  $m_r = 2\pi r \rho V_r c_i dx + Q_{i,d} 2\pi r dx$ , where  $c_i$  and  $Q_{i,d}$  are the concentration and the diffusion flux of the  $i$ -th component, respectively, evaluated per unit area.

The flux of the  $i$ -th component through the outer surface is

$$m_r + \frac{\partial m_r}{\partial r} dr = m_r + \frac{\partial (\rho V_r r c_i)}{\partial r} 2\pi dr dx + \frac{\partial (Q_{i,d} r)}{\partial r} 2\pi dr dx$$

Consequently, the flow of the component into the volume being considered is

$$[\partial (\rho V_r r c_i) / \partial r] 2\pi dr dx + [\partial (Q_{i,d} r) / \partial r] 2\pi dr dx$$

**Fig. 3.2.1**

An elementary gas particle in an axisymmetric three-dimensional flow

Disregarding the diffusion flux of the substance along the  $x$ -axis, we find the rate of flow of the gas through the left-hand face of the element normal to this axis:

$$m_x = 2\pi\rho V_x c_i r dr$$

and through the right-hand one

$$m_x + (\partial m_x / \partial x) dx = m_x + [\partial (\rho V_x r c_i) / \partial x] 2\pi dr dx$$

Hence, the flow of the component into the volume is

$$2\pi [\partial (\rho V_x r c_i) / \partial x] dr dx$$

Since the amount of gas in the volume does not change, the total flow of the component into the volume equals its outflow because of chemical reactions. If the rate of formation of the  $i$ -th component in a unit volume caused by chemical reactions is  $(W_{ch})_i$ , the consumption of the component in the elementary volume is  $2\pi (W_{ch})_i r \times r dr dx$ . Therefore, the balance of mass of the  $i$ -th component in the volume being considered is

$$\partial (\rho V_x r c_i) / \partial x + \partial (\rho V_r r c_i) / \partial r = -\partial (Q_{i,d} r) / \partial r + (W_{ch})_i r \quad (3.2.4)$$

This equation is known as the diffusion equation in a cylindrical coordinate system. In a similar way, we can obtain a diffusion equation in the Cartesian coordinates  $x$  and  $y$  for a plane flow:

$$\partial (\rho V_x c_i) / \partial x + \partial (\rho V_y c_i) / \partial y = -\partial Q_{i,d} / \partial y + (W_{ch})_i \quad (3.2.5)$$

where  $Q_{i,d}$  is found from (3.2.3).

If we consider a binary mixture of atoms and molecules, then  $\sum c_i = c_A + c_M = 1$  and, consequently,  $Q_{A,d} = -Q_{M,d}$ . We determine the value of  $(W_{ch})_i$  for a given reaction in a dissociating gas by the formulas of chemical kinetics.

### Energy Equation

Together with the equations of state, motion, and continuity, the energy equation belongs to the system of fundamental differential equations as a result of whose solution we completely determine the motion of a gas.

Let us consider a system of rectangular Cartesian coordinates and compile an energy equation for a fluid particle in the form of an elementary parallelepiped. This equation expresses the law of energy conservation, according to which the change in the total energy of a particle, consisting of its kinetic and internal energy, during the time  $dt$  equals the work of the external forces applied to the particle plus the influx of heat from the surroundings.

The kinetic energy of a particle of volume  $\tau = dx dy dz$  is  $(\rho V^2/2) \tau$ , and its internal energy is  $u\rho\tau$  ( $u$  is the internal energy of a unit mass of the gas). Consequently, the change in the total energy during the time  $dt$  is

$$\frac{d}{dt} \left[ \left( \frac{\rho V^2}{2} + \rho u \right) \tau \right] dt = \rho \tau \frac{d}{dt} \left( \frac{V^2}{2} + u \right) dt$$

The work of the external mass (volume) forces in the displacement of the particle during the time  $dt$  can be represented in the form of the dot product  $\mathbf{G} \cdot \mathbf{V}$  multiplied by the mass of the particle  $\rho\tau$  and the time  $dt$ . The mass force vector is  $\mathbf{G} = X\mathbf{i} + Y\mathbf{j} + Z\mathbf{k}$ , consequently,

$$(\mathbf{G} \cdot \mathbf{V}) \rho\tau dt = (XV_x - YV_y + ZV_z) \rho\tau dt$$

Let us calculate the work of the surface forces. First we shall consider the work done during the time  $dt$  by the forces induced by the stresses acting on the right-hand and left-hand faces. The work done by the forces acting on the left-hand face equals the dot product  $\sigma_x \cdot \mathbf{V}$  multiplied by the area  $dy dz$  and the time  $dt$ . In the dot product, the vector of the surface forces is

$$\sigma_x = p_{xx}\mathbf{i} + \tau_{xy}\mathbf{j} + \tau_{xz}\mathbf{k}$$

The work done by the surface forces acting on the right-hand face is

$$\left[ \sigma_x \mathbf{V} + \frac{\partial (\sigma_x \mathbf{V})}{\partial x} dx \right] dy dz dt$$

Having in view that the forces for the left-hand and right-hand faces are directed oppositely, we must assume that the work done by these forces is opposite in sign, for example, positive for the right-hand and negative for the left-hand face. Accordingly, the work of all the surface forces applied to the left-hand and right-hand faces is

$$\frac{\partial (\sigma_x \mathbf{V})}{\partial x} \tau dt = \left[ \frac{\partial}{\partial x} (p_{xx}V_x + \tau_{xy}V_y + \tau_{xz}V_z) \right] \tau dt \quad (3.2.6)$$

We obtain expressions for the work done by the surface forces acting on the lower and upper, and also on the front and rear faces, in a similar way:

$$[\partial(\sigma_y V)/\partial y] \tau dt \text{ and } [\partial(\sigma_z V)/\partial z] \tau dt$$

Considering that the vectors of the surface forces acting on the lower and rear faces are, respectively,

$$\sigma_y = \tau_{yx}\mathbf{i} + p_{yy}\mathbf{j} + \tau_{yz}\mathbf{k}, \quad \sigma_z = \tau_{zx}\mathbf{i} + \tau_{zy}\mathbf{j} + p_{zz}\mathbf{k}$$

we obtain the following expressions for the work:

$$\frac{\partial(\sigma_y V)}{\partial y} \tau dt = \left[ \frac{\partial}{\partial y} (\tau_{yx}V_x + p_{yy}V_y + \tau_{yz}V_z) \right] \tau dt \quad (3.2.6')$$

$$\frac{\partial(\sigma_z V)}{\partial z} \tau dt = \left[ \frac{\partial}{\partial z} (\tau_{zx}V_x + \tau_{zy}V_y + p_{zz}V_z) \right] \tau dt \quad (3.2.6'')$$

In expressions (3.2.6), (3.2.6'), and (3.2.6''), the stresses are determined by relations (3.1.5) and (3.1.16), respectively.

The influx of heat to the particle occurs owing to heat conduction, diffusion, and radiation. Let  $q_x dy dz$  (where  $q_x$  is the specific heat flow) be the amount of heat due to heat conduction or diffusion transferred to the particle through the left-hand face in unit time. During the time  $dt$ , the heat flux  $q_x dy dz dt$  is supplied to the particle. The heat flux through the right-hand face is  $-[q_x + (\partial q_x/\partial x) dx] dy dz dt$ . The amount of heat transferred to the particle through both faces is  $-(\partial q_x/\partial x) \tau dt$ . We obtain similar expressions for the faces perpendicular to the  $y$ - and  $z$ -axes. Hence, the total heat flux transferred to the particle is  $-(\partial q_x/\partial x + \partial q_y/\partial y + \partial q_z/\partial z) \tau dt$ .

If we consider the supply of heat caused by conduction, the specific heat flows, equal to the heat fluxes along the relevant coordinate directions through a unit area, are expressed by the Fourier law

$$q_{T,x} = -\lambda \partial T / \partial x, \quad q_{T,y} = -\lambda \partial T / \partial y, \quad q_{T,z} = -\lambda \partial T / \partial z \quad (3.2.7)$$

With this taken into account, we have

$$-(\partial q_{T,x}/\partial x + \partial q_{T,y}/\partial y + \partial q_{T,z}/\partial z) \tau dt = \operatorname{div}(\lambda \operatorname{grad} T) \tau dt \quad (3.2.8)$$

where  $\operatorname{grad} T = (\partial T / \partial x)\mathbf{i} + (\partial T / \partial y)\mathbf{j} + (\partial T / \partial z)\mathbf{k}$ .

The energy supplied to a gas particle at the expense of diffusion is

$$q_{d,x} = \sum_i Q_{t,d,x} i_t, \quad q_{d,y} = \sum_i Q_{t,d,y} i_t, \quad q_{d,z} = \sum_i Q_{t,d,z} i_t$$

where  $i_t$  is the generalized enthalpy component of the gas mixture.

Hence,

$$-\left(\frac{\partial q_{d,x}}{\partial x} + \frac{\partial q_{d,y}}{\partial y} + \frac{\partial q_{d,z}}{\partial z}\right) \tau dt = -\left(\sum_i i_t \frac{\partial Q_{i,d,x}}{\partial x}\right. \\ \left.+ \sum_i i_t \frac{\partial Q_{i,d,y}}{\partial y} + \sum_i i_t \frac{\partial Q_{i,d,z}}{\partial z}\right) \tau dt = \left(-\sum_i i_t \operatorname{div} \mathbf{Q}_{i,d}\right) \tau dt$$

Introducing into this equation the value of  $\mathbf{Q}_{i,d}$  from (3.2.3), we obtain

$$-(\partial q_{d,x}/\partial x + \partial q_{d,y}/\partial y + \partial q_{d,z}/\partial z) \tau dt \\ = \sum_i i_t \operatorname{div} (\rho D \operatorname{grad} c_i) \tau dt \quad (3.2.9)$$

In addition to the energy transferred to a particle by conduction and diffusion, it also receives heat owing to radiation, equal to  $\varepsilon \tau dt$  ( $\varepsilon$  is the heat flux due to radiation absorbed by unit volume).

By equating the change in the energy of a particle during the time  $dt$  to the sum of the work done by the mass and surface forces and the influx of heat because of conduction, diffusion, and radiation, we obtain the energy equation:

$$\rho \frac{d}{dt} \left( \frac{V^2}{2} + u \right) = \rho (X V_x + Y V_y + Z V_z) + \frac{\partial}{\partial x} (p_{xx} V_x \\ + \tau_{xy} V_y + \tau_{xz} V_z) + \frac{\partial}{\partial y} (\tau_{yx} V_x + p_{yy} V_y + \tau_{yz} V_z) \\ + \frac{\partial}{\partial z} (\tau_{zx} V_x + \tau_{zy} V_y + p_{zz} V_z) + \operatorname{div} (\lambda \operatorname{grad} T) \\ + \sum_i i_t \operatorname{div} (\rho \bar{D} \operatorname{grad} c_i) + \varepsilon \quad (3.2.10)$$

Upon the motion of a chemically reacting mixture of gases, the energy equation expresses the condition of the heat balance including the heat that may appear as a result of chemical reactions. If we take into account, however, that upon the proceeding of reactions the generalized enthalpy of the gas mixture  $\sum c_i i_t$  does not change, then upon introducing the generalized enthalpy into Eq. (3.2.10), we can no longer take into account separately the release or absorption of heat because of chemical reactions.

Introducing into (3.2.10) the expressions for the stresses (3.1.5) and (3.1.16) and excluding the term taking into account the work done by the mass forces, after transformations we obtain an energy equation for a gas:

$$\rho \frac{d}{dt} \left( \frac{V^2}{2} + u \right) = -\operatorname{div} (p \mathbf{V}) - \frac{2}{3} \operatorname{div} (\mu \mathbf{V} \operatorname{div} \mathbf{V}) \\ + \frac{\partial}{\partial x} \left( \mu \frac{\partial V_x^2}{\partial x} \right) + \frac{\partial}{\partial y} \left( \mu \frac{\partial V_y^2}{\partial y} \right) + \frac{\partial}{\partial z} \left( \mu \frac{\partial V_z^2}{\partial z} \right)$$

$$\begin{aligned}
 & + 2 \frac{\partial}{\partial x} [\mu (V_y \varepsilon_z + V_z \varepsilon_y)] + 2 \frac{\partial}{\partial y} [\mu (V_x \varepsilon_z + V_z \varepsilon_x)] \\
 & + 2 \frac{\partial}{\partial z} [\mu (V_x \varepsilon_y + V_y \varepsilon_x)] + \operatorname{div} (\lambda \operatorname{grad} T) \\
 & + \sum_i i_i \operatorname{div} (\rho \bar{D} \operatorname{grad} c_i) + \varepsilon
 \end{aligned} \tag{3.2.11}$$

Equation (3.2.11) shows what causes the kinetic energy of a fluid to change. In addition to conduction, diffusion, and radiation, this energy changes at the expense of the work of compression  $\operatorname{div}(p\mathbf{V})$  and the work of the friction forces (the terms of the equation containing the dynamic viscosity  $\mu$ ). The dissipation of energy is associated with the losses of mechanical energy for overcoming the friction forces. Energy dissipation consists in that the mechanical energy in part transforms irreversibly into heat. Accordingly, the friction forces are called **dissipative**. The terms on the right-hand side of (3.2.11) containing  $\mu$  form the **dissipative function**.

For two-dimensional plane motion of a viscous fluid, the energy equation is

$$\begin{aligned}
 \rho \frac{\partial}{\partial t} \left( \frac{V^2}{2} + u \right) = & - \operatorname{div}(p\mathbf{V}) - \frac{2}{3} \operatorname{div}(\mu \mathbf{V} \operatorname{div} \mathbf{V}) \\
 & + \frac{\partial}{\partial x} \left( \mu \frac{\partial V_x^2}{\partial x} \right) + \frac{\partial}{\partial y} \left( \mu \frac{\partial V_y^2}{\partial y} \right) \\
 & + 2 \frac{\partial}{\partial x} (\mu V_y \varepsilon_z) + 2 \frac{\partial}{\partial y} (\mu V_x \varepsilon_z) + \operatorname{div} (\lambda \operatorname{grad} T) \\
 & + \sum_i i_i \operatorname{div} (\rho \bar{D} \operatorname{grad} c_i) + \varepsilon
 \end{aligned} \tag{3.2.12}$$

where

$$\begin{aligned}
 \mathbf{V} &= V_x \mathbf{i} + V_y \mathbf{j}, \quad \operatorname{div} \mathbf{V} = \partial V_x / \partial x + \partial V_y / \partial y, \\
 \operatorname{grad} T &= (\partial T / \partial x) \mathbf{i} + (\partial T / \partial y) \mathbf{j}, \quad \operatorname{grad} c_i = (\partial c_i / \partial x) \mathbf{i} + (\partial c_i / \partial y) \mathbf{j}
 \end{aligned}$$

Let us transform the energy equation (3.2.12). To do this, we multiply the first equation (3.1.20) by  $V_x$ , the second one by  $V_y$ , and sum up the results. We obtain

$$\begin{aligned}
 \rho \frac{d}{dt} \left( \frac{V^2}{2} \right) = & - \left( V_x \frac{\partial p}{\partial x} + V_y \frac{\partial p}{\partial y} \right) \\
 + V_x \frac{\partial}{\partial x} \left[ \mu \left( 2 \frac{\partial V_x}{\partial x} - \frac{2}{3} \operatorname{div} \mathbf{V} \right) \right] + V_y \frac{\partial}{\partial y} \left[ \mu \left( 2 \frac{\partial V_y}{\partial y} - \frac{2}{3} \operatorname{div} \mathbf{V} \right) \right] \\
 & + 2 \left[ V_x \frac{\partial}{\partial y} (\mu \varepsilon_z) + V_y \frac{\partial}{\partial x} (\mu \varepsilon_z) \right]
 \end{aligned} \tag{3.2.13}$$

We can show by simple transformations that

$$V_x \frac{\partial p}{\partial x} + V_y \frac{\partial p}{\partial y} = \operatorname{div}(p\mathbf{V}) - p \operatorname{div} \mathbf{V}$$

where we find  $p \operatorname{div} \mathbf{V}$  by using the continuity equation

$$p \operatorname{div} \mathbf{V} = -(p/\rho) d\rho/dt, \text{ or } p \operatorname{div} \mathbf{V} = \rho (d/dt) (p/\rho) - dp/dt$$

We transform the sum of the other two terms on the right-hand side of the equation to the form

$$\begin{aligned} V_x \frac{\partial}{\partial x} \left[ \mu \left( 2 \frac{\partial V_x}{\partial x} - \frac{2}{3} \operatorname{div} \mathbf{V} \right) \right] + V_y \frac{\partial}{\partial y} \left[ \mu \left( 2 \frac{\partial V_y}{\partial y} - \frac{2}{3} \operatorname{div} \mathbf{V} \right) \right] \\ = \frac{\partial}{\partial x} \left( \mu \frac{\partial V_x^2}{\partial x} \right) + \frac{\partial}{\partial y} \left( \mu \frac{\partial V_y^2}{\partial y} \right) - 2\mu \left[ \left( \frac{\partial V_x}{\partial x} \right)^2 + \left( \frac{\partial V_y}{\partial y} \right)^2 \right] \\ - \frac{2}{3} \operatorname{div} (\mu \mathbf{V} \operatorname{div} \mathbf{V}) + \frac{2}{3} \mu (\operatorname{div} \mathbf{V})^2 \end{aligned}$$

For the last term in (3.2.13), we have the expression

$$2 \left[ V_x \frac{\partial}{\partial y} (\mu \varepsilon_z) + V_y \frac{\partial}{\partial x} (\mu \varepsilon_z) \right] = 2 \frac{\partial}{\partial x} (\mu V_y \varepsilon_z) + 2 \frac{\partial}{\partial y} (\mu V_x \varepsilon_z) - 4\mu \varepsilon_z^2$$

Let us make the relevant substitution in (3.2.13) and subtract the obtained equation from (3.2.12). Having in view that  $i = u + p/\rho$ , we obtain

$$\begin{aligned} \rho \frac{di}{dt} = \frac{dp}{dt} + 2\mu \left\{ \left[ \left( \frac{\partial V_x}{\partial x} \right)^2 + \left( \frac{\partial V_y}{\partial y} \right)^2 \right] - \frac{2}{3} (\operatorname{div} \mathbf{V})^2 + 4\varepsilon_z^2 \right\} \\ + \operatorname{div} (\lambda \operatorname{grad} T) + \sum_i i_i \operatorname{div} (\rho \bar{D} \operatorname{grad} c_i) + \varepsilon \quad (3.2.14) \end{aligned}$$

In the absence of heat transfer by diffusion and radiation, we can write the energy equation in the form

$$\begin{aligned} \rho \frac{di}{dt} = \frac{dp}{dt} + 2\mu \left\{ \left[ \left( \frac{\partial V_x}{\partial x} \right)^2 + \left( \frac{\partial V_y}{\partial y} \right)^2 \right] - \frac{2}{3} (\operatorname{div} \mathbf{V})^2 + 4\varepsilon_z^2 \right\} \\ + \operatorname{div} (\lambda \operatorname{grad} T) \quad (3.2.15) \end{aligned}$$

At low gas velocities, when the work of the friction forces is not great, we may disregard the dissipative terms. In addition, the work done by the pressure forces is also insignificant ( $dp/dt \approx 0$ ). In the given case, instead of (3.2.15), we have

$$dT/dt = (\lambda/\rho c_p) \operatorname{div} (\operatorname{grad} T) \quad (3.2.16)$$

The quantity  $\lambda/(\rho c_p) = a$ , called the **thermal diffusivity**, characterizes the intensity of molecular heat transfer.

### 3.3. System of Equations of Gas Dynamics. Initial and Boundary Conditions

The investigation of the motion of a gas, i.e. the determination of the parameters characterizing this motion for each point of space, consists in solving the relevant equations that relate these parameters to one another. All these equations are independent and form a **system of equations of gas dynamics**. We determine the number of independent equations by the number of unknown parameters of the gas being sought.

Let us consider the motion of an ideal compressible gas. If the velocities of the flow are not high, we may ignore the change in the specific heats with the temperature and take no account of radiation. In this case, the gas flow is a thermodynamically isolated system and is adiabatic. The unknown quantities for the flow being considered are the three velocity components  $V_x$ ,  $V_y$ , and  $V_z$ , and also the pressure  $p$ , density  $\rho$ , and temperature  $T$ . Consequently, the system of equations of gas dynamics must include six independent ones. Among them are the equations of motion, continuity, state, and energy, which are customarily called the **fundamental equations of gas dynamics**.

Before compiling this system of equations, let us consider separately the energy equation. In accordance with our assumption on the adiabatic nature of the flow, we transform the energy equation (3.2.14) as follows:

$$di = dp/\rho \quad (3.3.1)$$

If we take into consideration the equation  $di = c_p dT$ , and also the expressions  $c_p - c_v = R$  and  $p = R\rho T$ , from which we can find

$$c_p = \frac{(c_p/c_v) R}{c_p/c_v - 1} = \frac{k}{k-1} R, \quad dT = \frac{1}{R} d \left( \frac{p}{\rho} \right)$$

then (3.3.1) is reduced to the form  $dp/p = k d\rho/\rho$ .

Hence

$$p = A \rho^k \quad (3.3.2)$$

where  $A$  is a constant characteristic of the given conditions of gas flow.

Equation (3.3.2) is known as the equation of an adiabat (isentrope). Hence, in the case being considered, the energy equation coincides with that of an adiabat. Having the energy equation in this

form, we shall write all the equations of the system:

$$\left. \begin{aligned} \frac{dV_x}{dt} &= -\frac{1}{\rho} \cdot \frac{\partial p}{\partial x}, & \frac{dV_y}{dt} &= -\frac{1}{\rho} \cdot \frac{\partial p}{\partial y} \\ \frac{dV_z}{dt} &= -\frac{1}{\rho} \cdot \frac{\partial p}{\partial z}, & \frac{d\rho}{dt} + \rho \operatorname{div} \mathbf{V} &= 0 \\ p &= R\rho T, & A\rho^{k-1} &= RT \end{aligned} \right\} \quad (3.3.3)$$

Let us consider the system of equations for the more general case of the motion of an inviscid gas at high speeds when the specific heats change with the temperature, and dissociation and ionization may occur in the gas. For generality, we shall retain the possibility of the heated gas radiating energy. Now the thermodynamic process in the gas flow will not be adiabatic. Accordingly, the quantity  $\epsilon$  determining the radiation heat flux remains on the right-hand side of energy equation (3.2.14). We shall note that the equation of state must be adopted in the form of (1.5.8) taking into account the change in the mean molar mass  $\mu_m$  with the temperature and pressure. In accordance with the above, and also taking into account that the equations of motion and continuity do not change in form, we shall give the fundamental equations of the system:

$$\left. \begin{aligned} \frac{dV_x}{dt} &= -\frac{1}{\rho} \cdot \frac{\partial p}{\partial x}, & \frac{\partial V_u}{dt} &= -\frac{1}{\rho} \cdot \frac{\partial p}{\partial y} \\ \frac{dV_z}{dt} &= -\frac{1}{\rho} \cdot \frac{\partial p}{\partial z}, & \frac{d\rho}{dt} + \rho \operatorname{div} \mathbf{V} &= 0 \\ p &= \frac{R_n}{\mu_m} \rho T, & \rho \frac{di}{dt} &= \frac{dp}{dt} + \epsilon \end{aligned} \right\} \quad (3.3.4)$$

We can see that in the given system in addition to the six unknown quantities indicated above ( $V_x$ ,  $V_y$ ,  $V_z$ ,  $p$ ,  $\rho$ , and  $T$ ) three more have appeared: the enthalpy  $i$ , mean molar mass of the gas  $\mu_m$ , and the heat flux  $\epsilon$  produced by radiation. Besides these quantities, when studying the flow of a gas, we must also determine the entropy  $S$  and the speed of sound  $a$ . Hence, the total number of unknown parameters characterizing a gas flow and being additionally sought is five. Therefore, we must add this number of independent relations for the additional unknowns to the system of fundamental equations. These expressions can be written in the form of general relations determining the unknown quantities as functions of the pressure and temperature:

$$i = f_1(p, T) \quad (3.3.5)$$

$$S = f_2(p, T) \quad (3.3.6)$$

$$\mu_m = f_3(p, T) \quad (3.3.7)$$

$$a = f_4(p, T) \quad (3.3.8)$$

$$\epsilon = f_5(p, T) \quad (3.3.9)$$

The finding of these functions is the subject of special branches of physics and thermodynamics.

The solution of Eqs. (3.3.4)-(3.3.9) determines the parameters of flow of an inviscid dissociating and ionizing gas with account taken of the radiation effect. Such flow is studied by the aerodynamics of a radiating gas.

Let us consider a more general case of flow characterized by the action of friction forces and heat transfer. We shall assume that chemical reactions occur in the gas. Therefore, the fundamental equations of the system (for simplification we shall consider two-dimensional plane flow) will include two differential equations (3.1.20) of motion of a viscous compressible fluid with a varying dynamic viscosity ( $\mu \neq \text{const}$ ), and also continuity equation (2.4.1). These equations must be supplemented with equation of state (1.5.8) relating to the general case of a dissociated and ionized gas, and with expression (3.2.14) that is the energy equation for a two-dimensional compressible gas flow in which heat transfer by diffusion and radiation occur. These equations describe the general case of unsteady motion and characterize the unsteady thermal processes occurring in a gas flow. Hence, we have

$$\left. \begin{aligned} \frac{dV_x}{dt} &= -\frac{1}{\rho} \cdot \frac{\partial p}{\partial x} + \frac{1}{\rho} \cdot \frac{\partial}{\partial x} \left[ \mu \left( 2 \frac{\partial V_x}{\partial x} - \frac{2}{3} \operatorname{div} \mathbf{V} \right) \right] \\ &\quad + \frac{2}{\rho} \cdot \frac{\partial}{\partial y} (\mu \varepsilon_z) \\ \frac{dV_y}{dt} &= -\frac{1}{\rho} \cdot \frac{\partial p}{\partial y} + \frac{1}{\rho} \cdot \frac{\partial}{\partial y} \left[ \mu \left( 2 \frac{\partial V_y}{\partial y} - \frac{2}{3} \operatorname{div} \mathbf{V} \right) \right] \\ &\quad + \frac{2}{\rho} \cdot \frac{\partial}{\partial x} (\mu \varepsilon_z) \\ \frac{dp}{dt} + \rho \operatorname{div} \mathbf{V} &= 0; \quad p = \frac{R_0}{\mu_m} \rho T \\ \rho \frac{di}{dt} &= \frac{dp}{dt} + 2\mu \left\{ \left[ \left( \frac{\partial V_x}{\partial x} \right)^2 + \left( \frac{\partial V_y}{\partial y} \right)^2 \right] - \frac{2}{3} (\operatorname{div} \mathbf{V})^2 + 4\varepsilon_z^2 \right\} \\ &\quad + \operatorname{div} (\lambda \operatorname{grad} T) + \sum_i i_i \operatorname{div} (\rho \bar{D} \operatorname{grad} c_i) + \varepsilon \end{aligned} \right\} \quad (3.3.10)$$

This system must be supplemented with relations (3.3.5)-(3.3.9), and also with the general relations for the thermal conductivity

$$\lambda = f_6(p, T) \quad (3.3.11)$$

the dynamic viscosity

$$\mu = f_7(p, T) \quad (3.3.12)$$

and the specific heats

$$c_p = f_8(p, T), \quad c_v = f_9(p, T) \quad (3.3.13)$$

The last two quantities are not contained explicitly in Eqs. (3.3.10), but they are nevertheless used in solving them because when studying the flow of a gas its thermodynamic characteristics are determined. Since the energy equation also takes into account heat transfer by diffusion, equation (3.2.5) has to be included additionally. It must be taken into account simultaneously that the concentration  $c_i$  in the energy and diffusion equations is a function of the pressure and temperature, and it can be written in the form of the general relation

$$c_i = f_{10}(p, T) \quad (3.3.14)$$

The above system of equations including the fundamental equations of gas dynamics and the corresponding number (according to the number of unknowns being sought) of additional relations is considered in the aerodynamics of a viscous gas and allows one to find the distribution of the normal and shear stresses, and also the aerodynamic heat fluxes from the heated gas to the wall over which it flows. In specific cases, for which a definite schematization of the flow process is possible, the above system is simplified, and this facilitates the solution of the differential equations.

When solving the equations, it becomes necessary to involve additional relations used for determining the characteristic parameters of motion. Among them are, for example, relations for determining the specific heats and the degree of dissociation depending on the pressure and temperature, and formulas for calculating the shear stress depending on the velocity.

The solution of a system of gas-dynamic equations describing the flow over a given surface must satisfy definite initial and boundary conditions of this flow.

**The initial conditions** are determined by the values of the gas parameters for a certain instant and have sense, evidently, for unsteady motion.

The **boundary conditions** are superposed on the solution of the problem both for steady and for unsteady motion and must be observed at every instant of this motion. According to one of them, the solution must be such that the parameters determined by it equal the values of the parameters for the undisturbed flow at the boundary separating the disturbed and undisturbed flow regions.

The second boundary condition is determined by the nature of gas flow over the relevant surface. If the gas is inviscid and does not penetrate through such a surface, the flow is said to be without separation (a free streamline flow). In accordance with this condition, the normal velocity component at each point of the surface is zero, while the vector of the total velocity coincides with the direction of a tangent to the surface.

It is general knowledge that the vector  $\text{grad } F$  [here  $F(q_1, q_2, q_3) = 0$  is the equation of the surface in the flow, and  $q_1, q_2, q_3$  are the generalized curvilinear coordinates] coincides in direction with a normal to the surface. Hence, for conditions of flow without separation, the dot product of this vector and the velocity vector  $\mathbf{V}$  is zero.

Consequently, the condition of flow without separation can be written in a mathematical form as follows:

$$\mathbf{V} \cdot \text{grad } F = 0$$

Taking into account that

$$\text{grad } F = \frac{1}{h_1} \cdot \frac{\partial F}{\partial q_1} \mathbf{i}_1 + \frac{1}{h_2} \cdot \frac{\partial F}{\partial q_2} \mathbf{i}_2 + \frac{1}{h_3} \cdot \frac{\partial F}{\partial q_3} \mathbf{i}_3 \quad (3.3.15)$$

the condition of flow without separation can be written as

$$\frac{1}{h_1} \cdot \frac{\partial F}{\partial q_1} V_1 + \frac{1}{h_2} \cdot \frac{\partial F}{\partial q_2} V_2 + \frac{1}{h_3} \cdot \frac{\partial F}{\partial q_3} V_3 = 0 \quad (3.3.16)$$

For Cartesian coordinates, we have

$$\text{grad } F = (\partial F / \partial x) \mathbf{i}_1 + (\partial F / \partial y) \mathbf{i}_2 + (\partial F / \partial z) \mathbf{i}_3$$

Consequently, for (3.3.16)

$$V_x \frac{\partial F}{\partial x} + V_y \frac{\partial F}{\partial y} + V_z \frac{\partial F}{\partial z} = 0 \quad (3.3.17)$$

For two-dimensional plane flow

$$\frac{V_y}{V_x} = - \frac{\partial F / \partial x}{\partial F / \partial y} \quad (3.3.17')$$

If the equation of the surface is given in cylindrical coordinates, we have

$$\text{grad } F = \frac{\partial F}{\partial x} \mathbf{i}_1 + \frac{\partial F}{\partial r} \mathbf{i}_2 + \frac{1}{r} \cdot \frac{\partial F}{\partial \gamma} \mathbf{i}_3$$

therefore, the condition of flow without separation has the form

$$\frac{\partial F}{\partial x} V_x + \frac{\partial F}{\partial r} V_r + \frac{1}{r} \cdot \frac{\partial F}{\partial \gamma} V_\gamma = 0 \quad (3.3.18)$$

In a particular case, when a surface of revolution is in the flow, we obtain the equation

$$V_x \frac{\partial F}{\partial x} + V_r \frac{\partial F}{\partial r} = 0 \quad (3.3.18')$$

from which we find the condition for the velocity ratio:

$$\frac{V_r}{V_x} = - \frac{\partial F / \partial x}{\partial F / \partial r} \quad (3.3.19)$$

Other boundary conditions can also be formulated. They are determined for each specific problem, the boundary conditions for

a viscous gas differing from the conditions for an ideal fluid. Particularly, when studying the flow of a viscous gas in a boundary layer, the solutions of the pertinent equations must satisfy the conditions on the surface of the body and at the edge of the boundary layer. According to experimental data, the gas particles adhere, as it were, to the surface, and therefore the velocity on it is zero. At the boundary layer edge, the velocity becomes the same as in free (inviscid) flow, and the shear stress equals zero.

### 3.4. Integrals of Motion for an Ideal Fluid

The differential equations derived for the general case of motion of a gas are non-integrable in the finite form. Integrals of these equations can be obtained only for the particular case of an ideal (inviscid) gas flow.

The equation of motion of an ideal gas in the vector form is

$$\partial \mathbf{V} / \partial t + \text{grad } (V^2/2) + \text{curl } \mathbf{V} \times \mathbf{V} = -(1/\rho) \text{grad } p \quad (3.4.1)$$

This equation can be obtained from vector relation (3.1.22') in which the terms on the right-hand side taking into account the influence of the viscosity should be taken equal to zero.

In its form (3.4.1), the equation of motion was first obtained by the Russian scientist prof. I. Gromeka. With a view to the mass forces, Gromeka's equation becomes

$$\partial \mathbf{V} / \partial t + \text{grad } (V^2/2) + \text{curl } \mathbf{V} \times \mathbf{V} = \mathbf{G} - (1/\rho) \text{grad } p \quad (3.4.2)$$

Let us assume that the unsteady flow will be potential, hence  $\text{curl } \mathbf{V} = 0$  and  $\mathbf{V} = \text{grad } \varphi$ . In addition, let us assume that the mass forces have the potential  $U$ , therefore the vector

$$\mathbf{G} = -\text{grad } U$$

where  $\text{grad } U = (\partial U / \partial x)\mathbf{i} + (\partial U / \partial y)\mathbf{j} + (\partial U / \partial z)\mathbf{k}$ .

If a fluid has the property of barotropy characterized by an unambiguous relation between the pressure and density (this occurs, for example, in an adiabatic flow, for which  $p = A\rho^k$ ), then the ratio  $dp/\rho$  equals the differential of a certain function  $P$  and, therefore,

$$(1/\rho) \text{grad } p = \text{grad } P$$

With a view to this equation, expression (3.4.2) becomes

$$\partial(\text{grad } \varphi) / \partial t + \text{grad } (V^2/2) = -\text{grad } U - \text{grad } P$$

Substituting the quantity  $\text{grad } (\partial \varphi / \partial t)$  for the derivative  $\partial(\text{grad } \varphi) / \partial t$ , we obtain

$$\text{grad } (\partial \varphi / \partial t) + \text{grad } (V^2/2) = -\text{grad } U - \text{grad } P \quad (3.4.3)$$

Going over from the relation for the gradients to one between the corresponding scalar functions, we find

$$\partial\varphi/\partial t + V^2/2 + P + U = C(t) \quad (3.4.4)$$

where

$$P = \int dp/\rho \quad (3.4.5)$$

Expression (3.4.4) is known as the **Lagrange equation or integral**. The right-hand side of (3.4.4) is a function that *depends on the time*, but does not depend on the coordinates, i.e. is *identical for any point of a potential flow*. The terms on the left-hand side of (3.4.4) have a simple physical meaning:  $V^2/2$  is the kinetic energy,  $P = \int dp/\rho$  is the potential energy due to the pressure for a unit mass, and  $U$  is the potential energy due to the position of the fluid particles and related to their mass.

To reveal the physical meaning of the first term, let us use the expression for the potential function  $\partial\varphi/\partial s = V_s$ , where  $V_s$  is the projection of the velocity vector onto a certain direction  $s$ . We can determine the function  $\varphi$  from the condition  $\varphi = \int_{s_0}^s V_s ds$  (where  $s_0$  and  $s$  are the coordinates of a fixed and an arbitrary point, respectively). The derivative  $\partial\varphi/\partial t = \int_{s_0}^s (\partial V_s/\partial t) ds$ .

The local acceleration  $\partial V_s/\partial t$  can be considered as the projection of the inertia force due to the presence of local acceleration and related to unit mass, and the product  $(\partial V_s/\partial t) ds$  as the work done by this force on the section  $ds$ . Accordingly, the derivative  $\partial\varphi/\partial t$  equals the work done by the inertia force on the section between points  $s_0$  and  $s$  and can be considered as the energy of unit mass due to the change in time of the velocity and the pressure associated with it at the given point.

With a view to the above, the expression on the left-hand side of (3.4.4) is the total energy of a unit mass of the gas. Hence, the Lagrange equation establishes the fact that the total energy of unit mass at a given instant is a quantity identical for all points of the potential flow.

For an incompressible fluid whose motion occurs under the action of mass and pressure forces, integral (3.4.4) has the form

$$\partial\varphi/\partial t + V^2/2 + p/\rho + U = C(t) \quad (3.4.6)$$

If, particularly, the  $y$ -axis is directed vertically upward, then  $U = gy$ , and

$$\partial\varphi/\partial t + V^2/2 + p/\rho + gy = C(t) \quad (3.4.6')$$

Of major practical significance is the particular case of a steady potential flow for which  $\partial\phi/\partial t = 0$  and the function  $C(t) = \text{const}$ , i.e. is independent of the time. In this case, Eq. (3.4.4) is reduced to the form

$$V^2/2 + \int dp/\rho + U = \text{const} \quad (3.4.7)$$

This partial form of the Lagrange equation is called the **Euler equation**. It expresses the law according to which *the total energy of a unit mass is a constant quantity for all points of the steady potential flow*. Hence, the constant in the Euler equation is the same not only for the entire region of a flow, but also, unlike the function  $C(t)$  of the Lagrange integral, *is independent of the time*.

The Euler equation for an incompressible fluid ( $\rho = \text{const}$ ) has the same form as (3.4.7), the only difference being that instead of  $\int dp/\rho$  it includes the ratio  $p/\rho$ .

Let us consider the more general case of a non-potential steady flow of a gas. The equation of this motion has the form

$$\text{grad } (V^2/2) + \text{curl } \mathbf{V} \times \mathbf{V} = -\text{grad } P - \text{grad } U \quad (3.4.8)$$

or

$$\text{grad } (V^2/2 + \int dp/\rho + U) = -\text{curl } \mathbf{V} \times \mathbf{V} \quad (3.4.8')$$

The right-hand side of (3.4.8') equals zero if the vectors  $\text{curl } \mathbf{V}$  and  $\mathbf{V}$  are parallel, i.e. provided that a vortex line and streamline coincide. In this case, we have

$$V^2/2 + \int dp/\rho + U = C_1 \quad (3.4.9)$$

This equation was first obtained by I. Gromeka. The constant  $C_1$  is the same for the entire region where the condition of the coincidence of the vortex lines and streamlines is observed. Such regions, to study which the Gromeka equation is used, appear, for example, in a flow past a finite-span wing. This flow is characterized by the formation of vortices virtually coinciding in direction near the wing with the streamlines. A flow does not always contain such regions, however. A flow is customarily characterized by the presence of vortex lines and streamlines not coinciding with one another. The family of vortex lines is given by Eq. (2.6.1), and that of the streamlines (pathlines), by Eq. (2.1.6). The flow being considered is described by Eq. (3.4.8').

Let us take the vector of the arc in the form  $d\mathbf{s} = dx\mathbf{i} + dy\mathbf{j} + dz\mathbf{k}$  belonging to a streamline or vortex line, and determine the dot product

$$d\mathbf{s} \cdot \text{grad } (V^2/2 + \int dp/\rho + U) = -d\mathbf{s} \cdot (\text{curl } \mathbf{V} \times \mathbf{V})$$

The left-hand side in this equation is the total differential of the trinomial in parentheses, consequently,

$$d(V^2/2 + \int dp/\rho + U) = -ds \cdot (\text{curl } \mathbf{V} \times \mathbf{V}) \quad (3.4.10)$$

The product  $\text{curl } \mathbf{V} \times \mathbf{V}$  is a vector perpendicular to the vectors  $\text{curl } \mathbf{V}$  and  $\mathbf{V}$ . The dot product of this vector and the vector  $ds$  is zero in two cases: *when the vector  $ds$  coincides with the direction of a streamline (pathline) or when this vector coincides with the direction of a vortex*. In these two cases, the following solution of the equation of motion is valid:

$$V^2/2 + \int dp/\rho + U = C_2 \quad (3.4.11)$$

where the value of the constant  $C_2$  depends on what pathline or vortex line is being considered.

Relation (3.4.11) is known as the **Bernoulli equation**. It is obvious that for various vortex lines passing through points on a given streamline, the constant is the same as for the streamline. In exactly the same way, the constants are identical for a family of streamlines (pathlines) and the vortex through whose points a streamline passes.

One must clearly understand the distinction between the Gromeka and Bernoulli equations considered above. They are both derived for a vortex (non-potential) flow, however the first of them reflects the fact that the total energy of a unit mass of the gas is constant *in the entire region* where the vortex lines and streamlines coincide, while the second equation establishes the law according to which this energy is constant along a given *streamline or vortex line*. Accordingly, in the Gromeka equation, the constant is the same for the entire flow region being considered, whereas in the Bernoulli equation it relates to a given streamline or vortex line. Naturally, in the general case, the two constants  $C_1$  and  $C_2$  are not the same. From the above, there also follows a distinction, on the one hand, between these equations, and, on the other, between the Lagrange and Euler equations relating to an *unsteady and steady vortex-free (potential) flow*, respectively, and also between each of the considered equations.

When studying the flow of a fluid, investigators give the greatest favour to the Bernoulli equation related to the conditions on the streamlines (pathlines). It is known that the constant  $C_2$  in this equation (3.4.11) is determined for every streamline being considered. If, however, a steady flow is also vortex-free (potential), the Bernoulli equation coincides with the Euler equation, and, therefore, the constant is identical for all the streamlines, i.e. for the entire flow region.

Let us consider some specific forms of the Bernoulli equation. For an incompressible fluid and provided that the function  $U = gy$ ,

we shall write this equation in the form

$$V^2/2 + p/\rho + yg = C_2 \quad (3.4.12)$$

When studying the motion of a gas, we may disregard the influence of the mass forces. Consequently, we must assume that  $U = 0$  in Eq. (3.4.11) and the other integrals. Particularly, instead of (3.4.12), we have

$$V^2/2 + p/\rho = C_2 \quad (3.4.13)$$

Let us consider the motion of an ideal compressible gas. In such a gas, heat transfer processes due to viscosity (heat conduction, diffusion) are absent. Assuming also that the gas does not radiate energy, we shall consider its adiabatic (isentropic) motion. Examination of energy equation (3.2.14) reveals that Eq. (3.3.1) holds for such an inviscid gas in the absence of radiation ( $\epsilon = 0$ ). Consequently, the Bernoulli integral is

$$V^2/2 + i = C \quad (3.4.14)$$

In this form, the Bernoulli integral is an energy equation for an isentropic flow. According to this equation, the sum of the kinetic energy and enthalpy of a gas particle is constant. Assuming that  $i = c_p T = c_p p / (\rho R)$ ,  $c_p - c_v = R$ , and  $k = c_p/c_v$ , we find

$$i = [k/(k-1)] p/\rho \quad (3.4.15)$$

Consequently,

$$V^2/2 + [k/(k-1)] p/\rho = C \quad (3.4.16)$$

or

$$V^2/2 + kRT/(k-1) = C \quad (3.4.16')$$

The Bernoulli equation for an ideal compressible gas is the theoretical foundation for investigating the laws of isentropic flows of a gas.

### 3.5. Aerodynamic Similarity

#### Concept of Similarity

The aerodynamic characteristics of craft or their individual elements can be determined both theoretically and experimentally. The theoretical approaches are based on the use of a system of equations of gas dynamics that is solved as applied to a body in a flow, the body having a given configuration and arbitrary absolute dimensions.

When running experiments intended for obtaining aerodynamic parameters that can be used directly for further ballistic calculations or for verifying the results of theoretical investigations, it is not always possible to use a full-scale body because of its large size, and a smaller-size model of the body has to be used. In this con-

nection, the question appears on the possibility of transferring the experimental results obtained to full-scale bodies. The answer to this question is given by the **dimensional analysis and similarity method**. The latter establishes the conditions that must be observed in scale-model experiments and indicates characteristic and convenient parameters determining the basic effects and flow conditions.

Let us assume that measurements in a wind tunnel yielded a drag force which in accordance with (1.3.5) is  $X_{\text{mod}} = c_{x,\text{mod}} q_{\text{mod}} S_{\text{mod}}$ . Now let us see when we can use the result obtained to determine the drag force of a full-scale body in accordance with the formula  $X_{\text{fs}} = c_{x,\text{fs}} q_{\text{fs}} S_{\text{fs}}$  in which the drag coefficient  $c_{x,\text{fs}}$  for this body is an unknown quantity, while the velocity head  $q_{\text{fs}}$  and the reference or characteristic area  $S_{\text{fs}}$  are given. From the two formulas for  $X_{\text{fs}}$  and  $X_{\text{mod}}$ , we obtain

$$X_{\text{fs}} = X_{\text{mod}} (c_{x,\text{fs}}/c_{x,\text{mod}}) (q_{\text{fs}} S_{\text{fs}}/q_{\text{mod}} S_{\text{mod}}) \quad (3.5.1)$$

A glance at this expression reveals that the experimental value  $X_{\text{mod}}$  can be used to evaluate the full-scale force  $X_{\text{fs}}$  only upon the equality of the aerodynamic coefficients  $c_{x,\text{mod}}$  and  $c_{x,\text{fs}}$  because the quantities  $q_{\text{mod}} S_{\text{mod}}$  and  $q_{\text{fs}} S_{\text{fs}}$  are determined unambiguously by the given values of the velocity heads and the reference areas.

Here both flows—the model and full-scale ones—have the property of **dynamic similarity**. It consists in this case in that the preset force characteristic of one flow (the drag  $X_{\text{mod}}$ ) is used to find the characteristic of the other flow (the force  $X_{\text{fs}}$ ) by simple conversion, similar to the transition from one system of units of measurement to another.

The requirements whose satisfaction in the given case ensures the equality  $c_{x,\text{mod}} = c_{x,\text{fs}}$ , and in the general case of other dimensionless aerodynamic coefficients too, are established in the dimensional analysis and similarity method proceeding either from the physical nature of the phenomenon being studied or from the corresponding differential equations of aerodynamics.

Considering the expression for the aerodynamic coefficient

$$c_{x,a} = \int_{(S)} [\bar{p} \cos(nx_a) + c_{f,x} \cos(\hat{t}x_a)] \frac{dS}{S_r} \quad (3.5.2)$$

obtained from (1.3.2), we can see that this coefficient depends on dimensionless geometric parameters, and also on dimensionless quantities such as the pressure coefficient and local friction factor. Hence it follows that the aerodynamic coefficients for a full-scale object and an experimental one with different absolute dimensions remain constant if these bodies are geometrically similar and an identical distribution of the coefficients  $\bar{p}$  and  $c_{f,x}$  over their surface is ensured.

If we consider a steady uniform flow over a body in the absence of heat transfer, the coefficients  $\bar{p}$  and  $c_{f,x}$  with a given configuration

of the body in the flow and known values of the angle of attack and the sideslip angle, as well as of the rudder and elevator angles, will be functions of the free stream velocity  $V_\infty$ , the pressure  $p_\infty$ , the density  $\rho_\infty$ , the dynamic viscosity  $\mu_\infty$ , the specific heats  $c_p\infty$  and  $c_v\infty$  of the gas, as well as of a certain characteristic (reference) linear dimension of the body  $L$ . Consequently, the drag coefficient will also depend on these parameters, and we can compile a functional relation for it in the form  $c_x = f(V_\infty, p_\infty, \rho_\infty, \mu_\infty, c_p\infty, c_v\infty, L)$ . Since this coefficient is a dimensionless quantity, it must also be a function of dimensionless parameters. From the general considerations of the dimensional method, it follows that the seven different arguments of the function  $c_x$  can be reduced to three. The latter are dimensionless combinations compiled from  $V_\infty, p_\infty, \rho_\infty, \mu_\infty, c_p\infty, c_v\infty$ , and  $L$  because there are four independent units of measurement, namely, mass, length, time, and temperature. These dimensionless combinations have the following form:  $V_\infty \sqrt{k_\infty p_\infty / \rho_\infty} = V_\infty / a_\infty = M_\infty$ —the Mach number for an undisturbed flow;  $V_\infty \rho_\infty L / \mu_\infty = Re_\infty$ —the Reynolds number based on the parameters of an undisturbed flow and the characteristic linear dimension  $L$ ;  $c_p\infty / c_v\infty = k_\infty$ —the adiabatic exponent.

In the expression for  $M_\infty$ , it is assumed that  $\sqrt{k_\infty p_\infty / \rho_\infty} = a_\infty$  is the speed of sound in the undisturbed flow. Indeed, in accordance with the general expression for the speed of sound  $a^2 = dp/d\rho$ , and also with a view to the adiabatic nature of propagation of sonic disturbances in a gas, according to which  $p = A\rho^k$ , we have  $a^2 = d(A\rho^k)/d\rho = kp/\rho$ . Accordingly, the square of the speed of sound in an undisturbed flow is  $a_\infty^2 = k_\infty p_\infty / \rho_\infty$ . Hence, the ratio  $V_\infty / \sqrt{k_\infty p_\infty / \rho_\infty} = V_\infty / a_\infty$ . All other dimensionless combinations except for  $M_\infty$ ,  $Re_\infty$ , and  $k_\infty$  formed from the seven parameters indicated above or in general from any quantities that can be determined by them are functions of the combinations  $M_\infty$ ,  $Re_\infty$ , and  $k_\infty$ . Consequently, the drag coefficient is

$$c_x = f(M_\infty, Re_\infty, k_\infty) \quad (3.5.3)$$

Similar expressions can be obtained for the other aerodynamic coefficients. It follows from these expressions that when the numbers  $M_\infty$ ,  $Re_\infty$  and the parameter  $k_\infty$  for a model and a full-scale flows are equal, the aerodynamic coefficients for geometrically similar bodies are the same. Hence, an important conclusion can be made in the dimensional analysis and similarity method in accordance with which the necessary and sufficient condition for aerodynamic similarity is the constancy of the numerical values of the dimensionless combinations forming what is called a base, i.e. a system of dimensionless quantities determining all the other parameters of a flow. These dimensionless combinations are called **similarity criteria**.

The similarity criteria given above have a definite physical meaning. In accordance with the expression  $a^2 = dp/d\rho$ , the speed of sound can be considered as a criterion depending on the property of compressibility, i.e. on the ability of a gas to change its density with a change in the pressure. Consequently, the Mach number is the similarity criterion that is used to characterize the *influence of compressibility on the flow of a gas*. The Reynolds number is a parameter used to appraise the *influence of viscosity on a gas in motion*, while the parameter  $k_\infty = c_{p\infty}/c_{r\infty}$  determines the features of a flow due to the *thermodynamic properties of a gas*.

#### Similarity Criteria Taking Account of the Viscosity and Heat Conduction

In the more general conditions of flow characterized by the influence of a number of other physical and thermodynamic parameters on the aerodynamic properties of craft, the dynamic similarity criteria are more complicated and diverse. To establish these criteria, we can use a different approach of the dimensional analysis and similarity method based on the use of the equation of motion of a viscous heat-conducting gas.

Let us write these equations in the dimensionless form, i.e. in a form such that the parameters (velocity, pressure, temperature, etc.) in the equations are related to reference parameters. The latter are constants for a given flow and determine its scale. We shall take as references the parameters of the free stream: its velocity  $V_\infty$ , pressure  $p_\infty$ , density  $\rho_\infty$ , temperature  $T_\infty$ , dynamic viscosity  $\mu_\infty$  (or, respectively, the kinematic viscosity  $v_\infty$ ), and so on. It must be remembered that of the three parameters  $p_\infty$ ,  $\rho_\infty$ , and  $T_\infty$ , two may be set arbitrarily, while the third one is determined from the first two with the aid of an equation of state. The quantity  $t_\infty$  is the reference time characterizing unsteady flow conditions, while a characteristic linear dimension  $L$  (for example, the length of the body in the flow) is the reference length. The acceleration of free fall  $g$  can be chosen as the reference acceleration of the mass forces. The dimensionless variables for the length and time have the form

$$\bar{x} = x/L, \bar{y} = y/L, \bar{z} = z/L, \bar{t} = t/t_\infty \quad (3.5.4)$$

while those for the velocity, pressure, density, viscosity, and mass forces have the following form:

$$\left. \begin{aligned} \bar{V}_x &= V_x/V_\infty, & \bar{V}_y &= V_y/V_\infty, & \bar{V}_z &= V_z/V_\infty, & \bar{p} &= p/p_\infty, \\ \bar{\rho} &= \rho/\rho_\infty \\ \bar{\mu} &= \mu/\mu_\infty, & \bar{v} &= v/v_\infty, & \bar{X} &= X/g, & \bar{Y} &= Y/g, & \bar{Z} &= Z/g \end{aligned} \right\} \quad (3.5.5)$$

Let us introduce dimensionless variables into the equation of motion (3.1.17) and the continuity equation (2.4.2). We shall use only the first equation of system (3.1.17) for transformation because the other two equations are compiled in a similar way. Let us write the indicated equations using dimensionless variables:

$$\begin{aligned} \frac{V_\infty}{t_\infty} \cdot \frac{\partial \bar{V}_x}{\partial t} + \frac{V_\infty^2}{L} \left( \bar{V}_x \frac{\partial \bar{V}_x}{\partial \bar{x}} + \bar{V}_y \frac{\partial \bar{V}_x}{\partial \bar{y}} + \bar{V}_z \frac{\partial \bar{V}_x}{\partial \bar{z}} \right) &= g \bar{X} \\ - \frac{\rho_\infty}{\rho_\infty L} \cdot \frac{1}{\bar{\rho}} \cdot \frac{\partial \bar{p}}{\partial \bar{x}} + \frac{v_\infty V_\infty}{L^2} \left\{ \bar{v} \Delta \bar{V}_x + \frac{\bar{v}}{3} \cdot \frac{\partial}{\partial \bar{x}} \operatorname{div} \mathbf{V} \right. \\ + \frac{1}{\bar{\rho}} \left[ \frac{\partial \bar{\mu}}{\partial \bar{x}} \left( 2 \frac{\partial \bar{V}_x}{\partial \bar{x}} - \frac{2}{3} \operatorname{div} \mathbf{V} \right) + \frac{\partial \bar{\mu}}{\partial \bar{y}} \left( \frac{\partial \bar{V}_x}{\partial \bar{y}} + \frac{\partial \bar{V}_y}{\partial \bar{x}} \right) \right. \\ \left. \left. + \frac{\partial \bar{\mu}}{\partial \bar{z}} \left( \frac{\partial \bar{V}_x}{\partial \bar{z}} + \frac{\partial \bar{V}_z}{\partial \bar{x}} \right) \right] \right\} \\ \frac{\rho_\infty}{t_\infty} \cdot \frac{\partial \bar{p}}{\partial \bar{t}} + \frac{\rho_\infty V_\infty}{L} \left[ \frac{\partial (\bar{\rho} \bar{V}_x)}{\partial \bar{x}} + \frac{\partial (\bar{\rho} \bar{V}_y)}{\partial \bar{y}} + \frac{\partial (\bar{\rho} \bar{V}_z)}{\partial \bar{z}} \right] &= 0 \end{aligned}$$

where  $\operatorname{div} \mathbf{V} = \partial \bar{V}_x / \partial \bar{x} + \partial \bar{V}_y / \partial \bar{y} + \partial \bar{V}_z / \partial \bar{z}$ .

From the reference quantities in these equations, we can form dimensionless numbers characterizing the similarity of gas flows. These numbers, named after the scientists who were the first to obtain them, are given in the following form:

$$\left. \begin{aligned} \mathbf{Sh} &= V_\infty t_\infty / L \text{ — the Strouhal number;} \\ \mathbf{Fr} &= V_\infty^2 / (gL) \text{ — the Froude number;} \\ \mathbf{M} &= V_\infty / a_\infty \text{ — the Mach number;} \\ \mathbf{Re} &= V_\infty \rho_\infty L / \mu_\infty = V_\infty L / v_\infty \text{ — the Reynolds number} \\ (\text{the subscript "}\infty\text{" on } \mathbf{M} \text{ and } \mathbf{Re} \text{ has been omitted.)} \end{aligned} \right\} \quad (3.5.6)$$

Here  $a_\infty = \sqrt{k_\infty R T_\infty}$  is the speed of sound in an undisturbed flow ( $k_\infty$  and  $T_\infty$  are the adiabatic exponent and the temperature of a gas in the undisturbed flow, respectively). Introducing these numbers into the equation of motion and the continuity equation, we obtain:

$$\begin{aligned} \mathbf{Sh}^{-1} \frac{\partial \bar{V}_x}{\partial \bar{t}} + \bar{V}_x \frac{\partial \bar{V}_x}{\partial \bar{x}} + \bar{V}_y \frac{\partial \bar{V}_x}{\partial \bar{y}} + \bar{V}_z \frac{\partial \bar{V}_x}{\partial \bar{z}} &= \frac{1}{\mathbf{Fr}} \bar{X} \\ - \frac{1}{k_\infty \mathbf{M}} \cdot \frac{1}{\bar{\rho}} \cdot \frac{\partial \bar{p}}{\partial \bar{x}} + \frac{1}{\mathbf{Re}} \left\{ \bar{v} \Delta \bar{V}_x + \frac{\bar{v}}{3} \cdot \frac{\partial}{\partial \bar{x}} \operatorname{div} \mathbf{V} \right. \\ \left. - \frac{1}{\mathbf{Sh} \mathbf{M}} \left( 2 \frac{\partial \bar{V}_x}{\partial \bar{x}} - \frac{2}{3} \operatorname{div} \mathbf{V} \right) \right\} &= 0 \end{aligned}$$

$$+ \frac{1}{\rho} \left[ \frac{\partial \bar{\mu}}{\partial \bar{x}} \left( 2 \frac{\partial \bar{V}_x}{\partial \bar{x}} - \frac{2}{3} \operatorname{div} \mathbf{V} \right) + \frac{\partial \bar{\mu}}{\partial \bar{y}} \left( \frac{\partial \bar{V}_x}{\partial \bar{y}} + \frac{\partial \bar{V}_y}{\partial \bar{x}} \right) + \frac{\partial \bar{\mu}}{\partial \bar{z}} \left( \frac{\partial \bar{V}_x}{\partial \bar{z}} + \frac{\partial \bar{V}_z}{\partial \bar{x}} \right) \right] \} \quad (3.5.7)$$

$$Sh \frac{\partial \bar{p}}{\partial \bar{t}} + \frac{\partial (\bar{\rho} \bar{V}_x)}{\partial \bar{x}} + \frac{\partial (\bar{\rho} \bar{V}_y)}{\partial \bar{y}} + \frac{\partial (\bar{\rho} \bar{V}_z)}{\partial \bar{z}} = 0 \quad (3.5.8)$$

Let us transform the energy equation (3.2.14) in which we shall exclude terms taking into account radiation and diffusion. We introduce the dimensionless variables

$$\bar{T} = T/T_\infty, \bar{c}_p = c_p/c_{p\infty}, \bar{\lambda} = \lambda/\lambda_\infty \quad (3.5.9)$$

where  $c_{p\infty}$  and  $\lambda_\infty$  are the specific heat and the heat conductivity of a gas in the undisturbed flow, respectively.

Having in view that  $di = c_p dT$  and expanding the total derivative  $dT/dt$ , we obtain after the corresponding substitutions:

$$\begin{aligned} & \frac{\rho_\infty c_{p\infty} T_\infty}{t_\infty} \bar{\rho} \bar{c}_p \frac{\partial \bar{T}}{\partial \bar{t}} + \frac{\rho_\infty c_{p\infty} V_\infty T_\infty}{L} \bar{\rho} \bar{c}_p \left( \bar{V}_x \frac{\partial \bar{T}}{\partial \bar{x}} \right. \\ & \left. + \bar{V}_y \frac{\partial \bar{T}}{\partial \bar{y}} + \bar{V}_z \frac{\partial \bar{T}}{\partial \bar{z}} \right) = \frac{p_\infty}{t_\infty} \cdot \frac{dp}{d\bar{t}} + \frac{\mu_\infty V_\infty^2}{L^2} \bar{\mu} \\ & \times \left\{ \left[ \left( \frac{\partial \bar{V}_x}{\partial \bar{x}} \right)^2 + \left( \frac{\partial \bar{V}_y}{\partial \bar{y}} \right)^2 \right] - \frac{2}{3} \bar{\mu} (\operatorname{div} \mathbf{V})^2 + 4\bar{\mu} \bar{\varepsilon}_z^2 \right\} \\ & + \frac{\lambda_\infty T_\infty}{L^2} \operatorname{div} (\bar{\lambda} \operatorname{grad} \bar{T}) \end{aligned} \quad (3.5.10)$$

Let us introduce the dimensionless Prandtl number

$$Pr = \mu_\infty c_{p\infty} / \lambda_\infty \quad (3.5.11)$$

by means of which we shall compare the relative effect of the viscosity and heat conduction, or, in other words, appraise the relation between the heat flux due to skin friction and the molecular transfer of heat. Hence, taking into account that  $p_\infty/\rho_\infty = RT_\infty = c_{p\infty}(1 - 1/k_\infty) \times T_\infty$ , we have:

$$\begin{aligned} & \bar{\rho} \bar{c}_p \left( Sh^{-1} \frac{\partial \bar{T}}{\partial \bar{t}} + \bar{V}_x \frac{\partial \bar{T}}{\partial \bar{x}} + \bar{V}_y \frac{\partial \bar{T}}{\partial \bar{y}} + \bar{V}_z \frac{\partial \bar{T}}{\partial \bar{z}} \right) \\ & = Sh^{-1} \frac{k_\infty - 1}{k_\infty} \cdot \frac{dp}{d\bar{t}} + \frac{M^2(k_\infty - 1)}{Re} \left\{ \left[ \left( \frac{\partial \bar{V}_x}{\partial \bar{x}} \right)^2 + \left( \frac{\partial \bar{V}_y}{\partial \bar{y}} \right)^2 \right] \right. \\ & \left. - \frac{2}{3} \bar{\mu} (\operatorname{div} \mathbf{V})^2 + 4\bar{\mu} \bar{\varepsilon}_z^2 \right\} + \frac{1}{Re Pr} \operatorname{div} (\bar{\lambda} \operatorname{grad} \bar{T}) \quad (3.5.10') \end{aligned}$$

Let us convert several additional relations of the system of equations of gas dynamics (see Sec. 3.3) to the dimensionless form:

$$\bar{p} = \bar{\rho} \bar{T} \quad (3.5.12)$$

$$\bar{\mu}_m = f_3(p_\infty \bar{p}, T_\infty \bar{T}) (1/\mu_{m\infty}) \quad (3.5.13)$$

$$\bar{\lambda} = f_6(p_\infty \bar{p}, T_\infty \bar{T}) (1/\lambda_\infty) \quad (3.5.14)$$

$$\bar{\mu} = f_7(p_\infty \bar{p}, T_\infty \bar{T}) (1/\mu_\infty) \quad (3.5.15)$$

$$\bar{c}_p = f_8(p_\infty \bar{p}, T_\infty \bar{T}) (1/c_{p\infty}) \quad (3.5.16)$$

Assume that we are investigating two flows over geometrically similar surfaces. For such surfaces, the dimensionless coordinates of analogous points are identical, which is a necessary condition for the aerodynamic similarity of flows. To observe the sufficient condition for such similarity, we must ensure equality of the dimensionless values of the gas-dynamic parameters (velocity, pressure, density, etc.) at analogous points. Since the dimensionless variables are simultaneously solutions of the system of equations (3.5.7), (3.5.8), (3.5.10'), and (3.5.12)-(3.5.16), the indicated equality is evidently observed provided that the systems of dimensionless equations, and also the dimensionless boundary and initial conditions for each flow are the same.

When considering systems of dimensionless equations for two flows, we see that both these systems are identical if:

(1) the similarity criteria are equal:

$$Fr_1 = Fr_2, Re_1 = Re_2, M_1 = M_2, Sh_1 = Sh_2 \quad (3.5.17)$$

(2) the equality of the Prandtl numbers  $Pr_1 = Pr_2$  is observed, i.e.

$$(c_{p\infty} \mu_\infty / \lambda_\infty)_1 = (c_{p\infty} \mu_\infty / \lambda_\infty)_2 \quad (3.5.18)$$

and also the equality of the specific heat ratios for the two gas flows

$$k_{\infty 1} = k_{\infty 2} \quad (3.5.19)$$

(3) each of the equations (3.5.13)-(3.5.16) determines the dependences for the dimensionless variables  $\bar{\mu}_m$ ,  $\bar{\lambda}$ ,  $\bar{\mu}$ , or  $\bar{c}_p$  on the relative quantities  $\bar{p}$  and  $\bar{T}$ , and also on the variables (3.5.17)-(3.5.19). Such relations do not exist for a dissociated gas because similarity criteria of the form of (3.5.17)-(3.5.19) or of some other form cannot be found. This is why the corresponding dimensionless equations (3.5.13)-(3.5.16) are not the same for a full-scale and a model flows, and complete dynamic similarity cannot be ensured.

Two particular cases can be indicated when this similarity is ensured. The first is the flow of an undissociated gas for which the mean molar mass remains constant ( $\mu_{m1} = \mu_{m2}$ ), while the specific

heats, heat conductivity, and viscosity vary depending on the temperature according to a power law of the kind  $y = aT^x$ . In this case, Eqs. (3.5.14)-(3.5.16) for the quantities  $\bar{\lambda}$ ,  $\bar{\mu}$ , and  $\bar{c}_p$  are replaced by the corresponding dependences only on the dimensionless temperature  $\bar{T} = T/T_\infty$ . The second case is the flow of a gas at low speeds when the parameters  $\lambda$ ,  $\mu$ , and  $c_p$  do not depend on the temperature. The corresponding values of these parameters are identical for the full-scale and model flows. For this case, the system of equations includes the dimensionless equations of Navier-Stokes, continuity, energy, and also an equation of state.

The boundary conditions imposed on the solutions of the dimensionless equations give rise to additional similarity criteria. This does not relate to the condition of flow without separation, which does not introduce new similarity criteria. Indeed, this condition in the dimensionless form is

$$\bar{V}_x \frac{\partial \bar{F}}{\partial \bar{x}} + \bar{V}_y \frac{\partial \bar{F}}{\partial \bar{y}} + \bar{V}_z \frac{\partial \bar{F}}{\partial \bar{z}} = 0$$

and is the same both for a full-scale and for a model flow because of the geometrical similarity of the surfaces. But the temperature boundary condition according to which the solution for the temperature must satisfy the equality  $T = T_w$  (here  $T_w$  is the temperature of the wall) introduces an additional similarity criterion. In reality, it follows from the boundary conditions for a full-scale and model surfaces having the form  $T_1 = (T_w)_1$  and  $T_2 = (T_w)_2$ , respectively, that the dimensionless temperatures are  $\bar{T}_1 = (\bar{T}_w)_1$  and  $\bar{T}_2 = (\bar{T}_w)_2$ . From the condition of similarity,  $\bar{T}_1 = \bar{T}_2$ , therefore the equality  $(\bar{T}_w)_1 = (\bar{T}_w)_2$  must be observed. Hence, the boundary condition for the wall temperature leads to an additional similarity criterion:

$$(T_w/T_\infty)_1 = (T_w/T_\infty)_2 \quad (3.5.20)$$

The dimensionless gas-dynamic variables on the surface of a body in a flow, as can be seen from the system of **dimensionless equations** [provided that Eqs. (3.5.13)-(3.5.16) determine  $\bar{\mu}_m$ ,  $\bar{\lambda}$ ,  $\bar{\mu}$ , and  $\bar{c}_p$  as a function of  $\bar{T}$ ] depend on the dimensionless coordinates and the time, and also on the similarity criteria (3.5.17)-(3.5.19). Particularly, the dimensionless pressure can be represented as the function

$$p/p_\infty = \varphi_1 (Fr, Re, M, Sh, Pr, k_\infty, \bar{T}_w, \bar{x}, \bar{y}, \bar{z}, \bar{t}) \quad (3.5.21)$$

We can use the known pressure distribution to determine the dimensionless drag force coefficient for a given instant:

$$c_{x_*} = X_a/(q_\infty S) = \varphi_2 (Fr, Re, M, Sh, Pr, k_\infty, \bar{T}_w) \quad (3.5.22)$$

This expression determines the dependence of the aerodynamic drag coefficient on the dimensionless similarity criterion more completely than (3.5.3). But relation (3.5.22) does not reflect all the features of flow of a dissociated gas because it was obtained from the simplified equations (3.5.13)-(3.5.16). Consequently, formula (3.5.22) is less accurate for such a flow than for that of an undisassociated gas, and determines only partial similarity.

The similarity criteria on which a dimensionless aerodynamic variable depends have a definite physical meaning and characterize the real factors affecting the aerodynamic force.

The Froude number  $Fr$  is a similarity criterion taking into account the influence of the mass force (force of gravity) on the drag. It can be seen from the equation of motion given in the dimensionless form that the number  $Fr$  equals the ratio of the quantity  $V_\infty^2/L$  due to the influence of the inertia forces to the scaling of the mass forces  $g$ . The equality of the Froude numbers  $Fr$  for a full-scale body and its geometrically similar model signifies that they have identical drag coefficients due to the influence of the force of gravity of the fluid. This similarity criterion is of no significance when studying gas flows because the influence of the force of gravity of a gas on motion is negligibly small. But the importance of this criterion may be appreciable in hydrodynamics, particularly in the experimental investigation of the wave resistance of various navigable vessels.

When a body moves in a real fluid, the aerodynamic forces depend on the viscosity. The viscous force is characterized by the Reynolds number  $Re$  that can be obtained as the ratio of the quantity  $V_\infty^2/L$  describing the influence of inertia forces to the parameter  $v_\infty V_\infty/L^2$  determining the influence of the viscosity. If the equality of the Reynolds numbers for two geometrically similar flows is observed, the condition of partial aerodynamic similarity with account taken of the influence of viscosity is satisfied. In this condition, the friction factors for a full-scale and a model bodies are equal.

The similarity with respect to the Mach number is obtained from the ratio of the quantity  $V_\infty^2/L$  to the parameter  $p_\infty/(\rho_\infty L)$  that takes into account the influence of the pressure forces depending on the compressibility of the gas. The partial similarity of two flows of a compressible gas flowing over geometrically similar bodies is observed when the Mach numbers are equal.

When investigating unsteady flow, similarity with respect to the Strouhal number is significant. It is obtained by comparing the inertia forces and the forces due to the influence of the unsteadiness, i.e. from the ratio of the quantities  $V_\infty^2/L$  and  $V_\infty/t_\infty$ . Two unsteady flows around a full-scale body and a model have partial aerodynamic similarity with identical values of the Strouhal number.

The similarity criteria with respect to the Prandtl number  $Pr$

and the ratio of the specific heats are due to definite requirements to the physical properties of the gases in the full-scale and model flows. The gases may differ, but their physical properties must observe the equalities  $Pr_1 = Pr_2$  and  $k_{\infty 1} = k_{\infty 2}$ . The Prandtl number depends on the dynamic viscosity and the heat conductivity. The dynamic viscosity reflects the properties of a gas which the molecular transfer of the momentum depends on, while the heat conductivity characterizes the intensity of the molecular transfer of heat. Consequently, the Prandtl number  $Pr = \mu c_p \infty / \lambda \infty$  is the measure of the transformation of the energy of molecular transfer into heat. For a gas,  $Pr < 1$ .

A dimensionless variable of the aerodynamic force or heat transfer is a composite function of a number of similarity criteria, each of which reflects the influence of a definite physical process. Complete similarity of a full-scale and a model flows can be ensured only when equality of all the similarity criteria is observed. In practice, this cannot be done because some of these criteria are contradictory.

Let us consider, for example, the Reynolds, Froude, and Mach numbers. For the observance of similarity with respect to the skin friction forces, it is essential that  $V_1 L_1 / v_1 = V_2 L_2 / v_2$ . If we assume that for a full-scale and model flows the coefficients  $v_1 = v_2$ , then the speed of the model flow  $V_2 = V_1 (L_1 / L_2)$ , i.e. it is greater than the speed of the full-scale flow the same number of times that the model of the body in the flow is less than the full-scale one.

To ensure similarity with respect to the forces of gravity, it is necessary to ensure equality of the Froude numbers, i.e.  $V_1^2 / (L_1 g_1) = V_2^2 / (L_2 g_2)$ , whence it follows that if experiments were run at identical values of  $g$ , then the speed of the model flow is  $V_2 = V_1 \sqrt{L_2 / L_1}$ . We can see that in the given case the speed  $V_2$  for the small-size model must be smaller than  $V_1$  instead of greater as in the previous example.

Upon equality of the Mach numbers, we have  $V_1 / a_1 = V_2 / a_2$ . Assuming for simplification that  $a_2 = a_1$ , we obtain the condition for equality of the speeds of the model and full-scale flows.

It is natural that all these conditions for the speed cannot be observed simultaneously, therefore we can consider only incomplete similarity. We must note, however, that in practice there is no need to satisfy all the similarity criteria because their influence in a specific case of motion is not the same. For example, the forces of skin friction and pressure have a more significant influence on the flow of a gas over a body than the forces of gravity, and accordingly the numbers  $Re$  and  $M$  are more significant than  $Fr$ . In this connection, the Froude number is not taken into consideration as a similarity criterion in such cases.

If at the same time the speeds are not great, then the influence of the pressure forces due to compressibility of the gas is negligibly small, and, consequently, no account may be taken of the similarity criterion with respect to the Mach number, assuming that the aerodynamic coefficient depends on the Reynolds number.

The aerodynamic force, moment, or heat flux from a gas to a surface is the result of the action of a moving gas on a body. Various processes occur simultaneously in the gas: skin friction, compression (or expansion), heating, a change in the physical properties, etc. Therefore, one must try to satisfy the maximum number of similarity criteria. For example, it is expedient that the equality of the Reynolds and Mach numbers for a full-scale and model flows be retained simultaneously, i.e.  $Re_1 = Re_2$  and  $M_1 = M_2$ . This is especially important when studying aerodynamic forces, which for bodies with a large surface may consist of equivalent components depending on the friction and pressure due to compressibility. This condition can be ensured when running experiments in variable density wind tunnels.

If tests are being performed in a gas flow in which the speed of sound is the same as in the full-scale flow ( $a_2 = a_1$ ), it follows from the equality of the Mach numbers that  $V_2 = V_1$ . Having this in view and using the equality  $Re_1 = Re_2$  or, which is the same,  $V_2 \rho_2 L_2 / \mu_2 = V_1 \rho_1 L_1 / \mu_1$ , we obtain  $L_2 \rho_2 / \mu_2 = L_1 \rho_1 / \mu_1$ . Assuming that  $\mu_2 = \mu_1$ , we find that the density of the gas in the wind tunnel flow is  $\rho_2 = \rho_1 (L_1 / L_2)$ . Assuming that the temperature of the full-scale and model flows is the same ( $T_2 = T_1$ ) and using an equation of state, we obtain the condition  $p_2 = p_1 (L_1 / L_2)$ . Hence, to simultaneously ensure similarity with respect to the forces of skin friction and of pressure with account taken of compressibility, i.e. to observe the equalities  $Re_1 = Re_2$  and  $M_1 = M_2$ , it is essential that the static pressure in the flow of a gas produced by a wind tunnel be greater than the pressure in the full-scale flow by the same number of times by which the model is smaller than the full-scale body. The design of a wind tunnel makes it possible within known limits to control the static pressure in the model flow of a gas depending on the size of the model.

With a known approximation, the influence of heat transfer may not be taken into account when determining the force interaction. Here the aerodynamic coefficients will depend on the numbers  $Re$ ,  $M$ , and  $Sh$ . If in addition the tests are conducted in a gas for which  $k_{\infty 2} = k_{\infty 1}$ , we have

$$c_x = f(Re, M, Sh) \quad (3.5.23)$$

For a steady flow

$$c_x = f(Re, M) \quad (3.5.24)$$

### 3.6. Isentropic Gas Flows

#### Configuration of Gas Jet

Let us consider the steady motion of an ideal (inviscid) gas in a stream or jet with a small expansion and a slight curvature. Motion in such a jet can be studied as one-dimensional, characterized by the change in the parameters depending on one linear coordinate measured along the axis of the jet. For a steady flow, the parameters determining this flow are identical in each cross section at any instant. If the width of the jet is small in comparison with the radius of curvature of the centre line, the lateral pressure gradient may be disregarded, and one may consider that the pressure at each point of the jet cross section is the same.

The consideration of such a one-dimensional steady flow of a compressible gas leads to the simplest approximate solution of the equations of gas dynamics. Condition (2.4.51) of a constant mass flow is retained along the jet, i.e.  $\rho_1 V_1 S_1 = \rho_2 V_2 S_2 = \rho_3 V_3 S_3 = \dots$ , or  $\rho V S = \text{const}$ , where the subscripts 1, 2, 3 signify the corresponding parameters of the gas at the control surfaces. Cross sections of the channel with an area of  $S_1$ ,  $S_2$ , and  $S_3$  have been chosen as these surfaces. Taking logarithms, we obtain  $\ln \rho + \ln V + \ln S = \text{const}$ . Differentiation of this expression yields

$$d\rho/\rho + dV/V + dS/S = 0$$

whence

$$\frac{dS}{dV} = -S \left( \frac{1}{V} + \frac{1}{\rho} \cdot \frac{d\rho}{dV} \right) \quad (3.6.1)$$

Let us use relation (3.4.14), by differentiation of which we have

$$V \cdot dV = -di \quad (3.6.2)$$

Substituting  $d\rho/\rho$  for  $di$ , we find

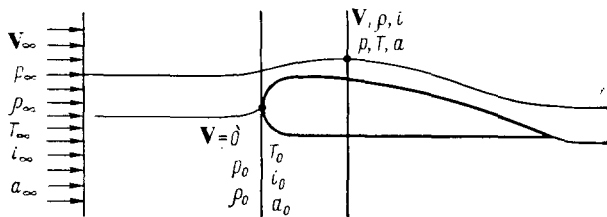
$$V \cdot dV = -dp/\rho \quad (3.6.3)$$

Taking the speed of sound  $a = \sqrt{dp/d\rho}$  into account and using relation (3.6.3), we transform (3.6.1) to the form

$$dS/dV = (S/V)(M^2 - 1) \quad (3.6.4)$$

where  $M = V/a$  is the Mach number in the given cross section of the jet.

Let us assume that the velocity along the jet grows ( $dV > 0$ ), but remains subsonic and, consequently,  $M < 1$ . A glance at (3.6.4) reveals that for this case the derivative  $dS/dV < 0$ . This indicates that the jet converges downstream. Conversely, for a subsonic

**Fig. 3.6.1**

Parameters of a gas flowing over a body

flow with a diminishing velocity ( $M < 1$ ,  $dV < 0$ ), the cross section increases, which is indicated by the inequality  $dS > 0$  following from (3.6.4).

Let us consider a supersonic flow ( $M > 1$ ). If the velocity decreases, then, as can be seen from (3.6.4), the differential  $dS < 0$ , and, consequently, the jet converges. Conversely, when the velocity grows, the value of  $dS > 0$ , i.e. the jet diverges.

Let us take a nozzle that first has the shape of a converging, and then of a diverging channel. In definite conditions in the converging part of the nozzle, a subsonic flow is accelerated, reaching the speed of sound in the narrowest cross section [here  $dS = 0$  and, as follows from (3.6.4),  $M = 1$ ], and then becomes supersonic. This is how nozzles are designed in rocket engines, gas turbines, and wind tunnels intended for obtaining supersonic flows.

### Flow Velocity

Let us consider a gas jet flowing over a surface (Fig. 3.6.1). We shall denote the free-stream parameters by  $V_\infty$ ,  $p_\infty$ ,  $\rho_\infty$ ,  $T_\infty$ ,  $i_\infty$ , and  $a_\infty$ , and the parameters for the part of the jet in the disturbed region by the same symbols without subscripts. To find the velocity in an arbitrary cross section of the jet, we shall use Eq. (3.4.14) in which we shall determine the constant  $C$  according to the preset parameters of the free stream:

$$C = V_\infty^2/2 + i_\infty \quad (3.6.5)$$

With this in view, we have

$$V^2/2 + i = V_\infty^2/2 + i_\infty$$

whence

$$V = \sqrt{V_\infty^2/2 + 2(i_\infty - i)} \quad (3.6.6)$$

At the stagnation point,  $V = 0$ , consequently the enthalpy is

$$i = i_0 = V_\infty^2/2 + i_\infty \quad (3.6.7)$$

Hence, the constant  $C$  as regards its physical meaning can be considered as the stagnation enthalpy. With a view to this value of  $C$ , the velocity in the jet is

$$V = \sqrt{2(i_0 - i)} \quad (3.6.8)$$

The stagnation pressure  $p_0$  and density  $\rho_0$  correspond to the enthalpy  $i_0$ . They are determined from the condition

$$i_0 = \frac{k}{k-1} \cdot \frac{p_0}{\rho_0} = \frac{V_\infty^2}{2} + i_\infty = \frac{V_\infty^2}{2} + \frac{k}{k-1} \cdot \frac{p_\infty}{\rho_\infty} \quad (3.6.9)$$

We can rewrite Eq. (3.6.9) as follows:

$$\frac{V^2}{2} + \frac{k}{k-1} \cdot \frac{p}{\rho} = \frac{k}{k-1} \cdot \frac{p_0}{\rho_0} \quad (3.6.10)$$

Since the flow is isentropic, we have

$$p/\rho^k = p_0/\rho_0^k \quad (3.6.11)$$

consequently

$$V = \sqrt{\frac{2k}{k-1} \cdot \frac{p_0}{\rho_0} \left[ 1 - \left( \frac{p}{p_0} \right)^{(k-1)/k} \right]} \quad (3.6.12)$$

Seeing that for conditions of stagnation the speed of sound is  $a_0 = \sqrt{kp_0/\rho_0}$ , we find

$$V = a_0 \sqrt{\frac{2}{k-1} \left[ 1 - \left( \frac{p}{p_0} \right)^{(k-1)/k} \right]} \quad (3.6.13)$$

Examination of (3.6.8) reveals that the velocity along the jet grows with diminishing of the enthalpy, and therefore more and more of the heat is converted into kinetic energy. The maximum velocity is reached provided that the enthalpy  $i = 0$ , i.e. all the heat is spent to accelerate the gas. The value of this velocity is

$$V_{\max} = \sqrt{2i_0} \quad (3.6.14)$$

or with a view to (3.6.9):

$$V_{\max} = \sqrt{\frac{2k}{k-1} \cdot \frac{p_0}{\rho_0}} = a_0 \sqrt{\frac{2}{k-1}} \quad (3.6.15)$$

Accordingly, the velocity in an arbitrary section is

$$V = V_{\max} \sqrt{1 - i/i_0} \quad (3.6.16)$$

or

$$V = V_{\max} \sqrt{1 - (p/p_0)^{(k-1)/k}} \quad (3.6.17)$$

In the narrowest, critical, cross section of the jet, the velocity equals the local speed of sound. The latter is called critical and is

designated by  $a^*$ . The critical pressure  $p^*$  and density  $\rho^*$  correspond to the critical speed. It follows from the Bernoulli equation that for the critical section we have

$$\frac{a^{*2}}{2} + \frac{k}{k-1} \cdot \frac{p^*}{\rho^*} = \frac{k}{k-1} \cdot \frac{p_0}{\rho_0}$$

Having in view that  $k p^*/\rho^* = a^{*2}$ , the critical speed is

$$a^* = \sqrt{\frac{2k}{k+1} \cdot \frac{p_0}{\rho_0}} = a_0 \sqrt{\frac{2}{k+1}} \quad (3.6.18)$$

or, taking into account (3.6.15),

$$a^* = V_{\max} \sqrt{(k-1)/(k+1)} \quad (3.6.19)$$

To determine the **local sound speed**  $a$ , we shall use Eq. (3.6.10). Performing the substitutions  $a^2 = kp/\rho$  and  $a_0^2 = kp_0/\rho_0$  in it, we obtain

$$a^2 = a_0^2 - \frac{k-1}{2} V^2 \quad (3.6.20)$$

or

$$a^2 = \frac{k+1}{2} a^{*2} - \frac{k-1}{2} V^2 \quad (3.6.21)$$

$$a^2 = \frac{k-1}{2} (V_{\max}^2 - V^2) \quad (3.6.22)$$

Let us introduce the **velocity ratio (relative velocity)**  $\lambda = V/a^*$ . Dividing Eq. (3.6.21) by  $V^2$  and having in view that the ratio  $V/a = M$ , we can establish the relation between  $\lambda$  and  $M$ :

$$\lambda^2 = [(k+1)/2] M^2 / \{1 + [(k-1)/2] M^2\} \quad (3.6.23)$$

Hence it follows that in the cross section of the jet where  $V_{\max}$  is reached, the number  $M = \infty$ . We find the corresponding value of  $\lambda = \lambda_{\max}$  from (3.6.23) provided that  $M \rightarrow \infty$ :

$$\lambda_{\max} = \sqrt{(k+1)/(k-1)} \quad (3.6.24)$$

Evidently, in the critical section where  $M = 1$ , we also have  $\lambda = 1$ . In an arbitrary section characterized by the values  $1 \leq M \leq \infty$ , the velocity ratio is

$$1 \leq \lambda \leq \sqrt{(k+1)/(k-1)} \quad (3.6.25)$$

### Pressure, Density, and Temperature

It follows from (3.6.17) that the pressure in an arbitrary cross section of the jet is

$$p = p_0 (1 - V^2/V_{\max}^2)^{k/(k-1)} \quad (3.6.26)$$

By (3.6.22), the difference

$$1 - \frac{V^2}{V_{\max}^2} = \left( 1 + \frac{k-1}{2} M^2 \right)^{-1} \quad (3.6.27)$$

consequently,

$$p = p_0 \left( 1 + \frac{k-1}{2} M^2 \right)^{-k/(k-1)} = p_0 \pi(M) \quad (3.6.28)$$

where the function  $\pi$  of the argument  $M$  is determined by the pressure ratio  $p/p_0$ .

For the conditions of the free-stream flow, formula (3.6.28) yields:

$$p_0 = p_\infty \left( 1 + \frac{k-1}{2} M_\infty^2 \right)^{k/(k-1)} = \frac{p_\infty}{\pi(M_\infty)} \quad (3.6.29)$$

Consequently,

$$p = p_\infty \left\{ \frac{1 + [(k-1)/2] M_\infty^2}{1 + [(k-1)/2] M^2} \right\}^{k/(k-1)} = p_\infty \frac{\pi(M)}{\pi(M_\infty)} \quad (3.6.30)$$

From the equation of an adiabat  $p \rho^k = p_0 \rho_0^k$ , in which  $p$  is replaced in accordance with formulas (3.6.26) and (3.6.28), we find a relation for the density

$$\rho = \rho_0 \left( 1 - \frac{V^2}{V_{\max}^2} \right)^{1/(k-1)} = \rho_0 \left( 1 + \frac{k-1}{2} M^2 \right)^{-1/(k-1)} = \rho_0 \varepsilon(M) \quad (3.6.31)$$

where the function  $\varepsilon$  of the argument  $M$  is determined by the ratio of the densities  $\rho/\rho_0$ .

Using the equation of state

$$p/p_0 = (\rho/\rho_0) T/T_0 \quad (3.6.32)$$

and also Eqs. (3.6.26) and (3.6.28) for the pressure and (3.6.31) for the density, we have

$$T = T_0 \left( 1 - \frac{V^2}{V_{\max}^2} \right) = T_0 \left( 1 + \frac{k-1}{2} M^2 \right)^{-1} = T_0 \tau(M) \quad (3.6.33)$$

where the function  $\tau$  of the argument  $M$  is determined by the ratio of the temperatures  $T/T_0$ .

Tables of the gas-dynamic functions  $\pi(M)$ ,  $\varepsilon(M)$ , and  $\tau(M)$  for values of the exponent  $k$  from 1.1 to 1.67 are given in [12].

We shall determine the corresponding relations for the density  $\rho_0$  and temperature  $T_0$  by means of expressions (3.6.31) and (3.6.33). For the conditions of a free-stream flow, these expressions yield:

$$\rho_0 = \rho_\infty \left( 1 + \frac{k-1}{2} M_\infty^2 \right)^{1/(k-1)} = \frac{\rho_\infty}{\varepsilon(M_\infty)} \quad (3.6.34)$$

$$T_0 = T_\infty \left( 1 + \frac{k-1}{2} M_\infty^2 \right) = \frac{T_\infty}{\tau(M_\infty)} \quad (3.6.35)$$

In the critical cross section of the stream,  $M = 1$ . Consequently, from (3.6.28), (3.6.31), and (3.6.33), we obtain the following formulas for the critical values of the pressure  $p^*$ , density  $\rho^*$ , and temperature  $T^*$ :

$$p^* = p_0 \left( \frac{2}{k+1} \right)^{k/(k-1)} = p_0 \pi(1) \quad (3.6.36)$$

$$\rho^* = \rho_0 \left( \frac{2}{k+1} \right)^{1/(k-1)} = \rho_0 \varepsilon(1) \quad (3.6.37)$$

$$T^* = T_0 \left( \frac{2}{k+1} \right) = T_0 \tau(1) \quad (3.6.38)$$

where  $\pi(1)$ ,  $\varepsilon(1)$ , and  $\tau(1)$  are the values of the gas-dynamic functions at  $M = 1$ .

The above formulas, suitable for any speeds, can give us approximate relations for cases when the numbers  $M$  are very large. A glance at (3.6.30) reveals that when  $M \gg 1$  and  $M_\infty \gg 1$ , we have

$$p/p_\infty = (M_\infty/M)^{2k/(k-1)} \quad (3.6.39)$$

Similar relations for the density and temperature have the form

$$\rho/\rho_\infty = (M_\infty/M)^{2/(k-1)} \quad (3.6.40)$$

$$T/T_\infty = (M_\infty/M)^2 \quad (3.6.41)$$

Using relation (3.6.27) for the velocity of the free-stream flow,

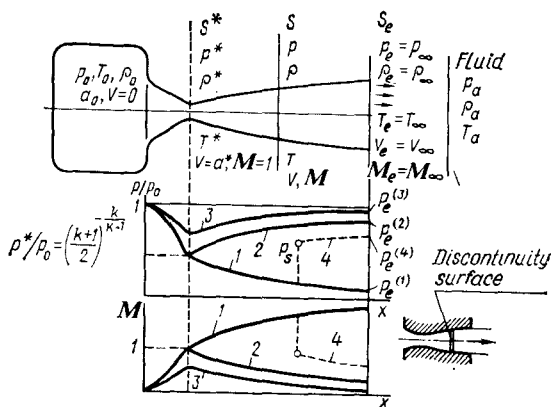
$$1 - \frac{V_\infty^2}{V_{\max}^2} = \left( 1 + \frac{k-1}{2} M_\infty^2 \right)^{-1} \quad (3.6.27')$$

for the conditions  $M_\infty \gg 1$  and  $M \gg 1$ , we obtain the following approximate formula for the local velocity:

$$\frac{V}{V_\infty} = 1 + \frac{1}{k-1} \left( \frac{1}{M_\infty^2} - \frac{1}{M^2} \right) \quad (3.6.42)$$

### Flow of a Gas from a Reservoir

Formula (3.6.12) allows us to determine the velocity of a gas flowing out through a nozzle from a reservoir (Fig. 3.6.2) in which the parameters are determined by the conditions of stagnation corresponding to a velocity of the gas in the reservoir of  $V \approx 0$ . Such conditions are ensured in practice if the critical cross section of the nozzle is sufficiently small in comparison with the cross-sectional dimension of the reservoir. In the critical section of the nozzle, which the value of the derivative  $dS/dV = 0$  corresponds

**Fig. 3.6.2**

Parameters of a gas flowing from a reservoir

to, the Mach number, as can be seen from (3.6.4), equals unity, i.e. the velocity in this section equals the local speed of sound:

$$V = a^* = \sqrt{\frac{2k}{k+1} \cdot \frac{p_0}{\rho_0}} = a_0 \sqrt{\frac{2}{k+1}} = \sqrt{\frac{2kRT_0}{k+1}}$$

Such a speed is ensured provided that the pressure in the reservoir according to (3.6.36) is not lower than the value

$$p_0 = p^* \left( \frac{k+1}{2} \right)^{k/(k-1)} \quad (3.6.43)$$

If the nozzle communicates with the atmospheric air whose pressure is  $p_a = 10^5$  Pa (this pressure is called the backpressure), flow through the nozzle is possible when  $p^* \geq 10^5$  Pa. Assuming that  $p^* = 10^5$  Pa and  $k = 1.4$ , we obtain the pressure needed to ensure the speed of sound at the outlet of a converging nozzle:

$$p_0 = 10^5 \left( \frac{1.4+1}{2} \right)^{1.4/(1.4-1)} \approx 1.9 \times 10^5 \text{ Pa}$$

When the critical parameters are reached in the throat of a nozzle, a further reduction of the backpressure ( $p_a < p^*$ ) no longer affects the values of  $a^*$  and  $p^*$ , which depend on the state of the gas in the reservoir. But here conditions are created for the appearance of a supersonic speed of the gas in the diverging part of the nozzle. In Fig. 3.6.2, these conditions of isentropic motion are characterized by curves 1 determining the change in the ratio  $p/p_0$  and in the number  $M$  along the nozzle. Such conditions are realized when the backpressure  $p_a$  equals the pressure  $p_e^{(1)}$  at the exit of the expanding nozzle or is less than it. A change in the backpressure does not affect the parameters of the gas in the outlet cross section.

Let us consider another set of possible conditions of isentropic flow along a nozzle. Let us assume that the backpressure grows to the value  $p_a^{(2)} > p_e^{(1)}$  at which the pressure  $p_e^{(2)}$  at the exit reaches the same value as  $p_a^{(2)}$ . The subsonic flow formed in this case is characterized by curves 2 shown in Fig. 3.6.2. We find the velocity ratio  $\lambda(M)$  of this flow by Eq. (3.6.23), choosing from the two solutions for  $\lambda$  the one that is less than unity.

Upon a further increase in the backpressure to the value  $p_a^{(3)}$ , conditions appear in which the pressure  $p_e^{(3)}$  at the exit will equal the backpressure, i.e.  $p_e^{(3)} = p_a^{(3)}$ , while the pressure in the throat will exceed the critical pressure  $p^*$ ; the relevant speed in this cross section is subsonic ( $V < a^*$ ). Consequently, in the diverging part of the nozzle, the speed lowers, remaining subsonic (curve 3 in Fig. 3.6.2).

At pressures at the exit smaller than  $p_e^{(2)}$  and larger than  $p_e^{(1)}$ , the isentropic nature of the flow is disturbed. At a certain cross section of the nozzle, a jump (discontinuity of the parameters) occurs, the transition through which is attended by sharp deceleration of the flow. As a result of this deceleration, having an *irreversible adiabatic nature*, the supersonic flow *transforms abruptly* into a subsonic one. The change in the pressure and in the number  $M$  along the nozzle in these flow conditions is characterized by curves 4 (Fig. 3.6.2). The surface of discontinuity of the parameters (shock) must be in a cross section with a Mach number  $M$  such that would correspond to the pressure  $p_s$  past this surface ensuring a gas pressure of  $p_e^{(4)}$  ( $p_e^{(1)} < p_e^{(4)} < p_e^{(2)}$ ) at the exit as a result of further expansion of the gas. Hence, in the given case, the flow of the gas must be analysed with the aid of the shock-wave theory whose fundamentals are treated in Chap. 4.

In an arbitrary cross section of the nozzle, including its outlet section, we determine the supersonic speed by (3.6.12). At  $M_e = M_\infty$  and a pressure of  $p_e = p_\infty$  in the outlet section, the required pressure  $p_0$  in the reservoir is determined by (3.6.29).

The mass flow rate equation has the form

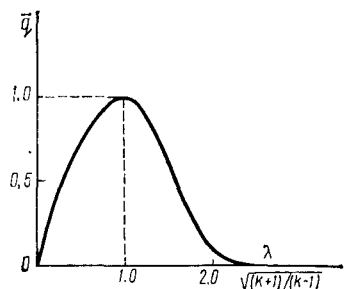
$$\rho S V = \rho^* S^* a^* \quad (3.6.44)$$

from which we find that the ratio of the mass velocity (the specific mass flow rate)  $q = \rho V$  through the cross section  $S$  being considered to the mass velocity  $q^* = \rho^* a^*$  through the critical section  $S^*$  is

$$\bar{q} = q/q^* = \rho V / (\rho^* a^*) = S^*/S \quad (3.6.45)$$

With a view to relations (3.6.19) and (3.6.31), we find

$$\begin{aligned} \rho &= \rho_0 \left( 1 - \frac{V^2}{V_{\max}^2} \right)^{1/(k-1)} = \rho_0 \left( 1 - \frac{k-1}{k+1} \cdot \frac{V^2}{a^{*2}} \right)^{1/(k-1)} \\ &= \rho_0 \left( 1 - \frac{k-1}{k+1} \lambda^2 \right)^{1/(k-1)} \end{aligned}$$

**Fig. 3.6.3**

Change in the mass velocity ratio when a gas flows out from a reservoir

After now determining the ratio  $\rho_0/\rho^*$  from (3.6.37), we obtain relation (3.6.45) in the following form:

$$\bar{q}(\lambda) = \lambda \left( 1 - \frac{k-1}{k+1} \lambda^2 \right)^{1/(k-1)} \left( \frac{k+1}{2} \right)^{1/(k-1)} = \frac{S^*}{S} \quad (3.6.46)$$

The function  $\bar{q}(\lambda)$  is called the **reduced mass density**. Taking formula (3.6.23) into account, we can determine this function of the argument  $M$ :

$$\bar{q}(M) = M \left[ \frac{2}{k+1} \left( 1 + \frac{k-1}{2} M^2 \right) \right]^{-(k+1)/[2(k-1)]} = \frac{S^*}{S} \quad (3.6.46')$$

Tabulated values of the function  $\bar{q}$  within the range of values of  $k$  from 1.1 to 1.67 are given in [12]. It follows from these relations that the number  $\lambda$  (or  $M$ ) in a certain section  $S$  of a nozzle is a function of only the ratio of the areas  $S^*/S$  and does not depend on the parameters of the gas in the reservoir.

The dependence of the mass velocity ratio  $\bar{q}$  (or of the ratio  $S^*/S$  of the areas) on  $\lambda$  is shown in Fig. 3.6.3. At a given critical nozzle section in the subsonic region ( $\lambda < 1$ ), the speed grows at the expense of the reduction in the area  $S$ , while in the supersonic region, conversely, it grows at the expense of the increase in the area. In accordance with the above, a decrease in the pressure in the reservoir does not affect the value of  $\lambda$  or  $M$  at the nozzle exit. In the case being considered, as follows from (3.6.29), a change in the pressure  $p_0$  is attended by a proportional change in the pressure at the exit  $p_e = p_\infty$ .

The mass flow rate of a gas from a reservoir can be determined by the formula

$$G_{\text{sec}} = \rho^* a^* S^*$$

Evaluation of  $\rho^*$  and  $a^*$  by formulas (3.6.37) and (3.6.18), respectively, yields

$$G_{\text{sec}} = S^* \left( \frac{2}{k+1} \right)^{1/(k-1)} \sqrt{\frac{2k}{k+1} p_0 \rho_0} \quad (3.6.47)$$

where  $\rho_0$  is the density of the gas in the reservoir.

Upon the motion of an incompressible fluid, the mass flow rate equation in accordance with (2.4.51) and provided that  $\rho = \text{const}$  becomes

$$VS = \text{const} \quad (3.6.48)$$

Kinematic equation (3.6.48) completely characterizes the one-dimensional flow of an incompressible fluid. It shows that the flow velocity is inversely proportional to the cross-sectional area of the channel. The pressure in steady flow is calculated by the Bernoulli equation (3.4.12) or (3.4.13).

## Shock Wave Theory

### 4.1. Physical Nature of Shock Wave Formation

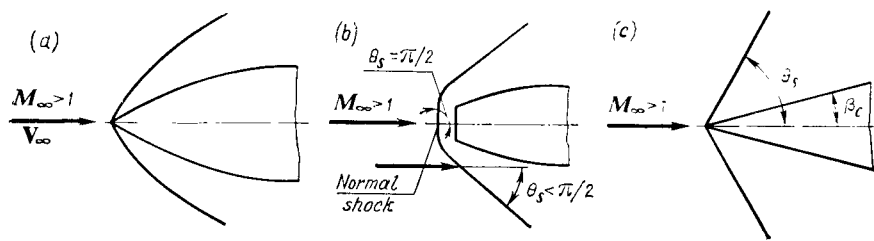
A feature of supersonic gas flows is that deceleration is attended by the formation of discontinuity surfaces in them. When a gas passes through these surfaces, its parameters change abruptly: the velocity sharply diminishes, and the pressure, temperature, and density grow. Such continuity surfaces moving relative to a gas are often referred to as **shock waves**, while the immovable discontinuity surfaces are called **stationary shock waves** or simply **shocks**. Below we consider the conditions of gas flow after stationary shock waves, and we shall use the term "shock", as a rule.

In the most general case, a shock has a curved shape. Figure 4.1.1a shows schematically an **attached curved shock** formed in a flow past a sharp-nosed body, and Fig. 4.1.1b—a **detached curved shock** appearing in front of a blunt surface in a supersonic flow. Upon the supersonic flow past a sharp-nosed body with straight walls, an **attached straight shock** may appear (Fig. 4.4.1c).

A glance at Fig. 4.1.1b reveals that the surfaces of shocks may be oriented along a normal to the free-stream velocity (the shock angle  $\theta_s = \pi/2$ ) or inclined at an angle other than a right one ( $\theta_s < \pi/2$ ). In the first case, the shock is said to be **normal**, in the second—**oblique**. An attached curved shock can evidently be considered as a set of oblique shocks, and a detached shock as consisting of a normal shock and a system of oblique shocks.

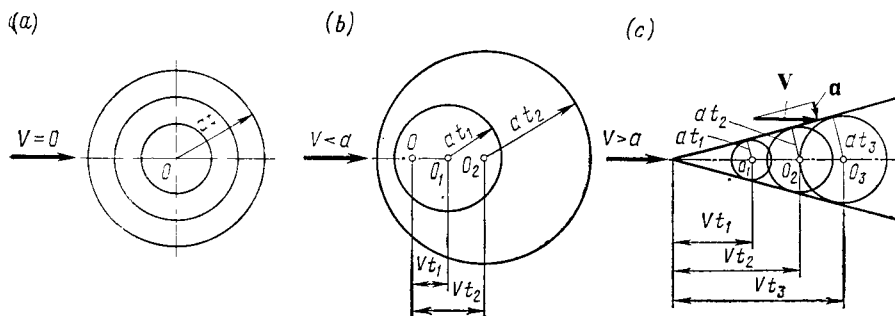
The formation of shocks is due to the specific nature of propagation of disturbances in a supersonic gas flow. By a disturbance is meant a local compression causing a pressure increase. The latter appears in a flow passing around an obstacle called a **source of disturbances**.

Let us consider a source of infinitely small disturbances at point  $O$  (Fig. 4.1.2). Such disturbances propagate in a gas at rest ( $V = 0$ ) in all directions at the speed of sound  $a$  in the form of spherical waves in space or circular waves in a plane (Fig. 4.1.2a). At the instant  $t$ , the radius of a wave is  $r = at$ . If a subsonic gas flow is

**Fig. 4.1.1**

Shocks:

a—attached curved shock; b—detached curved shock; c—attached straight shock

**Fig. 4.1.2**

Propagation of disturbances in a gas:

a—gas at rest; b—subsonic flow; c—supersonic flow

incident on a source ( $V < a$ , Fig. 4.1.2b), the waves are carried downstream: the centre of a wave travels at a speed of  $V < a$ , while the wave propagates at the speed of sound. During a certain time  $t$ , the centre of the wave travels the distance  $Vt$ , while the radius of the wave  $r = at$ , here  $at > Vt$ . Hence, in a subsonic flow, disturbances also propagate upstream.

In the particular case of a sonic velocity ( $V = a$ ), the front of spherical or circular disturbance waves is limited by a flat vertical surface or straight line tangent to a sphere or circle, respectively, and passing through point  $O$  because in this case the distance over which the centre of the wave travels during the time  $t$  equals its radius at the same instant  $t$ .

Let us assume that the free-stream velocity is supersonic ( $V > a$ ). During the time  $t$ , the centre of the wave travels the distance  $Vt$ , while a sound wave covers the distance  $at$ . Since  $at < Vt$ , for all the spherical sound waves we can draw an enveloping conical surface (Fig. 4.1.2c), i.e. a **disturbance cone** (or **Mach cone**). On a plane, **disturbance lines** (or **Mach lines**) are envelopes of the family of circular waves. The disturbances are the densest on the disturbance

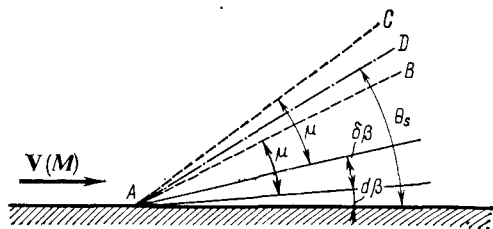


**Fig. 4.1.3**  
Origination of a shock

cone or lines that are boundaries of a disturbed and undisturbed region because all the sound waves on this cone are in the same phase of oscillation—the compression phase. Such disturbed regions—conical or plane waves confined within straight Mach lines, are called **simple pressure waves** or **Mach waves**.

The angle  $\mu$  formed by the generatrix of a conical wave or line of disturbances is determined from the condition (Fig. 4.1.2c) that  $\sin \mu = at/(Vt)$ , whence

$$\sin \mu = 1/M \quad (4.1.1)$$

The angle  $\mu$  is called the **Mach angle**. A supersonic flow carries all the sound disturbances downstream, limiting their propagation by the Mach cone or lines inclined at the angle  $\mu$ . The front of a pressure wave propagates at the same speed of sound as the front of a spherical (or circular) wave. This is why the projection of the free-stream velocity onto a normal to the wave front equals the speed of sound (Fig. 4.1.2c).

In a simple pressure wave, as in a sound one, the gas parameters (pressure, density, etc.) change by an infinitely small magnitude, which is indicated, particularly, by the relation for the speed of sound  $a = \sqrt{dp/d\rho}$  known from physics. In the disturbed region, the velocity remains virtually the same as in the undisturbed flow. Therefore, a simple pressure wave can be considered as a shock (or shock wave) of an infinitely small strength, and we can assume for practical purposes that the parameters do not change when traversing it. This is why such a simple pressure wave is also called a **weak shock wave**, while its front (Mach line) is called a **line of weak disturbances** or a **wavelet**.

It is natural to assume that the formation of a shock of a finite strength is associated with the superposition of simple pressure waves and, as a result, with their mutual amplification. Let us consider the process of formation of such a shock taking an oblique shock as an example. Let us assume that a supersonic flow initially travels along a level and smooth surface (Fig. 4.1.3). We create artificially a local pressure increment at point A by turning the flow through the infinitely small angle  $d\beta$ . This produces a simple press-

ure wave  $AB$  emerging from point  $A$  as from the source of disturbance and inclined to the surface at the angle  $\mu$ . If we again turn the flow slightly through the angle  $\delta\beta$ , a new simple wave  $AC$  is formed that emerges from the same point  $A$ , but is higher than the first wave. But in a supersonic flow, as shown above, waves cannot propagate upstream, therefore the wave  $AC$  will drift downstream until it coincides with the first one. A more intensive wave is formed that is considerably amplified upon a further turning of the flow. The shock of a finite strength formed in this way has a speed of propagation higher than the speed of sound at which the simple pressure wave travels. Therefore, the shock of finite strength must deviate from the simple wave  $AB$  to the left and occupy the new position  $AD$ . Here it is kept in equilibrium because the speed of its propagation equals the component of the free-stream velocity along a normal to the shock front  $V \sin \theta_s$ , where  $\theta_s$  is the angle of inclination of the shock. It follows that the angle of inclination of a shock of finite strength is larger than that of the Mach line (cone), i.e.  $\theta_s > \mu$ .

#### 4.2. General Equations for a Shock

We shall consider the more general case when the gas behind a shock, owing to substantial heating, experiences physicochemical transformations and *changes its specific heat*. Of major significance when studying shocks behind which oscillations are generated and dissociation, ionization, and chemical reactions occur are the rates of the physicochemical transformations.

Processes behind shock waves are characterized by a fraction of the kinetic energy of the moving gas virtually instantaneously transforming into the internal energy of the gas. In these conditions, we cannot ignore the fact that thermodynamic equilibrium is achieved after a certain time elapses only in conditions of such equilibrium do *all the parameters experiencing discontinuities* (the pressure, density, temperature) *become time-independent*. The analysis of these phenomena is a more involved problem and is associated primarily with studying of the mechanism of non-equilibrium processes, and with a knowledge, particularly, of the rates of chemical reactions in the air.

The simplest case is characterized by an infinitely high rate of the physicochemical transformations and, consequently, by the instantaneous setting in of thermodynamic equilibrium. Such processes behind shock waves are possible physically, which is confirmed by experimental studies.

Let us consider the basic theoretical relations allowing one to evaluate the equilibrium parameters behind a shock wave.

### Oblique Shock

A shock formed in real conditions is characterized by a certain thickness. The parameters of the gas in such a shock change not instantaneously, but during a certain time interval. As shown by theoretical and experimental investigations, however, the thickness of a shock is very small and is of the order of the mean free path of the molecules.

For atmospheric conditions, calculations yielded the following values of the thickness of a shock measured in the direction of the free-stream velocity:

Mach number $M_\infty$	.....	1.5	2	3	10
Thickness, mm	.....	$4.5 \times 10^{-4}$	$1.2 \times 10^{-4}$	$0.7 \times 10^{-4}$	$0.2 \times 10^{-4}$

For  $M_\infty = 2$ , the thickness of a shock equals about four molecular free paths, and for  $M_\infty = 3$ —about three. Therefore, when studying a shock in an ideal fluid, this thickness may be disregarded and the shock represented in the form of a geometric discontinuity surface for the gas parameters, assuming these parameters to change instantaneously.

Our task consists in determining the unknown parameters of a gas behind a shock according to the preset parameters characterizing the flow of the gas ahead of the shock.

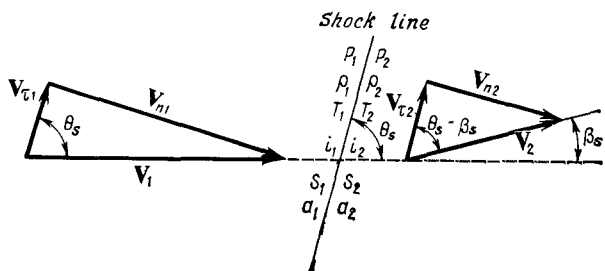
For an oblique shock formed in a dissociating and ionizing gas, there are nine unknown parameters: the pressure  $p_2$ , density  $\rho_2$ , temperature  $T_2$ , velocity  $V_2$ , enthalpy  $i_2$ , entropy  $S_2$ , speed of sound  $a_2$ , the mean molar mass  $\mu_{m2}$ , and the shock angle  $\theta_s$  (or the flow deviation angle  $\beta_s$ ). Consequently, it is necessary to compile nine simultaneous equations. The parameters ahead of a shock will be the known ones in these equations, namely, the pressure  $p_1$ , density  $\rho_1$ , velocity  $V_1$ , etc. Instead of the velocity  $V_2$  behind a shock, we can determine its components along a normal  $V_{n2}$  and a tangent  $V_{\tau 2}$  to the shock. This will increase the number of equations needed to ten. These equations include the fundamental equations of gas dynamics (of motion, continuity, energy, and state), a number of kinematic relations for the velocities, and also thermodynamic relations characterizing the properties of a gas. Let us consider each equation of this system.

Figure 4.2.1 shows triangles of the flow velocities ahead of a shock (the parameters with the subscript 1) and behind it (the subscript 2). We shall use the figure to determine the following relations for these components:

$$V_{\tau 2} = V_2 \cos (\theta_s - \beta_s), \quad V_{n2} = V_2 \sin (\theta_s - \beta_s) \quad (4.2.1)$$

This yields the first equation of the system of simultaneous ones:

$$V_{n2}/V_{\tau 2} = \tan (\theta_s - \beta_s) \quad (4.2.2)$$



**Fig. 4.2.1**  
Oblique shock

The continuity equation (or the mass flow equation) is the second one. It determines the amount of fluid passing through unit surface of a shock in unit time:

$$\rho_1 V_{1n} = \rho_2 V_{2n} \quad (4.2.3)$$

here  $V_{1n} = V_1 \sin \theta_s$  is the normal component of the velocity ahead of the shock (Fig. 4.2.1).

Let us use the equation of motion reduced to the form of an equation of momentum for the conditions of the passage through a shock. This is the third equation of the system. We shall obtain it by assuming that the change in the momentum of the fluid passing in unit time through unit surface area of the shock in the direction of a normal to this surface equals the impulse of the pressure forces:

$$\rho_1 V_{1n}^2 - \rho_2 V_{2n}^2 = p_2 - p_1 \quad (4.2.4)$$

With a view to Eq. (4.2.3), we can write this equation in the form

$$\rho_1 V_{1n} (V_{1n} - V_{2n}) = p_2 - p_1 \quad (4.2.4')$$

Equation (4.2.4) can also be written as

$$p_1 + \rho_1 V_{1n}^2 = p_2 + \rho_2 V_{2n}^2 \quad (4.2.4'')$$

In this form, the equation expresses the law of momentum conservation when passing through a shock. If we consider the change in the momentum in a direction tangent to the shock surface, then, taking into account that the pressure gradient in this direction is zero, we obtain the following relation:

$$\rho_1 V_{1n} V_{1t} - \rho_2 V_{2n} V_{2t} = 0$$

whence, when  $\rho_1 V_{1n} = \rho_2 V_{2n}$ , we have

$$V_{1t} = V_{2t} \quad (4.2.5)$$

Equation (4.2.5) is the fourth one of the system. It indicates that the tangential components of the velocity when passing through

a shock do not change. A glance at Fig. 4.2.1 reveals that  $V_{\tau 1} = V_1 \cos \theta_s$ , therefore we can write (4.2.5) in the form

$$V_{\tau 2} = V_1 \cos \theta_s = V_{n1}/\tan \theta_s \quad (4.2.5')$$

We can write the equation of energy conservation in the form

$$i_1 + V_1^2/2 = i_2 + V_2^2/2$$

Provided that

$$V_1^2 = V_{n1}^2 + V_{\tau 1}^2, \quad V_2^2 = V_{n2}^2 + V_{\tau 2}^2, \quad \text{and} \quad V_{\tau 1} = V_{\tau 2}$$

the equation of energy conservation can be transformed:

$$i_1 + V_{n1}^2/2 = i_2 + V_{n2}^2/2 \quad (4.2.6)$$

By combining the equations of state for the conditions ahead of the shock and behind it, we obtain the relation

$$p_2 - p_1 = R_2 \rho_2 T_2 - R_1 \rho_1 T_1$$

or, taking into account that  $R = R_0/\mu_m$ , we have

$$p_2 - p_1 = R_0 (\rho_2 T_2 / \mu_{m2} - \rho_1 T_1 / \mu_{m1}) \quad (4.2.7)$$

We can write four equations of the system being considered that allow us to determine the enthalpy, entropy, mean molar mass, and speed of sound in a dissociating gas in the form of general dependences of these parameters on the pressure and temperature:

$$i_2 = f_1 (p_2, T_2) \quad (4.2.8)$$

$$S_2 = f_2 (p_2, T_2) \quad (4.2.9)$$

$$\mu_{m2} = f_3 (p_2, T_2) \quad (4.2.10)$$

$$a_2 = f_4 (p_2, T_2) \quad (4.2.11)$$

These functions are not expressed analytically in the explicit form and are determined by means of experimental investigations or with the aid of rather involved calculations based on the solution of the relevant thermodynamic equations. The relations for these functions are usually constructed in the form of graphs, and their values are tabulated in special tables of thermodynamic functions for air at high temperatures (see [6, 7, 13]).

Let us express the basic parameters behind a shock wave in terms of the relative change in the normal components of the velocity, i.e. in terms of the quantity

$$\Delta \bar{V}_n = \Delta V_n / V_{n1} = (V_{n1} - V_{n2}) / V_{n1} \quad (4.2.12)$$

From (4.2.3), we find the ratio of the densities:

$$\rho_2 / \rho_1 = 1 / (1 - \Delta \bar{V}_n) \quad (4.2.13)$$

and from (4.2.4'), the ratio of the pressures:

$$p_2/p_1 = 1 + (\rho_1 V_{n1}^2/p_1) \Delta \bar{V}_n \quad (4.2.14)$$

Introducing the concept of the "normal component" of the number  $M_1$  as the ratio  $M_{n1} = V_{n1}/a_1$  or  $M_{n1} = M_1 \sin \theta_s$ , and assuming that ahead of a shock the gas is not dissociated and the speed of sound for it is  $a_1 = \sqrt{k_1 p_1 / \rho_1}$ , we obtain

$$p_2/p_1 = 1 + k_1 M_{n1}^2 \Delta \bar{V}_n \quad (4.2.15)$$

instead of (4.2.14).

We find the ratio of the enthalpies  $i_2/i_1$  from (4.2.6):

$$i_2/i_1 = 1 + (1/2i_1) (V_{n1}^2 - V_{n2}^2)$$

Let us write the difference of the velocity squares in the form

$$\begin{aligned} V_{n1}^2 - V_{n2}^2 &= V_{n1}^2 (1 - V_{n2}/V_{n1}) (1 + V_{n2}/V_{n1}) \\ &= V_{n1}^2 \Delta \bar{V}_n (2 - \Delta \bar{V}_n) \end{aligned}$$

Hence

$$i_2/i_1 = 1 + (V_{n1}^2/2) (\Delta \bar{V}_n/i_1) (2 - \Delta \bar{V}_n) \quad (4.2.16)$$

To determine the ratio of the temperatures  $T_2/T_1$ , we shall use the equations of state for the conditions ahead of a shock and behind it, from which

$$T_2/T_1 = (p_2/p_1) (\mu_{m2}/\mu_{m1}) \rho_1/\rho_2 \quad (4.2.17)$$

Substituting for the ratio of the densities and pressures in this equation their values from Eqs. (4.2.13) and (4.2.15), respectively, we obtain

$$T_2/T_1 = (1 + k_1 M_{n1}^2 \Delta \bar{V}_n) (1 - \Delta \bar{V}_n) \mu_{m2}/\mu_{m1} \quad (4.2.17')$$

To determine the velocity behind a shock, we shall use the relations

$$V_2^2 = V_\tau^2 + V_{n2}^2 \text{ and } V_1^2 = V_\tau^2 + V_{n1}^2$$

from which we find

$$V_2^2/V_1^2 = 1 - (V_{n1}^2/V_1^2) \Delta \bar{V}_n (2 - \Delta \bar{V}_n) \quad (4.2.18)$$

Since

$$V_{n1}/V_1 = \sin \theta_s$$

then

$$V_2^2/V_1^2 = 1 - \sin^2 \theta_s \Delta \bar{V}_n (2 - \Delta \bar{V}_n) \quad (4.2.18')$$

Let us find a relation for the flow deviation angle behind a shock. By (4.2.2) and (4.2.5'), we have

$$\Delta \bar{V}_n = 1 - \tan (\theta_s - \beta_s)/\tan \theta_s \quad (4.2.19)$$

Hence, having in view that

$$\tan(\theta_s - \beta_s) = (\tan \theta_s - \tan \beta_s)/(1 + \tan \theta_s \tan \beta_s)$$

we obtain

$$\tan \beta_s = \tan \theta_s \frac{\Delta \bar{V}_n}{1 - \Delta \bar{V}_n} \left( \frac{1}{1 - \bar{V}_n} + \tan^2 \theta_s \right)^{-1} \quad (4.2.20)$$

The relative change in the velocity  $\Delta \bar{V}_n$  is determined in accordance with (4.2.13) by the dimensionless density

$$\Delta \bar{V}_n = 1 - \rho_2/\rho_1 \quad (4.2.21)$$

This shows that the ratios of the pressures, temperatures, and enthalpies, and also the flow deviation angle  $\beta_s$  can be written as functions of the relative density  $\rho_2/\rho_1$ . In addition, we can introduce the values  $V_{n1} = V_1 \sin \theta_s$  and  $M_{n1} = M_1 \sin \theta_s$  into the formulas instead of the quantities  $V_{n1}$  and  $M_{n1}$ , respectively.

Hence, the solution of the problem on an oblique shock when its angle of inclination  $\theta_s$  is known consists in finding the ratio of the densities  $\rho_2/\rho_1$ , or, which is the same, in determining the function  $\Delta \bar{V}_n$ . This function is determined with the aid of expressions (4.2.16) and (4.2.17'), each of which can be written in the form of a quadratic equation in  $\Delta \bar{V}_n$ . From the first quadratic equation, we have

$$\Delta \bar{V}_n = 1 - \sqrt{1 - 2(i_2 - i_1)/V_{n1}^2} \quad (4.2.22)$$

and from the second

$$\Delta \bar{V}_n = A + \sqrt{A^2 - B} \quad (4.2.23)$$

where

$$A = \frac{k_1 M_{n1}^2 - 1}{2k_1 M_{n1}^2}, \quad B = \frac{1}{k_1 M_{n1}^2} \left( \frac{T_2}{T_1} \cdot \frac{\mu_{m1}}{\mu_{m2}} - 1 \right) \quad (4.2.24)$$

The signs of the square roots—minus in (4.2.22) and plus in (4.2.23)—were chosen with a view to the fact that the velocity behind a shock is always lower than ahead of it, and, consequently,  $\Delta \bar{V}_n < 1$ . The plus sign in (4.2.23) also indicates that physically the larger of the two values of  $\Delta \bar{V}_n < 1$  is real.

Equations (4.2.22) and (4.2.23) are solved by the method of successive approximations. The problem of an oblique shock can be solved if the angle  $\beta_s$  is given. Here the angle  $\theta_s$  is calculated with the aid of relation (4.2.20), in accordance with which

$$\tan^2 \theta_s - \frac{\tan \theta_s}{\tan \beta_s} \frac{\Delta \bar{V}_n}{1 - \Delta \bar{V}_n} + \frac{1}{1 - \Delta \bar{V}_n} = 0$$

The solution of this equation yields

$$\tan \theta_s = \cot \beta_s \left[ \frac{1}{2} \cdot \frac{\Delta \bar{V}_n}{1 - \Delta \bar{V}_n} \pm \sqrt{\frac{1}{4} \cdot \frac{\Delta \bar{V}_n^2}{(1 - \Delta \bar{V}_n)^2} - \frac{\tan^2 \beta_s}{1 - \Delta \bar{V}_n}} \right] \quad (4.2.25)$$

One of the solutions (the plus sign before the root) determines the larger value of the angle  $\theta_s$  realized in a detached curved shock, and the other (the minus sign) determines the smaller value realized in an attached shock with a lower strength.

To facilitate calculations, we can evaluate the angles  $\theta_s$  beforehand from the given values of  $\beta_s$ , and compile a corresponding table or plot a graph. With their aid, for a value of  $\Delta \bar{V}_n$  which previously calculated values of the ratios  $p_2/p_1$ ,  $\rho_2/\rho_1$ , etc. correspond to, we can find one of the angles  $\theta_s$  or  $\beta_s$  from the other known one.

The velocity  $V_1$  and the number  $M_1$  of the free stream at which the parameters are realized in a shock with the given values of the angle  $\theta_s$  (or  $\beta_s$ ), and also  $V_{n1}$  (or  $M_{n1}$ ) are calculated by the formulas

$$V_1 = V_{n1}/\sin \theta_s, \quad M_1 = M_{n1}/\sin \theta_s \quad (4.2.26)$$

### Normal Shock

The formulas for calculating a normal shock can be obtained from the above relations for an oblique one if we assume that  $\theta_s = \pi/2$  and  $\beta_s = 0$ . Accordingly, the velocity  $V_{n1} = V_1$ , and the number  $M_{n1} = M_1$ . Now the basic relations acquire the following form:

$$p_2/p_1 = 1 + k_1 M_1^2 \Delta \bar{V} \quad (4.2.27)$$

$$i_2/i_1 = 1 + (V_1^2/2) (\Delta \bar{V}/i_1) (2 - \Delta \bar{V}) \quad (4.2.28)$$

$$T_2/T_1 = (1 + k_1 M_1^2 \Delta \bar{V}) (1 - \Delta \bar{V}) \mu_{m2} \mu_{m1} \quad (4.2.29)$$

$$V_2^2/V_1^2 = 1 - \Delta \bar{V} (2 - \Delta \bar{V}) \quad (4.2.30)$$

where the change in the relative velocity

$$\Delta \bar{V} = \Delta V/V_1 = (V_1 - V_2)/V_1 \quad (4.2.31)$$

is determined with the aid of expressions (4.2.22)-(4.2.24):

$$\Delta \bar{V} = 1 - \sqrt{1 - 2(i_2 - i_1)/V_1^2} \quad (4.2.32)$$

$$\Delta \bar{V} = A + \sqrt{A^2 - B} \quad (4.2.33)$$

in which

$$A = \frac{k_1 M_1^2 - 1}{2k_1 M_1^2}, \quad B = \frac{1}{k_1 M_1^2} \left( \frac{T_2}{T_1} \cdot \frac{\mu_{m1}}{\mu_{m2}} - 1 \right) \quad (4.2.34)$$

The relation between  $\Delta \bar{V}$  and the relative density is determined by the formula

$$\Delta \bar{V} = 1 - \rho_1/\rho_2 \quad (4.2.35)$$

We have given the general relations for shocks. Now let us use them to analyse the nature of flow and the ways of calculating the parameters of a gas behind shocks for *constant specific heats* and then consider in greater detail practical ways of calculating similar parameters for a dissociating fluid, i.e. for the more general case of *varying specific heats*.

### 4.3. Shock in the Flow of a Gas with Constant Specific Heats

Of major theoretical and practical interest is the problem on the flow of a gas behind a shock when the specific heats  $c_p$  and  $c_v$  are constant. Although such a flow is considered to be a particular (idealized) case of the flow of a gas whose physicochemical properties change to a greater or smaller extent when passing through a shock, nevertheless the results obtained in solving this problem make it possible to comprehend the general *qualitative* nature of a shock transition. The relations characterizing the change in the parameters of a gas when passing through a shock are obtained here in the explicit form. They can also be used for an approximate *quantitative* estimation of these parameters when the more general case of varying specific heats is being treated. The problem being considered also has an independent significance because its solution can be used directly for determining the parameters of a gas behind a shock in a flow at comparatively low supersonic velocities at which the change in the specific heats in the compressed gas is negligibly small. These velocities, which are determined for the most intensive (normal) shock, correspond approximately to Mach numbers  $M_\infty < 3-4$ .

#### System of Equations

The method of calculating an oblique shock treated below is based on the use of a system of equations that is a particular case of the system (4.2.2)-(4.2.11).

If in a shock transition the specific heats do not change, it should also be assumed that the mean molar mass remains constant, and the speed of sound and the enthalpy depend only on the temperature. Equations (4.2.8), (4.2.10), and (4.2.11) accordingly acquire the following form:

$$i_2 = c_p T_2 \quad (4.3.1)$$

$$\mu_{m2} = \mu_{m1} = \mu_m = \text{const} \quad (4.3.2)$$

$$a_2^2 = kRT_2 \quad (4.3.3)$$

Instead of Eq. (4.2.9), it is necessary to use the thermodynamic equation for the entropy of a non-dissociating perfect gas:

$$dS = di/T - dp/(\rho T)$$

Having in view the equations  $di = c_p dT$  and  $dp = d(R\rho T) = R\rho dT + RT d\rho$ , we obtain

$$dS = c_p d \ln T = R d \ln T - R d \ln \rho$$

But

$$c_p - R = c_v \text{ and } R/c_v = (c_p - c_v)/c_v = k - 1$$

Consequently,

$$dS = c_v [d \ln T - (k - 1) d \ln \rho]$$

Integrating this equation at  $k = \text{const}$ , we find

$$S = c_v \ln (T/\rho^{k-1}) + \text{const} \quad (4.3.4)$$

It follows from the equation of state  $p = R\rho T$  that

$$T/\rho^{k-1} = p/(\rho^k R), \text{ and } \ln [p/(\rho^k R)] = \ln (p/\rho^k) - \ln R$$

Introducing the quantity  $\ln R$  into the constant on the right-hand side of (4.3.4), we obtain a relation for the entropy in the form

$$S = c_v \ln (p/\rho^k) + \text{const} \quad (4.3.5)$$

By applying this equation to the conditions ahead of a shock and behind it, and then determining the difference between the entropies, we obtain instead of (4.2.9) the equation for the entropy used in the theory of an oblique shock:

$$S_2 - S_1 = c_v \ln [(p_2/p_1)(\rho_1^k/\rho_2^k)] \quad (4.3.6)$$

Equation of state (4.2.7) for the case of constant specific heats being considered is simplified:

$$p_2 - p_1 = R (\rho_2 T_2 - \rho_1 T_1) \quad (4.3.7)$$

Equations (4.2.2)-(4.2.6) of the system are retained with no alterations.

#### Formulas for Calculating the Parameters of a Gas Behind a Shock

To calculate the density, pressure, and enthalpy, the formulas needed are (4.2.13), (4.2.15) and (4.2.16), respectively. To determine the temperature, the formula needed is (4.2.17') with the assumption made that  $\mu_{m2} = \mu_{mi}$ :

$$T_2/T_1 = (1 + kM_{n1}^2 \Delta \bar{V}_n) (1 - \Delta \bar{V}_n) \quad (4.3.8)$$

The unknown quantity in all these expressions is the change in the relative velocity  $\Delta \bar{V}_n$ . Let us determine it by assuming that the shock angle  $\theta_s$  and the free-stream Mach number  $M_1$  are known. We shall use Eq. (4.2.4') for this purpose. After dividing it by  $\rho_1 V_{n1} = \rho_2 V_{n2}$ , we obtain

$$\frac{p_2}{(\rho_2 V_{n2})} - \frac{p_1}{(\rho_1 V_{n1})} = V_{n1} - V_{n2} \quad (4.3.9)$$

Inserting  $a_2^2/k$  and  $a_1^2/k$  here instead of  $p_2/\rho_2$  and  $p_1/\rho_1$ , respectively, and using Eq. (3.6.21) for the speed of sound, we find

$$\begin{aligned} \frac{1}{kV_{n2}} \left( \frac{k+1}{2} a^{*2} - \frac{k-1}{2} V_2^2 \right) - \frac{1}{kV_{n1}} \left( \frac{k+1}{2} a^{*2} - \frac{k-1}{2} V_1^2 \right) \\ = V_{n1} - V_{n2} \end{aligned}$$

Introducing the values of  $V_2^2 = V_{n2}^2 + V_\tau^2$  and  $V_1^2 = V_{n1}^2 + V_\tau^2$  and multiplying both sides of the equation by  $V_{n1}V_{n2}$ , we obtain after simple transformations

$$\begin{aligned} \frac{k+1}{2k} a^{*2} (V_{n1} - V_{n2}) - \frac{k-1}{2k} V_\tau^2 (V_{n1} - V_{n2}) \\ + \frac{k-1}{2k} V_{n1}V_{n2} (V_{n1} - V_{n2}) = V_{n1}V_{n2} (V_{n1} - V_{n2}) \end{aligned}$$

Excluding the trivial solution  $V_{n1} = V_{n2} = 0$  corresponding to the absence of a shock, we obtain

$$V_{n1}V_{n2} = a^{*2} - \frac{k-1}{k+1} V_\tau^2 \quad (4.3.10)$$

This equation is used to determine the velocity behind a shock. It is called the **basic equation of an oblique shock**, and allows us to find the relative change in the velocity  $\Delta \bar{V}_n = (V_{n1} - V_{n2})/V_{n1}$ . For this purpose, let us write  $V_{n1}V_{n2} = V_{n1}^2 (V_{n2}/V_{n1})$  and use the relations  $V_{n1} = V_1 \sin \theta_s$  and  $V_\tau = V_1 \cos \theta_s$ . After the relevant substitutions in (4.3.10), we obtain

$$\sin^2 \theta_s (1 - \Delta \bar{V}_n) = \frac{1}{\lambda_1^2} - \frac{k-1}{k+1} (1 - \sin^2 \theta_s)$$

where  $\lambda_1 = V_1/a^*$ .

Substituting Eq. (3.6.23) for  $\lambda_1$  and performing transformations, we find

$$\Delta \bar{V}_n = \frac{2}{k+1} \left( 1 - \frac{1}{M_1^2 \sin^2 \theta_s} \right) \quad (4.3.11)$$

Let us introduce the symbol

$$\delta = (k-1)/(k+1) \quad (4.3.12)$$

with a view to which formula (4.3.11) becomes

$$\Delta \bar{V}_n = (1 - \delta) [1 - 1/(M_1^2 \sin^2 \theta_s)] \quad (4.3.11')$$

By inserting this quantity into (4.2.13), we can determine the density ratio:

$$\rho_2/\rho_1 = M_1^2 \sin^2 \theta_s / (1 - \delta + \delta M_1^2 \sin^2 \theta_s) \quad (4.3.13)$$

To determine the pressure ratio  $p_2/p_1$ , we shall use formula (4.2.15). We shall assume in it that  $M_{n1} = M_1 \sin \theta_s$ , substitute expression (4.3.11') for  $\Delta \bar{V}_n$ , and replace the quantity  $k$  in accordance with (4.3.12) by the value

$$k = (1 + \delta)/(1 - \delta) \quad (4.3.14)$$

The result is the parameter

$$p_2/p_1 = (1 + \delta) M_1^2 \sin^2 \theta_s - \delta \quad (4.3.15)$$

that characterizes the **shock strength**. We may also use the following relation for this purpose:

$$(p_2 - p_1)/p_1 = \Delta p/p_1 = (1 + \delta) (M_1^2 \sin^2 \theta_s - 1) \quad (4.3.15')$$

Formula (4.3.15') can be used to obtain another parameter characterizing the shock strength, namely, the pressure coefficient  $\bar{p}_2 = (p_2 - p_1)/q_1$ , where  $q_1 = [(1 + \delta)/(1 - \delta)] p_1 M_1^2/2$ . By subtracting unity from both the left-hand and right-hand sides of (4.3.15') and relating the expression obtained to  $q_1$ , we have

$$\bar{p}_2 = [2(1 - \delta)/M_1^2] (M_1^2 \sin^2 \theta_s - 1) \quad (4.3.15'')$$

Eliminating the quantity  $M_1^2 \sin^2 \theta_s$  from Eqs. (4.3.15) and (4.3.13), we find the relation for the pressure-to-density ratios—the **Hugoniot equation**:

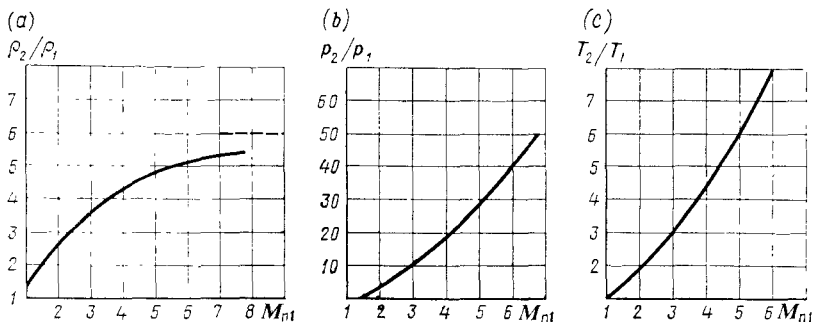
$$p_2/p_1 = (\rho_2/\rho_1 - \delta)/(1 - \delta \rho_2/\rho_1) \quad (4.3.13')$$

This relation is also known as the **shock adiabat**. Unlike the conventional equation of an adiabat (isentrope) of the form  $p = A\rho^k$ , it shows how the parameters change in a transition through a shock wave. This transition process is attended by a growth in the entropy determined from Eq. (4.3.6).

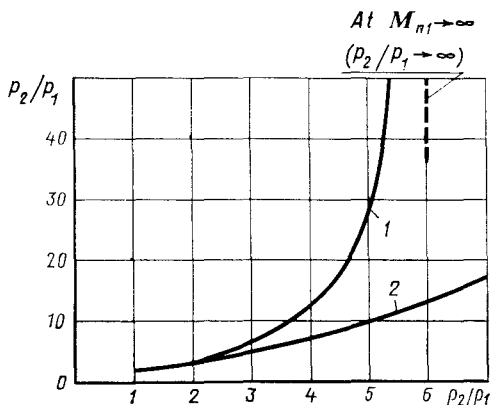
Hence, the process of the transition through a shock is **non-isentropic**. In accordance with the change in the indicated parameters, the temperature behind a shock grows. Its value is calculated by the equation of state

$$\frac{T_2}{T_1} = \frac{p_2}{p_1} \cdot \frac{\rho_1}{\rho_2} = \frac{[(1 + \delta) M_1^2 \sin^2 \theta_s - \delta]}{M_1^2 \sin^2 \theta_s} \frac{(1 - \delta + \delta M_1^2 \sin^2 \theta_s)}{(1 - \delta)} \quad (4.3.16)$$

The dependences of the ratios of the gas parameters behind a shock and ahead of it ( $\rho_2/\rho_1$ ,  $p_2/p_1$ ,  $T_2/T_1$ ) on the quantity  $M_{n1} = M_\infty \sin \theta_s$  for  $k = 1.4$  ( $\delta = 1/6$ ) are shown graphically in Fig. 4.3.1, and the Hugoniot equation (4.3.13'), in Fig. 4.3.2.

**Fig. 4.3.1**

Dependences of the ratios of the gas parameters behind a shock and ahead of it on the value of  $M_{n1} = M_\infty \sin \theta_s$  for  $k = 1.4$  ( $\delta = 1/6$ ):  
 a—density ratio  $\rho_2/\rho_1$ ; b—pressure ratio  $p_2/p_1$ ; c—temperature ratio  $T_2/T_1$

**Fig. 4.3.2**

Shock adiabat (1) and isentropic (2)  
 $(k = 1.4, \delta = 1/6)$

The special form of the transition through a shock, differing from an isentropic process, manifests itself in the different nature of the change in the gas parameters. It follows from (4.3.15) and (4.3.16) that at  $M_1 \rightarrow \infty$ , the pressure and temperature grow without a limit. It also follows from (4.3.13) that for the same condition  $M_1 \rightarrow \infty$  the density tends to a certain definite value equal to  $(\rho_2/\rho_1)_{M_1 \rightarrow \infty} = 1/\delta$ . When  $k = 1.4$ , this yields the value of  $1/\delta = 6$ . It follows from the formula  $p = A\rho^k$  or  $T = B\rho^{k-1}$  ( $A$  and  $B$  are constants) that in an isentropic process an infinite increase in the density and temperature corresponds to an infinite pressure increase. A comparison allows us to arrive at the conclusion that with an identical change in the pressure in both a shock and isentropic processes, the former is attended by greater heating of the gas, and this is just what facilitates a certain drop in the density.

Formula (4.3.16) determines the ratio of the squares of the sound speed in accordance with the relation

$$a_2^2/a_1^2 = T_2/T_1 \quad (4.3.17)$$

Using this relation, and also Eq. (4.2.18'), we can determine the number  $M_2$  behind a shock. Inserting expression (4.2.21) for  $\Delta\bar{V}_n$  into (4.2.18'), we find

$$V_2^2/V_1^2 = \cos^2 \theta_s + (\rho_1/\rho_2)^2 \sin^2 \theta_s \quad (4.3.18)$$

Dividing Eq. (4.3.18) by (4.3.17), we obtain an expression for the ratio of the squares of the Mach numbers:

$$M_2^2/M_1^2 = (T_1/T_2) [\cos^2 \theta_s + (\rho_1/\rho_2)^2 \sin^2 \theta_s] \quad (4.3.19)$$

where  $T_1/T_2$  and  $\rho_1/\rho_2$  are found from formulas (4.3.16) and (4.3.13), respectively.

The formula for calculating  $M_2$  can be obtained in a somewhat different form with the aid of momentum equation (4.2.4''). Let us write it in the form

$$\frac{p_1}{p_2} \left( 1 + \frac{\rho_1}{\rho_2} V_1^2 \sin^2 \theta_s \right) = 1 + \frac{\rho_2}{p_2} V_2^2 \sin^2 (\theta_s + \beta_s)$$

Taking into account that  $kp/\rho = [(1 + \delta)/(1 - \delta)] p/\rho$ , and determining  $p_2/p_1$  by the Hugoniot equation (4.3.13'), we obtain

$$\frac{1 - \delta(\rho_2/\rho_1)}{\rho_2/\rho_1 - \delta} \left( 1 + \frac{1 + \delta}{1 - \delta} M_1^2 \sin^2 \theta_s \right) = 1 + \frac{1 + \delta}{1 - \delta} M_2^2 \sin^2 (\theta_s - \beta_s)$$

After substituting for  $M_1^2 \sin^2 \theta_s$  its value found from (4.3.13), we obtain the relation

$$M_2^2 \sin^2 (\theta_s - \beta_s) = (1 - \delta) (\rho_2/\rho_1 - \delta)^{-1} \quad (4.3.19')$$

Let us determine the stagnation pressure for the conditions of a flow behind a shock. Considering the flow of a gas behind a shock and ahead of it to be isentropic, we can compile the thermodynamic relations:

$$p_2/\rho_2^k = p'_0/\rho'_0^k, \quad p_1/\rho_1^k = p_0/\rho_0^k$$

where  $p_0$  and  $p'_0$ ,  $\rho_0$  and  $\rho'_0$  are the stagnation pressure and density in the regions of the flow ahead of the shock and behind it, respectively. These relations yield the **pressure recovery ratio across a shock wave**:

$$v_0 = p'_0/p_0 = (p_2/p_1) (\rho_1/\rho_2)^k (\rho'_0/\rho_0)^k$$

Multiplying both sides of this equation by the ratio  $(p_0/p'_0)^k$ , we obtain

$$v_0^{1-k} = \left( \frac{p'_0}{p_0} \right)^{1-k} = \frac{p_2}{p_1} \left( \frac{\rho_1}{\rho_2} \right)^k \left( \frac{\rho'_0}{p'_0} \cdot \frac{p_0}{\rho_0} \right)$$

Let us use the energy equation  $V^2/2 + c_p T = \text{const}$  and write it for the conditions ahead of and behind a shock:

$$V_1^2/2 + c_p T_1 = V_2^2/2 + c_p T_2$$

At points of stagnation,  $V_1 = V_2 = 0$ . It follows from the energy equation that the temperatures at these points are identical, i.e.  $T_0 = T'_0$  or, which is the same,  $p_0/\rho_0 = p'_0/\rho'_0$ .

Consequently,

$$v_0 = p'_0/p_0 = (p_1/p_2)^{1/(k-1)} (\rho_2/\rho_1)^{k/(k-1)} \quad (4.3.20)$$

or

$$v_0 = p'_0/p_0 = (p_1/p_2)^{(1-\delta)/2\delta} (\rho_2/\rho_1)^{(1-\delta)/2\delta} \quad (4.3.20')$$

where  $p_1/p_2$  and  $\rho_2/\rho_1$  are found by (4.3.15) and (4.3.13), respectively.

By (3.6.28), the stagnation pressure is

$$p_0 = p_1 \left( 1 + \frac{\delta}{1-\delta} M_1^2 \right)^{(1+\delta)/2\delta} \quad (4.3.21)$$

Consequently,

$$\begin{aligned} \frac{p'_0}{p_1} & [ (1+\delta) M_1^2 \sin^2 \theta_s - \delta ]^{(\delta-1)/2\delta} (M_1 \sin \theta_s)^{(1+\delta)/\delta} \\ & \times (1-\delta)^{-(1+\delta)/2\delta} \frac{\left( 1 + \frac{\delta}{1-\delta} M_1^2 \right)^{(1+\delta)/2\delta}}{\left( 1 + \frac{\delta}{1-\delta} M_1^2 \sin^2 \theta_s \right)^{(1+\delta)/2\delta}} \end{aligned} \quad (4.3.22)$$

Let us determine the stagnation pressure coefficient behind an oblique shock

$$\begin{aligned} \bar{p}_0 &= \frac{p'_0 - p_1}{q_1} = \frac{2(1-\delta)}{(1+\delta) M_1^2} \left\{ [ (1+\delta) M_1^2 \sin^2 \theta_s - \delta ]^{(\delta-1)/2\delta} \right. \\ &\quad \times (M_1 \sin \theta_s)^{(1+\delta)/\delta} (1-\delta)^{-(1+\delta)/2\delta} \\ &\quad \times \left. \frac{\left( 1 + \frac{\delta}{1-\delta} M_1^2 \right)^{(1+\delta)/2\delta}}{\left( 1 + \frac{\delta}{1-\delta} M_1^2 \sin^2 \theta_s \right)^{(1+\delta)/2\delta}} - 1 \right\} \end{aligned} \quad (4.3.23)$$

An analysis of relation (4.3.20) shows that behind a shock of finite strength the pressure ratio  $p'_0/p_0$  is always less than unity. The stronger the shock, the larger are the stagnation pressure losses and, consequently, the smaller is the ratio  $p'_0/p_0$ .

When establishing the physical nature of these losses, we cannot consider a shock as a discontinuity surface; we must take into account that a real compression process occurs in a layer with a small thickness of the order of the molecular free path. It is exactly such a process

of transition through a shock in a layer that is possible because the existence of two contacting regions with a finite difference of their temperatures, pressures, and densities cannot be visualized. It is only a mathematical abstraction.

The transition through a shock having a small thickness is characterized by so great velocity and temperature gradients that in the compression regions the *influence of skin friction and heat conduction* becomes quite substantial. It thus follows that the irreversible losses of the kinetic energy of gas in a transition through a shock are associated with the work done by the friction forces, and also with the heat conduction. The action of these dissipative forces and also heat transfer within the compression zone cause an *increase in the entropy* and a resulting *reduction in the pressure* in the flow behind the shock in comparison with an isentropic compression process.

### Oblique Shock Angle

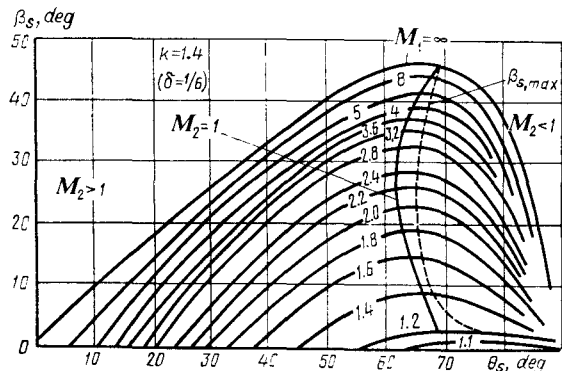
The parameters behind an oblique shock are determined by the number  $M_1$  and the shock angle  $\theta_s$ . Its magnitude, determined by the same number  $M_1$  and the flow deflection angle  $\beta_s$ , can be calculated by using Eq. (4.2.19). Substituting for  $\Delta \bar{V}_n$  in it its value from (4.2.21), we obtain a working relation:

$$\tan \theta_s / \tan (\theta_s - \beta_s) = \rho_2 / \rho_1 \quad (4.3.24)$$

Determining  $\rho_1 / \rho_2$  from (4.3.13), we find

$$\tan \theta_s / \tan (\theta_s - \beta_s) = M_1^2 \sin^2 \theta_s / (1 - \delta + \delta M_1^2 \sin^2 \theta_s) \quad (4.3.25)$$

On the other hand, this relation allows us to find the flow deflection angle  $\beta_s$  behind a shock according to the known shock angle. Figure 4.3.3 presents graphically the relation between the angles  $\theta_s$  and  $\beta_s$  for various values of the number  $M_1$ . In the region to the left of the dashed line, which corresponds to the maximum values of the angle  $\beta_s$  (i.e.,  $\beta_{s, \max}$ ), the value of the angle  $\theta_s$  diminishes with decreasing  $\beta_s$ , and to the right, conversely, it grows with decreasing  $\beta_s$ . This nature of the relation is due to the different form of a shock. In the first case, the change in the angle  $\theta_s$  corresponds to an attached curved shock ahead of a sharp-nosed body. As the body becomes blunter (the nose angle increases), the flow deflection angle grows, and, consequently, the shock angle increases. The maximum flow deflection angle  $\beta_s = \beta_{s, \max}$  is determined only by the given value of  $M_1$ . This angle is also called the **critical flow deflection (deviation) angle**  $\beta_{c,r}$ . The points corresponding to its values are connected in Fig. 4.3.3 by a dashed line. Investigations show that a flow behind an attached shock is stable as long as in the entire region behind it the flow deflection angle is smaller than the critical one. This flow is accordingly referred to as a **subcritical one**.

**Fig. 4.3.3**

Change in the flow deflection angle  $\beta_s$  depending on the shock angle  $\theta_s$  for various numbers  $M_1$

Upon a further growth of the nose angle, the angle  $\beta_s$  may become critical. According to Fig. 4.3.3, its value grows with an increase in the number  $M_1$ . From the physical viewpoint, this is explained by an increase in the strength of a shock, a greater density behind it, and, as a result, by the shock coming close to the surface of the body, which leads to deflection of the flow through a larger angle.

At a still larger nose angle, the flow behind an attached shock becomes unstable, as a result of which the shock moves away from the nose. Behind such a detached shock, a new stable flow region appears. It is characterized by deflection through an angle also less than the critical one. But unlike a subcritical flow, this one is called **supercritical**. This definition corresponds to the fact that the nose angle of the body in the flow exceeds the value at which a shock is still attached.

A detached shock changes its shape absolutely, which can be seen especially clearly in the example of a flow over a sharp-nosed cone or wedge (Fig. 4.3.4). As long as the flow is subcritical, the shock is attached to the nose and the generatrix of its surface is straight. The flow around thick wedges or cones may become supercritical, upon which the shock detaches and acquires a curved shape. At the point of intersection of the shock surface with the flow axis, the shock angle  $\theta_s = \pi/2$  and, consequently, the parameters change according to the law of a normal shock. In practice, there is a section of such a normal shock near the axis.

With an increase in the distance from the axis, the shock angle  $\theta_s$  in accordance with Fig. 4.3.4 diminishes, remaining on a certain section larger than the value that a subcritical flow corresponds to. The change in the flow deflection angle is of the opposite nature.

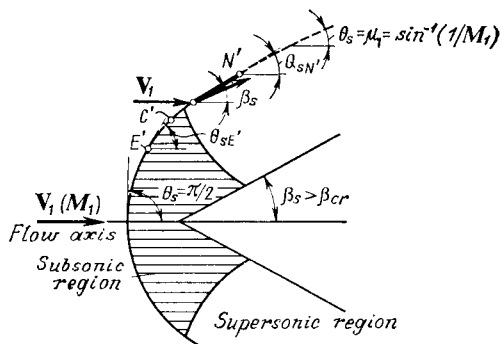


Fig. 4.3.4

Detached shock ahead of a sharp-nosed body

At the apex of the detached wave behind its straight part,  $\beta_s = 0$ , and then it grows. At a certain point on the surface, the angle  $\beta_s$  becomes critical, and then it again diminishes together with the shock angle. As follows from (4.3.25), at the limit when  $\beta_s \rightarrow 0$ , the angle  $\theta_s$  tends to the value  $\mu_1 = \sin^{-1}(1/M_1)$ . Hence, the shock angles at a preset number  $M_1$  vary within the interval  $\mu_1 \leq \theta_s \leq \pi/2$ . A shock of an infinitely small strength that is a simple pressure wave corresponds to the value  $\theta_s = \mu_1$ .

On a curved shock (see Fig. 4.3.3), we can find two points corresponding to two different angles  $\theta_s$  that at a given  $M_1$  determine the same value of the angle  $\beta_s$ . This angle is calculated by formula (4.2.20), which after introducing into it the value of  $\Delta \bar{V}_n$  from (4.3.11) acquires the form

$$\tan \beta_s = \cot \theta_s (M_1^2 \sin^2 \theta_s - 1) \left[ 1 + \left( \frac{1}{1-\delta} - \sin^2 \theta_s \right) M_1^2 \right]^{-1} \quad (4.3.26)$$

A strong shock with a subsonic flow behind it corresponds to a larger value of the angle  $\theta_s$ , and a weak shock with a supersonic flow behind it (if we exclude the vicinity of the shock with angles  $\beta_s$  close to the critical ones, where the flow may be subsonic) corresponds to a smaller value of the angle  $\theta_s$ .

An oblique shock angle can be evaluated by using formula (4.2.25). Substituting the relative density from (4.2.21) for  $\Delta \bar{V}_n$ , we obtain

$$\begin{aligned} \tan \theta_s &= \cot \beta_s \left[ \frac{1}{2} \left( \frac{\rho_2}{\rho_1} - 1 \right) \right. \\ &\quad \left. \pm \sqrt{\frac{1}{4} \left( \frac{\rho_2}{\rho_1} - 1 \right)^2 - \tan^2 \beta_s \frac{\rho_2}{\rho_1}} \right] \end{aligned} \quad (4.3.27)$$

On each curve shown in Fig. 4.3.3, we can indicate a point corresponding to the value of  $M_2 = 1$  behind a curved shock. By connecting these points with a solid curve, we obtain the boundary of

two flow conditions behind such a shock: to the left of the curve the flow will be supersonic ( $M_2 > 1$ ), and to the right of it—subsonic ( $M_2 < 1$ ).

#### 4.4. Hodograph

In addition to an analytical solution of the problem of determining the flow parameters behind an oblique shock, there is a graphical method based on the concept of a hodograph.

A **hodograph** is a curve forming the locus of the tips of the velocity vectors in the plane behind a shock. Let us consider the equation of a hodograph. Let point  $A$  (Fig. 4.4.1) be the tip of the velocity vector  $\mathbf{V}_2$  and be located, consequently, on a hodograph constructed in a coordinate system whose horizontal axis coincides with the direction of the velocity  $\mathbf{V}_1$  ahead of a shock. Hence, the inclination of the velocity vector  $\mathbf{V}_2$  is determined by the angle  $\theta_s$ . Let us designate the vertical and horizontal components of this velocity by  $w$  and  $u$ , respectively. A glance at Fig. 4.4.1 reveals that  $u$  and  $w$  can be expressed in terms of the normal  $V_{n2}$  and tangential  $V_\tau$  components of the velocity  $\mathbf{V}_2$  to the plane of the shock as follows:

$$u = V_\tau \cos \theta_s + V_{n2} \sin \theta_s, \quad w = V_\tau \sin \theta_s - V_{n2} \cos \theta_s \quad (4.4.1)$$

We determine the component  $V_{n2}$  from formula (4.3.10) in which we assume that  $V_{n1} = V_1 \sin \theta_s$  and  $V_\tau = V_1 \cos \theta_s$ . Accordingly,

$$u = V_1 \cos^2 \theta_s + \left( a^{*2} - \frac{k-1}{k+1} V_1^2 \cos^2 \theta_s \right) / V_1 \quad (4.4.2)$$

Let us eliminate the angle  $\theta_s$  from this equation. For this purpose, we shall use Eqs. (4.4.1). Multiplying the first of them by  $\cos \theta_s$ , the second by  $\sin \theta_s$  and summatting them, we obtain

$$u \cos \theta_s + w \sin \theta_s = V_\tau$$

Having in view that  $V_\tau = V_1 \cos \theta_s$ , we find

$$\tan \theta_s = (V_1 - u)/w \quad (4.4.3)$$

Substituting for  $\tan \theta_s$  its value from (4.4.3) into the trigonometric relation  $\cos^2 \theta_s = (1 + \tan^2 \theta_s)^{-1}$ , we obtain

$$\cos^2 \theta_s = [1 + (V_1 - u)^2/w^2]^{-1}$$

Introduction of this value into (4.4.2) yields

$$u = \frac{V_1}{1 + [(V_1 - u)/w]^2} + \left\{ a^{*2} - \frac{k-1}{k+1} V_1^2 \left[ 1 + \left( \frac{V_1 - u}{w} \right)^2 \right]^{-1} \right\} / V_1$$

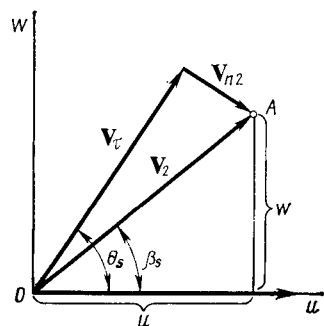


**Fig. 4.4.1**  
To the derivation of the hodograph equation

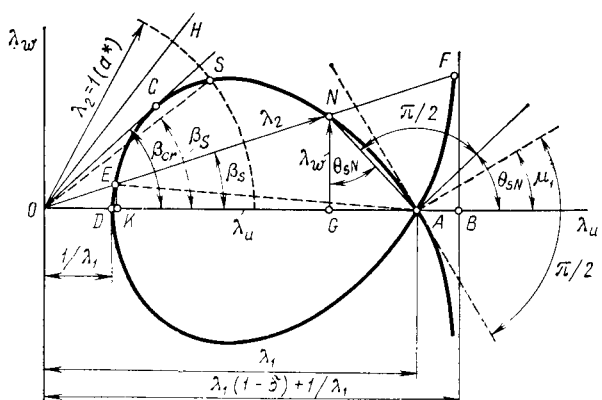


**Fig. 4.4.2**  
Strophoid (shock polar)

This expression, relating the variables  $w$  and  $u$ , is an **equation of a hodograph**. It is usually written in the form

$$\frac{w^2}{(V_1 - u)^2} = \left( u - a^{*2}/V_1 \right) / \left( \frac{2}{k+1} V_1 + \frac{a^{*2}}{V_1} - u \right) \quad (4.4.4)$$

Let us introduce the dimensionless quantities  $\lambda_u = u/a^*$ ,  $\lambda_w = w/a^*$ ,  $\lambda_1 = V_1/a^*$ , and the parameter  $\delta = (k-1)/(k+1)$ . The hodograph equation now becomes

$$\lambda_w^2/(\lambda_1 - \lambda_u)^2 = (\lambda_u \lambda_1 - 1)/[(1 - \delta) \lambda_1^2 + 1 - \lambda_1 \lambda_u] \quad (4.4.4')$$

Equation (4.4.4') graphically depicts on the plane  $\lambda_w$ ,  $\lambda_u$  a curve known as a **strophoid** (Fig. 4.4.2). Let us determine certain characteristic points of a strophoid. Particularly, let us calculate the coordinates of points  $A$  and  $D$  of intersection of the strophoid with the axis  $\lambda_u$ . Examination of (4.4.4') reveals that the condition  $\lambda_w$  is

satisfied if  $\lambda_u = \lambda_1$  or  $\lambda_u = 1/\lambda_1$ . The value  $\lambda_u = \lambda_1$  determines the coordinate of point  $A$  and makes it possible to obtain a solution corresponding to a shock of an infinitely small strength behind which the velocity does not change. The value  $\lambda_u = 1/\lambda_1$  determines the coordinate of intersection point  $D$  closest to the origin of coordinates and is the solution for a normal shock.

It follows from the construction of a strophoid that its two branches to the right of point  $A$  extend to infinity, asymptotically approaching the straight line passing through point  $B$  and parallel to the vertical axis. The coordinate of this point can be obtained from (4.4.4') by a limit transition at  $\lambda_u \rightarrow \infty$ . The result is the condition  $(1 - \delta) \lambda_1^2 + 1 - \lambda_1 \lambda_u = 0$ , from which we find the coordinate of point  $B$ , i.e.  $\lambda_u = \lambda_1 (1 - \delta) + 1/\lambda_1$ .

Any point on a strophoid branch extending to infinity formally yields a solution for a shock. Considering, for example, point  $F$  in Fig. 4.2.2, we may assume that for a shock behind which the direction of the velocity changes by a preset value of the angle  $\beta_s$ , the velocity increases abruptly to the value  $\lambda_2$  determined by the length of segment  $OF$ . The pressure and density would also decrease abruptly. In other words, in the given case there would be not a compression shock, but an expansion one. But the formation of such shocks is impossible physically. To prove this, let us use formula (4.3.6) for the change in the entropy. Applying the ratios  $p_2/p_2^k = p_0'/(\rho_0')^k$ ,  $p_1/p_1^k = p_0/\rho_0^k$ , and taking into account that  $p_0' p_0 = \rho_0' \rho_0$ , from formula (4.3.6) we obtain

$$S_2 - S_1 = R \ln (p_0/p_0') \quad (4.4.5)$$

When there is a compression shock,  $p_0 > p_0'$  and, consequently,  $S_2 - S_1 > 0$ . This conclusion corresponds to the second law of thermodynamics, according to which the entropy of an isolated system with compression shocks increases.

Let us now consider the reverse situation when a gas passes from a state characterized by the stagnation pressure  $p_0'$  (the parameters with the subscript 2) into a state with the stagnation pressure  $p_0$  (the parameters with the subscript 1) through an expansion shock. In this case, by analogy with (4.4.5), the change in the entropy is

$$S_1 - S_2 = R \ln (p_0'/p_0)$$

Hence, when the condition  $p_0' < p_0$  is retained, the entropy should diminish, but this contradicts the second law of thermodynamics. It thus follows that expansion shocks cannot appear.

In accordance with the above, the passage of a gas through a shock, which is adiabatic in its nature because it occurs in a thermally insulated system, is an irreversible adiabatic non-isentropic process.

Equation (4.3.6) can be used to verify that a real process of an increase in the entropy ( $S_2 - S_1 > 0$ ) corresponds to a supersonic

flow [ $M_1 > 1$  (a normal shock),  $M_1 \sin \theta_s > 1$  (an oblique shock)], while the physically impossible phenomenon of a decrease in the entropy ( $S_2 - S_1 < 0$ ), to a subsonic flow ( $M_1 < 1$  and  $M_1 \sin \theta_s < 1$ ). Hence, *shocks can appear only in a supersonic flow*. We must note that the relations obtained for the change in the entropy are valid when an irreversible process of transition through a shock is attended by an isentropic flow of the gas both ahead of a shock and behind it.

It follows from the above that the branches of a strophoid extending to infinity have no physical meaning. The part of a strophoid (to the left of point  $A$ , Fig. 4.4.2) having a physical meaning is called a **shock polar**. Such a curve is constructed for a given number  $\lambda_1$  (or  $M_1$ ). Several curves constructed for various values of  $\lambda_1$  form a family of shock polars allowing one to calculate graphically the velocity of a flow behind a shock and the flow deflection angle.

Let us consider an attached shock ahead of a wedge-shaped surface with the half-angle  $\beta_s$  (see Fig. 4.1.1c). To determine the velocity behind such a shock, we construct a shock polar corresponding to the given number  $\lambda_1$  (or  $M_1$ ) and draw a straight line from point  $O$  (Fig. 4.4.2) at the angle  $\beta$ . Point of intersection  $N$  with the shock polar determines the vector  $\vec{ON}$  whose magnitude shows the value of the velocity ratio  $\lambda_2$  behind the shock. By formula (4.4.3), which we shall write in the form

$$\tan \theta_s = (\lambda_1 - \lambda_u)/\lambda_w \quad (4.4.3')$$

the angle  $ANG$  on the shock polar equals the shock angle  $\theta_{sN}$ . We must note that this angle can also be determined as the angle between the horizontal axis and a normal to the straight line connecting the tips of the velocity vectors ahead of a shock and behind it (points  $A$  and  $N$ , respectively, in Fig. 4.4.2).

When considering the shock polar, we can arrive at the conclusion that a decrease in the angle  $\beta_s$  (point  $N$  moves along the curve toward point  $A$ ) is attended by a decrease in the shock angle  $\theta_{sN}$ . At the limit, when  $\beta_s \rightarrow 0$ , point  $N$  merges with point  $A$ , which physically corresponds to the transformation of the shock wave into an **infinitesimal shock wave**, i.e. into a **line of weak disturbances**. The shock angle for such a shock  $\theta_s = \mu_1$  is determined as the angle between the horizontal axis and the straight line perpendicular to a tangent to the shock polar at point  $A$  (Fig. 4.4.2).

A growth in the flow deflection angle (in Fig. 4.4.2 this corresponds to point  $N$  moving away from  $A$ ) leads to an increase in the shock angle and to a higher strength of the shock. A glance at the shock polar shows that at a certain angle  $\beta_s$  a straight line drawn from point  $O$  will be tangent to the curve at point  $C$ . The angle of inclination of this tangent determines the maximum flow deflection angle, called the critical one above ( $\beta_s = \beta_{cr}$ ). Assume that the wedge

angle  $\beta_s > \beta_{cr}$ . In the graph, solid line  $OH$  drawn from point  $O$  and not intersecting the shock polar corresponds to this angle.

Therefore, when  $\beta_s > \beta_{cr}$ , we cannot find a graphical solution for a shock with the aid of a shock polar. This is due to the fact that the inequality  $\beta_s > \beta_{cr}$  does not correspond to the assumptions (on the basis of which we obtained equations for a shock) consisting in that a shock is straight and should be attached to a nose. Physically—in the given case of the wedge angle  $\beta_s$  exceeding the critical deflection angle  $\beta_{cr}$ —the compression shock detaches and becomes curved.

The determination of the shape of such a curved shock and of its distance to the body is the task of a special problem of aerodynamics associated, particularly, with the conditions of supercritical flow past a wedge. If such a problem is not solved, then with the aid of a polar in the field of definition from point  $D$  to  $A$  we can give only a qualitative appraisal of the change in the parameters in a region ahead of the surface in the flow. If, on the other hand, the shape of the shock is determined for preset flow conditions (in addition to calculations, this can also be done with the aid of blowing in a wind tunnel), it is possible to establish quantitative correspondence between the points of a shock polar and the shock surface.

Assume, for example, that we have set the angle  $\beta_s$  and points  $E$  and  $N$  on a shock polar (Fig. 4.4.2). The shock angle  $\theta_{sN} = \angle ANG$  corresponds to point  $N$ , and the angle  $\theta_{sE} = \angle AEK$  ( $EK \perp OB$ ) to point  $E$ . If the configuration of the shock wave front is known, then by direct measurement we can find on it a point  $N'$  with the wave angle  $\theta_{sN'}$  and a point  $E'$  with the angle  $\theta_{sE'}$  (see Fig. 4.3.4). In the same way, we can find a point  $C'$  on the shock that corresponds to the critical (maximum) deflection angle  $\beta_{cr}$ .

On a preset surface of a detached shock, point  $D$  on the shock polar corresponds to the shock apex (a normal shock), and terminal point  $A$  of the polar corresponds to the remotest part of the shock that has transformed into a line of weak disturbances.

For an attached shock ( $\beta_s < \beta_{cr}$ ), we can indicate two solutions, as can be seen on the shock polar. One of them (point  $E$ ) corresponds to a lower velocity behind the shock, and the other (point  $N$ ), to a higher one. Observations show that attached shocks with a higher velocity behind them, i.e. shocks with a lower strength are possible physically.

If we draw on the graph the arc of a circle whose radius is unity (in the dimensional axes  $w$  and  $u$  this corresponds to a radius equal to the critical speed of sound  $a^*$ ), we can determine the regions of the flow—subsonic and supersonic—which points on the shock polar to the left and right of the arc correspond to. In Fig. 4.3.4, the section of the flow corresponding to a subsonic velocity is hatched. A close look at the shock polar reveals that the velocity is always

subsonic behind a normal shock. On the other hand, behind an oblique (curved) shock, the velocity may be either supersonic (the relevant points on the shock polar are to the right of point  $S$ ) or subsonic (the points on the polar are to the left of point  $S$ ). Points on the polar between  $S$  and  $C$  correspond to an attached shock behind which the velocities are subsonic. Experimental investigations show that for wedge angles  $\beta_s$  less than the critical one  $\beta_{cr}$  or larger than  $\angle SOB$ , a shock remains attached, but it becomes curved. The theoretical values for the angle  $\theta_s$  and the gas velocity  $\lambda_2$  on the entire section behind such a curved shock found on the polar according to the wedge angle  $\beta_s$  do not correspond to the actual values.

#### 4.5. A Normal Shock in the Flow of a Gas with Constant Specific Heats

We shall obtain the corresponding relations for a normal shock from the condition that  $\theta_s = \pi/2$  and, consequently,  $V_{n1} = V_1$  and  $V_{n2} = V_2$ . Basic equation (4.3.10) becomes

$$V_1 V_2 = a^{*2} \quad (4.5.1)$$

or

$$\lambda_1 \lambda_2 = 1 \quad (4.5.1')$$

where  $\lambda_1 = V_1/a^*$  and  $\lambda_2 = V_2/a^*$ .

We find the relative change in the velocity from (4.3.11'):

$$\Delta \bar{V} = (V_1 - V_2)/V_1 = (1 - \delta)(1 - 1/M_1^2) \quad (4.5.2)$$

We obtain the corresponding relations for the ratios of the densities, pressures, and temperatures from (4.3.13), (4.3.15), and (4.3.16):

$$\rho_2/\rho_1 = M_1^2/(1 - \delta + \delta M_1^2) \quad (4.5.3)$$

$$p_2/p_1 = (1 + \delta) M_1^2 - \delta \quad (4.5.4)$$

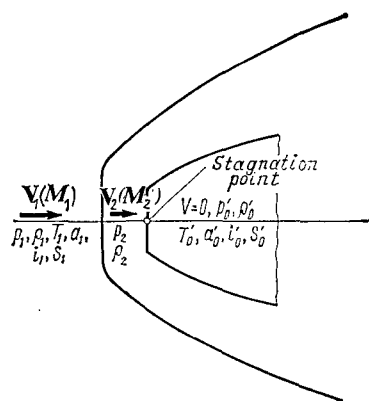
$$T_2/T_1 = [(1 + \delta) M_1^2 - \delta] (1 - \delta + \delta M_1^2)/M_1^2 \quad (4.5.5)$$

By eliminating  $M_1^2$  from (4.5.3) and (4.5.4), we obtain an equation of a shock adiabat for a normal shock that in its appearance differs in no way from the similar equation for an oblique shock [see (4.3.13')].

Assuming in (4.3.19) that  $\theta_s = \pi/2$ , we find the relation for the Mach number behind a normal shock:

$$M_2^2/M_1^2 = (T_1/T_2) (\rho_1/\rho_2)^2 \quad (4.5.6)$$

Let us consider the parameters of a gas at the point of stagnation (at the critical point) of a blunt surface behind a normal shock (Fig. 4.5.1). The pressure  $p'_0$  at this point is determined by formula

**Fig. 4.5.1**

Parameters of a gas at the stagnation point behind a normal shock

(4.3.20') in which the ratios  $\rho_2/\rho_1$  and  $p_2/p_1$  are found from (4.5.3) and (4.5.4), respectively. With this in view, we have

$$p'_0/p_0 = [(1 + \delta) M_1^2 - \delta]^{(\delta-1)/2\delta} [M_1^2/(1 - \delta + \delta M_1^2)]^{(1+\delta)/2\delta} \quad (4.5.7)$$

Determining  $p_0$  by (4.3.21), we find

$$p'_0/p_1 = [(1 + \delta) M_1^2 - \delta]^{(\delta-1)/2\delta} M_1^{(1+\delta)/\delta} (1 - \delta)^{-(1+\delta)/2\delta} \quad (4.5.8)$$

Knowing the absolute pressure  $p'_0$ , we can determine the dimensionless quantity  $\bar{p}_0 = (p'_0 - p_1)/q_1$ —the pressure coefficient at the stagnation point. Taking into account that the velocity head is

$$q_1 = \frac{k p_1 M_1^2}{2} = \frac{1 + \delta}{2(1 - \delta)} p_1 M_1^2$$

we obtain

$$\begin{aligned} \bar{p}_0 &= \frac{2(1 - \delta)}{(1 + \delta) M_1^2} \{[(1 + \delta) M_1^2 - \delta]^{(\delta-1)/2\delta} M_1^{(1+\delta)/\delta} \\ &\quad \times (1 - \delta)^{-(1+\delta)/2\delta} - 1\} \end{aligned} \quad (4.5.9)$$

It is proved in Sec. 4.3 that the stagnation temperature behind a shock does not change, i.e.  $T'_0 = T_0$ . Consequently, at the stagnation point, we have

$$T'_0 = T_1 \left( 1 + \frac{\delta}{1 - \delta} M_1^2 \right) \quad (4.5.10)$$

Let us use the expression  $i'_0 = c_p T'_0$  and  $i_1 = c_p T_1$  to determine the enthalpy. Accordingly, at the stagnation point, we have

$$i'_0 = i_1 \left( 1 + \frac{\delta}{1 - \delta} M_1^2 \right) \quad (4.5.11)$$

#### 4.6. A Shock at Hypersonic Velocities and Constant Specific Heats of a Gas

At hypersonic (very high) velocities, which values of  $M_1 \sin \theta_s \gg \gg 1$  correspond to, the dimensionless parameters of a gas behind a shock are very close to their limiting values obtained at  $M_1 \sin \theta_s \rightarrow \infty$ . It follows from (4.3.11') that for this condition, we have

$$\Delta \bar{V}_n = 1 - \delta \quad (4.6.1)$$

Consequently, the limiting ratio of the densities by (4.2.13) is

$$\rho_1 / \rho_2 = 1 - \Delta \bar{V}_n = \delta \quad (4.6.2)$$

Introducing this value into (4.3.27), we obtain the following expression at the limit when  $M_1 \sin \theta_s \rightarrow \infty$ :

$$\tan \theta_s = (\cot \beta_s / 2\delta) [1 - \delta \pm \sqrt{(1 - \delta)^2 - 4\delta \tan^2 \beta_s}] \quad (4.6.3)$$

Let us find the limiting value of the pressure coefficient. For the conditions directly behind a shock, as follows from (4.3.15"), when  $M_1 \sin \theta_s \rightarrow \infty$  and  $M_1 \rightarrow \infty$ , we have

$$\bar{p}_2 = 2(1 - \delta) \sin^2 \theta_s \quad (4.6.4)$$

We obtain the corresponding quantity for the point of stagnation from (4.3.23):

$$\bar{p}_0 = 2(1 - \delta)^{(\delta-1)/2\delta} (1 + \delta)^{-(1+\delta)/2\delta} \sin^2 \theta_s \quad (4.6.5)$$

The ratio of the pressure coefficients is

$$\bar{p}_0 / \bar{p}_2 = (1 - \delta^2)^{-(1+\delta)/2\delta} \quad (4.6.6)$$

In the particular case when  $\delta = 1/6$  ( $k = 1.4$ ), the ratio  $\bar{p}_0 / \bar{p}_2 = 1.09$ . The limiting value of the number  $M_2$  can be found from (4.3.19), using relation (4.3.16) for  $T_2 / T_1$ . A passage to the limit when  $M_1 \sin \theta_s \rightarrow \infty$  and  $M_1 \rightarrow \infty$  yields

$$M_2^2 = \{1 / [\delta(1 + \delta)]\} (\cot^2 \theta_s + \delta^2) \quad (4.6.7)$$

To find the limiting parameters behind a normal shock, we must assume that  $\theta_s = \pi/2$  in the above relations. As a result, from (4.6.4) and (4.6.5) we have:

$$\bar{p}_2 = 2(1 - \delta) \quad (4.6.4')$$

$$\bar{p}_0 = 2(1 - \delta)^{(\delta-1)/2\delta} (1 + \delta)^{-(1+\delta)/2\delta} \quad (4.6.5')$$

We can see that the ratio  $\bar{p}_0/\bar{p}_2$  is the same as for an oblique shock. The limiting Mach number behind a normal shock is

$$M_2 = \sqrt{\delta/(1-\delta)} \quad (4.6.7')$$

For  $\delta = 1/6$  ( $k = 1.4$ ), the number  $M_2 = \sqrt{1/7} \approx 0.38$ . The actual values of the dimensionless parameters behind a shock at finite, although very large, Mach numbers depend on  $M_1$ .

Let us consider the corresponding working relations for the case when attached shocks originate ahead of slender wedges, and the shock angles are therefore low. Assuming in (4.3.25) that  $\tan \theta_s \approx \approx \theta_s$  and  $\tan(\theta_s - \beta_s) \approx \theta_s - \beta_s$ , we obtain

$$(\theta_s - \beta_s) \theta_s = (1 - \delta + \delta M_1^2 \theta_s^2) (M_1^2 \theta_s^2)$$

Introducing the symbol  $K = M_1 \beta_s$ , after transformations, we find

$$\frac{\theta_s^2}{\beta_s^2} - \frac{1}{1-\delta} \cdot \frac{\theta_s}{\beta_s} - \frac{1}{K^2} = 0 \quad (4.6.8)$$

Solving this equation for  $\theta_s/\beta_s$  and taking into account that the condition  $\theta_s/\beta_s > 1$  is physically possible, we find

$$\frac{\theta_s}{\beta_s} = \frac{1}{2(1-\delta)} + \sqrt{\frac{1}{4(1-\delta)^2} + \frac{1}{K^2}} \quad (4.6.9)$$

Inspection of Eq. (4.6.9) reveals that the parameters determining the flow in a shock at very high velocities are combined into functional groups such that they are *a solution of the problem of a shock for a broad range of numbers  $M_\infty$  and values of the angle  $\beta_s$  in the form of a single curve*. Equation (4.6.9) is an example of a similarity relation. In accordance with this equation for the ratio  $\theta_s/\beta_s$ , the quantity  $K = M_1 \beta_s$  is a similarity criterion. This similarity must be understood in the sense that regardless of the absolute value of the quantities characterizing hypersonic flows, when such flows have identical parameters  $K$ , the ratios of the angles  $\theta_s/\beta_s$  are also identical. When  $K \rightarrow \infty$ , the ratio  $\theta_s/\beta_s$  tends to a limit equal to

$$\theta_s/\beta_s = 1/(1-\delta) \quad (4.6.10)$$

Let us consider the relation for the pressure coefficient. At low values of  $\theta_s$ , formula (4.3.15'') acquires the form

$$\bar{p}_2 = 2(1-\delta)(\theta_s^2 - 1/M_1^2)$$

or

$$\bar{p}_2 = 2(1-\delta)\beta_s^2(\theta_s^2/\beta_s^2 - 1/K^2) \quad (4.6.11)$$

Introducing the value of  $1/K^2$  from (4.6.8), we obtain

$$\bar{p}_2 = 2\beta_s \theta_s \quad (4.6.11)$$

Substituting for the angle  $\theta_s$  the value determined from (4.6.9), we find

$$\frac{\bar{p}_2^2}{\beta_s^2} = \frac{1}{1-\delta} \left[ 1 + \sqrt{1 + \frac{4(1-\delta)^2}{K^2}} \right] \quad (4.6.12)$$

This formula shows that  $K$  is also a similarity criterion for the ratio  $\bar{p}_2/\beta_s^2$ . At the limit when  $K \rightarrow \infty$ , this ratio becomes

$$\bar{p}_2/\beta_s^2 = 2/(1-\delta) \quad (4.6.13)$$

In accordance with (4.3.13), at small value of  $\theta_s$ , the density ratio is

$$\rho_2/\rho_1 = K_s^2/(1-\delta + \delta K_s^2) \quad (4.6.14)$$

where the parameter  $K_s = M_1 \theta_s$  is determined with the aid of (4.6.9) in the following form:

$$K_s = \frac{K}{2(1-\delta)} \left[ 1 + \sqrt{1 + \frac{4(1-\delta)^2}{K^2}} \right] \quad (4.6.15)$$

We can see from (4.3.18) that at low values of  $\theta_s$  the second term on the right-hand side may be ignored, and we can thus consider that  $V_2 \approx V_1$ . With this in view, the ratio of the squares of the Mach numbers in accordance with (4.3.19) is  $M_2^2/M_1^2 = T_1/T_2$ . Substituting for the ratio  $T_1/T_2$  here its value from formula (4.3.16) in which we assume that  $\sin \theta_s \approx \theta_s$ , we obtain

$$\theta_s^2 M_2^2 = K_s^4 / \{[(1+\delta) K_s^2 - \delta](1-\delta + \delta K_s^2)\} \quad (4.6.16)$$

When  $K_s \rightarrow \infty$ , we have

$$\theta_s^2 M_2^2 \rightarrow 1/[\delta(1+\delta)] \quad (4.6.16')$$

#### 4.7. A Shock in a Flow of a Gas with Varying Specific Heats and with Dissociation and Ionization

When solving a problem on a shock in a dissociated and ionized gas, the parameters of the air at an altitude  $H$  (the pressure  $p_1$ , temperature  $T_1$ , density  $\rho_1$ , speed of sound  $a_1$ , etc.), and also the value of the normal velocity component  $V_{n1}$  (or the number  $M_{n1} = V_{n1}/a_1$ ) are taken as the initial data. Hence, an oblique shock in the given case is treated as a normal one. Assuming in a first approximation that the value of  $\Delta \bar{V}_n \approx 0.9-0.95$ , which corresponds to setting a relative density for a shock of  $\rho_2/\rho_1 = (1 - \Delta \bar{V}_n)^{-1} \approx 10-20$ , from (4.2.15) we find the pressure  $p_2$ , and from (4.2.16), the enthalpy  $i_2$  that is evidently close to the stagnation enthalpy  $i'_0$ .

By next using an  $i$ - $S$  diagram (see [6, 8]), we determine the temperature  $T_2$ , and then from Fig. 1.5.7, the mean molar mass  $\mu_{m2}$ . Instead of the diagram, one may use suitable tables of the thermodynamic functions of air (see [7]), which will increase the accuracy of the calculations.

By inserting the found values of  $p_2$ ,  $T_2$ , and  $\mu_{m2}$  into the equation of state (1.5.8), we can determine the density  $\rho_2$  and define the value of  $\Delta\bar{V}_n$  more precisely by (4.2.21). We next use this value in a second approximation to find the pressure and enthalpy, respectively, by formulas (4.2.15) and (4.2.16). According to these values and with the aid of tables and graphs, we define the temperature and mean molar mass more exactly. We use the refined values of  $p_2$ ,  $T_2$ , and  $\mu_{m2}$  to find the density in the second approximation by the equation of state. The approximations are terminated when the preset accuracy is achieved.

We can evaluate the shock angle corresponding to a given velocity  $V_1$  by the formula  $\sin \theta_s = V_{n1}/V_1$ . By introducing the value of  $\theta_s$  and also the number  $M_1 = V_1/a_1$  into (4.3.26), we determine the flow deviation angle  $\beta_s$  behind the shock.

An oblique shock can also be calculated when the values of the free-stream parameters (including the number  $M_1$ ) and the angle  $\beta_s$  are known. In a first approximation, we determine the shock angle  $\theta_s$  for an undissociating gas [see (4.3.27)], and then find the corresponding values of  $\Delta\bar{V}_n$ ,  $p_2$ , and  $i_2$  by formulas (4.2.19), (4.2.15), and (4.2.16). Using these values, we determine the temperature  $T_2$  and the mean molar mass  $\mu_{m2}$  from tables [7] or graphs [6, 8]. Next by formulas (4.2.23) and (4.2.24), we define  $\Delta\bar{V}_n$  more precisely, and by expression (4.2.25),  $\tan \theta_s$  and the angle  $\theta_s$ . We refine the other parameters according to the relevant formulas.

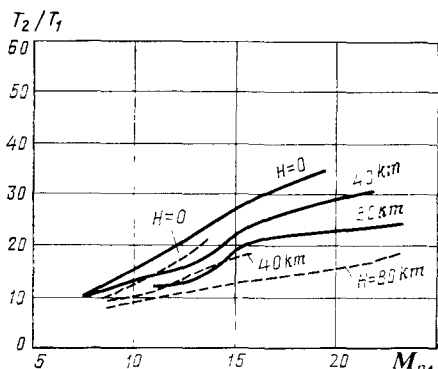
We calculate the parameters of a gas behind a normal shock in a similar way with the use of tables or graphs of the thermodynamic functions for high temperatures. We assume that  $\theta_s = \pi/2$  and  $\beta_s = 0$  and, therefore, use (4.2.27)-(4.2.35).

When dissociation and ionization occur, the relative values of the parameters of a gas behind a shock wave depend not only on the temperature, which is characteristic of varying specific heats, but also on the pressure. These relations are shown graphically in Figs. 4.7.1-4.7.3. The ratios of the temperatures and densities are calculated for averaged values of the temperature  $T_1$  of 220 and 350 K. These values equal, respectively, the probable minimum and maximum that are chosen depending on the change in the air temperature with altitude for decreased and increased annual average values. Available data show that dissociation and ionization give rise to a substantial change in the equilibrium temperature and density in comparison with constant specific heats ( $k = 1.4 = \text{const}$ ). The pressure depends to a considerably smaller extent

**Fig. 4.7.1**

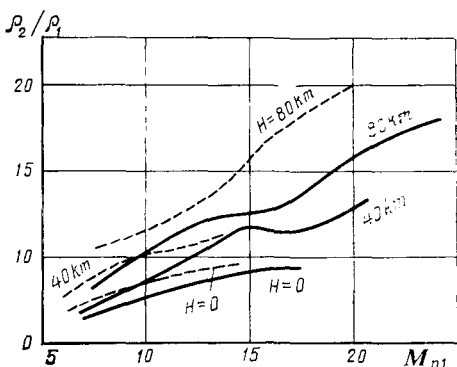
Ratio of the air temperatures behind and ahead of a shock with account taken of dissociation and ionization:

solid lines— $T_1 = 220 \text{ K}$ , dashed lines— $T_1 = 350 \text{ K}$

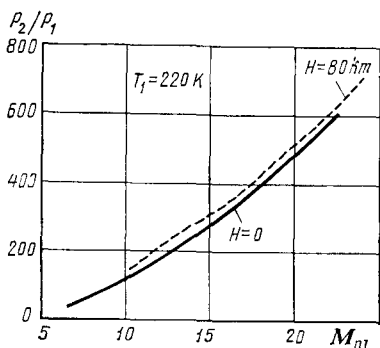
**Fig. 4.7.2**

Ratio of the air densities behind and ahead of a shock with account taken of dissociation and ionization:

solid lines— $T_1 = 220 \text{ K}$ , dashed lines— $T_1 = 350 \text{ K}$

**Fig. 4.7.3**

Ratio of the air pressures behind and ahead of a shock with account taken of dissociation and ionization



on the physicochemical transformations of the air. The ratio  $p_2/p_1$  differs only slightly from the maximum value of  $p_2/p_1 = 1 + k_1 M_{n1}^2$  determined only by the conditions of the oncoming flow, but not by the change in the structure and physicochemical properties of the air behind a shock wave.

The temperature behind a shock in a dissociated gas is lower than that with constant specific heats (Fig. 4.7.1). The explanation is the loss of energy on the thermal dissociation of the molecules.

The lowering of the temperature due to this phenomenon causes the density to grow (Fig. 4.7.2). This greater "yielding" of the gas to compression reduces the space between a shock and a surface in the flow, thus diminishing the shock angle. And conversely, at the same angle  $\theta_s$  in a real heated gas, the flow deflection (the angle  $\beta_s$ ) is greater than in a perfect gas ( $k = \text{const}$ ). The result is that in a heated gas a detached shock forms with a certain delay in comparison with a cold gas. Particularly, the wedge angle (critical angle) at which detachment of a shock begins is larger in a heated gas than in a cold one.

Account of the influence of dissociation leads to a certain increase in the pressure behind a shock in comparison with a gas having constant specific heats (Fig. 4.7.3). This is explained by the increase in the number of particles in the gas owing to dissociation and by the increase in the losses of kinetic energy when they collide. But the drop in the temperature in a dissociated gas causes an opposite effect, but smaller in magnitude. As a result, the pressure increases, although only slightly.

The theory of a normal shock has an important practical application when determining the parameters of a gas at the point of stagnation. The procedure is as follows. According to the found values  $i_2$  and  $p_2$  with account taken of dissociation and ionization, we find the entropy  $S_2$  from an  $i$ - $S$  diagram or tables of thermodynamic functions for air. Considering the flow behind a shock to be isentropic, we assume that the entropy  $S'_0$  at the stagnation point equals the value  $S_2$  behind the shock wave. In addition, for this point we can find the enthalpy  $i'_0 = i_1 + 0.5V_1^2$ . Now knowing  $S'_0$  and  $i'_0$ , we can use an  $i$ - $S$  diagram or thermodynamic tables to find the other parameters, namely,  $p'_0$ ,  $T'_0$ ,  $\rho'_0$ , etc.

The results of the calculations correspond to the preset flight altitude. A change in the altitude is attended by a change in the conditions of flow past a body and, consequently, in the parameters at the point of stagnation. This relation is shown graphically in Fig. 4.7.4. The curves allow us to determine the temperature  $T'_0$  and pressure  $p'_0$  as a function of the velocity  $V_1$  and the flight altitude  $H$ .

The value of  $p'_0$ , in turn, can be used to calculate the pressure coefficient at the point of stagnation:  $\bar{p}_0 = 0.5kM_\infty^2 (p'_0/p_\infty - 1)$ . Its value grows somewhat in a dissociating flow. For example, at an altitude of 10 km at  $M_\infty = 16.7$ , its value is  $\bar{p}_0 = 2.08$ , whereas without account taken of dissociation  $\bar{p}_0 = 1.83$  (for  $k = c_p/c_r = 1.4$ ). The pressure coefficient can be seen to grow by about 13%.

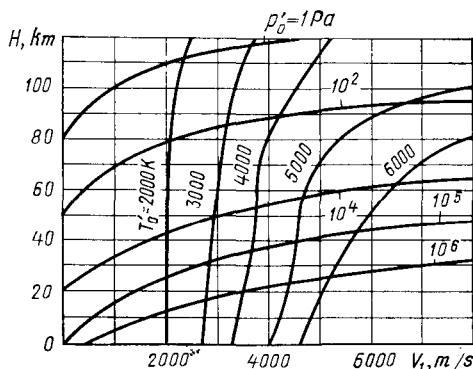


**Fig. 4.7.4**  
Pressure and temperature at the point of stagnation

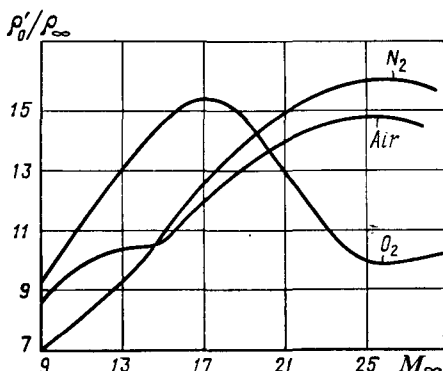


**Fig. 4.7.5**  
Density at the point of stagnation on the surface of a sphere for nitrogen, oxygen, and air ( $p_{\infty} = 10^3$  Pa,  $T_{\infty} = 290$  K)

The results of calculating the density at the point of stagnation with account taken of dissociation and ionization for air, and also for pure oxygen and nitrogen, are given in Fig. 4.7.5. An analysis of these results allows us to arrive at the following conclusion. At  $M_{\infty} = 18$ , when oxygen is already noticeably dissociated, the quantity  $\rho'_0/\rho_{\infty}$  reaches its maximum value. Upon a further increase in  $M_{\infty}$ , the gas completely dissociates, and the density drops. Next a growth in  $M_{\infty}$  is attended by primary ionization of the oxygen. This leads to an increase in the specific heat and, consequently, to a certain growth in the density.

The influence of the varying nature of the specific heat on the change in the density of nitrogen is observed only at very large numbers  $M_{\infty}$  when dissociation and ionization take place. These processes run not consecutively, as in oxygen, but virtually simultaneously, which is due to the smaller difference between the energies of dissociation and ionization of nitrogen. This is why the curve  $\rho'_0/\rho_{\infty}$  for nitrogen is more monotonic than for oxygen.

At  $M_\infty < 13$ , what mainly occurs in the air is dissociation of oxygen, and the density curve for air is closer to the relevant curve for oxygen. At  $M_\infty > 13$ , when the dissociation of the nitrogen becomes appreciable, the dependence of  $\rho'/\rho_\infty$  on  $M_\infty$  for air reminds one of the similar relation for gaseous nitrogen because the latter is the predominating component in the air.

The calculation of the parameters of a gas behind a shock with a view to the varying nature of the specific heats is described in greater detail in [14].

#### 4.8. Relaxation Phenomena

Section 4.7 deals with ways of calculating the parameters of a gas behind a shock with account taken of the physicochemical transformations for conditions of equilibrium of the thermodynamic processes. In a more general case, however, these processes are characterized by non-equilibrium, which has a definite influence on the gas flow behind shocks.

##### Non-Equilibrium Flows

It is known from thermodynamics that the assumption of thermodynamic equilibrium consists in agreement between the levels of the internal degrees of freedom and the parameters characterizing the state of a gas. For example, at comparatively low temperatures (low velocities), equilibrium sets in between the temperature and the vibrational degree of freedom, which corresponds to equilibrium between the temperature and the specific heat. At high temperatures (high velocities), when a gas dissociates, the equilibrium state is reached as follows. As dissociation develops, the probability of triple collisions grows (for a binary mixture of diatomic gases) because the number of gas particles increases. This leads to the acceleration of recombination and the retardation of the rate of dissociation. At a certain instant and temperature, the rates of the direct and reverse reactions become equal, and the gas arrives at an equilibrium state. The latter is characterized by a constant composition and agreement between the degree of dissociation, on the one hand, and the temperature and pressure, on the other. At still higher temperatures (very high velocities), equilibrium processes of excitation of the electron levels and ionization can be considered.

Upon a sudden change in the temperature in an equilibrium flow, the corresponding internal degrees of freedom also set in instantaneously; dissociation and ionization can be considered as the manifestation of new degrees of freedom. Consequently, in these cases, there is no delay in establishing the degrees of freedom, i.e. the time needed for achieving equilibrium is zero.

In practice, an equilibrium flow is observed under supersonic flows past bodies at Mach numbers of  $M_\infty = 4\text{-}5$  in conditions corresponding to altitudes of 10-15 km and less. The explanation is that at the maximum temperatures of the order of 1000-1500 K appearing in these conditions, the main part of the internal energy falls to the share of the translational and rotational degrees of freedom, which upon sudden changes in the temperature are established virtually instantaneously because only a few molecular collisions are needed to achieve equilibrium. This is why the translational and rotational degrees of freedom are usually called "active" degrees. With an increase in the velocities and, consequently, in the temperatures, a substantial part of the internal energy is spent on vibrations, then on dissociation, excitation of the electron levels, and ionization.

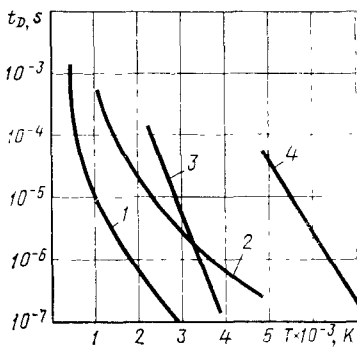
Actual processes are such that these energy levels set in more slowly than the translational and rotational ones because a much greater number of collisions is needed. For this reason, the vibrational and dissociative degrees of freedom are sometimes called "inert" degrees. Hence, the inert degrees are featured by a delay in the achievement of equilibrium called **relaxation**. The time in which equilibrium sets in, i.e. correspondence between the temperature and the energy level is established, is called the **relaxation time**.

*The relaxation time characterizes the rate of attenuation of departures of a gas state from an equilibrium one, which in a general case manifests itself in the form of a change in the energy distribution among the different degrees of freedom.*

Relaxation processes are determined by what degree of freedom is excited. If upon a sudden change in the temperature, vibrations appear, the corresponding non-equilibrium process is called **vibrational relaxation**. It is characterized by a lag in the specific heat when the temperature changes. If the temperature rises, the specific heat grows because of the appearance of vibrations of the atoms in the molecules. The time during which vibrational motion reaches equilibrium is called the **vibrational relaxation time**.

In a non-equilibrium dissociating gas upon a sudden change in the temperature, a delay occurs in the change in the degree of dissociation. This phenomenon is called **dissociative relaxation**. Owing to the difference between the rates of formation of the atoms and their vanishing (the rate of dissociation is higher than that of recombination), a gradual increase in the degree of dissociation occurs. The equilibrium value of the degree of dissociation is achieved at the instant when the rates of the direct and reverse reactions become equal. The time needed to obtain an equilibrium degree of dissociation is called the **dissociative relaxation time**.

Experimental data on the relaxation time for oxygen and nitrogen are given in Fig. 4.8.1.

**Fig. 4.8.1**

Experimental (1, 2) curves of the vibrational relaxation time and calculated (3, 4) curves of the relaxation time for the dissociation of oxygen and nitrogen, respectively, at atmospheric pressure

At temperatures approximately up to 10 000 K, the vibrational and dissociative relaxation processes are the main ones. The relaxation phenomena associated with the excitation of the electron levels of the molecules and atoms, and also with ionization, may be disregarded because a small fraction of the internal energy falls to the share of these degrees of freedom at the indicated temperatures.

A non-equilibrium state has a substantial influence on the various processes attending the flow of a gas at very high velocities. Particularly, vibrational and dissociative relaxations change the parameters of a gas in a transition through shock waves and in the flow past bodies. This, in turn, affects the processes of friction, heat exchange, and also the redistribution of the pressure.

The studying of non-equilibrium flows consists in the joint investigation of the motion of the fluid and of the chemical processes occurring at finite velocities. This is expressed formally in that an equation for the rate of chemical reactions is added to the usual system of equations of gas dynamics.

### **Equilibrium Processes**

Equilibrium flows have been studied better than non-equilibrium ones both from the qualitative and the quantitative standpoints. The regions of a flow in which equilibrium sets in are different because of the different relaxation times for the excitation levels. The duration of the establishment of equilibrium relative to the vibrational degrees of freedom is longer by several orders than relative to the translational and rotational ones. Equilibrium sets in even more slowly relative to the composition of a gas mixture when dissociation and ionization occur. Accordingly, the scheme of a non-equilibrium process is such that the attainment of equilibrium of one degree of freedom may be attended by the beginning of a relax-

ation phenomenon of another one. In more general case, overlapping of the regions of establishing equilibrium is observed.

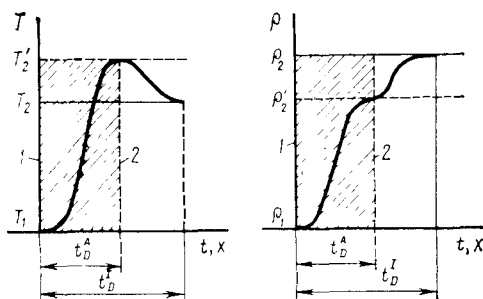
An approximate model of the process can be conceived on the basis of the "freezing" principle. It is considered that a region of achievement of equilibrium relates to one or several degrees of freedom, while the others are not excited. The sequence of these regions of equilibrium can be represented by degrees of freedom with elevation of the temperature in the following order: translational, rotational, and vibrational degrees, dissociation, excitation of electron levels, and ionization. When considering, for example, the process of establishing equilibrium of vibrations, the first two degrees of freedom can be considered to be completely excited. This process occurs in conditions of "frozen" dissociation and ionization.

Such a scheme is not suitable for certain gases, particularly nitrogen at high temperatures, because ionization begins before dissociation is completed. This is explained by the fact that the energies of dissociation and ionization of nitrogen differ from each other only one-and-a-half times. In this case, the regions of attainment of equilibrium overlap. A similar phenomenon is observed in the air at comparatively low temperatures. At temperatures exceeding 3200 K, the relaxation time for the dissociation of oxygen is lower than the duration of setting in of nitrogen vibrations. Consequently, equilibrium in the dissociation of oxygen is established before the vibrations of the nitrogen are in equilibrium.

Investigation of the flow of a non-equilibrium gas over bodies is facilitated if the characteristic time of this process is considerably lower than the relaxation time of one of the inert processes and conditions of a frozen flow occurring without the participation of this inert process appear. Particularly, if the duration of flow over a section of a surface is small in comparison with the time needed for chemical equilibrium to set in, but is commensurable with the vibrational relaxation time, a process with frozen dissociation and ionization may be considered on this section.

#### Relaxation Effects In Shock Waves

In the transition of a gas through a shock wave, a portion of the kinetic energy is converted into the energy of active and inert degrees of freedom. For the active degrees (superscript "A")—translational and rotational—equilibrium sets in during the relaxation time  $t_D^A$  commensurable with the time taken by the gas to pass through the thickness of the shock. Since this time is very small, we can consider in practice that the active degrees are excited instantaneously. At the same time, dissociation does not yet begin because during a small time interval the number of collisions of the molecules is not

**Fig. 4.8.2**

Relaxation process in a shock wave:

(the hatched region determines the thickness of the shock wave):  
1 and 2—front and rear surfaces of the shock wave, respectively

large. Hence, directly behind a shock wave, the temperature  $T'_2$  is the same as in a gas with constant specific heats.

In accordance with this scheme, no inert degrees of freedom (super-script "I") are excited directly after a shock. Since these degrees have a finite relaxation time  $t_D^I$  considerably greater than the time  $t_D^A$  and the duration of transition through the thickness of a real shock, then *the temperature lowers* until the inert degrees of freedom (first vibrations, then dissociation, excitation of the electron levels, and ionization) reach equilibrium.

In Fig. 4.8.2, schematically illustrating a relaxation process, the relaxation time  $t_D^A$  measured from the instant of the beginning of motion on the front surface of the shock wave ahead of which the temperature of the undisturbed gas is  $T_1$  corresponds to the temperature  $T'_2$ . The figure also shows the density  $\rho'_2$  corresponding to the temperature  $T'_2$ , while the equilibrium state is established at a temperature of  $T_2 < T'_2$ . A non-equilibrium process of gas flow behind a shock is attended by an *increase in the density* to the equilibrium value  $\rho_2 > \rho'_2$ . Here a small *growth in the pressure* is observed in comparison with an ideal gas. Simultaneously *the degree of dissociation* (and at very high temperatures, the degree of ionization) grows from zero to its equilibrium value.

The investigation of the non-equilibrium flow behind a shock consists in determining the length of the non-equilibrium zone, or the relaxation length, and also in estimating the non-equilibrium parameters. The system of equations describing such motion includes equations of the momentum, energy, state, and an equation for the rate of chemical reactions.

The initial conditions upon its integration are determined by the parameters directly behind the shock wave, which are found with the assumption that dissociation is absent. At the end of the

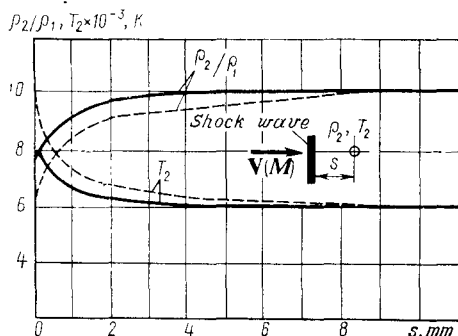


Fig. 4.8.3

Influence of non-equilibrium dissociation on the density and temperature behind a shock wave.

$(M_1 = 14.2, T_1 = 300 \text{ K}, p_1 = 120 \text{ Pa})$

relaxation length, these parameters reach equilibrium values corresponding to the equilibrium degree of dissociation.

The results of such investigations of a non-equilibrium flow of a gaseous mixture of oxygen and nitrogen behind a shock wave are given in Fig. 4.8.3. The solid curves were obtained on the assumption of instantaneous vibrational excitation, and the dashed ones in the absence of excitation. These results reveal that vibrations have an appreciable significance in direct proximity to a shock. For example, without account of excitations, the temperature behind a shock is 12 000 K, while for a completely excited state it is about 9800 K, i.e. considerably lower. At the end of the relaxation zone, vibrational excitation is of virtually no importance. Therefore in calculations of equilibrium dissociation, we can assume that the rates of vibrational excitation are infinitely high, thus considering a gas before the beginning of dissociation to be completely excited. It is shown in Fig. 4.8.3 that the length of the non-equilibrium zone is comparatively small and is approximately 8-10 mm.

The data of investigations of the relaxation in shock waves can be used to determine the nature of non-equilibrium flow in the vicinity of a blunt nose in a hypersonic flow. Here we find the length of the relaxation (non-equilibrium) zone and determine whether such a zone reaches the vicinity of the point of stagnation. In accordance with this, the stagnation parameters are calculated, and with a view to their values, similar parameters are evaluated for the peripheral sections of the surface in the flow.

The length of the non-equilibrium zone is found as the relaxation length calculated by means of the expression

$$x_D = 0.5 V_C t_D \quad (4.8.1)$$

where  $V_C$  is the velocity directly behind the normal part of the shock wave, and  $t_D$  is the relaxation time.

The relaxation time can be found by the formula

$$t_D \approx 2.8 \times 10^{-7} (1 - \alpha_e) \{ [f(H) \bar{\rho}]^2 \alpha_e (3 - \alpha_e) \}^{-1} \quad (4.8.2)$$

in which  $f(H) = \rho_{\infty H}/\rho_{\infty E}$  is a function of the altitude ( $\rho_{\infty H}$  and  $\rho_{\infty E}$  are the densities of the atmosphere at the altitude  $H$  and at the Earth's surface, respectively),  $\bar{\rho} = \rho/\rho_{\infty H}$  [the density  $\rho = 0.5(\rho_C + \rho_e)$ , where  $\rho_C$  and  $\rho_e$  are the densities behind the shock in the undissociated gas and for equilibrium dissociation, respectively].

If the length  $x_D$  is smaller than the distance  $s_0$  between a shock wave and the point of stagnation, the non-equilibrium zone is near the wave and does not include the body in the flow. Consequently, the condition for equilibrium in the vicinity of a blunted surface will be  $x_D < s_0$ , or  $0.5V_0 t_D < s_0$ . Hence we can also find the inequality  $t_D < s_0/(0.5V_0)$  in which the term on the right-hand side is the characteristic time  $t_{s_0}$  spent by a particle in the compression zone. If  $t_{s_0} > t_D$ , a particle of the gas will have time to reach the state of equilibrium before it reaches the surface.

It is not difficult to see from formula (4.8.2) that the relaxation time grows with increasing flight altitude  $H$  and, consequently, the length of the non-equilibrium zone increases. At the same time,  $t_D$  diminishes with an increase in the intensity of a compression shock for very high supersonic velocities of the flow (here the relative density behind a shock  $\bar{\rho} = \rho/\rho_{\infty H}$  becomes larger).

A non-equilibrium state substantially affects the distance between a shock wave and a body. With a completely non-equilibrium flow behind a shock (the degree of dissociation  $\alpha = 0$ ), this distance can be appreciably larger than in equilibrium dissociation ( $\alpha = \alpha_e > 0$ ). It decreases in the real conditions of a gradual transition from a non-equilibrium state to an equilibrium flow behind a shock wave, i.e. when the degree of dissociation changes from 0 behind the wave to the equilibrium value  $\alpha = \alpha_e$  at the end of the relaxation zone.

## Method of Characteristics

### 5.1. Equations for the Velocity Potential and Stream Function

An important place in aerodynamics is occupied by the **method of characteristics**, which allows one to calculate the disturbed flow of an ideal (inviscid) gas. This method makes it possible to design correctly the contours of nozzles for supersonic wind tunnels, determine the parameters of supersonic flow over airfoils and craft bodies.

The method of characteristics has been developed comprehensively for solving the system of equations of steady supersonic two-dimensional (plane or spatial axisymmetric) vortex and vortex-free gas flows. Investigations associated with the use of the method of characteristics for calculating the three-dimensional flow over bodies are being performed on a broad scale. Below we consider the method of characteristics and its application to problems on supersonic two-dimensional flows.

Equations for a two-dimensional plane steady flow of an inviscid gas are obtained from (3.1.20) provided that  $\mu = 0$ ,  $\partial V_x / \partial t = \partial V_y / \partial t = 0$  and have the following form:

$$\left. \begin{aligned} V_x \frac{\partial V_x}{\partial x} + V_y \frac{\partial V_x}{\partial y} &= -\frac{1}{\rho} \cdot \frac{\partial p}{\partial x} \\ V_x \frac{\partial V_y}{\partial x} + V_y \frac{\partial V_y}{\partial y} &= -\frac{1}{\rho} \cdot \frac{\partial p}{\partial y} \end{aligned} \right\} \quad (5.1.1)$$

For a two-dimensional axisymmetric flow, the equations of motion obtained from (3.1.36) for similar conditions ( $v = 0$ ,  $\partial V_x / \partial t = \partial V_y / \partial t = 0$ ) can be written in the form

$$\left. \begin{aligned} V_x \frac{\partial V_x}{\partial x} + V_r \frac{\partial V_x}{\partial r} &= -\frac{1}{\rho} \cdot \frac{\partial p}{\partial x} \\ V_x \frac{\partial V_r}{\partial x} + V_r \frac{\partial V_r}{\partial r} &= -\frac{1}{\rho} \cdot \frac{\partial p}{\partial r} \end{aligned} \right\} \quad (5.1.2)$$

The continuity equations for plane and axisymmetric flows having respectively the form of (2.4.5) and (2.4.32) can be generalized as

follows:

$$\partial(\rho V_x y^\epsilon) / \partial x + \partial(\rho V_y y^\epsilon) / \partial y = 0 \quad (5.1.3)$$

When  $\epsilon = 0$ , this equation coincides with the continuity equation for a two-dimensional plane flow in the Cartesian coordinates  $x$  and  $y$ . If  $\epsilon = 1$ , we have a continuity equation for a two-dimensional axisymmetric flow in the cylindrical coordinates  $y(r)$ ,  $x$ . Accordingly, for both kinds of flow, we may consider that the equations of motion (5.1.1) are written in a generalized form.

Having determined the partial derivatives in continuity equation (5.1.3), we obtain

$$\left( V_x \frac{\partial \rho}{\partial x} + V_y \frac{\partial \rho}{\partial y} \right) y^\epsilon + \rho y^\epsilon \left( \frac{\partial V_x}{\partial x} + \frac{\partial V_y}{\partial y} \right) + \rho V_y \epsilon y^{\epsilon-1} = 0 \quad (5.1.4)$$

We can replace the partial derivative  $\partial \rho / \partial x$  with the expression  $\partial \rho / \partial x = (\partial p / \partial p) \partial p / \partial x$ , in which  $\partial \rho / \partial p = 1/a^2$ , while the derivative  $\partial p / \partial x$  is found from (5.1.1) in the form

$$\frac{\partial p}{\partial x} = -\rho \left( V_x \frac{\partial V_x}{\partial x} + V_y \frac{\partial V_x}{\partial y} \right)$$

With this in view, we have

$$\frac{\partial \rho}{\partial x} = -\frac{\rho}{a^2} \left( V_x \frac{\partial V_x}{\partial x} + V_y \frac{\partial V_x}{\partial y} \right) \quad (5.1.5)$$

An expression for the derivative  $\partial \rho / \partial y$  is found in a similar way:

$$\frac{\partial \rho}{\partial y} = -\frac{\rho}{a^2} \left( V_x \frac{\partial V_y}{\partial x} + V_y \frac{\partial V_y}{\partial y} \right) \quad (5.1.6)$$

Substitution of the values of these derivatives into (5.1.4) yields

$$(V_x^2 - a^2) \frac{\partial V_x}{\partial x} + V_x V_y \left( \frac{\partial V_x}{\partial y} + \frac{\partial V_y}{\partial x} \right) + (V_y^2 - a^2) \frac{\partial V_y}{\partial y} - \frac{a^2 V_y \epsilon}{y} = 0 \quad (5.1.7)$$

This equation is the fundamental differential equation of gas dynamics for a two-dimensional (plane or spatial axisymmetric) steady flow which the velocity components  $V_x$  and  $V_y$  must satisfy. Since this equation relates the velocities, it is also referred to as the **fundamental kinematic equation**.

If a flow is potential, then

$$V_x = \partial \phi / \partial x, \quad V_y = \partial \phi / \partial y, \quad \partial V_x / \partial y = \partial V_y / \partial x = \partial^2 \phi / \partial x \partial y$$

therefore, Eq. (5.1.7) can be transformed as follows:

$$(V_x^2 - a^2) \frac{\partial^2 \phi}{\partial x^2} + 2V_x V_y \frac{\partial^2 \phi}{\partial x \partial y} + (V_y^2 - a^2) \frac{\partial^2 \phi}{\partial y^2} - \frac{a^2 V_y \epsilon}{y} = 0 \quad (5.1.8)$$

where

$$a^2 = \frac{k-1}{2} \left[ V_{\max}^2 - \left( \frac{\partial \psi}{\partial x} \right)^2 - \left( \frac{\partial \psi}{\partial y} \right)^2 \right]$$

Equation (5.1.8) is the fundamental differential equation of gas dynamics for a two-dimensional potential steady flow and is called an **equation for the velocity potential**. Hence, unlike (5.1.7), Eq. (5.1.8) is used only for studying vortex-free gas flows.

If a two-dimensional gas flow is a *vortex* one, the stream function  $\psi$  has to be used for studying it. The velocity components expressed in terms of the function  $\psi$  have the form of (2.5.5). Replacing  $\rho$  in accordance with formula (3.6.31) in which the stagnation density  $\rho_0$  along a given streamline is assumed to be constant, expressions (2.5.5) can be written as follows:

$$V_x = y^{-\varepsilon} (1 - \bar{V}^2)^{-1/(k-1)} \frac{\partial \psi}{\partial y}, \quad V_y = -y^{-\varepsilon} (1 - \bar{V}^2)^{-1/(k-1)} \frac{\partial \psi}{\partial x} \quad (5.1.9)$$

where  $\bar{V} = V/V_{\max}$ .

The calculation of a vortex gas flow consists in solving a differential equation for the stream function  $\psi$ . To obtain this equation, let us differentiate (5.1.9) with respect to  $y$  and to  $x$ :

$$\begin{aligned} \frac{\partial V_x}{\partial y} &= -\varepsilon y^{-\varepsilon-1} (1 - \bar{V}^2)^{-1/(k-1)} \frac{\partial \psi}{\partial y} + y^{-\varepsilon} \frac{1}{k-1} \\ &\times (1 - \bar{V}^2)^{-1/(k-1)-1} \frac{\partial \bar{V}^2}{\partial y} \cdot \frac{\partial \psi}{\partial y} + y^{-\varepsilon} (1 - \bar{V}^2)^{-1/(k-1)} \frac{\partial^2 \psi}{\partial y^2} \\ \frac{\partial V_y}{\partial x} &= -y^{-\varepsilon} \frac{1}{k-1} (1 - \bar{V}^2)^{-1/(k-1)-1} \frac{\partial \bar{V}^2}{\partial x} \cdot \frac{\partial \psi}{\partial x} - y^{-\varepsilon} (1 - \bar{V}^2)^{-1/(k-1)} \frac{\partial^2 \psi}{\partial x^2} \end{aligned}$$

Taking into account expression (3.6.22) for the square of the speed of sound, and also relations (5.1.9), we can write the expressions obtained for the derivatives  $\partial V_x/\partial y$  and  $\partial V_y/\partial x$  as follows:

$$\frac{\partial V_x}{\partial y} = -\frac{\varepsilon}{y} V_x + \frac{V_x}{2a^2} \cdot \frac{\partial V^2}{\partial y} + y^{-\varepsilon} (1 - \bar{V}^2)^{-1/(k-1)} \frac{\partial^2 \psi}{\partial x^2} \quad (5.1.10)$$

$$\frac{\partial V_y}{\partial x} = \frac{V_y}{2a^2} \cdot \frac{\partial V^2}{\partial x} - y^{-\varepsilon} (1 - \bar{V}^2)^{-1/(k-1)} \frac{\partial^2 \psi}{\partial x^2} \quad (5.1.11)$$

We shall determine the derivatives  $\partial V^2/\partial y$  and  $\partial V^2/\partial x$  in Eqs. (5.1.10) and (5.1.11) with the aid of relations (5.1.9). Combining these relations, we obtain

$$(\partial \psi / \partial x)^2 + (\partial \psi / \partial y)^2 = V^2 y^{2\varepsilon} (1 - \bar{V}^2)^{2/(k-1)} \quad (5.1.12)$$

By differentiating (5.1.12) with respect to  $x$  and  $y$ , we find the relevant relations:

$$2 \frac{\partial \psi}{\partial x} \cdot \frac{\partial^2 \psi}{\partial x^2} + 2 \frac{\partial \psi}{\partial y} \cdot \frac{\partial^2 \psi}{\partial x \partial y} = \frac{\partial V^2}{\partial x} y^{2\varepsilon} (1 - \bar{V}^2)^{2/(k-1)}$$

$$- V^2 y^{2\varepsilon} \frac{2}{k-1} (1 - \bar{V}^2)^{2/(k-1)-1} \frac{\partial \bar{V}^2}{\partial x}$$

$$2 \frac{\partial \psi}{\partial x} \cdot \frac{\partial^2 \psi}{\partial x \partial y} + 2 \frac{\partial \psi}{\partial y} \cdot \frac{\partial^2 \psi}{\partial y^2} = \frac{\partial V^2}{\partial y} y^{2\varepsilon} (1 - \bar{V}^2)^{2/(k-1)}$$

$$+ 2\varepsilon V^2 y^{2\varepsilon-1} (1 - \bar{V}^2)^{2/(k-1)} - V^2 y^{2\varepsilon} \frac{2}{k-1} (1 - \bar{V}^2)^{2/(k-1)-1} \frac{\partial \bar{V}^2}{\partial y}$$

We transform these relations with a view to Eq. (3.6.22) for the square of the speed of sound and to relations (5.1.9):

$$- V_y \frac{\partial^2 \psi}{\partial x^2} + V_x \frac{\partial^2 \psi}{\partial x \partial y} = \frac{y^\varepsilon}{2} \cdot \frac{\partial V^2}{\partial x} (1 - \bar{V}^2)^{1/(k-1)} \left( 1 - \frac{V^2}{a^2} \right) \quad (5.1.13)$$

$$- V_y \frac{\partial^2 \psi}{\partial x \partial y} + V_x \frac{\partial^2 \psi}{\partial y^2} = \frac{y^\varepsilon}{2} \cdot \frac{\partial V^2}{\partial y} (1 - \bar{V}^2)^{1/(k-1)} \\ \times \left( 1 - \frac{V^2}{a^2} \right) + \frac{\varepsilon}{y^{1-\varepsilon}} V^2 (1 - \bar{V}^2)^{1/(k-1)} \quad (5.1.14)$$

Determining the derivatives  $\partial V^2 / \partial y$  and  $\partial V^2 / \partial x$  from these expressions and inserting them into (5.1.10) and (5.1.11), respectively, we obtain

$$\frac{y^\varepsilon}{2} (1 - \bar{V}^2)^{1/(k-1)} \left( 1 - \frac{V^2}{a^2} \right) \frac{\partial V_x}{\partial y} = - \frac{\varepsilon}{2y^{1-\varepsilon}} V_x (1 - \bar{V}^2)^{1/(k-1)} \\ \times \left( 1 - \frac{V^2}{a^2} \right) + \frac{V_x}{2a^2} \left[ - V_y \frac{\partial^2 \psi}{\partial x \partial y} + V_x \frac{\partial^2 \psi}{\partial y^2} \right. \\ \left. - \frac{\varepsilon}{y^{1-\varepsilon}} V^2 (1 - \bar{V}^2)^{1/(k-1)} \right] + \frac{1}{2} \left( 1 - \frac{V^2}{a^2} \right) \frac{\partial^2 \psi}{\partial y^2} \\ \frac{y^\varepsilon}{2} (1 - \bar{V}^2)^{1/(k-1)} \left( 1 - \frac{V^2}{a^2} \right) \frac{\partial V_y}{\partial x} \\ = \frac{V_y}{2a^2} \left( - V_y \frac{\partial^2 \psi}{\partial x^2} + V_x \frac{\partial^2 \psi}{\partial x \partial y} \right) - \frac{1}{2} \left( 1 - \frac{V^2}{a^2} \right) \frac{\partial^2 \psi}{\partial x^2}$$

Subtraction of the first equation from the second one yields a relation for a *vortex*:

$$\frac{\partial V_y}{\partial x} - \frac{\partial V_x}{\partial y} = \frac{V_y}{a^2 - V^2} \cdot \frac{1}{y^\varepsilon} \left( - V_y \frac{\partial^2 \psi}{\partial x^2} \right. \\ \left. + V_x \frac{\partial^2 \psi}{\partial x \partial y} \right) (1 - \bar{V}^2)^{-1/(k-1)} - \frac{1}{y^\varepsilon} (1 - \bar{V}^2)^{-1/(k-1)} \frac{\partial^2 \psi}{\partial x^2}$$

$$-\frac{V_x}{a^2 - V^2} \cdot \frac{1}{y^\varepsilon} \left( -V_y \frac{\partial^2 \Psi}{\partial x \partial y} + V_x \frac{\partial^2 \Psi}{\partial y^2} \right) (1 - \bar{V}^2)^{-1/(k-1)} \\ - \frac{1}{y^\varepsilon} (1 - \bar{V}^2)^{-1/(k-1)} \frac{\partial^2 \Psi}{\partial y^2} + \frac{\varepsilon}{y} \cdot \frac{a^2}{a^2 - V^2} V_x \quad (5.1.15)$$

A vortex can also be determined with the aid of Eq. (3.1.22') transformed for the conditions of the steady flow of an ideal gas and having the form

$$\operatorname{grad} (V^2/2) + \operatorname{curl} \mathbf{V} \times \mathbf{V} = - (1/\rho) \operatorname{grad} p \quad (5.1.16)$$

By applying the grad operation to the energy equation (3.4.14), we have:

$$\operatorname{grad} (V^2/2) = -\operatorname{grad} i \quad (5.1.17)$$

Consequently, Eq. (5.1.16) can be written in the form

$$\operatorname{curl} \mathbf{V} \times \mathbf{V} = \operatorname{grad} i - (1/\rho) \operatorname{grad} p \quad (5.1.18)$$

Vortex supersonic gas flows can be characterized thermodynamically by the change in the entropy when going over from one streamline to another. This is why it is convenient to introduce into the calculations a parameter that reflects this change in the entropy as a feature of vortex flows.

In accordance with the second law of thermodynamics

$$T dS = di - dp/\rho$$

or in the vector form,

$$T \operatorname{grad} S = \operatorname{grad} i - (1/\rho) \operatorname{grad} p \quad (5.1.19)$$

Combining (5.1.18) and (5.1.19), we obtain

$$\operatorname{curl} \mathbf{V} \times \mathbf{V} = T \operatorname{grad} S \quad (5.1.20)$$

Let us calculate the cross product  $\operatorname{curl} \mathbf{V} \times \mathbf{V}$ , having in view that by (2.2.12) the vector

$$\operatorname{curl} \mathbf{V} = (\partial V_y / \partial x - \partial V_x / \partial y) \mathbf{i}_3$$

(here  $\mathbf{i}_3$  is a unit vector), and, therefore, the projections  $(\operatorname{curl} \mathbf{V})_x = (\operatorname{curl} \mathbf{V})_y = 0$ . Let us use a third-order determinant:

$$\operatorname{curl} \mathbf{V} \times \mathbf{V} = \begin{vmatrix} \mathbf{i}_1 & \mathbf{i}_2 & \mathbf{i}_3 \\ 0 & 0 & (\operatorname{curl} \mathbf{V})_3 \\ V_x & V_y & 0 \end{vmatrix}$$

in which the projection

$$(\operatorname{curl} \mathbf{V})_3 = \partial V_y / \partial x - \partial V_x / \partial y$$

Calculations yield

$$\operatorname{curl} \mathbf{V} \times \mathbf{V} = -V_y \left( \frac{\partial V_y}{\partial x} - \frac{\partial V_x}{\partial y} \right) \mathbf{i}_1 + V_x \left( \frac{\partial V_y}{\partial x} - \frac{\partial V_x}{\partial y} \right) \mathbf{i}_2 \quad (5.1.21)$$

Accordingly, for the projection of the vector  $\operatorname{curl} \mathbf{V} \times \mathbf{V}$  onto a normal  $n$  to a streamline, we obtain the relation

$$\begin{aligned} (\operatorname{curl} \mathbf{V} \times \mathbf{V})_n^2 &= (\operatorname{curl} \mathbf{V} \times \mathbf{V})_x^2 + (\operatorname{curl} \mathbf{V} \times \mathbf{V})_y^2 \\ &= V^2 (\partial V_y / \partial x - \partial V_x / \partial y)^2 \end{aligned} \quad (5.1.22)$$

Examination of (5.1.20) reveals that this projection can also be written in the form

$$(\operatorname{curl} \mathbf{V} \times \mathbf{V})_n = T dS/dn$$

or, with a view to (5.1.22)

$$V (\partial V_y / \partial x - \partial V_x / \partial y) = T \partial S / \partial n \quad (5.1.23)$$

Since  $a^2 = kRT$ , then, taking (3.6.22) into account, we find an expression for the temperature:

$$T = \frac{a^2}{kR} = \frac{k-1}{2k} \cdot \frac{1}{R} (V_{\max}^2 - V^2) = \frac{k-1}{2k} \cdot \frac{V_{\max}^2}{R} (1 - \bar{V}^2)$$

Introducing this relation into (5.1.23), we obtain

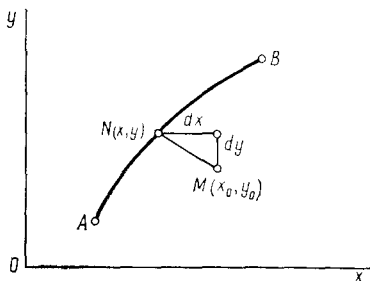
$$\frac{\partial V_y}{\partial x} - \frac{\partial V_x}{\partial y} = \frac{k-1}{2k} \cdot \frac{V_{\max}^2}{RV} (1 - \bar{V}^2) \frac{dS}{dn} \quad (5.1.24)$$

By introducing the vortex according to this expression into (5.1.15), we find a differential equation for the stream function:

$$\begin{aligned} (V_x^2 - a^2) \frac{\partial^2 \psi}{\partial x^2} + 2V_x V_y \frac{\partial^2 \psi}{\partial x \partial y} + (V_y^2 - a^2) \frac{\partial^2 \psi}{\partial y^2} \\ + \frac{\varepsilon}{y^{1-\varepsilon}} a^2 V_x (1 - \bar{V}^2)^{1/(k-1)} \\ = \frac{k-1}{2k} \cdot \frac{V_{\max}^2}{RV} (1 - \bar{V}^2)^{k/(k-1)} y^\varepsilon (a^2 - V^2) \frac{dS}{dn} \end{aligned} \quad (5.1.25)$$

## 5.2. The Cauchy Problem

Equations (5.1.8) for the velocity potential and (5.1.25) for the stream function are inhomogeneous non-linear second-order partial differential equations. The solutions of these equations  $\varphi = \varphi(x, y)$  and  $\psi = \psi(x, y)$  are depicted geometrically by integral surfaces in a space determined by the coordinate systems  $x, y, \varphi$  or  $x, y, \psi$ . In these systems, the plane  $x, y$  is considered as the basic one and is called the **physical plane** or the **plane of independent variables**.

**Fig. 5.2.1**

Initial curve  $AB$ ; the required function and its first derivatives with respect to  $x$  and  $y$  are known on it

The Cauchy problem consists in finding such solutions in the vicinity of an initial curve  $y = y(x)$  satisfying the additional conditions set on this curve. The values of the required function  $\varphi(x, y)$  or  $\psi(x, y)$  and the first derivatives  $\varphi_x$  ( $\psi_x$ ) or  $\varphi_y$  ( $\psi_y$ ) are such additional conditions. They are known as Cauchy's initial conditions.

From the geometric viewpoint, the Cauchy problem consists in finding an integral surface in the space  $x, y, \varphi$  (or  $x, y, \psi$ ) that passes through a preset spatial curve. It is just the projection of this curve onto the plane  $y, x$  that is the initial curve  $y = y(x)$  on this plane. The solution of the Cauchy problem as applied to the investigation of supersonic gas flows and the development of the corresponding method of characteristics are the results of work performed by the Soviet scientist, prof. F. Frankl.

To consider the Cauchy problem, let us write Eqs. (5.1.8) and (5.1.25) in the general form

$$Au + 2Bs + Ct + H = 0 \quad (5.2.1)$$

where  $u = \varphi_{xx}$  (or  $\psi_{xx}$ ),  $s = \varphi_{xy}$  (or  $\psi_{xy}$ ), and  $t = \varphi_{yy}$  (or  $\psi_{yy}$ ) are second partial derivatives, the values of  $A$ ,  $B$ , and  $C$  equal the coefficients of the corresponding second partial derivatives, and the quantity  $H$  is determined by the free terms in Eqs. (5.1.8) and (5.1.25).

We shall find a solution of Eq. (5.2.1) in the vicinity of the initial curve  $AB$  (Fig. 5.2.1) in the form of a series. At a point  $M(x_0, y_0)$ , the required function is

$$\begin{aligned} \varphi(x_0, y_0) &= \varphi(x, y) + \sum_{n=1}^{\infty} \frac{1}{n!} \left[ (\Delta x)^n \frac{\partial^n \varphi}{\partial x^n} \right. \\ &+ \frac{n}{1} (\Delta x)^{n-1} \Delta y \frac{\partial^n \varphi}{\partial x^{n-1} \partial y} + \frac{n(n-1)}{1 \cdot 2} (\Delta x)^{n-2} (\Delta y^2) \\ &\times \left. \frac{\partial^n \varphi}{\partial x^{n-2} \partial y^2} + \dots + (\Delta y)^n \frac{\partial^n \varphi}{\partial y^n} \right] \end{aligned} \quad (5.2.2)$$

where  $\varphi(x, y)$  is the value of this function at the given point  $N(x, y)$  on the initial curve,  $\Delta x = x_0 - x$ , and  $\Delta y = y_0 - y$ . The function  $\psi$  may be used in (5.2.2) instead of  $\varphi$ .

Series (5.2.2) yields the required solution if values of the functions  $\varphi$  (or  $\psi$ ) and also their derivatives of any order exist on a given curve and are known. Since the first derivatives on this curve [we shall denote them by  $p = \varphi_x$  (or  $\psi_x$ ) and  $q = \varphi_y$  (or  $\psi_y$ )] are given, our task consists in finding the second derivatives on it, and also derivatives of a higher order. Hence, the solution of the Cauchy problem is associated with finding of the conditions in which the higher derivatives on the given curve can be determined. We shall limit ourselves to determination of the second derivatives. Since these derivatives are three in number ( $u$ ,  $s$ , and  $t$ ), we have to compile the same number of independent equations to find them. Equation (5.2.2), which is satisfied on the initial curve  $AB$ , is the first of them. The other two are obtained from the following known relations for the total differentials of the functions of two independent variables on this curve:

$$\begin{aligned} dp &= (\partial p / \partial x) dx + (\partial p / \partial y) dy = u dx + s dy \\ dq &= (\partial q / \partial x) dx + (\partial q / \partial y) dy = s dx + t dy \end{aligned}$$

Hence, we can write the system of equations for determining the second derivatives in the form

$$\left. \begin{array}{l} Au + 2Bs + Ct + H = 0 \\ dx u + dy s + 0 \cdot t - dp = 0 \\ 0 \cdot u + dx s + dy t - dq = 0 \end{array} \right\} \quad (5.2.3)$$

This system of equations is solved for the unknowns  $u$ ,  $s$ , and  $t$  with the aid of determinants. If we introduce the symbols  $\Delta$  and  $\Delta_u$ ,  $\Delta_s$ ,  $\Delta_t$  for the principal and partial determinants, respectively, we have

$$u = \Delta_u / \Delta, \quad s = \Delta_s / \Delta, \quad t = \Delta_t / \Delta \quad (5.2.4)$$

where

$$\Delta = \begin{vmatrix} A & 2B & C \\ dx & dy & 0 \\ 0 & dx & dy \end{vmatrix}; \quad \Delta_u = \begin{vmatrix} -H & 2B & C \\ dp & dy & 0 \\ dq & dx & dy \end{vmatrix} \quad \left. \right\} \quad (5.2.4')$$

$$\Delta_s = \begin{vmatrix} A & -H & C \\ dx & dp & 0 \\ 0 & dq & dy \end{vmatrix}; \quad \Delta_t = \begin{vmatrix} A & 2B & -H \\ dx & dy & dp \\ 0 & dx & dq \end{vmatrix} \quad \left. \right\}$$

It follows from these relations that if the principal determinant  $\Delta$  does not equal zero on the initial curve  $AB$ , the second derivatives  $u$ ,  $s$ , and  $t$  are calculated *unambiguously*.

Let us assume that the curve has been chosen so that the principal determinant on it is zero, i.e.  $\Delta = 0$ . Hence

$$A(dy/dx)^2 - 2B(dy/dx) + C = 0 \quad (5.2.5)$$

It is known from mathematics that when the principal determinant  $\Delta$  of the system of equations (5.2.3) is zero on the curve given by Eq. (5.2.5), the second derivatives  $u$ ,  $s$ , and  $t$  (5.2.4) are either determined *ambiguously*, or in general *cannot be determined* in terms of  $\varphi$ ,  $p$ , and  $q$ .

Let us consider quadratic equation (5.2.5). Solving it for the derivative  $dy/dx$ , we obtain

$$(dy/dx)_{1,2} = y'_{1,2} = (1/A)(B \pm \sqrt{B^2 - AC}) \quad (5.2.6)$$

This equation determines the slope of a tangent at each point of the initial curve on which the principal determinant  $\Delta = 0$ . It is not difficult to see that (5.2.6) is a differential equation of two families of real curves if  $B^2 - AC > 0$ . Such curves, at each point of which the principal determinant of system (5.2.3) is zero, are called **characteristics**, and Eq. (5.2.5) is called a **characteristic one**.

From the above, there follows a condition in which the unambiguous determination of the second derivatives on the initial curve is possible: no arc element of this curve should coincide with the characteristics. The same condition  $\Delta \neq 0$  holds for the unambiguous determination of the higher derivatives in series (5.2.2). Consequently, if  $\Delta \neq 0$ , all the coefficients of series (5.2.2) are determined unambiguously according to the data on the initial curve.

Consequently, the condition  $\Delta \neq 0$  is necessary and sufficient to solve the Cauchy problem. This problem has a fundamental significance in the theory of partial differential equations, and formula (5.2.2) can be used to calculate the flow of a gas. But from the viewpoint of the physical applications, particularly of the calculation of supersonic gas flows, of greater interest is the problem of determining the solution according to the characteristics, i.e. the **method of characteristics**. This method can be obtained from an analysis of the Cauchy problem and consists in the following. Let us assume that the initial curve  $AB$  coincides with one of the characteristics, and not only the principal determinant of the system (5.2.3) equals zero along it, but also the partial determinants  $\Delta_u = \Delta_s = \Delta_t = 0$ . It can be proved here that if, for example, the determinants  $\Delta$  and  $\Delta_t$  equal zero, i.e.

$$Ay'^2 - 2By' + C = 0 \quad (5.2.5')$$

$$A(y'q' - p') - 2Bq' - H = 0 \quad (5.2.7)$$

where  $p' = dp/dx$ ,  $q' = dq/dx$ , then the equality to zero of the other determinants is satisfied automatically.

According to the theory of systems of algebraic equations, the equality to zero of the principal and all the partial determinants signifies that solutions of system (5.2.3), although they are *ambiguous*, can exist. If one of the solutions, for example, that for  $u$ , is finite, then the solutions for  $s$  and  $t$  are also finite.

### 5.3. Characteristics

#### Compatibility Conditions

Equations (5.2.5) and (5.2.7) determining the conditions in which solutions, although ambiguous, exist for  $u$ ,  $s$ , and  $t$  are known as the **compatibility conditions**. Geometrically, the first of these equations represents two families of curves that are characteristics in the physical plane  $x$ ,  $y$ , and the second equation two families of curves that are characteristics in the plane  $p$ ,  $q$ .

Any solution of the problem on the supersonic flow of a gas found by solving equations of characteristics (or compatibility conditions) is a *solution of the fundamental equation of gas dynamics* (5.1.8) or (5.1.25). The proof follows from what is known as the **equivalence theorem**, according to which the equations of characteristics (5.2.5) and (5.2.7) are equivalent to the fundamental equation (5.1.8) or (5.1.25) (a proof of this theorem is given in [15]).

From the geometric viewpoint, the proved equivalence signifies that the solution of the equations of the characteristics also gives the image of a plane  $x$ ,  $y$  on the plane  $p$ ,  $q$  when points of the curves determined by differential equation (5.1.8) correspond to points of the curves determined by differential equation (5.1.25).

Hence, a definite point on a characteristic in the plane  $p$ ,  $q$  corresponds to each point on a characteristic in the plane  $x$ ,  $y$ . This correspondence can evidently be established in different ways depending on the preset boundary conditions, and, as will be shown below, it is just this correspondence that makes it possible to use characteristics for calculating gas flows.

Accordingly, a feature of characteristics is that the initial conditions cannot be set arbitrarily along them, while they can along a curve that is not a characteristic.

#### Determination of Characteristics

**Kind of Characteristics.** A close look at (5.2.6) reveals that the roots of quadratic characteristic equation (5.2.5) may be real (equal or not equal in magnitude) and also complex conjugate. The difference between the roots is determined by the expression  $B^2 - AC = \delta$ . When  $\delta > 0$ , Eq. (5.2.5) gives two different families of real

characteristics; the value of  $\delta = 0$  determines two identical roots, which corresponds to two coinciding families of characteristics, i.e. actually to one characteristic; when  $\delta < 0$ , the roots of the equation are a pair of imaginary characteristics.

Since the roots of a characteristic equation depend on the coefficients  $A$ ,  $B$ , and  $C$  of differential equation (5.2.1), it is customary practice to establish the type of these equations depending on the kind of characteristics. When  $\delta > 0$ , Eq. (5.2.1) is a **hyperbolic** one, when  $\delta = 0$ , a **parabolic**, and when  $\delta < 0$ , an **elliptic** one.

The coefficients  $A$ ,  $B$ , and  $C$  in Eqs. (5.1.8) for the velocity potential and (5.1.25) for the stream function are determined identically:

$$A = V_x^2 - a^2, \quad B = V_x V_y, \quad C = V_y^2 - a^2 \quad (5.3.1)$$

Consequently,

$$\delta = B^2 - AC = a^2 (V^2 - a^2) \quad (5.3.2)$$

where  $V = \sqrt{V_x^2 + V_y^2}$  is the total velocity.

Therefore, for the regions of a gas flow with supersonic velocities ( $V > a$ ), hyperbolic equations are employed, and for regions of a flow with subsonic velocities ( $V < a$ ), elliptic ones. At the boundary of these regions, the velocity equals that of sound ( $V = a$ ), and the equations will be parabolic.

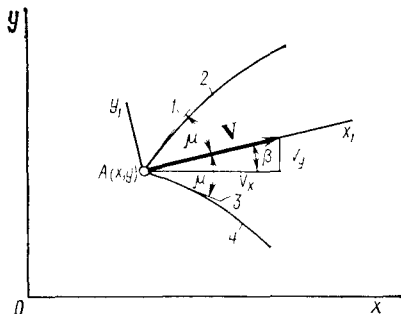
**Characteristics in a Physical Plane.** Characteristics in the plane  $x, y$  are determined from the solution of the differential equation (5.2.6) in which the plus sign corresponds to the characteristics of the first family, and the minus sign to those of the second one.

The quantity  $\lambda_1 = dy/dx$  directly calculated by expression (5.2.6) and the plus sign in this expression determine the angular coefficient of the **characteristic of the first family**, and  $\lambda_2 = dy/dx$  and the minus sign—that of the **characteristic of the second family**. Both these characteristics are customarily referred to as **conjugate**. With a view to expressions (5.3.1) and (5.3.2), we obtain the following expression for the characteristics in the plane  $x, y$ :

$$\lambda_{1,2} = dy/dx = [1/(V_x^2 - a^2)] (V_x V_y \pm a \sqrt{V^2 - a^2}) \quad (5.3.3)$$

The characteristics in the plane  $x, y$  have a definite physical meaning that can be determined if we find the angle  $\mu$  between the velocity vector  $\mathbf{V}$  at a point  $A$  of the flow (Fig. 5.3.1) and the direction of the characteristic at this point. The angle is determined with the aid of Eq. (5.3.3) if we use the local system of coordinates  $x_1, y_1$  with its origin at point  $A$  and with the  $x_1$ -axis coinciding with the direction of the vector  $\mathbf{V}$ . With such a choice of the coordinate axes,  $V_x = V$ ,  $V_y = 0$ , and, consequently,

$$\lambda_{1,2} = \tan \mu_{1,2} = \pm (M^2 - 1)^{-1/2}$$

**Fig. 5.3.1**

To the explanation of the physical meaning of a characteristic:

1—direction of a characteristic of the first family at point  $A$ ; 2—characteristic of the first family with the angular coefficient  $\lambda_1$ ; 3—direction of a characteristic of the second family at point  $A$ ; 4—characteristic of the second family with the angular coefficient  $\lambda_2$ .

It thus follows that  $\mu$  is the Mach angle. We have therefore established an important property of characteristics consisting in that at every point belonging to a characteristic, the angle between a tangent to it and the velocity vector at this point *equals the Mach angle*. Consequently, a characteristic is a **line of weak disturbances** (or a **Mach line**) having the shape of a curve in the general case.

The definition of a characteristic as a Mach line has a direct application to a two-dimensional plane supersonic flow. If we have to do with a two-dimensional spatial (axisymmetric) supersonic flow, the Mach lines (characteristics) should be considered as the **generatrices of a surface of revolution enveloping the Mach cones** issuing from vertices at the points of disturbance (on the characteristics). A surface confining a certain region of disturbance is called a **wave surface or three-dimensional Mach wave**.

We already know that pressure waves appear in a gas whose supersonic flow is characterized by a *growth in the pressure*. But such a flow may be attended by *lowering of the pressure*, i.e. there will be a supersonic expanding flow, and the Mach lines will characterize expansion waves. The relevant characteristics, which in the general case are curved lines (for a plane flow) or surfaces formed by the rotation of these lines (for a spatial axisymmetric flow) coincide with these Mach lines. If a flow contains Mach lines (characteristics) in the form of straight lines, then **simple expansion waves** whose velocity of propagation has one direction correspond to them. When Mach lines correspond to expansion waves, we call them lines of weak disturbances, using the terminology adopted for weak pressure waves. It must be remembered here that no other expansion waves except weak ones appear in an expanding supersonic flow, because otherwise we would have to assume the possibility of the formation of "strong" expansion waves (expansion shocks) which in real flow conditions cannot exist.

If at a point of a physical plane the flow velocity and speed of sound are known, the above property of characteristics makes it possible

to determine their directions at this point by calculating the Mach angle by the formula  $\mu = \pm \sin^{-1}(1/M)$ . We determine the angular coefficients of the characteristics in the coordinates  $x, y$  (Fig. 5.3.1) from the equation

$$\lambda_{1,2} = dy/dx = \tan(\beta \pm \mu) \quad (5.3.4)$$

where  $\beta$  is the angle of inclination of the velocity vector to the  $x$ -axis; the plus sign relates to the characteristic of the first family, and the minus sign to that of the second family.

Equation (5.3.4) is a differential equation for the characteristics in a physical plane.

**Characteristics in the Plane  $p, q$ .** If we substitute for  $y'$  in Eq. (5.2.7) the first root of the characteristic equation (5.2.5) equal to  $y' = \lambda_1$ , the equation obtained, namely,

$$A(\lambda_1 q' - p') - 2Bq' - H = 0 \quad (5.3.5)$$

is the first family of characteristics in the plane  $p, q$ . A similar substitution for  $y'$  of the second root  $y' = \lambda_2$  yields an equation for the second family of characteristics in the same plane:

$$A(\lambda_2 q' - p') - 2Bq' - H = 0 \quad (5.3.6)$$

Equations (5.3.5) and (5.3.6) for the characteristics can be transformed by using the property of the roots of quadratic equation (5.2.5) according to which

$$\lambda_1 + \lambda_2 = 2B/A \quad (5.3.7)$$

By considering the first family of characteristics and by introducing the relation  $A\lambda_1 - 2B = -\lambda_2 A$  obtained from (5.3.7) into (5.3.5), we compile the equation

$$A(\lambda_2 q' + p') + H = 0 \quad (5.3.8)$$

Similarly, for a characteristic of the second family, we have

$$A(\lambda_1 q' + p') + H = 0 \quad (5.3.9)$$

With a view to expression (5.3.4), Eqs. (5.3.8) and (5.3.9) can be written in the form

$$\frac{dp}{dx} + \tan(\beta \mp \mu) \frac{dq}{dx} + \frac{H}{A} = 0 \quad (5.3.10)$$

where the minus sign relates to characteristics of the first family, and the plus sign to those of the second one. Equation (5.3.10) determines the **conjugated characteristics** in the plane  $p, q$ .

### Orthogonality of Characteristics

If we replace the differentials in the equations for the characteristics with finite differences, the equations obtained will be ones of straight lines in the corresponding planes  $x, y$  and  $p, q$ .

Let us consider the equations, particularly, for the characteristics of the first family in the plane  $x, y$  and of the second family in the plane  $p, q$ . It follows from (5.3.4) that for an element of a characteristic—a straight line in the plane  $x, y$ —the equation has the form

$$y - y_0 = (x - x_0) \lambda_1 \quad (5.3.4')$$

where  $x_0, y_0$  are the coordinates of a fixed point,  $\lambda_1$  is an angular coefficient calculated from the parameters of the gas at this point, and  $x, y$  are the running coordinates.

Let us compile an equation for an element of a characteristic of the second family in the plane  $p, q$  in accordance with (5.3.9):

$$A\lambda_1(q - q_0) + A(p - p_0) + H(x - x_0) = 0 \quad (5.3.9')$$

where  $p_0, q_0$  are the values of the functions  $p$  and  $q$  at point  $x_0, y_0$  of the physical plane, the angular coefficient  $\lambda_1$  and also the values of  $A$  and  $H$  are calculated according to the parameters of the gas at this point, and  $p$  and  $q$  are running coordinates.

Examination of Eqs. (5.3.4') and (5.3.9') reveals that the inclination of a straight line in the plane  $x, y$  is determined by the angular coefficient  $\lambda_1$ , and in the plane  $p, q$  by the angular coefficient  $-1/\lambda_1$ . It can be proved similarly that an element of a characteristic of the second family in the plane  $x, y$  has the angular coefficient  $\lambda_2$ , and an element of a characteristic of the first family in the plane  $p, q$ —the angular coefficient  $-1/\lambda_2$ . It thus follows that *the characteristics of different families in the two planes are perpendicular to each other*.

This property makes it possible to determine the direction of the characteristics in the plane  $p, q$  if the direction of the conjugate characteristics in the physical plane is known. Assume that for a point  $P(x_0, y_0)$  of the plane  $x, y$  we know the velocity components  $V_{x0}, V_{y0}$  and the values of the functions  $p_0, q_0$ . We can determine the directions of the Mach lines at this point (Fig. 5.3.2) by (5.3.4'). To an element of characteristic  $PN$  of the first family in the plane  $x, y$  there corresponds an element of a characteristic of the second family—a straight line in the plane  $p, q$  set by Eq. (5.3.9'). This line is perpendicular to line  $PN$ , but does not pass through point  $P'$  with the coordinates  $p_0, q_0$ , which is indicated by the presence of a free term in Eq. (5.3.9'). Consequently, to construct an element of a characteristic according to the rules of analytic geometry, we must first determine the distance  $\delta_1$  to it from point  $P'$ . A characteristic

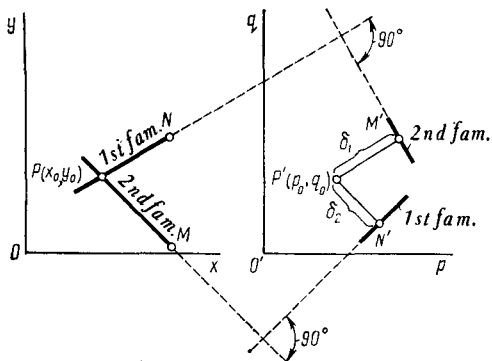


**Fig. 5.3.2**  
Property of orthogonality of  
characteristics

of the first family is constructed in a similar way in the plane  $p, q$  perpendicular to straight line  $PM$  and at a distance of  $\delta_2$  from point  $P'$  (Fig. 5.3.2).

The property of orthogonality of characteristics belonging to different families manifests itself in the case of a potential flow for the planes  $x, y$  and  $V_x, V_y$  (the hodograph plane), and also in the case of a vortex flow, for which the plane  $p, q$  is replaced with the same hodograph plane  $V_x, V_y$ .

#### Transformation of the Equations for Characteristics in a Hodograph

Let us transform Eq. (5.3.10) to a form such that it will determine the characteristics in a hodograph where the velocity components  $V_x, V_y$  are the coordinates or independent variables. For this purpose, by differentiating expressions (5.1.9) with respect to  $x$ , we calculate the derivatives  $dp/dx$  and  $dq/dx$ :

$$\begin{aligned} \frac{dp}{dx} &= \frac{d}{dx} \left( \frac{\partial \Psi}{\partial x} \right) = -V_y \varepsilon y^{\varepsilon-1} \frac{dy}{dx} (1 - \bar{V}^2)^{1/(k-1)} \\ &\quad - y^\varepsilon \frac{dV_y}{dx} (1 - \bar{V}^2)^{1/(k-1)} \\ &\quad + \frac{2y^\varepsilon}{k-1} V_y (1 - \bar{V}^2)^{1/(k-1)-1} \bar{V} \frac{d\bar{V}}{dy} \end{aligned} \quad (5.3.11)$$

$$\begin{aligned} \frac{dq}{dx} &= \frac{d}{dx} \left( \frac{\partial \Psi}{\partial y} \right) = V_x \varepsilon y^{\varepsilon-1} \frac{dy}{dx} (1 - \bar{V}^2)^{1/(k-1)} + y^\varepsilon \frac{dV_x}{dx} \\ &\quad \times (1 - \bar{V}^2)^{1/(k-1)} - \frac{2y^\varepsilon}{k-1} V_x (1 - \bar{V}^2)^{1/(k-1)-1} \bar{V} \frac{d\bar{V}}{dx} \end{aligned} \quad (5.3.12)$$

A glance at Eq. (5.1.25) reveals that

$$\left. \begin{aligned} H &= \varepsilon y^{\varepsilon-1} a^2 V_x (1 - \bar{V}^2)^{1/(k-1)} - \frac{k-1}{2k} \\ &\times \frac{V_{\max}^2}{RV} (1 - \bar{V}^2)^{k/(k-1)} y^\varepsilon (a^2 - V^2) \frac{dS}{dn}; \quad A = V_x^2 - a^2 \end{aligned} \right\} \quad (5.3.13)$$

After introducing (5.3.11)-(5.3.13) into (5.3.10) and replacing the quantities  $dy/dx$  with the angular coefficients  $\lambda_{1,2}$  of the characteristics, and the functions  $\tan(\beta \mp \mu)$  with the corresponding values of  $\lambda_{2,1}$ , we obtain

$$\begin{aligned} &\varepsilon y^{\varepsilon-1} \lambda_{1,2} (1 - \bar{V}^2)^{1/(k-1)} (V_x \lambda_{2,1} - V_y) + y^\varepsilon (1 - \bar{V}^2)^{1/(k-1)} \\ &\times \left( \frac{dV_x}{dx} \lambda_{2,1} - \frac{dV_y}{dx} \right) + \frac{2y^\varepsilon}{k-1} (1 - \bar{V}^2)^{1/(k-1)-1} \bar{V} \frac{d\bar{V}}{dx} (V_y - V_x \lambda_{2,1}) \\ &+ \frac{1}{V_x^2 - a^2} \left[ \varepsilon y^{\varepsilon-1} a^2 V_x (1 - \bar{V}^2)^{1/(k-1)} - \frac{k-1}{2k} \right. \\ &\times \left. \frac{V_{\max}^2}{RV} (1 - \bar{V}^2)^{k/(k-1)} y^\varepsilon (a^2 - V^2) \frac{dS}{dn} \right] = 0 \end{aligned}$$

After cancelling quantities where possible and introducing the dimensionless variables

$$\bar{V}_x = V_x/V_{\max}, \quad \bar{V}_y = V_y/V_{\max}, \quad \bar{V} = V/V_{\max}, \quad V/a = M$$

we can write this equation in the form

$$\begin{aligned} &\frac{\varepsilon}{y} \lambda_{1,2} (\bar{V}_x \lambda_{2,1} - \bar{V}_y) + \left( \frac{d\bar{V}_x}{dx} \lambda_{2,1} - \frac{d\bar{V}_y}{dx} \right) \\ &+ \frac{2\bar{V}}{k-1} \cdot \frac{\bar{V}_y - \bar{V}_x \lambda_{2,1}}{1 - \bar{V}^2} \cdot \frac{d\bar{V}}{dx} - \frac{\varepsilon}{y} \cdot \frac{\bar{V}_x}{1 - V_x^2/a^2} \\ &- \frac{k-1}{2k} \cdot \frac{1}{R\bar{V}} \cdot (1 - \bar{V}^2) \frac{M^2 - 1}{1 - V_x^2/a^2} \cdot \frac{dS}{dn} = 0 \end{aligned} \quad (5.3.14)$$

By introducing the polar angle  $\beta$ , we obtain the following expressions for the projections of the velocity vector:

$$\bar{V}_x = \bar{V} \cos \beta, \quad \bar{V}_y = \bar{V} \sin \beta \quad (5.3.15)$$

Let us differentiate these expressions with respect to  $x$ :

$$\left. \begin{aligned} d\bar{V}_x/dx &= (d\bar{V}/dx) \cos \beta - \bar{V} \sin \beta \frac{d\beta}{dx} \\ d\bar{V}_y/dx &= (d\bar{V}/dx) \sin \beta + \bar{V} \cos \beta \frac{d\beta}{dx} \end{aligned} \right\} \quad (5.3.16)$$

Introducing (5.3.15) and (5.3.16) into (5.3.14) and taking into account that  $\tan^2 \mu = (M^2 - 1)^{-1}$  and  $\sin^2 \mu = M^{-2}$ , we have

$$\frac{d\bar{V}}{dx} \left( \frac{2\bar{V}^2}{k-1} \cdot \frac{\sin \beta - \lambda_{1,2} \cos \beta}{1 - \bar{V}^2} + \lambda_{2,1} \cos \beta - \sin \beta \right)$$

$$-\bar{V} \frac{d\beta}{dx} (\lambda_{2,1} \sin \beta + \cos \beta) + \frac{\epsilon}{y} \bar{V} \left[ \lambda_{1,2} (\lambda_{2,1} \cos \beta - \sin \beta) - \frac{\cos \beta}{1 - \cos^2 \beta / \sin^2 \mu} \right] - \frac{k-1}{2k} \cdot \frac{1}{R\bar{V}} (1 - \bar{V}^2) \frac{\cot^2 \mu}{1 - \cos^2 \beta / \sin^2 \mu} \cdot \frac{dS}{dn} = 0$$

Having in view that  $[(k-1)/2] (1 - V^2/V_{\max}^2) = a^2/V_{\max}^2 = \bar{V}^2 \sin^2 \mu$ , we find

$$\begin{aligned} & \frac{dV}{V} + d\beta \frac{(\lambda_{2,1} \sin \beta + \cos \beta) \tan^2 \mu}{\lambda_{2,1} \cos \beta - \sin \beta} - \epsilon \frac{dx}{y} \\ & \times \left[ \lambda_{1,2} - \frac{\sin^2 \mu \cos \beta}{(\lambda_{2,1} \cos \beta - \sin \beta) (\sin^2 \mu - \cos^2 \beta)} \right] \tan^2 \mu \\ & + \frac{dx}{kR} \cdot \frac{\sin^4 \mu}{(\sin^2 \mu - \cos^2 \beta) (\lambda_{2,1} \cos \beta - \sin \beta)} \frac{dS}{dn} = 0 \end{aligned} \quad (5.3.17)$$

Performing the substitutions  $\lambda_{2,1} = \tan(\beta \mp \mu)$  and  $\lambda_{1,2} = \tan(\beta \pm \mu)$ , we transform the individual expressions contained in (5.3.17) to the following form:

$$\frac{\lambda_{2,1} \sin \beta + \cos \beta}{\lambda_{2,1} \cos \beta - \sin \beta} = \frac{1}{\mp \tan \mu} \quad (5.3.18)$$

$$\lambda_{1,2} - \frac{\sin^2 \mu \cos \beta}{(\lambda_{2,1} \cos \beta - \sin \beta) (\sin^2 \mu - \cos^2 \beta)} = \frac{\sin \beta \cos \mu}{\cos(\beta \pm \mu)} \quad (5.3.19)$$

$$\frac{\sin^4 \mu}{(\sin^2 \mu - \cos^2 \beta) (\lambda_{2,1} \cos \beta - \sin \beta)} = \pm \frac{\sin^3 \mu}{\cos(\beta \pm \mu)} \quad (5.3.20)$$

With a view to (5.3.18)-(5.3.20), Eq. (5.3.17) for the characteristics of the first and second families, respectively, acquire the form

$$\begin{aligned} & \frac{dV}{V} - \tan \mu d\beta - \epsilon \frac{dx}{y} \cdot \frac{\sin \mu \sin \beta \tan \mu}{\cos(\beta + \mu)} \\ & + \frac{dx}{kR} \cdot \frac{\sin^3 \mu}{\cos(\beta + \mu)} \cdot \frac{dS}{dn} = 0 \end{aligned} \quad (5.3.21)$$

$$\begin{aligned} & \frac{dV}{V} + \tan \mu d\beta - \epsilon \frac{dx}{y} \cdot \frac{\sin \mu \sin \beta \tan \mu}{\cos(\beta - \mu)} \\ & - \frac{dx}{kR} \cdot \frac{\sin^3 \mu}{\cos(\beta - \mu)} \cdot \frac{dS}{dn} = 0 \end{aligned} \quad (5.3.22)$$

The entropy gradient  $dS/dn$  can be calculated according to the value of the derivative of the stagnation pressure  $dp'_0/dn$ . For this purpose, we shall use relations (4.3.6) and (4.3.20) from which we obtain the following formula for the difference of the entropies:

$$S_2 - S_1 = -c_v (k-1) \ln(p'_0/p_0) \quad (5.3.23)$$

Since  $c_v (k-1) = R$ , then by calculating the derivative with respect to  $n$  and designating  $dS_2/dn$  by  $dS/dn$ , we find

$$\frac{1}{R} \cdot \frac{dS}{dn} = - \frac{1}{p'_0} \cdot \frac{dp'_0}{dn} \quad (5.3.24)$$

For our further transformations, we shall introduce the new variable

M

$$\omega = \int_{a^*}^V \cot \mu \frac{dV}{V} \quad (5.3.25)$$

that is an angle. We shall express the ratio  $dV/V$  in the form  $d\lambda/\lambda$ . ( $\lambda = V/a^*$ ), and  $\cot \mu$  with the aid of (3.6.23) in the form

$$\cot \mu = \sqrt{M^2 - 1} = \sqrt{(\lambda^2 - 1) / \left(1 - \frac{k-1}{k+1} \lambda^2\right)} \quad (5.3.26)$$

Consequently,

$$\omega = \int_1^\lambda \sqrt{(\lambda^2 - 1) / \left(1 - \frac{k-1}{k+2} \lambda^2\right)} \frac{d\lambda}{\lambda} \quad (5.3.27)$$

Integration of (5.3.27) yields

$$\begin{aligned} \omega = & \sqrt{\frac{k+1}{k-1}} \tan^{-1} \sqrt{\frac{k-1}{k+1} \cdot \frac{\lambda^2 - 1}{1 - \frac{k-1}{k+1} \lambda^2}} \\ & - \tan^{-1} \sqrt{\frac{\lambda^2 - 1}{1 - \frac{k-1}{k+1} \lambda^2}} \end{aligned} \quad (5.3.28)$$

Having in view that  $\lambda_{\max} = V_{\max}/a^* = \sqrt{(k+1)/(k-1)}$ , we obtain

$$\omega = \sqrt{\frac{k+1}{k-1}} \tan^{-1} \sqrt{\frac{\lambda^2 - 1}{\lambda_{\max}^2 - \lambda^2}} - \tan^{-1} \sqrt{\frac{k+1}{k-1} \cdot \frac{\lambda^2 - 1}{\lambda_{\max}^2 - \lambda^2}} \quad (5.3.29)$$

Substituting  $M$  for  $\lambda$  in (5.3.28) in accordance with (5.3.26), we have

$$\omega = \sqrt{\frac{k+1}{k-1}} \tan^{-1} \sqrt{\frac{k-1}{k+1} (M^2 - 1)} - \tan^{-1} \sqrt{M^2 - 1} \quad (5.3.30)$$

Examination of Eqs. (5.3.29) and (5.3.30) reveals that the angle  $\omega$  is a function only of the number  $\lambda$  (or  $M$ ), and, consequently, it can be evaluated beforehand, which facilitates calculations of supersonic gas flows by the method of characteristics.

The values of  $\omega$  for various numbers  $M$  at  $k = 1.4$  are contained in Table 5.3.1, which also gives the angles of inclination of the disturbance line calculated by the formula  $\mu = \sin^{-1}(1/M)$ .

Table 5.3.1

$M$	$\omega$ , deg	$\mu$ , deg	$M$	$\omega$ , deg	$\mu$ , deg	$M$	$\omega$ , deg	$\mu$ , deg
1.00	0.000	90.000	4.00	65.785	14.478	7.00	90.973	8.213
1.10	1.336	65.380	4.10	67.082	14.117	7.10	91.491	8.097
1.20	3.558	56.443	4.20	68.333	13.774	7.20	91.997	7.984
1.30	6.170	50.285	4.30	69.541	13.448	7.30	92.490	7.873
1.40	8.987	45.585	4.40	70.706	13.137	7.40	92.970	7.776
1.50	11.905	41.810	4.50	71.832	12.814	7.50	93.440	7.662
1.60	14.861	38.682	4.60	72.919	12.556	7.60	93.898	7.561
1.70	17.810	36.032	4.70	73.970	12.284	7.70	94.345	7.462
1.80	20.725	33.749	4.80	74.986	12.025	7.80	94.781	7.366
1.90	23.586	31.757	4.90	75.969	11.776	7.90	95.208	7.272
2.00	26.380	30.000	5.00	76.920	11.537	8.00	95.625	7.181
2.10	29.097	28.437	5.10	77.841	11.308	8.20	96.430	7.005
2.20	31.732	27.036	5.20	78.732	11.087	8.40	97.200	6.837
2.30	34.283	25.771	5.30	79.596	10.876	8.60	97.936	6.677
2.40	36.746	24.624	5.40	80.433	10.672	8.80	98.642	6.525
2.50	39.124	23.578	5.50	81.245	10.476	9.00	99.318	6.379
2.60	41.415	22.620	5.60	82.032	10.287	9.20	99.967	6.240
2.70	43.621	21.738	5.70	82.796	10.104	9.40	100.589	6.107
2.80	45.746	20.925	5.80	83.537	9.928	9.60	101.188	5.979
2.90	47.790	20.171	5.90	84.256	9.758	9.80	101.763	5.857
3.00	49.757	19.471	6.00	84.955	9.594	10.00	102.316	5.739
3.10	51.650	18.819	6.10	85.635	9.435	10.20	102.849	5.626
3.20	53.470	18.210	6.20	86.296	9.282	10.40	103.362	5.518
3.30	55.222	17.640	6.30	86.937	9.133	10.60	103.857	5.413
3.40	56.907	17.105	6.40	87.561	8.989	10.80	104.335	5.313
3.50	58.530	16.602	6.50	88.168	8.850	11.00	104.796	5.216
3.60	60.091	16.128	6.60	88.759	8.715	11.20	105.241	5.133
3.70	61.595	15.680	6.70	89.335	8.584	11.40	105.671	5.032
3.80	63.044	15.258	6.80	89.895	8.457	11.60	106.087	4.945
3.90	64.440	14.857	6.90	90.441	8.333	11.80	106.489	4.861
						12.00	106.879	4.780

Introducing the angle  $\omega$  into (5.3.21) and (5.3.22), we obtain the following equation for the characteristics:

$$d(\omega \mp \beta) - \varepsilon \frac{dx}{y} \cdot \frac{\sin \beta \sin \mu}{\cos(\beta \pm \mu)} \pm \frac{dx}{kR} \cdot \frac{\sin^2 \mu \cos \mu}{\cos(\beta \pm \mu)} \cdot \frac{dS}{dn} = 0 \quad (5.3.31)$$

Equation (5.3.31) corresponds to the most general case of supersonic two-dimensional (plane or spatial) vortex (non-isentropic) flow of a gas.

**Equations for Characteristics  
in a Hodograph for Particular  
Cases of Gas Flow**

The form of Eq. (5.2.5) for characteristics in a physical plane is the same for all cases of gas flow if the latter is supersonic and two-dimensional. But in a hodograph, the equations for the characteristics differ and depend on the kind of flow.

If a two-dimensional flow is vortex-free, then according to (5.1.23) at all points of space occupied by the gas, the entropy is constant ( $dS/dn = 0$ ), and, therefore, the equation for the characteristics acquires a simpler form:

$$d(\omega \mp \beta) - \varepsilon \frac{dx}{y} \cdot \frac{\sin \beta \sin \mu}{\cos(\beta \pm \mu)} = 0 \quad (5.3.32)$$

For a plane non-isentropic flow ( $\varepsilon = 0$ ), we have

$$d(\omega \mp \beta) \pm \frac{dx}{kR} \cdot \frac{\sin^2 \mu \cos \mu}{\cos(\beta \pm \mu)} \cdot \frac{dS}{dn} = 0 \quad (5.3.33)$$

In the simplest case of a plane vortex-free flow ( $dS/dn = 0$ ), we have

$$d(\omega \mp \beta) = 0 \quad (5.3.34)$$

Integration of (5.3.34) yields  $\beta = \pm \omega + \text{const}$ . Introducing fixed values of the angles  $\beta_1$  and  $\beta_2$  instead of the constant, where  $\beta_1$  corresponds to the plus sign of  $\omega$ , and  $\beta_2$  to the minus sign, we find an equation for the characteristics in the form

$$\beta = \pm \omega + \beta_{1,2} \quad (5.3.35)$$

Introducing instead of  $\omega$  relation (5.3.29), we obtain

$$\begin{aligned} \beta = & \pm \left( \sqrt{\frac{k+1}{k-1}} \tan^{-1} \sqrt{\frac{\lambda^2 - 1}{\lambda_{\max}^2 - \lambda^2}} \right. \\ & \left. - \tan^{-1} \sqrt{\frac{k+1}{k-1} \cdot \frac{\lambda^2 - 1}{\lambda_{\max}^2 - \lambda^2}} \right) + \beta_{1,2} \end{aligned} \quad (5.3.36)$$

Hence, unlike Eq. (5.2.5) for characteristics in a physical plane and Eqs. (5.3.31), (5.3.32) or (5.3.33) for characteristics in a hodograph in a differential form, the corresponding equation (5.3.36) for the characteristics of a plane isentropic flow has an explicit form. Geometrically, this equation defines two families of curves—characteristics in a ring whose inner radius is  $\lambda = 1$  and whose outer one is  $\lambda_{\max} = [(k+1)/(k-1)]^{1/2}$  (Fig. 5.3.3). The integration constant  $\beta_1$  and the plus sign in front of the function  $\omega(\lambda)$  correspond to a characteristic of the first family, while the constant  $\beta_2$  and the minus sign, to the second one. These curves are **epicycloids**.

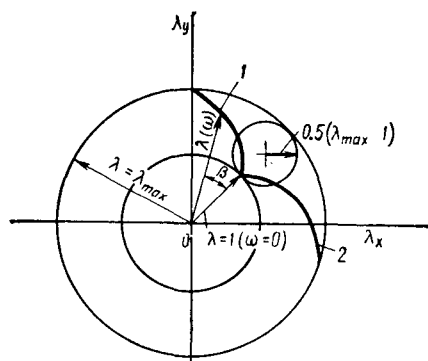


Fig. 5.3.3

Epicycloids—characteristics of a plane supersonic flow:

1—characteristic of the first family;  
2—characteristic of the second family

and can be obtained as the path of a point on a circle of radius  $0.5(\lambda_{\max} - 1)$  travelling along the inner (or outer) circle of the ring (Fig. 5.3.3). The angle  $\beta$  of inclination of the velocity vector and the speed ratio  $\lambda$  are the polar coordinates of points on an epicycloid.

By analysing a graph depicting a network of epicycloids, we can conclude that angles  $\beta$  larger in their magnitude, i.e. a more considerable deflection of the flow from its initial direction, correspond to an increase in the velocity due to expansion of the flow. A smaller deflection of the flow is observed at lower velocities.

The angle of inclination of the velocity vector is determined directly by the angle  $\omega$  whose physical meaning can be established from (5.3.35). Assume that the integration constants  $\beta_{1,2} = 0$ . This signifies that expansion of the flow begins when  $\beta = 0$  and  $M = 1$ . In accordance with this, the quantity  $\beta = \pm \omega(M)$  is the angle of deflection of the flow upon its isentropic expansion from the point where  $M = 1$  to a state characterized by an arbitrary number  $M > 1$  equal to the upper limit when evaluating integral (5.3.27).

Hence, there is a difference between the angle of deflection of a flow with the number  $M > 1$  from a certain initial direction and the angle  $\beta = \pm \omega$  determining the complete turning of the flow upon its expansion from a state characterized by the number  $M = 1$ .

The angle of flow deflection in an arbitrary cross section can be determined as follows. Let us assume that we know the initial number  $M_1 > 1$  which as a result of expansion of the flow increases and reaches the value  $M_2 > M_1$ . The angles  $\omega_1$  and  $\omega_2$  of deflection of the flow from its direction at a point with the number  $M = 1$  correspond to the numbers  $M_1$  and  $M_2$ . The angles  $\omega_1$  and  $\omega_2$  can be determined graphically with the aid of an epicycloid from expression (5.3.30) or Table 5.3.1. We use their values to find the angle of inclination of the velocity vectors. Considering, particularly, a characteristic of the first family, we obtain  $\beta_1 = \omega_1(M_1)$  and  $\beta_2 = \omega_2(M_2)$ . Conse-

quently, the angle of deflection from the initial direction is

$$\Delta\beta = \beta_2 - \beta_1 = \omega_2(M_2) - \omega_1(M_1) \quad (5.3.37)$$

The calculations can be performed in the opposite sequence, determining the local number  $M_2$  according to the known angle  $\Delta\beta$  of deflection of the flow and the initial number  $M_1$ . For this purpose, from (5.3.37) (in the given example we also consider a characteristic of the first family), we find

$$\omega_2(M_2) = \Delta\beta + \omega_1(M_1) \quad (5.3.38)$$

We find the corresponding values of  $\lambda_2$  or  $M_2$  from Fig. 5.3.3 or Table 5.3.1 according to the value of  $\omega_2$ .

Of interest is the calculation of the **ultimate flow angle** or the angle of deflection of the flow needed to obtain the maximum velocity  $V_{\max}$ . Assume that deviation begins from the initial number  $M = 1$ . In this case, we find the ultimate flow angle by formula (5.3.30) in which we must adopt a value of  $M$  corresponding to  $V_{\max}$  equal to infinity:

$$\omega_{\max} = (\pi/2) [\sqrt{(k+1)/(k-1)} - 1] \quad (5.3.39)$$

for  $k = 1.4$ , the value of  $\omega_{\max} = 0.726\pi = 130.46^\circ$ .

Consequently, a supersonic flow cannot turn through an angle larger than  $\omega_{\max}$ , and theoretically part of space remains unfilled with the gas.

If the initial number  $M$  from which the deflection begins is larger than unity, the angle of this deflection measured from the direction at  $M = 1$  will be  $\omega(M)$ , while the ultimate flow angle corresponding to this number is

$$\beta_{\max} = \omega_{\max} - \omega(M) = (\pi/2) [\sqrt{(k+1)/(k-1)} - 1] - \omega(M) \quad (5.3.40)$$

for  $k = 1.4$ , the angle  $\beta_{\max} = 130.46^\circ - \omega(M)$ .

For hypersonic velocities, the calculation of the function  $\omega$  and, consequently, of the angles of deflection is simplified. Indeed, for  $M \gg 1$ , the terms in (5.3.30) can be represented in the following form with an accuracy within quantities of a higher order of infinitesimal:

$$\begin{aligned} \sqrt{\frac{k+1}{k-1}} \tan^{-1} \sqrt{\frac{k-1}{k+1}} (M^2 - 1) &\approx \sqrt{\frac{k+1}{k-1}} \left( \frac{\pi}{2} - \frac{1}{M} \sqrt{\frac{k+1}{k-1}} \right) \\ \tan^{-1} \sqrt{M^2 - 1} &\approx \pi/2 - 1/M. \end{aligned}$$

Accordingly,

$$\omega = \frac{\pi}{2} \left( \sqrt{\frac{k+1}{k-1}} - 1 \right) - \frac{2}{k-1} \cdot \frac{1}{M} \quad (5.3.41)$$

The formula corresponding to (5.3.37) acquires the form

$$\Delta\beta = \beta_2 - \beta_1 = -\frac{2}{k-1} \left( \frac{1}{M_2} - \frac{1}{M_1} \right) \quad (5.3.37')$$

All the above relations have been found for a perfect gas. At very low pressures, however, a gas is no longer perfect. This is why the calculated ultimate flow angles are not realized and have only a theoretical significance.

#### 5.4. Outline of Solution of Gas-Dynamic Problems According to the Method of Characteristics

The determination of the parameters of a disturbed supersonic flow is associated with the solution of a system of equations for the characteristics in a physical plane and in a hodograph if the initial conditions in some way or other are set in the form of Cauchy's conditions. In the general case of a two-dimensional non-isentropic flow, this system has the form:

for characteristics of the first family

$$dy = dx \tan(\beta + \mu) \quad (5.4.1)$$

$$d(\omega - \beta) - \varepsilon(dx/y)l + (dx/kR)(dS/dn)c = 0 \quad (5.4.2)$$

for characteristics of the second family

$$dy = dx \tan(\beta - \mu) \quad (5.4.3)$$

$$d(\omega + \beta) - \varepsilon(dx/y)m - (dx/kR)(dS/dn)t = 0 \quad (5.4.4)$$

where the coefficients are

$$l = \sin \beta \sin \mu / \cos(\beta + \mu), \quad c = \sin^2 \mu \cos \mu / \cos(\beta + \mu) \quad (5.4.5)$$

$$m = \sin \beta \sin \mu / \cos(\beta - \mu), \quad t = \sin^2 \mu \cos \mu / \cos(\beta - \mu) \quad (5.4.6)$$

For a two-dimensional isentropic flow, we have

$$dS/dn = 0 \quad (5.4.7)$$

therefore the system of equations is simplified:

for characteristics of the first family

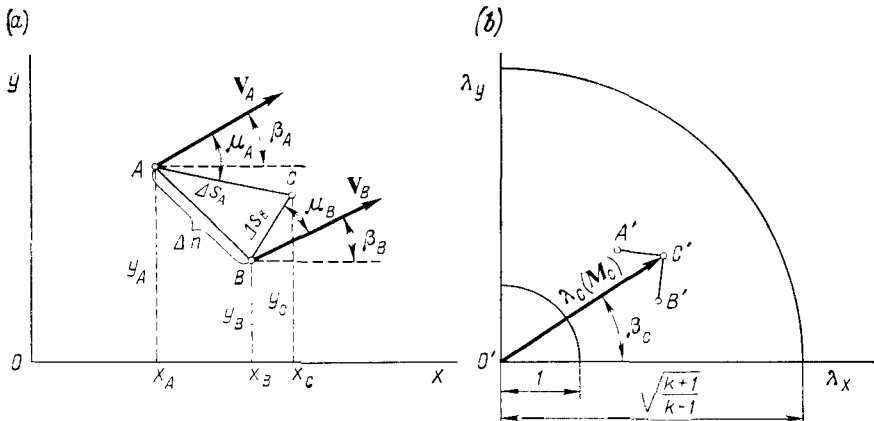
$$dy = dx \tan(\beta + \mu); \quad d(\omega - \beta) - \varepsilon(dx/y)l = 0 \quad (5.4.8)$$

for characteristics of the second family

$$dy = dx \tan(\beta - \mu); \quad d(\omega + \beta) - \varepsilon(dx/y)m = 0 \quad (5.4.9)$$

For a plane flow, we assume that  $\varepsilon = 0$  in the equations, for a spatial axisymmetric flow,  $\varepsilon = 1$ , and we introduce  $r$  instead of  $y$ .

A solution according to the method of characteristics of any problem on the flow over a body consists of the solution of three particular problems.

**Fig. 5.4.1**

Calculation of the velocity at the intersection point of two characteristics of different families:

a—physical plane; b—plane of hodograph

The first problem is associated with the determination of the velocity and other parameters at the point of intersection of characteristics of different families issuing from two close points.

Assume that we are determining the parameters at point  $C$  (velocity  $\mathbf{V}_C$ , number  $M_C$ , flow deflection angle  $\beta_C$ , entropy  $S_C$ , etc.) at the intersection of elements of characteristics of the first and second families drawn from points  $A$  and  $B$  (Fig. 5.4.1a). At these points, which are on different streamlines, we know the velocities  $\mathbf{V}_A$ ,  $\mathbf{V}_B$ , and other parameters, including the entropies  $S_A$  and  $S_B$ .

All the calculations are based on the use of Eqs. (5.4.1)-(5.4.4) for the characteristics, which in finite differences have the form:

for the first family

$$\Delta y_B = \Delta x_B \tan(\beta_B + \mu_B) \quad (5.4.10)$$

$$\Delta \omega_B - \Delta \beta_B - \varepsilon (\Delta x_B/y_B) l_B + (\Delta x_B/kR) (\Delta S/\Delta n) c_B = 0 \quad (5.4.11)$$

for the second family

$$\Delta y_A = \Delta x_A \tan(\beta_A - \mu_A) \quad (5.4.12)$$

$$\Delta \omega_A + \Delta \beta_A - \varepsilon (\Delta x_A/y_A) m_A - (\Delta x_A/kR) (\Delta S/\Delta n) t_A = 0 \quad (5.4.13)$$

where

$$\left. \begin{aligned} \Delta y_B &= y_C - y_B, & \Delta x_B &= x_C - x_B, & \Delta \omega_B &= \omega_C - \omega_B, \\ && \Delta \beta_B &= \beta_C - \beta_B \\ \Delta y_A &= y_C - y_A, & \Delta x_A &= x_C - x_A, & \Delta \omega_A &= \omega_C - \omega_A, \\ && \Delta \beta_A &= \beta_C - \beta_A \end{aligned} \right\} \quad (5.4.14)$$

$$\left. \begin{aligned} l_B &= \sin \beta_B \sin \mu_B / \cos (\beta_B + \mu_B) \\ c_B &= \sin^2 \mu_B \cos \mu_B / \cos (\beta_B + \mu_B) \\ m_A &= \sin \beta_A \sin \mu_A / \cos (\beta_A - \mu_A) \\ t_A &= \sin^2 \mu_A \cos \mu_A / \cos (\beta_A - \mu_A) \end{aligned} \right\} \quad (5.4.15)$$

Equations (5.4.10)-(5.4.13) were derived assuming that the coefficients  $l$ ,  $m$ ,  $c$ , and  $t$  remain *constant* upon motion along characteristic elements  $BC$  and  $AC$  and equal their values at the initial points  $B$  and  $A$ .

The change in the entropy per unit length of a normal  $\Delta S / \Delta n$  is calculated as follows. It is shown in Fig. 5.4.1a that the distance between points  $B$  and  $A$  is

$$\Delta n \approx (AC) \sin \mu_A + (BC) \sin \mu_B$$

where

$$AC = (x_C - x_A) / \cos (\beta_A - \mu_A), \quad BC = (x_C - x_B) / \cos (\beta_B - \mu_B)$$

Introducing the notation

$$e = (x_C - x_A) \sin \mu_A \cos (\beta_B + \mu_B), \quad f = (x_C - x_B) \sin \mu_B \cos \times (\beta_A - \mu_A)$$

we obtain

$$\Delta S / \Delta n = (S_A - S_B) \cos (\beta_B + \mu_B) \cos (\beta_A - \mu_A) / (f + e) \quad (5.4.16)$$

The entropy at point  $C$  is determined from the relation

$$S_C = \Delta S_B + S_B = \frac{\Delta S}{\Delta n} (BC) \sin \mu_B + S_B = \frac{(S_A - S_B) f}{f + e} + S_B \quad (5.4.17)$$

The entropy gradient may be replaced with the stagnation pressure gradient in accordance with (5.3.24):

$$\frac{1}{R} \cdot \frac{\Delta S}{\Delta n} = - \frac{1}{p'_0} \cdot \frac{\Delta p'_0}{\Delta n} = - \frac{(p'_{0,A} - p'_{0,B}) \cos (\beta_B + \mu_B) \cos (\beta_A - \mu_A)}{(f + e) p'_{0,B}} \quad (5.4.18)$$

The stagnation pressure at point  $C$  is

$$p'_{0,C} = (p'_{0,A} - p'_{0,B}) f / (f + e) + p'_{0,B} \quad (5.4.19)$$

To find the coordinates  $x_C$  and  $y_C$  of point  $C$ , we have to solve the simultaneous equations (5.4.10) and (5.4.12) for the elements of the characteristics in a physical plane:

$$y_C - y_B = (x_C - x_B) \tan (\beta_B + \mu_B);$$

$$y_C - y_A = (x_C - x_A) \tan (\beta_A - \mu_A)$$

A graphical solution of these equations is shown in Fig. 5.4.1a. We use the found value of  $x_C$  to determine the differences  $\Delta x_B =$

$= x_C - x_B$  and  $\Delta x_A = x_C - x_A$  in Eqs. (5.4.11) and (5.4.13). The increments  $\Delta\omega_B$ ,  $\Delta\omega_A$ ,  $\Delta\beta_B$ , and  $\Delta\beta_A$  are the unknowns in these equations, but the latter are only two in number. The number of unknowns can be reduced to two in accordance with the number of equations in the system. For this purpose, we compile the obvious relations

$$\left. \begin{aligned} \Delta\omega_A &= \omega_C - \omega_A = \Delta\omega_B + \omega_B - \omega_A \\ \Delta\beta_A &= \beta_B - \beta_A = \Delta\beta_B + \beta_B - \beta_A \end{aligned} \right\} \quad (5.4.20)$$

With account taken of these relations, Eq. (5.4.13) is transformed as follows:

$$\Delta\omega_B + \omega_B - \omega_A + \Delta\beta_B + \beta_B - \beta_A - \varepsilon \frac{\Delta x_A}{y_A} m_A - \frac{\Delta x_A}{kR} \cdot \frac{\Delta S}{\Delta n} t_A = 0 \quad (5.4.21)$$

By solving this equation simultaneously with (5.4.11) for the variable  $\Delta\beta_B$ , we obtain

$$\Delta\beta_B = \frac{1}{2} \left[ \frac{1}{kR} \cdot \frac{\Delta S}{\Delta n} (\Delta x_A t_A + \Delta x_B c_B) + \varepsilon \left( \frac{\Delta x_A}{y_A} m_A - \frac{\Delta x_B}{y_B} l_B \right) - (\omega_B - \omega_A) - (\beta_B - \beta_A) \right] \quad (5.4.22)$$

We use the found value of  $\Delta\beta_B$  to evaluate the increment of the function  $\omega$  by (5.4.11):

$$\Delta\omega_B = \Delta\beta_B + \varepsilon \frac{\Delta x_B}{y_B} l_B - \frac{\Delta x_B}{kR} \cdot \frac{\Delta S}{\Delta n} c_B \quad (5.4.23)$$

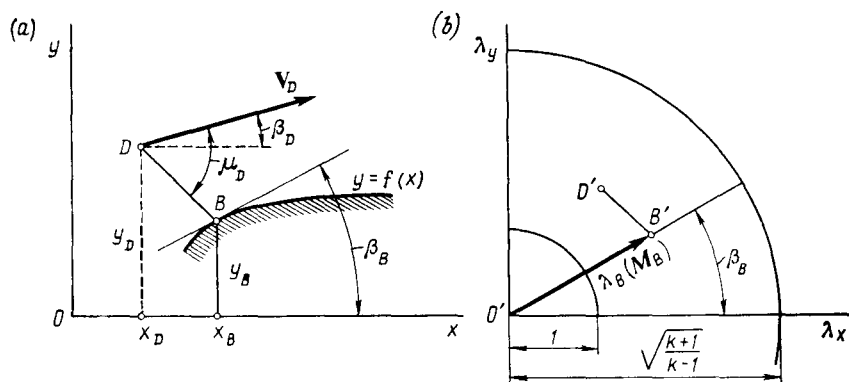
Now we can calculate the angles for point *C*:

$$\beta_C = \Delta\beta_B + \beta_B; \quad \omega_C = \Delta\omega_B + \omega_B \quad (5.4.24)$$

According to the found value of  $\omega_C$ , we determine the number  $M_C$  and the Mach angle  $\mu_C$  at point *C* from Table 5.3.1.

A graphical solution of the system of equations for characteristics in a hodograph as a result of which the angle  $\beta_C$  and the number  $\lambda_C$  ( $M_C$ ) are determined is shown in Fig. 5.4.1b, where  $B'C'$  and  $A'C'$  are elements of the characteristics of the first and second families corresponding to elements of the conjugate characteristics  $BC$  and  $AC$  in a physical plane. The found number  $M_C$  (or  $\lambda_C$ ) when necessary can be used to determine parameters such as the pressure, density, and temperature.

The calculated parameters can be determined more precisely if we substitute for  $l_B$ ,  $m_A$ ,  $c_B$ , and  $t_A$  in Eqs. (5.4.10)-(5.4.13) the quantities obtained from the values of the angles  $\beta$  and  $\mu$  that are the average between the ones set at points *A* and *B*, and those found

**Fig. 5.4.2**

Calculation of the velocity at the intersection point of a characteristic with a surface in a flow:

a—physical plane; b—plane of hodograph

at point *C* in the first approximation, i.e. from the values:

$$\left. \begin{aligned} \mu_A^{(2)} &= (\mu_A + \mu_C)/2, \quad \mu_B^{(2)} = (\mu_B + \mu_C)/2 \\ \beta_A^{(2)} &= (\beta_A + \beta_C)/2, \quad \beta_B^{(2)} = (\beta_B + \beta_C)/2 \end{aligned} \right\} \quad (5.4.25)$$

We find the more precise coordinates  $x_C$  and  $y_C$  of point *C* from the equations

$$\left. \begin{aligned} \Delta y_B &= \Delta x_B \tan(\beta_B^{(2)} + \mu_B^{(2)}); \\ \Delta y_A &= \Delta x_A \tan(\beta_A^{(2)} - \mu_A^{(2)}) \end{aligned} \right\} \quad (5.4.26)$$

The **second problem** consists in calculating the velocity at the point of intersection of a characteristic with a surface in a flow. Assume that point *B* is located at the intersection with linear element *DB* of a characteristic of the second family drawn from point *D* near a surface (Fig. 5.4.2). The velocity at this point (both its magnitude and direction), the entropy, and the coordinates of the point are known.

The velocity at point *B* is determined directly with the aid of Eq. (5.4.4) for a characteristic of the second family. If we relate this equation to the conditions along characteristic element *DB* and express it in finite differences, we have

$$\Delta \omega_D = -\Delta \beta_D + \varepsilon (\Delta x_D/y_D) m_D - (\Delta x_D/kR) (\Delta S/\Delta n) t_D \quad (5.4.27)$$

where

$$\left. \begin{aligned} \Delta \omega_D &= \omega_B - \omega_D, \quad \Delta \beta_D = \beta_B - \beta_D, \quad \Delta x_D = x_B - x_D \\ m_D &= \sin \beta_D \sin \mu_D / \cos(\beta_D - \mu_D) \\ t_D &= \sin^2 \mu_D \cos \mu_D / \cos(\beta_D - \mu_D) \end{aligned} \right\} \quad (5.4.28)$$

$$\Delta S / \Delta n = (S_B - S_D) \cos (\beta_D - \mu_D) / (x_D - x_B) \sin \mu_D$$

or

$$\frac{\Delta S}{\Delta n} = - \frac{R}{p'_{0,D}} \cdot \frac{\Delta p'_0}{\Delta n} = - \frac{R}{p'_{0,D}} \frac{(p'_{0,B} - p'_{0,D}) \cos (\beta_D - \mu_D)}{(x_D - x_B) \sin \mu_D} \quad (5.4.29)$$

The coordinates  $x_B$  and  $y_B$  of point  $B$  are determined by the simultaneous solution of the equation for a characteristic of the second family and the equation of the wall contour:

$$y_B - y_D = (x_B - x_D) \tan (\beta_D - \mu_D); \quad y_B = f(x_D) \quad (5.4.30)$$

A graphical solution of these equations is shown in Fig. 5.4.2a.

We use the found coordinates  $x_B$  and  $y_B$  to evaluate the angle  $\beta_B$  from the equation

$$\tan \beta_B = (dy/dx)_B \quad (5.4.31)$$

The entropy  $S_B$  (or the stagnation pressure  $p'_{0,B}$ ) at point  $B$  is considered to be a known quantity and equal to its value on the streamline coinciding with a tangent to the surface. The entropy is considered to be constant along an element of the tangent.

Upon calculating the increment  $\Delta \omega_D$  by (5.4.27), we can find the angle  $\omega_B = \Delta \omega_D + \omega_D$ , and then determine the number  $M_B$  from Table 5.3.1. How the velocity at point  $B$  is determined is shown graphically in Fig. 5.4.2b, where element  $D'B'$  of a characteristic of the second family in a hodograph corresponds to an element of a characteristic of the same family in a physical plane.

The **third problem** consists in calculating the velocity at the intersection of the characteristics with a shock and in determining the change in the inclination of the shock at this point. Since a characteristic in its nature is a line of weak disturbances, this intersection physically corresponds to the interaction of a weak wave with a compression shock. Assume that closely arranged expansion waves, which characteristics of the first family correspond to, fall at points  $J$  and  $H$  on compression shock  $N$  of a preset shape  $y = f(x)$  (Fig. 5.4.3a). As a result, the strength diminishes, as does the inclination angle of the shock. Since points  $J$  and  $H$  are sources of disturbances, expansion waves appear, and characteristics of the second family can be drawn through these points. One of such characteristics, passing through point  $J$ , intersects the neighbouring conjugate characteristic at point  $F$  called the **nodal point of the characteristics**.

To determine the change in the inclination of the shock and in the velocity behind it, one must use the properties of the characteristics  $JF$  and  $FH$  passing through nodal point  $F$ , and also the relations for calculating a compression shock. Since length  $JH$  of the shock is small, this section may be assumed to be linear. The angle of inclination of the shock on this section and the corresponding pa-

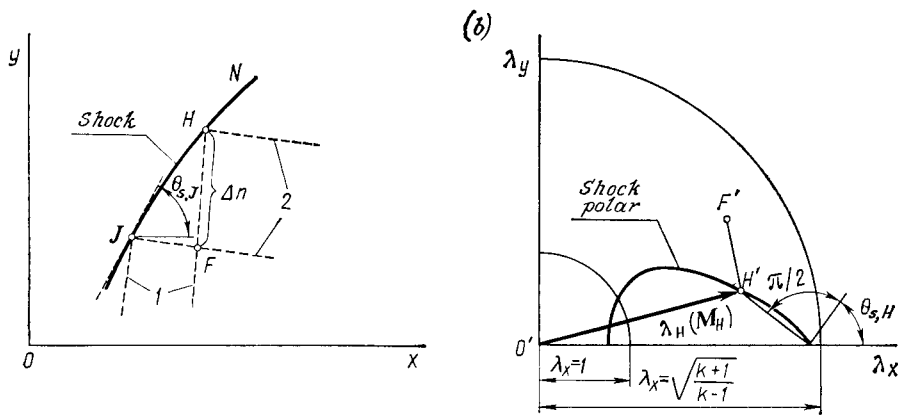


Fig. 5.4.3

Calculation of the velocity at the intersection of characteristics with a shock:  
 a—physical plane; b—plane of hodograph; 1—characteristics of the first family; 2—characteristics of the second family

parameters of the gas are approximately equal to their values at intersection point  $H$  of element  $FH$  of a first family characteristic with the shock.

One of the unknown parameters is the angle of inclination  $\beta_H$  of the velocity vector at this point, which can be written as  $\beta_H = \Delta\beta_F + \beta_F$ , where  $\Delta\beta_F = \beta_H - \beta_F$ , and  $\beta_F$  is the known angle of inclination of the velocity vector at point  $F$ . To evaluate the second unknown (the number  $M_H$  at the same point) we shall use the formula

$$M_H = M_J + (dM/d\beta)_J \Delta\beta_{JH} \quad (5.4.32)$$

in which  $(dM/d\beta)_J$  is a derivative calculated with the aid of the relevant expressions for a compression shock according to the known parameters at point  $J$ , and the quantity  $\Delta\beta_{JH}$  determined by the change in the angle  $\beta$  along a shock element equals the difference  $\beta_H - \beta_J$ . We may assume that this quantity approximately equals the change in the angle  $\beta$  along the element  $FH$  of a characteristic of the first family  $\Delta\beta_{FH} = \Delta\beta_F = \beta_H - \beta_F$ .

The derivative  $dM/d\beta$  is evaluated as a result of differentiation of (4.3.19'):

$$\begin{aligned} \frac{dM}{d\beta} &= \frac{dM_2}{d\beta_s} = -M_2 \left[ \cot(\theta_s - \beta_s) \left( \frac{d\theta_s}{d\beta_s} - 1 \right) \right. \\ &\quad \left. + \frac{M_2^2}{2(1-\delta)} \sin^2(\theta_s - \beta_s) \frac{d}{d\beta_s} \left( \frac{\rho_2}{\rho_1} \right) \right] \end{aligned} \quad (5.4.33)$$

We shall calculate the derivative  $d(\rho_2/\rho_1)/d\beta_s$  on the right-hand side by differentiating (4.3.13):

$$\frac{d}{d\beta_s} \left( \frac{\rho_2}{\rho_1} \right) = 2 \cot \theta_s \left( 1 - \delta \frac{\rho_2}{\rho_1} \right) \frac{\rho_2}{\rho_1} \cdot \frac{d\theta_s}{d\beta_s} \quad (5.4.34)$$

We determine the derivative  $d\theta_s/d\beta_s$  as follows. We differentiate (4.3.24):

$$\frac{d}{d\beta_s} \left( \frac{\rho_2}{\rho_1} \right) = \frac{\rho_2}{\rho_1} \left\{ \frac{d\theta_s}{d\beta_s} \left[ \frac{1}{\sin \theta_s \cos \theta_s} - \frac{1}{\sin(\theta_s - \beta_s) \cos(\theta_s - \beta_s)} \right. \right. \\ \left. \left. + \frac{1}{\sin(\theta_s - \beta_s) \cos(\theta_s - \beta_s)} \right] \right\}$$

This relation can be transformed somewhat by using (4.3.24):

$$\frac{d}{d\beta_s} \left( \frac{\rho_2}{\rho_1} \right) = \frac{\rho_2}{\rho_1} \cdot \frac{1}{\tan \theta_s \cos^2(\theta_s - \beta_s)} \\ \times \left\{ \frac{d\theta_s}{d\beta_s} \left[ \frac{\cos^2(\theta_s - \beta_s)}{\cos^2 \theta_s} - \frac{\rho_2}{\rho_1} \right] + \frac{\rho_2}{\rho_1} \right\} \quad (5.4.35)$$

Equating the right-hand sides of (5.4.34) and (5.4.35) and solving the equation obtained for the derivative  $d\theta_s/d\beta_s$ , we obtain:

$$\frac{d\theta_s}{d\beta_s} = \frac{\rho_2}{\rho_1} \left[ 2 \cos^2(\theta_s - \beta_s) \left( 1 - \delta \frac{\rho_2}{\rho_1} \right) \right. \\ \left. - \frac{\cos^2(\theta_s - \beta_s)}{\cos^2 \theta_s} + \frac{\rho_2}{\rho_1} \right]^{-1} \quad (5.4.36)$$

Let us derive an expression for the change in the number  $M$  when travelling along the characteristics from point  $F$  to point  $H$ , i.e. for the quantity  $\Delta M_F = M_H - M_F$ . To do this, we shall substitute expression (5.4.32) here for  $M_H$ :

$$\Delta M_F = M_J + (dM/d\beta)_J \Delta \beta_F - M_F \quad (5.4.37)$$

We can go over from the number  $M$  to the function  $\omega$  determined by relation (5.3.30):

$$\Delta \omega_F = \omega_J + (d\omega/d\beta)_J \Delta \beta_F - \omega_F \quad (5.4.38)$$

where

$$(d\omega/d\beta)_J = (dM/d\beta)_J (d\omega/dM)_J \quad (5.4.39)$$

The derivative  $d\omega/dM$  is determined as a result of differentiating (5.3.30):

$$\frac{d\omega}{dM} = \sqrt{M^2 - 1} \left[ M \left( 1 + \frac{k-1}{1} M^2 \right) \right]^{-1} \quad (5.4.40)$$

Equation (5.4.41) for a characteristic of the first family applied along element  $FH$  yields

$$\Delta \omega_F - \Delta \beta_F - \varepsilon (\Delta x_F/y_F) l_F + (\Delta x_F/kR) (\Delta S/\Delta n) c_F = 0 \quad (5.4.41)$$

where

$$\left. \begin{aligned} \Delta \omega_F &= \omega_H - \omega_F, \quad \Delta \beta_F = \beta_H - \beta_P, \quad \Delta x_F = x_H - x_F \\ l_F &= \sin \beta_F \sin \mu_F / \cos(\beta_F + \mu_F) \\ c_F &= \sin^2 \mu_F \cos \mu_F / \cos(\beta_F + \mu_F) \end{aligned} \right\} \quad (5.4.42)$$

The distance along a normal to a streamline between points  $F$  and  $H$  is

$$\Delta n = (FH) \sin \mu_F = \frac{x_H - x_F}{\cos \beta_F + \mu_F} \sin \mu_F \quad (5.4.43)$$

Consequently, the entropy gradient in (5.4.41) is

$$\Delta S / \Delta n = (S_H - S_F) \cos (\beta_F + \mu_F) / (x_H - x_F) \sin \mu_F \quad (5.4.44)$$

or

$$\frac{\Delta S}{\Delta n} = - \frac{R}{p'_{0,F}} \cdot \frac{(p'_{0,H} - p'_{0,F}) \cos (\beta_F + \mu_F)}{(x_H - x_F) \sin \mu_F} \quad (5.4.45)$$

where  $p'_{0,H}$  is found according to the number  $M_H$  from the shock theory.

The entropy  $S_F$  or the stagnation pressure  $p'_{0,F}$  at point  $F$  can be adopted approximately equal to the corresponding values at point  $J$  on the shock, i.e.  $S_F \approx S_J$  and  $p'_{0,F} \approx p'_{0,J}$ .

Solving Eqs. (5.4.38) and (5.4.41) for  $\Delta\beta_F$ , we obtain

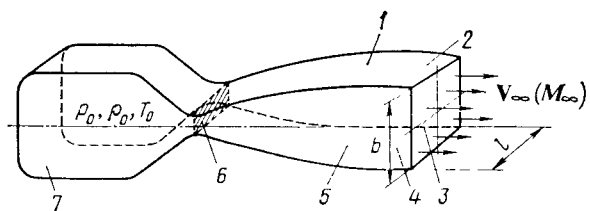
$$\Delta\beta_F = \left[ \left( \frac{d\omega}{d\beta} \right)_J - 1 \right]^{-1} \left( \omega_F - \omega_J + \varepsilon \frac{\Delta x_F}{y_F} l_F - \frac{\Delta x_F}{kR} \cdot \frac{\Delta S}{\Delta n} c_F \right) \quad (5.4.46)$$

Inserting the value of  $\Delta\beta_F$  into (5.4.38), we can find  $\Delta\omega_F$ , calculate the angle  $\omega_H = \Delta\omega_F + \omega_F$ , and determine more precisely the number  $M_H$ . By calculating the angle  $\beta_H = \Delta\beta_F + \beta_F$ , we use the values of this angle, and also of the preset number  $M_\infty$  to find the shock angle  $\theta_{s,H}$  at point  $H$  and, consequently, to determine the shape of the shock more accurately on section  $JH$ . If necessary, the calculations can be performed in a second approximation, adopting instead of the parameters at point  $J$  their average values between points  $J$  and  $H$ . Particularly, instead of the angles  $\omega_J$  and  $\beta_J$ , we take the relevant average values of  $0.5(\omega_J + \omega_H)$  and  $0.5(\beta_J + \beta_H)$ .

Figure 5.4.3b shows how the problem is solved graphically. Point  $H'$  on a hodograph, corresponding to point  $H$  on a physical plane, is determined as a result of the intersection of element  $F'H'$  of a first family characteristic with a shock polar constructed for the given free-stream number  $M_\infty$ . The vector  $O'H'$  determines the velocity  $\lambda_H$  at point  $H$ .

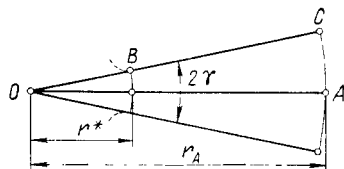
## 5.5. Applications of the Method of Characteristics to the Solution of the Problem on Shaping the Nozzles of Supersonic Wind Tunnels

The method of characteristics allows us to solve one of the most important problems of gas dynamics associated with the determination of the shape of a wind tunnel nozzle intended for producing a two-dimensional plane parallel supersonic flow at a preset velocity.

**Fig. 5.5.1**

Nozzle of supersonic tunnel:

1—top wall; 2 and 5—side walls; 3—exit section; 4—bottom wall; 6—critical section; 7—receiver

**Fig. 5.5.2**

Unshaped two-dimensional supersonic nozzle with a radial flow

The nozzle ensuring such a flow is a mouthpiece whose side walls are flat, while its top and bottom walls have a specially shaped **contour** (Fig. 5.5.4).

In addition to determining the shape of its curved contour, the design of a nozzle includes calculation of the parameters of the gas in the receiver (the parameters of stagnation) and in the critical section, and also its area  $S^*$ . The parameters of the gas at the nozzle exit are usually preset, namely, the number  $M_\infty$ , the pressure  $p_\infty$ , the area of the exit section  $S = lb$ , and the temperature of the gas in the receiver  $T_0$ . The area of the critical nozzle section is found from flow rate equation (3.6.44) which we shall write in the form  $\rho_\infty V_\infty S = \rho^* a^* S^*$ . Hence  $S^* = (\rho_\infty V_\infty / \rho^* a^*) S = \bar{q} S$ .

It follows from (3.6.46') that the parameter  $\bar{q}$  is determined by the preset number  $M_\infty$  at the nozzle exit. According to this value of  $M_\infty$  and the pressure  $p_\infty$  at the exit, and by using formula (3.6.29), we can find the pressure  $p_0$  in the receiver needed to ensure the preset number  $M_\infty$  at the exit.

Next the angle  $2\gamma$  of an unshaped nozzle is set (Fig. 5.5.2). Experimental investigations show that this angle is generally chosen equal to  $30\text{--}35^\circ$ .

If the section of the inlet part of a nozzle changes sufficiently gradually, the flow downstream of the critical section can be considered as an **expanding radial flow** from a source at point  $O$ . Such a flow has the property that its direction coincides with that of radial lines emerging from point  $O$ . The change in the parameters of the gas in magnitude along each of these lines is of the same nature. The length of the subsonic portion of the nozzle of unit width is de-

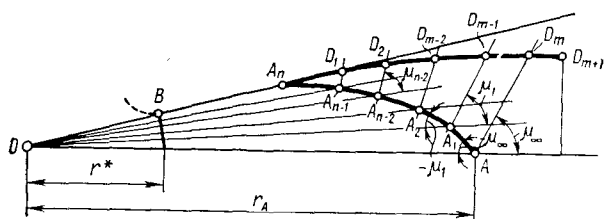


Fig. 5.5.3

Construction of a  $\lambda$ -shaped supersonic two-dimensional nozzle

terminated by the quantity  $r^* = S^* [360/(2\pi \cdot 2\gamma \cdot 1)]$ , while the distance to the exit section  $r_A = S [360/(2\pi \cdot 2\gamma \cdot 1)]$ .

In the region of the nozzle confined by two circles of radii  $r^*$  and  $r_A$ , i.e. beyond the limits of the critical section, the gas flow is supersonic. Shaping of the nozzle consists in replacing straight wall  $BC$  in this region with a curved contour ensuring the gradual transition of the radial flow into a *plane parallel flow at the exit at a preset velocity*. For this purpose, let us draw through point  $O$  a number of closely arranged lines and determine the velocities (the numbers  $M$ ) on these lines at their intersection points  $A_1, \dots, A_n$  with a characteristic of one of the families  $AA_n$  (let us consider it to be a characteristic of the second family) emerging from point  $A$  on an arc of radius  $r_A$  (Fig. 5.5.3). Point  $A_1$  is at the intersection of ray  $r_1 = OA_1$  with the element of characteristic  $AA_1$  drawn at an angle of  $\mu_\infty = -\sin^{-1}(1/M_\infty)$ .

We find the number  $M_1$  at point  $A_1$  with the aid of the expression  $\bar{q}_1 = S^*/S_1$ . Since  $S_1 = 2\pi r_1 \cdot 1 (2\gamma/360)$ , and  $S^* = 2\pi r^* \cdot 1 (2\gamma/360)$ , we have  $\bar{q}_1 = r^*/r_1$ . Employing (3.6.46), we can find  $\lambda_1$  and the corresponding number  $M_1$ .

We determine in a similar way the coordinates of intersection point  $A_2$  of the adjacent ray  $r_2 = OA_2$  with the element of characteristic  $AA_1A_2$  inclined to straight line  $OA_1$  at the angle  $\mu_1 = -\sin^{-1}(1/M_1)$ , the number  $M_2$  at point  $A_2$ , and so on. As a result, we can construct a characteristic of the second family in the form of broken line  $AA_1 \dots A_{n-1}A_n$  intersecting straight wall  $BA_n$  of the nozzle at point  $A_n$ . For this point, as for the other points  $A_{n-2}, A_{n-1}$ , and  $A_n$  of intersection of the characteristic with the straight lines emerging from source  $O$ , we can calculate the relevant Mach numbers and the angles  $\mu = -\sin^{-1}(1/M)$ .

The flow region  $OAA_n$  with a known velocity field confined by the characteristic  $AA_n$  and the straight walls of the nozzle is called a **triangle of definiteness**. The shape of this flow is preserved if we change the wall behind point  $A_n$  so that the radial flow on the Mach line gradually transforms into a plane parallel flow at the exit.

With a view to this condition, we can construct a characteristic of the first family emerging from point  $A$  and having the form of a straight line. If we now determine the field of velocities between the characteristics  $AA_n$  and  $AD_m$ , we can find the relevant streamlines. It is exactly the streamline passing through point  $A_n$  that coincides with the shaped contour of the nozzle.

To determine the velocity field, we shall assume that in the two-dimensional flow being considered all the characteristics of the first family emerging from points  $A_{n-2}$ ,  $A_{n-1}$ , as well as the characteristic  $AD_m$  are straight lines (Fig. 5.5.3). The inclination of each characteristic to a radial line is determined by the corresponding Mach angle  $\mu_1 = \sin^{-1}(1/M_1)$ ,  $\mu_2 = \sin^{-1}(1/M_2)$ , etc., while the velocity along a characteristic is determined by its relevant value at the initial points  $A_1$ ,  $A_2$ , . . .

Let us consider the streamline emerging from point  $A_n$ . The initial part of this line coincides with the direction of the velocity at point  $A_n$  and is a straight line that is an extension of contour  $BA_n$  up to its intersection point  $D_1$  with the characteristic of the first family  $A_{n-1}A_n$ . Behind point  $D_1$ , the streamline element coincides with the direction of the velocity at point  $D_1$  equal to the velocity at point  $A_{n-1}$ . Drawing through point  $D_1$  a straight line parallel to ray  $OA_{n-1}$  up to its intersection point  $D_2$  with the characteristic  $A_{n-2}D_2$ , we obtain the next part of the streamline. Behind point  $D_2$ , part  $D_2D_{m-2}$  of the streamline (point  $D_{m-2}$  is on the characteristic of the first family  $A_2D_{m-2}$ ) is parallel to straight line  $OA_{n-2}$ . The remaining parts of the streamline are constructed similarly. Behind point  $D_m$ , which is on the characteristic  $AD_m$ , the part of the streamline is parallel to the axis of the nozzle. The contour of the nozzle coinciding with the streamline  $A_nD_{m+1}$  and constructed in the form of a smooth curve ensures a parallel supersonic flow with the preset number  $M_\infty$  at the nozzle exit.

## Airfoil and Finite-Span Wing in an Incompressible Flow

Let us consider the problems associated with the application of the aerodynamic theory to calculating the flow past an airfoil. A feature of this flow is the formation of a two-dimensional disturbed flow over the airfoil. We shall use simpler equations of aerodynamics than for three-dimensional flows to investigate it.

The flow over an airfoil treated as a two-dimensional one is idealized. Actually, the flow past an airfoil belonging to a real finite-span wing is three-dimensional. This is why the aerodynamic characteristics of an airfoil cannot be transferred directly to a wing. But these characteristics can be among the basic parameters used in calculating similar characteristics of real wings. At the same time, the solution of the problem on an airfoil has an independent significance because cases are possible when on individual parts of wings the flow past airfoils is practically of a two-dimensional nature.

We shall investigate the flow of an incompressible fluid past an airfoil. We shall simultaneously consider the problem of a finite-span wing in a similar flow. The results obtained, which have an independent significance in low-speed aerodynamics, can be used for aerodynamic investigations at high speeds.

### 6.1. Thin Airfoil in an Incompressible Flow

Let us consider the method of calculating the steady flow of an incompressible fluid past a thin slightly bent airfoil at a small angle of attack (Fig. 6.1.1). The aerodynamic characteristics of the airfoil obtained as a result of these calculations can be used directly for flight at low subsonic speeds ( $M_\infty < 0.3-0.4$ ) when the air may be considered as an incompressible fluid. They can also be used as

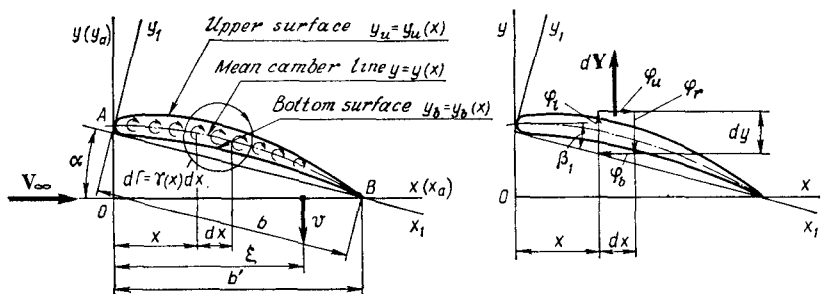


Fig. 6.1.1

Thin airfoil in an incompressible flow

the initial data when performing aerodynamic calculations of airfoils having a given configuration in a subsonic compressible flow.

Since the airfoil is thin, and the angle of attack is not large, the velocity of the flow near it differs only slightly from that of the undisturbed flow. Such a flow is called **nearly uniform**.

We can write the following condition for the velocity of a nearly uniform flow:

$$V_x = V_\infty + u \quad (u \ll V_\infty), \quad V_y = v \quad (v \ll V_\infty) \quad (6.1.1)$$

where  $u$  and  $v$  are the components of the **velocity of small disturbances**.

In accordance with this condition,

$$V^2 = V_x^2 + V_y^2 = (V_\infty + u)^2 + v^2 \approx V_\infty^2 + 2V_\infty u \quad (6.1.2)$$

Let us now determine the pressure in a nearly uniform flow. From the Bernoulli equation (3.4.13), in which we assume that the constant  $C_2$  equals  $p_\infty/\rho_\infty + V_\infty^2/2$  and  $\rho = \text{const}$ , we obtain the excess pressure

$$p - p_\infty = \rho_\infty (V_\infty^2/2 - V^2/2) = -\rho_\infty V_\infty u \quad (6.1.3)$$

We define  $u$  in terms of the velocity potential,  $u = \partial\varphi/\partial x$ :

$$p - p_\infty = -\rho_\infty V_\infty \partial\varphi/\partial x \quad (6.1.4)$$

The corresponding pressure coefficient is

$$\bar{p} = (p - p_\infty)/q_\infty = -2u/V_\infty = -(2/V_\infty) \partial\varphi/\partial x \quad (6.1.5)$$

By (6.1.4), the excess pressure on the bottom surface of the airfoil is

$$p_b - p_\infty = -(\partial\varphi_b/\partial x) V_\infty \rho_\infty$$

and on its upper surface is

$$p_u - p_\infty = -(\partial\varphi_u/\partial x) V_\infty \rho_\infty$$

where  $\varphi_b$  and  $\varphi_u$  are the velocity potentials on the bottom and upper surfaces, respectively. Consequently, the lift force produced by the pressure acting on an element of area is

$$dY_{a,ic} = (p_b - p_u) dx = -V_\infty \rho_\infty (\partial \varphi_b / \partial x - \partial \varphi_u / \partial x) dx$$

while the lift force for the entire airfoil with the chord  $b$  is

$$Y_{a,ic} = -V_\infty \rho_\infty \int_0^{b'} \left( \frac{\partial \varphi_b}{\partial x} - \frac{\partial \varphi_u}{\partial x} \right) dx$$

Assuming the upper limit  $b'$  of the integral to be approximately equal to the chord  $b$  (because of the smallness of the angle of attack), we find the corresponding lift coefficient:

$$c_{y_a,ic} = \frac{Y_{a,ic}}{q_\infty b} = -\frac{2}{V_\infty b} \int_0^b \left( \frac{\partial \varphi_b}{\partial x} - \frac{\partial \varphi_u}{\partial x} \right) dx \quad (6.1.6)$$

Let us consider the circulation of the velocity over a contour that is a rectangle with the dimensions  $dx$  and  $dy$  and encloses an element of the airfoil. In accordance with Fig. 6.1.1, the circulation is

$$d\Gamma = \left( V_\infty + \frac{\partial \varphi_u}{\partial x} \right) dx - \left( V_\infty + \frac{\partial \varphi_b}{\partial x} \right) dx + \left( \frac{\partial \varphi_l}{\partial y} - \frac{\partial \varphi_r}{\partial y} \right) dy$$

where  $\varphi_l$  and  $\varphi_r$  are the velocity potentials on the left and right surfaces, respectively.

Let us introduce the concept of the **intensity of circulation (of a vortex)** determined by the derivative  $d\Gamma/dx = \gamma(x)$ . The magnitude of this intensity is

$$\gamma(x) = \frac{\partial \varphi_u}{\partial x} - \frac{\partial \varphi_b}{\partial x} + \frac{dy}{dx} \left( \frac{\partial \varphi_l}{\partial y} - \frac{\partial \varphi_r}{\partial y} \right)$$

Since for a thin airfoil, the angular coefficient  $dy/dx$  is small, the product of this coefficient and the difference of the vertical component of the velocities is a second-order infinitesimal and, consequently,

$$\gamma(x) = \partial \varphi_u / \partial x - \partial \varphi_b / \partial x \quad (6.1.7)$$

Hence, (6.1.6) can be written in the form

$$c_{y_a,ic} = \frac{2}{V_\infty b} \int_0^b \gamma(x) dx \quad (6.1.8)$$

We calculate the moment coefficient in a similar way:

$$m_{z_a,ic} = -\frac{2}{V_\infty b^2} \int_0^b \gamma(x) x dx \quad (6.1.9)$$

In accordance with formulas (6.1.8) and (6.1.9), the coefficients of the lift force and the moment produced by the pressure depend on the distribution of the intensity of the circulation along the airfoil. This signifies that the flow over an airfoil can be calculated by replacing it with a system of continuously distributed vortices.

According to the Biot-Savart formula (2.7.12), an element of a distributed vortex with the circulation  $d\Gamma = \gamma(x) dx$  induces the vertical velocity at a point with the abscissa  $\xi$  (Fig. 6.1.1)

$$dv = d\Gamma/[2\pi(x - \xi)] = \gamma(x) dx/[2\pi(x - \xi)]$$

The velocity induced at this point by all the vortices is

$$v = \frac{1}{2\pi} \int_0^b \frac{\gamma(x) dx}{x - \xi} \quad (6.1.10)$$

According to the boundary condition,  $v/(V_\infty + \partial\varphi/\partial x) = dy/dx$ . Taking into account that the airfoil is thin, we can assume that  $V_\infty + \partial\varphi/\partial x \approx V_\infty$ , and calculate the derivative  $dy/dx$  from the equation of the mean camber line

$$y = y(x) = 0.5(y_u + y_b) \quad (6.1.11)$$

where  $y_u = y_u(x)$  and  $y_b = y_b(x)$  are the equations of the upper and bottom contours of the airfoil, respectively.

Hence, the intensity of vortex circulation  $\gamma(x)$  is determined by the integral equation

$$\frac{1}{2\pi V_\infty} \int_0^b \frac{\gamma(x) dx}{x - \xi} = \left( \frac{dy}{dx} \right)_\xi \quad (6.1.12)$$

Let us introduce instead of  $x$  a new independent variable  $\theta$  determined by the equation

$$x = (b/2)(1 - \cos \theta) \quad (6.1.13)$$

We find the solution of Eq. (6.1.12) in the form of a trigonometric Fourier series:

$$\gamma(\theta_0) = 2V_\infty \left[ A_0 \cot \frac{\theta_0}{2} + \sum_{n=1}^{\infty} A_n \sin(n\theta_0) \right] \quad (6.1.14)$$

in which the variable  $\theta_0$  in accordance with (6.1.13) is related to the coordinate  $x = \xi$  by the equation

$$\xi = (b/2)(1 - \cos \theta_0) \quad (6.1.15)$$

We change the variables in (6.1.12). By differentiation of (6.1.13), we find

$$dx = (b/2) \sin \theta d\theta \quad (6.1.16)$$

Substitutions yield

$$\frac{A_0}{\pi} \int_0^\pi \frac{\cot(\theta/2) \sin \theta d\theta}{\cos \theta_0 - \cos \theta} + \frac{1}{\pi} \sum_{n=1}^{\infty} A_n \int_0^\pi \frac{\sin(n\theta) \sin \theta d\theta}{\cos \theta_0 - \cos \theta} = \beta(\theta_0) \quad (6.1.17)$$

where  $\beta(\theta_0) = (dy/dx)_\xi$ .

After introducing the values of the integrals in (6.1.17) calculated in [16], we find

$$-A_0 + \sum_{n=1}^{\infty} A_n \cos(n\theta_0) = \beta(\theta_0). \quad (6.1.18)$$

By integrating both sides of Eq. (6.1.18) from 0 to  $\pi$ , we obtain a relation for the coefficient  $A_0$  of the Fourier series:

$$A_0 = -\frac{1}{\pi} \int_0^\pi \beta(\theta) d\theta \quad (6.1.19)$$

By multiplying (6.1.19) in turn by  $\cos \theta$ ,  $\cos 2\theta$ , . . . ,  $\cos(n\theta)$ , we find expressions for the coefficients  $A_1$ ,  $A_2$ , . . . ,  $A_n$ , respectively. Hence,

$$A_n = \frac{2}{\pi} \int_0^\pi \beta(\theta) \cos(n\theta) d\theta \quad (6.1.20)$$

Let us consider relation (6.1.8) for the lift coefficient. Going over to the variable  $\theta$  and introducing (6.1.16), we obtain

$$c_{y_a,ic} = \frac{1}{V_\infty} \int_0^\pi \gamma(\theta) \sin \theta d\theta \quad (6.1.21)$$

With a view to (6.1.14)

$$c_{y_a,ic} = 2A_0 \int_0^\pi \cot \frac{\theta}{2} \sin \theta d\theta + 2 \sum_{n=1}^{\infty} A_n \int_0^\pi \sin(n\theta) \sin \theta d\theta$$

Integration yields

$$c_{y_a,ic} = 2\pi (A_0 + A_1/2) \quad (6.1.22)$$

Hence, the lift coefficient depends on the first two coefficients of the series. Introducing into (6.1.22) expression (6.1.19) and formula (6.1.20) in which  $n = 1$ , we have

$$c_{y_a,ic} = -2 \int_0^\pi \beta(\theta) (1 - \cos \theta) d\theta \quad (6.1.23)$$

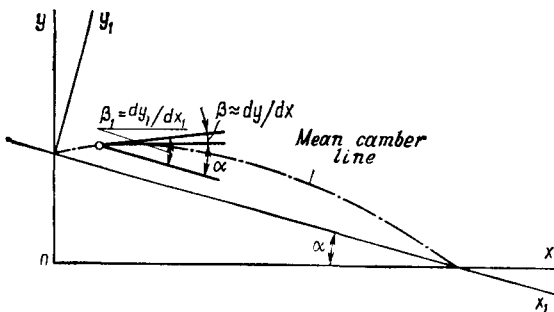


**Fig. 6.1.2**  
Mean camber line of an airfoil

We change the variables in (6.1.9) for the moment coefficient:

$$m_{z_a, \text{ic}} = \frac{-1}{2V_\infty} \int_0^\pi \gamma(\theta) (1 - \cos \theta) \sin \theta d\theta \quad (6.1.24)$$

With a view to expression (6.1.14) for  $\gamma(\theta)$ , we have

$$m_{z_a, \text{ic}} = -A_0 \int_0^\pi (1 - \cos \theta)^2 d\theta - \sum_{n=1}^{\infty} A_n \int_0^\pi \sin(n\theta)(1 - \cos \theta) \sin \theta d\theta$$

Integration yields

$$m_{z_a, \text{ic}} = -(\pi/2)(A_0 + A_1 - A_2/2) \quad (6.1.25)$$

With a view to (6.1.22), we have

$$m_{z_a, \text{ic}} = -(\pi/4)(A_1 - A_2) - (1/4)c_{y_a, \text{ic}} \quad (6.1.26)$$

By determining  $A_1$  and  $A_2$  from (6.1.20) and introducing their values into (6.1.26), we obtain

$$m_{z_a, \text{ic}} = -\frac{1}{2} \int_0^\pi \beta(\theta) (\cos \theta - \cos 2\theta) d\theta - \frac{1}{4} c_{y_a, \text{ic}} \quad (6.1.27)$$

Let us consider the body axis coordinates  $x_1$  and  $y_1$  in which the equation of the mean camber line is  $y_1 = y_1(x_1)$ , and the slope of a tangent is determined by the derivative  $dy_1/dx_1$ . This angle (Fig. 6.1.2) is  $\beta_1 = \beta + \alpha$ , where  $\beta \approx dy/dx$ . Hence we determine the angle  $\beta = \beta_1 - \alpha$  and introduce its value into (6.1.23) and (6.1.27):

$$c_{y_a, \text{ic}} = 2\pi(\alpha + \epsilon_0) \quad (6.1.28)$$

$$m_{z_a, \text{ic}} = -2\left(\frac{\pi}{4}\epsilon_0 - \mu_0\right) - \frac{1}{4}c_{y_a, \text{ic}} \quad (6.1.29)$$

where

$$\varepsilon_0 = \frac{1}{\pi} \int_0^\pi \beta_1 (1 - \cos \theta) d\theta; \quad \mu_0 = -\frac{1}{4} \int_0^\pi \beta_1 (1 - \cos 2\theta) d\theta \quad (6.1.30)$$

A glance at (6.1.28) reveals that when  $\alpha = -\varepsilon_0$ , the lift coefficient equals zero. The angle  $\alpha = -\varepsilon_0$  is called the **angle of zero lift**. The coefficients  $\varepsilon_0$  and  $\mu_0$  are evaluated according to the given equation of the mean camber line of the airfoil provided that in the expression for the function  $\beta_1(\bar{x}_1)$  the variable  $\bar{x}_1 = x_1/b$  is replaced according to (6.1.13) with the relation  $\bar{x}_1 = (1/2)(1 - \cos \theta)$ .

We can use the found values of  $m_{z_a}$  and  $c_{y_a}$  to approximately determine the coefficient of the centre of pressure  $c_p = x_p/b$  and the relative coordinate of the aerodynamic centre  $x_{AC} = x_{AC}/b$ :

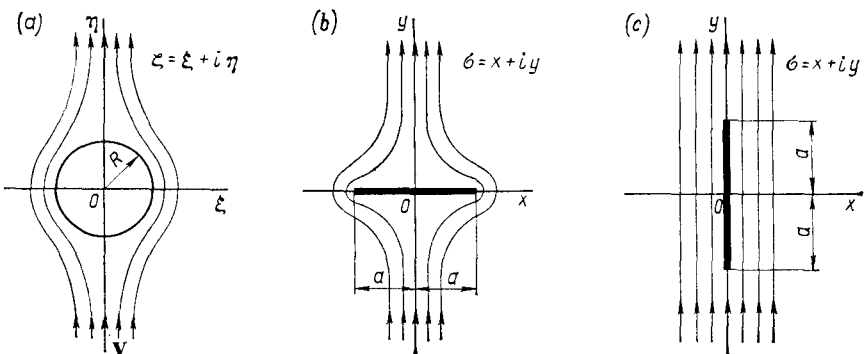
$$c_p = -\frac{m_{z_a}}{c_{y_a}} = \frac{1}{4} + \frac{(\pi/4)\varepsilon_0 - \mu_0}{\pi(\alpha + \varepsilon_0)}, \quad \bar{x}_{AC} = -\frac{\partial m_{z_a}}{\partial c_{y_a}} = \frac{1}{4} \quad (6.1.31)$$

It follows from these relations that the coordinate of the centre of pressure depends on the angle of attack and the shape of the airfoil, whereas the aerodynamic centre is at a fixed point at a distance of one-fourth of the chord length from the leading edge. For a symmetric airfoil  $\varepsilon_0 = \mu_0 = 0$  [which follows from formulas (6.1.30) in which  $\beta_1 = dy_1/dx_1 = 0$ ], therefore the value of  $c_p$ , like that of the relative coordinate of the aerodynamic centre, is 1/4.

## 6.2. Transverse Flow over a Thin Plate

Let us consider the flow of an incompressible fluid over a very simple airfoil in the form of a thin plate arranged at right angles to the direction of the free-stream velocity. We can solve this problem by means of the **conformal transformation (or mapping) method**. We shall use the results of the solution in real cases to determine the aerodynamic characteristics of finite-span wings.

Let us arrange the plate in the plane of the complex variable  $\sigma = x + iy$  along the real axis  $x$  (Fig. 6.2.1b). Now the free-stream velocity vector  $V$  will coincide with the direction of the imaginary axis  $y$ . In this case, the flow over such a plate can be obtained by conformal transformation of the flow over a circular cylinder on the plane  $\zeta = \xi + i\eta$  (Fig. 6.2.1a). If we know the function  $W = f(\zeta)$  that is a complex potential for the flow over a circular cylinder and the analytical function  $\zeta = F(\sigma)$  of the complex variable  $\sigma = x + iy$  (known as the **conformal function**) that transforms the contour of a circle on the plane  $\zeta$  into a segment of a straight line placed across

**Fig. 6.2.1**

Conformal transformation of the flow past a round cylinder (a) into a flow past a flat plate arranged (b) at right angles to the direction of the free-stream velocity, or (c) along the flow

the flow on the plane  $\sigma$ , then the function  $W = f[F(\sigma)]$  is the complex potential for the flow over the plate.

Let us see how we can determine the complex potential for the flow over a circular cylinder. For this purpose, we shall again revert to the method of conformal transformation, using the known function of the complex potential for the flow over a plate arranged along it. This function has the form

$$W = \varphi + i\psi = -iV(x + iy) = iV\sigma \quad (6.2.1)$$

We shall show that the conformal function

$$\sigma = \zeta - R^2/\zeta \quad (6.2.2)$$

transforms a segment of a straight line arranged along the flow on the plane  $\sigma$  into a circle on the plane  $\zeta$  (Fig. 6.2.1c, a). Indeed, examination of (6.2.2) reveals that since for points satisfying the conditions  $-a \leq y \leq a$ ,  $x = 0$ , and  $a = 2R$ , we have  $\sigma = iy$ , then from the solution of the quadratic equation  $\zeta^2 - \sigma\zeta - R^2 = 0$ , we obtain

$$\zeta = iy/2 \pm \sqrt{R^2 - y^2/4} = \xi + i\eta \quad (6.2.3)$$

Separating the real and imaginary parts, we obtain

$$\eta = y/2, \quad \xi = \pm \sqrt{R^2 - y^2/4}$$

whence  $\xi^2 + \eta^2 = R^2$ .

Consequently, points on the circle in the plane  $\zeta$  correspond to points in the plane  $\sigma$  on the vertical segment. Substituting for  $\sigma$  in (6.2.1) its value from (6.2.2), we obtain the complex potential of the flow over a circular cylinder of radius  $R$  in a plane parallel flow

at the velocity  $V$ :

$$W = iV (\zeta - R^2/\zeta) \quad (6.2.4)$$

To obtain the complex potential for the flow over a plate arranged across the flow (Fig. 6.2.1b), let us substitute for  $\zeta$  in (6.2.4) the following value obtained from the conformal formula  $\sigma = \zeta + R^2/\zeta$  transforming a circle of radius  $R$  (plane  $\zeta$ ) into a segment of a straight line across the flow (plane  $\sigma$ ):

$$\zeta = \sigma/2 \pm \sqrt{\sigma^2/4 - R^2} \quad (6.2.5)$$

Therefore,

$$W = -iV \left( \frac{\sigma}{2} \pm \sqrt{\frac{\sigma^2}{4} - R^2} - \frac{R^2}{\sigma/2 \pm \sqrt{\sigma^2/4 - R^2}} \right) \quad (6.2.6)$$

Since for points on the plate we have  $\sigma = x$ , where  $-a \leq x \leq a$  and  $a = 2R$ , then

$$W = \varphi + i\psi = -iV \left( \frac{x}{2} \pm i \sqrt{\frac{R^2}{4} - \frac{x^2}{4}} - \frac{R^2}{x/2 \pm i \sqrt{R^2 - x^2/4}} \right)$$

whence the potential function is

$$\varphi = \pm V \sqrt{4R^2 - x^2} = \pm V \sqrt{a^2 - x^2} \quad (6.2.7)$$

where the plus sign corresponds to the upper surface, and the minus sign to the bottom one.

By evaluating the derivatives  $\partial\varphi/\partial x$ , we can find the velocity on the plate and calculate the pressure. It follows from the data obtained that the pressure on the upper and bottom sides of the plate is the same. Consequently, in the case being considered of the transverse free streamline flow of an ideal (inviscid) fluid over a plate, drag of the plate is absent. This interesting aerodynamic effect is considered below in Sec. 6.3 using the example of flow over a flat plate arranged at a certain finite angle of attack.

A flow characterized by the potential function (6.2.7) is shown in Fig. 6.2.1b. It is a **non-circulatory flow** past the plate obtained upon the superposition onto an undisturbed flow with the potential

$$W_\infty = -iV\zeta \quad (6.2.8)$$

of the flow from a doublet with the potential

$$W_d = iVR^2/\zeta \quad (6.2.9)$$

where  $\zeta$  is determined by the conformal function (6.2.5).

### 6.3. Thin Plate at an Angle of Attack

Let us calculate the potential function for the disturbed flow of an incompressible fluid over a thin plate at the angle of attack  $\alpha$  using, as in the preceding problem, the method of conformal transformation. We arrange the plate in the plane of the complex variable  $\sigma = x + iy$  along the real axis  $x$ .

If we assume that the flow being considered is a non-circulatory one, the complex potential of such a flow can be written as the sum of the potentials of the longitudinal  $W_1 = V_\infty \sigma$  and transverse  $W_2$  flows at the velocity of the undisturbed flow  $V = \alpha V_\infty$  (Fig. 6.3.1). The total complex potential is

$$W = W_1 + W_2 = V_\infty \sigma - i\alpha V_\infty \left[ \frac{\sigma}{2} \pm \sqrt{\frac{\sigma^2}{4} - R^2} - R^2 \left( \frac{\sigma}{2} \pm \sqrt{\frac{\sigma^2}{4} - R^2} \right)^{-1} \right] = V_\infty \sigma \pm i\alpha V_\infty \sqrt{\sigma^2 - 4R^2} \quad (6.3.1)$$

With account taken of formula (6.2.7), the total velocity potential on the plate is

$$\varphi = V_\infty x \pm \alpha V_\infty \sqrt{a^2 - x^2} \quad (6.3.2)$$

We use this value of the potential to find the velocity component

$$V_x = V_\infty \mp \alpha V_\infty x / \sqrt{a^2 - x^2} \quad (6.3.3)$$

The second velocity component on the thin plate  $V_y = 0$ .

A close look at (6.3.3) reveals that at the leading ( $x = -a$ ) and trailing ( $x = a$ ) edges, the velocity  $V_x$  is infinite. Physically, such a flow is impossible. The velocity at one of the edges, for example, the trailing one, can be restricted by superposition of a **circulatory flow** onto the flow being considered. In the plane  $\zeta$ , the potential of the circulatory flow is determined in accordance with (2.9.22) by the expression

$$W_3 = -(i\Gamma/2\pi) \ln \zeta \quad (6.3.4)$$

Let us substitute for  $\zeta$  its value from (6.2.5):

$$W_3 = -\frac{\Gamma i}{2\pi} \ln \left( \frac{\sigma}{2} \pm \sqrt{\frac{\sigma^2}{4} - R^2} \right) \quad (6.3.5)$$

Summation of (6.3.1) and (6.3.5) yields the complex potential of a **circulatory-forward flow** over an inclined plate:

$$W = W_1 + W_2 + W_3 = V_\infty \sigma \pm i\alpha V_\infty \sqrt{\sigma^2 - 4R^2} - \frac{\Gamma i}{2\pi} \ln \left( \frac{\sigma}{2} \pm \sqrt{\frac{\sigma^2}{4} - R^2} \right) \quad (6.3.6)$$

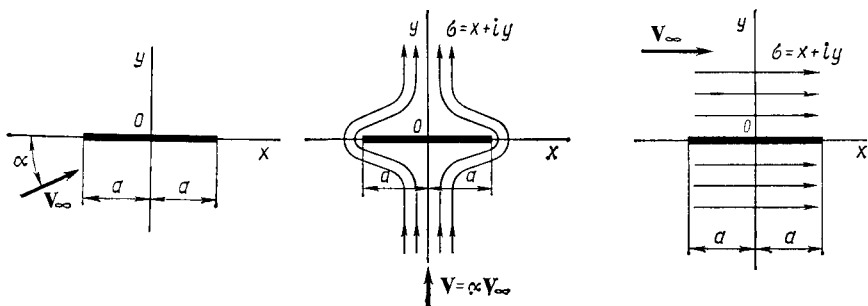


Fig. 6.3.1

Flow over a flat plate at an angle of attack

We determine the circulation  $\Gamma$  on the basis of the **Zhukovsky-Chaplygin hypothesis**, according to which the velocity at the trailing edge of the plate is finite. This value of the velocity can be obtained, as we already know from the theory of conformal transformation, in the form of the derivative  $d\bar{W}/d\sigma$  of the complex potential  $\bar{W}$  for a cylinder. This potential, in turn, makes it possible to find the complex velocity at the relevant point on the cylinder as the derivative  $d\bar{W}/d\zeta$ , which according to the rules of differentiation of a complex function is

$$d\bar{W}/d\zeta = (dW/d\sigma) d\sigma/d\zeta \quad (6.3.7)$$

where  $\bar{W}$  and  $W$  are the complex potentials for the cylinder and plate, respectively.

According to the Zhukovsky-Chaplygin hypothesis, the quantity  $dW/d\sigma$  is limited in magnitude. Since the derivative  $d\sigma/d\zeta$  calculated by the formula

$$d\sigma/d\zeta = 1 - R^2/\zeta^2$$

equals zero on the cylinder at the point  $\zeta = R$  corresponding to a point on the trailing edge of the plate, the derivative  $d\bar{W}/d\zeta = 0$ .

The complex potential for a cylinder is

$$\bar{W} = \bar{W}_1 + \bar{W}_2 + \bar{W}_3$$

The potential  $\bar{W}_1$  characterizes the flow in an axial direction corresponding to the flow over the plate in the same direction at the velocity  $V_\infty$ . It is obtained by substituting the value  $\sigma = \zeta + R^2/\zeta$  for  $\sigma$  in the formula  $W_1 = V_\infty \sigma$ :

$$\bar{W}_1 = V_\infty (\zeta + R^2/\zeta)$$

The complex potentials  $\bar{W}_2$  and  $\bar{W}_3$  are determined by Eqs. (6.2.4) and (6.3.4), respectively. We shall substitute  $\alpha V_\infty$  for  $V$  in the first of them and find the total complex potential:

$$\bar{W} = V_\infty (\zeta + R^2/\zeta) - i\alpha V_\infty (\zeta - R^2/\zeta) - (i\Gamma/2\pi) \ln \zeta \quad (6.3.8)$$

We calculate the derivative:

$$d\bar{W}/d\zeta = V_\infty (1 - R^2/\zeta^2) - i\alpha V_\infty (1 + R^2/\zeta^2) - i\Gamma/(2\pi\zeta) \quad (6.3.8')$$

For the coordinate  $\zeta = R$  corresponding to a point on the trailing edge of the plate, the derivative  $d\bar{W}/d\zeta$  is zero, i.e.

$$2i\alpha V_\infty - i\Gamma/(2\pi R) = 0$$

Hence

$$\Gamma = -4\pi\alpha RV_\infty \quad (6.3.9)$$

or, since  $2R = a$ ,

$$\Gamma = -2\pi\alpha a V_\infty \quad (6.3.9')$$

After inserting this result into (6.3.6) and differentiating with respect to  $\sigma$ , we find the complex velocity:

$$\begin{aligned} \frac{dW}{d\sigma} &= V_x - iV_y = V_\infty \pm \frac{i\alpha V_\infty \sigma}{\sqrt{\sigma^2 - 4R^2}} \\ &+ \frac{2\pi i\alpha a V_\infty}{2\pi} \cdot \frac{2}{\sigma \pm \sqrt{\sigma^2 - 4R^2}} \left( \frac{1}{2} \pm \frac{\sigma}{\sqrt{\sigma^2 - 4R^2}} \right) \end{aligned}$$

Simple transformations and the substitution  $2R = a$  yield

$$dW/d\sigma = V_x - iV_y = V_\infty (1 \mp i\alpha \sqrt{(\sigma - a)/(\sigma + a)}) \quad (6.3.10)$$

On the surface of the plate ( $\sigma = x$ )

$$dW/d\sigma = V_x - iV_y = V_\infty (1 \mp i\alpha \sqrt{(x - a)/(x + a)}) \quad (6.3.11)$$

Since  $|x| \leq a$ , we have

$$dW/d\sigma = V_x - iV_y = V_\infty (1 \pm \alpha \sqrt{(a - x)/(a + x)}) \quad (6.3.11')$$

whence it follows that the total velocity on the plate is

$$V = V_x = V_\infty (1 \pm \alpha \sqrt{(a - x)/(a + x)}) \quad (6.3.12)$$

The plus sign relates to the upper surface, and the minus sign to the bottom one.

The velocity on the trailing edge ( $x = a = 2R$ ) is  $V_\infty$ , and on the leading edge ( $x = -a$ ) it is found to be infinite. In real conditions, the thickness of the leading edge is not zero; particularly, the nose may have a *finite*, although small, radius of curvature. Therefore the velocities on such an edge have high, but finite values.

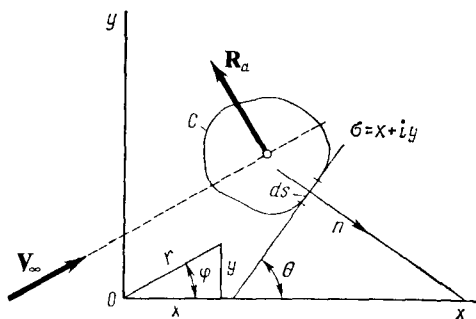


Fig. 6.3.2

Contour in the flow of an incompressible fluid

To determine the force acting on the plate, we shall use the general expression for the principal vector of the hydrodynamic pressure forces applied to a stationary cylindrical body of an arbitrary shape in the steady flow of an incompressible fluid. By analogy with the complex velocity, let us introduce the concept of the complex force  $\bar{R}_a = X - iY$ , determining this force as the mirror reflection of the principal vector  $R_a$  of the pressure forces with respect to the real axis.

The vector  $\bar{R}_a$  being considered is determined by formulas (1.3.2) and (1.3.3) in which the friction coefficient  $c_{f,x}$  is taken equal to zero:

$$\begin{aligned}\bar{R}_a &= X - iY = - \oint_C p [\cos(\hat{n}, \hat{x}) - i \cos(\hat{n}, \hat{y})] ds \\ &= - \oint_C p (\sin \theta + i \cos \theta) ds = - i \oint_C p e^{-i\theta} ds\end{aligned}\quad (6.3.13)$$

where  $n$  is the direction of an outward normal to contour  $C$  of the body in the flow, and  $\theta$  is the angle between the element  $ds$  of the contour and the  $x$ -axis (Fig. 6.3.2).

Since

$$\begin{aligned}d\sigma &= dx + i dy = ds (\cos \theta + i \sin \theta) = e^{i\theta} ds \\ d\bar{\sigma} &= dx - i dy = ds (\cos \theta - i \sin \theta) = e^{-i\theta} ds\end{aligned}\quad \left.\right\} \quad (6.3.14)$$

and the pressure is determined by the Bernoulli equation

$$p = p_\infty + \rho V_\infty^2/2 - \rho V^2/2 = C_2 - \rho V^2/2 \quad (6.3.15)$$

then

$$\bar{R}_a = -iC_2 \oint_C d\bar{\sigma} + \frac{i\rho}{2} \oint_C V^2 d\bar{\sigma} = \frac{i\rho}{2} \oint_C V^2 d\bar{\sigma}$$

Taking into account that by (6.3.14) we have  $d\bar{\sigma} = e^{-2i\theta} d\sigma$ , and also that in accordance with the condition of flow without separa-

tion the complex velocity at the point of the contour being considered is

$$\bar{V} = V_x - iV_y = V \cos \theta - iV \sin \theta = Ve^{-i\theta} \quad (6.3.16)$$

we find

$$\bar{R}_a = X - iY = \frac{i\rho}{2} \oint_C \bar{V}^2 d\sigma \quad (6.3.17)$$

Since for a potential flow, the complex velocity is  $\bar{V} = dW/d\sigma$ , we have

$$\bar{R}_a = X - iY = \frac{i\rho}{2} \oint_C \left( \frac{dW}{d\sigma} \right)^2 d\sigma \quad (6.3.18)$$

Expression (6.3.18) is called the **Zhukovsky-Chaplygin formula**.

Integration in (6.3.18) can be performed over another contour enveloping the given contour  $C$  of the body in the flow, for example, over a circle  $K$  whose complex velocity in the plane  $\sigma$  is written as follows:

$$dW/d\sigma = \bar{V}_\infty - i\Gamma/(2\pi\sigma) + A/\sigma^2 \quad (6.3.19)$$

where  $\bar{V}_\infty = V_{x_\infty} - iV_{y_\infty} = V_\infty e^{-i\theta_\infty}$ , and  $A$  is a coefficient determined with the aid of an equation similar to (6.3.8).

The square of the complex velocity is

$$\left( \frac{dW}{d\sigma} \right)^2 = \bar{V}_\infty^2 - \frac{i\Gamma\bar{V}_\infty}{\pi\sigma} + \frac{2A\bar{V}_\infty - \Gamma^2/(4\pi^2)}{\sigma^2} + \dots$$

Introducing this value into (6.3.18), we find

$$\begin{aligned} \bar{R}_a &= X - iY = \frac{i\rho}{2} \left[ \bar{V}_\infty^2 \oint_K d\sigma - \frac{i\Gamma\bar{V}_\infty}{\pi} \oint_K \frac{d\sigma}{\sigma} \right. \\ &\quad \left. + \left( 2A\bar{V}_\infty - \frac{\Gamma^2}{4\pi^2} \right) \oint_K \frac{d\sigma}{\sigma^2} + \dots \right] \end{aligned}$$

Here the first and third integrals equal zero. The integral  $\oint_K d\sigma/\sigma$  is evaluated with a view to the formula  $\sigma = x + iy = re^{i\varphi}$  (Fig. 6.3.2) and equals

$$\oint_K \frac{d\sigma}{\sigma} = \ln \sigma |_K = \ln (re^{i\varphi}) |_K = 2\pi i$$

Hence,

$$\bar{R}_a = X - iY = i\rho\bar{V}_\infty\Gamma \quad \text{or} \quad X - iY = i\rho V_\infty \Gamma e^{-i\theta_\infty} \quad (6.3.20)$$

where  $V_\infty$  is the magnitude of the free-stream velocity.

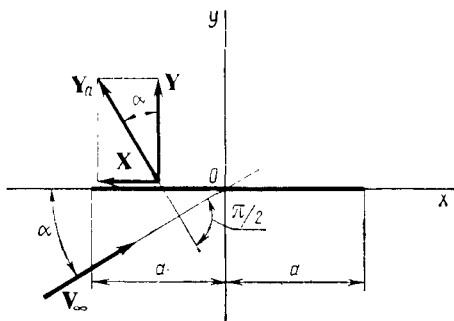
**Fig. 6.3.3**

Diagram of the forces acting on a plate (X is the suction force)

If its direction coincides with the horizontal axis ( $\theta_\infty = \pi$ ), we have

$$\bar{R}_a = X - iY = -i\rho V_\infty \Gamma \quad (6.3.21)$$

whence it follows that

$$|\bar{R}_a| = Y = Y_a = \rho V_\infty \Gamma \quad (6.3.22)$$

Expression (6.3.22) is known as the **Zhukovsky formula**.

It follows from (6.3.21) that the force is a vector perpendicular to the free-stream velocity vector, and, therefore, is a lift force. Its direction coincides with that of the vector obtained by turning the velocity vector  $V_\infty$  through the angle  $\pi/2$  against the circulation.

A glance at (6.3.21) reveals that  $X = X_a = 0$ . Hence, when an inviscid incompressible fluid flows over a surface without separation, the resistance associated with the distribution of the pressure is zero. This aerodynamic effect is known as the **Euler-D'Alembert paradox**. This name corresponds to the fact that actually resistance is present because there always occurs a relevant redistribution of the pressure caused by separation of the flow and the action of skin friction (viscosity).

Let us use formula (6.3.22) to evaluate the lift force of a flat plate. Taking into account the value of the circulation (6.3.9'), we obtain (Fig. 6.3.3)

$$Y_a = 2\pi\alpha a \rho V_\infty^2 \quad (6.3.23)$$

Let us determine the normal  $Y$  and longitudinal  $X$  components of the force  $Y_a$ :

$$Y = Y_a \cos \alpha \approx Y_a = 2\pi\alpha a \rho V_\infty^2 \quad (6.3.24)$$

$$X = -Y_a \sin \alpha \approx -Y_a \alpha = -2\pi\alpha^2 a \rho V_\infty^2 \quad (6.3.25)$$

The arising of the force  $X$  acting along the plate opposite to the flow seems to be paradoxical because all the elementary forces produced by the pressure are directed along a normal to the surface.

This component is called the **suction force**. The physical nature of its appearance consists in the following. Assume that the leading edge is slightly rounded. Now the velocities near it will be considerable, but not infinitely high as at the leading edge of a plate. In accordance with the Bernoulli equation, the difference between the pressure at the edge and that at infinity will be negative. The resulting rarefaction is exactly what causes the suction force. Its limiting value is given by expression (6.3.25) relating to the case of flow over a plate when the velocity near its leading edge is determined by formula (6.3.12). In accordance with this formula, the longitudinal component of the disturbed velocity at the indicated point of the plate is

$$V'_x = \pm \alpha V_\infty \sqrt{(a-x)/(a+x)} \quad (6.3.26)$$

The expression for the suction force can be generalized for an arbitrary velocity near the leading edge. For this purpose, we shall transform (6.3.25) to the form

$$T = -X = \pi \rho c^2 \quad (6.3.27)$$

where

$$c^2 = 2a\alpha^2 V_\infty^2 \quad (6.3.28)$$

We shall write the quantity  $c^2$  in the form of the limit

$$c^2 = \lim_{x \rightarrow x_{l.e.}} [V'_x^2 (x - x_{l.e.})] \quad (6.3.28')$$

where  $x_{l.e.}$  is the abscissa of the leading edge ( $x_{l.e.} = -a$ ),  $x$  is the running abscissa of points of the plate, and  $V'_x$  is the longitudinal component of the disturbed velocity on the upper surface of a wing.

Formula (6.3.28') can be shown to be correct. For this purpose, we shall insert expression (6.3.26) into (6.3.28'):

$$c^2 = \lim_{x \rightarrow -a} \left[ V_\infty^2 \alpha^2 \left( \frac{a-x}{a+x} \right) (x+a) \right] = 2a\alpha^2 V_\infty^2$$

By introducing this value into (6.3.27), we obtain formula (6.3.25).

The conclusions on an incompressible circulatory-forward flow over an airfoil in the form of a thin plate are used in studying the aerodynamic characteristics of airfoils encountered in practice, and also of finite-span wings in flows of an incompressible fluid or of a compressible gas.

#### 6.4. Finite-Span Wing in an Incompressible Flow

Up to now, we considered an airfoil in an incompressible flow. We can presume that such an airfoil relates to an elementary part of a lifting surface belonging to an **infinite-span wing** in a plane parallel

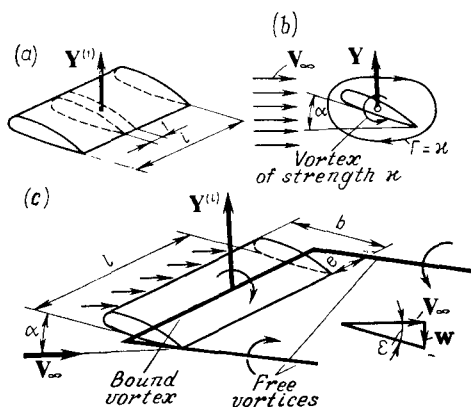


**Fig. 6.4.1**  
System of equivalent vortices  
for a rectangular wing

flow. Hence, the theory of this flow is also a foundation of the aerodynamics of an infinite-span wing.

By formula (6.3.22), the lift force of a unit-span wing part is  $Y^{(1)} = \rho_\infty V_\infty \Gamma$  (Fig. 6.4.1a). Consequently, there is a circulation flow around the airfoil with the velocity circulation  $\Gamma$ . If the circulation is clockwise, the velocities on the upper surface of the airfoil are higher (a circulation flow having the same direction as the oncoming one is superposed on it), while on the bottom surface they are lower (the circulation flow does not coincide with the direction of the oncoming flow). Therefore, in accordance with the Bernoulli equation, the pressure from above is lower than from below, and the lift force is directed upward as shown in Fig. 6.4.1b.

Since by (2.7.8) and (2.7.8'), the circulation equals the vorticity (vortex strength)  $\nu$ , the part of the wing can be replaced with an equivalent vortex of the indicated strength passing along its span. N. Zhukovsky used the term **bound** to designate this vortex. Hence, in the hydrodynamic sense, an infinite-span wing is equivalent to a bound vortex.

Let us now consider an *approximate scheme of the flow past a finite-span wing* with a rectangular planform. As established by S. Chaplygin, a bound vortex near the side edges turns and is cast off the wing in the form of a pair of vortex cores approximately coinciding with the direction of the free-stream velocity. The distance  $e$  (Fig. 6.4.1c) from a vortex core to the relevant side edge depends on the geometry of the wing. Consequently, the hydrodynamic effect of a finite-span wing can be obtained by replacing it with a bound vortex and a pair of free horseshoe vortices. This wing pattern is called **Chaplygin's horseshoe one**.

A vortex system equivalent to a finite-span wing induces **additional velocities** in the flow and thus causes downwash, which is a fea-

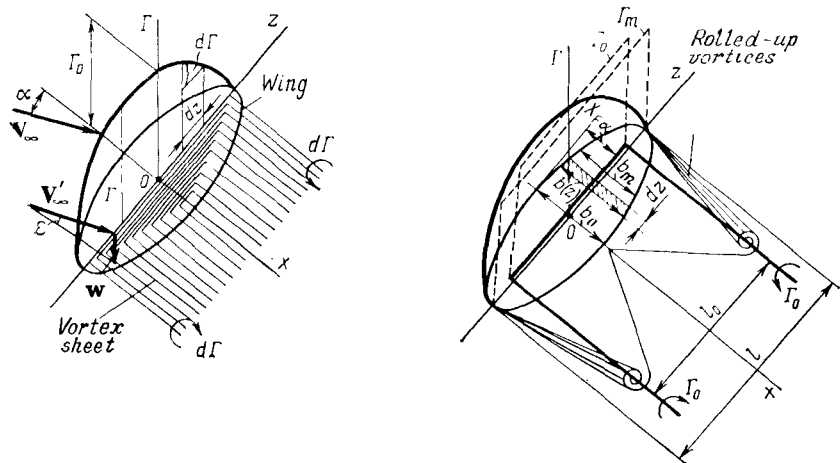


**Fig. 6.4.2**  
Vortex sheet and rolled-up vortices behind a wing

ture of flow past a finite-span wing. The calculations of the induced velocities and the downwash angle caused by the free vortices are based on the following theorems formulated by H. Helmholtz:

- (1) the strength along a vortex does not change in magnitude, and as a result, a vortex cannot end somewhere in a fluid. It must either be closed or reach the boundary of the fluid;
- (2) the strength of a vortex does not depend on the time;
- (3) a vortex is not disrupted in an ideal fluid.

In the considered scheme of a rectangular wing, the circulation along the span was presumed to be constant in accordance with the assumption that the lift force of each elementary part of the wing is identical. Actually, the lift force along the span of a wing having such a rectangular planform varies. This change is not great in the middle part of the wing and is more noticeable at the side edges. For a wing with an arbitrary planform, the change in the circulation is clearly expressed and is due to the different dimensions of the elementary parts and, consequently, to different values of the lift force. We can obtain the vortex pattern of flow over a wing with a system of horseshoe vortices forming a **vortex sheet** (Fig. 6.4.2). The circulation along each vortex will be constant, but changes when going over from one vortex to another. For the section at the middle of the wing, the lift force is maximum, therefore the strength of the relevant vortex and the circulation will be maximum.

Now let us see what changes the downwash introduces into the flow over a wing arranged at the geometric angle of attack  $\alpha$  (the angle between the chord of a wing section and the vector  $V_\infty$  is also

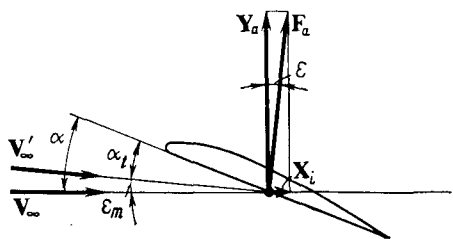


Fig. 6.4.3

Flow downwash at a wing and the appearance of induced drag

called the **setting angle**). The appearance of downwash of the flow behind the wing at the angle  $\epsilon$  leads to the fact that the flow over the wing in the section being considered is characterized by values of the velocity  $V'_\infty$  and the angle of attack  $\alpha_t$  differing from the corresponding values of  $V_\infty$  and  $\alpha$  that determine the flow over an infinite-span wing. *The true angle of attack  $\alpha_t$  of a section of a finite-span wing is smaller than the setting angle by the magnitude of the downwash angle  $\epsilon$*  (Fig. 6.4.3), i.e.  $\alpha_t = \alpha - \epsilon$ . The downwash angle  $\epsilon = -w/V_\infty$  varies along the span of the wing, increasing toward its tips. For convenience, the concept of the span-averaged downwash

angle is introduced, determined by the formula  $\epsilon_m = \frac{1}{l} \int_{-l/2}^{l/2} \epsilon dz$ .

Accordingly, the true angle of attack of the wing is

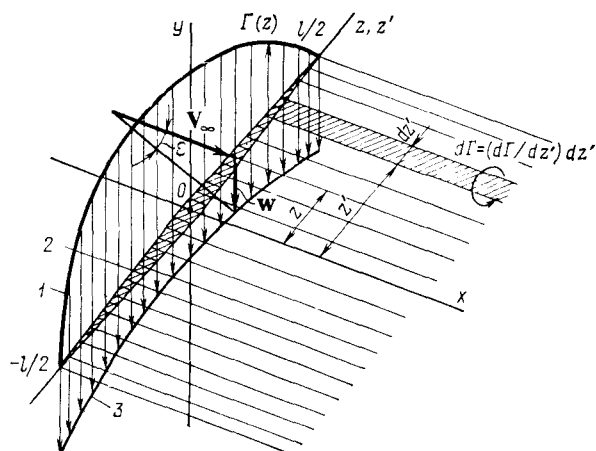
$$\alpha_t = \alpha - \epsilon_m \quad (6.4.1)$$

The existence of a downwash angle leads to a change in the forces acting on a body in the flow. If flow downwash is absent, the vector of the aerodynamic force by (6.3.21) is normal to the direction of the velocity of the **undisturbed flow**  $V_\infty$ . If downwash is present, the vector of the resultant aerodynamic force is oriented along a normal to the direction of the **true velocity**  $V'_\infty$  (Fig. 6.4.3). Such deviation of the resultant force through the angle  $\epsilon_m$  causes the component  $X_i$  to appear in the direction of the undisturbed flow. This additional force  $X_i$  appearing as a result of flow downwash is called the **induced resistance** or **induced drag**. From the physical viewpoint, an induced drag is due to losses of a portion of the kinetic energy of a moving wing spent on the formation of vortices cast off its trailing edge. The magnitude of this drag is determined in accordance with Fig. 6.4.3 from the expression

$$X_i = Y_a \epsilon_m \quad (6.4.2)$$

The lift force  $Y_a$ , owing to the smallness of the downwash, is determined in the same way as for an infinite-span wing. If we divide  $X_i$  by the quantity  $(\rho_\infty V_\infty^2/2) S_w$ , we obtain the **induced drag coefficient**

$$c_{x,i} = 2X_i / (\rho_\infty V_\infty^2 S_w) = c_{y_a} \epsilon_m \quad (6.4.3)$$

**Fig. 6.4.4**

Replacement of a finite-span wing with a loaded line:

1—distribution of circulation; 2—loaded line; 3—distribution of induced velocities or downwash angles

We shall determine this coefficient on the basis of the theory of a "loaded line". According to this theory, a finite-span wing is replaced with a single bound vortex (a loaded line). The circulation  $\Gamma(z)$  for the loaded line is the same as for the corresponding sections of the wing itself (Fig. 6.4.4). Upon such a replacement, a plane vortex sheet begins directly on the loaded line and has a strength  $d\Gamma(z)/dz$  that varies along the span. The flow downwash in a given section is determined for a semi-infinite vortex core having the strength  $[d\Gamma(z)/dz] dz$ . Accordingly, the total downwash angle for a section, as can be seen from Fig. 6.4.4, is

$$\varepsilon = -\frac{w}{V_\infty} = -\frac{1}{4\pi V_\infty} \int_{-l/2}^{l/2} \frac{d\Gamma(z')}{dz'} \cdot \frac{dz'}{z' - z} \quad (6.4.4)$$

Here the improper integral must be considered in the sense of its principal value.

By (6.4.4), the mean downwash angle over a span is

$$\varepsilon_m = -\frac{1}{4\pi V_\infty l} \int_{-l/2}^{l/2} \left[ \int_{-l/2}^{l/2} \frac{d\Gamma(z')}{dz'} \cdot \frac{dz'}{z' - z} \right] dz \quad (6.4.5)$$

The lift force coefficient  $c_{y_a}$  can be determined according to the known law of circulation distribution along the span. With such a determination, we can proceed from the hypothesis of plane sections according to which the flow over a wing element being considered is

the same as over the corresponding airfoil belonging to a cylindrical infinite-span wing. Calculations on the basis of this hypothesis give a satisfactory accuracy for wings with a low sweep and an aspect ratio of  $\lambda_w > 3-4$ .

According to the Zhukovsky formula, the lift force of an airfoil is

$$dY_a = \rho_\infty V_\infty \Gamma(z) dz \quad (6.4.6)$$

its total value for a wing is

$$Y_a = \rho_\infty V_\infty \int_{-l/2}^{l/2} \Gamma(z) dz \quad (6.4.6')$$

and the corresponding aerodynamic coefficient is

$$c_{y_a} = \frac{Y}{q_\infty S_w} = \frac{2}{V_\infty S_w} \int_{-l/2}^{l/2} \Gamma(z) dz \quad (6.4.6'')$$

To find the law of circulation distribution  $\Gamma(z)$ , let us consider an airfoil in an arbitrary section of a wing for which the lift force can be written in the form

$$dY_a = c_y(z) q_\infty b(z) dz \quad (6.4.7)$$

where  $b(z)$  is the chord of the airfoil in the section being considered.

With a view to the Zhukovsky formula (6.4.6), we find a **coupling equation** determining the relation for the velocity circulation in a given section:

$$\Gamma(z) = 0.5 c_{y_a}(z) b(z) V_\infty \quad (6.4.8)$$

According to the hypothesis of plane sections, the lift coefficient  $c_{y_a}(z)$  of a section being considered is the same as for the corresponding infinite-span cylindrical wing. Its magnitude can be determined with account taken of the downwash angle by the formula

$$c_{y_a}(z) = c_{y_a}^\alpha(z) (\alpha - \varepsilon) \quad (6.4.9)$$

where the derivative  $c_{y_a}^\alpha(z) = \partial c_{y_a}(z) / \partial \alpha$  is determined for an infinite-span wing and a range of angles of attack corresponding to the linear section of the curve  $c_{y_a}(\alpha)$ . After inserting into (6.4.8) the values from (6.4.4) and (6.4.9), we obtain

$$\Gamma(z) = (1/2) c_{y_a}^\alpha(z) b(z) V_\infty \left( \alpha + \frac{1}{4\pi V_\infty} \int_{-l/2}^{l/2} \frac{d\Gamma(z')}{az'} \cdot \frac{dz'}{z' - z} \right) \quad (6.4.10)$$

This equation is called the **fundamental integro-differential equation** of a finite-span wing. It allows one to find the law of circulation distribution  $\Gamma(z)$  for a given wing shape according to the known conditions of its flight. The angle of attack  $\alpha$  in (6.4.10) may be fixed

(i.e. the same for all sections) or may vary along the span if geometric warp of the wing is present.

One of the most favoured ways of solving Eq. (6.4.10) is based on expanding the required function  $\Gamma(z)$  into a trigonometric series (the Glauert-Trefftz method)

$$\Gamma(z) = 2lV_\infty \sum_{n=1}^{\infty} A_n \sin(n\theta) \quad (6.4.11)$$

where the new variable  $\theta$  is related to the variable  $z$  by the expression  $z = -(l/2) \cos \theta$  (see Fig. 6.5.1), and  $A_n$  are constant coefficients determined with the aid of Eq. (6.4.10).

Since the series (6.4.11) is a rapidly descending one, a small number  $m$  of terms is usually sufficient. To determine the unknown coefficients  $A_m$ , we compile  $m$  algebraic equations (according to the number of selected sections). Each of these equations is obtained by introducing into (6.4.10) the value of the circulation  $\Gamma(z) =$

$$= 2lV_\infty \sum_{n=1}^m A_n \sin(n\theta) \text{ for the corresponding section.}$$

For conventional wings that are symmetric about the central (root) chord, the distribution of the circulation over the span is also symmetric, i.e. the equality  $\Gamma(\theta) = \Gamma(\pi - \theta)$  holds (see Fig. 6.5.1). Accordingly, the terms of the series with even indices equal zero, and the circulation can be written in the approximate form

$$\Gamma = 2lV_\infty [A_1 \sin \theta + A_3 \sin(3\theta) + \dots + A_m \sin(m\theta)]$$

Consequently, the number of algebraic equations needed to determine the coefficients  $A_m$  diminishes. The procedure followed to determine these coefficients is set out in detail in [16].

Using the found law of distribution of the circulation in the form of a series, we can determine the flow downwash and the corresponding aerodynamic coefficients (see [13]). By going over in (6.4.6") from the variable  $z$  to the variable  $\theta$  in accordance with the expression  $dz = (l/2) \sin \theta d\theta$ , introducing the formula for the circulation in the form of a series, and taking into account that  $l^2/S_w = \lambda_w$ , we find a relation for the lift coefficient:

$$c_{y_a} = \pi \lambda_w A_1 \quad (6.4.12)$$

Using (6.4.5), we determine the mean downwash angle:

$$\epsilon_m = (c_{y_a}/\pi \lambda_w) (1 + \tau) \quad (6.4.13)$$

where  $\tau$  is a coefficient taking into account the influence of the aspect ratio:

$$\tau = \sum_{n=2}^m A_n/A_1 \quad (6.4.14)$$

From (6.4.3), we obtain the relevant induced drag coefficient. Its value can be determined more precisely, however, by going over from the mean downwash angle to its local value in accordance with the expression  $dX_1 = \varepsilon dY_a$ . By introducing into this expression instead of  $\varepsilon$  and  $dY_a$  their values from (6.4.4) and (6.4.6), integrating, and determining the induced drag coefficient, we obtain

$$c_{x,1} = \frac{-1}{2\pi V_\infty^2 S_w} \int_{-l/2}^{l/2} \Gamma(z) \left[ \int_{-l/2}^{l/2} \frac{d\Gamma(z')}{dz'} \cdot \frac{dz'}{z' - z} \right] dz \quad (6.4.15)$$

Introducing the value of  $\Gamma(z)$  and substituting  $\lambda_w$  for  $l^2/S_w$ , we have

$$c_{x,1} = (c_{y_a}^2 / \pi \lambda_w) (1 + \delta) \quad (6.4.16)$$

where the coefficient  $\delta$  taking into account the influence of the aspect ratio on the drag depending on the lift is

$$\delta = \sum_{n=2}^m n A_n^2 / A_1^2 \quad (6.4.17)$$

The coefficients  $\tau$  and  $\delta$  for wings of various planforms can be determined according to the data given in [13, 16].

The results of the general theory of a loaded line obtained can be seen to be characterized by a comparative simplicity of the aerodynamic relations, provide a clear notion of the physical phenomena attending flow past finite-span wings, and allow one to reveal the mechanism of formation of the lift force and induced drag. The application of this theory, however, is limited to wings with a sufficiently small sweep and a relatively large aspect ratio. In modern aerodynamics, more accurate and more general solutions are worked out. They are described in special literature.

At the same time, the development of ways of evaluating the aerodynamic properties of wings by constructing approximate models of the flow over finite-span wings is of practical significance. Let us consider one of them based on the representation of the aerodynamic scheme of a wing in the form of a bound and a pair of free vortex cores. This representation is based on experimental data according to which a vortex sheet is not stable and at a comparatively short distance from the wing rolls up into two parallel vortex cores (see Fig. 6.4.2).

The basic element of this problem is the finding of the distance  $l_0$  between the free (rolled up) vortices. We proceed here from the fact that for a wing with a span of  $l$ , the vortex pattern of the wing may be replaced with a single horseshoe vortex with the constant circulation  $\Gamma_0$  corresponding to the root section. We also assume that the bound vortex (the loaded line) passes through the aerodynamic cen-

tre of the wing with the coordinate  $x_{Fa}$ . The magnitude of this circulation can be determined by a coupling equation according to which

$$\Gamma_0 = 0.5c_{y_a} b_0 V_\infty \quad (6.4.18)$$

where  $c_{y_a}$  and  $b_0$  are the lift coefficient and the section chord, respectively.

A similar expression can be compiled for the mean circulation over the span, the same as in the section with the chord  $b_m$ :

$$\Gamma_m = 0.5c_{y_a} b_m V_\infty \quad (6.4.19)$$

where  $c_{y_a}$  is the lift coefficient of the wing.

From Eqs. (6.4.18) and (6.4.19), we find the relation between the circulations:

$$\Gamma_0 = \Gamma_m c_{y_a} b_0 / (c_{y_a} b_m) \quad (6.4.20)$$

As stipulated, the adopted vortex systems  $\Gamma_m$  and  $\Gamma_0$  correspond to the same lift force ( $Y_a = \rho_\infty V_\infty \Gamma_m l = \rho_\infty V_\infty \Gamma_0 l_0$ ), hence  $\Gamma_m l = \Gamma_0 l_0$ . Therefore, by Eq. (6.4.20), we have

$$l_0 = l b_m c_{y_a} / (b_0 c_{y_a}) \quad (6.4.21)$$

Now, according to the known arrangement of the horseshoe vortex system, we can use formula (2.7.13) to determine the downwash angle at each point behind a wing, also taking into account the induction of the bound vortex.

To find the induced drag coefficient by formula (6.4.3), we must find the mean downwash angle  $\varepsilon_m = (1/l) \int_{-l/2}^{l/2} \varepsilon dz$  on the loaded line, taking account only of a pair of free vortices with the aid of formula (2.7.13). According to calculations (see [13]), this angle is

$$\varepsilon_m = -\frac{\Gamma_0}{2\pi l V_\infty} \ln \frac{l_0 + l}{l_0 - l} \quad (6.4.22)$$

where  $\Gamma_0$  is determined by (6.4.18). Having in view that  $l/b_0 = \lambda_w (b_m/b_0)$ , we finally obtain

$$\varepsilon_m = -\frac{c_{y_a} b_0}{4\pi \lambda_w b_m} \ln \frac{l_0 + l}{l_0 - l} = -\frac{c_{y_a}}{\pi \lambda_w} \cdot \frac{l}{4l_0} \ln \frac{l_0 + l}{l_0 - l} \quad (6.4.23)$$

We can use this downwash angle to estimate the value of the induced drag coefficient with the aid of (6.4.3). In a particular case for an infinite-span wing ( $\lambda_w \rightarrow \infty$ ), the downwash angle is absent and, consequently, the induced drag vanishes.

## 6.5. Wing with Optimal Planform

**Conversion of Coefficients  
 $c_y$  and  $c_{x,1}$  from  
 One Wing Aspect Ratio  
 to Another**

A finite-span lifting plane having the minimum induced drag is called a **wing with the optimal planform**. A glance at formula (6.4.16) reveals that at the given values of  $c_{y_a}$  and  $\lambda_w$ , the value of  $c_{x,1}$  will

be minimum when the coefficient  $\delta = 0$ , or  $\sum_{n=2}^m nA_n^2/A_1^2 = 0$ . It follows

from this equality that all the coefficients of the expansion of the circulation  $\Gamma$  into a series (6.4.11), except for  $A_1$ , equal zero ( $A_3 = A_5 = \dots = 0$ ). Hence, the circulation in an arbitrary section is

$$\Gamma(\theta) = 2lV_\infty A_1 \sin \theta \quad (6.5.1)$$

For the central section ( $\theta = \pi/2$ ), the circulation is maximum and equals  $\Gamma_0 = 2lV_\infty A_1$ . Hence,  $\Gamma(\theta) = \Gamma_0 \sin \theta$ . Inserting into this formula  $\sin \theta = \sqrt{1 - (2z/l)^2}$ , we obtain

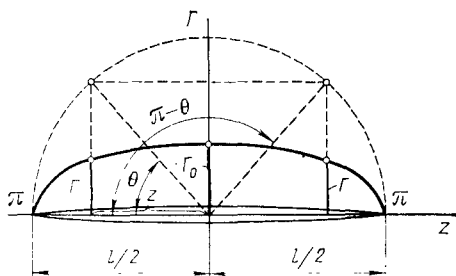
$$\Gamma^2(z)/\Gamma_0^2 + z^2/(0.5l)^2 = 1 \quad (6.5.2)$$

This equation determines the **elliptic law** of distribution of the circulation over the span of a wing having the optimal planform (Fig. 6.5.1). For such a wing, the induced drag coefficient  $c_{x,1} = c_{y_a}^2/(\pi\lambda_w)$ , while the mean flow downwash angle  $\epsilon_m = c_{y_a}/(\pi\lambda_w)$ ; by analysing (6.4.4), we can convince ourselves that the quantity  $\epsilon_m$  exactly equals the downwash angle in an arbitrary section. In other words, the downwash angle does not change along the span in a wing with the minimum induced drag.

In accordance with the coupling equation, for an arbitrary wing section, we have  $\Gamma(z) = 0.5c_{y_a} b(z) V_\infty$ , and for a central one, we have  $\Gamma_0 = 0.5c_{y_a} b_0 V_\infty$ . Now we can use Eq. (6.5.2) to find the following expression for the chord in a wing section with the optimal planform:

$$b(z) = b_0 (c_{y_a} / c_{y_a}) \sqrt{1 - (z/0.5l)^2} \quad (6.5.3)$$

Let us consider a wing at the angle of attack  $\alpha$  having section profiles that are identical along the span. We shall assume that the sections of the wing are arranged at the same local geometric angle of attack determined by the given value of  $\alpha$ . Since the downwash angle does not change from one section to another for a wing with an elliptical distribution of the circulation, the true angles of attack

**Fig. 6.5.1**

Elliptical distribution of the circulation and a geometric interpretation of the constants  $\alpha_t$  and  $\theta$

are the same:  $\alpha_t = \alpha - \varepsilon$ , and, therefore, the lift coefficients of the profiles are the same, i.e. the ratio  $c_{y_a}/c_{y_{a0}} = 1$ . Hence, the local chord of the wing is determined by the relation

$$b(z) = b_0 \sqrt{1 - (z/0.5l)^2} \quad (6.5.4)$$

In accordance with the result obtained, a wing with the minimum induced drag has an elliptical planform. In the case being considered, a constant coefficient  $c_{y_a} = c_{y_{a0}}^{\alpha} \alpha_t$  is ensured as a result of the constancy along the span of the quantity  $\alpha_t$  and the derivative  $c_{y_a}^{\alpha}$  identical for the same profiles. For a wing with an elliptical planform, the same effect can be achieved by varying the parameters  $c_{y_a}^{\alpha}$  and  $\alpha_t$ , i.e. by selecting the corresponding profiles in combination with geometric warp (upon which the sections are set at different geometric angles of attack).

It must be noted that just such a method of varying the geometric and aerodynamic parameters is used to achieve an elliptical (or close to it) distribution of the circulation on modern wings. Here three factors change in the corresponding way simultaneously. These factors, namely,  $c_{y_a}^{\alpha}(z)$ ,  $\alpha_t(z)$ , and  $b(z)$  characterize the circulation  $\Gamma(z) = 0.5c_{y_a}^{\alpha}\alpha_t b V_{\infty}$  that is distributed according to the elliptical law (6.5.2).

In the simplest case of a wing with a rectangular planform,  $b = \text{const}$ , this law of circulation distribution is ensured by only varying the values of  $c_{y_a}^{\alpha}$  and  $\alpha_t$  (by selecting the profiles and warping, respectively). It must be borne in mind that for wings of a non-elliptical planform, including rectangular ones, an elliptical distribution of the circulation can be achieved only at a definite angle of attack, and the distribution will be different if the value of the angle is changed.

It is interesting to appraise by how much wings with a different planform differ from their elliptical counterparts in their aerodynamic properties. Table 6.5.1 gives the results of evaluating the coeffi-

Table 6.5.1

Planform of wing	$\delta$	$\tau$
Elliptical	0	0
Trapezoidal ( $\eta_w = 2-3$ )	0	0
Rectangular ( $\lambda_w = 5-8$ )	0.053	0.179
Rectangular with rounded tips	0	0.147

cients  $\delta$  and  $\tau$ , called corrections for wings of a non-elliptical planform. These coefficients depend mainly on the planform of a wing and its aspect ratio. A glance at the table reveals that trapezoidal wings do not virtually differ from elliptical ones. A slight deviation in the values of  $\delta$  and  $\tau$  is observed in rectangular wings with straight tips. Rounding of these tips leads to complete analogy with an elliptical wing as regards the value of  $\delta$  and to a smaller difference in the coefficients  $\tau$ .

The relations obtained for determining the aerodynamic coefficients of finite-span wings make it possible to solve an important problem associated with the finding of these coefficients when going over from one wing aspect ratio  $\lambda_{w1}$  to another one  $\lambda_{w2}$ . This solution appreciably facilitates aerodynamic calculations because it makes it possible to use the data obtained when testing serial models of wings with the adopted (standard) value of the aspect ratio in wind tunnels.

Let us assume that for a wing with the aspect ratio  $\lambda_{w1}$  we know the coefficients  $c_{y_a}$  and  $c_{x_1}$  and we have to convert these coefficients to another aspect ratio  $\lambda_{w2}$  of a wing having the same set of sections, but differing in its planform. If both of these wings have the same lift coefficient  $c_{y_a}$ , the mean downwash angles behind them are

$$\varepsilon_{m1} = (c_{y_a}/\pi\lambda_{w1}) (1 + \tau_1), \quad \varepsilon_{m2} = (c_{y_a}/\pi\lambda_{w2}) (1 + \tau_2)$$

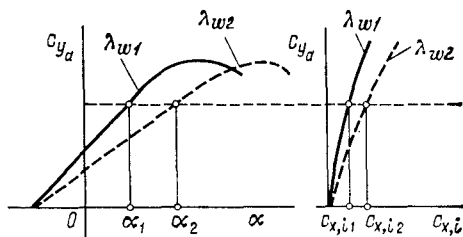
Identical values of  $c_{y_a}$  for wings are determined by identical true angles of attack, i.e.  $\alpha_{t1} = \alpha_{t2}$ , where

$$\alpha_{t1} = \alpha_1 - \varepsilon_{m1}, \quad \alpha_{t2} = \alpha_2 - \varepsilon_{m2}$$

Consequently, for the setting angle of the second wing, we obtain the expression

$$\alpha_2 = \alpha_1 - (c_{y_a}/\pi) [(1 + \tau_1)/\lambda_{w1} - (1 + \tau_2)/\lambda_{w2}] \quad (6.5.5)$$

According to this formula for converting the lift coefficient, a wing with a smaller aspect ratio ( $\lambda_{w2} < \lambda_{w1}$ ) having a larger down-

**Fig. 6.5.2**

Conversion of aerodynamic coefficients of a wing from one aspect ratio to another

wash angle ( $\epsilon_{w2} > \epsilon_{w1}$ ) must have an increased setting angle ( $\alpha_2 > \alpha_1$ ) to obtain the same coefficient  $c_{y_a}$ .

The induced drag coefficients for two wings with the aspect ratios  $\lambda_{w1}$  and  $\lambda_{w2}$  and with identical coefficients  $c_{y_a}$  are determined by the following formulas, respectively:

$$c_{x,i1} = (c_{y_a}/\pi\lambda_{w1}) (1 + \delta_1), \quad c_{x,i2} = (c_{y_a}/\pi\lambda_{w2}) (1 + \delta_2)$$

Accordingly, for a wing with the aspect ratio  $\lambda_{w2}$ , the induced drag coefficient is

$$c_{x,i2} = c_{x,i1} - (c_{y_a}/\pi) [(1 + \delta_1)/\lambda_{w1} - (1 + \delta_2)/\lambda_{w2}] \quad (6.5.6)$$

This formula is used to convert the value of  $c_{x,i1}$  for a wing with the aspect ratio  $\lambda_{w1}$  to its value for the aspect ratio  $\lambda_{w2}$ . If this new ratio is smaller than the given one ( $\lambda_{w2} < \lambda_{w1}$ ), a large downwash appears ( $\epsilon_{m2} > \epsilon_{m1}$ ), and, consequently, the induced drag coefficient grows ( $c_{x,i2} > c_{x,i1}$ ).

Figure 6.5.2 shows graphically how the coefficients  $c_{y_a}$  and  $c_{x,i1}$  are converted from the aspect ratio  $\lambda_{w1}$  to  $\lambda_{w2}$  in accordance with formulas (6.5.5) and (6.5.6). First the curves  $c_{y_a} = f_1(\alpha_1)$  and  $c_{y_a} = \varphi_1(c_{x,i1})$  are plotted for a wing with the given aspect ratio  $\lambda_{w1}$ . Next, setting a number of values of  $c_{y_a}$ , we use the plot to determine the corresponding values of  $\alpha_1$  and  $c_{x,i1}$ , and then calculate the angles of attack  $\alpha_2$  and the coefficients  $c_{x,i2}$  for the second wing by formulas (6.5.5) and (6.5.6). The corresponding points are laid off, and the curves  $c_{y_a} = f_2(\alpha_2)$  and  $c_{y_a} = \varphi_2(c_{x,i2})$  are plotted.

For wings with smaller aspect ratios ( $\lambda_{w2} < \lambda_{w1}$ ), these curves will be to the right of those of the ratio  $\lambda_{w1}$  because with the same true angle of attack, the increase in the downwash angle  $\epsilon_{w2}$  for the second wing with a smaller  $\lambda_{w2}$  is compensated by the growth in the setting angle of attack ( $\alpha_2 > \alpha_1$ ); in turn, an increased coefficient  $c_{x,i2}$  corresponds to the greater downwash angle  $\epsilon_{w2}$ , and this is exactly what is shown in Fig. 6.5.2.

The plots in Fig. 6.5.2 can be used to convert  $c_{y_a}$  and  $c_{x,i1}$  to a wing with an infinitely large aspect ratio (airfoil). For this purpose,

the second terms in the brackets in formulas (6.5.5) and (6.5.6) must be taken equal to zero. The converted curves  $c_{y_a} = f_2(\alpha_2)$  and  $c_{y_a} = \varphi_2(c_{x,12})$  will occupy a position at the extreme left of the corresponding curves  $c_{y_a} = f_1(\alpha_1)$  and  $c_{y_a} = \varphi_1(c_{x,11})$ .

**Mean Aerodynamic Chord.** When performing aerodynamic calculations of finite-span wings, the **mean aerodynamic chord** is selected as the characteristic geometric dimension of the span. Such a chord belongs to a conditional wing having a rectangular planform for which the planform area, the aerodynamic force, and the pitching moment are the same as for a wing of the given planform. The mean aerodynamic chord allows us to compare the moment characteristics of various wings with a varying chord along their span. One of such characteristics is the pitching moment coefficient determined as  $m_{zA} = M_z/(b_A q S_w)$ , where  $b_A$  is the mean aerodynamic chord. The quantity  $m_{zA}$  is sufficiently stable when the planform of a wing and its dimensions change.

The value of the chord  $b_A$ , and those of the coordinates of its leading point  $x_A, y_A$  (relative to coordinate axes passing through the apex of the given wing), are usually determined approximately assuming equality of the aerodynamic coefficients (of the moment, drag, and lift) of a wing as a whole and its individual section (profile). Accordingly, we have

$$\left. \begin{aligned} b_A &= \frac{2}{S_w} \int_0^{l/2} b^2(z) dz, & x_A &= \frac{2}{S_w} \int_0^{l/2} xb(z) dz \\ y_A &= \frac{2}{S_w} \int_0^{l/2} yb(z) dz \end{aligned} \right\} \quad (6.5.7)$$

where  $x, y$  are the longitudinal and vertical coordinates of the leading point of a section with the varying chord  $b(z)$ . Evidently, knowing  $x_A$  and the equation of the leading edge of a given wing, we can determine the lateral coordinate  $z_A$  of the mean aerodynamic chord.

Formulas (6.5.7) make it possible to calculate the magnitude of the chord  $b_A$  by numerical or graphical integration and determine its position. The middle of  $b_A$  coincides with the centre of gravity of the wing area.

For a broad range of wings having a trapezoidal planform, we can find analytical relations for  $b_A, x_A, y_A$ , and  $z_A$ . For such wings

$$\left. \begin{aligned} b(z) &= b_0 [1 - (\eta_w - 1) \bar{z}/\eta_w] \\ S_w &= b_0 l (\eta_w + 1)/(2\eta_w) \\ x &= z \tan \kappa_0; \quad y = z \tan \psi \end{aligned} \right\} \quad (6.5.8)$$

where  $\eta_w = b_0/b_A$  is the taper ratio of the wing,  $\alpha_0$  is the sweep angle of the leading edge,  $\psi$  is the dihedral angle, and  $\bar{z} = 2z/l$ .

Introduction of (6.5.8) into (6.5.7) yields

$$\left. \begin{aligned} b_A &= 4S_w [1 - \eta_w/(\eta_w + 1)^2]/(3l) \\ x_A &= l (\eta_w + 2) \tan \alpha_0/[6 (\eta_w + 1)] \\ y_A &= l (\eta_w + 2) \tan \psi/[6 (\eta_w + 1)] \end{aligned} \right\} \quad (6.5.9)$$

The lateral coordinate of the chord  $b_A$  is found from the formula  $z_A = x_A / \tan \alpha_0$ . If a wing has no dihedral, the coordinate  $y_A$  is evidently zero.

## An Airfoil in a Compressible Flow

### 7.1. Subsonic Flow over a Thin Airfoil

#### Linearization of the Equation for the Velocity Potential

The calculation of a subsonic flow over an airfoil is associated with solution of the equation for the velocity potential of a plane two-dimensional flow that is obtained from (5.1.8) provided that  $\varepsilon = 0$  and has the form

$$(V_x^2 - a^2) \frac{\partial^2 \varphi}{\partial x^2} + 2V_x V_y \frac{\partial^2 \varphi}{\partial x \partial y} + (V_y^2 - a^2) \frac{\partial^2 \varphi}{\partial y^2} = 0. \quad (7.1.1)$$

This partial differential equation of the second order is **non-linear** in the unknown function  $\varphi$  and describes the flow past sufficiently thick airfoils. The latter cause large disturbances of the gas upon which the flow velocities  $V$  and the speeds of sound  $a$  differ appreciably from the relevant free-stream flow parameters.

If an airfoil is thin and the disturbances it produces are small, Eq. (7.1.1) can be simplified by reducing it to a linear equation with constant coefficients of the second partial derivatives. Such a simplification is called **linearization**, while the obtained equation and the nearly uniform flow it describes are called **linearized**.

For a linearized flow, conditions (6.1.1) for the velocities are satisfied, and equation (6.1.2) holds. Since the disturbance velocities  $u$  and  $v$  (6.1.1) are infinitesimal, the equation for the speed of sound obtained from (3.6.20) can be transformed as follows:

$$a^2 = a_\infty^2 + [(k - 1)/2] (V_\infty^2 - V^2) \quad (7.1.2)$$

Substituting for  $V^2$  its value from (6.1.2), we obtain

$$a^2 = a_\infty^2 - (k - 1) V_\infty u \quad (7.1.2')$$

Inserting into (7.1.1) the value of  $a^2$  from (7.1.2'), and also  $V_x = V_\infty + u$ ,  $V_y = v$ ,  $V_x^2 = V_\infty^2 + 2V_\infty u$ ,  $V_y^2 \approx v^2$ , and taking into account that the total velocity potential of a linearized flow can be written in the form  $\varphi = \varphi_\infty + \varphi'$ , where  $\varphi_\infty$  is the velocity potential of the oncoming flow, while the additional potential according to

condition (6.1.1) is  $\varphi' \ll \varphi_\infty$ , we obtain

$$\begin{aligned} [V_\infty^2 - a_\infty^2 + (k+1)V_\infty u] \frac{\partial^2 \varphi'}{\partial x^2} + 2(V_\infty + u)v \frac{\partial^2 \varphi'}{\partial x \partial y} \\ + [v^2 - a_\infty^2 + (k-1)V_\infty u] \frac{\partial^2 \varphi'}{\partial y^2} = 0 \end{aligned} \quad (7.1.3)$$

The second partial derivatives of the potential  $\varphi'$  with respect to the coordinates  $x$  and  $y$  are first-order infinitesimals:

$$\frac{\partial^2 \varphi'}{\partial x^2} = \frac{\partial u}{\partial x}, \quad \frac{\partial^2 \varphi'}{\partial x \partial y} = \frac{\partial u}{\partial y} = \frac{\partial v}{\partial x}, \quad \frac{\partial^2 \varphi'}{\partial y^2} = \frac{\partial v}{\partial y}$$

With this in view, in (7.1.3), we can determine the group of terms that are second- and third-order infinitesimals; disregarding them, we obtain a linearized equation in the following form:

$$(a_\infty^2 - V_\infty^2) \frac{\partial^2 \varphi'}{\partial x^2} + a_\infty^2 \frac{\partial^2 \varphi'}{\partial y^2} = 0 \quad (7.1.4)$$

or

$$(1 - M_\infty^2) \frac{\partial^2 \varphi'}{\partial x^2} + \frac{\partial^2 \varphi'}{\partial y^2} = 0 \quad (7.1.4')$$

where  $M_\infty = V_\infty/a_\infty$ .

Let us consider the expression for the pressure in a linearized flow. To do this, we shall use formula (3.6.26), which we shall write in the form

$$p/p_\infty = (1 - V^2/V_{\max}^2)^{k/(k-1)} (1 - V_\infty^2/V_{\max}^2)^{-k/(k-1)}$$

Inserting the value of  $V^2$  from (6.1.2), we have

$$p/p_\infty = [1 - 2V_\infty u/(V_{\max}^2 - V_\infty^2)]^{k/(k-1)}$$

Taking into account that by formula (3.6.22)

$$V_{\max}^2 - V_\infty^2 = \frac{2}{k-1} a_\infty^2 = \frac{2k}{k-1} \cdot \frac{p_\infty}{\rho_\infty}$$

we find

$$\frac{p}{p_\infty} = \left(1 - \frac{k-1}{k} \cdot \frac{\rho_\infty V_\infty u}{p_\infty}\right)^{k/(k-1)} \quad (7.1.5)$$

Let us expand the expression on the right-hand side into a binomial series and retain the second term in the expansion:

$$p/p_\infty = 1 - \rho_\infty V_\infty u / p_\infty \quad (7.1.5')$$

Hence we find the excess pressure  $p - p_\infty = -\rho_\infty V_\infty u$  and the pressure coefficient  $p = -2u/V_\infty$ , i.e. we obtain the same relations (6.1.3) and (6.1.5) as for an incompressible fluid. But when using these relations for high subsonic velocities, one must take into account that the disturbance velocity  $u = \partial \varphi' / \partial x$  is determined with a view to compressibility.

**Relation Between  
the Parameters of a Compressible  
and Incompressible Fluid Flow  
over a Thin Airfoil**

The flow over a thin airfoil at a small angle of attack in a compressible subsonic flow is investigated with the aid of Eq. (7.1.4') in which  $M_\infty < 1$ . Let us change the variables in this equation in accordance with the relations

$$x_0 = x, \quad y_0 = y \sqrt{1 - M_\infty^2}, \quad \varphi'_0 = \varphi' \gamma V_{\infty 0} / V_\infty \quad (7.1.6)$$

where  $\gamma$  is an arbitrary parameter, and  $V_{\infty 0}$  is the velocity of a conditional flow (fictitious velocity) that in the general case differs from the velocity  $V_\infty$  of a given flow.

By introducing (7.1.6) into (7.1.4'), we obtain the Laplace equation for determining the velocity potential  $\varphi'_0$  of an incompressible flow in the plane  $x_0, y_0$ :

$$\partial^2 \varphi'_0 / \partial x_0^2 + \partial^2 \varphi'_0 / \partial y_0^2 = 0 \quad (7.1.4'')$$

Hence, the problem of a compressible flow over a given airfoil can be solved by using the results of solving the problem on an incompressible flow at the fictitious velocity  $V_{\infty 0}$  over a modified airfoil. Let us find the relation between the corresponding parameters of flow over the airfoils and between their geometric characteristics. The relation between the disturbance velocities  $u_0$  in the incompressible and  $u$  in the compressible flows is established in accordance with (7.1.6) as follows:

$$u_0 = \frac{\partial \varphi'_0}{\partial x_0} = \frac{\partial \varphi'}{\partial x} \gamma \frac{V_{\infty 0}}{V_\infty} = u \gamma \frac{V_{\infty 0}}{V_\infty} \quad (7.1.7)$$

Using (6.1.5), we find the pressure coefficients in an incompressible fluid  $\bar{p}_{1c} = -2u_0/V_{\infty 0}$  and in a compressible gas  $\bar{p} = -2u/V_\infty$ . Consequently, with a view to (7.1.7), we obtain

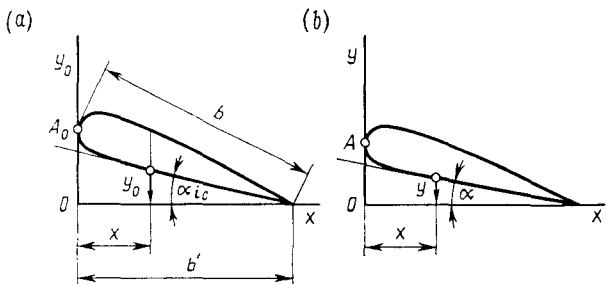
$$\bar{p}_{1c} = \gamma \bar{p} \quad (7.1.8)$$

From the formulas  $c_{y,1c} = \oint p_{1c} d\bar{x}_0$ ,  $m_{z,1c} = \oint \bar{p}_{1c} \bar{x}_0 d\bar{x}_0$ , in which  $\bar{x}_0 = x/b$ , and expression (7.1.8), we find the relation between the corresponding lift and moment coefficients:

$$c_{y_a1c} = \gamma \oint \bar{p} d\bar{x} = \gamma c_{y_a}; \quad m_{z_a1c} = \gamma \oint \bar{p} \bar{x} d\bar{x} = \gamma m_{z_a} \quad (7.1.9)$$

where  $\bar{x} = x/b$ .

Let us establish the relation between the configurations of airfoils and the angles of attack. For this purpose, we shall first determine

**Fig. 7.1.1**

Airfoils in a nearly uniform incompressible (a) and compressible (b) flows:  
A and \$A\_0\$—stagnation points

the relation between the vertical velocity components. In accordance with (7.1.6), we have

$$v_0 = \frac{\partial \Phi'_0}{\partial y_0} = \frac{\partial \Phi'}{\partial y} \cdot \frac{1}{\sqrt{1 - M_\infty^2}} \cdot \frac{V_{\infty 0}}{V_\infty} = v \frac{\gamma}{\sqrt{1 - M_\infty^2}} \cdot \frac{V_{\infty 0}}{V_\infty} \quad (7.1.10)$$

In an incompressible fluid by Eq. (3.3.17'), in which the function  $F$  is taken equal to  $y_0 - f_0(x_0)$  if  $y_0 = f_0(x_0)$ , we may consider for an airfoil that  $v_0/(V_{\infty 0} + u_0) = dy_0/dx_0$  or, taking into account that  $u_0 \ll V_{\infty 0}$ , assume that  $v_0/V_{\infty 0} = dy_0/dx_0$ . Similarly, we find for an airfoil in a compressible gas that  $v/V_\infty = dy/dx$ . Consequently,  $(v_0/v)(V_\infty/V_{\infty 0}) = (dy_0/dy) dx/dx_0$ . Taking (7.1.6) and (7.1.10) into account, we find  $dy_0/dy = \gamma/\sqrt{1 - M_\infty^2}$ . Integration for the condition that for  $y = 0$  the quantity  $y_0 = 0$  yields an equation relating the vertical coordinates of the fictitious and given airfoils:

$$y_0 = y\gamma/\sqrt{1 - M_\infty^2} \quad (7.1.11)$$

At the same time, as follows from (7.1.6), the horizontal coordinates of the airfoils do not change. With this in view, the angles of attack can be written in the form

$$\alpha_{1c} = y_0/(b' - x) \text{ and } \alpha = y/(b' - x)$$

where  $b'$  is the distance to the trailing edge of the airfoil, and  $x$  is the horizontal coordinate (Fig. 7.1.1).

Hence, by (7.1.11), we have

$$\alpha_{1c} = \alpha\gamma/\sqrt{1 - M_\infty^2} \quad (7.1.12)$$

Let us assume that the arbitrary parameter  $\gamma = 1$ . Therefore,

$$\left. \begin{aligned} \bar{p} &= \bar{p}_{1c}, & y &= y_0\sqrt{1 - M_\infty^2}, & \alpha &= \alpha_{1c}\sqrt{1 - M_\infty^2} \\ c_{y_a} &= c_{y_{a1c}}, & m_{z_a} &= m_{z_{a1c}} \end{aligned} \right\} \quad (7.1.13)$$

Consequently, if the pressure coefficients are the same at corresponding points of thin airfoils in compressible and incompressible flows, then in the compressible flow the airfoil is thinner than in the incompressible one  $\sqrt{1 - M_\infty^2}$  times. The angle of attack decreases to the same extent.

Let us consider the case when  $\gamma = \sqrt{1 - M_\infty^2}$  and, therefore,

$$\left. \begin{aligned} \bar{p} &= \bar{p}_{1c}/\sqrt{1 - M_\infty^2}, & y &= y_0, & \alpha &= \alpha_{1c} \\ c_{y_a} &= c_{y_{1c}}/\sqrt{1 - M_\infty^2}, & m_{z_a} &= m_{z_{1c}}/\sqrt{1 - M_\infty^2} \end{aligned} \right\} \quad (7.1.14)$$

According to the results obtained, for two identical airfoils at the same angle of attack, the pressure coefficients at corresponding points of the airfoils, and also their overall lift and moment coefficients in a compressible flow are *larger* than those in an incompressible one  $1/\sqrt{1 - M_\infty^2}$  times. Hence follows the conclusion that compressibility leads to *an increase* in the pressure and lift force. The coefficient  $1/\sqrt{1 - M_\infty^2}$  is known as the **Prandtl-Glauert correction** (for the compressibility effect). The corresponding relation (7.1.14) for  $\bar{p}$  is known as the Prandtl-Glauert formula. It can be considered as a first approximation when calculating the pressure coefficient in a compressible flow according to the relevant value of  $\bar{p}_{1c}$ . More accurate results relating to thickened airfoils and increased angles of attack are obtained by the **Kármán-Tsien formula**

$$\bar{p} = \bar{p}_{1c} \left( \sqrt{1 - M_\infty^2} + \frac{M_\infty^2}{1 + \sqrt{1 - M_\infty^2}} \frac{\bar{p}_{1c}}{2} \right)^{-1} \quad (7.1.15)$$

The use of formulas (7.1.14) and (7.1.15) for  $\bar{p}$  leads to quite a large error when determining the pressure coefficient at the stagnation point where the velocities and, consequently, the local Mach number, equal zero. For example, for this point, at which  $\bar{p}_{01c} = 1$ , formula (7.1.14) when  $M_\infty = 0.8$  yields a coefficient  $\bar{p}_0 = 1.67$ , and formula (7.1.15),  $\bar{p}_0 = 1.26$  instead of the actual value of 1.17.

At the stagnation point, the pressure coefficient  $\bar{p}_0 = 2(p_0 - p_\infty)/(kp_\infty M_\infty^2)$  for arbitrary numbers  $M_\infty < 1$  is evaluated with the aid of an expression obtained from (3.6.30) provided that  $M = 1$ :

$$\bar{p}_0 = \frac{2}{kM_\infty^2} \left[ \left( 1 + \frac{k-1}{2} M_\infty^2 \right)^{k/(k-1)} - 1 \right] \quad (7.1.16)$$

When  $M_\infty < 1$ , the quantity in parentheses can be written in the form of a series in which the first three terms are retained:

$$\bar{p}_0 = 1 + \frac{M_\infty^2}{4} + \frac{2-k}{24} M_\infty^2 \quad (7.1.17)$$

This relation is suitable for quite a broad range of values of  $0 \leqslant M_\infty \leqslant 1$ .

## 7.2. Khristianovich Method

### Content of the Method

If an airfoil or another body in a flow introduces finite disturbances into it, the linearized equations are not suitable. Non-linear equations of gas dynamics must be used when studying such a flow.

Many problems on supersonic flow can be solved by employing, particularly, the method of characteristics. The number of solvable problems of supersonic aerodynamics increases still more owing to the numerical methods of integrating the equations of motion. It is much more difficult to analyse subsonic flow. This is explained mathematically by the different nature of the equations: for supersonic flows they are hyperbolic, and for subsonic ones, elliptic.

The use of imaginary characteristics in the elliptic equations does not yield appreciable simplifications. The more complicated nature of studying subsonic flows is explained physically by the fact that disturbances in them propagate into all the regions of motion, whereas the disturbances in supersonic flows are confined within conical surfaces issuing from the point of disturbance and propagating only downstream. Owing to the linearized nature of the equations, the investigation of nearly uniform subsonic flows is somewhat simpler than of subsonic flows with finite disturbances over, for example, thick airfoils.

A method of studying such flows is described by Academician S. Chaplygin [17]. He gives equations forming the mathematical basis of the theory of potential subsonic flows. They are known in gas dynamics as the **Chaplygin equations**. Their feature is that they describe the flow of a gas not in the plane  $y$ ,  $x$ , but in that of the special coordinates  $\tau$  and  $\beta$  ( $\tau = V^2$  is the square of the total velocity at a given point in the flow, and  $\beta$  is the polar angle determined from the condition  $V_x = V \cos \beta$ ). Unlike the conventional equations, they are *linear* because the coefficients of the equations are functions of the independent variables  $\tau$  and  $\beta$ . These equations were solved by Chaplygin for a number of cases of flow at high subsonic velocities.

The Chaplygin equations underlie many other methods in the field of high-speed aerodynamics. Academician S. Khristianovich, using these equations, developed a method making it possible to take into account the influence of compressibility on the subsonic flow over airfoils of an arbitrary configuration. The theoretical tenets of this method are described in detail in [3]. We shall consider the basic content of the method and its application to the solution of various problems of a compressible subsonic flow over airfoils.

When considering a compressible flow over an airfoil of a given configuration, Khristianovich showed that the flow equations can be

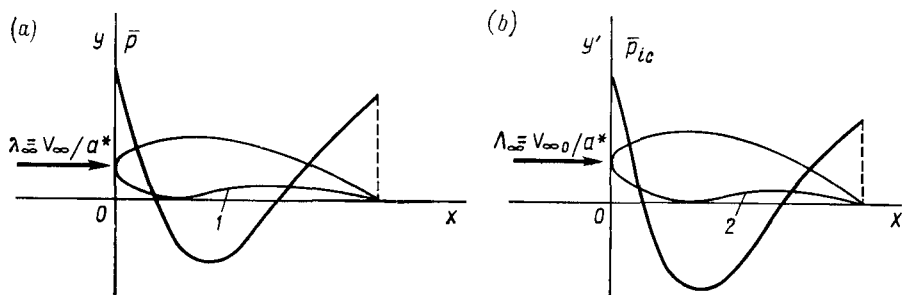


Fig. 7.2.1

Calculation of the pressure on an airfoil in a compressible flow:  
 $a$ —true flow;  $b$ —fictitious flow; 1—given airfoil; 2—fictitious airfoil

reduced to *equations of an incompressible flow over an airfoil with a modified configuration* (Fig. 7.2.1). Hence, according to Khristianovich's approach, first the relatively simple problem of a *conditional (fictitious) incompressible flow over a fictitious airfoil is solved, and then the parameters obtained are converted to the conditions of a compressible flow over the given airfoil.*

Table 7.2.1

$\lambda$	0	0.05	0.10	0.15	0.20	0.25	0.30	0.35
$\Lambda$	0	0.0500	0.0998	0.1493	0.1983	0.2467	0.2943	0.3410
$\lambda$	0.40	0.45	0.50	0.55	0.60	0.625	0.650	0.675
$\Lambda$	0.3862	0.4307	0.4734	0.5144	0.5535	0.5722	0.5904	0.6080
$\lambda$	0.700	0.725	0.750	0.775	0.800	0.825	0.850	0.875
$\Lambda$	0.6251	0.6413	0.6568	0.6717	0.6857	0.6988	0.7110	0.7223
$\lambda$	0.900		0.925		0.950		0.975	1
$\Lambda$	0.7324		0.7413		0.7483		0.7546	0.7577

This conversion is based on the use of a **functional relation** between the true speed ratio  $\lambda = V/a^*$  of a compressible flow and the fictitious speed ratio  $\Lambda = V_0/a^*$  at the corresponding points of the given and fictitious airfoils (Table 7.2.1). The method being considered makes it possible to *reconstruct the given airfoil to the fictitious one.*

As shown by Khristianovich, for prolate airfoils, the difference between the configurations of the given and fictitious airfoils may be disregarded. In this case, the **Khristianovich method** allows one to convert the parameters of the flow over an airfoil (pressure, velocity) to any number  $M_\infty > 0$ , i.e. to take account of compressibility, if the distribution of these parameters over the same airfoil is known for a low-speed flow when the influence of compressibility is absent ( $M_\infty \approx 0$ ). In addition, this method allows us to convert the flow parameters from one number  $M_{\infty 1} > 0$  to another one  $M_{\infty 2} > 0$ .

The Khristianovich method is suitable provided that the velocity is subsonic over the entire airfoil. This condition is satisfied if the Mach number of the oncoming flow is less than the **critical value**  $M_{\infty, cr}$ . Consequently, before performing calculations, one must find this critical value and determine the number  $M_\infty < M_{\infty, cr}$  for which calculations are possible. The critical number  $M_{\infty, cr}$  can also be found by the Khristianovich method.

**Conversion of the Pressure Coefficient  
for an Incompressible Fluid  
to the Number  $M_\infty > 0$**

Assume that we know the distribution of the pressure coefficient over an airfoil in an incompressible flow, i.e. we know the form of the function  $\bar{p}_{ic} = \bar{p}_{ic}(x)$  (Fig. 7.2.2). This function is converted to the number  $M_{\infty, cr} > M_\infty > 0$  as follows.

We determine the speed ratio according to the given number  $M_\infty > 0$ :

$$\lambda_\infty := \left[ \frac{k+1}{2} M_\infty^2 \left( 1 + \frac{k-1}{2} M_\infty^2 \right)^{-1} \right]^{1/2} \quad (7.2.1)$$

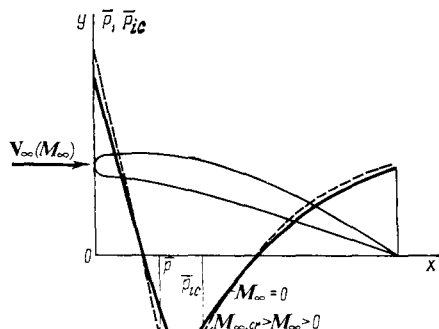
From Table 7.2.1, we find the fictitious speed ratio  $\Lambda_\infty$  of an incompressible flow corresponding to the value  $\lambda_\infty$ , and for the chosen value of  $\bar{p}_{ic}$  from the Bernoulli equation

$$\bar{p}_{ic} = 1 - (\Lambda/\Lambda_\infty)^2 \quad (7.2.2)$$

we determine the local fictitious speed ratio

$$\Lambda = \Lambda_\infty \sqrt{1 - \bar{p}_{ic}} \quad (7.2.2')$$

Knowing  $\Lambda$ , we use Table 7.2.1 to find the local true speed ratio  $\lambda$  of the compressible flow, and we calculate the pressure  $p$  by formula (3.6.26) in which it is necessary to assume that  $V^2/V_{max}^2 = [(k-1)/(k+1)] \lambda^2$ . We determine the pressure coefficient by the

**Fig. 7.2.2**

Nature of the pressure distribution on one side of an airfoil at different values of  $M_{\infty}$

formula  $\bar{p} = 2(p/p_{\infty} - 1)/(kM_{\infty}^2)$ . The curve  $\bar{p} = \bar{p}(x)$  converted to the given number  $M_{\infty}$  is shown by a dashed line in Fig. 7.2.2.

#### Conversion of the Pressure Coefficient from $M_{\infty 1} > 0$ to $M_{\infty 2} > 0$

Assume that we know the distribution of the pressure coefficient of a compressible fluid  $\bar{p}_1 = \bar{p}_1(x)$  at a certain number  $M_{\infty 1}$  (where  $M_{\infty,cr} > M_{\infty 1} > 0$ ). To convert this distribution to the number  $M_{\infty 2} > 0$ , it is necessary to first calculate the speed ratios  $\lambda_{\infty 1}$  and  $\lambda_{\infty 2}$  corresponding to the numbers  $M_{\infty 1}$  and  $M_{\infty 2}$  by formula (7.2.1) and use Table 7.2.1 to find the speed ratios  $\Lambda_{\infty 1}$  and  $\Lambda_{\infty 2}$  of the fictitious incompressible flow.

After assigning a value to the pressure coefficient  $\bar{p}_1$ , from the formula  $\bar{p}_1 = 2(p_1 - p_{\infty})/(kM_{\infty 1}p_{\infty 1})$  we find the absolute pressure:

$$p_1 = p_{\infty 1} [\bar{p}_1 (kM_{\infty 1}^2/2) + 1] \quad (7.2.3)$$

and evaluate the local speed ratio of the given flow:

$$\lambda_1 = \left\{ \frac{k+1}{k-1} \left[ 1 - \left( \frac{p_1}{p_0} \right)^{(k-1)/k} \right] \right\}^{1/2} \quad (7.2.4)$$

From Table 7.2.1 according to the value of  $\lambda_1$ , we find the local speed ratio of the fictitious incompressible flow, and from the Bernoulli equation (7.2.2), we calculate the corresponding pressure coefficient:

$$\bar{p}_{ic} = 1 - (\Lambda_1/\Lambda_{\infty 1})^2$$

The pressure coefficient  $\bar{p}_2$  for the number  $M_{\infty 2}$  is determined according to this value of  $\bar{p}_{ic}$  in the same way as the pressure coefficient of an incompressible flow is converted to the number  $M_{\infty} > 0$  according to the procedure set out previously.

### Determination of the Critical Number $M$

According to Khristianovich's hypothesis, a local sonic velocity, which the critical Mach number  $M_{\infty, cr}$  of the oncoming flow corresponds to, appears near an airfoil where the maximum rarefaction is observed in an incompressible flow. Khristianovich established the relation between the minimum coefficient  $\bar{p}_{ic, \min}$  corresponding to this maximum rarefaction and the number  $M_{\infty, cr}$ .

Hence, to find the critical Mach number, it is necessary in some way or other, for example, by blowing air over a model in a low-speed wind tunnel, to determine the magnitude of the maximum rarefaction  $\bar{p}_{ic, \min}$ . If as a result we find the distribution of the pressure with account taken of the compressibility for  $M_{\infty, cr} > M_{\infty} > 0$ , we can determine the value of  $\bar{p}_{ic, \min}$  by the conversion of  $p_{ic, \min}$  to the number  $M_{\infty} = 0$ .

Assume that we know the value of the maximum rarefaction  $\bar{p}_{ic, \min}$ . Since  $\lambda = 1$  where a sonic velocity appears, from Table 7.2.1 we can find the corresponding value of the local speed ratio of the fictitious incompressible flow, i.e.  $\Lambda = 0.7577$ . Using the Bernoulli equation  $\bar{p}_{ic, \min} = 1 - (\Lambda/\Lambda_{\infty})^2$  we can find the speed ratio for the fictitious oncoming flow:

$$\Lambda_{\infty} = \Lambda / \sqrt{1 - \bar{p}_{ic, \min}} = 0.7577 / \sqrt{1 - \bar{p}_{ic, \min}} \quad (7.2.5)$$

while using Table 7.2.1 and the value of  $\Lambda_{\infty}$ , we can determine the critical speed ratio  $\lambda_{\infty, cr}$  of the compressible flow. The corresponding critical Mach number is

$$M_{\infty, cr} = \lambda_{\infty, cr} \left( \frac{k+1}{2} - \frac{k-1}{2} \lambda_{\infty, cr}^2 \right)^{-1/2} \quad (7.2.6)$$

A plot of the critical Mach number versus  $\bar{p}_{ic, \min}$  constructed according to the results of the above calculation is shown in Fig. 7.2.3.

An increase in the airfoil thickness is attended by a decrease in the number  $M_{\infty, cr}$ . The explanation is that such an increase leads to contraction of the stream filament and to an increase in the local flow velocity. Consequently, sonic velocity on a thickened airfoil is achieved at a lower free-stream velocity, i.e. at a lower value of  $M_{\infty} = M_{\infty, cr}$ . This conclusion follows directly from Fig. 7.2.3 in accordance with which at an increased local velocity lower values of  $M_{\infty, cr}$  correspond to a lower value of the coefficient  $\bar{p}_{ic, \min}$ . Upon an increase in the angle of attack, the number  $M_{\infty, cr}$  diminishes, which is also explained by the greater contraction of the stream filaments and by the associated increase in the local subsonic velocity.

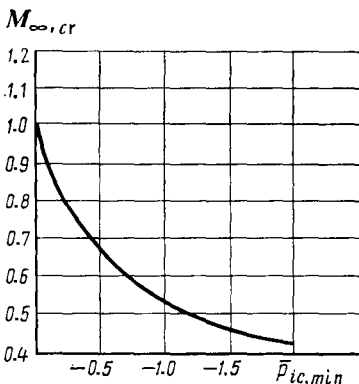


**Fig. 7.2.3**  
A Khristianovich curve for determining the critical Mach number

#### Aerodynamic Coefficients

Khristianovich's investigations made it possible to obtain more accurate relations for the lift and moment coefficients than relations (7.1.14) found on the basis of the Prandtl-Glauert formula for the pressure coefficient. These relations are as follows:

$$c_{y_a} = c_{y, 1c} L / \sqrt{1 - M_\infty^2}; \quad m_{z_a} = m_{z_a 1c} L^2 / \sqrt{1 - M_\infty^2} \quad (7.2.7)$$

where

$$L = 1 + 0.05 M_\infty^2 / M_{\infty, cr}^2$$

Compressibility changes the position of the centre of pressure of an airfoil (the coordinate  $x_p$  of this centre is measured from the leading edge along the chord). It follows from (7.2.7) that in a compressible flow, the coefficient of the centre of pressure is

$$c_p = c_{p, 1c} L \quad (7.2.8)$$

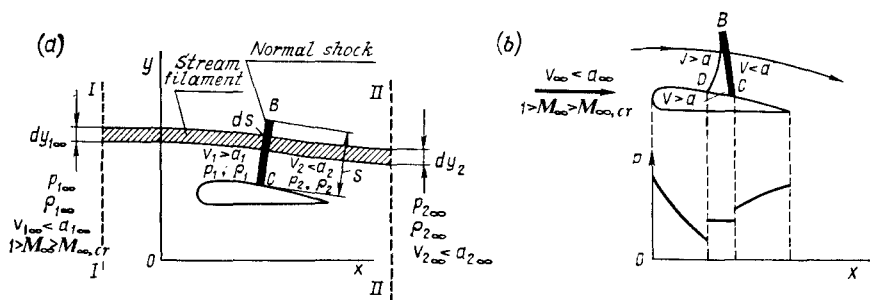
where

$$c_p = x_p / b = -m_{z_a} / c_{y_a}, \quad c_{p, 1c} = -m_{z_a 1c} / c_{y_a 1c}$$

Examination of (7.2.8) reveals that the centre of pressure in a compressible flow in comparison with an incompressible one is displaced toward the trailing edge. This is explained by the increase in the aerodynamic load on the tail sections of an airfoil at increased flow speeds and, as a consequence, by the appearance of an additional stabilizing effect.

### 7.3. Flow at Supercritical Velocity over an Airfoil ( $M_\infty > M_{\infty, cr}$ )

Subsonic flow over an airfoil can be characterized by two cases. In the first one, the local velocity of the flow on a surface does not exceed the speed of sound anywhere. This case is **purely subsonic**.

**Fig. 7.3.1**

Subsonic flow over an airfoil at a supercritical velocity:

a—diagram of the flow used for calculations when a local normal shock is present; b—distribution of the pressure over the airfoil when a local  $\lambda$ -shaped shock forms

**flow.** It is general knowledge that at such a velocity, no shocks can form at any point on an airfoil, while the lift force and drag are determined with a view to the compressibility and in the general case depend on the normal pressure and skin friction forces. Such a drag, including that produced by the normal stress (pressure) and the friction drag is called the **profile drag**.

In the second case, called **supercritical flow**, at which the number  $M$  of the oncoming flow is larger than the critical one, i.e.  $M_\infty > M_{\infty, \text{cr}}$ , the local velocity at some points in the vicinity of an airfoil becomes higher than the speed of sound, and a zone of local **supersonic velocities** appears. Here the flow over an airfoil is characterized by the fact that both behind it and ahead of the leading edge the local velocity is lower than the speed of sound. Hence, local compression shocks form in the transition from supersonic velocities to subsonic ones in the vicinity of the wing (Fig. 7.3.1). Such  $\lambda$ -shaped shocks consist, as it were, of two shocks: a front curved (oblique) one  $DB$  and a rear almost straight one  $CB$  (Fig. 7.3.1b).

Local shocks that may form on both the upper and bottom sides of an airfoil substantially change the distribution of the pressure and lead to the appearance of an additional wave drag  $X_w$ . Hence, the total drag of an airfoil  $X_a$  consists of the profile  $X_{\text{pr}}$  and the wave  $X_w$  drags, i.e.  $X_a = X_{\text{pr}} + X_w$ , or  $c_{x,a} = c_{x,\text{pr}} + c_{x,w}$ , where  $c_{x,a}$  is the total drag coefficient of the airfoil,  $c_{x,\text{pr}}$  and  $c_{x,w}$  are the profile and wave drag coefficients, respectively.

Let us consider a simple method of calculating wave drag proposed by Prof. G. Burago [16]. Let us assume that a local supersonic zone closed by nearly normal shock  $BC$  is formed on the upper side of an airfoil (Fig. 7.3.1a). Let us separate a stream filament passing through this shock in the flow. The parameters of the gas in the filament directly ahead of the shock are  $V_1$ ,  $p_1$ ,  $\rho_1$ , and  $M_1$ , and behind it are

$V_2$ ,  $p_2$ ,  $\rho_2$ , and  $M_2$ . Let us introduce two control surfaces  $I-I$  and  $II-II$  to the left and right of the airfoil at a sufficiently large distance from it; let the parameters of the gas along the left plane be  $V_{1\infty}$ ,  $p_{1\infty}$ , and  $\rho_{1\infty}$ , and along the right plane be  $V_{2\infty}$ ,  $p_{2\infty}$ , and  $\rho_{2\infty}$ .

Using the theorem of the change in the momentum of the mass of a gas when flowing through the control surfaces, we obtain

$$\int_{-\infty}^{\infty} V_{2\infty} dm_{2\infty} - \int_{-\infty}^{\infty} V_{1\infty} dm_{1\infty} = \int_{-\infty}^{\infty} (p_{1\infty} - p_{2\infty}) dy - X_w \quad (7.3.1)$$

where  $p_{1\infty}$  and  $p_{2\infty}$  are the forces acting on the left and right surfaces,  $X_w$  is the force of the wave drag with which the airfoil acts on the flow, and  $dm_{1\infty} = \rho_{1\infty} V_{1\infty} dy_{1\infty}$ ,  $dm_{2\infty} = \rho_{2\infty} V_{2\infty} dy_{2\infty}$  are the rates of flow of the gas along the stream filaments that according to the condition of the constancy of the flow rate are equal, i.e.

$$\rho_{1\infty} V_{1\infty} dy_{1\infty} = \rho_{2\infty} V_{2\infty} dy_{2\infty} \quad (7.3.2)$$

Let us assume (see [16]) that levelling out of the velocities occurs behind the wing at a large distance from it, i.e.  $V_{2\infty} \rightarrow V_{1\infty}$ . Accordingly, and by (7.3.2), we have

$$\int_{-\infty}^{\infty} V_{2\infty} dm_{2\infty} - \int_{-\infty}^{\infty} V_{1\infty} dm_{1\infty} = \int_{-\infty}^{\infty} \rho_{1\infty} V_{1\infty} (V_{2\infty} - V_{1\infty}) dy_{1\infty} = 0$$

Consequently,

$$X_w = \int_{-\infty}^{\infty} (p_{1\infty} - p_{2\infty}) dy \quad (7.3.3)$$

We can assume that for stream filaments not intersecting the shock,  $p_{2\infty} = p_{1\infty}$  i.e. the pressure at a large distance from the airfoil behind it is restored to the value of the free-stream pressure. For the filaments that pass through the shock,  $p_{2\infty} < p_{1\infty}$ . Indeed, since

$$\left. \begin{aligned} p_{1\infty} &= p_0 (1 - V_{1\infty}^2/V_{\max}^2)^{h/(h-1)} \\ p_{2\infty} &= p'_0 (1 - V_{2\infty}^2/V_{\max}^2)^{h/(h-1)} = p'_0 (1 - V_{1\infty}^2/V_{\max}^2)^{h/(h-1)} \end{aligned} \right\} \quad (7.3.4)$$

where  $p'_0 < p_0$ , we have

$$p_{2\infty}/p_{1\infty} = p'_0/p_0 = v_0 < 1 \quad (7.3.5)$$

According to (7.3.5), formula (7.3.3) can be transformed by taking into account the flow rate equation  $\rho_{1\infty} V_{1\infty} dy_{1\infty} = \rho_1 V_1 ds$ , in accordance with which

$$dy_{1\infty} = ds = (\rho_1 V_1 / \rho_{1\infty} V_{1\infty}) ds$$

where  $s$  is the length of the shock.

As a result of transformations, the wave drag force is

$$X_w = p_{\infty} \int_0^S \frac{\rho_1 V_1}{\rho_{1\infty} V_{1\infty}} (1 - v_0) ds \quad (7.3.6)$$

and the coefficient of this force is

$$c_{x,w} = \frac{2X_w}{kp_{\infty} M_{\infty}^2 b} = \frac{2}{kM_{\infty}^2 b} \int_0^S \frac{\rho_1 V_1}{\rho_{1\infty} V_{1\infty}} (1 - v_0) ds \quad (7.3.6')$$

Let us expand the function  $v_0$  in (4.3.20) into a series in powers of  $n = M_1 - 1$ :

$$\begin{aligned} v_0(n) &= v_0(0) + \left( \frac{dv_0}{dn} \right)_{n=0} n + \frac{1}{2} \left( \frac{d^2v_0}{dn^2} \right)_{n=0} n^2 \\ &\quad + \frac{1}{6} \left( \frac{d^3v_0}{dn^3} \right)_{n=0} n^3 + \dots \end{aligned} \quad (7.3.7)$$

In expression (7.3.7), the quantity  $v_0(0) = 1$  because at  $M_1 = 1$  ( $n = 0$ ), the shock transforms into a wave of an infinitesimal strength, and the pressure  $p'_0 = p_0$ .

Using (4.3.13), (4.3.15), and (4.3.20), we can also show that

$$\left( \frac{dv_0}{dn} \right)_{n=0} = \left( \frac{dv_0}{dM_1} \right)_{M_1=1} = 0 \text{ and } \left( \frac{d^2v_0}{dn^2} \right)_{n=0} = \left( \frac{d^2v_0}{dM_1^2} \right)_{M_1=1} = 0$$

Having in view that for thin airfoils at small angles of attack, the difference  $M_1 - 1$  is small, we can limit ourselves to the fourth term in expansion (7.3.7):

$$v_0(n) = 1 + \frac{1}{6} \left( \frac{d^3v_0}{dM_1^3} \right)_{M_1=1} (M_1 - 1)^2 \quad (7.3.7')$$

Investigations have shown that for a given airfoil, the quantity  $M_1 - 1$  can be considered approximately proportional to the difference  $M_{\infty} - M_{\infty,cr}$ . Designating the relevant proportionality factor by  $A_1$  and including it in the overall coefficient  $A$  determined in the form

$$A = -\frac{A_1}{3kM_{\infty}^2 b} \left( \frac{d^3v_0}{dM_1^3} \right)_{M_1=1} \int_0^S \frac{\rho_1 V_1}{\rho_{1\infty} V_{1\infty}} ds \quad (7.3.8)$$

we obtain an expression from (7.3.6') and (7.3.7') for the wave drag coefficient:

$$c_{x,w} = A (M_{\infty} - M_{\infty,cr})^3 \quad (7.3.9)$$

The coefficient  $A$  in the general case depends on the configuration of the airfoil, the angle of attack, and the number  $M_{\infty}$ . It may be considered as approximately constant, however. Tests of modern airfoils installed at small angles of attack in wind tunnels show that

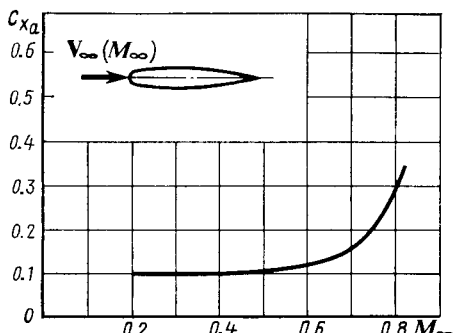


**Fig. 7.3.2**  
Drag of an airfoil in a nearly sonic flow

the coefficient  $A \approx 11$ . At this value, satisfactory results of calculations by formula (7.3.9) are obtained if the difference  $M_\infty - M_{\infty, cr}$  does not exceed 0.15.

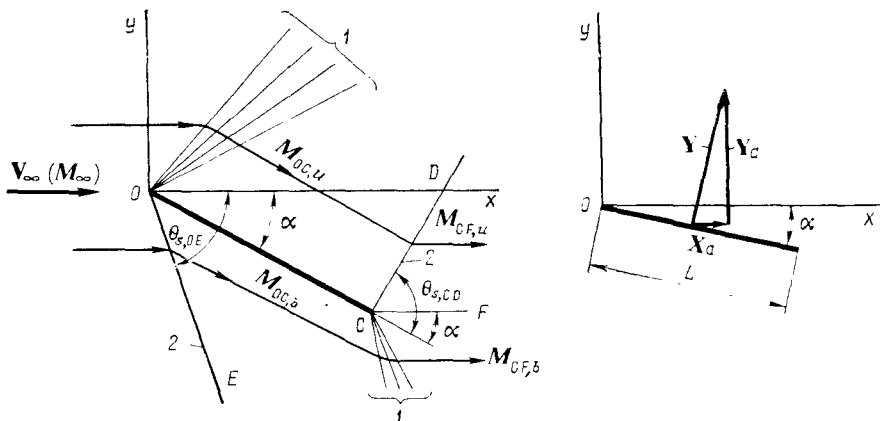
It follows from formula (7.3.9) that the wave drag coefficient increases with increasing  $M_\infty$ . This is due to the fact that upon a growth in the airspeed, the shocks formed on an airfoil become more and more intensive and extended. To lower  $c_{x, w}$  at a given  $M_\infty$ , one must ensure an increase in the number  $M_{\infty, cr}$ , which is achieved mainly by reducing the thickness of the airfoil. A similar result can be obtained when the angle of attack is made smaller.

Figure 7.3.2 shows an experimental curve characterizing the change in the drag coefficient  $c_{x_a} = c_{x, pr} + c_{x, w}$  in nearly sonic flow. For values of  $M_\infty < 0.45-0.5$ , only profile drag is observed, while at  $M_\infty > 0.5-0.55$  (supercritical flow velocities) a wave drag also appears that is due to local shocks.

#### 7.4. Supersonic Flow of a Gas with Constant Specific Heats over a Thin Plate

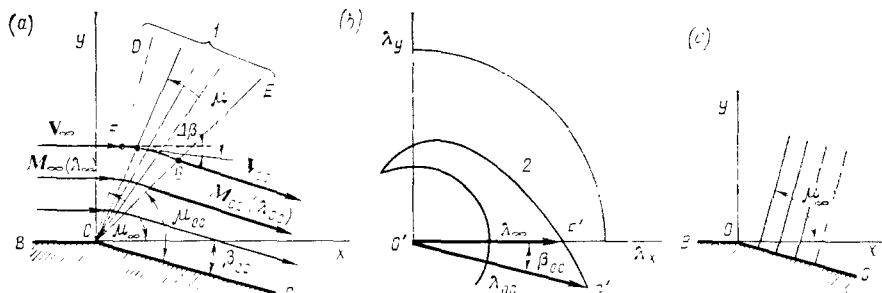
Let us consider a very simple airfoil in the form of an infinitely thin plate placed in a supersonic flow at the angle of attack  $\alpha$ . The flow over such a plate is shown schematically in Fig. 7.4.1. At its leading edge, the supersonic flow divides into two parts—an upper one (above the plate) and a bottom one (under it) that do not influence each other. This is why the supersonic flow over each side can be investigated independently.

Let us consider the upper side of the plate. The flow here is a plane supersonic flow over a surface forming an angle larger than  $180^\circ$  with the direction of the undisturbed flow. Such a flow is shown schematically in Fig. 7.4.2, where plane  $OC$  corresponds to the upper

**Fig. 7.4.1**

Supersonic flow over a thin plate:

1—expansion fan; 2—shock

**Fig. 7.4.2**

Prandtl-Meyer flow:

a—physical plane; b—hodograph plane; c—diagram of a nearly uniform flow; 1—expansion fan; 2—epicycloid

side of the plate. It was first investigated by L. Prandtl and T. Meyer and is called a **Prandtl-Meyer flow**.

In accordance with the flow diagram in Fig. 7.4.2a, the flow parallel to plane  $OB$  when passing around angle  $O$  gradually turns, expands, and acquires a new direction parallel to plane  $OC$ . The angle  $\beta_{OC}$  of inclination of this plane to the vector  $V_\infty$  corresponds to the angle of attack  $\alpha$  of the plate (see Fig. 7.4.1). The disturbed region of the expanding flow is limited at the left-hand side by Mach line  $OD$  inclined to the free-stream velocity vector  $V_\infty$  at the angle  $\mu_\infty = \sin^{-1}(1/M_\infty)$ , where  $M_\infty$  is the Mach number of the undisturbed flow. The expansion process terminates on Mach line  $OE$  inclined to

the disturbed velocity vector  $\mathbf{V}_{OC}$  at the angle  $\mu_{OC} = \sin^{-1}(1/M_{OC})$  determined from the Mach number  $o$  the disturbed flow along plane  $OC$ . The change in the direction of the flow between Mach lines  $OD$  and  $OE$  can be represented as a consecutive set of deflections of the streamlines through the small angles  $\Delta\beta$ . A straight Mach line issuing from point  $O$  corresponds to each of these deflections indicating the formation of an additional disturbance.

Hence, the turning flow is filled with an infinite multitude of Mach lines forming a "fan" of disturbance lines that characterizes a **centered expansion wave**. This centered wave, sometimes called a **Prandtl-Meyer fan**, is defined by straight Mach lines along each of which the flow parameters are constant, and this is why it belongs to the class of simple expansion waves.

The problem on the disturbed motion of a gas near an obtuse angle, which is associated with the formation of a centered expansion wave, can be solved according to the method of characteristics. Point  $F'$  on an epicycloid—a characteristic in a hodograph of the same family—corresponds to point  $F$  of intersection of a streamline belonging to the plane parallel oncoming flow (the inclination of a streamline at this point is  $\beta = 0$ ) with characteristic  $OD$  in a physical plane. To be specific, we can relate each of these characteristics to those of the first family. The equation  $\beta = \omega + \beta_1$  is used for a characteristic of this family in the hodograph. Since we have assumed that  $\beta = 0$ , the constant  $\beta_1 = -\omega_\infty (M_\infty)$ , where the angle  $\omega_\infty$  is found from (5.3.30) according to the known number  $M_\infty$ . Consequently, the equation for the characteristic has the form  $\beta = \omega - \omega_\infty$ , whence

$$\omega = \beta + \omega_\infty \quad (7.4.1)$$

By setting the inclination of a streamline on the small angle  $\beta = \Delta\beta$ , we can calculate the corresponding angle  $\omega = \Delta\beta + \omega_\infty$  and find the number  $M$  on the neighbouring Mach line inclined to the new direction of a streamline at the angle  $\mu = \sin^{-1}(1/M)$ . The Mach number on plane  $OC$  with an inclination of  $\beta = \beta_{OC} = \alpha$ , i.e. on the upper side of the plate, is determined according to the angle

$$\omega_{OC} = \beta_{OC} + \omega_\infty \quad (7.4.2)$$

The found value of the local number  $M_{OC}$  makes it possible to determine the Mach angle  $\mu_{OC} = \sin^{-1}(1/M_{OC})$ . A graphical solution of the problem on the Prandtl-Meyer flow is shown in Fig. 7.4.2b. The coordinate of point  $G'$  of intersection of the epicycloid with straight line  $O'G'$  parallel to plane  $OC$  determines the speed ratio  $\lambda_{OC}$  of the disturbed flow near plane  $OC$ . The point  $G$  of intersection of a streamline with characteristic  $OE$  corresponds to point  $G'$  in a physical plane.

According to the known number  $M_{OC}$  ( $\lambda_{OC}$ ), by using formula (3.6.30), we can determine the pressure on the upper side of the plate:

$$p_u = p_{OC, u} = p_\infty \left[ \left( 1 + \frac{k-1}{2} M_\infty^2 \right) / \left( 1 + \frac{k-1}{2} M_{OC}^2 \right) \right]^{k/(k-1)} \quad (7.4.3)$$

and the corresponding value of the pressure coefficient:

$$\bar{p}_u = \bar{p}_{OC, u} = 2 (p_{OC, u} - p_\infty) / (k M_\infty^2 p_\infty)$$

At hypersonic velocities ( $M_\infty \gg 1$ ), the calculation of the Prandtl-Meyer flow is simplified, because to determine the function  $\omega$  we can use formula (5.3.41). This allows us to determine the local number  $M$  directly. Substituting for the angles  $\omega_{OC}$  and  $\omega_\infty$  in (7.4.2) their values in accordance with (5.3.41), we obtain

$$M_u = M_{OC} = \left( \frac{1}{M_\infty} - \frac{k-1}{2} \beta_{OC} \right)^{-1} \quad (7.4.4)$$

The corresponding pressure can be determined by formula (3.6.39).

Let us consider the Prandtl-Meyer flow appearing at hypersonic velocities with small flow deflections  $\beta_{OC} = \alpha$ . At very large numbers  $M_\infty$ , the beam of Mach lines issuing from point  $O$  will be very narrow. We can consider to a sufficiently good approximation that the beam is compressed into a single line on which the flow immediately turns, with expansion. This line can therefore be conditionally considered as an "expansion shock" behind which the velocities (Mach numbers) grow and the pressures lower. The angle  $\mu'_{OC}$  of inclination of this line to the vector  $V_\infty$  is obtained if we take advantage of the analogy with a compression shock and calculate this angle by formula (4.6.9) provided that the angle  $\beta_s = \beta_{OC} = \alpha$  in this formula is negative. Assuming that  $\theta_s = \mu'_{OC}$ , we find

$$\frac{\mu'_{OC}}{|\beta_{OC}|} = \frac{1}{2(1-\delta)} + \sqrt{\frac{1}{4(1-\delta)^2} + \frac{1}{K^2}} \quad (7.4.5)$$

where  $|\beta_{OC}| = |\alpha|$  is the magnitude of the turning angle of the flow (the angle of attack), and  $K^2 = (M_\infty \beta_{OC})^2$ .

By using formula (4.6.11') to evaluate the pressure coefficient with a view to the sign of the angle  $\beta_{OC} = \alpha$ , we obtain

$$\frac{\bar{p}_u}{\alpha^2} = \frac{\bar{p}_{OC, u}}{\alpha^2} = \frac{1}{1-\delta} - \sqrt{\frac{1}{(1-\delta)^2} + \frac{4}{K^2}} \quad (7.4.6)$$

At low numbers  $M_\infty$  and small angles  $\beta_{OC} = \alpha$ , a nearly uniform Prandtl-Meyer flow appears near the deflected surface. For such a flow, relation (7.1.2') for the speed of sound holds. If we now find a formula for the Mach number from (7.1.2), namely,

$$M^2 = \frac{V^2}{a^2} = \frac{2}{k-1} \left( \frac{a_\infty^2}{a^2} - 1 \right) + \frac{V_\infty^2}{a^2}$$

and introduce the value of  $a^2$  from (7.1.2') into this formula, we obtain

$$\frac{V^2}{a^2} = M^2 = M_\infty^2 \left( 1 + \frac{2u}{V_\infty} \right) \left[ 1 - (k-1) \frac{u V_\infty}{a_\infty^2} \right]^{-1} \quad (7.4.7)$$

In accordance with this expression, we can assume in a first approximation that in a nearly uniform flow  $M \approx M_\infty$  and, consequently, the equation  $dy/dx = \tan(\beta \pm \mu_\infty)$  is used for the characteristics in a physical plane. Since the flow deflection angle  $\beta$  is small and  $\beta \ll \mu_\infty$ , then  $dy/dx \approx \pm \tan \mu_\infty$ . Consequently, the characteristics are Mach lines inclined to the  $x$ -axis at angles of  $\pm \mu_\infty$ . For a Prandtl-Meyer flow, we have a family of characteristics in the form of parallel lines inclined to the horizontal axis at the angle  $\mu_\infty$  (Fig. 7.4.2c).

We obtain difference equations for the characteristics in the hodograph of a supersonic flow from (5.3.21) and (5.3.22):

$$\Delta V/V \mp \tan \mu \Delta \beta = 0 \quad (7.4.8)$$

For a nearly uniform flow, we have

$$\Delta V = u, \quad V = V_\infty, \quad \Delta \beta = \beta, \quad \tan \mu = \tan \mu_\infty = (M_\infty^2 - 1)^{-1/2}$$

Consequently,

$$u/V_\infty = \pm \beta / \sqrt{M_\infty^2 - 1} \quad (7.4.8')$$

Inserting the value of  $u$  from (7.4.8') into (6.1.5), we obtain the pressure coefficient

$$\bar{p} = \mp 2\beta / \sqrt{M_\infty^2 - 1} \quad (7.4.9)$$

Since we are considering an expanding flow for which  $\bar{p} < 0$  and are having in view that the magnitude of the angle  $\beta$  is being found, we must take the minus sign in formula (7.4.9). Accordingly, on the upper side of the plate inclined at a small angle of attack  $\beta = \alpha$ , the pressure coefficient is

$$\bar{p}_u = \bar{p}_{OC,u} = -2\alpha / \sqrt{M_\infty^2 - 1} \quad (7.4.10)$$

Let us consider the *bottom* side of the plate. The flow over this side (see Fig. 7.4.1) is attended by the formation of shock  $OE$  issuing from a point on the leading edge and, consequently, by compression of the flow. To determine the angle  $\theta_{s,OE}$  of inclination of the shock, we should use formula (4.3.25) in which we must assume that  $M_1 = M_\infty$  and  $\beta_s = \alpha$ . According to the found value of  $\theta_{s,OE}$ , we find the Mach number  $M_2 = M_{OC,b}$  on the bottom side by (4.3.19) or (4.3.19').

When determining the nature of the flow in the region behind point  $C$  on the trailing edge, we can proceed from the following considerations. On the upper side of the plate, the number  $M_{OC,u}$  ahead of shock  $CD$  is larger than the number  $M_\infty$  ahead of shock  $OE$

formed on the leading edge from below. If we assume that behind point  $C$  the flow does not deflect from the direction of the undisturbed flow (streamline  $CF$  is parallel to the vector  $\mathbf{V}_\infty$ ), the losses in the upper shock will evidently be greater, and therefore  $M_{CF,u} < M_{OC,b}$ . The pressure in the region above line  $CF$  will be greater than in that below it.

A pressure jump cannot be retained on a boundary surface in a gas flow, although the velocities may remain different. Therefore, in real conditions, the direction of streamline  $CF$  differs from that of the free-stream velocity, i.e. a downwash of the flow forms behind the plate. It is clear from physical notions that line  $CF$  deviates in the direction of the bottom region. Here turning of the flow behind shock  $CD$  through a smaller angle is ensured, which is just what leads to lowering of the pressure.

Investigations show that the downwash angle is small, hence to a sufficiently good approximation we can proceed from the assumption that at point  $C$  the direction of the flow coincides with that of the free stream. Accordingly, the shock angle  $\theta_{s,CD}$  on the upper side is determined by formula (4.3.25) in which we assume that  $M_1 = M_{OC,u}$  and  $\beta_s = \alpha$ . The corresponding Mach number behind the shock  $M_2 = M_{CF,u}$  is determined from (4.3.19) or (4.3.19') according to the values of  $\theta_s = \theta_{s,CD}$ ,  $M_1 = M_{OC,u}$ , and  $\beta_s = \alpha$ .

Below line  $CF$  in the region behind the trailing edge, a Prandtl-Meyer flow appears with the Mach number  $M_{CF,b}$  determined with the aid of the formula  $\omega_{CF,b} = \omega_{OC,b} + \alpha$ .

The pressure  $p_u = p_{OC,u}$  on the upper side of the plate is determined by formula (7.4.3), while the corresponding pressure  $p_b = p_{OC,b}$  on the bottom side is calculated by expression (4.3.15) in which it is assumed that  $p_2 = p_b$ ,  $p_1 = p_\infty$ ,  $\theta_s = \theta_{s,OE}$ , and  $p_u < p_\infty < p_b$ .

If the length of the plate is  $L$ , and its width is taken equal to unity, the force produced by the normal pressure applied to the plate is  $Y = L(p_b - p_u)$ . Consequently, the lift force is  $Y_a = Y \cos \alpha$ , while the drag is  $X_a = Y \sin \alpha$ . The corresponding values of the lift and drag coefficients are  $c_{y_a} = Y/(q_\infty L)$  and  $c_{x_a} = X_a/(q_\infty L)$ . Introducing the pressure coefficients  $\bar{p}_u = (p_u - p_\infty)/q_\infty$  for the upper and  $\bar{p}_b = (p_b - p_\infty)/q_\infty$  for the lower sides, respectively, we obtain the following expressions for the aerodynamic coefficients:

$$c_{y_a} = (\bar{p}_b - \bar{p}_u) \cos \alpha, \quad c_{x_a} = (\bar{p}_b - \bar{p}_u) \sin \alpha \quad (7.4.11)$$

The force  $X_a$  appearing upon supersonic flow over the plate and caused by the formation of shock waves and ordinary disturbance waves is called the **wave drag**, and the corresponding quantity  $c_{x_a} = c_{xw}$  is called the **wave drag coefficient**. This drag does not equal zero even in an ideal (inviscid) fluid.

The fineness of the plate  $K = c_{y_a}/c_{x_a} = \cot \alpha$  can be seen to be a function of only the angle of attack. Owing to the uniform distribution of the pressure over the surface of the plate, the centre of pressure is at its middle. Consequently, the moment of the pressure forces about the leading edge is  $M_z = -YL/2$ , and the corresponding moment coefficient is

$$m_z = m_{z_a} = M_z/(q_\infty L^2) = -(\bar{p}_b - \bar{p}_u)/2 \quad (7.4.12)$$

At hypersonic velocities, the pressure coefficient for the upper side of the plate is determined approximately by (7.4.6), and for its lower side, by (4.6.12). With this in view and assuming in (4.6.12) that  $\beta_s = \alpha$ , we obtain for the difference of the pressure coefficients  $\bar{p}_b - \bar{p}_u$ , also known as the **pressure-drop coefficient**, the expression

$$(\bar{p}_b - \bar{p}_u)/\alpha^2 = 4\sqrt{1/[4(1-\delta)^2] + 1/K^2} \quad (7.4.13)$$

Consequently,

$$c_{y_a}/\alpha^2 = 4\sqrt{1/[4(1-\delta)^2] + 1/K^2} \quad (7.4.14)$$

$$c_{x_a}/\alpha^3 = 4\sqrt{1/[4(1-\delta)^2] + 1/K^2} \quad (7.4.15)$$

$$m_{z_a}/\alpha^2 = -2\sqrt{1/[4(1-\delta)^2] + 1/K^2} \quad (7.4.16)$$

Formulas (7.4.13)-(7.4.16) express the law of hypersonic similarity as applied to the flow over a thin plate. This law consists in that regardless of the values of  $M_\infty$  and  $\alpha$ , but at identical values of  $K = M_\infty \alpha$ , the corresponding quantities  $\bar{p}/\alpha^2$ ,  $c_{y_a}/\alpha^2$ ,  $c_{x_a}/\alpha^3$ , and  $m_{z_a}/\alpha^2$  for plates are identical. The parameter  $K = M_\infty \alpha$  is called the **hypersonic similarity criterion**.

Examination of formulas (7.4.13)-(7.4.16) reveals that the relations for the pressure, lift, and moment coefficients are quadratic, and for the drag coefficients—cubic functions of the angle of attack  $\alpha$ . At the limit, when  $K \rightarrow \infty$ , we have

$$(\bar{p}_b - \bar{p}_u)/\alpha^2 = c_{y_a}/\alpha^2 = c_{x_a}/\alpha^3 = 2/(1-\delta) \quad (7.4.17)$$

$$m_{z_a}/\alpha^2 = -1/(1-\delta) \quad (7.4.18)$$

For a plate in a nearly uniform (linearized) flow, the pressure coefficients are calculated by formula (7.4.9) in which we should assume that  $\beta = \alpha$ . The minus sign in this formula determines the pressure coefficient for the upper side, and the plus sign—for the bottom side. Accordingly, the difference between the pressure coefficients related to the angle of attack is

$$(\bar{p}_b - \bar{p}_u)/\alpha = 4/\sqrt{M_\infty^2 - 1} \quad (7.4.19)$$

Introducing (7.4.19) into formulas (7.4.11) and (7.4.12), we obtain

$$c_{y_a}/\alpha = 4/\sqrt{M_\infty^2 - 1} \quad (7.4.20)$$

$$c_{x_a}/\alpha^2 = 4/\sqrt{M_\infty^2 - 1} \quad (7.4.21)$$

$$m_{z_a}/\alpha = -2/\sqrt{M_\infty^2 - 1} \quad (7.4.22)$$

In the given case, the number  $M_\infty$  is the similarity criterion. When its value is retained, and regardless of the value of the angle of attack, the corresponding values of  $\bar{p}/\alpha$ ,  $c_{y_a}/\alpha$ ,  $c_{x_a}/\alpha^2$ , and  $m_{z_a}/\alpha$  are identical. If we consider a nearly uniform flow at very large numbers  $M_\infty \gg 1$ , formulas similar to (7.4.19)-(7.4.22) can be written in the form

$$(\bar{p}_b - \bar{p}_u)/\alpha^2 = c_{y_a}/\alpha^2 = c_{x_a}/\alpha^3 = 4/K \quad (7.4.23)$$

$$m_{z_a}/\alpha^2 = -2/K \quad (7.4.24)$$

Hence, the hypersonic similarity criterion  $K = M_\infty \alpha$  is also valid for a nearly uniform (linearized) flow with large Mach numbers. It is evident that such a flow can appear only at very small angles of attack.

### 7.5. Parameters of a Supersonic Flow over an Airfoil with an Arbitrary Configuration

#### Use of the Method of Characteristics

Let us consider a supersonic flow over a sharp-nosed airfoil with an arbitrary configuration (Fig. 7.5.1). The upper contour of the airfoil is given by the equation  $y_u = f_u(x)$ , and the bottom one by the equation  $y_b = f_b(x)$ . Assume that the angle of attack is larger than the angle  $\beta_{0,u}$  formed by a tangent to the airfoil contour on its upper side at point  $O$  on the leading edge. Consequently, a Prandtl-Meyer flow develops at this point. The flow passes through an *expansion fan* issuing from point  $O$  as from a source of disturbances, and acquires a direction tangent to the contour at this point. Further expansion of the flow occurs behind point  $O$  along the contour. Consequently, the flow near the airfoil can be considered as a *consecutive set of Prandtl-Meyer flows*. Since the turning angle at the points on the contour is infinitely small, individual Mach lines issue from them instead of a fan of expansion lines (Fig. 7.5.1).

We find the velocity at point  $O$  by formula (7.4.2), which we shall write in the form

$$\omega_0 = \omega_\infty + \alpha - \beta_{0,u} \quad (7.5.1)$$

where  $\beta_{0,u} = \tan^{-1}(dy_u/dx)_0$ .

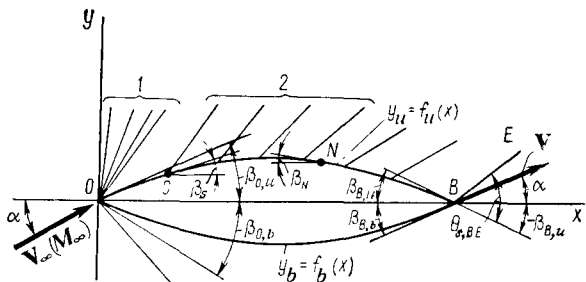


Fig. 7.5.1

Supersonic flow over a sharp-nosed airfoil:

1—expansion fan; 2—Mach lines

Using the value of  $\omega_0$ , we determine the corresponding number  $M_0$  from Table 5.3.1. At point  $C$ , which is at a small distance from the nose, the velocity of the gas is calculated as for a Prandtl-Meyer flow by the formula

$$\omega_C = \omega_\infty + \beta_{0,u} - \beta_C \quad (7.5.2)$$

where  $\beta_C = \tan^{-1}(dy_u/dx)_C$ .

Inserting Eq. (7.5.1) into (7.5.2), we obtain

$$\omega_C = \omega_\infty + \alpha - \beta_C \quad (7.5.3)$$

Hence, by (7.5.3) for any arbitrary point  $N$  on the contour, we have

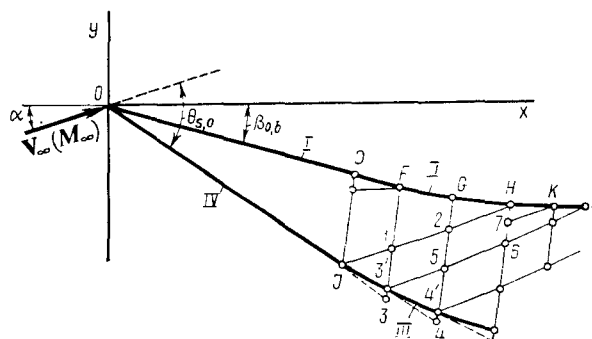
$$\omega_N = \omega_\infty + \alpha - \beta_N \quad (7.5.4)$$

where  $\beta_N = \tan^{-1}(dy_u/dx)_N$  is the angle calculated with a view to the sign (for the leading part of the contour the signs of the angles are positive, and for the trailing part, negative).

Let us assume, as for flow over a flat plate, that the flow behind point  $B$  approximately retains the direction of the free stream. Therefore, at point  $B$ , the flow moving near the contour at a velocity corresponding to the number  $M_{B,u}$  turns, and a shock  $BE$  appears issuing from point  $B$ . The angle  $\theta_{s,BE}$  of inclination of the shock and the parameters behind it are calculated with the aid of the relevant formulas of the shock theory according to the known values of the angle of attack  $\alpha$ , the number  $M_{B,u}$ , and the contour nose angle at point  $B$  on the upper side. The parameters on the upper side of the airfoil (pressure, velocity, etc.) are determined from the known value of the local Mach number with the aid of the relations for an isentropic flow of a gas.

If the angle of attack equals the angle  $\beta_{0,u}$ , we have the *limiting case* of a Prandtl-Meyer flow at point  $O$  where the Mach number is  $M_{0,b} = M_\infty$ . Formula (7.5.4) can be written as

$$\omega_N = \omega_\infty + \beta_{0,u} - \beta_N \quad (7.5.4')$$

**Fig. 7.5.2**

Supersonic flow over the bottom side of an airfoil with the formation of a shock:  
 I—straight part of the contour of the airfoil in the flow; II—curved part of the airfoil contour;  
 III—curved part of the shock; IV—straight part of the shock

Calculation of the flow over the bottom side of the airfoil (Fig. 7.5.2) begins with determination of the gas parameters at point  $O$ —directly behind the shock. For this purpose, using formula (4.3.25) and the values  $M_1 = M_\infty$  and  $\beta_C = \alpha + \beta_{0,b}$ , we calculate the shock angle  $\theta_{s,0}$ . We find the number  $M_{O,b} = M_2$  at point  $O$  from (4.3.19) or (4.3.19'). We may assume that this number remains constant within a very small neighbourhood of point  $O$  on straight line element  $OD$  of the contour. Straight element  $OJ$  of an oblique shock corresponds to  $OD$ . Its length is determined as the distance from point  $O$  to point  $J$  that is on the intersection of the shock with a first family characteristic issuing from point  $D$ .

The flow behind a straight shock is *vortex-free*, consequently there is an isentropic flow over part of the contour behind point  $D$ . To determine the velocity of such a flow at point  $F$ , we shall use Eq. (7.4.1), from which we find  $\omega_F = \omega_D - (\beta_D - \beta_F)$ , where  $\omega_D$  is the value of the angle  $\omega$  calculated by formula (5.3.30) for the number  $M$  on part  $OD$  of the contour. The values of the angles  $\beta_D$  and  $\beta_F$  are determined with a view to the sign (in the given case the angles  $\beta_D$  and  $\beta_F$  are negative on the leading part of the contour).

The flow near part  $DF$  of the contour can be considered as a Prandtl-Meyer flow, therefore disturbance line  $F-1-3$  issues from point  $F$  as from a perturbation source. It intersects the continuation of the normal shock at point  $3$  and curves it, as a result of which the actual direction of the shock is determined by point  $3$  of intersection of the shock and the characteristic.

Downstream, curving of the shock is due to its interaction with the characteristics issuing from points  $G$ ,  $H$ ,  $K$ , etc. Curving of the shock causes a *vortex flow* to form for whose calculation we must use relations on the characteristics for a non-isentropic plane flow. The

second family characteristic  $JH$  is the boundary of this vortex flow. The characteristic is gradually constructed in the form of a broken line according to the known values of the number  $M$  and the angles  $\beta$  along the straight second family characteristics issuing from contour points  $F$ ,  $G$ , etc. At point  $H$  of the contour, which is simultaneously on characteristic  $JH$ , the velocity is found from the expression  $\omega_H = \omega_D - (\beta_D - \beta_H)$ . At point  $K$  adjacent to  $H$ , the parameters are calculated according to the equations for the characteristics taking into account the vortex nature of the flow behind a shock. To determine the velocity at this point, it is sufficient to know the velocity and its direction (the angle  $\beta$ ) at point  $7$  near point  $K$  on element  $7-K$  of the second family characteristic. To find this velocity, it is necessary to calculate the curving of the shock behind point  $J$  on element  $J-3'$  and find the parameters on the shock at point  $3'$ . To do this, we have the following data at our disposal: the number  $M = M_1 = M_F$  and the angle  $\beta = \beta_F$  of deflection of the flow at point  $I$ , and also the parameters  $M_2 = M_J$  and  $\beta_s = \beta_{s,J}$  on the shock at point  $J$ . By using formula (5.4.46) and assuming that  $\epsilon = 0$ , we obtain the following expression for the change in the angle  $\beta$  along characteristic  $I-3$ :

$$\Delta\beta_1 = \left[ \left( \frac{d\omega}{d\beta} \right)_J - 1 \right]^{-1} \left( \omega_1 - \omega_J - \frac{\Delta x_1}{kR} \cdot \frac{\Delta S}{\Delta n} c_1 \right) \quad (7.5.5)$$

where  $\Delta\beta_1 = \beta_3 - \beta_1$ ,  $\Delta x_1 = x_3 - x_1$ ;

$$\frac{\Delta S}{\Delta n} = \frac{(S_3 - S_1) \cos(\beta_1 + \mu_1)}{(x_3 - x_1) \sin \mu_1}, \quad c_1 = \frac{\sin^2 \mu_1 \cos \mu_1}{\cos(\beta_1 + \mu_1)}$$

The derivative  $(d\omega/d\beta)_J$  is evaluated by (5.4.39) for the values of the relevant parameters at point  $I$ ; the angles  $\omega_1$  and  $\omega_J$  are determined from (5.3.30) according to the numbers  $M$  at points  $I$  and  $J$ , respectively.

Point  $3$  in Fig. 7.5.2 is at the intersection of the normal shock and characteristic  $I-3$ . Consequently, its coordinates are found as a result of the simultaneous solution of the equations

$$y_3 - y_1 = (x_3 - x_1) \tan(\beta_1 + \mu_1), \quad y_3 = x_3 \tan(\theta_{s,O} - \alpha) \quad (7.5.6)$$

The intersection of the characteristic with the shock at point  $3'$  is different because of *curving* of the shock. We shall find the new shock angle  $\theta_{s,J3'}$  on  $J-3'$  according to the flow deflection angle behind the shock  $\beta_s = \beta_{3'} = \Delta\beta_1 + \beta_1$  and the number  $M'_3$  calculated by means of the expression  $\omega'_3 = \Delta\omega_1 + \omega_1$  in which  $\Delta\omega_1$  is found from (5.4.38):

$$\Delta\omega_1 = \omega_J + (d\omega/d\beta)_J \Delta\beta_1 - \omega_1 \quad (7.5.7)$$

Consequently, the equation of the shock element  $J-3'$  has the form

$$y_{3'} - y_J = (x_{3'} - x_J) \tan(\theta_{s,J3'} - \alpha)$$

Owing to deflection of the flow at point  $3'$ , the characteristic on element  $1-3'$  changes its direction. The equation of the characteristic on this element has the form

$$y_{3'} - y_1 = (x_{3'} - x_1) \tan (\beta_{3'} + \mu_{3'})$$

By solving these two equations simultaneously, we find the coordinates  $x_{3'}$  and  $y_{3'}$  of point  $3'$ .

Let us consider point  $5$  at the intersection of characteristic elements  $2-5$  of the first and  $3'-5$  of the second family. We determine the coordinates  $y_5$  and  $x_5$  of this point from the solution of the equations for the elements of the corresponding characteristics:

$$\left. \begin{aligned} y_5 - y_2 &= (x_5 - x_2) \tan (\beta_2 + \mu_2) \\ y_5 - y_{3'} &= (x_5 - x_{3'}) \tan (\beta_{3'} - \mu_{3'}) \end{aligned} \right\} \quad (7.5.8)$$

We determine the change in the direction of the flow when passing from point  $2$  to point  $5$  along characteristic element  $2-5$  from Eq. (5.4.22) in which we assume that  $\epsilon = 0$ :

$$\Delta\beta_2 = \frac{1}{2} \left[ \frac{1}{kR} \cdot \frac{\Delta S}{\Delta n} (\Delta x_{3'} t_{3'} + \Delta x_2 c_2) - (\omega_2 - \omega_{3'}) - (\beta_2 - \beta_{3'}) \right] \quad (7.5.9)$$

where  $\Delta\beta_2 = \beta_5 - \beta_2$ ;  $\Delta x_{3'} = x_5 - x_{3'}$ ;

$$\frac{\Delta S}{\Delta n} = \frac{(S_{3'} - S_2) \cos (\beta_2 + \mu_2) \cos (\beta_{3'} - \mu_{3'})}{f + \epsilon}$$

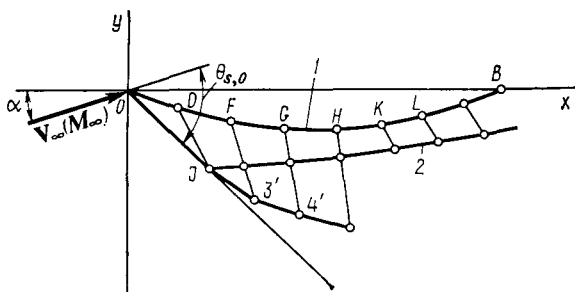
we assume that

$$f = (x_5 - x_2) \sin \mu_{3'} \cos (\beta_2 + \mu_2);$$

$$e = (x_5 - x_{3'}) \sin \mu_2 \cos (\beta_{3'} - \mu_{3'})$$

We determine the values of  $c_2$  and  $t_{3'}$  by (5.4.15). We find the number  $M$  at point  $5$  from (5.4.23) using  $\Delta\beta_2$ . Similarly, according to the known values of the gas parameters at point  $5$  and at point  $H$  on the wall, we determine the velocity at point  $6$  at the intersection of the characteristic elements  $H-6$  of the first family and  $5-6$  of the second one. We find the coordinates  $x_H$  and  $y_H$  of point  $H$  by solving the equations of the contour  $y_H = f_H(x_H)$  and of element  $2-H$  of the characteristic  $y_H - y_2 = (x_H - x_2) \tan (\beta_2 - \mu_2)$ .

Let us now choose arbitrary point  $7$  with the coordinates  $x_7$  and  $y_7$  on characteristic element  $H-6$ . We shall determine the parameters at this point by interpolation. For example, the angle  $\beta_7 = \beta_6 - (\beta_6 - \beta_H) l_{6-7} / l_{6-H}$ , where  $l_{6-7}$  and  $l_{6-H}$  are the distances from point  $6$  to point  $7$  and to point  $H$ , respectively. Similarly, we can find the number  $M_7$  and the corresponding Mach angle  $\mu_7$ . We choose point  $7$  so that characteristic element  $7-K$  drawn from this point at the angle  $\beta_7 - \mu_7$  will intersect the contour at point  $K$  at a small distance from point  $H$ . We determine the coordinates  $x_K$ ,  $y_K$  of this

**Fig. 7.5.3**

Supersonic isentropic flow over a curved sharp-nosed airfoil:  
1—contour of the body in the flow; 2—second family characteristic

point as a result of solving the equation  $y_K - y_7 = (x_K - x_7) \times \tan(\beta_7 - \mu_7)$  for the characteristic element  $7-K$  and the equation  $y_K = f_H(x_K)$  of the contour. Since the flow at point  $K$  is a vortex one, Eq. (5.4.27) must be used to calculate the velocity at this point. Assuming in the equation that  $\epsilon = 0$ , we obtain

$$\Delta\omega_7 = -\Delta\beta_7 - \frac{\Delta x_7}{kR} \cdot \frac{\Delta S}{\Delta n} t_7 \quad (7.5.10)$$

where  $\Delta\omega_7 = \omega_K - \omega_7$  and  $\Delta\beta_7 = \beta_K - \beta_7$ , the angle  $\beta_K = \tan^{-1}(dy_H/dx)_K$ . We determine the parameter  $t_7$  from (5.4.28) for the values  $\mu_7$  and  $\beta_7$  and evaluate the entropy gradient by the formula (5.4.29):

$$\Delta S/\Delta n = (S_7 - S_K) \cos(\beta_7 - \mu_7)/[(x_K - x_7) \sin \mu_7]$$

We find the entropy  $S_K$  at point  $K$  as a result of calculating its value at point  $O$  directly behind the shock, and the entropy  $S_7$  at point  $7$  by interpolation between its values at points  $H$  and  $G$ .

Similarly, by consecutively solving each of the three problems considered in Sec. 5.4, we determine the velocity field in the region between characteristic  $DJ$ , the contour, and curved shock  $J-3'-4'$ . We find the shape of this shock gradually in the form of a broken line, and fill the indicated region of the flow with a **network of characteristic curves (characteristics)**.

We can determine the pressure at the nodes of the network of characteristics according to the Mach number with the aid of formula (3.6.28). We calculate the corresponding stagnation pressure  $p_0 = p'_0$  needed in this formula by interpolation, using formula (5.4.19). We find the pressure at points on the contour using the corresponding Mach numbers and the stagnation pressure  $p_0 = p'_0$  evaluated by (4.3.22) for the angle  $\theta_{s,O}$  and the number  $M_\infty$ .

Calculation of the flow on the bottom side of an airfoil is simplified when a second family characteristic drawn from point  $J$  does not intersect the contour, and, consequently, this flow can be considered as an isentropic one (Fig. 7.5.3). We use Eq. (5.3.38) to calculate the Mach number at arbitrary point  $L$  of the contour:

$$\omega_b = \omega_D - (\beta_D - \beta_L) \quad (7.5.11)$$

Here we determine the angle  $\beta_L$  by the formula  $\beta_L = \tan^{-1}(dy_H/dx)_L$  with a view to the sign: at the leading edge of the contour it is negative, at the trailing edge, positive, the angle  $\beta_D$  is negative. We determine the shape of the shock by its angles  $\theta_s$  at points  $3'$  and  $4'$  at the intersection of the straight characteristics drawn from points  $F$  and  $G$ . We find the shock angle  $\theta_s$  at point  $3'$  approximately by formula (4.3.25), using the values of  $\beta_{3'} = \beta_F$  and  $M_\infty$ . We calculate the shock angle at point  $4'$  in a similar way.

We have considered the calculation of the flow at such angles of attack  $\alpha \geq \beta_{O,u}$  when there is an expanding flow all over the upper side. If this condition is not observed ( $\alpha < \beta_{O,u}$ ), the flow over the upper contour occurs with compression of the gas at the leading edge and the *formation of a compression shock*. Hence, such a flow should be calculated in the same way as for the bottom surface.

### Hypersonic Flow over a Thin Airfoil

If a thin sharp-nosed airfoil (see Fig. 7.5.1) is in a hypersonic flow at such small angles of attack that the local Mach numbers on its upper and bottom surfaces at all points considerably exceed unity and, in addition, the conditions of isentropic flow over the bottom contour (Fig. 7.5.3) are retained, we can use simplified relations for the characteristics to calculate the disturbance velocity.

If the angle of attack  $\alpha \geq \beta_{O,u}$ , to determine the number  $M$  at an arbitrary point  $N$  on the upper contour, we must use the formula

$$M_N = \left[ \frac{1}{M_\infty} - \frac{k-1}{2} (\alpha - \beta_N) \right]^{-1} \quad (7.5.12)$$

obtained from (7.4.4).

Since everywhere on the upper contour there is an *expanding flow*, the number  $M_N > M_\infty$ .

Flow over the bottom surface is attended by the formation of a shock and, therefore, by *compression of the gas*. We calculate the pressure coefficient at point  $O$  directly behind the shock with the aid of formula (4.6.12) as follows:

$$\bar{p}_b / (\alpha - \beta_{O,b})^2 = 1/(1-\delta) + \sqrt{1/(1-\delta)^2 + 4/K^2} \quad (7.5.13)$$

where  $K = M_\infty (\alpha - \beta_{O,b})$ ; we take the angle  $\beta_{O,b}$  with a minus sign.

From the formula  $\bar{p}_b = 2\theta_{s,0}(\alpha - \beta_{0,b})$ , we can calculate the shock angle  $\theta_{s,0}$ , and then using the value of  $K_s = M_\infty \theta_{s,0}$  we can find the Mach number at point  $O$ , using formula (4.6.16):

$$M_{O,b}^2/M_\infty^2 = K_s^2 / \{(1 + \delta) K_s^2 - \delta\} (1 - \delta + \delta K_s^2\} \quad (7.5.14)$$

Behind point  $O$ , expansion of the flow occurs, therefore to determine the velocity at an arbitrary point  $L$ , we can use the relation

$$M_L = \left[ \frac{1}{M_{O,b}} + \frac{k-1}{2} (\beta_{O,b} - \beta_L) \right]^{-1} \quad (7.5.15)$$

Hypersonic flow over a thin airfoil can be calculated approximately by using the **method of tangent wedges**. According to this method, we calculate the flow at an arbitrary point of a contour by the relevant formulas for a flat plate assuming that the latter is in a flow with the number  $M_\infty$  at an angle of attack equal to the angle between the vector  $V_\infty$  and a tangent to the contour at the point being considered. Hence, for a point  $N$  on the upper side, the pressure coefficient by (7.4.6) is

$$\bar{p}_N / (\alpha - \beta_N)^2 = 1/(1 - \delta) - \sqrt{1/(1 - \delta)^2 + 4/K_N^2} \quad (7.5.16)$$

where  $K_N = M_\infty(\alpha - \beta_N)$ .

For an arbitrary point  $L$  on the bottom side, with a view to (7.5.13), we have

$$\bar{p}_L / (\alpha - \beta_L)^2 = 1/(1 - \delta) + \sqrt{1/(1 - \delta)^2 + 4/K_L^2} \quad (7.5.17)$$

where  $K_L = M_\infty(\alpha - \beta_L)$ .

In formula (7.5.16), the angle  $\beta_N$  has a plus sign at the leading edge of the contour and a minus sign at the trailing edge, whereas in formula (7.5.17) the angle  $\beta_L$  has a minus sign at the leading edge and a plus sign at the trailing one.

At the limit, when  $K \rightarrow \infty$ , we have

$$\bar{p}_N = 0 \quad (7.5.18)$$

$$\bar{p}_L = 2(\alpha - \beta_L)^2 / (1 - \delta) \quad (7.5.19)$$

With a zero angle of attack, formulas (7.5.16), (7.5.17), and (7.5.19) acquire the following form:

$$\bar{p}_N / \beta_N^2 = 1/(1 - \delta) - \sqrt{1/(1 - \delta)^2 + 4/K_N^2} \quad (7.5.16')$$

$$\bar{p}_L / \beta_L^2 = 1/(1 - \delta) + \sqrt{1/(1 - \delta)^2 + 4/K_L^2} \quad (7.5.17')$$

$$\bar{p}_L = 2\beta_L^2 / (1 - \delta) \quad (7.5.19')$$

In formulas (7.5.16') and (7.5.17'),  $K_N = M_\infty \beta_N$  and  $K_L = M_\infty \beta_L$

**Nearly Uniform Flow  
over a Thin Airfoil**

At this case, we consider a flow over a thin airfoil at small angles of attack. This flow is featured by shocks of a finite intensity being absent and by the characteristics on the upper and bottom sides being *straight lines* with an angle of inclination of  $\mu_\infty = \sin^{-1}(1/M_\infty)$ .

To determine the pressure coefficient for the airfoil, we shall use Eq. (7.4.9). According to this equation, for an arbitrary point *N* on the upper side of the airfoil

$$\bar{p}_N = -2(\alpha - \beta_N)/\sqrt{M_\infty^2 - 1} \quad (7.5.20)$$

and for a point *L* on the bottom side

$$\bar{p}_L = 2(\alpha - \beta_L)/\sqrt{M_\infty^2 - 1} \quad (7.5.20')$$

For a zero angle of attack

$$\bar{p}_N = 2\beta_N/\sqrt{M_\infty^2 - 1}, \quad \bar{p}_L = -2\beta_L/\sqrt{M_\infty^2 - 1} \quad (7.5.20'')$$

An increase in the small angles of attack leads to a growth in the error when calculating the pressure on a thin airfoil in a nearly uniform flow. The accuracy of these calculations can be increased by using the *second-order aerodynamic theory*. According to the latter, the pressure coefficient is

$$\bar{p} = \pm c_1 \theta + c_2 \theta^2 \quad (7.5.21)$$

where

$$c_1 = 2(M_\infty^2 - 1)^{-1/2}, \quad c_2 = 0.5(M_\infty^2 - 1)^{-2} [(M_\infty^2 - 2)^2 + kM_\infty^4] \quad (7.5.22)$$

The plus sign in (7.5.21) relates to the bottom side of the plate ( $\bar{p}_L; \theta = \alpha - \beta_L$ ), and the minus sign, to the upper one ( $\bar{p}_N; \theta = \alpha - \beta_N$ ).

**Aerodynamic Forces  
and Their Coefficients**

To determine the aerodynamic pressure forces, we shall use formulas (1.3.2) and (1.3.3), relating them to the body axes *x*, *y* (see Fig. 7.5.1) and assuming that  $c_{f,x} = 0$ . In this condition, formula (1.3.2) determines the longitudinal force *X* for an airfoil, and (1.3.3), the normal force *Y* produced by the pressure:

$$X = q_\infty S_r \int \limits_{(S)} \bar{p} \cos(n, \hat{x}) \frac{dS}{S_r}, \quad Y = -q_\infty S_r \int \limits_{(S)} \bar{p} \cos(n, \hat{y}) \frac{dS}{S_r}$$

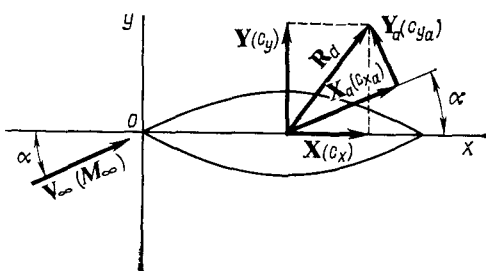


Fig. 7.5.4

Aerodynamic forces for an airfoil in a body axis and flight path coordinate systems

Adopting the quantity  $S_r = b \times 1$  as the characteristic area and taking into account that  $dS = dl \times 1$  ( $b$  is the chord of the airfoil, and  $dl$  is an arc element of the contour), we obtain the following expressions for the aerodynamic coefficients:

$$c_x = X/(q_\infty S_r) = \oint \bar{p} \cos(\hat{n}, \hat{x}) d\bar{l},$$

$$c_y = Y/(q_\infty S_r) = - \oint \bar{p} \cos(\hat{n}, \hat{y}) d\bar{l}$$

where  $d\bar{l} = dl/b$ , while the curvilinear integrals are taken along the contour of the airfoil (counterclockwise circumvention of the contour is usually taken as positive).

Let us introduce into this expression  $d\bar{l} = d\bar{x}/\sin(\hat{n}, \hat{x})$ ,  $\cos(\hat{n}, \hat{y}) d\bar{l} = d\bar{x}$ , where  $d\bar{x} = dx/b$ .

Next passing over from curvilinear integrals to ordinary ones, we obtain

$$c_x = - \int_0^1 \bar{p}_b \left( \frac{dy}{dx} \right)_b d\bar{x} + \int_0^1 \bar{p}_u \left( \frac{dy}{dx} \right)_u d\bar{x} \quad (7.5.23)$$

$$c_y = \int_0^1 (\bar{p}_b - \bar{p}_u) d\bar{x} \quad (7.5.24)$$

where  $\bar{p}_b$  and  $\bar{p}_u$  are the pressure coefficients for the bottom and upper sides of the airfoil, respectively.

Using the formula for conversion [see formula (1.2.3) and Table 1.2.1], we obtain the aerodynamic coefficients in a wind (flight path) coordinate system (Fig. 7.5.4):

$$c_{x_a} = c_x \cos \alpha + c_y \sin \alpha, \quad c_{y_a} = c_y \cos \alpha - c_x \sin \alpha \quad (7.5.25)$$

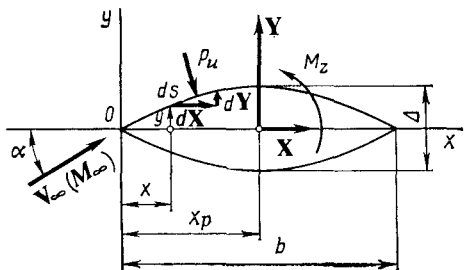


**Fig. 7.5.5**  
Determination of the moment of the forces for an airfoil

With flight angles of attack not exceeding the values of  $\alpha \approx 10\text{--}12$ , we have

$$c_{x_a} = c_x + c_y \alpha, \quad c_{y_a} \approx c_y \quad (7.5.25')$$

For the coefficient of the moment about the leading edge of the airfoil due to the pressure force (Fig. 7.5.5), by analogy with (1.3.6), we derive the formula

$$\begin{aligned} m_z &= \frac{M_z}{q_\infty S_r b} = \frac{1}{q_\infty S_r b} \left( \int x dY - \int y dX \right) \\ &= \frac{1}{b} \left\{ \int \bar{p}_x \cos(n, \hat{y}) \frac{dS}{S_r} - \int \bar{p}_y \cos(n, \hat{x}) \frac{dS}{S_r} \right\} \end{aligned}$$

or

$$m_z = \frac{M_z}{q_\infty b^2} = - \int_0^1 (\bar{p}_b - \bar{p}_u) \bar{x} d\bar{x} - \int_0^1 \left[ \bar{p}_b \bar{y}_b \left( \frac{dy}{dx} \right)_b - \bar{p}_u \bar{y}_u \left( \frac{dy}{dx} \right)_u \right] d\bar{x} \quad (7.5.26)$$

where  $\bar{y}_b = y_b/b$  and  $\bar{y}_u = y_u/b$ .

We determine the coefficient of the centre of pressure for the condition that the point of application of the resultant of the aerodynamic forces is on the chord of the airfoil. If its coordinate is  $x_p$ , we have

$$c_p = \frac{x_p}{b} = - \frac{m_z}{c_y} = - \frac{\int_0^1 (\bar{p}_b - \bar{p}_u) \bar{x} d\bar{x} + \int_0^1 \left[ \bar{p}_b \bar{y}_b \left( \frac{dy}{dx} \right)_b - \bar{p}_u \bar{y}_u \left( \frac{dy}{dx} \right)_u \right] d\bar{x}}{\int_0^1 (\bar{p}_b - \bar{p}_u) d\bar{x}} \quad (7.5.27)$$

For thin airfoils, we may disregard the second integral on the right-hand side of (7.5.26) and in the numerator of (7.5.27). Accord-

ingly,

$$m_z = - \int_0^1 (\bar{p}_b - \bar{p}_u) \bar{x} d\bar{x} \quad (7.5.26')$$

$$c_p = \int_0^1 (\bar{p}_b - \bar{p}_u) \bar{x} d\bar{x} \left[ \int_0^1 (\bar{p}_b - \bar{p}_u) d\bar{x} \right]^{-1} \quad (7.5.27')$$

By comparing the first and second terms on the right-hand side of (7.5.26), we can estimate the order of the discarded infinitesimals.

It is determined by the value of  $\int_0^1 \bar{y} (d\bar{y}/d\bar{x}) d\bar{x} \approx \bar{\Delta}^2$ , where  $\bar{\Delta} = \Delta/b$  is the relative thickness of the airfoil.

Using relation (7.5.21), we obtain the longitudinal-force coefficient (7.5.23) corresponding to the second-order aerodynamic theory:

$$c_x = c_1 K_1 + 2c_2 K_2 \alpha \quad (7.5.28)$$

where

$$K_1 = \int_0^1 (\beta_b^2 + \beta_u^2) d\bar{x}, \quad K_2 = \int_0^1 (\beta_b^2 - \beta_u^2) d\bar{x} \quad (7.5.29)$$

The normal force coefficient in accordance with (7.5.24) is

$$c_y = 2c_1 \alpha + c_2 K_2 \quad (7.5.30)$$

According to the results obtained, the drag and lift coefficients are  $c_{x_a} = 2c_1 \alpha^2 + 3c_2 K_2 \alpha + c_1 K_1$ ,  $c_{y_a} = 2c_1 \alpha + c_2 K_2$

In the particular case of a symmetric airfoil,  $\beta_b^2 = \beta_u^2 = \beta^2 = (dy/dx)^2$  and, consequently,  $K_1 = 2 \int_0^1 \beta^2 dx$  and  $K_2 = 0$ . Accordingly,

$$c_{x_a} = 2c_1 \alpha^2 + 2c_1 \int_0^1 \beta^2 d\bar{x}, \quad c_{y_a} = 2c_1 \alpha \quad (7.5.31')$$

From these two relations, we find

$$c_{x_a} = \frac{c_y^2}{2c_1} + 2c_1 \int_0^1 \beta^2 d\bar{x} \quad (7.5.32)$$

Equation (7.5.32) determines the relation between the drag and lift coefficients—what is called the polar of an airfoil.

We find the coefficient of the longitudinal moment about the leading edge by inserting (7.5.21) into (7.5.26'):

$$m_z = c_1 A_1 - c_2 B_2 + (2c_2 A_2 - c_1) \alpha \quad (7.5.33)$$

where

$$A_1 = \int_0^1 (\beta_b + \beta_u) \bar{x} d\bar{x}; \quad A_2 = \int_0^1 (\beta_b - \beta_u) \bar{x} d\bar{x} \quad (7.5.34)$$

$$B_2 = \int_0^1 (\beta_b^2 - \beta_u^2) \bar{x} d\bar{x} \quad (7.5.35)$$

For a symmetric airfoil,  $\beta_u = -\beta_b = \beta$ , therefore  $A_1 = B_2 = 0$ ;  $A_2 = 2 \int_0^1 \beta \bar{x} d\bar{x}$ . Accordingly,

$$m_z = \left( 4c_2 \int_0^1 \beta \bar{x} d\bar{x} - c_1 \right) \alpha \quad (7.5.33')$$

The coefficient of the centre of pressure, by (7.5.27'), is

$$c_p = -[c_1 A_1 - c_2 B_2 + (2c_2 A_2 - c_1) \alpha] / (2c_1 \alpha + c_2 K_2) \quad (7.5.36)$$

For a symmetric airfoil

$$c_p = 0.5 \left( 1 - 4 \frac{c_2}{c_1} \int_0^1 \beta \bar{x} d\bar{x} \right) \quad (7.5.36')$$

For a linearized flow (low supersonic velocities), the coefficient  $c_2$  should be taken equal to zero in the above relations.

With *hypersonic velocities* of a thin airfoil, formulas (7.4.6) and (4.6.12) can be used to calculate the pressure coefficients in (7.5.23), (7.5.24), (7.5.26') and (7.5.27'). The pressure coefficient for the bottom side in accordance with (4.6.12) is

$$\bar{p}_b = (\alpha - \beta_b)^2 [1/(1-\delta) + \sqrt{1/(1-\delta)^2 + 4/K_b^2}] \quad (7.5.37)$$

while for the upper side, the value of this coefficient by (7.4.6) is

$$\bar{p}_u = (\alpha - \beta_u)^2 [1/(1-\delta) - \sqrt{1/(1-\delta)^2 + 4/K_u^2}] \quad (7.5.38)$$

where  $K_b = M_\infty (\alpha - \beta_b)$  and  $K_u = M_\infty (\alpha - \beta_u)$ .

Let us find the relations for the aerodynamic coefficients of a wedge-shaped airfoil (Fig. 7.5.6). Since for the bottom contour we have  $(dy/dx)_b = \tan \beta_b$ , and for the upper one  $(dy/dx)_u = \tan \beta_u$ , and taking into account that the pressure coefficients  $p_b$  and  $p_u$

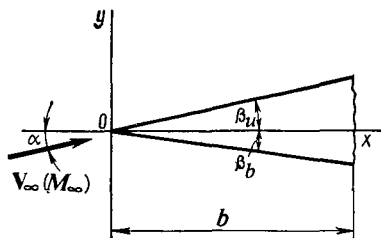


**Fig. 7.5.6**  
Wedge-shaped airfoil

are constant, we obtain from (7.5.23) and (7.5.24):

$$c_x = -\bar{p}_b \tan \beta_b + \bar{p}_u \tan \beta_u \quad (7.5.39)$$

$$c_y = \bar{p}_b - \bar{p}_u \quad (7.5.40)$$

The angle  $\beta_b$  should be considered negative in formula (7.5.39). We find the moment coefficient from (7.5.26):

$$m_z = -0.5 (\bar{p}_b - \bar{p}_u) - 0.5 (\bar{p}_b \tan^2 \beta_b - \bar{p}_u \tan^2 \beta_u) \quad (7.5.41)$$

while the coefficient of the centre of pressure by (7.5.27) is

$$c_p = 0.5 [1 + (\bar{p}_b \tan^2 \beta_b - \bar{p}_u \tan^2 \beta_u) / (\bar{p}_b - \bar{p}_u)] \quad (7.5.42)$$

For a symmetric airfoil, we have

$$\left. \begin{aligned} c_x &= (\bar{p}_b + \bar{p}_u) \tan \beta, & c_y &= \bar{p}_b - \bar{p}_u \\ m_z &= -0.5 (\bar{p}_b - \bar{p}_u) (1 + \tan^2 \beta), & c_p &= 0.5 (1 + \tan^2 \beta) \end{aligned} \right\} \quad (7.5.43)$$

In the above relations, the pressure coefficient  $\bar{p}_b$  is determined by accurate relations obtained in the theory of an oblique shock. We also use this theory to find the pressure coefficient  $\bar{p}_u$  for  $\alpha < \beta_u$ . For  $\alpha > \beta_u$ , the finding of  $\bar{p}_u$  is associated with calculation of the Prandtl-Meyer flow on the upper side of the airfoil.

The relations obtained for the aerodynamic coefficients of the airfoil relate to arbitrary values of the nose angle ( $\beta_b$ ,  $\beta_u$ ) and the angle of attack. If these values are not large, the second-order theory can be used to calculate the coefficients. According to this theory, in formulas (7.5.31) for  $c_{x_a}$  and  $c_{y_a}$ , we must assume that

$$K_1 = \beta_b^2 + \beta_u^2, \quad K_2 = \beta_b^2 - \beta_u^2$$

When calculating the moment coefficients (7.5.33) and (7.5.36), we must proceed from the fact that

$$A_1 = 0.5 (\beta_b + \beta_u), \quad A_2 = 0.5 (\beta_b - \beta_u), \quad B_2 = 0.5 (\beta_b^2 - \beta_u^2)$$

For a symmetric airfoil, we have

$$\left. \begin{aligned} c_{x_a} &= 2c_1(\alpha^2 + \beta^2), & c_{y_a} &= 2c_1\alpha \\ m_z &= (2c_2\beta - c_1)\alpha, & c_p &= 0.5 \left( 1 - 2 \frac{c_2}{c_1} \beta \right) \end{aligned} \right\} \quad (7.5.44)$$

where the angle  $\beta$  is chosen with a minus sign (for the bottom side).

The use of formulas (7.5.37), (7.5.38) allows us to determine the aerodynamic coefficients (7.5.39)-(7.5.43) corresponding to hypersonic velocities of a thin airfoil at a small angle of attack.

## 7.6. Sideslipping Wing Airfoil

### Definition of a Sideslipping Wing

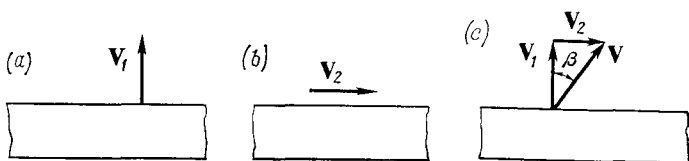
Let us assume that an infinite-span rectangular wing performs longitudinal motion at the velocity  $V_1$  (normal to the leading edge) and lateral motion along the span at the velocity  $V_2$ . The resultant velocity  $V = V_1 + V_2$  is directed toward the plane of symmetry of the wing at the sideslip angle  $\beta$ . A rectangular wing performing such motion is said to be a sideslipping one.

The flow over a sideslipping wing does not change if we consider inverted flow in which a rectangular wing encounters a stream of air at the velocity  $-V_1$  perpendicular to the leading edge, and a stream at the velocity  $-V_2$  in the direction of the wing span (Fig. 7.6.1).

The nature of the flow is the same if the resultant velocity  $V_\infty$  is parallel to the initial velocity  $-V_1$  (see Fig. 7.6.1) and the rectangular wing is turned through the angle  $\alpha = \beta$  (Fig. 7.6.2). Such a wing, which is also a sideslipping one, is usually called an infinite-span swept wing. The angle  $\alpha$  is determined as the sweep angle relative to the leading edge.

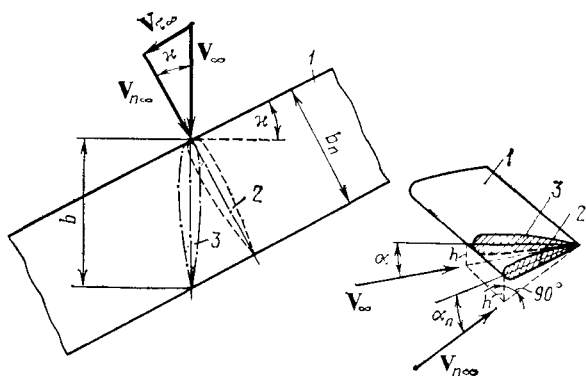
Let us consider some features of the flow over sideslipping wings. The flow about such wings can be divided into two flows: a longitudinal one (along the span of the wing) characterized by the velocity  $V_{\tau\infty} = V_\infty \sin \alpha$  parallel to the leading edge, and a lateral one depending on the magnitude of the normal velocity component to this edge  $V_{n\infty} = V_\infty \cos \alpha$ .

The distribution of the velocities and pressures along the wing does not depend on the longitudinal flow, and is due only to the lateral flow at the velocity  $V_{n\infty} = V_\infty \cos \alpha$ . The nature of this flow and, therefore, the pressure distribution change depending on the configuration of the airfoil in a plane normal to the leading edge, and on the angle of attack measured in this plane. Accordingly, the aerodynamic characteristics of the airfoil are the same as of a rectangular (unswept) wing airfoil in a flow with a free-stream velocity of  $V_{n\infty}$  at the indicated angle of attack.

**Fig. 7.6.1**

Motion of a wing with sideslipping:

a—longitudinal motion of an infinite-span rectangular wing; b—lateral motion; c—resultant motion at the sideslip angle<sub>β</sub>

**Fig. 7.6.2**

Sideslipping wing:

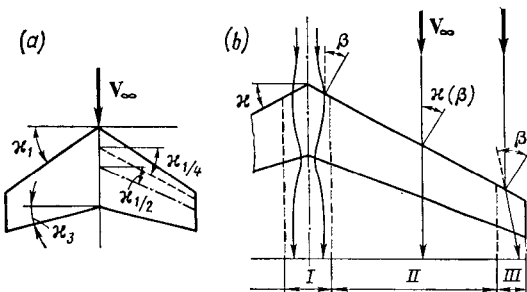
1—wing surface; 2—airfoil in a section along a normal; 3—airfoil in a section along the flow

This is exactly the content of the **sideslip effect** which to a considerable extent determines the aerodynamic properties of finite-span swept wings. The term **swept** is conventionally applied to a wing in which the line connecting the aerodynamic centres (foci) of the airfoils (the aerodynamic centre line) makes with a normal to the longitudinal plane of symmetry the angle  $\alpha$  (the sweep angle).

In aerodynamic investigations, the sweep angle is often measured from another characteristic line, for example, from the leading or trailing edge ( $x_1$ ,  $x_3$ ), from lines connecting the ends of selected elements of a chord ( $x_{1/4}$ ,  $x_{1/2}$ , . . .), from the lines of the maximum thickness of the airfoils, etc. (Fig. 7.6.3a).

If the leading edges are curved or have sharp bends, the sweep angle will be variable along the span.

The flow over swept wings in real conditions is distinguished by its very intricate nature, due primarily to the partial realization of the sideslip effect. Figure 7.6.3b shows a possible scheme of such flow over a swept finite-span wing with a sufficiently large aspect ratio.

**Fig. 7.6.3**

Finite-span swept wing:

a—designation of the sweep angles; b—subsonic flow over a swept wing

The middle region of the wing (region *I*) is characterized by the mutual influence of neighbouring airfoils reducing the sweep (sideslip) angle. Here the **mid-span effect** appears that detracts from the aerodynamic properties because of the decrease in the sideslip effect. In region *III*, the tip effect acts. It is due to an appreciable deflection of the streamlines in comparison with a sideslipping wing. And only in region *II*, distinguished by a more uniform flow, is the curvature of the streamlines relatively small, and the sideslip angles  $\beta$  are close to the sweep angle  $\alpha$ . In aerodynamic investigations, this region of the wing can be represented in the "pure" form as a region of a swept (sideslipping) infinite-span wing arranged in the flow at the sweep angle. It will be shown in Chap. 8 that the conclusions relating to such wings of a small thickness can be used to calculate the flow over separate parts of swept finite-span wings at supersonic velocities.

#### **Aerodynamic Characteristics of a Sideslipping Wing Airfoil**

When determining such characteristics, a sideslipping wing is considered as a straight one turned through the sideslip angle  $\alpha$ . In this case, the airfoil of a sideslipping wing in a normal section will evidently be the same as that of a straight one.

The airfoil and the angle of attack in a plane normal to the leading edge differ from the airfoil and angle of attack in the section along the flow (see Fig. 7.6.2). The chord in a normal section  $b_n$  and the chord  $b$  along the flow are related by the expression  $b_n = b \cos \alpha$ .

The angle of attack  $\alpha_n$  in a normal section is determined from the expression

$$\sin \alpha_n = h/b_n = h/(b \cos \alpha) = \sin \alpha / \cos \alpha \quad (7.6.1)$$

where  $\alpha$  is the angle of attack in the plane of the flow. It is evident that at small angles of attack we have

$$\alpha_n = \alpha / \cos \alpha \quad (7.6.1')$$

If at a point on a wing airfoil in flow without sideslipping at the velocity  $V_\infty$  the pressure coefficient is  $\bar{p}$ , then when the wing is turned through the angle  $\alpha$  the pressure coefficient  $\bar{p}_n$  at the corresponding point is the same, i.e.

$$2(p_n - p_\infty) / (\rho_\infty V_\infty^2 \cos^2 \alpha) = 2(p - p_\infty) / (\rho_\infty V_\infty^2)$$

Accordingly, for the airfoil of a sideslipping wing, the pressure coefficient calculated from the velocity head  $q_\infty = 0.5\rho_\infty V_\infty^2$  is

$$\bar{p}_\alpha = 2(p_n - p_\infty) / (\rho_\infty V_\infty^2) = \bar{p} \cos^2 \alpha \quad (7.6.2)$$

With a view to (7.6.2) and in accordance with (7.5.23), (7.5.24), and (7.5.26), the aerodynamic coefficients for the airfoil of a thin sideslipping wing are

$$c_{x,\alpha} = c_x \cos^2 \alpha, \quad c_{y,\alpha} = c_y \cos^2 \alpha, \quad m_{z,\alpha} = m_z \cos^2 \alpha \quad (7.6.3)$$

Evidently, by (7.5.25'), we have

$$c'_{x_a \alpha} = (c_x + c_y \alpha) \cos^2 \alpha = c_{x_a} \cos^2 \alpha$$

Since the drag force is determined not in the direction of the velocity component  $V_\infty \cos \alpha$ , but in the direction of the free-stream velocity  $V_\infty$ , the coefficient of this drag is

$$c_{x_a \alpha}^{**} = c'_{x_a \alpha} \cos \alpha = c_{x_a} \cos^3 \alpha \quad (7.6.4)$$

All these coefficients are determined for a velocity head of  $q_\infty = 0.5\rho_\infty V_\infty^2$ . Inspection of formulas (7.6.3) for  $c_{y,\alpha}$  and  $m_{z,\alpha}$  reveals that the coefficient of the centre of pressure  $c_p = -m_{z,\alpha}/c_{y,\alpha}$  corresponding to small angles of attack does not depend on the angle of attack, i.e.  $c_p = -m_z/c_y$ .

**Compressible Flow.** According to the linearized theory, the pressure coefficient for the airfoil of a sideslipping wing in a *subsonic compressible flow* can be obtained from the corresponding coefficient for the same wing in an incompressible fluid by the Prandtl-Glauert formula (7.1.14), substituting the number  $M_\infty \cos \alpha$  for  $M_\infty$  in it:

$$\bar{p}_\alpha = \bar{p}_{\alpha, \text{ic}} / \sqrt{1 - M_\infty^2 \cos^2 \alpha} \quad (7.6.5)$$

or, with a view to (7.6.2)

$$\bar{p}_\alpha = \bar{p}_{\alpha, \text{ic}} \cos^2 \alpha / \sqrt{1 - M_\infty^2 \cos^2 \alpha} \quad (7.6.5')$$

The relevant aerodynamic coefficients are obtained from (7.5.23), (7.5.24), and (7.5.26), and are found with the aid of formulas (7.6.3)

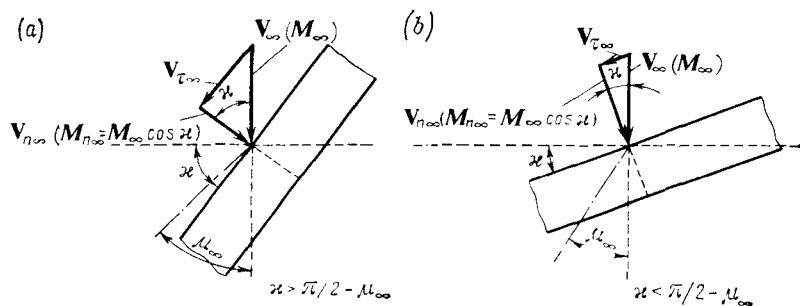


**Fig. 7.6.4**  
Sideslipping wing with subsonic (a) and supersonic (b) leading edges

and (7.6.4) whose right-hand sides contain the quantity  $\sqrt{1 - M_\infty^2 \cos^2 \alpha}$  in the denominator. Particularly, the coefficients of the normal force and the longitudinal moment are

$$c_{y,\alpha} = c_y \cos^2 \alpha / \sqrt{1 - M_\infty^2 \cos^2 \alpha}; \quad m_{z,\alpha} = m_z \cos^2 \alpha / \sqrt{1 - M_\infty^2 \cos^2 \alpha} \quad (7.6.6)$$

It follows from these relations that for thin airfoils, the coefficient of the centre of pressure  $c_p = -m_{z,\alpha}/c_{y,\alpha}$  depends neither on the sideslip (sweep) angle nor on the compressibility (the number  $M_\infty$ ).

The use of a sideslipping wing produces the same flow effect that appears when the free-stream velocity is lowered from  $V_\infty$  to  $V_\infty \cos \alpha$  (or the Mach number from  $M_\infty$  to  $M_\infty \cos \alpha$ ). Here, naturally, the local velocities on an airfoil of the sideslipping wing also decrease, and this, in turn, leads to diminishing of the rarefaction and, as a result, to an increase in the critical Mach number. The latter can be determined from its known value  $M_{\infty,c_r}$  for a straight wing of the same shape and angle of attack as the airfoil of the sideslipping wing in a normal section:

$$M_{\infty,c_r,\alpha} = M_{\infty,c_r} / \cos^2 \alpha \quad (7.6.7)$$

**Supersonic Velocities.** Let us assume that at a supersonic free-stream velocity ( $V_\infty > a_\infty$ ,  $M_\infty > 1$ ), the sweep angle satisfies the inequality  $\alpha > \pi/2 - \mu_\infty$ , according to which  $\cos \alpha < \sin \mu_\infty$  and, consequently,  $V_{n,\infty} < a_\infty = V_\infty \sin \mu_\infty$ , i.e. the normal component to the leading edge is subsonic. Hence, the flow over the sections of a sideslipping wing is subsonic in its nature. In the case being considered, the swept edge is called subsonic (Fig. 7.6.4a).

At increased flow velocities, the normal velocity component may become higher than the speed of sound ( $V_{n,\infty} > a_\infty = V_\infty \sin \mu_\infty$ ), so that  $\alpha < \pi/2 - \mu_\infty$  and  $\cos \alpha > \sin \mu_\infty$ . In this case, the flow

over the airfoils of a sideslipping wing is supersonic. Accordingly, the leading edge of such a wing is called **supersonic** (Fig. 7.6.4b).

Let us consider the calculation of the supersonic flow over a sideslipping wing in each of these cases.

*Supersonic Leading Edge.* The flow over such a wing can be calculated by the formulas obtained for an infinite-span thin plate provided that the free-stream velocity is  $V_{n\infty} = V_\infty \cos \alpha > a_\infty$ , and the corresponding number  $M_{n\infty} = M_\infty \cos \alpha > 1$ . The angle of attack of the plate  $\alpha_n$  is related to the given angle of attack  $\alpha$  of the sideslipping wing by expression (7.6.1), or at small angles of attack by (7.6.1').

Using formula (7.4.9) and substituting  $\alpha_n = \alpha / \cos \alpha$  for  $\beta$  and  $M_{n\infty} = M_\infty \cos \alpha$  for  $M_\infty$  in it, we obtain a relation for the pressure coefficient in a plane perpendicular to the leading edge:

$$\bar{p} = \pm 2\alpha / (\cos \alpha \sqrt{M_\infty^2 \cos^2 \alpha - 1})$$

In this formula, the pressure coefficient  $\bar{p}$  is related to the velocity head  $q_n = 0.5 \rho_\infty M_{n\infty}^2$ . To obtain the value of the pressure coefficient related to the free-stream velocity head  $q_\infty = 0.5 \rho_\infty M_\infty^2$ , we must use formula (7.6.2) according to which

$$\bar{p}_\alpha = \pm 2\alpha \cos \alpha / \sqrt{M_\infty^2 \cos^2 \alpha - 1} \quad (7.6.8)$$

In (7.6.8), the plus sign determines the pressure coefficient for the bottom side of a wing, and the minus sign for the upper side.

In accordance with formulas (7.4.20)-(7.4.22) (replacing  $\alpha$  with  $\alpha_n$  and  $M_\infty$  with  $M_\infty \cos \alpha$  in them), and also with a view to relations (7.6.3) and (7.6.4), we find a relation for the aerodynamic coefficients of a sideslipping wing airfoil

$$\left. \begin{aligned} c_{y_{a\alpha}} &= 4\alpha_n \cos^2 \alpha / \sqrt{M_\infty^2 \cos^2 \alpha - 1} \\ c_{x_{a\alpha}} &= 4\alpha_n^2 \cos^3 \alpha / \sqrt{M_\infty^2 \cos^2 \alpha - 1} \\ m_{z_{a\alpha}} &= -2\alpha_n \cos^2 \alpha / \sqrt{M_\infty^2 \cos^2 \alpha - 1} \end{aligned} \right\} \quad (7.6.9)$$

Upon analysing these relations, we can establish a feature of swept wings consisting in that in comparison with straight ones ( $\alpha = 0$ ), the lift force and drag coefficients, and also the coefficient of the longitudinal moment of airfoils (in their magnitude) are smaller at identical angles of attack  $\alpha_n$  along a normal to the leading edge. The physical explanation is that in flow over a sideslipping wing not the total velocity head  $q_\infty = 0.5 \rho_\infty V_\infty^2$  is realized, but only a part of it,  $q_n = q_\infty \cos^2 \alpha$ , and flow in the direction of the oncoming stream occurs at a smaller angle of attack than in the absence of sideslip ( $\alpha < \alpha_n$ ,  $\alpha_n = \alpha / \cos \alpha$ ).

*Subsonic Leading Edge.* The flow over sections corresponding to the motion of a straight wing with the number  $M_{n\infty} < 1$  is investi-

gated with the aid of the subsonic or transonic (combined) theory of flow over an airfoil. The drag and lift forces are determined by the laws of subsonic flows characterized by interaction of the flows on the upper and bottom sides of a wing that manifests itself in the gas flowing over from a region of high pressure into a zone with reduced pressure values. Wave losses may appear only in supercritical flow ( $M_{n\infty} > M_{\infty \text{ cr}}$ ) when shocks form on the surface. If  $M_{n\infty} < M_{\infty \text{ cr}}$ , then shocks and, therefore, wave drag are absent. This conclusion relates to an infinite-span wing. For finite-span wings, wave losses are always present because flow over their tips is affected by the velocity component  $V_\infty \sin \alpha$ . A result is the appearance of supersonic flow properties and of a wave drag. The three-dimensional theory of supersonic flow has to be used to study this drag.

### Suction Force

As we have established in Sec. 6.3, a suction force appears on the leading edge of an airfoil over which an incompressible fluid is flowing. The same effect occurs when an airfoil is in a subsonic flow of a compressible gas. The magnitude of the suction force is affected by the sweep of the leading edge of the wing.

To calculate this force, we shall use expression (6.3.25), which by means of the corresponding transformations can be made to cover the more general case of the flow over an airfoil of a wing with a swept leading edge (Fig. 7.6.5). Let us consider this transformation. In an inviscid flow, the free-stream velocity component tangent to the leading edge of a sideslipping wing does not change the field of the disturbed velocities, and it remains the same as for a straight wing in a flow at the velocity  $V_{n\infty} = V_\infty \cos \alpha$ . The forces acting on the wing also remain unchanged.

Therefore, the following suction force acts on a wing element  $dz_0$  with a straight edge (in the coordinates  $x_0, z_0$ ):

$$dT_0 = \pi \rho c_0^2 dz_0 \quad (7.6.10)$$

where in accordance with (6.3.28')

$$c_0^2 = \lim_{x_0 \rightarrow x_{s.e.0}} [u_0^2 (x_0 - x_{s.e.0})]$$

A glance at Fig. 7.6.3 reveals that  $dT_0 = dT / \cos \alpha$ ,  $dz_0 = dz / \cos \alpha$ ,  $u_0 = u / \cos \alpha$ , and  $x_0 - x_{s.e.0} = (x - x_{s.e.}) \cos \alpha$ .

Insertion of these values into (7.6.10) yields

$$dT/dz = \pi \rho c^2 \sqrt{1 + \tan^2 \alpha} \quad (7.6.11)$$

where

$$c^2 = \lim_{x \rightarrow x_{s.e.}} [u^2 (x - x_{s.e.})] \quad (7.6.12)$$

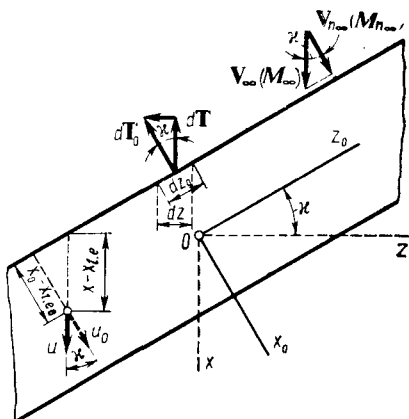


**Fig. 7.6.5**  
Suction force of a sideslipping wing

Expressions (7.6.11) and (7.6.12) can be generalized for compressible flows. For this purpose, we shall use expressions (8.2.4) relating the geometric characteristics of wings in a compressible and an incompressible flows. It follows from these relations that all the linear dimensions in the direction of the  $x$ -axis for a wing in a compressible flow are  $\sqrt{1 - M_\infty^2}$  times smaller than the relevant dimensions for a wing in an incompressible flow, whereas the thickness of the wing and its lateral dimensions (in the direction of the  $z$ -axis) do not change. Accordingly, we have

$$x = x_{ic} \sqrt{1 - M_\infty^2}, \quad b dz = b_{ic} dz_{ic} \sqrt{1 - M_\infty^2}$$

$$\tan \kappa = \tan \kappa_{ic} \sqrt{1 - M_\infty^2} \quad (7.6.13)$$

From the conditions that  $x = x_{ic} \sqrt{1 - M_\infty^2}$  and  $\varphi' = \varphi'_{ic}$ , we find

$$\frac{\partial \varphi'}{\partial x} = \frac{\partial \varphi'_{ic}}{\partial x_{ic}} \cdot \frac{1}{\sqrt{1 - M_\infty^2}}$$

i.e.

$$u = u_{ic} / \sqrt{1 - M_\infty^2} \quad (7.6.14)$$

Therefore, the pressure coefficient for a compressible flow is determined by the Prandtl-Glauert formula:

$$\bar{p} = \bar{p}_{ic} / \sqrt{1 - M_\infty^2} \quad (7.6.15)$$

The suction force  $T$  in its physical nature is a force produced by the action of the normal stress (pressure) and at low angles of attack is determined from the condition  $T \approx \alpha Y_a$ . The corresponding suction

force coefficient is  $c_{x,T} = T/(q_\infty S_w) = \alpha c_{y_a}$ . Since the dimensions of a wing in the direction of the  $y$ -axis do not change in a compressible and an incompressible flows, the angles of attack for both flows also do not change, i.e.  $\alpha = \alpha_{ic}$ . Consequently,  $c_{x,T}/c_{x,T,ic} = c_{y_a}/c_{y_a,ic}$ , or by (7.1.14)

$$c_{x,T} = c_{x,T,ic} / \sqrt{1 - M_\infty^2} \quad (7.6.16)$$

With a view to the relations for an airfoil of a sideslipping wing, we have

$$c_{x,T} \frac{\rho_\infty V_\infty^2}{2} b dz = \frac{c_{x,T,ic}}{\sqrt{1 - M_\infty^2}} \cdot \frac{\rho_\infty V_\infty^2}{2} b_{ic} \sqrt{1 - M_\infty^2} dz_{ic}$$

or

$$dT = dT_{ic}$$

But since  $dz = dz_{ic}$ , then

$$dT/dz = dT_{ic}/dz_{ic} \quad (7.6.17)$$

The right-hand side of Eq. (7.6.17) corresponding to an incompressible flow is determined by formulas (7.6.11) and (7.6.12):

$$dT_{ic}/dz_{ic} = \pi \rho_\infty c_{ic}^2 \sqrt{1 + \tan^2 \alpha_{ic}}$$

where

$$c_{ic}^2 = \lim_{x_{ic} \rightarrow x_{s.e. ic}} [u_{ic}^2 (x_{ic} - x_{s.e. ic})]$$

In accordance with (7.6.17), (7.6.13), and (7.6.14), we obtain

$$\begin{aligned} c_{ic}^2 &= \lim_{x \rightarrow x_{s.e.}} [u^2 (x - x_{s.e.})] \sqrt{1 - M_\infty^2}; \quad \sqrt{1 + \tan^2 \alpha_{ic}} \\ &= \sqrt{1 + \frac{\tan^2 \alpha}{1 - M_\infty^2}} \end{aligned}$$

Consequently,

$$dT/dz = \pi \rho_\infty c^2 \sqrt{1 + \tan^2 \alpha - M_\infty^2} \quad (7.6.18)$$

where

$$c^2 = \lim_{x \rightarrow x_{s.e.}} [u^2 (x - x_{s.e.})] \quad (7.6.19)$$

It follows from the above formulas that at a given value of the number  $M_\infty$ , the suction force depends on the sideslip angle and on the nature of the change in the velocity  $u$  within a very small vicinity of the leading edge. We can assume that a finite-span swept wing is also characterized by a similar relation for the suction force.

## A Wing in a Supersonic Flow

### 8.1. Linearized Theory of Supersonic Flow over a Finite-Span Wing

#### Linearization of the Equation for the Potential Function

Let us consider a thin slightly bent finite-span wing of an arbitrary planform in a supersonic flow at a small angle of attack. The disturbances introduced by such a wing into the flow are small, and for investigation of the flow we can use the linearized theory as when studying a nearly uniform flow near a thin airfoil (see Sec. 6.2). The conditions for such a flow are given for the velocities in the form of (6.1.1). If we are considering a linearized three-dimensional gas flow, these conditions are supplemented with a given velocity component along the  $z$ -axis. Accordingly, the following relations hold for a linearized three-dimensional disturbed flow:

$$V_x = V_\infty + u, \quad V_y = v, \quad V_z = w \quad (8.1.1)$$

where  $u$ ,  $v$ , and  $w$  are the disturbance velocity components along the  $x$ ,  $y$ , and  $z$  axes, respectively.

In accordance with the property of a linearized flow, we have

$$u \ll V_\infty, \quad v \ll V_\infty, \quad w \ll V_\infty \quad (8.1.2)$$

These conditions make it possible to linearize the equations of motion and continuity and thus simplify the solution of the problem on a thin wing in an inviscid steady flow. In the general form, the equations of motion of such a flow are obtained from system (3.1.17) in which  $\mu = 0$ ,  $\partial V_x / \partial t = \partial V_y / \partial t = \partial V_z / \partial t = 0$ :

$$\left. \begin{aligned} V_x \frac{\partial V_x}{\partial x} + V_y \frac{\partial V_x}{\partial y} + V_z \frac{\partial V_x}{\partial z} &= - \frac{1}{\rho} \cdot \frac{\partial p}{\partial x} \\ V_x \frac{\partial V_y}{\partial x} + V_y \frac{\partial V_y}{\partial y} + V_z \frac{\partial V_y}{\partial z} &= - \frac{1}{\rho} \cdot \frac{\partial p}{\partial y} \\ V_x \frac{\partial V_z}{\partial x} + V_y \frac{\partial V_z}{\partial y} + V_z \frac{\partial V_z}{\partial z} &= - \frac{1}{\rho} \cdot \frac{\partial p}{\partial z} \end{aligned} \right\} \quad (8.1.3)$$

We shall adopt the continuity equation in the form of (2.4.4). Calculation of the partial derivatives yields

$$\rho \left( \frac{\partial V_x}{\partial x} + \frac{\partial V_y}{\partial y} + \frac{\partial V_z}{\partial z} \right) + V_x \frac{\partial \rho}{\partial x} + V_y \frac{\partial \rho}{\partial y} + V_z \frac{\partial \rho}{\partial z} = 0 \quad (8.1.4)$$

It was shown in Sec. 5.1 that the equations of continuity and motion can be combined into a single equation relating the velocity components to one another. By performing transformations similar to those made in Sec. 5.1, we can write this equation in the form

$$\begin{aligned} & (V_x^2 - a^2) \frac{\partial V_x}{\partial x} + (V_y^2 - a^2) \frac{\partial V_y}{\partial y} + (V_z^2 - a^2) \frac{\partial V_z}{\partial z} \\ & + V_x V_y \left( \frac{\partial V_x}{\partial y} + \frac{\partial V_y}{\partial x} \right) + V_x V_z \left( \frac{\partial V_x}{\partial z} + \frac{\partial V_z}{\partial x} \right) \\ & + V_y V_z \left( \frac{\partial V_y}{\partial z} + \frac{\partial V_z}{\partial y} \right) = 0 \end{aligned} \quad (8.1.5)$$

Taking into account relations (2.3.2) for the potential function, and also the condition of equality of the cross partial derivatives ( $\partial^2 \varphi / \partial x \partial y = \partial^2 \varphi / \partial y \partial x$ , etc.), from (8.1.5) we derive an equation for the velocity potential:

$$\begin{aligned} & (V_x^2 - a^2) \frac{\partial^2 \Phi}{\partial x^2} + (V_y^2 - a^2) \frac{\partial^2 \Phi}{\partial y^2} + (V_z^2 - a^2) \frac{\partial^2 \Phi}{\partial z^2} \\ & + 2V_x V_y \frac{\partial^2 \Phi}{\partial x \partial y} + 2V_x V_z \frac{\partial^2 \Phi}{\partial x \partial z} + 2V_y V_z \frac{\partial^2 \Phi}{\partial y \partial z} = 0 \end{aligned} \quad (8.1.6)$$

Equations (8.1.5) and (8.1.6) are the *fundamental differential equations of gas dynamics for three-dimensional steady gas flows*. The first of them relates to the more general case of a *vortex (non-potential)* flow of a gas, while the second is used to investigate *only vortex-free (potential)* flows.

Since the flow over thin wings at small angles of attack is potential, we can use Eq. (8.1.6) for the velocity potential to investigate this flow. To linearize Eq. (8.1.6), which is a non-linear differential equation, we shall introduce into it expression (7.1.2') for the speed of sound, and also the values

$$\begin{aligned} V_x &= V_\infty + u, \quad V_y = v, \quad V_z = w \\ V_x^2 &= V_\infty^2 + 2V_\infty u, \quad V_y^2 \approx v^2, \quad V_z^2 = w^2; \\ \varphi &= \varphi_\infty + \varphi' \end{aligned}$$

After analysing the order of magnitude of the terms in the obtained equation in the same way as we did in Sec. 7.1 when considering a

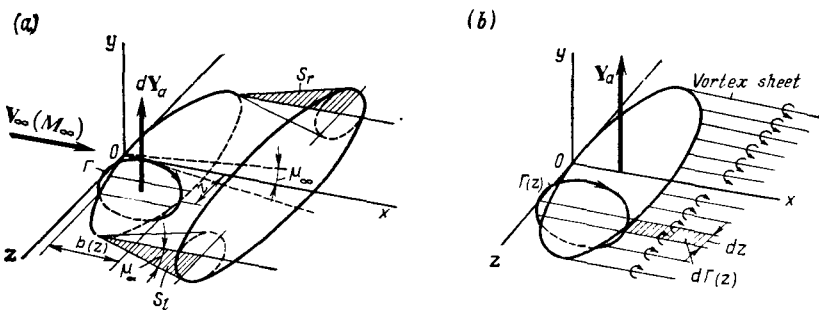


**Fig. 8.1.1**  
Thin wing in a linearized flow

nearly uniform plane flow, we obtain a linearized equation for the velocity potential of a three-dimensional disturbed flow in the following form:

$$(M_\infty^2 - 1) \frac{\partial^2 \varphi'}{\partial x^2} - \frac{\partial^2 \varphi'}{\partial y^2} - \frac{\partial^2 \varphi'}{\partial z^2} = 0 \quad (8.1.7)$$

#### Boundary Conditions

Investigation of the flow over a thin finite-span wing consists in solving the linearized partial differential equation (8.1.7) of the second order for the velocity potential  $\varphi'$  at the given boundary conditions. Let us consider these boundary conditions.

1. A wing in a linearized flow (Fig. 8.1.1a, b) causes disturbances that are concentrated inside the wave zone. This zone is limited by a surface that is the envelope of Mach cones issuing from points on the leading edge and having an apex (cone) angle of  $\mu_\infty = \sin^{-1}(1/M_\infty)$ . The boundary condition satisfied by the solution of Eq. (8.1.7) for the function  $\varphi'$  has the form

$$[\varphi'(x, y, z)]_\Sigma = 0 \quad (8.1.8)$$

According to this condition, on the wave surface (we shall designate this surface by  $\Sigma$ ) or outside of it, the disturbance velocities are zero.

2. The solution for the additional potential  $\varphi'$  also satisfies the boundary condition of flow over the wing surface  $S$  without separation, in accordance with which the normal velocity component at each point is zero, i.e.

$$\begin{aligned} (V_n)_S &= \left( \frac{\partial \varphi}{\partial n} \right)_S = \widehat{\frac{\partial \varphi}{\partial x}} \cos(\widehat{n}, \widehat{x}) \\ &+ \widehat{\frac{\partial \varphi}{\partial y}} \cos(\widehat{n}, \widehat{y}) + \widehat{\frac{\partial \varphi}{\partial z}} \cos(\widehat{n}, \widehat{z}) = 0 \end{aligned} \quad (8.1.9)$$

Here

$$\frac{\partial \Phi}{\partial x} = V_\infty + u = V_\infty + \frac{\partial \varphi'}{\partial x}, \quad \frac{\partial \Phi}{\partial y} = v = \frac{\partial \varphi'}{\partial y}, \quad \frac{\partial \Phi}{\partial z} = w = \frac{\partial \varphi'}{\partial z}$$

The direction cosines of an outward normal to the surface are found by formulas of analytical geometry:

$$\cos(\hat{n}, \hat{x}) = -A \frac{\partial f}{\partial x}, \quad \cos(\hat{n}, \hat{y}) = A; \quad \cos(\hat{n}, \hat{z}) = -A \frac{\partial f}{\partial z} \quad (8.1.10)$$

in which

$$A = [1 + (\partial f / \partial x)^2 + (\partial f / \partial z)^2]^{-1/2} \quad (8.1.11)$$

while the function  $f$  is determined by the shape of the wing surface [the function  $y = f_u(x, z)$  for the upper surface, and  $y = f_b(x, z)$  for the bottom one].

A linearized (nearly uniform) flow is realized provided that the wing is thin and, consequently,  $\partial f / \partial x \ll 1$  and  $\partial f / \partial z \ll 1$ . Accordingly,  $\cos(\hat{n}, \hat{x}) = -\partial f / \partial x$ ,  $\cos(\hat{n}, \hat{y}) = 1$ , and  $\cos(\hat{n}, \hat{z}) = -\partial f / \partial z$ . The conditions  $(\partial \varphi' / \partial x) \partial f / \partial x \ll 1$  and  $(\partial \varphi' / \partial z) \partial f / \partial z \ll 1$  are also observed in the flow over a thin wing. With this in view, (8.1.9) can be written as

$$-V_\infty \frac{\partial f}{\partial x} + \frac{\partial \varphi'}{\partial y} = 0;$$

whence the boundary condition is

$$\frac{\partial \varphi'}{\partial y} = V_\infty \frac{\partial f}{\partial x} \quad (8.1.12)$$

3. The flow over a wing may be attended by the developing of a lift force whose total magnitude is determined by integration over the surface of the values of the lift force acting on an elementary surface [a part of the wing having a width of  $dz$  and a chord length of  $b(z)$  (Fig. 8.1.1)]. In accordance with (6.1.8), and with the fact that

$\int_0^z \gamma(x) dx$  equals the circulation  $\Gamma$  in the section  $z$  being considered, the lift coefficient for an elementary surface equals the value  $c_{y_a}' = (2/V_\infty b) \Gamma(z)$ , whence the circulation in the given section is

$$\Gamma(z) = 0.5 c_{y_a}' V_\infty b \quad (8.1.13)$$

According to the coupling equation (8.1.13) [see (6.4.8)], upon moving to a neighbouring section with a different lift coefficient, the velocity circulation also changes. This change is

$$d\Gamma(z) = (d\Gamma/dz) dz = 0.5 V_\infty [d(c_{y_a}' b)/dz] dz \quad (8.1.14)$$

In accordance with the vortex model of a wing treated in Sec. 6.4, an *elementary bound vortex* belonging only to the section being con-

sidered passes within the contour enclosing the adjacent section. This vortex turns and is cast off the trailing edge in the form of a pair of elementary free vortices forming a vortex sheet behind the wing (Fig. 8.1.1). For a thin wing in a flow at a small angle of attack, we may assume that the width of this sheet equals the span of the wing, and that the direction of the free vortices coincides with the free-stream velocity.

Physical notions allow us to establish the following boundary conditions on a vortex sheet. The normal component of a particle's velocity  $v_n = \partial\varphi'/\partial n$  remains continuous on the sheet. Since the direction of a normal on the vortex sheet differs only slightly from the direction of the axis  $Oy$ , the derivative  $\partial\varphi'/\partial n$  equals the quantity  $\partial\varphi'/\partial y$ . Consequently, we can write the condition

$$(\partial\varphi'/\partial y)_{y=+0} = (\partial\varphi'/\partial y)_{y=-0} \quad (8.1.15)$$

in which the left-hand side corresponds to the velocity  $V_n$  directly above the vortex sheet ( $y = +0$ ), and the right-hand side, to the velocity under it ( $y = -0$ ). Hence, condition (8.1.15) expresses the continuity of the function  $\partial\varphi'/\partial y$  when passing through a vortex sheet.

In addition, the condition of the continuity of the pressure is satisfied on a vortex sheet. According to (7.1.5'), we obtain the relation

$$(\partial\varphi'/\partial x)_{y=+0} = (\partial\varphi'/\partial x)_{y=-0} \quad (8.1.16)$$

that also expresses the continuity of the partial derivative  $\partial\varphi'/\partial x$  when passing through a vortex sheet.

Let us consider the flow over a wing with a symmetric airfoil ( $y_u = -y_b$ ) at a zero angle of attack. In this case, there is no lift force and, consequently, no vortex sheet. Owing to the wing being symmetric, the vertical components of the velocity on its upper and bottom sides are equal in magnitude and opposite in sign, i.e.  $v(x, +y, z) = -v(x, -y, z)$ . On plane  $xOz$  outside the wing, the component  $v = 0$ , therefore

$$\partial\varphi'/\partial y = 0 \quad (8.1.17)$$

Let us assume further that we have a zero-thickness wing of the same planform in a flow at a small angle of attack. The equation of the wing's surface is  $y = f(x, z)$ . A glance at (8.1.12) reveals that the vertical velocity components  $V_n = \partial\varphi'/\partial y$  on the upper and bottom sides of the wing are identical at corresponding points. Since we are dealing with a sufficiently small angle of attack of the wing, the same condition can be related to the plane  $y = 0$ . At the same time, such a condition can be extended to the vortex sheet behind the wing, which is considered as a continuation of the vortices in the plane  $y = 0$ . Therefore, at points symmetric about this plane, the

components  $V_n$  are the same, i.e.  $\partial\varphi'(x, -y, z)/\partial y = \partial\varphi'(x, +y, z)/\partial y$ . Consequently, the additional potential  $\varphi'$  is an odd function relative to the coordinate  $y$ , i.e.

$$\varphi'(x, -y, z) = -\varphi'(x, +y, z) \quad (8.1.18)$$

Accordingly, the partial derivative  $\partial\varphi'/\partial x$  on the bottom side of the vortex sheet equals the value  $-\partial\varphi'/\partial x$  on the upper side. But the equality of the derivatives  $\partial\varphi'/\partial x$  was established from the condition of pressure continuity. This equality can be observed only when

$$\partial\varphi'/\partial x = 0 \quad (8.1.19)$$

on the vortex sheet.

4. To establish the last boundary condition, let us consider the disturbed regions  $S_r$  and  $S_1$  (Fig. 8.1.1) that are cut off from the plane  $y = 0$  by the Mach wave surface and located outside the wing and the vortex sheet. Over these regions of the plane  $y = 0$  and within the limits of the wave zone, the flow is continuous, therefore the potential  $\varphi'$  here is also a continuous function. At the same time, taking into account that by (8.1.18) the function  $\varphi'$  is odd, we should adopt the following equation for the plane  $y = 0$ :

$$\varphi'(x, 0, z) = 0 \quad (8.1.20)$$

#### Components of the Total Values of the Velocity Potentials and Aerodynamic Coefficients

The solution of Eq. (8.1.7) for the additional potential  $\varphi'$  must correspond to the considered boundary conditions. This solution can be obtained for a wing with a given planform by summation of two potentials: the first,  $\varphi'_1$ , is found for an idealized flat wing 1 (Fig. 8.1.2) of the same planform as the given one, but with a *symmetric airfoil*, and at a zero angle of attack ( $\alpha = 0$ ). The second potential,  $\varphi'_2$ , is evaluated for a different idealized *cambered wing 2 of zero thickness*, but for the given angle of attack  $\alpha$ .

The surface of an idealized symmetric airfoil wing can be given by the equation

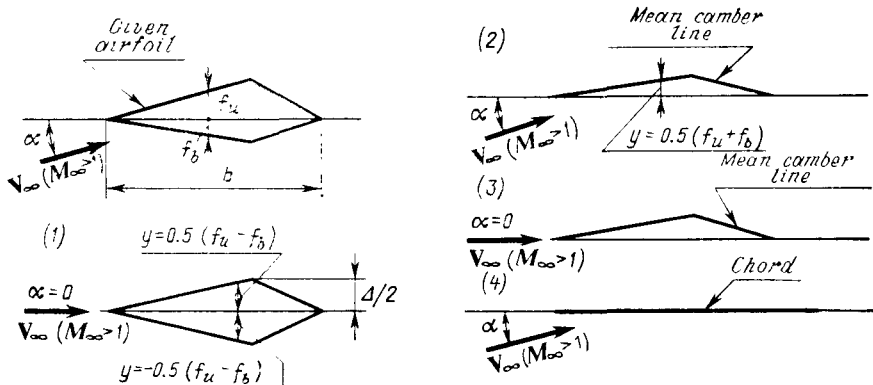
$$y = \pm 0.5 (f_u - f_b) \quad (8.1.21)$$

and of a zero-thickness airfoil wing, by the equation of the surface of the mean camber lines of the airfoil

$$y = 0.5 (f_u + f_b) \quad (8.1.22)$$

Hence, the total potential of the given wing is

$$\varphi' = \varphi'_1 + \varphi'_2 \quad (8.1.23)$$

**Fig. 8.1.2**

Linearized supersonic flow over a finite thickness airfoil at an angle of attack  $\alpha$ : 1— $\alpha = 0$ , symmetric airfoil, and given thickness distribution; 2— $\alpha \neq 0$ , zero thickness (the airfoil coincides with the mean camber line); 3— $\alpha = 0$ , zero thickness (the airfoil coincides with the mean camber line); 4— $\alpha \neq 0$ , zero thickness (the plate airfoil coincides with the chord)

The flow past wing 2, in turn, at  $\alpha \neq 0$  can be represented as a flow past wing 3 with a zero angle of attack and a surface equation  $y = 0.5(f_u + f_b)$  and an additional flow superposed onto this one. The additional flow is formed near wing 4 in the form of a zero thickness plate coinciding with the chord of the initial wing having an angle of attack  $\alpha$  (Fig. 8.1.2). In accordance with this flow scheme, the total potential for the given wing is

$$\varphi' = \varphi'_1 + \varphi'_3 + \varphi'_4 \quad (8.1.24)$$

We can use this value of the velocity potential to calculate the distribution of the pressure coefficient

$$\bar{p} = \bar{p}_1 + \bar{p}_3 + \bar{p}_4 \quad (8.1.25)$$

and then find the drag and lift forces. By (8.1.24) and (8.1.25), the total drag of the given wing is composed of the drags produced by wings 1, 3, and 4, i.e.

$$X_a = X_1 + X_3 + X_4 \quad (8.1.26)$$

Introducing the notation  $X_3 + X_4 = X_i$  and going over from the forces to the corresponding aerodynamic coefficients, we have

$$\frac{X_a}{q_\infty S_w} = \frac{X_1}{q_\infty S_w} + \frac{X_3 + X_4}{q_\infty S_w} = \frac{X_1}{q_\infty S_w} + \frac{X_i}{q_\infty S_w}$$

or

$$c_{x_a} = c_{x_0} + c_{x_3} + c_{x_4} = c_{x_0} + c_{x_i} \quad (8.1.27)$$

In accordance with (8.1.27), the wing drag coefficient  $c_{x_a}$  consists of the drag coefficient  $c_{x_0}$  of a symmetric wing at  $c_{y_a} = 0$  and the additional drag coefficient  $c_{x,i}$  due to the lift force and calculated for a zero-thickness wing at  $c_{y_a} \neq 0$ . The coefficient  $c_{x,i}$ , in turn, consists of the **induced wave drag coefficient** calculated for the case when the influence of vortices is absent and an additional **induced vortex drag coefficient** due to the span being finite and to the formation in this connection of a vortex sheet behind the trailing edge.

By analogy with expression (8.1.26) for the drag, let us give in the general form a relation determining the total magnitude of the lift force of a wing  $Y_a = Y_1 + Y_3 + Y_4$ . A glance at Fig. 8.1.2 reveals that wing 1 having a symmetric airfoil and arranged at a zero angle of attack does not create a lift force ( $Y_1 = 0$ ). Consequently, the total lift force of the wing is

$$Y_a = Y_3 + Y_4 \quad (8.1.28)$$

and the corresponding coefficient of this force is

$$c_{y_a} = c_{y_3} + c_{y_4} \quad (8.1.29)$$

Hence, according to the approximate linearized theory of flow, the thickness of a wing does not affect the lift force. Wing 3 produces a constant lift force that does not depend on the angle of attack. It corresponds to the value of this force at a zero angle of attack and a given concavity of a wing. A lift force due to the angle of attack is produced by wing 4 and, therefore, depends on the planform of the wing.

The finding of the pressure distribution, the resultant forces, and the relevant aerodynamic coefficients with a view to their possible resolution into components according to formulas (8.1.27) and (8.1.29) is the basic problem of the aerodynamics of a finite-span wing in a nearly uniform supersonic flow.

#### Features of Supersonic Flow over Wings

When determining the aerodynamic characteristics of wings, we must take account of the features of the supersonic flow over them. These features are due to the specific property of supersonic flows in which the disturbances propagate only downstream and within the confines of a disturbance (Mach) cone with an apex angle of  $\mu_\infty = \sin^{-1}(1/M_\infty)$ .

Let us consider a supersonic flow over a thin wing having an arbitrary planform (Fig. 8.1.3). Point  $O$  on the leading edge is a source of disturbances propagating downstream within the confines of a Mach cone. The Mach lines  $OF$  and  $OG$  are both ahead of the leading edges

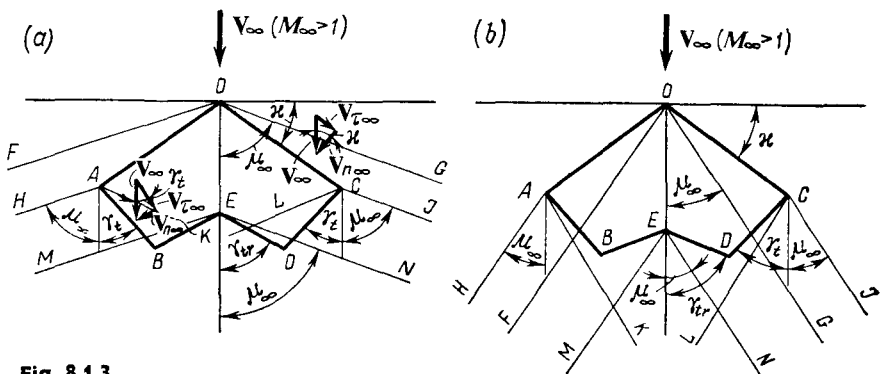


Fig. 8.1.3

Supersonic flow over a wing:

a—wing with subsonic edges; b—wing with supersonic edges

(Fig. 8.1.3a) and behind them (Fig. 8.1.3b). The arrangement of the Mach lines at a given wing planform depends on the number  $M_\infty$ . In the first case, the number  $M_\infty$  is smaller than in the second one, and the angle of inclination of the Mach line  $\mu_\infty > \pi/2 - \alpha$  ( $\alpha$  is the sweep angle). The normal velocity component to the leading edge is  $V_{n\infty} = V_\infty \cos \alpha$ . Since  $\cos \alpha < \sin \mu_\infty = 1/M_\infty$  and  $V_\infty/a_\infty = M_\infty$ , the normal component  $V_{n\infty}$  is evidently smaller than the speed of sound. The flow of a gas in the region of the leading edge of a swept wing for this case was considered in Sec. 7.6. This flow corresponds to the subsonic flow over an airfoil that is characterized by interaction between the upper and bottom surfaces occurring through the leading edge. Such a leading edge is called **subsonic** (Fig. 8.1.3a).

Upon an increase in the flow velocity, when the zone of disturbance propagation narrows and the Mach lines are behind the leading edges as shown in Fig. 8.1.3b, the normal velocity component becomes supersonic. Indeed, examination of Fig. 8.1.3b reveals that the angle of inclination of the Mach line  $\mu_\infty < \pi/2 - \alpha$ , hence  $\sin \mu_\infty = 1/M_\infty < \cos \alpha$ , and therefore  $V_{n\infty} = V_\infty \cos \alpha > a_\infty$ . Such a leading edge is called **supersonic**. The flow over airfoils in the region of the leading edge is of a supersonic nature whose feature is the absence of interaction between the bottom and the upper surfaces.

If the Mach line coincides with the leading edge ( $\alpha = \pi/2 - \mu_\infty$ ), such an edge is **sonic**. It is quite evident that in this case the magnitude of the normal velocity component to the edge equals the speed of sound.

Let us introduce the leading edge sweep parameter  $n = \tan \alpha / \cot \mu_\infty$ . For a supersonic leading edge,  $\cot \mu_\infty > \tan \alpha$ , therefore

$n < 1$ . For subsonic and sonic leading edges, we have  $n > 1$  and  $n = 1$ , respectively, because in the first case  $\cot \mu_\infty < \tan \alpha$  and in the second one  $\cot \mu_\infty = \tan \alpha$ .

By analogy with the leading edges, we can introduce the concept of subsonic, sonic, and supersonic tips (side edges) and trailing edges of a wing. *Tip CD with an angle of inclination  $\gamma_t$  to the direction of the free-stream velocity smaller than the Mach angle* (Fig. 8.1.3a) is called **subsonic**. The velocity component normal to a tip and equal to  $V_{n\infty} = V_\infty \sin \gamma_t$  is lower than the speed of sound in the given case. Indeed, since  $a_\infty = V_\infty \sin \mu_\infty$  and  $\mu_\infty > \gamma_t$ , we have  $V_{n\infty} < a_\infty$ . It is obvious that the leading edge sweep parameter  $n > 1$ . The part of the wing surface with a subsonic tip is inside the region cut off by the Mach cones issuing from corners A and C of the contour. Owing to a subsonic normal velocity component determining the flow over this part of the wing, air is observed to overflow the tips, the result being a change in the pressure distribution. Such an influence of the wing tips on the flow over the wing as a whole is not observed if the tips are supersonic, as when  $\gamma_t > \mu_\infty$  (Fig. 8.1.3b). In this case, the normal component  $V_{n\infty} = V_\infty \sin \gamma_t$  is higher than the speed of sound  $a_\infty = V_\infty \sin \mu_\infty$ .

Similar reasoning can be related to the trailing edge of the wing. Fig. 8.1.3a shows a subsonic trailing edge ( $\gamma_{tr} < \mu_\infty$ ;  $V_{n\infty} < a_\infty$ ), and Fig. 8.1.3b—a supersonic one ( $\gamma_{tr} > \mu_\infty$ ;  $V_{n\infty} > a_\infty$ ).

The above analysis allows one to establish the qualitative difference between supersonic and subsonic flow over wings. This difference manifests itself in the different influence of the tips and trailing edges on the flow over the entire wing surface. If in a supersonic flow, the tips and trailing edges do not affect the flow over the wing (Fig. 8.1.3b), or this influence is limited to the part of the surface adjoining these tips and edges (Fig. 8.1.3a), in a subsonic flow the action of the tips and trailing edges manifests itself on the entire surface because the disturbances can propagate both downstream and upstream.

## 8.2. Method of Sources

To solve the problem on determining the aerodynamic characteristics  $(\bar{p}_1, c_{x0})$  of a thin symmetric airfoil wing of an arbitrary planform in a nearly uniform supersonic flow at a zero angle of attack ( $c_y = 0$ ), we shall use the **method of sources**.

Sources in an incompressible fluid are treated in Sec. 2.9. The velocity potential of the incompressible flow from a point source at the origin of coordinates of the system  $x_{1c}, y_{1c}, z_{1c}$ , according to (2.9.14), is

$$\varphi_{1c} = -q_{1c}/(4\pi \sqrt{x_{1c}^2 + y_{1c}^2 + z_{1c}^2}) \quad (8.2.1)$$

where  $q_{ic}$  is the flow rate of the source, i.e. the volume of fluid flowing out of the source in unit time.

The method of sources deals not with individual point sources, but with sources continuously distributed over a part of a plane, usually the coordinate plane  $xOz$ .

Let  $dq_{ic}$  be the elementary volume flow rate of the fluid produced by the sources on the small area  $d\sigma_{ic} = d\xi_{ic} d\zeta_{ic}$  in the plane  $xOz$ . Hence the derivative  $dq_{ic}/d\sigma_{ic} = Q_{ic}$ , known as the **density (or intensity) of source distribution**, determines the strength of the sources per unit area.

If  $\pm v$  is the vertical component of the velocity on the area  $d\sigma_{ic}$  (the plus sign signifies that the fluid is discharged upward from the sources, and the minus sign—downward), the elementary volume flow rate is evidently  $dq_{ic} = 2v d\sigma_{ic}$  and, therefore,

$$Q_{ic} = 2v \quad (8.2.2)$$

The following potential corresponds to an elementary source:

$$d\varphi'_{ic} = -Q_{ic} d\sigma_{ic} / (4\pi \sqrt{x_{ic}^2 + y_{ic}^2 + z_{ic}^2}) \quad (8.2.3)$$

Using this expression, we can obtain a relation for the elementary potential of a source in a subsonic compressible flow. To do this, let us consider Eq. (8.1.7) and introduce the new variables

$$x_{ic} = x/\sqrt{1 - M_\infty^2}, \quad y_{ic} = y, \quad z_{ic} = z \quad (8.2.4)$$

With the aid of these variables, Eq. (8.1.7) is transformed as follows

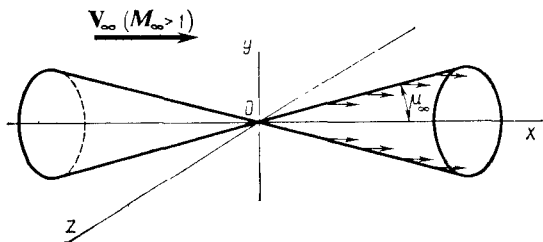
$$\partial^2 \varphi' / \partial x_{ic}^2 + \partial^2 \varphi' / \partial y_{ic}^2 + \partial^2 \varphi' / \partial z_{ic}^2 = 0 \quad (8.2.5)$$

This expression coincides with the continuity equation (2.4.8') for an incompressible flow. Consequently, the problem on the compressible disturbed flow in the coordinates  $x$ ,  $y$ , and  $z$  can be reduced to the problem on an incompressible disturbed flow in the coordinates  $x_{ic}$ ,  $y_{ic}$ , and  $z_{ic}$ , both systems of coordinates being related by conditions (8.2.4).

Accordingly, we can go over from potential (8.2.3) for an elementary source of an incompressible fluid to the relevant potential for a subsonic source of a compressible fluid. To do this, we shall find the relation between the small area  $d\sigma_{ic}$  on the plane  $x_{ic}Oz_{ic}$  in the incompressible flow and the area  $d\sigma$  on a corresponding plane in the compressible flow. Using (8.2.4) (with the substitution of  $\xi$  for  $x_{ic}$  and  $\zeta$  for  $z_{ic}$ ) and the expression  $d\sigma_{ic} = d\xi_{ic} d\zeta_{ic}$ , we find that  $d\sigma_{ic} = d\xi d\zeta (1/\sqrt{1 - M_\infty^2})$ , whence, taking into account that  $d\xi d\zeta = d\sigma$ , we find

$$d\sigma_{ic} = d\sigma / \sqrt{1 - M_\infty^2} \quad (8.2.6)$$

Let us transform the expression for  $Q_{ic}$  in (8.2.3). The component  $v_{ic} = \partial \varphi' / \partial y_{ic}$ , or with a view to (8.2.4),  $v_{ic} = \partial \varphi' / \partial y$ . It thus follows

**Fig. 8.2.1**

Disturbed flow due to a supersonic source:

at the right—a Mach (disturbance) cone in a real supersonic flow, at the left—an “inverted Mach cone”

that in a compressible flow, the velocity component  $v$  equals the component  $v_{lc}$  in an incompressible flow. Hence, the density of source distribution in a compressible and incompressible flows is the same, i.e.

$$Q_{lc} = Q = 2v_{lc} = 2v \quad (8.2.7)$$

With account taken of the relations obtained for a compressible flow, (8.2.3) is transformed to the following expression:

$$d\varphi' = Q d\sigma / [4\pi \sqrt{x^2 + (1 - M_\infty^2)(y^2 + z^2)}] \quad (8.2.8)$$

We can convince ourselves by direct substitution that the function  $\varphi'$  is an integral of Eq. (8.2.5). It does not matter whether the velocity is subsonic ( $M_\infty < 1$ ) or supersonic ( $M_\infty > 1$ ). In the latter case, it is convenient to write the expression for the elementary potential as

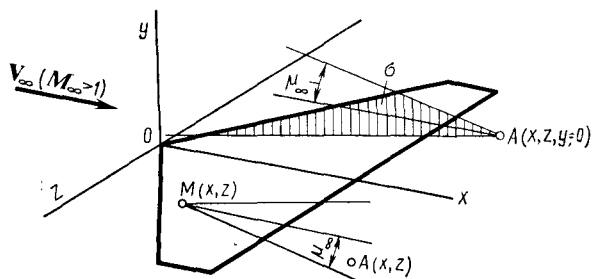
$$d\varphi' = -Q d\sigma / [4\pi \sqrt{x^2 - \alpha'^2(y^2 + z^2)}] \quad (8.2.9)$$

where  $\alpha'^2 = M_\infty^2 - 1$ .

Examination of expression (8.2.9) reveals that when  $M_\infty > 1$  it has real values in the region of space where  $x^2 \geq \alpha'^2(y^2 + z^2)$ . This signifies that the region of source influence, i.e. the region of disturbed flow experiencing the action of these sources, is inside the conical surface represented by the equation  $x^2 = \alpha'^2(y^2 + z^2)$ . If a point is outside this surface, the sources have no influence on it. Here there is no disturbed flow from a given source.

Formally, the equation  $x^2 = \alpha'^2(y^2 + z^2)$  determines the surfaces of two aligned cones (Fig. 8.2.1) with their vertices at the origin of coordinates, and, consequently, the strength of a source  $Q d\sigma$  is used to produce disturbed flows inside these cones. In a real case, supersonic disturbances propagate only downstream and only inside one cone (the right-hand one in Fig. 8.2.1).

The disturbed flow in such a cone is determined by a potential double that given by (8.2.9) because the entire strength of the source,

**Fig. 8.2.2**

Region of influence of supersonic sources

and not half of it, is realized in the flow confined within the Mach cone. Accordingly,

$$d\varphi' = -Q d\sigma / [2\pi \sqrt{x^2 - \alpha'^2 (y^2 + z^2)}] \quad (8.2.10)$$

In the considered case, the elementary area  $d\sigma = d\xi d\zeta$  with the sources is at the origin of coordinates. If it is displaced with respect to the origin of coordinates to a point with the coordinates  $x = \xi$  and  $z = \zeta$ , Eq. (8.2.10) has the form

$$d\varphi' = -Q d\sigma / \{2\pi \sqrt{(x - \xi)^2 - \alpha'^2 (y^2 + (z - \zeta)^2)}\} \quad (8.2.11)$$

When studying the flow over a wing, its surface is replaced with a **system of disturbed sources**. To obtain the potential due to these sources at arbitrary point  $A(x, y, z)$  (Fig. 8.2.2), we must integrate (8.2.11) over the region  $\sigma$  in which only part of the sources are located. Each of these sources influences point  $A(x, y, z)$  if it is inside a Mach cone with its vertex in the source. Hence, the region affected by the sources (the region of integration) is in the zone of intersection with the wing surface of an "inverted Mach cone" with its vertex at point  $A(x, y, z)$  being considered.

In a simpler case, point  $A$  and the source are located, as can be seen from Fig. 8.2.2, in the same plane  $y = 0$ . In this case, the affected zone coincides with the region of intersection of the wing and the Mach lines issuing from point  $M(x, z)$ , while the region of integration  $\sigma$  is on the wing and is the intersection of the wing surface with the inverted plane Mach wave having its vertex at point  $A(x, z)$ .

Having determined the integration region  $\sigma$ , we can evaluate the total potential at point  $A(x, y, z)$ :

$$\varphi'(x, y, z) = -\frac{1}{2\pi} \iint_{\sigma} \frac{Q(\xi, \zeta) d\xi d\zeta}{\sqrt{(x - \xi)^2 - \alpha'^2 (y^2 + (z - \zeta)^2)}} \quad (8.2.12)$$

By calculating the partial derivative of  $\varphi'$  (8.2.12) with respect to  $x$ , we find the additional axial velocity component:

$$\frac{\partial \varphi'}{\partial x} = u = \frac{1}{2\pi} \int \int_{\sigma} \frac{Q(\xi, \zeta)(x - \xi) d\xi d\zeta}{V \{(x - \xi)^2 - \alpha'^2 [y^2 + (z - \zeta)^2]\}^3} \quad (8.2.13)$$

We use this value to determine the pressure coefficient  $\bar{p} = -2u/V_{\infty}$  at the corresponding point.

Let us introduce the new coordinates

$$x_1 = x/\alpha', \quad y_1 = y, \quad z_1 = z \quad (8.2.14)$$

In these coordinates, expression (8.2.12) has the form

$$\varphi'(x_1, y_1, z_1) = -\frac{1}{2\pi} \int \int_{\sigma} \frac{Q(\xi, \zeta) d\xi d\zeta}{V(x_1 - \xi)^2 - y_1^2 - (z_1 - \zeta)^2} \quad (8.2.15)$$

In a particular case for points on the wing surface ( $y_1 = 0$ ), the additional potential is

$$\varphi'(x_1, 0, z_1) = -\frac{1}{2\pi} \int \int_{\sigma} \frac{Q(\xi, \zeta) d\xi d\zeta}{V(x_1 - \xi)^2 - (z_1 - \zeta)^2} \quad (8.2.16)$$

where by (8.2.7)

$$Q = 2v_{y_1=0} = 2 (\partial \varphi' / \partial y_1)_{y_1=0} \quad (8.2.17)$$

The expressions obtained for the potential function allow us to calculate the distribution of the velocity and pressure over the surface of a thin wing if its planform, airfoil configuration, and the free stream number  $M$  are given.

### 8.3. Wing with a Symmetric Airfoil and Triangular Planform

$$(\alpha = 0, c_{y_a} = 0)$$

#### Flow over a Wing Panel with a Subsonic Leading Edge

Let us consider a supersonic flow at a zero angle of attack over a wing panel with a symmetric airfoil that is a triangular surface in which one of the side edges is directed along the  $x$ -axis, while the trailing edge is removed to infinity (such a panel is also called an infinite triangular half-wing, Fig. 8.3.1). If such a surface has a *subsonic leading edge*, the Mach line issuing from vertex  $O$  is ahead of this edge.

The flow parameters at small angles of attack  $\alpha$  can be determined by replacing the surface in the flow with a system of distributed sources on the plane  $y = 0$ . Let us consider arbitrary point  $P$  on the surface and evaluate the velocity potential at this point by add-

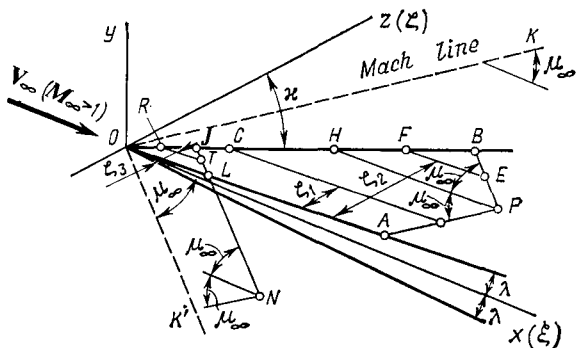


**Fig. 8.3.1**  
Triangular wing with a subsonic leading edge

ing up the action of the sources in region  $OAPB$  confined by the leading  $OA$  and side  $OB$  edges, and also by the Mach lines  $AP$  and  $BP$ .

We determine the strength  $Q(\xi, \zeta)$  of the sources by formula (8.2.7) in which according to the condition of flow without separation we have  $v = \lambda V_\infty$ , where  $\lambda = dy/dx$  is the angular coefficient of the wing surface. Hence

$$Q(\xi, \zeta) = 2\lambda V_\infty$$

The velocity potential at point  $P$  is determined by formula (8.2.12). Performing the substitution  $Q = 2\lambda V_\infty$  and assuming that  $y = 0$ , we obtain

$$\varphi' = -\frac{\lambda V_\infty}{\pi} \iint_{\sigma} \frac{d\xi d\zeta}{V(x_p - \xi)^2 - \alpha'^2(z_p - \zeta)^2} \quad (8.3.1)$$

where  $x_p$  and  $z_p$  are the coordinates of point  $P$ .

This integral takes into account the action on point  $P$  of sources located on the area  $\sigma$  equal to region  $OAPB$  that can be represented as the sum of two sections:  $OAPH$  and  $HPB$ . Accordingly, the integral  $\varphi'$  (8.3.1) can be written as the sum of two integrals:

$$\varphi' = \frac{\lambda V_\infty}{\pi} \left[ \iint_{OAPH} f(\xi, \zeta) d\xi d\zeta + \iint_{HPB} f(\xi, \zeta) d\xi d\zeta \right] \quad (8.3.2)$$

where

$$f(\xi, \zeta) = [(x_p - \xi)^2 - \alpha'^2(z_p - \zeta)^2]^{-1/2} \quad (8.3.3)$$

On section  $OAPH$ , integration with respect to  $\xi$  for each value of  $\zeta = \zeta_1$  must be performed from  $\xi = \xi_C = \zeta \tan \alpha$  to  $\xi = \xi_D = x_p - \alpha'(z_p - \zeta)$ , and integration with respect to  $\zeta$  from 0 to  $z_p$ . On section  $HPB$ , integration with respect to  $\xi$ , for which the value of  $\zeta = \zeta_2$ , must be performed from  $\xi = \xi_F = \zeta \tan \alpha$  to  $\xi = \xi_E = x_p - \alpha'(\zeta - z_p)$ , and integration with respect to  $\zeta$  from  $z_p$  to

$z_B = (x_P + \alpha' z_P) / (\alpha' + \tan \alpha)$ . Hence,

$$\begin{aligned} \varphi' = & -\frac{\lambda V_\infty}{\pi} \left[ \int_0^{z_P} d\xi \int_{\xi \tan \alpha}^{x_P - \alpha'(z_P - \xi)} f(\xi, \zeta) d\zeta \right. \\ & \left. + \int_{z_P}^{z_B} d\xi \int_{\xi \tan \alpha}^{x_P - \alpha'(\xi - z_P)} f(\xi, \zeta) d\zeta \right] \end{aligned} \quad (8.3.4)$$

The indefinite integral

$$\int f(\xi, \zeta) d\xi = \int \frac{d\xi}{\sqrt{(x_P - \xi)^2 - \alpha'^2(z_P - \zeta)^2}} = \cosh^{-1} \frac{x_P - \xi}{\alpha' (z_P - \zeta)} \quad (8.3.5)$$

Using this expression and introducing the main value of the integral, we obtain the following formula for the potential function:

$$\varphi' = \frac{\lambda V_\infty}{\pi} \int_0^{z_B} \cosh^{-1} \frac{x_P - \zeta \tan \alpha}{\alpha' |z_P - \zeta|} d\zeta \quad (8.3.6)$$

By calculating the partial derivative  $\partial \varphi' / \partial x$ , we find the component of the additional velocity at point  $P$  in the direction of the  $x$ -axis:

$$u = \frac{\partial \varphi'}{\partial x} = \frac{\lambda V_\infty}{\pi} \int_0^{z_B} \frac{d\zeta}{\sqrt{(x_P - \zeta \tan \alpha)^2 - \alpha'^2 (z_P - \zeta)^2}} \quad (8.3.7)$$

Taking into account that  $\tan \alpha > \alpha'$  ( $\cot \mu_\infty$ ), we find as a result of integration that

$$u = -\frac{\lambda V_\infty}{\pi \sqrt{\tan^2 \alpha - \alpha'^2}} \cosh^{-1} \frac{x_P \tan \alpha - \alpha'^2 z_P}{\alpha' (x_P - z_P \tan \alpha)} \quad (8.3.8)$$

To facilitate the calculations, we shall introduce the angle  $\theta$  determined from the condition  $\tan \theta = z_P/x_P$ , and the nose angle of the leading edge  $\gamma = \pi/2 - \alpha$  (Fig. 8.3.2). In addition, let us introduce the notation

$$n = \tan \alpha / \alpha' = \tan \mu_\infty / \tan \gamma,$$

$$\sigma = z_P \tan \alpha / x_P = \tan \theta / \tan \gamma$$

With this taken into account, we have

$$u = -\frac{\lambda V_\infty}{\pi \alpha' \sqrt{n^2 - 1}} \cosh^{-1} \frac{n^2 - \sigma}{n(1 - \sigma)} \quad (8.3.9)$$

and the pressure coefficient is

$$\bar{p} = -\frac{2u}{V_\infty} = \frac{2\lambda}{\pi \alpha' \sqrt{n^2 - 1}} \cosh^{-1} \frac{n^2 - \sigma}{n(1 - \sigma)} \quad (8.3.10)$$

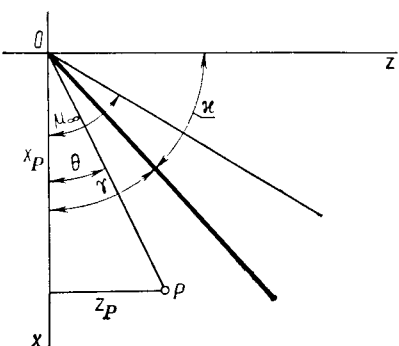


**Fig. 8.3.2**  
Angular parameters for a triangular wing

Now let us consider point  $N$  outside of the wing between the Mach line  $OK'$  and the  $x$ -axis (see Fig. 8.3.1) and calculate for it the velocity that is induced by the sources distributed over the wing surface. To do this, we shall use formula (8.3.1) determining the velocity potential. Taking into account that the action of the sources on point  $N$  is confined by the region  $\sigma = OLJ$ , we obtain the expression

$$\varphi' = -\frac{\lambda V_\infty}{\pi} \iint_{OLJ} f(\xi, \zeta) d\xi d\zeta \quad (8.3.11)$$

where the function  $f(\xi, \zeta)$  is determined by relation (8.3.3). Integration with respect to  $\xi$  for each value of  $\zeta = \zeta_3$  must be performed from  $\xi = \xi_R = \zeta \tan \alpha$  to  $\xi = \xi_T = x_N + \alpha'(z_N - \zeta)$ , and integration with respect to  $\zeta$ , from 0 to  $z_J$ . Hence,

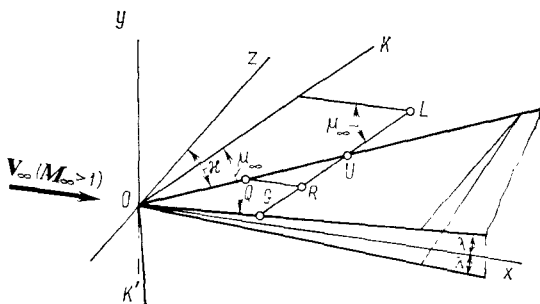
$$\varphi' = -\frac{\lambda V_\infty}{\pi} \int_0^{z_J} d\zeta \int_{\zeta \tan \alpha}^{x_N + \alpha'(z_N - \zeta)} f(\xi, \zeta) d\xi \quad (8.3.12)$$

where  $z_J = (x_N + \alpha' z_N)/(\alpha' + \tan \alpha)$ .

By integrating and using the main value of the integral, we obtain

$$\varphi' = \frac{\lambda V_\infty}{\pi} \int_0^{z_J} \cosh^{-1} \frac{x_N - \zeta \tan \alpha}{\alpha' |z_N - \zeta|} d\zeta$$

This expression is similar to (8.3.6) with the difference that the coordinate  $z_J$  is taken as the upper limit of the integral. By calculating the derivative  $\partial\varphi'/\partial x$  and integrating, we obtain relation (8.3.9) for the component of the additional velocity. We must assume in it that  $\sigma < 0$  because the coordinate  $z_N$  is negative. In calculations, the coordinate  $z_N$  may be assumed to be positive, and, consequently,  $\sigma > 0$ . If we take the magnitudes of  $\tan \alpha$ , then to determine the

**Fig. 8.3.3**

Influence of sources on the velocity outside a wing

induced velocity we may use Eq. (8.3.9) in which  $\sigma$  should be taken with the opposite sign. The working relation now becomes

$$u = -\frac{\lambda V_\infty}{\pi \alpha' \sqrt{n^2 - 1}} \cosh^{-1} \frac{n^2 + \sigma}{n(1 + \sigma)} \quad (8.3.13)$$

The pressure coefficient in the region being considered is

$$\bar{p} = -\frac{2u}{V_\infty} = \frac{2\lambda}{\pi \alpha' \sqrt{n^2 - 1}} \cosh^{-1} \frac{n^2 + \sigma}{n(1 + \sigma)} \quad (8.3.14)$$

The sources distributed over the wing also induce a velocity in the region between the Mach line  $OK$  and the leading subsonic edge (Fig. 8.3.3). The magnitude of this velocity at a point  $L$  is determined by the sources distributed on region  $OUG$ . We find the corresponding potential function by expression (8.3.12) in which we must introduce the coordinate  $z_U$  instead of  $z_J$ , and replace the quantity  $x_N + \alpha' (z_N - \xi)$  with the value  $x_L - \alpha' (z_L - \xi)$  equal to the longitudinal coordinate of point  $R$  (Fig. 8.3.3). Hence,

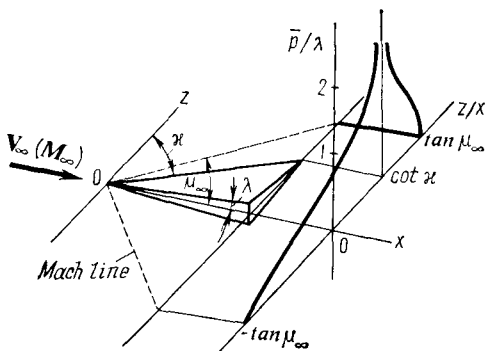
$$\varphi' = -\frac{\lambda V_\infty}{\pi} \int_0^{z_U} d\xi \int_{\xi \tan \alpha}^{x_L - \alpha'(z_L - \xi)} f(\xi, \xi) d\xi \quad (8.3.15)$$

where  $z_U = (x_L - \alpha' z_L) / (\tan \alpha - \alpha')$ .

Integration yields

$$\varphi' = \frac{\lambda V_\infty}{\pi} \int_0^{z_U} \cosh^{-1} \frac{x_L - \xi \tan \alpha}{\alpha' |z_L - \xi|} d\xi$$

By evaluating the derivative  $\partial \varphi' / \partial x$  and then performing integration provided that  $\sigma = z_L \tan \alpha / x_P > 1$ , we obtain the following

**Fig. 8.3.4**

Pressure field for a triangular wing with a subsonic leading edge

formula similar to (8.3.9) for the additional velocity component:

$$u = -\frac{\lambda V_\infty}{\pi \alpha' \sqrt{n^2 - 1}} \cosh^{-1} \frac{n^2 - \sigma}{n(\sigma - 1)} \quad (8.3.16)$$

where  $n > \sigma$ .

We use the value of this velocity to find the pressure coefficient:

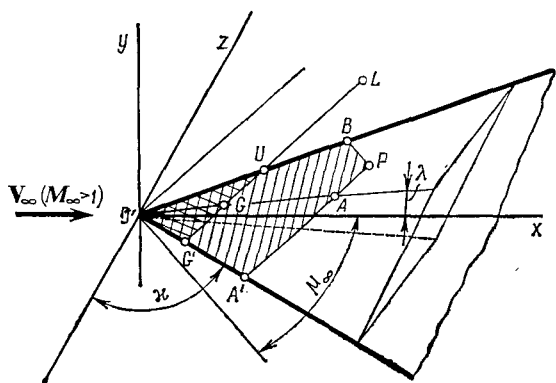
$$\bar{p} = -\frac{2u}{V_\infty} = \frac{2\lambda}{\pi \alpha' \sqrt{n^2 - 1}} \cosh^{-1} \frac{n^2 - \sigma}{n(\sigma - 1)} \quad (8.3.17)$$

Figure 8.3.4 shows the field of pressures for a wing with a triangular planform having a subsonic leading edge. The pressure coefficient along the Mach lines is zero. On the leading edge, the theoretical pressure coefficient equals infinity. The physically possible pressure can be considered to be sufficiently high, corresponding to the stagnation pressure at a subsonic velocity whose direction coincides with a normal to the leading edge.

#### Triangular Wing Symmetric about the $x$ -Axis with Subsonic Leading Edges

The velocity at point  $P$  of a triangular wing symmetric about the  $x$ -axis and having subsonic leading edges (Fig. 8.3.5) is determined by summing the action of sources in region  $OBPA'$  confined by leading edges  $OA'$  and  $OB$  and by Mach lines  $PA'$  and  $PB$ . The velocity induced by the sources distributed on section  $OAPB$  is determined by formula (8.3.9). The sources distributed in region  $OAA'$  produce at point  $P$  a velocity that is calculated by expression (8.3.13). The total value of the velocity is

$$u = -\frac{\lambda V_\infty}{\pi \alpha' \sqrt{n^2 - 1}} \left[ \cosh^{-1} \frac{n^2 - \sigma}{n(1 - \sigma)} + \cosh^{-1} \frac{n^2 + \sigma}{n(1 + \sigma)} \right]$$

**Fig. 8.3.5**

Triangular wing symmetric about the  $x$ -axis with subsonic leading edges

This expression can be transformed as follows:

$$u = -\frac{2\lambda V_\infty}{\pi\alpha' \sqrt{n^2-1}} \cosh^{-1} \sqrt{\frac{n^2-\sigma^2}{1-\sigma^2}} \quad (8.3.18)$$

Formula (8.3.18) is suitable for the conditions  $n > 1 > \sigma$ .

We can determine the pressure coefficient with the aid of (6.1.5) according to the known value of the additional velocity component:

$$\bar{p} = -\frac{2u}{V_\infty} = \frac{4\lambda}{\pi\alpha' \sqrt{n^2-1}} \cosh^{-1} \sqrt{\frac{n^2-\sigma^2}{1-\sigma^2}} \quad (8.3.19)$$

Point  $L$  located between the leading edge and the Mach wave (Fig. 8.3.5) is influenced by the sources distributed on section  $OUG'$  of the wing. The velocity induced by these sources can be calculated as the sum of the velocities induced by the sources in region  $OUG$  [formula (8.3.16)] and by the sources distributed in triangle  $OGG'$  [formula (8.3.13)].

Consequently,

$$u = -\frac{\lambda V_\infty}{\pi\alpha' \sqrt{n^2-1}} \left[ \cosh^{-1} \frac{n^2-\sigma}{n(\sigma-1)} + \cosh^{-1} \frac{n^2+\sigma}{n(1+\sigma)} \right]$$

or after transformations

$$u = -\frac{2\lambda V_\infty}{\pi\alpha' \sqrt{n^2-1}} \cosh^{-1} \sqrt{\frac{n^2-1}{\sigma^2-1}} \quad (8.3.20)$$

The corresponding pressure coefficient is

$$\bar{p} = \frac{4\lambda}{\pi\alpha' \sqrt{n^2-1}} \cosh^{-1} \sqrt{\frac{n^2-1}{\sigma^2-1}} \quad (8.3.21)$$

where  $n > \sigma > 1$ .

**Semi-Infinite Wing  
with a Supersonic Edge**

For such a wing (Fig. 8.3.6), Mach line  $OK$  issuing from a vertex is on its surface. Consequently,

$$\pi/2 - \alpha > \mu_\infty, \tan \alpha < \alpha', n = \tan \alpha / \alpha' < 1 (\alpha' = \cot \mu_\infty = \sqrt{M_\infty^2 - 1})$$

Let us consider the velocity at point  $L$  on the wing between the leading edge and Mach line  $OK$ . Since the side edge (tip) of the wing coinciding with the  $x$ -axis is outside the Mach line drawn through point  $L$ , no influence of the side edge is observed on the flow at this point. This flow is the same as over a flat plate in a flow directed along a normal to its leading edge at the supersonic velocity  $V_{n\infty} = V_\infty \cos \alpha > a_\infty$ . By expression (7.6.8) and the formula  $\bar{p} = -2u/V_\infty$ , the additional velocity component is

$$u = -\lambda V_\infty \cos \alpha / \sqrt{M_\infty^2 \cos^2 \alpha - 1}$$

Since

$$M_\infty^2 = \alpha'^2 + 1 \quad \text{and} \quad 1 - 1/\cos^2 \alpha = -\tan^2 \alpha$$

we have

$$u = -\lambda V_\infty / \sqrt{\alpha'^2 - \tan^2 \alpha}$$

whence

$$u = -\lambda V_\infty / (\alpha' \sqrt{1 - n^2}) \quad (8.3.22)$$

The relevant value of the pressure coefficient is

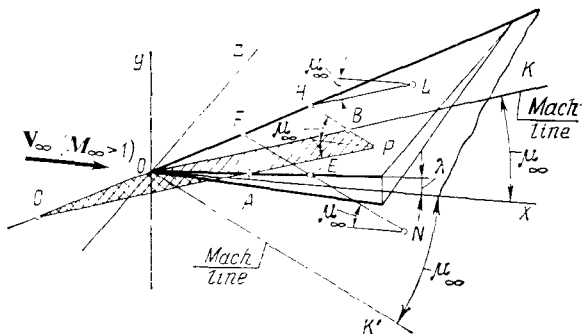
$$\bar{p} = -2u/V_\infty = 2\lambda / (\alpha' \sqrt{1 - n^2}) \quad (8.3.23)$$

Formulas (8.3.22) and (8.3.23) may be applied for  $n < 1$  and  $1 > \sigma > n$ .

Let us calculate the velocity and pressure at point  $P$  between Mach line  $OK$  and the side edge. If we assume that this point belongs to a wing whose vertex is at point  $C$  (Fig. 8.3.6), the velocity would be calculated with account taken of the influence of only the leading edge and, consequently, of the sources distributed in region  $PCH$ . By (8.3.22), this velocity is

$$u_{PCH} = -\lambda V_\infty / (\alpha' \sqrt{1 - n^2}) \quad (8.3.24)$$

To find the actual velocity at point  $P$  belonging to the wing with its vertex at point  $O$ , we must subtract from (8.3.24) the velocity induced by sources distributed in triangle  $ACO$  and having a strength of the opposite sign. The magnitude of this velocity is determined by means of formula (8.3.7). Substituting  $z_C = (x_P - \alpha' z_P) / (\tan \alpha - \alpha')$

**Fig. 8.3.6**

Triangular wing with a supersonic edge

for the upper limit  $z_B$  of the integral, after integration we obtain

$$u_{AOC} = \frac{\lambda V_\infty}{\pi} \int_0^{z_C} \frac{dz}{\sqrt{\zeta^2 (\tan^2 \alpha - \alpha'^2) - 2\zeta (x_P \tan \alpha - \alpha'^2 z_P) + x_P^2 - \alpha'^2 z_P^2}} \\ = - \frac{\lambda V_\infty}{\pi \sqrt{\alpha'^2 - \tan^2 \alpha}} \cos^{-1} \frac{\alpha'^2 z_P - x_P \tan \alpha}{\alpha' (x_P - z_P \tan \alpha)} \quad (8.3.25)$$

Taking into account that  $n = \tan \alpha / \alpha'$  and  $\sigma = z_P \tan \alpha / x_P$ , we find

$$u_{AOC} = - \frac{\lambda V_\infty}{\pi \alpha' \sqrt{1-n^2}} \cos^{-1} \frac{\sigma - n^2}{n(1-\sigma)} \quad (8.3.26)$$

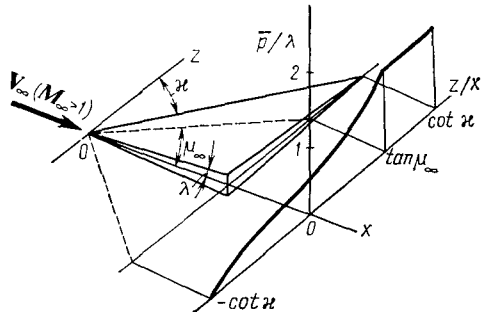
The total value of the additional velocity at point  $P$  is

$$u = u_{PCH} - u_{AOC} = - \frac{\lambda V_\infty}{\alpha' \sqrt{1-n^2}} \left[ 1 - \frac{1}{\pi} \cos^{-1} \frac{\sigma - n^2}{n(1-\sigma)} \right] \quad (8.3.27)$$

and the pressure coefficient is

$$\bar{p} = - \frac{2u}{V_\infty} = \frac{2\lambda}{\alpha' \sqrt{1-n^2}} \left[ 1 - \frac{1}{\pi} \cos^{-1} \frac{\sigma - n^2}{n(1-\sigma)} \right] \quad (8.3.28)$$

where  $\sigma < n < 1$ .The induced velocity at point  $N$ , between Mach wave  $OK'$  and the side edge is determined by summation of the action of the sources distributed on surface section  $OEF$  confined by leading edge  $OF$ , side edge  $OE$ , and Mach line  $EF$  drawn through point  $N$ .To calculate the velocity, we shall use formula (8.3.25), in which we shall replace the upper limit  $z_C$  of the integral with the quantity  $z_F = (x_N + \alpha' z_N) / (\tan \alpha + \alpha')$ , and the coordinates  $x_P$  and  $z_P$

**Fig. 8.3.7**

Pressure field for a semi-infinite triangular wing with a supersonic leading edge

with the relevant values  $x_N$  and  $z_N$ . Integration yields

$$u_{OEF} = -\frac{\lambda V_\infty}{\pi \sqrt{\alpha'^2 - \tan^2 \alpha}} \cos^{-1} \frac{x_N \tan \alpha - \alpha'^2 z_N}{\alpha' (x_N - z_N \tan \alpha)} \quad (8.3.29)$$

Introducing the symbols  $\sigma$  and  $n$ , we have

$$u_{OEF} = -\frac{\lambda V_\infty}{\pi \alpha' \sqrt{1-n^2}} \cos^{-1} \frac{n^2-\sigma}{n(1-\sigma)} \quad (8.3.30)$$

where  $\sigma < 0$ ,  $n < 1$ , and  $|\sigma| < n$ .

If we adopt positive values of  $z_N$  and  $\sigma = z_N \tan \alpha / x_N$  and take absolute values for  $n$ , the additional velocity is

$$u = -\frac{\lambda V_\infty}{\pi \alpha' \sqrt{1-n^2}} \cos^{-1} \frac{n^2+\sigma}{n(1+\sigma)} \quad (8.3.31)$$

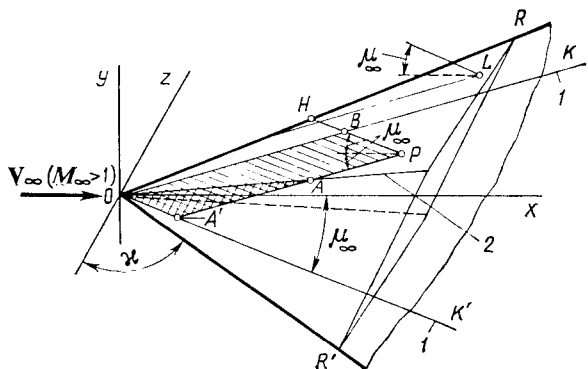
and the pressure coefficient is

$$\bar{p} = -\frac{2u}{V_\infty} = \frac{2\lambda}{\pi \alpha' \sqrt{1-n^2}} \cos^{-1} \frac{n^2+\sigma}{n(1+\sigma)} \quad (8.3.32)$$

The pressure field for a semi-infinite triangular wing with a supersonic leading edge is shown in Fig. 8.3.7. Between the leading edge and the internal Mach line, the pressure is constant, then it lowers, and on the external Mach line reaches the value of the free-stream pressure ( $\bar{p} = 0$ ).

#### Triangular Wing Symmetric about the $x$ -Axis with Supersonic Leading Edges

The velocity and the pressure coefficient at point  $L$  (Fig. 8.3.8) between Mach wave  $OK$  and the leading edge are determined by formulas (8.3.22) and (8.3.23), respectively, because the flow at this point is affected only by edge  $OR$ . These formulas may be applied for the conditions  $n < 1$  and  $1 > \sigma > n$ .

**Fig. 8.3.8**

Triangular wing symmetric about the  $x$ -axis with supersonic leading edges:  
1—Mach line; 2—maximum thickness line

The velocity at point  $P$  that is within the Mach angle is affected not only by the leading edge, but also by the trailing and side edges of the wing. The velocity due to the influence of the leading edge and part  $OA$  of the maximum thickness line (Fig. 8.3.8) is determined by formula (8.3.27), while the velocity induced by the sources distributed over region  $OA'A$  is evaluated by expression (8.3.31). Adding (8.3.27) and (8.3.31), we obtain the total velocity at point  $P$  of a symmetric wing:

$$u = -\frac{\lambda V_\infty}{\alpha' \sqrt{1-n^2}} \left[ 1 - \frac{1}{\pi} \cos^{-1} \frac{\sigma-n^2}{n(1-\sigma)} + \frac{1}{\pi} \cos^{-1} \frac{n^2+\sigma}{n(1+\sigma)} \right]$$

or after transformations,

$$u = -\frac{\lambda V_\infty}{\alpha' \sqrt{1-n^2}} \left( 1 - \frac{2}{\pi} \sin^{-1} \sqrt{\frac{n^2-\sigma^2}{1-\sigma^2}} \right) \quad (8.3.33)$$

The corresponding pressure coefficient is

$$\bar{p} = -\frac{2u}{V_\infty} = \frac{2\lambda}{\alpha' \sqrt{1-n^2}} \left( 1 - \frac{2}{\pi} \sin^{-1} \sqrt{\frac{n^2-\sigma^2}{1-\sigma^2}} \right) \quad (8.3.34)$$

#### 8.4. Flow over a Tetragonal Symmetric Airfoil Wing with Subsonic Edges at a Zero Angle of Attack

By using the formulas for determining the velocity and pressure on the surface of a triangular wing, we can calculate the flow at a zero angle of attack over wings with a symmetric airfoil and an arbi-

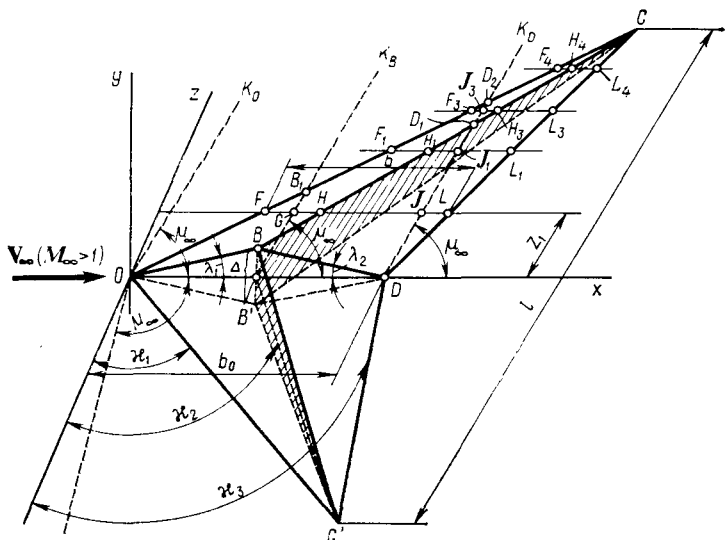


**Fig. 8.4.1**  
Tetragonal wing with a symmetriic airfoil and subsonic edges

trary planform. Let us consider the tetragonal wing shown in Fig. 8.4.1. A left-hand system of coordinates has been adopted here and in some other figures to facilitate the spatial depicting of the wing and the arrangement of both the sections being considered and the required notation. We shall assume that for such a wing the *leading* and *trailing edges*, and also *maximum thickness line*  $CBC'$  are subsonic. Accordingly, the sweep angles  $\alpha_1$ ,  $\alpha_3$  of the leading and trailing edges and the angle  $\alpha_2$  of the maximum thickness line are larger than  $\pi/2 - \mu_\infty$ .

The distribution of the velocity and pressure over an airfoil depends on where the latter is along the wing span, i.e. on the lateral coordinate  $z$  of the section.

**Airfoil  $FL$**  ( $z = z_1$ ). Four flow regions, namely,  $FG$ ,  $GH$ ,  $HJ$ , and  $JL$ , should be considered on the airfoil. Region  $FG$  is confined by point  $F$  on the leading edge and point  $G$  at the intersection of a Mach line with the coordinate plane  $z = z_1$ . Point  $G$  is considered to be on plane  $zOx$  and is determined, consequently, as the point of intersection of the Mach line issuing from the projection  $B'$  of point  $B$  onto plane  $zOx$  and of the straight line  $z = z_1$  (Fig. 8.4.1). The velocity and pressure coefficient in region  $FG$  behind Mach line  $OK_0$  on the surface of the wing are determined with the aid of the distribution of the sources in triangle  $OCC'$  by the relevant formulas (8.3.18) and (8.3.19).

Since the inclination of the surface is  $\lambda_1$  in accordance with (8.3.19) we have

$$\bar{p}_{FG} = \frac{4\lambda_1}{\pi\alpha' \sqrt{n_1^2 - 1}} \cosh^{-1} \sqrt{\frac{n_1^2 - \sigma_1^2}{1 - \sigma_1^2}} \quad (8.4.1)$$

where  $n_1 = \tan \alpha_1 / \alpha'$ ,  $\sigma_1 = z_1 \tan \alpha_1 / x_1$ , and  $x_1$  is the running coordinate of the point.

The drag coefficient of the airfoil corresponding to region  $FG$  is

$$c_{x, FG} = \frac{\lambda_1}{b} \int_{x_F}^{x_G} (\bar{p}_u + \bar{p}_b) dx_1 \quad (8.4.2)$$

where  $b$  is the local chord of the profile.

Since

$$\begin{aligned} \bar{p}_u + \bar{p}_b &= 2\bar{p}_{FG}, \quad \sigma_1 = \frac{z_1 \tan \alpha_1}{x_1}, \\ d\sigma_1 &= -\frac{z_1 \tan \alpha_1}{x_1^2} dx_1 = -\frac{dx_1}{z_1 \tan \alpha_1} \sigma_1^2 \end{aligned}$$

we have

$$c_{x, FG} = \frac{-8\lambda_1^2 z_1 \tan \alpha_1}{b\pi\alpha' \sqrt{n^2 - 1}} \int_{\sigma_{1F}}^{\sigma_{1G}} \cosh^{-1} \sqrt{\frac{n_1^2 - \sigma_1^2}{1 - \sigma_1^2}} \cdot \frac{d\sigma_1}{\sigma_1^2} \quad (8.4.3)$$

where  $\sigma_{1F} = z_1 \tan \alpha_1 / x_F = 1$ , and  $\sigma_{1G} = z_1 \tan \alpha_1 / x_G$ .

Region  $GH$  is acted upon by the distribution of the sources in triangle  $OCC'$  with a strength of  $Q = 2\lambda_1 V_\infty$  and in triangle  $BCC'$  where the strength of the sources  $Q = 2(\lambda_2 - \lambda_1) V_\infty$  (the sign of the angle  $\lambda_2$  is opposite to that of  $\lambda_1$ ).

Since region  $GH$  is behind Mach line  $OK_0$  within the limits of the wing, the pressure coefficient due to the distributed sources in region  $OCC'$  must be calculated with the aid of formula (8.3.19). The influence of the distribution of sources in triangle  $BCC'$  on the pressure coefficient should be taken into account with the aid of relation (8.3.21) because region  $GH$  is outside triangle  $BCC'$  between Mach wave  $B'K_B$  and edge  $BC$ . Hence,

$$\begin{aligned} \bar{p}_{GH} &= \frac{4\lambda_1}{\pi\alpha' \sqrt{n^2 - 1}} \cosh^{-1} \sqrt{\frac{n_1^2 - \sigma_1^2}{1 - \sigma_1^2}} \\ &+ \frac{4(\lambda_2 - \lambda_1)}{\pi\alpha' \sqrt{n_1^2 - 1}} \cosh^{-1} \sqrt{\frac{n_2^2 - 1}{\sigma_2^2 - 1}} \end{aligned} \quad (8.4.4)$$

where  $n_2 = \tan \alpha_2 / \alpha'$ ;  $\sigma_2 = z_1 \tan \alpha_2 / x_2$ , and  $x_2$  is the coordinate measured from point  $B$  and equal to  $x_2 = x_1 - x_B$ .

Using formulas (8.4.2) and (8.4.4), let us determine the drag coefficient corresponding to region  $GH$ :

$$c_x,_{GH} = -\frac{8\lambda_1^2 z_1 \tan \kappa_1}{b\pi\alpha' \sqrt{n_1^2 - 1}} \int_{\sigma_{1G}}^{\sigma_{1H}} \cosh^{-1} \sqrt{\frac{n_1^2 - \sigma_1^2}{1 - \sigma_1^2}} \cdot \frac{d\sigma_1}{\sigma_1^2}$$

$$-\frac{8(\lambda_2 - \lambda_1) \lambda_1 z_1 \tan \kappa_2}{b\pi\alpha' \sqrt{n_2^2 - 1}} \int_{\sigma_{2G}}^{\sigma_{2H}} \cosh^{-1} \sqrt{\frac{n_2^2 - 1}{\sigma_2^2 - 1}} \cdot \frac{d\sigma_2}{\sigma_2^2} \quad (8.4.5)$$

where  $\sigma_{2H}$  and  $\sigma_{2G}$  are evaluated relative to point  $B$ .

Summing (8.4.3) and (8.4.5) and taking into account that

$$\sigma_{1F} = \frac{z_1 \tan \kappa_1}{x_F} = 1, \quad \sigma_{1H} = \frac{z_1 \tan \kappa_1}{x_H} = \frac{z_1 \tan \kappa_1}{x_B + z_1 \tan \kappa_2}$$

$$\sigma_{2G} = \frac{z_1 \tan \kappa_2}{x_G} = \tan \mu_\infty \tan \kappa_2 = \frac{\tan \kappa_2}{\alpha'} = n_2, \quad \sigma_{2H} = \frac{z_1 \tan \kappa_2}{x_H} = 1$$

we obtain

$$c_x,_{FH} = c_x,_{FG} + c_x,_{GH}$$

$$= -\frac{8\lambda_1^2 z_1 \tan \kappa_1}{b\pi\alpha' \sqrt{n_1^2 - 1}} \int_1^{\frac{z_1 \tan \kappa_1}{x_B + z_1 \tan \kappa_2}} \cosh^{-1} \sqrt{\frac{n_1^2 - \sigma_1^2}{1 - \sigma_1^2}}$$

$$\times \frac{d\sigma_1}{\sigma_1^2} - \frac{8(\lambda_2 - \lambda_1) \lambda_1 z_1 \tan \kappa_2}{b\pi\alpha' \sqrt{n_2^2 - 1}} \int_{n_2}^1 \cosh^{-1} \sqrt{\frac{n_2^2 - 1}{\sigma_2^2 - 1}} \cdot \frac{d\sigma_2}{\sigma_2^2} \quad (8.4.6)$$

Let us assume that part of chord  $HL$  (we presume that point  $H$  is on line  $BC$ ) equals  $\bar{r}b$ , where  $\bar{r}$  is a dimensionless coefficient of proportionality determined from the condition  $\bar{r} = B'D/b_0$  (here  $b_0$  is the central chord). Therefore, for surface  $OBC$ , the part of chord  $FH$  will be  $(1 - \bar{r})b$ .

Since a part of central chord  $B'D$  equals  $\bar{r}b_0$ , the remaining part  $OB'$  equals  $(1 - \bar{r})b_0$ . The angles are

$$\lambda_1 = \bar{\Delta}/2(1 - \bar{r}), \quad \lambda_2 = -\bar{\Delta}/(2\bar{r}) \quad (8.4.7)$$

where  $\bar{\Delta} = \Delta/b_0$  is the relative thickness of the airfoil.

Taking into account the values of  $\lambda_1$  and  $\lambda_2$  we can write formula (8.4.6) as:

$$c_x,_{FH} = -\frac{2\bar{\Delta}^2 z_1}{b(1 - \bar{r})\pi\alpha'} \left[ \frac{\tan \kappa_1}{\sqrt{n_1^2 - 1}} \int_1^{\frac{z_1 \tan \kappa_1}{(1 - \bar{r})b_0 + z_1 \tan \kappa_2}} \cosh^{-1} \sqrt{\frac{n_1^2 - \sigma_1^2}{1 - \sigma_1^2}}$$

$$\times \frac{d\sigma_1}{\sigma_1^2} + \frac{\tan \kappa_2}{\bar{r}\sqrt{n_2^2 - 1}} \int_{n_2}^{n_2^2} \cosh^{-1} \sqrt{\frac{n_2^2 - 1}{\sigma_2^2 - 1}} \cdot \frac{d\sigma_2}{\sigma_2^2} \right] \quad (8.4.8)$$

The velocity on line  $HJ$  is induced by sources of the strength  $Q = 2\lambda_1 V_\infty$  distributed in triangle  $OCC'$  and by sources of the strength  $Q = 2(\lambda_2 - \lambda_1) V_\infty$  distributed over region  $BCC'$ . The first distribution of the sources gives rise to the pressure coefficient calculated by formula (8.3.19) in which we must assume that  $\lambda = \lambda_1$ ,  $n = n_1$ , and  $\sigma = \sigma_1$ . The pressure coefficient due to the influence of the second distribution of the sources is also found with the aid of formula (8.3.19) in which we must assume that  $\lambda = \lambda_2 - \lambda_1$ ,  $n = n_2$ , and  $\sigma = \sigma_2$ . Summation of the pressure coefficients yields

$$\bar{p}_{HJ} = \frac{4\lambda_1}{\pi\alpha' \sqrt{n_1^2 - 1}} \cosh^{-1} \sqrt{\frac{n_1^2 - \sigma_1^2}{1 - \sigma_1^2}} + \frac{4(\lambda_2 - \lambda_1)}{\pi\alpha' \sqrt{n_2^2 - 1}} \cosh^{-1} \sqrt{\frac{n_2^2 - \sigma_2^2}{1 - \sigma_2^2}} \quad (8.4.9)$$

Using formula (8.4.5) in which we must replace the value of  $\lambda_1$  with  $\lambda_2$  and taking into account that

$$\begin{aligned} \lambda_1 &= \bar{\Delta}/[2(1 - \bar{r})], \quad \lambda_2 - \lambda_1 = -\bar{\Delta}^2/[2\bar{r}(1 - \bar{r})], \quad \lambda_2 = -\bar{\Delta}(2\bar{r}) \\ n_1 &= \tan \alpha_1/\alpha', \quad n_2 = \tan \alpha_2/\alpha', \quad \sigma_1 = z_1 \tan \alpha_1/x_1 \\ \sigma_2 &= z_2 \tan \alpha_2/x'_2, \quad x_H \leq x_1 \leq x_J, \quad x'_2 = x_1 - x_H \end{aligned}$$

we obtain

$$\begin{aligned} c_{x, HJ} &= \frac{-2\bar{\Delta}^2 z_1}{br(1 - \bar{r})\pi\alpha'} \left[ \frac{\tan \alpha_1}{\sqrt{n_1^2 - 1}} \int_{\sigma_{1H}}^{\sigma_{1J}} \cosh^{-1} \sqrt{\frac{n_1^2 - \sigma_1^2}{1 - \sigma_1^2}} \cdot \frac{d\sigma_1}{\sigma_1^2} \right. \\ &\quad \left. - \frac{\tan \alpha_2}{\sqrt{n_2^2 - 1}} \int_{\sigma_{2H}}^{\sigma_{2J}} \cosh^{-1} \sqrt{\frac{n_2^2 - \sigma_2^2}{1 - \sigma_2^2}} \cdot \frac{d\sigma_2}{\sigma_2^2} \right] \quad (8.4.10) \end{aligned}$$

where  $\sigma_2$  is evaluated relative to point  $B$ .

On  $JL$ , we take into account the influence of three distributions of the sources, namely, on triangular surfaces  $OCC'$ ,  $BCC'$  and  $DCC'$ . The first two distributions give rise to the pressure coefficient determined with the aid of formula (8.4.9) in which  $\sigma_1$  and  $\sigma_2$  are calculated relative to points  $O$  and  $D$ , respectively. The additional coefficient of pressure induced by the sources distributed over region  $DCC'$  with a strength of  $-\lambda_2$  is found with the aid of formula (8.3.21) in which we must assume that  $\lambda = \lambda_2$ ,  $n = n_3$ , and  $\sigma = \sigma_3$ .

Summing the pressure coefficients due to all three source distributions, we obtain

$$\begin{aligned} \bar{p}_{JL} &= \frac{4\lambda_1}{\pi\alpha' \sqrt{n_1^2 - 1}} \cosh^{-1} \sqrt{\frac{n_1^2 - \sigma_1^2}{1 - \sigma_1^2}} + \frac{4(\lambda_2 - \lambda_1)}{\pi\alpha' \sqrt{n_2^2 - 1}} \\ &\quad \times \cosh^{-1} \sqrt{\frac{n_2^2 - \sigma_2^2}{1 - \sigma_2^2}} - \frac{4\lambda_2}{\pi\alpha' \sqrt{n_3^2 - 1}} \cosh^{-1} \sqrt{\frac{n_3^2 - 1}{\sigma_3^2 - 1}} \quad (8.4.11) \end{aligned}$$

where  $n_3 = \tan \kappa_3 / \alpha'$ ; the values of  $\sigma_1$ ,  $\sigma_2$ , and  $\sigma_3$  are calculated relative to points  $O$ ,  $B$  and  $D$ .

Introducing the value of  $p_{JL}$  into formula (8.4.2) and substituting  $\lambda_2$  for  $\lambda_1$  in it, we obtain

$$\begin{aligned} c_x, JL &= -\frac{2\bar{\Delta}^2 z_1}{b\bar{r}\pi\alpha'} \left[ \frac{\tan \kappa_1}{(1-\bar{r}) \sqrt{n_1^2 - 1}} \int_{\sigma_{1J}}^{\sigma_{1L}} \cosh^{-1} \sqrt{\frac{n_1^2 - \sigma_1^2}{1 - \sigma_1^2}} \cdot \frac{d\sigma_1}{\sigma_1^2} \right. \\ &\quad - \frac{\tan \kappa_2}{\bar{r}(1-\bar{r}) \sqrt{n_2^2 - 1}} \int_{\sigma_{2J}}^{\sigma_{2L}} \cosh^{-1} \sqrt{\frac{n_2^2 - \sigma_2^2}{1 - \sigma_2^2}} \cdot \frac{d\sigma_2}{\sigma_2^2} \\ &\quad \left. + \frac{\tan \kappa_3}{\bar{r} \sqrt{n_3^2 - 1}} \int_{\sigma_{3J}}^{\sigma_{3L}} \cosh^{-1} \sqrt{\frac{n_3^2 - 1}{\sigma_3^2 - 1}} \cdot \frac{d\sigma_3}{\sigma_3^2} \right] \end{aligned} \quad (8.4.12)$$

Summing (8.4.10) and (8.4.12), we have

$$\begin{aligned} c_x, HL &= -\frac{2\bar{\Delta}^2 z_1}{b\bar{r}\pi\alpha'} \left[ \frac{\tan \kappa_1}{(1-\bar{r}) \sqrt{n_1^2 - 1}} \int_{\sigma_{1H}}^{\sigma_{1L}} \cosh^{-1} \sqrt{\frac{n_1^2 - \sigma_1^2}{1 - \sigma_1^2}} \cdot \frac{d\sigma_1}{\sigma_1^2} \right. \\ &\quad - \frac{\tan \kappa_2}{\bar{r}(1-\bar{r}) \sqrt{n_2^2 - 1}} \int_{\sigma_{2H}}^{\sigma_{2L}} \cosh^{-1} \sqrt{\frac{n_2^2 - \sigma_2^2}{1 - \sigma_2^2}} \cdot \frac{d\sigma_2}{\sigma_2^2} \\ &\quad \left. + \frac{\tan \kappa_3}{\bar{r} \sqrt{n_3^2 - 1}} \int_{\sigma_{3J}}^{\sigma_{3L}} \cosh^{-1} \sqrt{\frac{n_3^2 - 1}{\sigma_3^2 - 1}} \cdot \frac{d\sigma_3}{\sigma_3^2} \right] \end{aligned} \quad (8.4.13)$$

In this expression

$$\left. \begin{aligned} \sigma_{1H} &= \frac{z_1 \tan \kappa_1}{(1-\bar{r}) b_0 + z_1 \tan \kappa_2}, & \sigma_{1L} &= \frac{z_1 \tan \kappa_1}{b_0 + z_1 \tan \kappa_3} \\ \sigma_{2H} &= 1, & \sigma_{2L} &= \frac{z_1 \tan \kappa_2}{\bar{r} b_0 + z_1 \tan \kappa_3} \\ \sigma_{3J} &= \frac{z_1 \tan \kappa_3}{x'_J} = n_3, & \sigma_{3L} &= \frac{z_1 \tan \kappa_3}{x'_L} = 1 \end{aligned} \right\} \quad (8.4.13')$$

where  $x'_J = z_1 \cot \mu_\infty = z_1 \alpha'$ , and  $x'_L = z_1 \tan \kappa_3$ .

We take the integrals in formulas (8.4.8) and (8.4.13) by parts. These formulas hold (see Fig. 8.4.1) when

$$0 < z_1 < z_{B1} < z_{D1} \quad (8.4.14)$$

where

$$z_{B1} = (1 - \bar{r}) b_0 / (\tan \kappa_1 - \alpha'), \quad z_{D1} = \bar{r} b_0 / (\tan \kappa_2 - \alpha') \quad (8.4.15)$$

or (Fig. 8.4.2) when

$$0 < z_1 < z_{D_1} < z_{B_1} \quad (8.4.16)$$

The drag coefficient of the airfoil determined by formula (8.4.13) has been related to the local chord  $b$ . We calculate the value of the drag coefficient  $c_{x,0}$  related to the central chord  $b_0$  by the formula  $c_{x,0} = c_x (b/b_0)$ .

**Airfoil in the Mid-Span Section ( $z = 0$ ).** We determine the values of the aerodynamic coefficients for this airfoil as follows. On airfoil section  $OB$  (see Fig. 8.4.1) with a length of  $(1 - \bar{r}) b_0$ , the velocity is induced by sources having a strength of  $Q = 2\lambda_1 V_\infty$  distributed in triangle  $OCC'$ .

Accordingly, we evaluate the pressure coefficient by formula (8.3.19). Assuming that  $\sigma = z_1 \tan \alpha_1 / x_1 = 0$ , we obtain

$$\bar{p}_{OB} = \frac{4\lambda_1}{\pi\alpha' \sqrt{n_1^2 - 1}} \cosh^{-1} n_1 \quad (8.4.17)$$

Airfoil section  $DB$  with a length of  $\bar{r}b_0$  experiences the action of sources with a strength of  $Q = 2\lambda_1 V_\infty$  distributed over region  $OCC'$  and with a strength of  $Q = 2(\lambda_2 - \lambda_1) V_\infty$  distributed in triangle  $BCC'$ . In accordance with this, we determine the pressure coefficients. Using formula (8.3.19) at  $\sigma = 0$ , we find

$$\bar{p}_{BD} = \frac{4\lambda_1}{\pi\alpha' \sqrt{n_1^2 - 1}} \cosh^{-1} n_1 + \frac{4(\lambda_2 - \lambda_1)}{\pi\alpha' \sqrt{n_2^2 - 1}} \cosh^{-1} n_2 \quad (8.4.18)$$

The drag coefficient of the airfoil with account taken of the upper and bottom surfaces related to the central chord  $b_0$  is

$$c_x = \frac{2}{b_0} \int_0^{(1-\bar{r})b_0} \bar{p}_{OB} \lambda_1 dx + \frac{2}{b_0} \int_0^{\bar{r}b_0} \bar{p}_{BD} \lambda_2 dx \quad (8.4.19)$$

Introducing the value of  $\bar{p}_{OB}$  from (8.4.17), of  $\bar{p}_{BD}$  from (8.4.18), and having in view that  $\lambda_2 = -\bar{\Delta}/(2\bar{r})$ ,  $\lambda_2 - \lambda_1 = -\bar{\Delta}/[2\bar{r}(1 - \bar{r})]$  and also that  $(1 - r)\lambda_1 = \bar{\Delta}/2$  and  $r\bar{\lambda}_2 = -\bar{\Delta}/2$ , we obtain

$$c_x = \frac{2\bar{\Delta}^2}{\pi\alpha' \bar{r}(1 - \bar{r}) \sqrt{n_2^2 - 1}} \cosh^{-1} n_2 \quad (8.4.20)$$

where  $\cosh^{-1} n_2 = \ln(n_2 + \sqrt{n_2^2 - 1})$ .

**Airfoil  $F_1L_1$ .** Let us calculate the drag coefficient of an airfoil (see Fig. 8.4.1) whose coordinate  $z_1$  satisfies the inequality  $z_{B_1} < z_1 < z_{D_1}$ . Section  $F_1H_1$  of the airfoil experiences the action of sources with the strength  $Q = 2\lambda_1 V_\infty$  distributed in region  $OCDC'$ , and with the strength  $Q = 2(\lambda_2 - \lambda_1) V_\infty$  distributed in  $BCC'$ . Therefore, we may use formula (8.4.4) to calculate the pressure

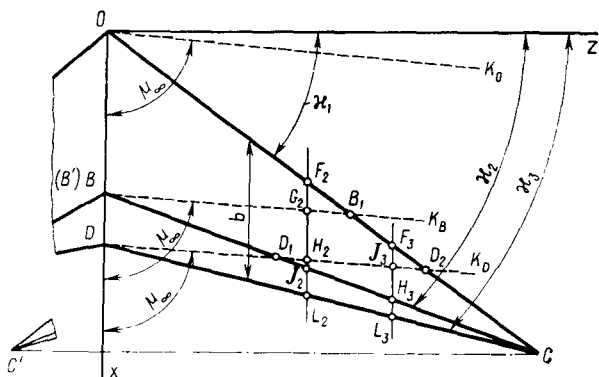


**Fig. 8.4.2**  
Arrangement of Mach lines

coefficient, and relation (8.4.5) to determine the drag coefficient. For airfoil section  $F_1H_1$ , relation (8.4.5) has the form

$$c_{x, F_1H_1} = - \frac{8\lambda_1^2 z_1 \tan \kappa_1}{b\pi\alpha' \sqrt{n_1^2 - 1}} \int_{\sigma_1 F_1}^{\sigma_1 H_1} \cosh^{-1} \sqrt{\frac{n_1^2 - \sigma_1^2}{1 - \sigma_1^2}} \cdot \frac{d\sigma_1}{\sigma_1^2}$$

$$- \frac{8(\lambda_2 - \lambda_1) \lambda_1 z_1 \tan \kappa_2}{b\pi\alpha' \sqrt{n_2^2 - 1}} \int_{\sigma_2 F_1}^{\sigma_2 H_1} \cosh^{-1} \sqrt{\frac{n_2^2 - 1}{\sigma_2^2 - 1}} \cdot \frac{d\sigma_2}{\sigma_2^2} \quad (8.4.21)$$

where  $\sigma_1$  and  $\sigma_2$  are calculated relative to points  $O$  and  $B$ , respectively.

We determine the pressure on airfoil section  $H_1L_1$  in the same way as on  $HL$  with the aid of formulas (8.4.9) and (8.4.11). We find the corresponding drag coefficient  $c_{x, H_1 L_1}$  from expression (8.4.13) in which we replace the limits  $\sigma_{1H}$  and  $\sigma_{1L}$  with the quantities  $\sigma_{1H_1}$  and  $\sigma_{1L_1}$ , the limits  $\sigma_{2H}$  and  $\sigma_{2L}$  with the quantities  $\sigma_{2H_1}$  and  $\sigma_{2L_1}$ , and the limits  $\sigma_{3J}$  and  $\sigma_{3L}$  with the quantities  $\sigma_{3J_1}$  and  $\sigma_{3L_1}$ , respectively, determined by formulas (8.4.13'). The overall drag coefficient for the airfoil  $F_1L_1$  related to the central chord  $b_0$  is

$$c_{x, F_1 L_1} = c_{x, F_1 H_1} + c_{x, H_1 L_1}$$

Airfoil  $F_2L_2$ . Let us consider the airfoil between points  $D_1$  and  $B_2$  (Fig. 8.4.2) with the coordinate  $z_1$  satisfying the inequality  $z_{D_1} < z_1 < z_{B_1}$ . The flow over this airfoil is of a more intricate nature. The velocity on section  $F_2G_2$  is induced by sources having the strength  $Q = 2\lambda_1 V_\infty$  distributed in triangle  $OCC'$ . Consequently, the pressure coefficient on this section is determined with the aid of formula (8.4.1), and the corresponding drag coefficient  $c_{x, F_2 G_2}$  from expression (8.4.3) in which the integral is taken between the limits  $\sigma_{1F_2}$  and  $\sigma_{1G_2}$ .

The pressure on section  $G_2H_2$  depends on the influence of sources having a strength of  $Q = 2\lambda_1 V_\infty$  distributed over section  $OCC'$ , and also of sources having a strength of  $Q = 2(\lambda_2 - \lambda_1) V_\infty$  in region  $BCC'$ . Consequently, we calculate the pressure coefficient by formula (8.4.4), and the drag coefficient  $c_{x, G_2H_2}$  from expression (8.4.5) in which we take the first integral between the limits  $\sigma_{1G_2}$  and  $\sigma_{1H_2}$ , and the second between  $\sigma_{2G_2}$  and  $\sigma_{2H_2}$ .

Section  $H_2J_2$  experiences the simultaneous action of sources distributed in region  $OCC'$  ( $Q = 2\lambda_1 V_\infty$ ), and also in triangle  $BCC'$  [ $Q = 2(\lambda_2 - \lambda_1) V_\infty$ ] and on surface  $BCC'$ , where the strength  $Q = -2\lambda_2 V_\infty$ . The first distribution results in a pressure coefficient determined by formula (8.3.19), and the second two distributions result in the coefficient calculated by expression (8.3.21).

The total value of the pressure coefficient on this section of the airfoil is

$$\bar{p}_{H_2J_2} = \frac{4\lambda_1}{\pi\alpha' \sqrt{n_1^2 - 1}} \cosh^{-1} \sqrt{\frac{n_1^2 - \sigma_1^2}{1 - \sigma_1^2}} + \frac{4(\lambda_2 - \lambda_1)}{\pi\alpha' \sqrt{n_1^2 - 1}} \\ \times \cosh^{-1} \sqrt{\frac{n_2^2 - 1}{\sigma_2^2 - 1}} - \frac{4\lambda_2^2}{\pi\alpha' \sqrt{n_3^2 - 1}} \cosh^{-1} \sqrt{\frac{n_3^2 - 1}{\sigma_3^2 - 1}} \quad (8.4.22)$$

where  $\sigma_1$ ,  $\sigma_2$ , and  $\sigma_3$  are determined relative to points  $O$ ,  $B$ , and  $D$ , respectively.

By using the formula

$$c_{x, H_2J_2} = \frac{2}{b_0} \int_{x_{H_2}}^{x_{J_2}} \bar{p}_{H_2J_2} \lambda_2 dx \quad (8.4.23)$$

we can calculate the drag coefficient for the section of the airfoil being considered related to the length  $b_0$  of the centre chord.

The flow over the last airfoil section  $J_2L_2$  is the result of induction by the sources distributed in the same regions of the wing as for airfoil section  $H_2J_2$ . Here account must be taken of the feature that the velocity induced by the sources in region  $BCC'$  is determined by formula (8.3.18), where  $\lambda$  is replaced by the angular coefficient  $\lambda_2 - \lambda_1$ . Therefore, the pressure coefficient should be calculated by formula (8.4.11), and the drag coefficient  $c_{x, J_2L_2}$  from expression (8.4.12) in which we take the integrals between the limits  $\sigma_{nJ_2}$  and  $\sigma_{nL_2}$  ( $n = 1, 2, 3$ ).

We obtain the total drag coefficient by summation of the coefficients for all four sections of the airfoil:

$$c_{x, F_2L_2} = c_{x, F_2G_2} + c_{x, G_2H_2} + c_{x, H_2J_2} + c_{x, J_2L_2}$$

provided that the value of  $z_1$  satisfies the inequality

$$\frac{\bar{r}b_0}{\tan \chi_1 - \alpha'} < z_1 < \frac{(1 - \bar{r})b_0}{\tan \chi_1 - \alpha'}$$

Airfoil  $F_3L_3$ . Let us consider section  $F_3L_3$  (Fig. 8.4.2) with the coordinate  $z_1$  satisfying the inequality

$$z_{D_1} < z_1 < z_{D_2}, \quad (8.4.24)$$

where

$$z_{D_1} = b_0 / (\tan \kappa_1 - \alpha') \quad (8.4.25)$$

The pressure on section  $F_3J_3$  of the airfoil is due to the action of sources distributed on the triangular surfaces  $OCC'$  ( $Q = 2\lambda_1 V_\infty$ ) and  $BCC'$  [ $Q = 2(\lambda_2 - \lambda_1) V_\infty$ ]. We shall therefore calculate the pressure coefficient by expression (8.4.4), and the drag coefficient by formula (8.4.5) in which we replace the limits  $\sigma_{n,G}$  and  $\sigma_{n,H}$  with the values  $\sigma_{n,F_3}$  and  $\sigma_{n,J_3}$ , ( $n = 1, 2$ ).

Airfoil section  $J_3H_3$ , in addition to the indicated source distributions in regions  $OCC'$  and  $BCC'$ , also experiences the action of sources having a strength of  $Q = -2\lambda_2 VL$  distributed in triangle  $DCC'$ . Consequently, the pressure coefficient equals the value calculated by formula (8.4.4) plus the additional value calculated by formula (8.3.21) in which we assume that  $\lambda = -\lambda_2$ .

Flow over section  $H_3L_3$  is characterized by the induction of sources distributed in three regions of the wing, namely,  $OCC'$ ,  $BCC'$ , and  $DCC'$ . Accordingly, the pressure coefficient on this section should be calculated with the aid of formula (8.4.11).

By calculating the relevant components of the drag coefficient for all three sections and summing them, we obtain the total drag coefficient:

$$c_{x,F_3L_3} = c_{x,F_3J_3} + c_{x,J_3H_3} + c_{x,H_3L_3}$$

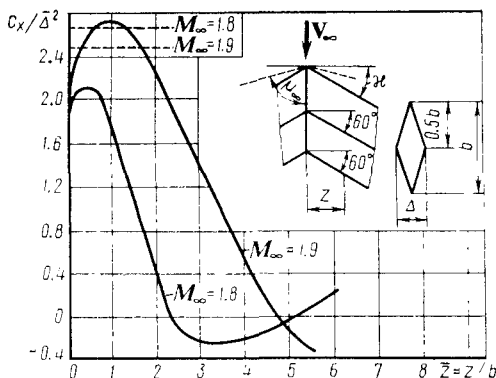
The relevant expression is suitable for calculating the drag coefficient of the airfoil between points  $D_1$  and  $D_2$  (Fig. 8.4.2) with the coordinate  $z_1$  that satisfies the inequality

$$\frac{\bar{r}b_0}{\tan \kappa_2 - \alpha'} < z_1 < \frac{b_0}{\tan \kappa_1 - \alpha'} \quad (8.4.26)$$

Airfoil  $F_4L_4$ . Let us consider section  $F_4L_4$  (see Fig. 8.4.1) with coordinate

$$z_1 > z_{D_2} \quad (8.4.27)$$

Three source distributions simultaneously act on this section, namely,  $OCC'$  ( $Q = 2\lambda_1 V_\infty$ ),  $BCC'$  [ $Q = 2(\lambda_2 - \lambda_1) V_\infty$ ], and  $DCC'$  ( $Q = -2\lambda_2 V_\infty$ ). Airfoil section  $F_4H_4$  is behind Mach line  $OK_0$  within the confines of the wing, therefore to calculate the pressure produced by the distribution of the sources in  $OCC'$  we must use formula (8.3.19) in which we assume that  $\lambda = \lambda_1$ . The second distribution of the sources in  $BCC'$  acts on section  $F_4H_4$  located beyond the confines of the surface between the Mach line and edge  $BC$ . Therefore, to calculate the additional pressure due to the influence of the distribution of the sources in  $BCC'$ , we must use formula (8.3.21) with the substitution of  $\lambda_2 - \lambda_1$  for  $\lambda$ .

**Fig. 8.4.3**

Distribution of the drag coefficient over the span of a swept constant chord wing with subsonic edges

(the dashed line shows an unswept wing)

The second section of airfoil  $H_4L_4$  is located within the confines of the wing surface, i.e. at the same side from the Mach lines and the relevant edges  $OC$  and  $BC$ . Consequently, to determine the pressure coefficient resulting from the distributions of the sources in  $OCC'$  and  $BCC'$ , we use formula (8.3.19) in which the value  $\lambda = \lambda_1$  corresponds to the distribution in  $OCC'$ , and the value  $\lambda = \lambda_2 - \lambda_1$  to the distribution in  $BCC'$ .

Section  $H_4L_4$  is at both sides of Mach line  $DK_D$  and trailing edge  $DC$ , i.e. it is beyond the confines of triangular surface  $DCC'$  where the strength of the sources is  $Q = -2\lambda_2 V_\infty$ . Hence, to calculate the pressure coefficient produced by these sources, we should use formula (8.3.21) with the substitution of  $-\lambda_2$  for  $\lambda$ .

Using the obtained value of the pressure coefficient, we can determine the relevant drag coefficient for airfoil  $F_4L_4$ :

$$c_{x, F_4L_4} = c_{x, F_4H_4} + c_{x, H_4L_4}$$

Figure 8.4.3 shows the results of calculating the distribution of the drag coefficient  $c_x / \bar{\Delta}^2$  ( $\bar{\Delta} = \Delta/b$ ) over the span of a swept constant chord ( $b$ ) wing ( $\alpha_1 = \alpha_2 = \alpha_3 = 60^\circ$ ) with a symmetric rhomboid airfoil ( $\bar{r} = 1/2$ ) for  $M_\infty = 1.8$  and  $1.9$ . A glance at the figure reveals that with an increase in the distance from the centre chord, the drag coefficient first grows somewhat, and then sharply drops. For purposes of comparison, the figure shows the value of the function  $c_x / \bar{\Delta}^2$  for an airfoil belonging to an unswept wing.

To determine the total drag coefficient of the wing, we must integrate the distribution of the drag coefficients  $c_{x,k}$  of the airfoils over the span, using the formula

$$c_x = \frac{2}{l} \int_0^{l/2} c_{x,k} dz \quad (8.4.28)$$

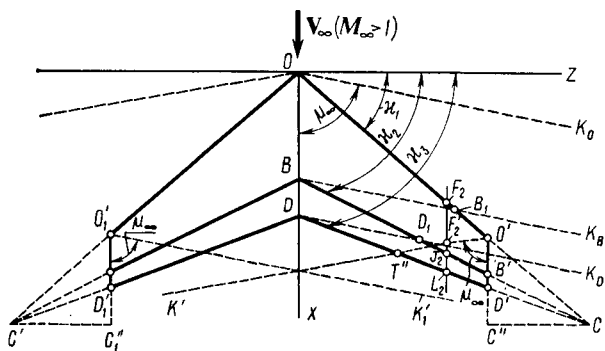


**Fig. 8.4.4**  
Wing with side edges

**Influence of a Side Edge on the Flow over a Wing.** If a wing has a wide tip or side edge (Fig. 8.4.4), its influence on the pressure distribution and the drag coefficient must be taken into account. The flow over such a hexagonal wing is calculated as follows. First the velocities and pressures in region  $O O' D' D$  produced by the distribution of the sources on triangular area  $O C D$  are calculated. The calculations in this case are performed similar to those of a wing with a tetragonal planform (see Fig. 8.4.1) having no side edges. Next the calculated velocities and pressures are determined more precisely with account taken of the influence of side edge  $O' C''$ , which is equivalent to the action of sources distributed in triangle  $O' C D'$ . The strength of these sources has a sign opposite to that of the sources corresponding to a wing of area  $O' C D'$ . The action of the sources distributed in triangle  $O' C D'$  extends to the wing within the area  $O' T' D'$  confined by Mach line  $O' K'$ , the side edge, and the trailing edge. For example, for airfoil  $F_2 L_2$ , the action of the sources is confined by section  $F'_2 L_2$  (point  $F'_2$  is at the intersection of chord  $F_2 L_2$  and Mach line  $O' K'$ ).

Let us see how the pressure is evaluated on section  $J_2 L_2$  of this airfoil. Taking into consideration only the distribution of the sources in region  $O C C'$ , we can determine the pressure coefficient by formula (8.4.11). We can introduce the correction  $\bar{\Delta p}$  for the action of sources of opposite signs in triangle  $O' C D'$ , so that

$$\bar{p}_{J_2 L_2} = \bar{p}_{J L} - \bar{\Delta p} \quad (8.4.29)$$

When finding the correction  $\bar{\Delta p}$  we must take account of the position of airfoil section  $J_2 L_2$  relative to Mach line  $O'_1 K'_1$  that passes through point  $O'_1$  belonging to the opposite side edge (Fig. 8.4.4). If this line does not intersect  $J_2 L_2$ , the latter is influenced only by the distribution of the sources in region  $O' C D'$  of one side of the

wing, whereas the influence of the sources in  $O'C'D'$  is excluded. The induced velocity is calculated by formula (8.3.13), and the corresponding additional value of the pressure coefficient by the formula  $\Delta\bar{p} = -2u/V_\infty$ . We shall write this additional value in the form of the sum

$$\Delta\bar{p} = \Delta\bar{p}_1 + \Delta\bar{p}_2 + \Delta\bar{p}_3 \quad (8.4.30)$$

where  $\Delta\bar{p}_1$  depends on the distribution of the sources in  $O'CC''$  ( $Q = 2\lambda_1 V_\infty$ ), while  $\Delta\bar{p}_2$  and  $\Delta\bar{p}_3$  depend on the distribution of the sources in  $B'CC''$  [ $Q = 2(\lambda_2 - \lambda_1) V_\infty$ ] and  $D'CC''$  ( $Q = -2\lambda_2 V_\infty$ ).

Hence, by using formula (8.3.14), we obtain

$$\begin{aligned} \Delta\bar{p} = & \frac{2\lambda_1}{\pi\alpha' \sqrt{n_1^2 - 1}} \cosh^{-1} \frac{n_1^2 + \sigma_1}{n_1(1 + \sigma_1)} \\ & + \frac{2(\lambda_2 - \lambda_1)}{\pi\alpha' \sqrt{n_2^2 - 1}} \cosh^{-1} \frac{n_2^2 + \sigma_2}{n_2(1 + \sigma_2)} \\ & - \frac{2\lambda_2}{\pi\alpha' \sqrt{n_3^2 - 1}} \cosh^{-1} \frac{n_3^2 + \sigma_3}{n_3(1 + \sigma_3)} \end{aligned} \quad (8.4.31)$$

where  $\sigma_1$ ,  $\sigma_2$  and  $\sigma_3$  are calculated relative to points  $O'$ ,  $B'$ , and  $D'$ .

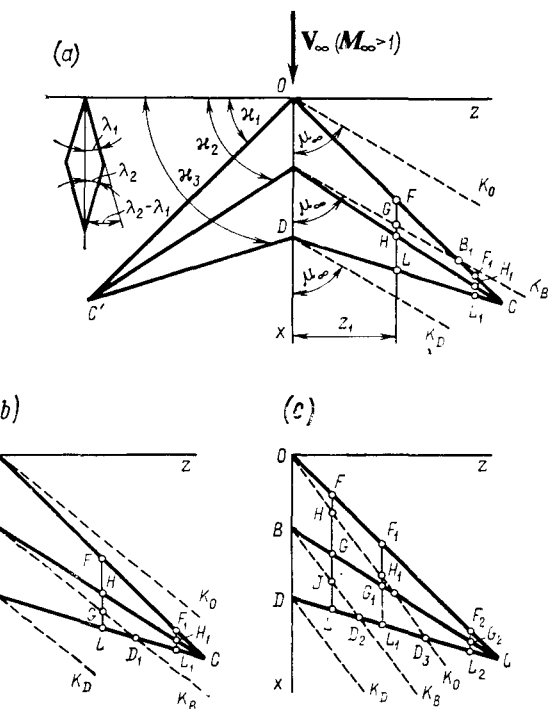
If Mach line  $O'_1K'_1$  intersects chord  $F_2L_2$ , then simultaneously with the action of sources  $O'CC''$  account must also be taken of the influence of the sources distributed in triangle  $O'_1C'C_1$  at the opposite side of the wing. The same formula (8.3.13) is used to calculate the induced velocity.

## 8.5. Flow over a Tetragonal Symmetric Airfoil Wing with Edges of Different Kinds (Subsonic and Supersonic)

**Leading and Middle Edges Are Subsonic  
Trailing Edge Is Supersonic**

The disturbances from the trailing supersonic edges of a wing (Fig. 8.5.1a) propagate downstream within the confines of the Mach cone with the generatrix  $DK_D$  and therefore do not affect the flow over the wing surface. The velocities and pressures depend on the influence of the leading and middle subsonic edges.

Let us consider profile  $FL$  with the coordinate  $z_1 < z_{B_1}$ . The pressure coefficient on section  $FG$ , which depends on the action of sources having a strength of  $Q = 2\lambda_1 V_\infty$  that are distributed in triangle  $OCC'$ , is determined from (8.4.1), and the corresponding drag coefficient  $c_{x_{FG}}$ , from (8.4.3). On the following section  $GH$  experiencing the influence of the sources distributed in triangles  $OCC'$  ( $Q = 2\lambda_1 V_\infty$ ) and  $BCC'$  [ $Q = 2(\lambda_2 - \lambda_1) V_\infty$ ], the pressure

**Fig. 8.5.1**

Tetragonal wing in a supersonic flow:

*a*—the leading and middle edges are subsonic, the trailing edge is supersonic; *b*—the leading edge is subsonic, the middle and trailing edges are supersonic; *c*—all the edges are supersonic

coefficient is calculated by (8.4.4). The corresponding value of the drag coefficient  $c_{x, GH}$  for this section is determined from (8.4.5).

The action of the same source distributions is observed on section  $HL$  as on section  $GH$ . But taking into account that section  $HL$  is below Mach line  $BK_B$  (on the wing surface), the pressure coefficient  $\bar{p}_{HL}$  must be calculated from (8.4.9), and the drag coefficient  $c_{x, HL}$ , from (8.4.10). The total drag coefficient of the airfoil is

$$c_{x, FL} = c_{x, FG} + c_{x, GH} + c_{x, HL} \quad (8.5.1)$$

When considering section  $F_1L_1$  with the coordinate  $z_1 > z_{B_1}$ , account must be taken simultaneously of the source distributions in  $OCC'$  and  $BCC'$ . For section  $F_1H_1$ , the drag coefficient  $c_{x, F_1H_1}$  is determined by formula (8.4.21). For section  $H_1L_1$  the drag coefficient  $c_{x, H_1L_1}$  is found by expression (8.4.13) in which the third term in the brackets is taken equal to zero, while the limits  $\sigma_{n,H}$  and  $\sigma_{n,L}$

are replaced with the values  $\sigma_{n_1 H_1}$  and  $\sigma_{n_1 L_1}$  ( $n = 1, 2$ ), respectively. The total drag coefficient for airfoil  $F_1 L_1$  is

$$c_{x, F_1 L_1} = c_{x, F_1 H_1} + c_{x, H_1 L_1} \quad (8.5.2)$$

**Leading Edge Is Subsonic,  
Middle and Trailing Edges  
are Supersonic**

A feature of the flow over the wing (Fig. 8.5.1b) consists in that the sources distributed in region  $BDD_1$  do not affect the distribution of the velocities and pressures on the remaining part of the wing above Mach line  $BK_B$ .

Let us consider airfoil  $FL$  with the coordinate  $z_1 < z_{D_1}$ . Section  $FH$  of this airfoil is acted upon by the sources distributed in triangle  $OCC'$  (Fig. 8.5.1a); consequently, the pressure distribution can be found from (8.4.1), and the corresponding drag coefficient  $c_{x, FH}$ , from (8.4.3) in which  $\sigma_{1H}$  is substituted for the upper limit  $\sigma_{1G}$ . The second section  $HG$  is influenced by subsonic leading edge  $OC$  (and, therefore, the distribution of the sources in  $OCC'$ ) and by supersonic middle edge  $BC$ . The corresponding pressure coefficient is determined as the sum of two coefficients, the first of which is evaluated by expression (8.4.1), and the second by (8.3.23) where we assume  $\lambda = \lambda_2 - \lambda_1$  and  $n = n_2$ . Consequently,

$$\bar{p}_{HG} = \frac{4\lambda_1}{\pi\alpha' \sqrt{n_1^2 - 1}} \cosh^{-1} \sqrt{\frac{n_1^2 - \sigma_1^2}{1 - \sigma_1^2}} + \frac{2(\lambda_2 - \lambda_1)}{\alpha' \sqrt{1 - n_2^2}} \quad (8.5.3)$$

On section  $GL$ , the velocity is induced by the sources distributed in triangles  $OCC'$  and  $BCC'$  (Fig. 8.5.1a). By using formulas (8.5.3) and (8.3.34), we obtain the following working relation for the pressure coefficient:

$$\begin{aligned} \bar{p}_{GL} = & \frac{4\lambda_1}{\pi\alpha' \sqrt{n_1^2 - 1}} \cosh^{-1} \sqrt{\frac{n_1^2 - \sigma_1^2}{1 - \sigma_1^2}} \\ & + \frac{2(\lambda_2 - \lambda_1)}{\alpha' \sqrt{1 - n_2^2}} \left( 1 - \frac{2}{\pi} \sin^{-1} \sqrt{\frac{n_2^2 - \sigma_2^2}{1 - \sigma_2^2}} \right) \end{aligned} \quad (8.5.4)$$

The drag coefficient of the airfoil is

$$c_{x, FL} = \frac{2}{b} \left( \int_{x_F}^{x_H} \bar{p}_{FH} \lambda_1 dx + \int_{x_H}^{x_G} \bar{p}_{HG} \lambda_2 dx + \int_{x_G}^{x_L} \bar{p}_{GL} \lambda_2 dx \right) \quad (8.5.5)$$

Airfoil  $F_1 L_1$  is below Mach line  $OK_O$ , therefore it is influenced by the distribution of sources with a strength of  $Q = 2\lambda_1 V_\infty$  in triangle

$OCC'$ . In addition, section  $H_1L_1$  is acted upon by the distribution of sources with a strength of  $Q = 2(\lambda_2 - \lambda_1) V_\infty$  in triangle  $BCC'$  that produces an additional pressure evaluated by formula (8.3.23), where we assume  $\lambda = \lambda_2 - \lambda_1$ . Accordingly, the pressure coefficient  $\bar{p}_{F_1H_1}$  on section  $F_1H_1$  is evaluated by expression (8.4.1), and the pressure coefficient  $\bar{p}_{H_1L_1}$  on section  $H_1L_1$ , with the aid of formula (8.5.3). The drag coefficient of the airfoil is

$$c_{x, F_1L_1} = \frac{2}{b} \left( \int_{x_{F_1}}^{x_{H_1}} \bar{p}_{F_1H_1} \lambda_1 dx + \int_{x_{H_1}}^{x_{L_1}} \bar{p}_{H_1L_1} \lambda_2 dx \right) \quad (8.5.6)$$

#### Wing with All Supersonic Edges

For such a wing (Fig. 8.5.1c), Mach lines  $OK_O$ ,  $BK_B$ , and  $DK_D$  drawn from points  $O$ ,  $B$ , and  $D$  are below the corresponding edges  $OC$ ,  $BC$  and  $DC$ , therefore formulas (8.3.23) and (8.3.34) are used to calculate the pressure coefficient.

Let us consider airfoil  $FL$  with the coordinate  $0 < z_1 < z_{D_s}$ . Section  $FH$  is between leading edge  $OC$  and Mach line  $OK_O$ . Therefore, the other edge  $OC'$  (Fig. 8.5.1a) does not affect the flow on this section, which is considered as plane supersonic. Taking into account that section  $FH$  is influenced by the sources in triangle  $OCC'$  having a strength of  $Q = 2\lambda_1 V_\infty$ , the pressure coefficient  $\bar{p}_{FH}$  can be determined by formula (8.3.23) in which we assume  $\lambda = \lambda_1$  and  $n = n_1$ . The additional pressure on section  $HG$  is due to the influence of edge  $OC'$ . The pressure coefficient  $\bar{p}_{HG}$  on this section is found from expression (8.3.34) in which it is assumed that  $n = n_1$  and  $\sigma = \sigma_1$ .

Section  $GJ$ , in addition to the distribution of the sources in  $OCC'$ , is affected by the source distribution in  $BCC'$  having a strength of  $Q = 2(\lambda_2 - \lambda_1) V_\infty$ . Using formulas (8.3.34) and (8.3.23), we obtain an expression for the pressure coefficient:

$$\bar{p}_{GJ} = \frac{2\lambda_1}{\alpha' \sqrt{1-n_1^2}} \left( 1 - \frac{2}{\pi} \sin^{-1} \sqrt{\frac{n_1^2 - \sigma_1^2}{1-\sigma_1^2}} \right) + \frac{2(\lambda_2 - \lambda_1)}{\alpha' \sqrt{1-n_1^2}} \quad (8.5.7)$$

The last airfoil section  $JL$  is influenced additionally by opposite edge  $BC'$ . Accordingly, the pressure coefficient on section  $JL$  on which sources having a strength of  $Q = 2(\lambda_2 - \lambda_1) V_\infty$  act is

$$\begin{aligned} \bar{p}_{JL} = & \frac{2\lambda_1}{\alpha' \sqrt{1-n_1^2}} \left( 1 - \frac{2}{\pi} \sin^{-1} \sqrt{\frac{n_1^2 - \sigma_1^2}{1-\sigma_1^2}} \right) \\ & + \frac{2(\lambda_2 - \lambda_1)}{\alpha' \sqrt{1-n_2^2}} \left( 1 - \frac{2}{\pi} \sin^{-1} \sqrt{\frac{n_2^2 - \sigma_2^2}{1-\sigma_2^2}} \right) \end{aligned} \quad (8.5.8)$$

The drag coefficient of airfoil  $FL$  is

$$c_{x, FL} = \frac{2}{b} \left( \int_{x_F}^{x_H} \bar{p}_{FH} \lambda_1 dx + \int_{x_H}^{x_G} \bar{p}_{HG} \lambda_1 dx \right. \\ \left. + \int_{x_G}^{x_J} \bar{p}_{GJ} \lambda_2 dx + \int_{x_J}^{x_L} \bar{p}_{JL} \lambda_2 dx \right) \quad (8.5.9)$$

The pressure coefficient  $\bar{p}_{F_1H_1}$  on section  $F_1H_1$  of airfoil  $F_1L_1$  with the coordinate  $z_D < z_1 < z_{D_1}$  is determined by formula (8.3.23) in which  $\lambda = \lambda_1$  and  $n = n_1$ . To determine the pressure coefficient  $\bar{p}_{H_1G_1}$  for the neighbouring section  $H_1G_1$ , we use formula (8.3.34) in which  $\lambda = \lambda_1$ ,  $n = n_1$ , and  $\sigma = \sigma_1$ . On the last section  $G_1L_1$ , the pressure is due to the influence of source distributions in  $OCC'$  ( $Q = 2\lambda_1 V_\infty$ ) and  $BCC'$  [ $Q = 2(\lambda_2 - \lambda_1) V_\infty$ ]. Consequently, to calculate the pressure coefficient  $\bar{p}_{G_1L_1}$ , we can use formula (8.5.7). The drag coefficient of airfoil  $F_1L_1$  is

$$c_{x, F_1L_1} = \frac{2}{b} \left( \int_{x_{F_1}}^{x_{H_1}} \bar{p}_{F_1H_1} \lambda_1 dx + \int_{x_{H_1}}^{x_{G_1}} \bar{p}_{H_1G_1} \lambda_1 dx + \int_{x_{G_1}}^{x_{L_1}} \bar{p}_{G_1L_1} \lambda_2 dx \right) \quad (8.5.10)$$

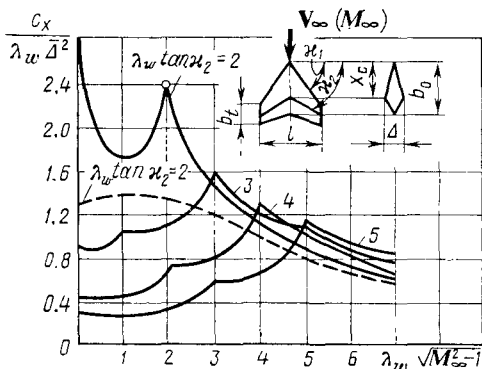
The flow near airfoil  $F_2L_2$  in the section  $z_{D_2} < z_1$  is plane supersonic, therefore the pressure coefficient for it is determined by formula (8.3.23). The sources in triangle  $OCC'$  having a strength of  $Q = 2\lambda_1 V_\infty$  act on section  $F_2G_2$ , therefore the pressure coefficient  $\bar{p}_{F_2G_2}$  is found by formula (8.3.23) in which  $\lambda = \lambda_1$  and  $n = n_1$ . The second section  $G_2L_2$  is additionally influenced by the sources having a strength of  $Q = 2(\lambda_2 - \lambda_1) V_\infty$  distributed in triangle  $BCC'$ . Therefore, the pressure coefficient on this section is

$$\bar{p}_{G_2L_2} = \frac{2\lambda_1}{\alpha' \sqrt{1-n_2^2}} + \frac{2(\lambda_2 - \lambda_1)}{\alpha' \sqrt{1-n_2^2}} \quad (8.5.11)$$

The drag coefficient for airfoil  $F_2L_2$  is

$$c_{x, F_2L_2} = \frac{2}{b} \left( \int_{x_{F_2}}^{x_{G_2}} \bar{p}_{F_2G_2} \lambda_1 dx + \int_{x_{G_2}}^{x_{L_2}} \bar{p}_{G_2L_2} \lambda_2 dx \right) \quad (8.5.12)$$

If a tetragonal wing has an extended tip or side edge ( $b_t \neq 0$ ), the flow parameters are calculated with account taken of the influence of the side edge on them. The part of the wing where this influence is observed is below the Mach line issuing from the front point of the side edge (see Fig. 8.4.4). The velocity and pressure on

**Fig. 8.5.2**

Drag coefficient of wings with a symmetric rhombiform airfoil:  
 $\bar{x}_C = x_C/b_0 = 0.5$ ;  $\eta_w = b_0/b_t = 5$ ;  
 $\lambda_w = l^2/S_w$ ;  $\tan \alpha_2 = \tan \alpha_1 - (2/\lambda_w)(\eta_w - 1)/(\eta_w + 1)$ ;  $\bar{\Delta} = \Delta/b_0$   
(the dashed curve is an experimental one)

this section are calculated by the method set out in Sec. 8.4 with account taken of the kind of the leading and middle edges (i.e. depending on whether they are subsonic or supersonic) by means of the relevant relations similar to (8.4.31).

By integrating over the span, we can determine the wave-drag coefficients in each of the cases of flow over a hexagonal or tetragonal rhombiform airfoil wing considered in Secs. 8.4 and 8.5. According to the relations obtained, these coefficients depend on the number  $M_\infty$  and on the configuration and relative dimensions of the wing:

$$c_x = f_1 (M_\infty, \lambda_w, \alpha_1, \eta_w, \bar{x}_C, \bar{\Delta}) \quad (8.5.13)$$

Here in addition to the known notation, we have introduced the quantity  $\bar{x}_C = x_C/b$ —the dimensionless distance to the spot with the maximum airfoil thickness.

The number of independent variables in (8.5.13) can be reduced by using the relation

$$c_x/(\lambda_w \bar{\Delta}^2) = f_2 (\lambda_w \sqrt{M_\infty^2 - 1}, \lambda_w \tan \alpha_2, \eta_w, \bar{x}_C) \quad (8.5.14)$$

where  $\tan \alpha_2$  is the tangent of the sweep angle along the maximum thickness line (i.e. of the middle edge).

Figure 8.5.2 shows a family of curves constructed in accordance with formula (8.5.14) for the following conditions:  $\eta_w = b_0/b_t = 5$  and  $x_C = 0.5$ . The salient points of the curves correspond to sonic edges. Particularly, for the curve corresponding to the value of  $\lambda_w \tan \alpha_2 = 3$ , the salient point for the smallest value of  $\lambda_w \sqrt{M_\infty^2 - 1}$  corresponds to a sonic trailing edge, and the second and third points to a sonic middle (the maximum thickness line) and trailing edges.

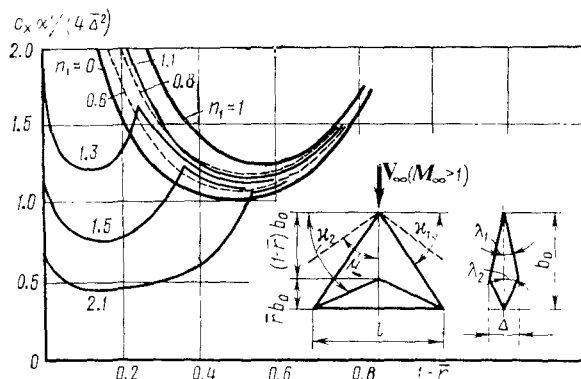


Fig. 8.5.3

Drag of triangular wings with a symmetric rhombiform airfoil in a supersonic flow

$$(n_1 = \tan \alpha_1 / \alpha')$$

A comparison shows that the experimental and theoretical values of the wave-drag coefficients differ, especially near values of  $\lambda_w \sqrt{M_\infty^2 - 1} \approx \lambda_w \tan \alpha_2$ , i.e. when the maximum thickness line becomes sonic. In this case, the linear theory cannot be applied. The discrepancy between the indicated values diminishes when this line is supersonic ( $\lambda_w \sqrt{M_\infty^2 - 1} > \lambda_w \tan \alpha_2$ ).

From the relations found for a tetragonal planform wing, we can obtain the relations for the aerodynamic characteristics of a triangular wing as a particular case (Fig. 8.5.3). The trailing edge of such a wing is supersonic and straight ( $\alpha_3 = 0$ ). The leading edge and the maximum thickness line (the middle edge) may be either subsonic or supersonic and, consequently, inclined at different angles  $\alpha_1$  and  $\alpha_2$ . Depending on this, we determine the local velocities and pressures, and also the total drag coefficient  $c_x$ .

Figure 8.5.3 shows the results of calculating the function  $c_x \alpha' / (4 \Delta^2)$  for triangular wings with a subsonic ( $n_1 > 1$ ) and supersonic ( $n_1 < 1$ ) leading edges depending on  $1 - \bar{r}$  for various values of  $n_1$  (the sweep angle  $\alpha_1$ ). The values of  $c_x \alpha' / (4 \Delta^2)$  at  $n_1 = 0$  correspond to a straight wing with a symmetric airfoil.

Figure 8.5.3 can be used to appraise the influence of the location of the maximum airfoil thickness on the drag. We can indicate the value of  $\bar{r}$  which the minimum drag coefficient corresponds to. The salient points of the curves correspond to values of  $\bar{r}$  at which the maximum thickness line becomes sonic ( $n_2 = n_1$  and  $\bar{r} = 1$ ).

**General Relation  
for Calculating the Drag**

The total drag coefficient of a wing can be written in the form

$$c_{x_a} = c_{x, f} + c_{x, w_0} + A c_{y_a}^2 \quad (8.5.15)$$

where  $A$  is a coefficient determined by the kind of the leading edge; if it is supersonic, the coefficient  $A$  equals the reciprocal of the derivative of the lift coefficient with respect to the angle of attack [ $A = (c_{y_a}^\alpha)^{-1}$ ]; with a subsonic edge  $A < (c_{y_a}^\alpha)^{-1}$  because a suction force appears that decreases the drag. The quantity  $A c_{y_a}^2$  is the induced drag depending on the lift force.

The coefficient of friction drag  $c_{x, f}$  can be evaluated for an equivalent rectangular wing whose chord equals the mean aerodynamic chord of the given lifting surface. We may consider here that the boundary layer near the leading edge of such a wing is laminar and on the remaining part is turbulent.

Let us consider the second component of the total drag coefficient,  $c_{x, w_0}$ , which is the wave-drag coefficient of the wing at  $\alpha = 0$ . We shall use formula (7.5.31) to evaluate it. According to this formula, at  $\alpha = 0$ , the wave-drag coefficient of an airfoil is  $c_{x, w} =$

$$= c_1 K_1 = c_1 \int_0^1 (\beta_b^2 + \beta_u^2) dx, \quad \text{therefore for a symmetric wedge}$$

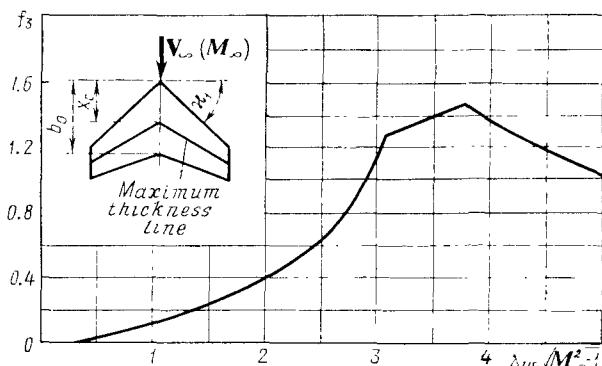
we have  $c_{x, w} = 0.5 c_1 \bar{\Delta}^2$ . Such a relation, characterizing the change in the wave-drag coefficient proportional to the square of the relative thickness of the airfoil [ $\bar{\Delta}^2 = (\Delta/b)^2$ ], can be applied for a thin airfoil of an arbitrary configuration. By comparing the above relation for  $c_{x, w}$  with (8.5.14), we can determine the ratio

$$c_{x, w_0}/c_{x, w} = f_3(\lambda_w \sqrt{M_\infty^2 - 1}, \lambda_w \tan \alpha, \eta_w, \bar{x}_C) \quad (8.5.16)$$

in which  $c_{x, w}$  is the wave-drag coefficient of the airfoil oriented in the direction of the oncoming flow (see Sec. 7.5),  $\lambda_w$  and  $\eta_w$  are the speed ratio and taper ratio of the wing, respectively.

The function  $f_3$  in (8.5.16) is similar to the function  $f_2$  in (8.5.14) and is determined with the aid of the method of sources set out above. The quantity  $\alpha$  may be taken equal to one of the characteristic angles of the given wing (the angle of inclination of the leading and trailing edges or of the maximum thickness line).

Figure 8.5.4 shows a curve characterizing the change in the function  $f_3$  for a swept wing with a taper ratio of  $\eta_w = 2$  a relative coordinate of  $\bar{x}_C = 0.5$  and the quantity  $\lambda_w \tan \alpha_1 = 3.67$ . The first

**Fig. 8.5.4**

Change in drag function  $f_3$  by formula (8.5.16)

salient point corresponds to the transformation of the trailing edge, and the second, of the leading edge into a sonic one.

### 8.6. Field of Application of the Source Method

The method of sources, as we already know, is used to calculate the flow in order to find the drag force of a wing with a symmetric airfoil at a *zero angle of attack*, i.e. in the absence of a lift force. Investigations reveal that the field of application of this method in aerodynamic research can be extended. Let us consider cases when the method of sources can be used to determine a nearly uniform flow over a thin wing at a *non-zero angle of attack*, and we can thus find the lift force in addition to the drag.

Let us take two wings with different leading edges. One of them has a curved edge with a finite supersonic section (Fig. 8.6.1), while the other has completely subsonic leading edges (Fig. 8.6.2).

In Fig. 8.6.1, the supersonic section is bounded by points  $E$  and  $E'$  at which a tangent to the contour coincides with the generatrices of the Mach cones. Let us consider the velocity potential at a point  $M$  in the region confined by edges  $ED$  and the Mach lines drawn in plane  $xOz$  from points  $E$ ,  $D$ ,  $D'$ , and  $E'$ .

By formula (8.2.16) in which the integration region  $\sigma$  should be taken equal to  $\sigma = S_1 + S_2$ , the velocity potential at the point being considered is

$$\begin{aligned} \varphi' = & -\frac{1}{2\pi} \iint_{S_1} \frac{Q_1(\xi, \zeta) d\xi d\zeta}{V(x_1 - \xi)^2 - (z_1 - \zeta)^2} \\ & -\frac{1}{2\pi} \iint_{S_2} \frac{Q_2(\xi, \zeta) d\xi d\zeta}{V(x_1 - \xi)^2 - (z_1 - \zeta)^2} \end{aligned} \quad (8.6.1)$$

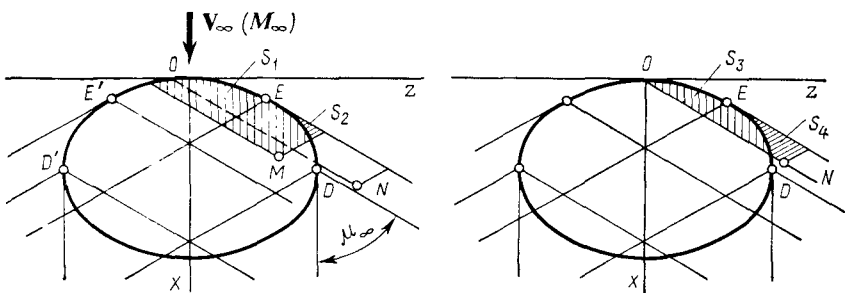


**Fig. 8.6.1**  
Wing with a finite section of a supersonic leading edge

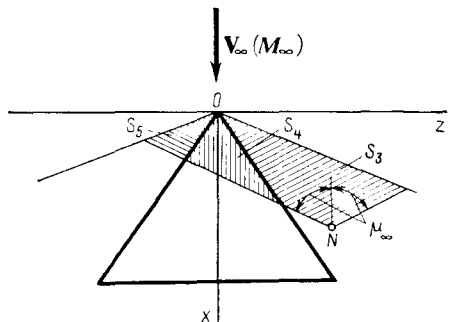


**Fig. 8.6.2**  
Wing with subsonic leading edges

In (8.6.1), the function  $Q_1(x, z) = 2(\partial\varphi'/\partial y)_{y=0}$ . This follows from (8.2.17). This function is determined from the condition of flow over the wing surface without separation (8.1.12). Since the equation of this surface is given, the function  $Q_1(x, z)$  is known. In the particular case of a wing in the form of a plate in a flow at the angle of attack  $\alpha$ , the function  $Q_1 = 2V_\infty\alpha$ . Hence, the determination of  $\varphi'$  by formula (8.6.1) is associated with the finding of the unknown function  $Q_2$  determining the intensity of source distribution on section  $S_2$ .

To find this function  $Q_2$ , let us take an arbitrary point  $N(x, O, z)$  in the region between the Mach lines issuing from points  $E$  and  $D$ . At this point, according to (8.1.20), the velocity potential is zero, therefore in accordance with the notation (see Fig. 8.6.1), we have

$$0 = -\frac{1}{2\pi} \iint_{S_3} \frac{Q_1(\xi, \zeta) d\xi d\zeta}{V(x_1 - \xi)^2 - (z_1 - \zeta)^2} + \frac{1}{2\pi} \iint_{S_4} \frac{Q_2(\xi, \zeta) d\xi d\zeta}{V(x_1 - \xi)^2 - (z_1 - \zeta)^2} \quad (8.6.2)$$

The first term on the right-hand side of this integral equation is a known function of the coordinates of a point because the strength  $Q_1$  on area  $S_3$  has been determined from the boundary conditions. We can therefore use the equation to determine the unknown function  $Q_2$  that is the strength of the sources in region  $S_4$ .

Hence, if the leading edge of a symmetric airfoil wing is completely or partly supersonic, the method of sources is suitable for investigating the flow over the wing at a non-zero angle of attack. The same conclusion evidently also relates to a wing with similar edges and a non-symmetric airfoil in a flow either at the angle  $\alpha \neq 0$  or at  $\alpha = 0$ .

Now let us consider a wing with subsonic leading edges. We can derive the following relation for a similar point  $N$  (Fig. 8.6.2):

$$0 = -\frac{1}{2\pi} \iint_{S_5} \frac{Q_3(\xi, \zeta) d\xi d\zeta}{V(x_1 - \xi)^2 - (z_1 - \zeta)^2} - \frac{1}{2\pi} \iint_{S_3} \frac{Q_1(\xi, \zeta) d\xi d\zeta}{V(x_1 - \xi)^2 - (z_1 - \zeta)^2} \\ - \frac{1}{2\pi} \iint_{S_4} \frac{Q_2(\xi, \zeta) d\xi d\zeta}{V(x_1 - \xi)^2 - (z_1 - \zeta)^2} \quad (8.6.3)$$

We have obtained an equation with two unknown functions  $Q_3$  and  $Q_2$ . Similar to  $Q_2$ , the function  $Q_3$  is the strength of the sources on area  $S_5$  belonging to the region located between the left-hand leading edge and the Mach line issuing from the wing vertex.

Hence, if a wing has a subsonic leading edge, the source method cannot be used to investigate the flow over a thin symmetric airfoil wing at an angle of attack, or the flow over a non-symmetric airfoil wing at a zero angle of attack or when  $\alpha \neq 0$ .

## 8.7. Doublet Distribution Method

It has been established that the application of the source method for investigating supersonic flow is restricted to wings with completely or partly supersonic leading edges. In other cases associated with the investigation of the supersonic aerodynamic characteristics of wings with subsonic leading edges with a non-zero angle of attack (or of similar non-symmetric airfoil wings and at  $\alpha = 0$ ), the **doublet distribution method** must be used.

Let us consider a doublet in a supersonic flow. To do this, we shall determine the velocity potential of the flow produced by an elementary source and an elementary sink of the same strength  $Q$  having coordinates  $x = \xi$ ,  $z = \zeta$ ,  $y = \varepsilon$ , and  $x = \xi$ ,  $z = \zeta$ ,  $y = -\varepsilon$ , respectively. The chosen source is located above the plane  $y = 0$  at the small distance  $\varepsilon$  from it, and the sink is under this plane at the same small distance  $-\varepsilon$ . Expressing (8.2.11) as a difference equation, we shall write the potential produced by the source and sink

in the form

$$\Delta\varphi = \frac{Q\Delta\sigma}{2\pi} \left\{ \frac{-1}{\sqrt{(x-\xi)^2 - \alpha'^2 [(y-\varepsilon)^2 + (z-\zeta)^2]}} + \frac{1}{\sqrt{(x-\xi)^2 - \alpha'^2 [(y+\varepsilon)^2 + (z-\zeta)^2]}} \right\}$$

Introducing the symbol  $\rho = \sqrt{(x-\xi)^2 - \alpha'^2 [y^2 + (z-\zeta)^2]}$  and disregarding the quantity  $\alpha'^2\varepsilon^2$ , we obtain

$$\Delta\varphi = \frac{Q\Delta\sigma}{2\pi\rho} \left( \frac{-1}{\sqrt{1+2\alpha'^2ye/\rho^2}} + \frac{1}{\sqrt{1-2\alpha'^2ye/\rho^2}} \right)$$

Using the expansion of the square roots into a series and deleting the second and higher order infinitesimals, we find

$$\Delta\varphi = \frac{\alpha'^2 Q y \varepsilon \Delta\sigma}{\pi \rho^3} = \frac{\alpha'^2 Q y \varepsilon d\sigma}{\pi \{(x-\xi)^2 - \alpha'^2 [y^2 + (z-\zeta)^2]\}^{3/2}}$$

By calculating the limit of  $\Delta\varphi$  at  $\varepsilon \rightarrow 0$  and assuming that the quantity  $M = Q\varepsilon$  called the **moment** (or power) of the doublet remains constant, we obtain an expression for the differential of the potential function of a doublet

$$d\varphi_{\text{doub}} = \frac{My d\sigma}{\pi \{(x-\xi)^2 - \alpha'^2 [y^2 + (z-\zeta)^2]\}^{3/2}}$$

This expression can be written in the form

$$d\varphi_{\text{doub}} = \frac{M d\sigma}{\pi} \cdot \frac{\partial}{\partial y} \left\{ \frac{1}{\sqrt{(x-\xi)^2 - \alpha'^2 [y^2 + (z-\zeta)^2]}} \right\}$$

Integrating over the region  $\sigma$  which the influence of the doublets extends to, we obtain for the potential function

$$\varphi_{\text{doub}} = \frac{\partial}{\partial y} \int \int \frac{M(\xi, \zeta) d\xi d\zeta}{\sqrt{(x-\xi)^2 - \alpha'^2 [y^2 + (z-\zeta)^2]}} \quad (8.7.1)$$

where the number  $\pi$  has been included in the doublet distribution function.

It can be shown that function (8.7.1) satisfies Eq. (8.1.7). To do this, let us differentiate (8.1.7) with respect to  $y$ :

$$(M_\infty^2 - 1) \frac{\partial}{\partial y} \left( \frac{\partial^2 \varphi'}{\partial x^2} \right) - \frac{\partial}{\partial y} \left( \frac{\partial^2 \varphi'}{\partial y^2} \right) - \frac{\partial}{\partial y} \left( \frac{\partial^2 \varphi'}{\partial z^2} \right) = 0$$

We can write this equation as

$$(M_\infty^2 - 1) \frac{\partial^2}{\partial x^2} \left( \frac{\partial \varphi'}{\partial y} \right) - \frac{\partial^2}{\partial y^2} \left( \frac{\partial \varphi'}{\partial y} \right) - \frac{\partial^2}{\partial z^2} \left( \frac{\partial \varphi'}{\partial y} \right) = 0 \quad (8.7.2)$$

Now let us consider expression (8.7.1) for the potential of a doublet. If we include the quantity  $-1/(2\pi)$  into the expression for this

potential, then in accordance with (8.2.12) the double integral can be considered as the potential of sources whose distribution over area  $\sigma$  is set by a function  $M$ . Consequently,

$$\varphi_{\text{doub}} = \partial\varphi'/\partial y \quad (8.7.3)$$

Comparing (8.7.2) and (8.7.3), we see that the function  $\varphi_{\text{doub}}$  does indeed satisfy Eq. (8.1.7) for the velocity potential.

Knowing the configuration of the surface in the flow, the free-stream velocity, and the angle of attack, we can find the doublet distribution function  $M$  and thus determine the potential  $\varphi_{\text{doub}}$  of the doublets. The derivative of the function  $\varphi_{\text{doub}}$  with respect to  $x$  yields the additional longitudinal component of the disturbed velocity  $u = \partial\varphi_{\text{doub}}/\partial x$  that is used to calculate the pressure coefficient  $p = -2u/V_\infty$  on the lifting surface and the lift force produced by this surface.

### 8.8. Flow over a Triangular Wing with Subsonic Leading Edges

A plane triangular wing with subsonic leading edges is *inside a Mach cone* (Fig. 8.8.1). To find the lift force of such a wing, we shall use the doublet distribution method and the relevant relation (8.7.1) for the velocity potential of doublets.

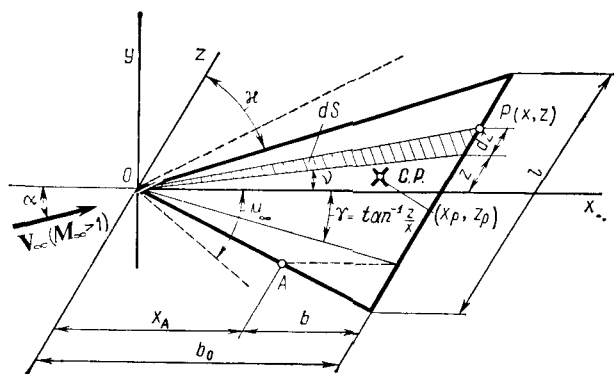
It is general knowledge that the additional velocity  $u$  induced by sources distributed over an inclined triangular surface with subsonic edges depends only on the function  $\sigma = z\alpha'/x$  [see, for example, formula (8.3.18)]. This signifies that along the ray issuing from the salient point of the leading edge of the wing at the angle  $\gamma = \tan^{-1}(z/x)$  the velocity is *constant*. This ray can be considered as the generatrix of a cone with its vertex coinciding with the salient point of the leading edge.

A flow retaining a constant velocity and, therefore, other constant parameters along a generatrix of such a conical surface is called a **conical flow**. We can consider that the additional velocity  $u$  for such a flow in the plane  $y = 0$  is a function of the ratio  $z/x$ , i.e.  $u = f(z/x)$ . It thus follows that the potential produced by the sources for a conical flow also depends on this ratio.

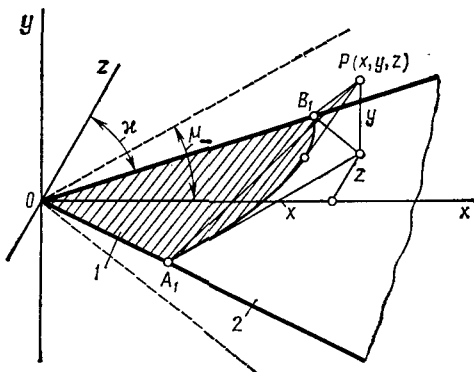
Considering the flow set up by doublets near a triangular surface as a conical one, its potential can be written for point  $P$  in the plane  $y = 0$  (Fig. 8.8.1) as follows:

$$\varphi_{\text{doub}} = xF_{\text{doub}}(z/x) \quad (8.8.1)$$

where  $F_{\text{doub}}(z/x)$  is a function depending only on the angle of the conical surface  $\gamma = \tan^{-1}(z/x)$ .

**Fig. 8.8.1**

Plane triangular wing with subsonic edges

**Fig. 8.8.2**

Region of doublet influence on the flow over a wing with subsonic leading edges:

1—region of doublet influence; 2—triangular wing

For a point with the coordinates  $x, y, z$  we shall write the potential of a conical flow in a more general form:

$$\varphi_{\text{doub}} = x F_{\text{doub}}(z/x, y/x) \quad (8.8.2)$$

In accordance with Eq. (8.8.1), the relation characterizing the distribution of the doublets in the plane  $y = 0$  (on the wing surface) is such that

$$M(\xi, \zeta) = \xi m(h) \quad (8.8.3)$$

where  $h = \zeta/\xi$ , and  $m(h)$  is a function of the argument  $h$ .

Let us transform Eq. (8.7.1). We shall express the elementary area occupied by a doublet in the form  $d\sigma = d\xi d\zeta = \xi dh d\xi$  because  $d\zeta = \xi dh$ . Therefore

$$\varphi_{\text{doub}} = \int_{-\cot \alpha}^{\cot \alpha} m(h) dh \frac{\partial}{\partial y} \int_0^{\xi_1} \frac{\xi^2 d\xi}{\sqrt{(x-\xi)^2 - \alpha'^2 [y^2 + (z-h\xi)^2]}} \quad (8.8.4)$$

where  $\xi_1$  is the coordinate of a doublet that may influence the flow at point  $P(x, y, z)$ . This doublet is on the curve confining the region of doublet influence (Fig. 8.8.2) and obtained as a result of the intersection of the plane  $y = 0$  with the Mach cone issuing upstream from point  $P$ . This curve is parabola  $A_1B_1$  described by the equation

$$(x - \xi_1)^2 - \alpha'^2 [y^2 + (z - \xi_1)^2] = 0 \quad (8.8.5)$$

in the coordinates  $\xi_1, \xi_1$ . We shall write the radicand in (8.8.4) in the form

$$(x - \xi)^2 - \alpha'^2 [y^2 + (z - h\xi)^2] = a\xi^2 + b\xi + c \quad (8.8.6)$$

where

$$\begin{aligned} a &= 1 - \alpha'^2 h^2, \quad b = 2x \left( \alpha'^2 h \frac{z}{x} - 1 \right), \\ c &= x^2 \left[ 1 - \alpha'^2 \left( \frac{y^2}{x^2} + \frac{z^2}{x^2} \right) \right] \end{aligned} \quad (8.8.7)$$

The integral in the case being considered is

$$\begin{aligned} \int_0^{\xi_1} \frac{\xi^2 d\xi}{\sqrt{a\xi^2 + b\xi + c}} &= \left( \frac{\xi}{2a} - \frac{3b}{4a^2} \right) \sqrt{a\xi^2 + b\xi + c} \Big|_0^{\xi_1} \\ &+ \frac{3b^2 - 4ac}{8a^2} \int_0^{\xi_1} \frac{d\xi}{\sqrt{a\xi^2 + b\xi + c}} \end{aligned} \quad (8.8.8)$$

¶ Taking into account that  $a = 1 - \alpha'^2$  and  $h^2 > 0$ , we find the integral on the right-hand side of (8.8.8):

$$\int_0^{\xi_1} \frac{d\xi}{\sqrt{a\xi^2 + b\xi + c}} = \frac{1}{\sqrt{a}} \ln [2 \sqrt{a(a\xi^2 + b\xi + c)} + 2a\xi + b] \Big|_0^{\xi_1} \quad (8.8.9)$$

By (8.8.5), the value of  $a\xi_1^2 + b\xi_1 + c = 0$ , consequently,

$$\begin{aligned} \int_0^{\xi_1} \frac{\xi^2 d\xi}{\sqrt{a\xi^2 + b\xi + c}} &= \frac{3b}{4a^2} \sqrt{c} \\ &+ \frac{3b^2 - 4ac}{8a^2 \sqrt{a}} [\ln (2a\xi_1 + b) - \ln (2\sqrt{ac} + b)] \end{aligned} \quad (8.8.10)$$

Solving Eq. (8.8.5) in the form

$$a\xi_1^2 + b\xi_1 + c = 0, \quad (8.8.11)$$

we obtain

$$\xi_1 = (-b + \sqrt{b^2 - 4ac})/2a \quad (8.8.12)$$

Accordingly,

$$\ln (2a\xi_1 + b) = \ln \sqrt{b^2 - 4ac} \quad (8.8.13)$$

The difference of the logarithms in (8.8.10) with a view to (8.8.13) is

$$\begin{aligned} \ln(2a\xi_1 + b) - \ln(2\sqrt{ac} + b) &= \ln \frac{\sqrt{b^2 - 4ac}}{2\sqrt{ac} + b} = \frac{1}{2} \ln \frac{b^2 - 4ac}{(2\sqrt{ac} + b)^2} \\ &= \frac{1}{2} \ln \frac{b - 2\sqrt{ac}}{b + 2\sqrt{ac}} = -\operatorname{th}^{-1} \frac{b}{2\sqrt{ac}} \end{aligned} \quad (8.8.14)$$

Therefore,

$$\int_0^{\xi_1} \frac{\xi^2 d\xi}{\sqrt{a\xi^2 + b\xi + c}} = \frac{3b\sqrt{c}}{4a^2} - \frac{3b^2 - 4ac}{8a^2\sqrt{a}} \operatorname{th}^{-1} \frac{b}{2\sqrt{ac}} \quad (8.8.15)$$

We calculate the derivative with respect to  $y$  from (8.8.15):

$$\begin{aligned} \frac{\partial}{\partial y} \int_0^{\xi_1} \frac{\xi^2 d\xi}{\sqrt{a\xi^2 + b\xi + c}} &= N \\ = \frac{1}{2a\sqrt{a}} \cdot \frac{\partial c}{\partial y} \left( \frac{b}{4\sqrt{ac}} \cdot \frac{8ac}{4ac - b^2} \right. &\left. + \operatorname{th}^{-1} \frac{b}{2\sqrt{ac}} \right) \end{aligned}$$

Introducing the symbol

$$v = b/(2\sqrt{ac}) \quad (8.8.16)$$

and having in view that  $\partial c/\partial y = -2y\alpha'^2$  [see formula (8.8.7)], we obtain

$$N = \frac{-y\alpha'^2}{a\sqrt{a}} \left( \frac{v}{1-v^2} + \operatorname{th}^{-1} v \right) \quad (8.8.17)$$

We introduce this expression into (8.8.4):

$$\varphi_{\text{doub}} := \int_{-\cot \kappa}^{\cot \kappa} N m(h) dh \quad (8.8.18)$$

To determine the form of the doublet distribution function, we shall use the condition of flow without separation, in accordance with which

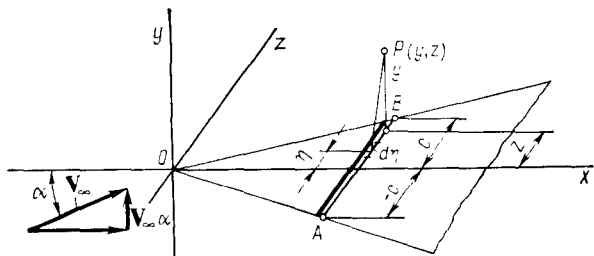
$$v_{y=0} = V_\infty \alpha = (\partial \varphi_{\text{doub}} / \partial y)_{y=0} \quad (8.8.19)$$

The partial derivative  $(\partial \varphi_{\text{doub}} / \partial y)_{y=0}$  is determined in accordance with (8.8.18) in the form

$$\left( \frac{\partial \varphi_{\text{doub}}}{\partial y} \right)_{y=0} = \int_{-\cot \kappa}^{\cot \kappa} \left( \frac{\partial N}{\partial y} \right)_{y=0} m(h) dh \quad (8.8.20)$$

Introducing this expression into (8.8.19), we find

$$V_\infty \alpha = \int_{-\cot \kappa}^{\cot \kappa} \left( \frac{\partial N}{\partial y} \right)_{y=0} m(h) dh \quad (8.8.21)$$

**Fig. 8.8.3**

Incompressible two-dimensional cross flow at the velocity  $V_\infty \alpha$  over flat plate  $AB$  belonging to a triangular wing

Differentiation of (8.8.17) with respect to  $y$  yields

$$\left( \frac{\partial N}{\partial y} \right)_{y=0} = - \frac{\alpha'^2}{a \sqrt{a}} \left( \frac{v}{1-v^2} + \operatorname{th}^{-1} v \right)_{y=0} \quad (8.8.22)$$

Let us calculate the partial derivative with respect to  $z/x$  from (8.8.20) with a view to (8.8.22):

$$0 = \int_{-\cot \alpha}^{\cot \alpha} \frac{1}{(1-v^2)^2} \cdot \frac{\partial v}{\partial(z/x)} \Big|_{y=0} m(h) dh \quad (8.8.23)$$

We calculate the value of the derivative  $\partial v / \partial(z/x)|_{y=0}$  by (8.8.16) and determine the quantity  $(1-v^2)^2|_{y=0}$  by using (8.8.7) and (8.8.16). After the corresponding substitutions into (8.8.23), we obtain the equation

$$\int_{-\cot \alpha}^{\cot \alpha} \frac{m(h) dh}{\left( h - \frac{z}{x} \right)^3} = 0 \quad (8.8.24)$$

We shall show that this equation has the same form as the one obtained when using the doublet distribution method to solve the problem on the flow of an incompressible fluid over a flat plate of infinite length installed at right angles to the direction of the free-stream velocity. We can determine the velocity potential for a plate that is a part of a wing in section  $AB$  with the coordinates  $z_A = -c$ ,  $z_B = c$ , and over which an incompressible fluid flows in a lateral direction at the velocity  $v = V_\infty \alpha$  (Fig. 8.8.3) with the aid of Eq. (2.9.16). We shall write the latter in accordance with the coordinate system chosen in Fig. 8.8.3 in the form

$$\varphi_{\text{doub}} = y / [(z - \eta)^2 + y^2] \quad (8.8.25)$$

This expression determines the potential at point  $P(y, z)$  produced by a two-dimensional point doublet with a unit moment

( $M = 1$ ). If the moment of the doublet differs from unity and the doublet distribution over the span of the plate is set by the function  $M(\eta)$ , the velocity potential induced by the doublets on the wing section  $d\eta$  is

$$d\varphi_{\text{doub}} = M(\eta) y d\eta / [(z - \eta)^2 + y^2] \quad (8.8.26)$$

The velocity potential at point  $P$  due to the influence of the doublets located along the span of the plate on the section from  $z_A = -c$  to  $z_B = c$  is

$$\varphi_{\text{doub}} = \int_{-c}^c \frac{M(\eta) y d\eta}{(z - \eta)^2 + y^2} \quad (8.8.27)$$

The vertical component of the velocity  $v = \partial\varphi_{\text{doub}}/\partial y$  on the surface of the wing is

$$v_{y=0} = \left( \frac{\partial \varphi_{\text{doub}}}{\partial y} \right)_{y=0} = \left[ \frac{\partial}{\partial y} \int_{-c}^c \frac{M(\eta) y d\eta}{(z - \eta)^2 + y^2} \right]_{y=0} = \int_{-c}^c \frac{M(\eta) d\eta}{(z - \eta)^2} \quad (8.8.28)$$

Since the component  $v_{y=0}$  does not change over the span of the plate, we have

$$\left( \frac{\partial v}{\partial z} \right)_{y=0} = \frac{\partial}{\partial z} \int_{-c}^c \frac{M(\eta) d\eta}{(z - \eta)^2} = 0 \quad (8.8.29)$$

Differentiation yields

$$\int_{-c}^c \frac{M(\eta) d\eta}{(z - \eta)^3} = 0 \quad (8.8.30)$$

A comparison of Eqs. (8.8.24) and (8.8.30) reveals that they are both of a single type, therefore it is possible to take the doublet distribution function  $m(h)$  in a supersonic linearized flow of the same appearance as the corresponding function  $M(\eta)$  in an incompressible flow.

To determine the form of the function  $M(\eta)$ , we shall use the solution of the problem on finding the potential function for a plane plate over which an incompressible fluid flows in a lateral direction (see Sec. 6.2). According to this solution, the velocity potential on the plate is determined by formula (6.2.7). The relevant potential difference on both sides of it is  $\Delta\varphi = 2V\sqrt{a^2 - z^2}$ . The flow of an incompressible fluid near the plate is considered as the result of superposition of the flow produced by the doublets onto the undisturbed flow [see formula (6.3.6)]. Consequently, *the distribution of doublets for a plane plate in a non-circulatory flow of an incompressible fluid is equivalent to the potential difference  $\Delta\varphi$* . Having in view that

the doublet distribution function  $m(h)$  in a compressible flow has the same form as for an incompressible one, we can consider the expression for this function in the form

$$m(h) = L \sqrt{H^2 - h^2} \quad (8.8.31)$$

where  $H^2 = \cot^2 \alpha$  and  $L$  is a proportionality coefficient.

We shall use Eq. (8.8.21) to find the coefficient  $L$ . Inserting (8.8.22) and (8.8.31) into it, we obtain

$$\alpha V_\infty = -\alpha'^2 L \int_{-\cot \alpha}^{\cot \alpha} \frac{1}{a \sqrt{a}} \left( \frac{v}{1-v^2} + \operatorname{th}^{-1} v \right)_{y=0} \sqrt{\cot^2 \alpha - h^2} dh \quad (8.8.32)$$

To simplify the calculation of the coefficient  $L$ , we can integrate (8.8.32) along a longitudinal coordinate on the wing. Having in view that along the  $x$ -axis the coordinates  $z = 0$  and  $y = 0$ , we determine the value of  $|v/(1-v^2) + \operatorname{th}^{-1} v|_{y=0}$  in accordance with (8.8.7) and (8.8.16), and the value of  $a \sqrt{a}$  by (8.8.7). Integration yields

$$\alpha V_\infty = \pi L \int_0^{\pi/2} \sqrt{1 - (1 - \alpha'^2 \cot^2 \alpha) \sin^2 \varphi} d\varphi \quad (8.8.33)$$

The integral

$$\int_0^{\pi/2} \sqrt{1 - (1 - \alpha'^2 \cot^2 \alpha) \sin^2 \varphi} d\varphi = E(k) \quad (8.8.34)$$

is a complete elliptic integral of the second order with the parameter

$$k = \sqrt{1 - \alpha'^2 \cot^2 \alpha} \quad (8.8.35)$$

The values of integral (8.8.34) are determined with the aid of the previously calculated tables depending on the parameter  $k$ .

The doublet distribution can be expressed by function (8.8.3) provided that  $m(h)$  is replaced by (8.8.31) and with account taken of the value for  $L$  determined from (8.8.33). As a result, we have

$$M(\xi, \zeta) = \xi \sqrt{\cot^2 \alpha - h^2} \frac{\alpha V_\infty}{\pi E(k)} \quad (8.8.36)$$

Let us find the component of the induced velocity produced by the doublets on the surface of the wing for  $y = 0$ . From (8.7.3), we have

$$(\varphi_{\text{doub}})_{y=0} = (\partial \varphi' / \partial y)_{y=0} = (v_{y=0})_{\text{source}} \quad (8.8.37)$$

i.e. the potential of the doublets on the wing is determined by the magnitude of the vertical component of the velocity induced by the

sources. A comparison of (8.2.12) and (8.7.1) reveals that  $M(\xi, \zeta)$  can be considered as a function similar to the function  $Q(\xi, \zeta)$  determining the distribution of the sources over the surface of a wing having a given planform and angle of attack. Consequently, if we take into account that in (8.7.1) the number  $\pi$  is included in  $M(\xi, \zeta)$  in accordance with (8.2.7), (8.8.36), and (8.8.37), we can compile the equation

$$(\varphi_{\text{doub}})_{y=0} = \pi M(\xi, \zeta) = \frac{\alpha V_\infty \xi}{E(k)} \sqrt{\cot^2 \alpha - h^2} \quad (8.8.38)$$

where  $h = \zeta/\xi$  (or  $h = z/x$ ).

The component of the induced velocity due to the doublets is

$$\begin{aligned} u &= \left( \frac{\partial \varphi_{\text{doub}}}{\partial x} \right)_{y=0} = \frac{\alpha V_\infty}{E(k)} \cdot \frac{\partial}{\partial x} \left( x \sqrt{\cot^2 \alpha - \frac{z^2}{x^2}} \right) \\ &= \frac{\alpha V_\infty \cot^2 \alpha}{E(k) \sqrt{\cot^2 \alpha - h^2}} \end{aligned} \quad (8.8.39)$$

The corresponding value of the pressure coefficient with a view to the possible signs in front of the square root is

$$\bar{p} = \frac{2(p - p_\infty)}{\rho_\infty V_\infty^2} = - \frac{2u}{V_\infty} = \frac{\pm 2\alpha \cot^2 \alpha}{E(k) \sqrt{\cot^2 \alpha - h^2}} \quad (8.8.40)$$

where the plus sign determines the pressure on the bottom, and the minus sign on the upper side of the wing. *The field of pressures corresponds to a conical flow relative to the vertex of the wing* at which the pressure coefficient  $\bar{p} = \text{const}$  for all the values of  $z/x = \text{const}$ .

The lift force acting on a triangular wing consists of the force produced by the pressure on the bottom surface, and of the suction force equal to it in magnitude and caused by the rarefaction on the upper side. The elementary lift force acting on area  $dS = 0.5xdz$  (see Fig. 8.8.1) is

$$dY_a = 2(p - p_\infty) dS = (p - p_\infty) x dz \quad (8.8.41)$$

The total force is obtained as a result of integration over the entire surface of the wing  $S_w = x^2 \cot \alpha$ :

$$Y_a = \int_{S_w} 2(p - p_\infty) dS \quad (8.8.42)$$

The lift coefficient is

$$\begin{aligned} c_{y_a} &= \frac{2Y_a}{\rho_\infty V_\infty^2 S_w} = \frac{1}{-\cot \alpha} \int_{-\cot \alpha}^{\cot \alpha} |\bar{p}| dh \\ &= \frac{2\alpha \cot \alpha}{E(k)} \int_{-\cot \alpha}^{\cot \alpha} \frac{dh}{\sqrt{\cot^2 \alpha - h^2}} \end{aligned} \quad (8.8.43)$$

After integration, we have

$$c_{y_a} = 2\alpha\pi \cot \alpha/E(k) \quad (8.8.44)$$

For a conical flow, the centre of pressure of each triangular element issuing from the apex is at a distance of two-thirds of the altitude from the apex. Therefore, the centre of pressure of the entire wing is on the root chord at a point that is at a distance of two-thirds of the chord from the apex. Accordingly, the coefficient of the pitching moment about the wing apex is

$$m_{z_a} = -c_{y_a} c_p = -(4/3) \alpha\pi \cot \alpha/E(k) \quad (8.8.45)$$

For a triangular low aspect ratio wing ( $\alpha \rightarrow \pi/2$ ), the quantity  $\alpha' \cot \alpha \ll 1$ , and we can take the value of the elliptic integral  $E(k) \approx 1$ . Consequently, for such a wing we have

$$c_{y_a} = 2\alpha\pi \cot \alpha; m_{z_a} = -(4/3) \alpha\pi \cot \alpha \quad (8.8.46)$$

Expressing  $\cot \alpha$  in terms of the wing aspect ratio  $\lambda_w = 4 \cot \alpha$ , we obtain

$$c_{y_a} = \alpha\pi\lambda_w/2; m_{z_a} = -(1/3) \alpha\pi\lambda_w \quad (8.8.46')$$

If the sweep angle  $\alpha$  is chosen such that  $\alpha = \pi/2 - \mu_\infty$ , and, consequently, the Mach line coincides with the leading edge, we have

$$\cot \alpha = \tan \mu_\infty \quad \text{and} \quad \alpha' \cot \alpha = \cot \mu_\infty \cot \alpha = 1$$

In the given case, the elliptic integral  $E(k) = \pi/2$ , therefore for a triangular wing with a sonic leading edge, we have

$$c_{y_a} = 4\alpha \cot \alpha \quad (8.8.47)$$

Since

$$\cot \alpha = \tan \mu_\infty = 1/\sqrt{M_\infty^2 - 1}$$

we obtain

$$c_{y_a} = 4\alpha/\sqrt{M_\infty^2 - 1} \quad (8.8.48)$$

This value coincides with the lift coefficient for a thin sharp-nosed airfoil in a linearized supersonic flow.

We shall show that the lift coefficient of a triangular wing with supersonic leading edges is expressed by the same relation (8.8.48). In accordance with (8.3.34), the pressure coefficient for the wing in the region between Mach cones is

$$\bar{p}_1 = \frac{\pm 2\alpha}{\alpha' \sqrt{1-n^2}} \left( 1 - \frac{2}{\pi} \sin^{-1} \sqrt{\frac{n^2-\sigma^2}{1-\sigma^2}} \right) \quad (8.8.49)$$

and on the section between the leading edge and a Mach cone [see (8.3.23)] it is

$$\bar{p}_2 = \pm 2\alpha/(\alpha' \sqrt{1-n^2}) \quad (8.8.50)$$

where  $n = \tan \alpha / \alpha'$ , and  $\sigma = z \tan \alpha / x = h \tan \alpha$ .

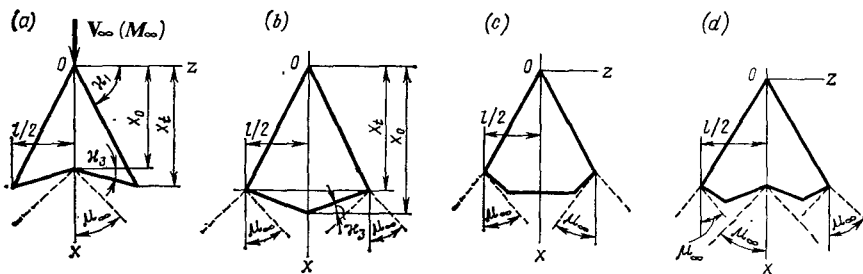


Fig. 8.8.4

Wings with supersonic trailing and side edges ( $x_0 = b_0$ ):

a—tetragonal wing with a dovetail; b—tetragonal wing with a vee-shaped appendage (rhombiform plate); c—pentagonal wing; d—hexagonal wing

According to (8.8.43), (8.8.49), and (8.8.50), the lift coefficient is

$$c_{y_a} = 2 \int_0^n |\bar{p}_1| d\sigma - 2 \int_0^n |\bar{p}_2| d\sigma = \frac{4\alpha}{\alpha' \sqrt{1-n^2}} \times \left[ \int_0^n \left( 1 - \frac{2}{\pi} \sin^{-1} \sqrt{\frac{n^2 - \alpha^2}{1 - \sigma^2}} \right) d\sigma - \int_1^n d\sigma \right]$$

Integration yields the relation  $c_{y_a} = 4\alpha/\alpha'$  that coincides with (8.8.48).

The methods of calculating the flow over triangular (delta) wings can be used to determine the aerodynamic characteristics of lifting surfaces in the form of tetragonal, pentagonal, and hexagonal plates with *supersonic* trailing and side edges (Fig. 8.8.4). The flow over them is characterized by the absence of zones of mutual influence of the tail and side regions confined by the intersection of Mach cones with the wing, i.e. when the flow at the side and trailing edges is supersonic. As a result, the coefficient of the pressure on the wing surface is the same as at the relevant point of a triangular plate. The formula for calculating it is chosen with account taken of the kind of leading edge (subsonic or supersonic). The lift and moment coefficients can be determined by integration according to the pressure distribution.

We shall give the results obtained for a tetragonal wing: with a subsonic leading edge

$$c_{y_a} = \frac{4\alpha \cot \kappa_1}{(1-\varepsilon) E(k)} [(1-\varepsilon)^{-1/2} \cos^{-1} \varepsilon - \varepsilon] \quad (8.8.51)$$

$$m_{z_a} = \frac{-4\alpha \cot \kappa_1}{3(1-\varepsilon) E(k)} \left[ \frac{2+\varepsilon^2}{(1+\varepsilon)^{3/2}} \cos^{-1} \varepsilon - \frac{\varepsilon(4-\varepsilon)^2}{1-\varepsilon^2} \right] \quad (8.8.52)$$

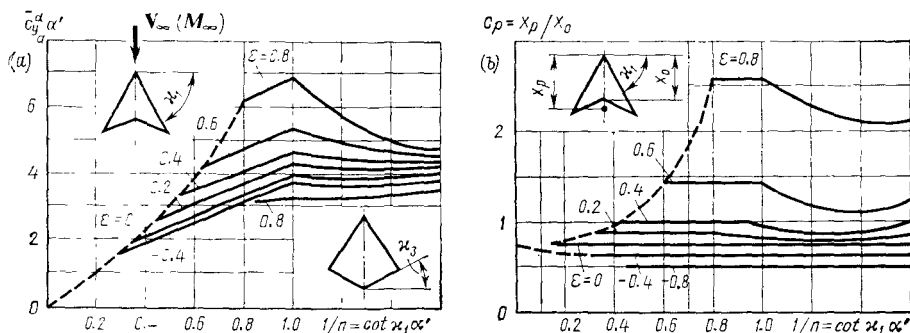


Fig. 8.8.5

Curves characterizing the change in the derivative of the lift coefficient (a) and centre-of-pressure coefficient (b) for a tetragonal wing

with supersonic edges

$$c_{y_a} = \frac{8\alpha}{(1-\varepsilon)\pi\alpha'} \left( \frac{1}{\sqrt{1-n_1^2}} \cos^{-1} n_1 - \frac{\varepsilon}{\sqrt{1-n^2}} \cos^{-1} n \right) \quad (8.8.53)$$

$$m_{z_a} = \frac{-8\alpha}{3(1-\varepsilon)\pi\alpha'} \left[ \frac{2-n_1^2(1+\varepsilon^2)}{(1+\varepsilon)^2(1-n_1^2)^{3/2}} \cos^{-1} n_1 - \frac{\varepsilon(3-\varepsilon^2)}{(1+\varepsilon)^2\sqrt{1-n^2}} \cos^{-1} n - \frac{n_1}{1-n_1^2} \right] \quad (8.8.54)$$

where  $\varepsilon = (x_t - x_0)/x_t = \tan x_3/\tan x_1$ ;  $n_1 = \tan x_3/\alpha' = \varepsilon n$ ;  $x_0$  and  $x_t$  are the dimensions shown in Fig. 8.8.4.

For dovetail wings (Fig. 8.8.4a), the quantity  $\varepsilon$  is positive, and for rhombiform plates (Fig. 8.8.4b), it is negative.

The relations for  $c_{y_a}$  and  $m_{z_a}$  allow us to determine the centre-of-pressure coefficient  $c_p = x_p/x_0 = -m_{z_a}/c_{y_a}$ .

Figure 8.8.5 shows curves characterizing the change in  $c_{y_a}^\alpha$  and  $c_p$  in accordance with the above relations. The dashed lines in this figure determine the values of the aerodynamic coefficients in the limiting case when  $1/n = \cot x_1 \alpha' = \varepsilon$  (a sonic trailing edge).

A salient point appears on the curves (Fig. 8.8.5) at a value of  $n = 1$  (when  $\cot x_1 \alpha' = 1$ ), i.e. when the leading edge is sonic. The coefficients  $c_{y_a}$  and  $c_p$  behind the salient point (with a supersonic leading edge) diminish with an increasing  $M_\infty$ .

Let us consider another limiting case corresponding to sufficiently high values of  $\cot x_1 \alpha' \gg 1$  ( $n \ll 1$ ,  $n_1 \ll 1$ ) at which the surface of a Mach cone is near the root chord. A glance at formula (8.8.53) reveals that the parameter  $\varepsilon$  does not virtually affect the coefficient  $c_{y_a}$ , and a dovetail or a V-shaped appendage (see the diagrams of the

wings in Fig. 8.8.5) alters the lift force of the wing almost in proportion to the change in the area of the plate.

It is not difficult to see that for  $\varepsilon = 0$  formulas (8.8.51)-(8.8.54) yield the values of the relevant coefficients for a triangular wing:  $c_{y_a} = c_{y_a \Delta}$  and  $m_{z_a} = m_{z_a \Delta}$ . The calculations by these formulas can be simplified if the tetragonal wings differ only slightly from triangular ones. In this case, provided that  $|\varepsilon| \ll 1$ , we have

$$c_{y_a} = c_{y_a \Delta} / (1 - \varepsilon), \quad m_{z_a} = m_{z_a \Delta} / (1 - \varepsilon) \quad (8.8.55)$$

### 8.9. Flow over a Hexagonal Wing with Subsonic Leading and Supersonic Trailing Edges

Let us find the aerodynamic characteristics in the more general case of the flow at a small angle of attack over a plane hexagonal wing *with subsonic leading and supersonic trailing edges* (Fig. 8.9.1). Such a kind of the trailing edges excludes the influence of the vortex sheet behind the wing on the flow over it.

To determine the velocity potential, let us use the results of solving the problem on the flow over a triangular wing with subsonic leading edges. Let us consider point  $A$  with the coordinates  $x, z$  in region  $I$  confined by the leading edges and the Mach lines issuing from points  $G$  and  $D$ . The velocity potential at this point can be expressed by analogy with (8.6.1) with the aid of the following formula:

$$\varphi'_I = -\frac{1}{2\pi} \iint_{\sigma} \frac{Q_1(\xi, \zeta) d\xi d\zeta}{\sqrt{(x-\xi)^2 - \alpha'^2(z-\zeta)^2}} + \Delta\varphi_2 + \Delta\varphi_3 \quad (8.9.1)$$

in which  $\sigma$  is the region of integration on the wing surface,  $\Delta\varphi_2$  and  $\Delta\varphi_3$  are the additional potentials determined by expressions similar to the second and third terms on the right-hand side of (8.6.3) when integrating over regions  $\sigma_1$  and  $\sigma_2$  (hatched in Fig. 8.9.1).

Taking into account that  $Q_1 = 2\lambda V_\infty = 2\alpha V_\infty$ , we can write Eq. (8.9.1) as follows:

$$\varphi'_I = -\frac{\alpha V_\infty \Omega}{\pi} \iint_{\sigma} \frac{d\xi d\zeta}{\sqrt{(x-\xi)^2 - \alpha'^2(z-\zeta)^2}} \quad (8.9.2)$$

where in accordance with (8.9.1)

$$\Omega = 1 - (\Delta\varphi_2 + \Delta\varphi_3) \left[ \frac{\alpha V_\infty}{\pi} \iint_{\sigma} \frac{d\xi d\zeta}{\sqrt{(x-\xi)^2 - \alpha'^2(z-\zeta)^2}} \right]^{-1} \quad (8.9.3)$$

For our further transformations, we shall introduce a characteristic system of coordinates whose axes  $r$  and  $s$  coincide with the

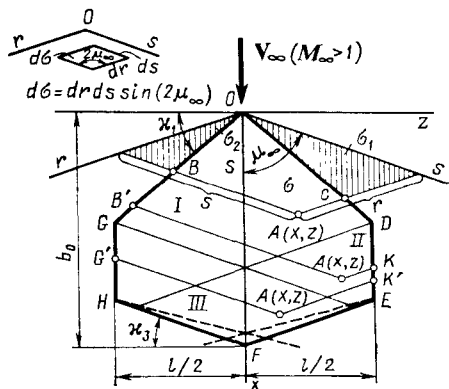


Fig. 8.9.1

Hexagonal wing with subsonic leading and supersonic trailing edges

directions of the Mach lines issuing from the vertex of the wing (Fig. 8.9.1):

$$r = (\mathbf{M}_\infty/2\alpha') (x - \alpha' z), \quad s = (\mathbf{M}_\infty/2\alpha') (x + \alpha' z) \quad (8.9.4)$$

The characteristic coordinates of point  $A(x_A, z_A)$  are as follows:

$$r_A = (\mathbf{M}_\infty/2\alpha') (x_A - \alpha' z_A), \quad s_A = (\mathbf{M}_\infty/2\alpha') (x_A + \alpha' z_A) \quad (8.9.4')$$

Let us convert Eq. (8.9.2) to the characteristic coordinates  $r$  and  $s$ . From (8.9.4), we find:

$$r + s = (\mathbf{M}_\infty/\alpha') x, \quad r - s = -\mathbf{M}_\infty z \quad (8.9.4'')$$

Consequently,

$$\left. \begin{aligned} x - \xi &= x_A - x = (\alpha'/\mathbf{M}_\infty) [(r_A + s_A) - (r + s)] \\ \alpha' (z - \zeta) &= \alpha' (z_A - z) = -(\alpha'/\mathbf{M}_\infty) [(r_A - s_A) - (r - s)] \end{aligned} \right\} \quad (8.9.5)$$

Introducing these expressions into (8.9.2) and taking into account that an area element in the coordinates  $r$  and  $s$  is  $d\sigma = dr ds \times \sin(2\mu_\infty)$  (Fig. 8.9.1), and that the integration limits are  $s_B$  and  $s_A$ ,  $r_C$  and  $r_A$ , we obtain an equation for the potential function:

$$\varphi'_I = -\frac{V_\infty \alpha \Omega}{\pi \mathbf{M}_\infty} \int_{r_C}^{r_A} \frac{dr}{\sqrt{r_A - r}} \int_{s_B}^{s_A} \frac{ds}{\sqrt{s_A - s}} \quad (8.9.6)$$

We shall express the coordinates  $s_B$  and  $r_C$  in terms of the coordinates  $r_A$  and  $s_A$  of point  $A$ . Since the equations of the leading edges in the coordinates  $z$  and  $x$  are  $z = \pm x \tan \alpha$ , then in accordance with (8.9.4'') these equations in the coordinates  $r$  and  $s$  are

transformed to the form:

$$r = sm \text{ for the starboard leading edge: } z = +x \cot \alpha \quad \left. \begin{array}{l} r = s/m \text{ for the port leading edge: } z = -x \cot \alpha \end{array} \right\} \quad (8.9.7)$$

where  $m = (n - 1)/(n + 1)$  and  $n = \tan \alpha_1 / \alpha'$ .

Therefore the coordinates  $r_C$  and  $s_B$  can be expressed as follows:

$$r_C = s_A m = s_A m \quad \text{and} \quad s_B = r_B m = r_A m \quad (8.9.8)$$

Substituting  $s_A m$  and  $r_A m$  for  $r_C$  and  $s_B$  in (8.9.6), respectively, after integration we obtain

$$\varphi'_I = -\frac{4\alpha V_\infty \Omega}{\pi M_\infty} \sqrt{(r_A - ms_A)(s_A - mr_A)} \quad (8.9.9)$$

Introducing into (8.9.9) the values of  $r_A$  and  $s_A$  from (8.9.4') and also the quantity

$$m = (n - 1)/(n + 1) \quad (8.9.10)$$

we find

$$\varphi'_I = -\frac{4\alpha V_\infty n x_A \Omega}{\pi(n+1)} \sqrt{\cot^2 \alpha - h^2} \quad (8.9.11)$$

where  $h = z_A/x_A$  (or  $h = \zeta/\xi$ ).

By comparing Eq. (8.9.11) with relation (8.8.38) for the potential function at the point being considered, we see that for matching of the results, in (8.9.11) we must assume that

$$\Omega = -\frac{\pi}{4} \cdot \frac{n+1}{n E(k)} \quad (8.9.12)$$

Hence, at point  $A$  located on the wing in region  $I$ , the velocity potential is

$$\varphi'_I = \frac{\alpha V_\infty x_A}{E(k)} \sqrt{\cot^2 \alpha - h^2} \quad (8.9.13)$$

Accordingly, the equation that must be used when determining the potential function on the wing has the following general form:

$$\varphi'_I = \frac{\alpha V_\infty (n+1)}{4n M_\infty E(k)} \iint_{\sigma} \frac{dr}{\sqrt{r_A - r}} \cdot \frac{ds}{\sqrt{s_A - s}} \quad (8.9.14)$$

Let us use Eq. (8.9.14) to determine the potential function at point  $A$  in region  $II$  that is confined by the Mach lines issuing from points  $D$  and  $G$ , the tips, (side edges) and partly the trailing edges. We shall write Eq. (8.9.14) in the following form:

$$\varphi'_{II} = \frac{\alpha V_\infty (n+1)}{4n M_\infty E(k)} \int_{r_K}^{r_A} \frac{dr}{\sqrt{r_A - r}} \int_{s_B'}^{s_A} \frac{ds}{\sqrt{s_A - s}} \quad (8.9.15)$$

By analogy with (8.9.8):

$$s_{B'} = r_{B'} m = r_A m \quad (8.9.16)$$

Point  $K$  is on a tip whose equation is  $z = l/2$ . In the coordinates  $r$  and  $s$ , the equation of a tip in accordance with (8.9.4'') is

$$r - s = -M_\infty l/2 \quad (8.9.17)$$

Therefore, for point  $K$ , the coordinate is

$$r_K = s_K - M_\infty l/2 = s_A - M_\infty l/2 \quad (8.9.18)$$

Taking also into account that  $s_{B'} = r_A m$ , after integration of (8.9.15) we obtain

$$\varphi'_{II} = \frac{\alpha V_\infty (n+1)}{n M_\infty E(k)} \sqrt{\left[ r_A - \left( s_A - \frac{M_\infty l}{2} \right) \right] (s_A - r_A m)} \quad (8.9.19)$$

Introducing instead of  $r_A$ ,  $s_A$  and  $m$  the relevant values from (8.9.4') and (8.9.10), we find

$$\varphi'_{II} = \frac{\alpha V_\infty}{n E(k)} \sqrt{\frac{n+1}{2} (l - 2z_A) \left( \frac{x_A}{\alpha'} + nz_A \right)} \quad (8.9.20)$$

The velocity potential for point  $A$  in region  $III$  is

$$\varphi'_{III} = \frac{\alpha V_\infty (n+1)}{4 n M_\infty E(k)} \int_{r_K'}^{r_A} \frac{dr}{\sqrt{r_A - r}} \int_{s_G'}^{s_A} \frac{ds}{\sqrt{s_A - s}} \quad (8.9.21)$$

Points  $K'$  and  $G'$  are on the tips whose equations are  $z = \pm l/2$  (the plus sign is for the starboard and the minus sign is for the port tip). In the coordinates  $r$  and  $s$ , the equations of these tips in accordance with (8.9.4) have the form:

$$\begin{aligned} r - s &= -M_\infty l/2 \text{ for the starboard tip} \\ r - s &= M_\infty l/2 \text{ for the port tip} \end{aligned} \quad \} \quad (8.9.22)$$

Consequently, for points  $K'$  and  $G'$ , we have, respectively:

$$\begin{aligned} r_{K'} &= s_{K'} - M_\infty l/2 = s_A - M_\infty l/2 \\ s_{G'} &= r_{G'} - M_\infty l/2 = r_A - M_\infty l/2 \end{aligned} \quad \} \quad (8.9.23)$$

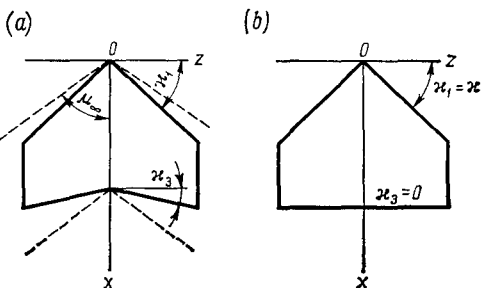
After the integration of (8.9.21), with a view to the values of the limits (8.9.23), we obtain

$$\varphi'_{III} = \frac{\alpha V_\infty (n+1)}{n M_\infty E(k)} \sqrt{\left( r_A - s_A + \frac{M_\infty l}{2} \right) \left( s_A - r_A - \frac{M_\infty l}{2} \right)} \quad (8.9.24)$$

We introduce into (8.9.24) the values of  $s_A$  and  $r_A$  from (8.9.4'):

$$\varphi'_{III} = \frac{\alpha V_\infty (n+1)}{2 n E(k)} \sqrt{l^2 - 4 z_A^2} \quad (8.9.25)$$

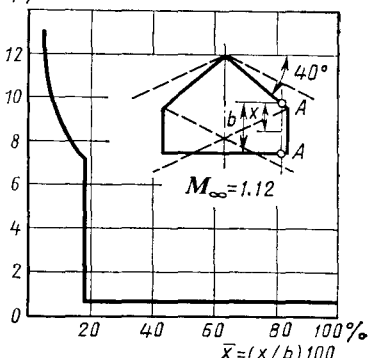
By calculating the partial derivatives with respect to  $x_A$ , we find the components of the disturbed velocity  $u = \partial \varphi'_n / \partial x_A$  ( $n = I, II$ ,

**Fig. 8.9.2**

Wings with subsonic leading edges and tips and with supersonic trailing edges:

a—hexagonal wing with a dovetail;  
b—plate with a straight trailing edge (a pentagonal wing)

$$\Delta \bar{p}/\alpha$$

**Fig. 8.9.3**

Distribution of the quantity  $\Delta \bar{p}/\alpha = (\bar{p}_b - \bar{p}_u)/\alpha$  near a tip of a pentagonal wing with subsonic leading edges (section AA')

III) and determine the pressure coefficients in the corresponding regions on the bottom and upper sides of the wing:

$$\left. \begin{aligned} \bar{p}_I &= -\frac{2}{V_\infty} \cdot \frac{\partial \varphi'_I}{\partial x_A} = \pm \frac{2\alpha \cot^2 \kappa}{E(k)} \cdot \frac{x_A}{\sqrt{x_A^2 \cot^2 \kappa - z_A^2}} \\ \bar{p}_{II} &= -\frac{2}{V_\infty} \cdot \frac{\partial \varphi'_{II}}{\partial x_A} = \pm \frac{\alpha}{nE(k)} \sqrt{\frac{(n+1)(l-2z_A)}{2\alpha'(x_A + z_A \tan \kappa)}} \\ \bar{p}_{III} &= -\frac{2}{V_\infty} \cdot \frac{\partial \varphi'_{III}}{\partial x_A} = 0 \end{aligned} \right\} \quad (8.9.26)$$

Here the plus sign on the right-hand side of the equations corresponds to the bottom side, and the minus sign, to the upper one.

The above relations for calculating the pressure coefficients can be used not only for triangular wings with a V-shaped appendage (Fig. 8.9.1), but also for similar wings with a dovetail and wings with a straight trailing edge (pentagonal plates shown in Fig. 8.9.2).

The change in the quantity  $\Delta \bar{p}/\alpha = (\bar{p}_b - \bar{p}_u)/\alpha$  near a tip as a function of the distance from the leading edge (in per cent of the

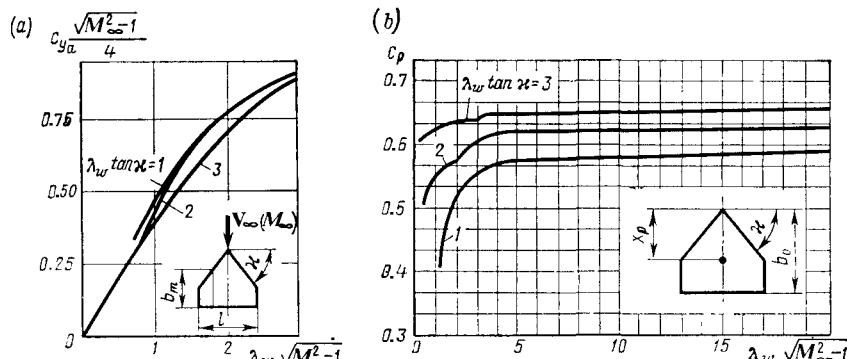


Fig. 8.9.4

Curves characterizing the change in the lift (a) and centre-of-pressure (b) coefficients for a pentagonal wing.

chord) calculated by the above formulas for a pentagonal wing with  $M_\infty = 1.12$  is shown in Fig. 8.9.3. On the surface of the tip Mach cone, a pressure discontinuity is observed due to the action of the corner point of the wing. The pressure is constant on the part between the tip and the tip Mach cone.

We use the known pressure to determine the lift and moment coefficients:

$$c_{y_a} = \frac{Y_a}{q_\infty S_w} = \frac{1}{S_w} \iint_{S_w} (\bar{p}_b - \bar{p}_u) dx dz \quad (8.9.27)$$

$$m_{z_a} = \frac{M_{z_a}}{q_\infty S_w b_0} = \frac{-1}{S_w b_0} \iint_{S_w} (\bar{p}_b - \bar{p}_u) x dx dz \quad (8.9.28)$$

where  $S_w$  and  $b_0$  are the area and the root chord of the wing, respectively, and  $\bar{p}_b$  and  $\bar{p}_u$  are the coefficients of the pressure on the bottom and upper sides determined by formulas (8.9.26).

According to the values of  $m_{z_a}$  and  $c_{y_a}$ , we can determine the centre-of-pressure coefficient  $c_p = x_p/b_0 = -m_{z_a}/c_{y_a}$ . Figure 8.9.4 shows theoretical curves characterizing the change in  $c_{y_a}$  and  $c_p$  for a wing in the form of a pentagonal plate. In this figure, the parts of the curves for which  $\lambda_w \sqrt{M_\infty^2 - 1} \ll \lambda_w \tan \alpha$  correspond to subsonic leading edges. A feature of the graphs characterizing the change in  $c_{y_a}$  is the absence of noticeable salient points on the corresponding curves in the transition to supersonic leading edges (i.e. when  $\lambda_w \sqrt{M_\infty^2 - 1} = \lambda_w \tan \alpha$ ).

### 8.10. Flow over a Hexagonal Wing with Supersonic Leading and Trailing Edges

To calculate the flow over arbitrary planform wings (including hexagonal ones with supersonic leading edges) in regions *I* and *II* (Fig. 8.10.1*a, b*) we can use the corresponding results for a triangular wing with the same leading edges (see Sec. 8.3).

According to these results, the pressure coefficient for point *A* ( $x_A, z_A$ ) in region *I* between the leading edge and the Mach lines issuing from the vertex of the wing and points *D* and *G* on its tips is determined by the formula

$$\bar{p}_I = \pm 2\alpha / (\alpha' \sqrt{1 - n^2}) \quad (8.10.1)$$

that has been obtained from (8.3.23) provided that  $\alpha$  has been substituted for  $\lambda$ . In the same condition, we find the corresponding relation for the pressure coefficient in region *II* confined by the Mach lines issuing from the vertex and the same points *D* and *G*. By (8.3.34), we have

$$\bar{p}_{II} = \pm \frac{4\alpha}{\alpha' \pi \sqrt{1 - n^2}} \left( \frac{\pi}{2} - \sin^{-1} \sqrt{\frac{n^2 - \sigma^2}{1 - \sigma^2}} \right) \quad (8.10.2)$$

The flow over the remaining part of the hexagonal wing (Fig. 8.10.1*c-h*) can be calculated with the aid of Eq. (8.3.1) for the velocity potential of the sources and sinks. We transform this equation to the following form in the new variables  $r$  and  $s$  [see (8.9.4)]

$$\varphi' = -\frac{\alpha V_\infty}{\pi M_\infty} \iint_{\sigma} \frac{dr ds}{\sqrt{(r_A - r)(s_A - s)}} \quad (8.10.3)$$

where  $r_A$  and  $s_A$  are the coordinates of point *A* on the surface of the hexagonal wing.

The coordinate lines  $r$  and  $s$  are directed along the Mach lines. The wing surface is divided into eight regions by these Mach lines, as well as by the lines of weak disturbances issuing from points *G* and *D*, and also from intersection points *G'* and *D'* of the coordinate lines  $r$  and  $s$  (the Mach lines) with the tips. For each of these eight regions, the velocity potential is calculated with the aid of Eq. (8.10.3).

Let us consider arbitrary point *A* in region *III* (Fig. 8.10.1*c*). When determining the velocity potential for this region, we must take into account the sources both on the surface of the wing (on areas  $S_1 = AD_1D_2A'$  and  $S_2 = A'D_2D$ ) and outside of it (area  $S_3 = A'DD''$ ).

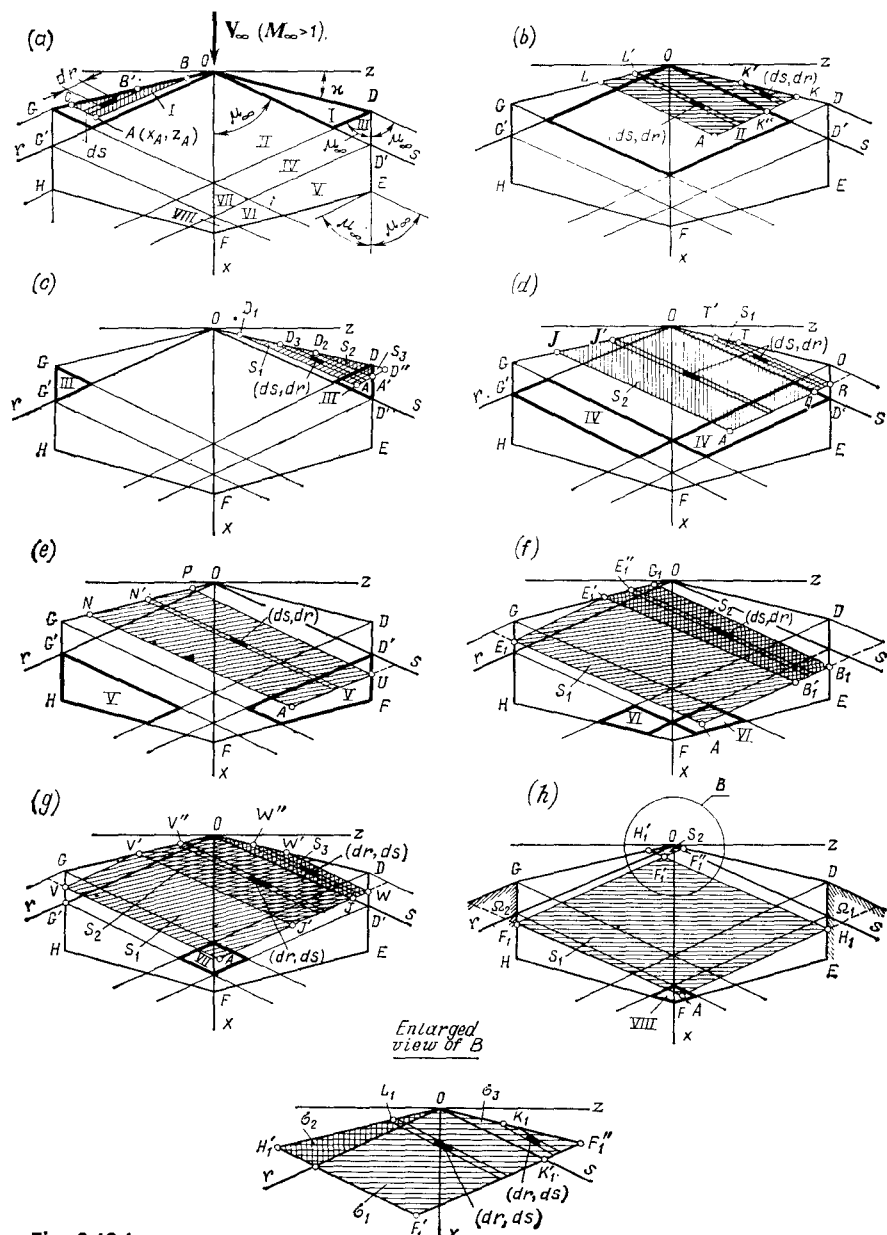


Fig. 8.10.1

Hexagonal wing with supersonic leading and trailing edges

Using (8.2.13), let us write the expression for  $\varphi'_{III}$  at point  $A(x, 0, z)$  in the form

$$\varphi'_{III} = -\frac{1}{2\pi} \iint_{S_1 + S_2 + S_3} \frac{Q(\xi, \zeta) d\xi d\zeta}{V(x - \xi)^2 - \alpha'^2(z - \zeta)^2} \quad (8.10.4)$$

On the wing area  $S_1 + S_2$ , the source strength is known and equals  $Q = 2v = 2\alpha V_\infty$ , therefore

$$\begin{aligned} \varphi'_{III} &= \frac{-\alpha V_\infty}{\pi} \iint_{S_1} \frac{d\xi d\zeta}{V(x - \xi)^2 - \alpha'^2(z - \zeta)^2} \\ &\quad - \frac{\alpha V_\infty}{\pi} \iint_{S_2} \frac{d\xi d\zeta}{V(x - \xi)^2 - \alpha'^2(z - \zeta)^2} \\ &\quad - \frac{1}{2\pi} \iint_{S_3} \frac{Q(\xi, \zeta) d\xi d\zeta}{V(x - \xi)^2 - \alpha'^2(z - \zeta)^2} \end{aligned} \quad (8.10.4')$$

where  $Q(\xi, \zeta)$  is a function determining the law of source distribution in region  $S_3$  outside the wing.

We can perform integration if we know the function  $Q(\xi, \zeta)$ . To determine it, let us use the boundary condition (8.1.20), in accordance with which the potential function on plane  $xOz$  in the region between the tip and the Mach line issuing from point  $D$  is zero. For point  $A'$  belonging to this region, the condition of the equality to zero of the potential function by analogy with (8.6.2) has the form

$$\begin{aligned} 0 &= \frac{-\alpha V_\infty}{\pi} \iint_{S_2} \frac{d\xi d\zeta}{V(x - \xi)^2 - \alpha'^2(z - \zeta)^2} \\ &\quad - \frac{1}{2\pi} \iint_{S_3} \frac{Q(\xi, \zeta) d\xi d\zeta}{V(x - \xi)^2 - \alpha'^2(z - \zeta)^2} \end{aligned}$$

A comparison of this equation with (8.10.4') reveals that to calculate the velocity potential at point  $A(x, 0, z)$ , it is sufficient to extend integration to region  $S_1$  in the main formula (8.10.4), i.e.

$$\varphi'_{III} = \frac{-\alpha V_\infty}{\pi} \iint_{S_1} \frac{d\xi d\zeta}{V(x - \xi)^2 - \alpha'^2(z - \zeta)^2} \quad (8.10.4'')$$

By this formula, the overall action on point  $A$  of the sources on sections  $S_2$  of the wing area and  $S_3$  of the area outside the wing equals zero (see [17]).

Using expression (8.10.4'') transformed to the form (8.10.3) in the coordinates  $r, s$ , we obtain

$$\varphi'_{III} = \frac{-\alpha V_\infty}{\pi M_\infty} \int_{r_{A'}}^{r_A} \frac{dr}{\sqrt{r_A - r}} \int_{s_{D3}}^{s_A} \frac{ds}{\sqrt{s_A - s}} \quad (8.10.5)$$

where in accordance with (8.9.8) for point  $D_3$  on the starboard tip, we have

$$s_{D_3} = r_{D_3}/m = r/m \quad (8.10.6)$$

We find the lower limit  $r_{A'}$  of the integral from the equation  $z = l/2$  for the tip. In the coordinates  $r$  and  $s$ , this equation has the form of (8.9.17). Consequently, the coordinate

$$r_{A'} = s_{A'} - M_\infty l/2 = s_A - M_\infty l/2 \quad (8.10.7)$$

With a view to (8.10.6), the integral

$$\int_{r/m}^{s_A} \frac{ds}{\sqrt{s_A - s}} = 2 \sqrt{s_A - \frac{r}{m}} = \frac{2}{\sqrt{\frac{m}{m}}} \sqrt{r - s_A m}$$

where  $m = (n - 1)/(n + 1)$ ;  $\bar{m} = (1 - m)/(n + 1)$ .

Hence

$$\varphi'_{III} = \frac{-2\alpha V_\infty}{\pi M_\infty \sqrt{\bar{m}}} \int_{r_{A'}}^{r_A} \sqrt{\frac{r - s_A m}{r_A - r}}$$

By calculating the integral, next inserting into it  $r_{A'}$  from (8.10.7), and taking into account expressions (8.9.4') for  $r_A$  and  $s_A$ , and also the values of  $m$  and  $\bar{m}$ , we find the potential

$$\begin{aligned} \varphi'_{III} = & \frac{-\alpha V_\infty}{\pi \sqrt{1-n^2}} \left\{ \sqrt{(l - 2z_A) [(x_A + \alpha' z_A) - \alpha' l (n+1)] \frac{n+1}{\alpha'}} \right. \\ & \left. + \frac{2(x_A - z_A \tan \alpha)}{\alpha'} \tan^{-1} \sqrt{\frac{\alpha' (n+1) (l - 2z_A)}{2(x_A + \alpha' z_A) - l(n+1) \alpha'}} \right\} \end{aligned} \quad (8.10.8)$$

We determine the derivative  $\partial \varphi'_{III} / \partial x_A$  and find the pressure coefficient:

$$\begin{aligned} \bar{p}_{III} = & -\frac{2}{V_\infty} \cdot \frac{\partial \varphi'_{III}}{\partial x_A} \\ = & \frac{\pm 4\alpha}{\pi \alpha' \sqrt{1-n^2}} \tan^{-1} \sqrt{\frac{\alpha' (n+1) (l - 2z_A)}{2(x_A + \alpha' z_A) - l(n+1) \alpha'}} \end{aligned} \quad (8.10.9)$$

The velocity potential for point  $A$  in region  $IV$  (Fig. 8.10.1d) is determined by the action of sources distributed over area  $AJOTR$ . We divide this area into two parts, namely,  $S_1 = OTRQ$  and  $S_2 = OQAJ$ , and find the potential at the point being considered as the sum of the potentials due to the action of the sources on areas  $S_1$  and  $S_2$ . By using formula (8.10.3), we obtain

$$\varphi'_{IV} = \frac{-\alpha V_\infty}{\pi M_\infty} \iint_{S_1 + S_2} \frac{dr ds}{\sqrt{(r_A - r)(s_A - s)}}$$

$$= \frac{-\alpha V_\infty}{\pi M_\infty} \int_{r_R}^0 \frac{dr}{\sqrt{r_A - r}} \\ \times \int_{s_{T'}}^{s_A} \frac{ds}{\sqrt{s_A - s}} - \frac{\alpha V_\infty}{\pi M_\infty} \int_0^{r_A} \frac{dr}{\sqrt{r_A - r}} \int_{s_{J'}}^{s_A} \frac{ds}{\sqrt{s_A - s}} \quad (8.10.10)$$

We determine the integration limits  $s_{T'}$  and  $s_{J'}$  with the aid of (8.9.8). For point  $T'$  on the starboard leading edge and point  $J'$  on the port one, we have

$$s_{T'} = r_{T'}/m = r/m, \quad s_{J'} = r_{J'}/m = rm \quad (8.10.11)$$

With a view to these values of the limits, we calculate the integrals:

$$\int_{s_{T'}}^{s_A} \frac{ds}{\sqrt{s_A - s}} = \frac{2}{\sqrt{\frac{m}{m}}} \sqrt{r - s_A m} \\ \int_{s_{J'}}^{s_A} \frac{ds}{\sqrt{s_A - s}} = 2 \sqrt{\frac{m}{m}} \sqrt{r - \frac{s_A}{m}}$$

Accordingly,

$$\varphi'_{IV} = \frac{-2\alpha V_\infty}{\pi M_\infty \sqrt{\frac{m}{m}}} \int_{r_R}^0 \sqrt{\frac{r - s_A m}{r_A - r}} dr \\ - \frac{2\alpha V_\infty \sqrt{\frac{m}{m}}}{\pi M_\infty} \int_0^{r_A} \sqrt{\frac{r - s_A / m}{r_A - r}} dr$$

where  $r_R$  is determined by formula (8.9.23):

$$r_R = s_R - M_\infty l/2 = s_A - M_\infty l/2$$

Integration and substitution of the values for  $s_A$  and  $r_A$  from (8.9.4'), and also  $m = -\bar{m} = (n-1)/(n+1)$  yield

$$\varphi'_{IV} = \frac{-2\alpha V_\infty}{\alpha' \pi \sqrt{1-n^2}} \left\{ (x_A - z_A \tan \alpha_i) \left[ -\tan^{-1} \sqrt{\frac{(n+1)(x_A - \alpha' z_A)}{(1-n)(x_A + \alpha' z_A)}} \right. \right. \\ \left. \left. + \tan^{-1} \sqrt{\frac{\alpha'(n+1)(l+2z_A)}{2(x_A + \alpha' z_A) - \alpha'l(n+1)}} \right] \right. \\ \left. + \frac{1}{2} \sqrt{(l-2z_A)[2(x_A + \alpha' z_A) - \alpha'l(n+1)](n+1)\alpha'} \right. \\ \left. + (x_A + z_A \tan \alpha_i) \tan^{-1} \sqrt{\frac{(1-n)(x - \alpha' z_A)}{(n+1)(x_A + \alpha' z_A)}} \right\} \quad (8.10.12)$$

Upon calculating the pressure coefficient  $\bar{p}_{IV} = -(2/V_\infty) \partial\phi'_{IV}/\partial x_A$  and using here the formula  $\tan^{-1} x - \tan^{-1} y = \tan^{-1} [(x-y)/(1+xy)]$ , we find

$$\bar{p}_{IV} = \frac{\pm 4\alpha}{\alpha'\pi \sqrt{1-n^2}} \left[ \tan^{-1} \sqrt{\frac{\alpha'(n+1)(l-2z_A)}{2(x_A - \alpha'z_A) - \alpha'l(n+1)}} \right. \\ \left. - \tan^{-1} \sqrt{\frac{n^2 - \sigma^2}{1-n^2}} \right] \quad (8.10.13)$$

Let us consider region  $V$ . For point  $A$  in this region (Fig. 8.10.1e), the potential is

$$\phi'_V = \frac{-\alpha V_\infty}{\pi M_\infty} \int_{r_U}^{r_A} \frac{dr}{\sqrt{r_A - r}} \int_{s_{N'}}^{s_A} \frac{ds}{\sqrt{s_A - s}} \quad (8.10.14)$$

By this formula, the velocity at point  $A$  is induced by the sources on section  $ANPU$  of the wing area. The inner integral in (8.10.14) whose lower limit  $s_{N'} = rm$ , is

$$\int_{s_{N'}}^{s_A} \frac{ds}{\sqrt{s_A - s}} = 2\sqrt{\bar{m}} \sqrt{r - \frac{s_A}{m}}$$

Consequently,

$$\phi'_V = \frac{-2\alpha V_\infty \sqrt{\bar{m}}}{\pi M_\infty} \int_{r_U}^{r_A} \sqrt{\frac{r - s_A/m}{r_A - r}} dr$$

Since  $r_U = s_A - M_\infty l/2$ , then, going over to conventional coordinates  $x$  and  $y$  and taking into account that  $m = (n-1)/(n+1)$  and  $\bar{m} = -m$ , after integration we find

$$\phi'_V = \frac{2\alpha V \sqrt{1-n}}{M_\infty \pi \sqrt{n+1}} \left\{ M_\infty \sqrt{\left(z_A - \frac{l}{2}\right)} \left[ (x_A + \alpha'z_A) \frac{1}{\alpha'(n-1)} + \frac{l}{2} \right] \right. \\ \left. - \frac{M_\infty (x_A + z_A \tan \alpha_1)}{\alpha'(n-1)} \tan^{-1} \sqrt{\frac{z_A - l/2}{(x_A + \alpha'z_A)/\alpha' (n-1) + l/2}} \right\} \quad (8.10.15)$$

After finding the derivative with respect to  $x_A$ , we determine the pressure coefficient:

$$\bar{p}_V = -\frac{2}{V_\infty} \cdot \frac{\partial \phi'_V}{\partial x_A} = \frac{\pm 4\alpha}{\pi \alpha' \sqrt{1-n^2}} \\ \times \tan^{-1} \sqrt{\frac{\alpha'(z_A - l/2)(n-1)}{x_A + \alpha'z_A + (l/2)(n-1)\alpha'}} \quad (8.10.16)$$

In region VI, the velocity potential is determined as follows (Fig. 8.10.1f):

$$\begin{aligned}\varphi'_{VI} &= \frac{-\alpha V_\infty}{\pi M_\infty} \iint_{S_1+S_2} \frac{dr ds}{\sqrt{(r_A - r)(s_A - s)}} \\ &= \frac{-\alpha V_\infty}{\pi M_\infty} \int_{r_{B'_1}}^{r_A} \frac{dr}{\sqrt{r_A - r}} \\ &\times \int_{s_{E'_1}}^{s_A} \frac{ds}{\sqrt{s_A - s}} - \frac{\alpha V_\infty}{\pi M_\infty} \int_{r_{B'_1}}^{r_A} \frac{dr}{\sqrt{r_A - r}} \int_{s_{E''_1}}^{s_A} \frac{ds}{\sqrt{s_A - s}} \quad (8.10.17)\end{aligned}$$

In accordance with (8.9.4) and (8.9.7), the limits of the integrals in expression (8.10.17) have the form

$$\left. \begin{aligned}s_{E''_1} &= mr, \quad s_{E_1} = r_{E_1} - \frac{M_\infty l}{2} = r_A - \frac{M_\infty l}{2} \\ r_{B'_1} &= r_{E'_1} = s_{E'_1}/m = s_{E_1}/m = (1/m)(r_A - M_\infty l/2) \\ r_{B_1} &= s_A - M_\infty l/2\end{aligned}\right\} \quad (8.10.18)$$

As a result of integration, we establish the corresponding relation for  $\varphi'_{VI}$  in the variables  $r_A$ ,  $s_A$ . Using their dependence on  $x_A$  and  $z_A$ , we find the velocity potential as a function of these coordinates. By calculating the derivative  $\partial\varphi'_{VI}/\partial x_A$  and inserting it into the formula  $\bar{p}_{VI} = -2(\partial\varphi'_{VI}/\partial x_A)/V_\infty$ , we obtain the following expression for the pressure coefficient in the region being considered:

$$\begin{aligned}\bar{p}_{VI} &= \frac{\pm 4\alpha}{\pi\alpha' \sqrt{1-n^2}} \left[ \tan^{-1} \sqrt{\frac{\alpha'(n-1)(z_A - l/2)}{x_A + \alpha' z_A + \left(\frac{l}{2}\right)(n-1)\alpha'}} \right. \\ &\quad \left. - \tan^{-1} \sqrt{\frac{(x_A - \alpha' z_A) - (l/2)\alpha'(n+1)}{\alpha'(l/2 + z_A)(n+1)}} \right] \quad (8.10.19)\end{aligned}$$

For point A in region VII (Fig. 8.10.1g), we have

$$\begin{aligned}\varphi'_{VII} &= \frac{-\alpha V_\infty}{\pi M_\infty} \iint_{S_1+S_2+S_3} \frac{dr ds}{\sqrt{(r_A - r)(s_A - s)}} \\ &= \frac{-\alpha V_\infty}{\pi M_\infty} \int_{r_{J'}}^{r_A} \frac{dr}{\sqrt{r_A - r}} \int_{s_V}^{s_A} \frac{ds}{\sqrt{s_A - s}}\end{aligned}$$

$$-\frac{\alpha V_\infty}{\pi M_\infty} \int_0^{r_{J'}} \frac{dr}{\sqrt{r_A - r}} \int_{s_{V''}}^{s_A} \frac{ds}{\sqrt{s_A - s}} \\ - \frac{\alpha V_\infty}{\pi M_\infty} \int_{r_W}^0 \frac{dr}{\sqrt{r_A - r}} \int_{s_{W''}}^{s_A} \frac{ds}{\sqrt{s_A - s}} \quad (8.10.20)$$

$$\left. \begin{aligned} s_V &= r_A - M_\infty l/2, & r_{J'} &= (1/m) \left( r_A - \frac{M_\infty l}{2} \right) \\ s_{V''} &= mr, & s_{W''} &= r/m, & r_W &= s_A - M_\infty l/2 \end{aligned} \right\} \quad (8.10.21)$$

The following pressure coefficient corresponds to the potential (8.10.20) calculated according to the values of the integration limits (8.10.21):

$$\bar{p}_{VII} = \frac{\pm 4\alpha}{\pi \alpha'} \sqrt{\frac{1+n}{1-n}} \left[ \tan^{-1} \sqrt{\frac{x_A - \alpha' z_A}{x_A + \alpha' z_A}} \right. \\ \left. - \tan^{-1} \sqrt{\frac{\alpha' (l/2 - z_A) (n+1)}{x_A + \alpha' z_A - (l/2) \alpha' (n+1)}} \right. \\ \left. + \tan^{-1} \sqrt{\frac{(x_A + \alpha' z_A) - (l/2) \alpha' (n+1)}{\alpha' (l/2 + z_A) (n+1)}} \right. \\ \left. - \tan^{-1} \sqrt{\frac{1-n}{n+1}} \sqrt{\frac{x_A - \alpha' z_A}{x_A + \alpha' z_A}} \right] \quad (8.10.22)$$

Let us now consider region *VIII* (Fig. 8.10.1*h*) for whose points the region of integration simultaneously intersects regions  $\Omega_1$  and  $\Omega_2$ ; disturbances manifest themselves in these regions that are produced by the flow over both tips *DE* and *GH*. To evaluate the velocity potential for point *A* that belongs to region *VIII*, it is sufficient to extend integration in formula (8.10.3) to the region  $S = S_1 + S_2$  hatched in Fig. 8.10.1*h*. Here the integral calculated over region  $S_2$  in formula (8.10.3) must be taken with the opposite sign, i.e. with the plus sign. Accordingly, we have

$$\varphi'_{VIII} = -\frac{\alpha V_\infty}{\pi M_\infty} \iint_{S_1} \frac{dr ds}{\sqrt{(r_A - r)(s_A - s)}} \\ + \frac{\alpha V_\infty}{\pi M_\infty} \iint_{S_2} \frac{dr ds}{\sqrt{(r_A - r)(s_A - s)}} \quad (8.10.23)$$

Here

$$\iint_{S_1} \frac{dr ds}{\sqrt{(r_A - r)(s_A - s)}} = \int_{r_{H_1}}^{r_A} \frac{dr}{\sqrt{r_A - r}} \int_{s_{F_1}}^{s_A} \frac{ds}{\sqrt{s_A - s}} \quad (8.10.24)$$

$$\begin{aligned} & \int \int_{S_2} \frac{dr ds}{V(r_A - r)(s_A - s)} = \int \int_{\sigma_1} \frac{dr ds}{V(r_A - r)(s_A - s)} \\ & + \int \int_{\sigma_2} \frac{dr ds}{V(r_A - r)(s_A - s)} + \int \int_{\sigma_3} \frac{dr ds}{V(r_A - r)(s_A - s)} \\ & = \int_0^{r_{F'_1}} \frac{dr}{V r_A - r} \int_{s_{L_1}}^{s_{F'_1}} \frac{ds}{V s_A - s} + \int_0^{r_{F''_1}} \frac{dr}{V r_A - r} \int_{s_{K_1}}^{s_{F'_1}} \frac{ds}{V s_A - s} \quad (8.10.25) \end{aligned}$$

The integration limits have the following values:

$$\left. \begin{aligned} r_{F'_1} &= r_{H_1} = s_A - M_\infty l/2, \quad s_{L_1} = mr, \quad s_{F'_1} = s_{F_1} = r_A - M_\infty l/2 \\ r_{F''_1} &= ms_{F''_1} = ms_{F_1} = m(r_A - M_\infty l/2), \quad s_{K_1} = r/m \end{aligned} \right\} \quad (8.10.26)$$

provided that

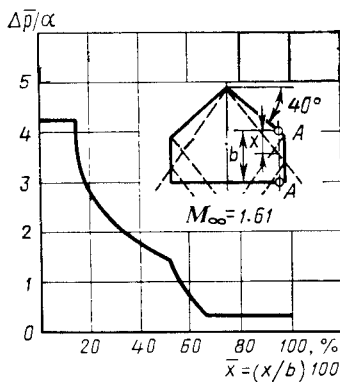
$$s_{F_1} = r_A - M_\infty l/2, \quad r_{H_1} = s_A - M_\infty l/2 \quad (8.10.26')$$

With a view to these values of the limits, we calculate integrals (8.10.24) and (8.10.25), and then find the velocity potential (8.10.23). The following pressure coefficient corresponds to this potential:

$$\begin{aligned} \bar{p}_{VIII} &= \frac{\pm 4\alpha}{\alpha' \pi \sqrt{1-n^2}} \left[ \tan^{-1} \sqrt{\frac{1+n}{1-n}} \sqrt{\frac{(x_A - \alpha' z_A) + (l/2) \alpha' (n-1)}{\alpha' (l/2 + z_A) (n+1)}} \right. \\ & - \tan^{-1} \sqrt{\frac{1+n}{1-n}} \sqrt{\frac{x_A - \alpha' z_A}{x_A + \alpha' z_A}} + \tan^{-1} \sqrt{\frac{1-n}{1+n}} \sqrt{\frac{x_A - \alpha' z_A}{x_A + \alpha' z_A}} \\ & \left. - \tan^{-1} \sqrt{\frac{1-n}{1+n}} \sqrt{\frac{\alpha' (l/2 - z_A) (n+1)}{x_A + \alpha' z_A + (l/2) \alpha' (n-1)}} \right] \quad (8.10.27) \end{aligned}$$

The above method of calculating the pressure distribution can be related not only to hexagonal wings with a V-shaped appendage (see Fig. 8.9.1), but also to other planforms, namely, to a wing with a dovetail and a pentagonal plate (see Fig. 8.9.2) provided that the tips are subsonic, while the leading and trailing edges are supersonic. The corresponding change in the quantity  $\Delta \bar{p}/\alpha = (\bar{p}_h - \bar{p}_u)/\alpha$  near a tip with the distance from the leading edge (in per cent of the chord) evaluated for a wing with a pentagonal planform at  $M_\infty = 1.61$  is shown in Fig. 8.10.2. The coefficient  $\Delta \bar{p}/\alpha$  is constant in the region between the leading edge and the Mach cones issuing from the vertex and tips of the wing, on the section confined by the tips and trailing edges, and also by the Mach wave reflected from a tip. A break in the curve characterizing a change in the pressure drop coefficient occurs on the Mach lines and is a result of the break in the configuration of the wing tip.

The found pressure distribution and formulas (8.9.27) and (8.9.28) are used to determine the lift, moment and centre-of-pressure coefficients. Figure 8.9.4 shows curves characterizing the change in the values of  $c_{y_a}$  and  $c_p$  for a pentagonal wing. These values should be

**Fig. 8.10.2**

Distribution of the quantity  $\Delta \bar{p}/\alpha = (\bar{p}_b - \bar{p}_u)/\alpha$  near a tip of a pentagonal wing with supersonic leading edges (section AA')

determined provided that  $\lambda_w \sqrt{M_\infty^2 - 1} > \lambda_w \tan \alpha_1$ , i.e. if the leading edge is supersonic. If a wing has subsonic leading edges (see Fig. 8.9.1), the flow over the section of the surface between the edges and the Mach lines issuing from points E and H is affected by a vortex sheet. The calculation of this flow is associated with solution of integral equation (8.2.16) and the use of boundary conditions (8.1.15) and (8.1.16). Such a solution is treated in detail in [17].

### 8.11. Drag of Wings with Subsonic Leading Edges

Let us consider the calculation of the drag of swept wings with *subsonic leading edges* in a supersonic flow at an angle of attack. We already know that the disturbed flow normal to the leading edge is subsonic near such wings. Such a flow is attended by the *overflow* of the gas from the region of increased pressure into the region where the pressure is reduced and is the cause of the corresponding force action on the wing. To calculate this action, we can use the results of investigating the disturbed flow of an incompressible fluid near an airfoil in the form of a flat plate arranged in the flow at an angle of attack (see Sec. 6.3).

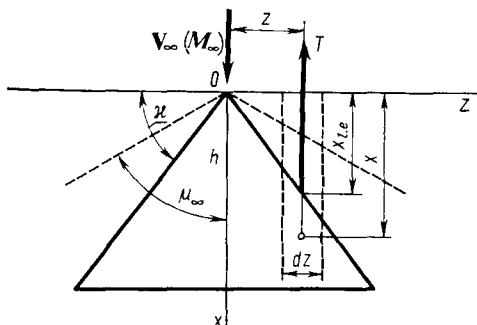
The drag coefficient for a thin wing with subsonic leading edges in a supersonic flow is

$$c_{x_a} = \alpha c_{y_a} - c_{x,T} \quad (8.11.1)$$

in which  $c_{x,T}$  is the coefficient of the wing suction force depending on the sweep angle  $\alpha$  of the leading edge and the number  $M_\infty$ :

$$c_{x,T} = T/(q_\infty S_w) \quad (8.11.2)$$

where  $T$  is the suction force,  $q_\infty = \rho_\infty V_\infty^2/2$  is the velocity head, and  $S_w$  is the area of the wing planform.

**Fig. 8.11.1**

To the calculation of the suction force for a triangular wing with subsonic leading edges

To determine the force  $T$ , we can use the relations obtained in Sec. 7.6 for an *infinite-span* swept wing. This follows from the fact that in accordance with (7.6.18) and (7.6.19), the suction force depends on the change in the axial component of the velocity in the close vicinity of the leading edge of the airfoil being considered, and also on the local sweep angle, and does not depend on the behaviour of this velocity far from the leading edge.

Using (7.6.18), we obtain

$$T = 2\pi\rho_\infty V \sqrt{1 + \tan^2 \kappa - M_\infty^2} \int_0^{l/2} c^2 dz \quad (8.11.3)$$

where  $c$  is a coefficient determined from (7.6.19).

Let us determine the drag for a triangular wing. For this purpose, we shall use expression (8.8.39) for the disturbed velocity. Assuming that  $\cot \kappa = z/x_{1,e}$ , we find

$$u = \frac{aV_\infty (z/x_{1,e})^2}{[E(k) \sqrt{1 - (x_{1,e}/z)^2}]}$$

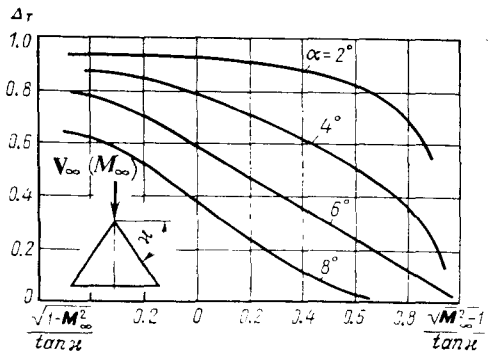
where  $x_{1,e}$  is the distance to the leading edge,  $z$  and  $x$  are the coordinates of a point on the wing (Fig. 8.11.1).

Introducing the value of  $u^2$  into (7.6.19) and taking into account that  $\lim_{x \rightarrow x_{1,e}} (x/x_{1,e}) = 1$ , we have

$$c^2 = \left[ \frac{\alpha V_\infty}{E(k)} \right]^2 \lim_{x \rightarrow x_{1,e}} \frac{z^2 (x/x_{1,e})^2 (x - x_{1,e})}{(x - x_{1,e})(x + x_{1,e})} = \frac{1}{2} \left[ \frac{\alpha V_\infty}{E(k)} \right]^2 z \cot \kappa$$

Introducing this expression into (7.6.18) and integrating, we find

$$\begin{aligned} T &= \frac{\pi \rho_\infty \cot \kappa}{2} \left[ \frac{\alpha V_\infty}{E(k)} \right]^2 2 \sqrt{1 + \tan^2 \kappa - M_\infty^2} \int_0^{l/2} z dz \\ &= \frac{\pi \rho_\infty \cot \kappa}{2} \left[ \frac{\alpha V_\infty}{E(k)} \right]^2 \frac{l^2}{4} \sqrt{1 + \tan^2 \kappa - M_\infty^2} \end{aligned}$$

**Fig. 8.11.2**

Change in the factor  $\Delta_T$  in formula (8.11.5) for calculating the suction force

The suction force coefficient by (8.11.2) is

$$c_{x,T} = \left[ \frac{\alpha \cot \alpha}{E(k)} \right]^2 \pi \sqrt{1 + \tan^2 \alpha - M_\infty^2} \quad (8.11.4)$$

Taking into account expression (8.8.44) for  $c_{y_a}$ , we have

$$c_{x,T} = (c_{y_a}^2 / 4\pi) \sqrt{1 + \tan^2 \alpha - M_\infty^2} \quad (8.11.4')$$

According to this formula, the suction force coefficient is proportional to  $c_{y_a}^2$ , i.e.  $c_{x,T} = c_T c_{y_a}^2$ . The proportionality coefficient, equal to  $c_T = (1/4\pi) \sqrt{1 + \tan^2 \alpha - M_\infty^2}$  for a triangular wing, changes when going over to another planform and depends not only on  $\alpha$  and  $M_\infty$ , but also on the taper ratio  $\eta_w$  and the aspect ratio  $\lambda_w$ . Investigations show, however, that the influence of these additional parameters is not great, and the suction force for an arbitrary planform wing can be calculated with the aid of (8.11.4').

With a supersonic leading edge ( $M_\infty \cos \alpha > 1$ ), and also when the leading edge becomes sonic ( $\tan \alpha = \cot \mu_\infty = \sqrt{M_\infty^2 - 1}$ ), the suction force coefficient equals zero. With a subsonic leading edge ( $M_\infty \cos \alpha < 1$ ), the quantity  $c_{x,T} = 0$ , but experimental investigations show that its actual value is lower than the calculated one. This is especially noticeable at large angles of attack or sweep when local separation of the flow (bubble) occurs in the vicinity of the leading edge and no further growth of the suction is observed. The decrease in the suction force can be taken into account by the correction factor  $\Delta_T$  in accordance with which

$$c_{x,T} = \bar{c}_T \Delta_T c_{y_a}^2 \quad (8.11.5)$$

Experimental data on the change in the quantity  $\Delta_T$  are contained in Fig. 8.11.2. According to these data, the suction force at subsonic velocities lowers less than in supersonic flow upon an increase in the

angle of attack because at such velocities the separation of the flow from the leading edge is less noticeable and the suction is greater. According to experimental investigations, at subsonic velocities the correction factor in (8.11.5) is determined by the formula (see [18])

$$\Delta_T = (c_{y_a}^\alpha)^{-1} - 1 / (\pi \lambda_w) \quad (8.11.6)$$

No suction force appears on wings with a sharp leading edge, i.e. the coefficient  $c_{x,T} = 0$ . Let us consider the total drag of a wing, which in accordance with (8.11.1), (8.11.5), and (8.8.44) can be written as

$$c_{x_a} = \alpha c_{y_a} - c_{x,T} = \frac{c_{y_a}^2}{4\pi \cot \alpha} [2E(k) - \Delta_T \sqrt{1 - \cot^2 \alpha (M_\infty^2 - 1)}]$$

Having in view that the aspect ratio of the wing is

$$\lambda_w = l^2/S_w = 4 \cot \alpha \quad (8.11.7)$$

we obtain

$$c_{x_a} = \frac{c_{y_a}^2}{\pi \lambda_w} [2E(k) - \Delta_T \sqrt{1 - \cot^2 \alpha (M_\infty^2 - 1)}] \quad (8.11.8)$$

Let us consider sonic flow. If  $M_\infty \rightarrow 1$ , then  $E(k) \rightarrow 1$ , and, consequently, the drag coefficient is

$$c_{x_a} = c_{y_a}^2 / (\pi \lambda_w) \quad (8.11.9)$$

Expression (8.11.9) coincides with formula (6.4.16) for the coefficient of the induced vortex drag of a finite-span wing (provided that  $\delta = 0$ ). Hence, *the physical nature of the drag force arising in a flow over a triangular wing with subsonic leading edges is due to induction by the vortices formed behind the wing*. Accordingly, the quantity determined by (8.11.8) is called the **induced drag coefficient**.

If the leading edge is sonic ( $\tan \alpha = \sqrt{M_\infty^2 - 1}$ ), the second term in the brackets in (8.11.8) is zero, while  $E(k) = E(0) = \pi/2$ ; consequently, the induced drag coefficient is

$$c_{x_a} = c_{x,1} = c_{y_a}^2 / \lambda_w \quad (8.11.10)$$

For a very thin wing ( $\alpha \rightarrow \pi/2$ ), we may assume that  $\cot \alpha \approx 0$  and  $E(k) \approx E(1) = 1$ . In this case, expression (8.11.8) coincides with (8.11.9).

In addition to triangular wings, formula (8.11.8) may be applied to wings having the form of tetra-, penta-, and hexagonal plates with subsonic leading edges, and supersonic trailing and side edges (tips) (see Fig. 8.8.4). Particularly, for tetragonal wings, the coefficient  $c_{y_a}$  in (8.11.8) is found from (8.8.51).

### 8.12. Aerodynamic Characteristics of a Rectangular Wing

Supersonic flow over a thin finite-span rectangular wing at a small angle of attack is characterized by the influence of the *leading supersonic edge and the subsonic tips* (side edges) on the disturbed flow near the surface. The simultaneous influence of the leading edge and one tip is present within the limits of Mach cones issuing from wing corners  $O$  and  $O'$  (Fig. 8.12.1a) if the generatrices of these cones intersect outside the wing. If these generatrices intersect on the surface of the wing (Fig. 8.12.1b), in addition to regions  $II$  and  $II'$  where the influence of one tip is observed, zone  $III$  appears in which both tips act simultaneously on the disturbed flow.

In region  $I$  on the wing between the leading edge and the Mach cones, the disturbed flow is due to the influence of only the leading edge. Here the pressure coefficient is determined by the formula for a flat plate:

$$\bar{p}_I = \pm 2\alpha/V M_\infty^2 - 1 \quad (8.12.1)$$

We shall use the method of sources to calculate the disturbed flow in region  $II$  (Fig. 8.12.1a). The velocity at point  $A$  in this region is induced by sources distributed over wing section  $ACOE$ . The total action of sources  $BCO$  and  $OBD$  on point  $A$  is zero, and, consequently, integration in (8.10.3) must be performed over region  $ABDE$ . Accordingly, the velocity potential at point  $A$  is

$$\begin{aligned} \varphi'_{II} &= \frac{-\alpha V_\infty}{\pi M_\infty} \iint_{ABDE} \frac{dr ds}{\sqrt{(r_A - r)(s_A - s)}} \\ &= \frac{-\alpha V_\infty}{\pi M_\infty} \int_{s_B}^{s_A} \frac{ds}{\sqrt{s_A - s}} \int_{r_F}^{r_A} \frac{dr}{\sqrt{r_A - r}} \end{aligned} \quad (8.12.2)$$

Point  $F$  is on the leading edge whose equation is  $x = 0$ . Hence, by (8.9.4), for this edge we have

$$r = -(M_\infty/2) z, \quad s = (M_\infty/2) z \quad (8.12.3)$$

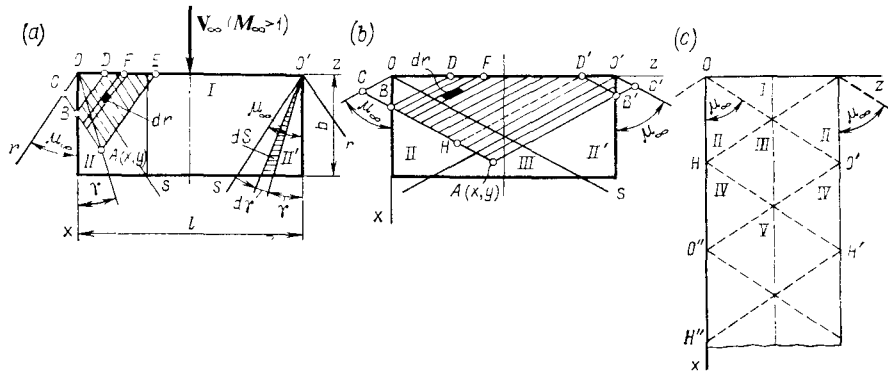
Consequently, the equation of the leading edge in the coordinates  $r$  and  $s$  has the form

$$r = -s \quad (8.12.4)$$

Therefore, for point  $F$ , the coordinate  $r_F = r = -s$ .

Point  $B$  is on the tip whose equation is  $z = 0$ . Hence, by (8.9.4), for this tip we have

$$r = (M_\infty/2\alpha')x, \quad s = (M_\infty/2\alpha')x \quad (8.12.5)$$

**Fig. 8.12.1**

Rectangular wing in a linearized supersonic flow

We can thus write the equation of the tip in the form

$$r = s \quad (8.12.6)$$

For point  $B$ , the coordinate  $s_B = r_B = r_A$ .

Performing integration in (8.12.2) with a view to the limits  $r_F = -s$  and  $s_B = r_A$ , after introducing the values of  $r_A$  and  $s_A$  from (8.9.4'), we obtain

$$\varphi'_{II} = \frac{-2\alpha V_\infty}{\pi} \left[ \sqrt{\frac{z_A}{\alpha'} (x_A - \alpha' z_A)} + \frac{x_A}{\alpha'} \tan^{-1} \sqrt{\frac{\alpha' z_A}{x_A - \alpha' z_A}} \right] \quad (8.12.7)$$

Let us calculate the corresponding pressure coefficient:

$$\bar{p}_{II} = -(2/V_\infty) \partial \varphi'_{II} / \partial x_A = \pm \frac{4\alpha}{\pi \alpha'} \tan^{-1} \sqrt{\frac{\alpha' z_A}{x_A - \alpha' z_A}} \quad (8.12.8)$$

On the boundary of the two regions  $I$  and  $II$  separated by a Mach line, the pressure coefficient determined by (8.12.8) equals the value (8.12.1). Indeed, since the equation of this boundary is  $z_A = x_A \tan \mu_\infty = x_A/\alpha'$ , from (8.12.8) we find

$$\bar{p}_{II} = \pm (4\alpha/\pi\alpha') \pi/2 = \bar{p}_I$$

It follows from (8.12.8) that at the tips of the wing, the pressure at the points along the lines whose equation is  $z/x = \text{const}$  is constant. These lines can be considered as the generatrices of conical surfaces and, consequently, the flow in the indicated region of the wing can be considered *conical*.

Let us calculate the aerodynamic coefficients of a wing. The lift force acting on an element of area of the end part of the wing is

$$dY = (\bar{p}_b - \bar{p}_u) (\rho_\infty V_\infty^2/2) dS \quad (8.12.9)$$

A glance at Fig. 8.12.1a reveals that the elementary area is

$$dS = \frac{1}{2} \cdot \frac{b^2}{c_s s^2} d\gamma \quad (8.12.10)$$

where  $\gamma$  is the angle measured from the wing tip.

Introducing into (8.12.9) the values of  $\bar{p}_b$  and  $-\bar{p}_u$  from (8.12.8), the value of  $dS$  from (8.12.10), and substituting  $\tan \gamma$  for  $z_A/x_A$ , we have

$$dY = \frac{4\alpha b^2}{\pi \alpha'} \cdot \frac{\rho_\infty V_\infty^2}{2} \tan^{-1} \sqrt{\frac{\alpha' \tan \gamma}{1 - \alpha' \tan \gamma}} \cdot \frac{d\gamma}{\cos^2 \gamma}$$

Dividing this expression by the product of the wing area confined within the Mach cone ( $S_{II} = b^2/2\alpha'$ ) and the velocity head ( $q_\infty = \rho_\infty V_\infty^2/2$ ) and performing integration, we obtain the lift coefficient for the wing tips:

$$c_y'' = \frac{Y_a}{S_{II} q_\infty} = \frac{8\alpha}{\pi} \int_0^{\mu_\infty} \tan^{-1} \sqrt{\frac{\alpha' \tan \gamma}{1 - \alpha' \tan \gamma}} \cdot \frac{d\gamma}{\cos^2 \gamma}.$$

Integration by parts yields

$$c_y'' = 2\alpha/\alpha' = 2\alpha \sqrt{M_\infty^2 - 1} \quad (8.12.11)$$

Let us determine the lift coefficient  $c_{yII}$  for the end parts of the wing related to its total area  $S_w = lb$ :

$$c_{yII} = c_y'' \frac{S_{II} + S_{II'}}{S_w} = c_y'' \frac{b^2}{lb\alpha'} = c_y'' \frac{1}{\lambda_w \alpha'} \quad (8.12.11')$$

where  $\lambda_w = l/b$ .

The lift coefficient for wing section I related to the area  $S_I$  of this section is

$$c_y' = 4\alpha/\alpha' = 4\alpha \sqrt{M_\infty^2 - 1} \quad (8.12.12)$$

The lift coefficient for this section related to the total wing surface is

$$c_{yI} = c_y' \frac{S_I}{S_w} = c_y' \frac{S_w - (S_{II} + S_{II'})}{S_w} = c_y' \left( 1 - \frac{1}{\lambda_w \alpha'} \right) \quad (8.12.13)$$

The total lift coefficient is

$$c_{y_a} = c_{yII} + c_{yI} = \frac{4\alpha}{\sqrt{M_\infty^2 - 1}} \left( 1 - \frac{1}{2\lambda_w \sqrt{M_\infty^2 - 1}} \right) \quad (8.12.14)$$

The wave drag coefficient is

$$c_{x, \text{wave}} = \alpha c_{y_a} = \frac{4\alpha^2}{V M_\infty^2 - 1} \left( 1 - \frac{1}{2\lambda_w \sqrt{M_\infty^2 - 1}} \right) \quad (8.12.15)$$

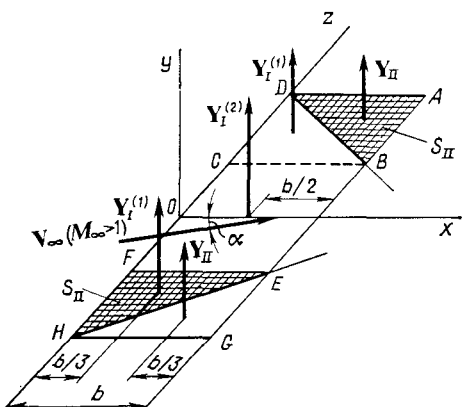


Fig. 8.12.2

To the determination of the aerodynamic moment for a rectangular wing

We can calculate the coefficient of the moment about the  $z$ -axis according to the known data on the pressure distribution and the lift coefficients for individual parts of the wing:

$$m_{z_a} = M_{z_a} / (q_\infty S_w b) \quad (8.12.16)$$

The moment  $M_{z_a}$  of the pressure forces distributed over the surface of the wing can be found as the sum of the moments of the lift forces about the  $z$ -axis acting on various parts of the wing (Fig. 8.12.2). Taking into account that on the triangular parts of the wing the point of application of the lift force coincides with the centre of mass of the area of the relevant part, we have the following expression for the moment:

$$-M_{z_a} = \frac{b}{3} 2Y_I^{(1)} + \frac{b}{2} Y_I^{(2)} + \frac{2b}{3} 2Y_{II} \quad (8.12.17)$$

where  $Y_I^{(1)}$ ,  $Y_I^{(2)}$ , and  $Y_{II}$  are the values of the lift force calculated for parts  $CDB$  ( $HEF$ ),  $EFCB$ , and  $ADB$  ( $GHE$ ), respectively. By (8.12.11) and (8.12.12), we have

$$\left. \begin{aligned} Y_I^{(1)} &= c'_y \frac{\rho_\infty V_\infty^2}{2} S_{II} = \frac{4\alpha}{\alpha'} \cdot \frac{\rho_\infty V_\infty^2}{2} S_{II} \\ Y_I^{(2)} &= c'_y \frac{\rho_\infty V_\infty^2}{2} S_{EFCB} = \frac{4\alpha}{\alpha'} \cdot \frac{\rho_\infty V_\infty^2}{2} (S_w - 4S_{II}) \\ Y_{II} &= c''_y \frac{\rho_\infty V_\infty^2}{2} S_{II} = \frac{2\alpha}{2} \cdot \frac{\rho_\infty V_\infty^2}{2} S_{II} \end{aligned} \right\} \quad (8.12.18)$$

Introducing (8.12.7) and (8.12.18) into (8.12.16) and taking into account the value  $S_{II} = S_w / (2\lambda_w \alpha')$ , we have

$$m_{z_a} = \frac{-2\alpha}{V M_\infty^2 - 1} \left( 1 - \frac{2}{3\lambda_w V M_\infty^2 - 1} \right) \quad (8.12.19)$$

The coefficient of the centre of pressure is

$$c_p = \frac{x_n}{b} = \frac{-M_{z_a}}{b Y_a} = \frac{-m_{z_a}}{c_{y_a}} = \frac{3\lambda_w \sqrt{M_\infty^2 - 1} - 2}{3(2\lambda_w \sqrt{M_\infty^2 - 1} - 1)} \quad (8.12.20)$$

If the number  $M_\infty$  for the flow over the wing shown in Fig. 8.12.1a is reduced, then at a certain value of this number the tip Mach cones intersect inside the wing. Here region III appears (see Fig. 8.12.1b) in which the disturbed flow is affected by the leading supersonic edge and both subsonic tips. The nature of the flow in regions I and II (II') is the same as in the corresponding zones I and II (II') of the wing whose diagram is shown in Fig. 8.12.1a.

Let us consider the flow at point A of region III (see Fig. 8.12.1b). The region of influence of the sources on this flow coincides with wing section ABDD'B'. The latter can be represented as the sum of areas HBDD' and AHD'B'. With this in view and according to (8.10.3), the velocity potential at point A is

$$\varphi'_{III} = \frac{-\alpha V_\infty}{\pi M_\infty} \left[ \iint_{HBDD'} \frac{dr ds}{V(r_A - r)(s_A - s)} + \iint_{AHD'B'} \frac{dr ds}{V(r_A - r)(s_A - s)} \right]$$

We can determine the integration limits directly from Fig. 8.12.1b. Hence,

$$\begin{aligned} \varphi'_{III} = & \frac{-\alpha V_\infty}{\pi M_\infty} \left[ \int_{s_B}^{s_H} \frac{ds}{\sqrt{s_A - s}} \int_{r_F}^{r_A} \frac{dr}{\sqrt{r_A - r}} \right. \\ & \left. + \int_{s_H}^{s_A} \frac{ds}{\sqrt{s_A - s}} \int_{r_{B'}}^{r_A} \frac{dr}{\sqrt{r_A - r}} \right] \end{aligned}$$

We calculate the first two integrals by analogy with (8.12.7), and the other two independently of each other because the region of integration is a parallelogram (see Fig. 8.12.1b). With this in view, we have

$$\begin{aligned} \varphi'_{III} = & \frac{-2\alpha V_\infty}{\pi M_\infty} \left\{ -V(r_A + s_H)(s_A - s_H) \right. \\ & + V\sqrt{2r_A(s_A - r_A)} - (s_A + r_A) \left( \tan^{-1} \sqrt{\frac{s_A - s_H}{r_A + s_H}} \right. \\ & \left. \left. - \tan^{-1} \sqrt{\frac{s_A - r_A}{2r_A}} \right) + 2V(s_A - s_H)(r_A - r_{B'}) \right\} \quad (8.12.21) \end{aligned}$$

Examination of Fig. 8.12.1b reveals that the coordinate  $s_H = s_{D'}$ , and in accordance with (8.12.4), the quantity  $s_{D'} = -r_{D'}$ . Consequently,  $s_H = -r_{D'} = -r_{B'}$ .

Point  $B'$  is on the starboard tip whose equation is  $z = l$ . From (8.9.4'), we can find the equation of this tip in the coordinates  $r$  and  $s$ :

$$r - s = -M_\infty l \quad (8.12.22)$$

Hence for point  $B'$

$$r_{B'} = s_{B'} - M_\infty l = s_A + M_\infty l \quad (8.12.23)$$

Accordingly, we have

$$s_H = -r_{B'} = -s_A + M_\infty l \quad (8.12.24)$$

Introducing into (8.12.21) the coordinates  $r_A$  and  $s_A$  from (8.9.4') and  $r_{B'}$  and  $s_H$  from (8.12.23) and (8.12.24), we find

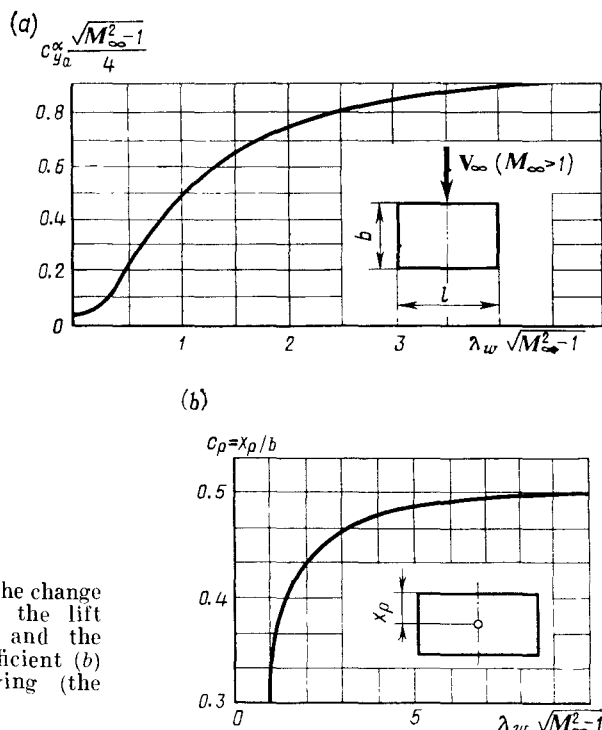
$$\begin{aligned} \varphi'_{III} = & \frac{-2\alpha V_\infty}{\pi\alpha'} \left\{ \sqrt{[(x_A - \alpha' z_A) - \alpha' l](l - z_A)} \alpha' \right. \\ & + \sqrt{\alpha' z_A (x_A - \alpha' z_A)} - x_A \left[ \tan^{-1} \sqrt{\frac{(x_A + \alpha' z_A) - \alpha' l}{(l - z_A)}} \alpha' \right. \\ & \left. \left. - \tan^{-1} \sqrt{\frac{\alpha' z_A}{x_A - \alpha' z_A}} \right] \right\} \end{aligned} \quad (8.12.25)$$

Using the formula  $\bar{p} = -(2/V_\infty) \partial\varphi'_{III}/\partial x_A$ , we find the pressure coefficient as a result of simple transformations:

$$\begin{aligned} \bar{p}_{III} = & \frac{\pm 4\alpha}{\pi\alpha'} \tan^{-1} \sqrt{\frac{\alpha' z_A}{x_A - \alpha' z_A}} \\ & \pm \frac{4\alpha}{\pi\alpha'} \tan^{-1} \sqrt{\frac{(l - z_A) \alpha'}{(x_A + \alpha' z_A) - \alpha' l}} \pm \frac{2\alpha}{\alpha'} \end{aligned} \quad (8.12.26)$$

The first and second terms in this expression are the pressure coefficients  $\bar{p}_{II}$  and  $\bar{p}_{II'}$  for the tip parts of the wing, respectively, while the third term is the pressure coefficient  $\bar{p}_I$  for region I where there is no influence of the tips.

The flow over a rectangular wing is of a still more intricate nature if it has a low aspect ratio and the quantity  $\lambda_w \sqrt{M_\infty^2 - 1} < 1$ . In this case (see Fig. 8.12.1c), new wave regions appear that are formed as a result of intersection of the disturbance waves incident on and reflected from the tips. For example, the disturbances travelling from section  $OH$  of the port tip reach the starboard one on section  $O'H'$  and over it propagate along Mach lines  $O'O''-H'H''$  in the opposite direction. This gives rise to new wave zones  $IV$  and  $V$  in which the nature of the flow changes substantially. This flow can be calculated by using the method of sources set out above and taking into consideration the indicated intricate nature of formation of the disturbance zones.

**Fig. 8.12.3**

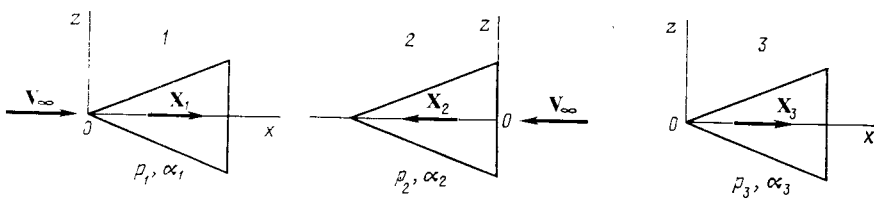
Curves characterizing the change in the derivative of the lift force coefficient (a) and the centre-of-pressure coefficient (b) for a rectangular wing (the aspect ratio  $\lambda_w = l/b$ )

The known pressure distribution and formulas (8.9.27) and (8.9.28) are used to calculate the coefficients of the lift force and moment, while the expressions  $c_p = -m_{z_a}/c_{y_a}$  and  $c_{x_a} = \alpha c_{y_a}$  are used to calculate the coefficients of the centre of pressure and drag of the wing being considered. Curves characterizing the change in the lift and centre-of-pressure coefficients of a rectangular wing with a various aspect ratio have been constructed in Fig. 8.12.3 according to the results of such calculations.

### 8.13. Reverse-Flow Method

Let us consider one of the methods of aerodynamic investigations, the **reverse-flow method**, that establishes relations between the aerodynamic characteristics of thin wings with an identical planform and located in oppositely directed flows.

Let us assume that one of such wings is in a *forward* flow at the angle of attack  $\alpha_1$ , and the other in an *reverse* flow at the angle of

**Fig. 8.13.1**

To the explanation of the reverse-flow method:

1—forward flow; 2—reverse flow; 3—combined flow

attack  $\alpha_2$  (Fig. 8.13.1). According to the theory of linearized flow, the excess pressure at a point of the surface is  $p - p_\infty = -\rho_\infty V_\infty u$ , while the pressure increment between the bottom and upper sides is

$$\Delta p = p_b - p_u = \rho_\infty V_\infty (u_u - u_b) = \rho_\infty V_\infty \Delta u \quad (8.13.1)$$

The magnitude of the drag force produced by the pressure increment is  $dX_a = \Delta p \alpha dS$ . Accordingly, the force for wing 1 in the forward flow is

$$X_{a1} = \iint_S \Delta p_1 \alpha_1 dS \quad (8.13.2)$$

and for wing 2 in the reverse flow is

$$X_{a2} = \iint_S \Delta p_2 \alpha_2 dS \quad (8.13.3)$$

The magnitudes of the pressure increment  $\Delta p_1$ ,  $\Delta p_2$  and of the local angles of attack  $\alpha_1$ ,  $\alpha_2$  are measured at the same point.

In the following, we shall disregard the suction force that can develop on the subsonic leading edge. This does not change the results. Since the flows in the vicinity of the wings are nearly uniform, by superposing them we can obtain a new flow with parameters satisfying the linearized equation for the velocity potential. We shall perform the superposition so that the free-stream velocities are subtracted. Now the contour of the new wing 3 (Fig. 8.13.1) coincides with the configuration of the given wings 1 and 2, but the camber of its surface is different.

This camber is determined by the local angle of attack  $\alpha_3$  equal to the sum of the angles of attack:

$$\alpha_3 = v_3/V_\infty = v_1/V_\infty + v_2/V_\infty = \alpha_1 + \alpha_2 \quad (8.13.4)$$

In accordance with (8.13.4), the vertical components of the velocity  $v$  at the corresponding points of the surfaces are added. The horizontal velocity components upon superposition are subtracted, therefore for the combined wing 3 we obtain  $\Delta u_3 = \Delta u_1 - \Delta u_2$ .

Hence the pressure increment between the bottom and upper sides of this wing is  $\Delta p_3 = \rho_\infty V_\infty \Delta u_3 = \rho_\infty V_\infty (\Delta u_1 - \Delta u_2)$ , or by (8.13.1):

$$\Delta p_3 = \Delta p_1 - \Delta p_2 \quad (8.13.5)$$

The drag of wing 3 is

$$X_{a3} = \iint_S (\Delta p_1 - \Delta p_2) (\alpha_1 - \alpha_2) dS \quad (8.13.6)$$

A drag in a wing is associated with a disturbed flow behind it. The latter is an infinitely long vortex sheet cast off the trailing edge. It is clear from physical considerations that there is strict correspondence between the disturbed state behind the wing and the drag force. Particularly, the force  $X_{a1}$  and the disturbed state behind wing 1, as well as the force  $X_{a2}$  and the disturbed state behind wing 2 are in such correspondence.

The flow near wing 3 obtained as a result of superposition of the flow patterns near wing 1 and wing 2 has the property that the disturbances ahead of it are the same as for wing 2, and behind it, the same as for wing 3. Hence, the drag force of combined wing 3 equals the difference between the drags of wings 1 and 2, i.e.

$$X_{a3} = X_{a1} - X_{a2} = \iint_S (\Delta p_1 \alpha_1 - \Delta p_2 \alpha_2) dS \quad (8.13.7)$$

Equating the right-hand sides of (8.13.6) and (8.13.7), we obtain

$$\iint_S \Delta p_1 \alpha_2 dS = \iint_S \Delta p_2 \alpha_1 dS \quad (8.13.8)$$

This relation is the *fundamental expression of the reverse-flow method*.

Going over to pressure coefficients in (8.13.8), we can write this relation as

$$\iint_S \Delta \bar{p}_1 \alpha_2 dS = \iint_S \Delta \bar{p}_2 \alpha_1 dS \quad (8.13.8')$$

where the pressure increment coefficients are  $\Delta \bar{p}_1 = \bar{p}_{1b} - \bar{p}_{1u}$  and  $\Delta \bar{p}_2 = \bar{p}_{2b} - \bar{p}_{2u}$ .

Using our right to choose the angle of attack arbitrarily, let us adopt the same constant values of  $\alpha_1$  and  $\alpha_2$  for all points on a wing surface, i.e.  $\alpha_1 = \alpha_2 = \alpha$ . We therefore find from (8.13.8') that

$$\iint_S \Delta \bar{p}_1 dS = \iint_S \Delta \bar{p}_2 dS, \text{ or } Y_{a1} = Y_{a2}$$

Hence, the reverse-flow method allows us to establish that the lift force of a flat plate in forward ( $Y_{a1}$ ) and reverse ( $Y_{a2}$ ) flow is the same at identical angles of attack and free-stream velocities.

## **Aerodynamic Characteristics of Craft in Unsteady Motion**

In the steady motion of craft, the aerodynamic forces and moments are independent of time and are determined for fixed rudders and elevators and for a given altitude and velocity only by the orientation of the craft relative to the velocity vector. Unsteady motion, when a craft experiences acceleration or deceleration and vibrates for various reasons, is the most general case. In inverted motion, this is equivalent to an unsteady flow of air over a craft. With such a flow, the aerodynamic properties of a craft are due not only to its position relative to the free-stream velocity, but also depend on the kinematic parameters characterizing motion, i.e. the aerodynamic coefficients are a function of time.

In unsteady flow, a craft experiences additional forces and moments. Their magnitudes in a number of cases are quite small in comparison with those encountered in steady motion. Particularly, in an axial accelerated supersonic flow over a body, the drag grows only insignificantly, which may be disregarded in practice (according to Frankl).

Many important problems relating to the motion of craft, including unsteady motion, can be solved by using the aerodynamic characteristics for a steady flow. A number of problems, however, are solved only by finding the aerodynamic characteristics with account taken of the unsteady nature of the flow.

The major problems include that of the **dynamic stability** of a craft. A craft has dynamic stability in given flight conditions if the deviation of the kinematic parameters produced by disturbing forces diminishes with time so that the disturbed motion attenuates and tends to the initial programmed flight.

If this condition is not realized, we have dynamic instability of a craft. Dynamic stability (or instability) is investigated on the basis of the equations for disturbed motion including time-dependent aerodynamic characteristics (what are called non-stationary aerodynamic characteristics).

The concept of **controllability**, i.e. the ability of a craft to respond to the controls and change its position in space and the corresponding flight characteristics sufficiently rapidly and without appreciable vibrations, is associated with the concept of stability.

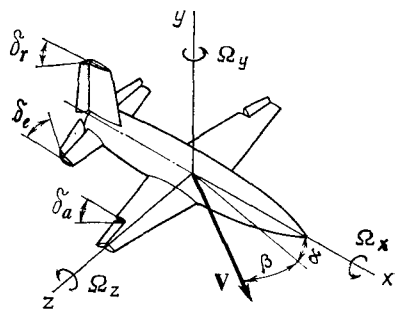
The problem of control is solved on the basis of equations of motion including non-stationary characteristics of a craft with account taken of the action of the control surfaces. These problems include the investigation of an unsteady flight for establishing and evaluating the **manoeuvrability** of a craft, i.e. its ability to change its speed, direction of flight, and orientation in space within a given interval of time.

### 9.1. General Relations for the Aerodynamic Coefficients

The aerodynamic forces or moments acting on a craft depend on the **kinematic variables** characterizing its motion. For a given configuration and altitude  $H$  of a craft, these forces and moments are determined by the flight velocity  $\mathbf{V} = -\mathbf{V}_\infty$  ( $\mathbf{V}_\infty$  is the free-stream velocity in inverted flow), the angular orientation relative to the velocity vector  $\mathbf{V}$  (the angles  $\alpha$  and  $\beta$ ), the angles of deflection of the control surfaces arranged in three mutually perpendicular planes ( $\delta_r$ ,  $\delta_e$  and  $\delta_a$  are the rudder, elevator, and aileron angles, respectively), and also the angular velocities of rotation about the body axes ( $\Omega_x$ ,  $\Omega_y$ ,  $\Omega_z$ , Fig. 9.1.1). In addition, in the general case it is necessary to take into account the influence of the angular and linear accelerations ( $\dot{\Omega}_x = d\Omega_x/dt$ ,  $\dot{\Omega}_y = d\Omega_y/dt$ ,  $\dot{\Omega}_z = d\Omega_z/dt$ ,  $\dot{V}_\infty = dV_\infty/dt$ ), of the rate of change in the angle of attack and the sideslip angle ( $\dot{\alpha} = d\alpha/dt$ ,  $\dot{\beta} = d\beta/dt$ ), and also of the rate of change in the angle of deflection of the control surfaces ( $\dot{\delta}_r = d\delta_r/dt$ ,  $\dot{\delta}_e = d\delta_e/dt$ ,  $\dot{\delta}_a = d\delta_a/dt$ ). Accordingly, the following general relation holds for a force or moment:

$$T = f_1(V_\infty, H, \alpha, \beta, \delta_r, \delta_e, \delta_a, \Omega_x, \Omega_y, \Omega_z, \dot{V}_\infty, \dot{\alpha}, \dot{\beta}, \dot{\delta}_r, \dot{\delta}_e, \dot{\delta}_a, \dot{\Omega}_x, \dot{\Omega}_y, \dot{\Omega}_z) \quad (9.1.1)$$

The aerodynamic force and moment coefficients are functions of dimensionless variables corresponding to the dimensional quantities in relation (9.1.1). As examples of such variables corresponding to the velocity  $V_\infty$  and altitude  $H$ , we can consider the Mach number  $M_\infty = V_\infty/a_\infty$  and Reynolds number  $Re = V_\infty l \rho_\infty / \mu_\infty$  (here  $a_\infty$ ,  $\rho_\infty$ , and  $\mu_\infty$  are the speed of sound, the density, and the dynamic viscosity, respectively, of the air at the altitude  $H$ , and  $l$  is a typical dimension of the craft).

**Fig. 9.1.1**

Designation of kinematic variables characterizing the motion of a craft

We can write the other dimensionless variables in the following form:

$$\left. \begin{aligned} \dot{\delta}_{r(e,a)} &= \dot{\delta}_{r(e,a)} l/V_\infty, & \dot{\alpha} &= \dot{\alpha} l/V_\infty, & \dot{\beta} &= \dot{\beta} l/V_\infty \\ \omega_x &= \Omega_x l/V_\infty, & \omega_y &= \Omega_y l/V_\infty, & \omega_z &= \Omega_z l/V_\infty, & \dot{V}_\infty &= \dot{V}_\infty l/V_\infty \\ \dot{\omega}_x &= \dot{\Omega}_x l^2/V_\infty^2, & \dot{\omega}_y &= \dot{\Omega}_y l^2/V_\infty^2, & \dot{\omega}_z &= \dot{\Omega}_z l^2/V_\infty^2 \end{aligned} \right\} \quad (9.1.2)$$

Hence, for an aerodynamic coefficient in any coordinate system, we have

$$c = f_2(M_\infty, Re_\infty, \alpha, \beta, \delta_r, \delta_e, \delta_a, \omega_x, \omega_y, \omega_z, \dot{V}_\infty, \dot{\alpha}, \dot{\beta}, \dot{\delta}_r, \dot{\delta}_e, \dot{\delta}_a, \dot{\omega}_x, \dot{\omega}_y, \dot{\omega}_z) \quad (9.1.3)$$

The variables  $M_\infty$ ,  $\alpha$ ,  $\beta$ ,  $\delta_r$ ,  $\delta_e$ ,  $\delta_a$ ,  $\omega_x$ ,  $\omega_y$ , and  $\omega_z$  determine the coefficients of the aerodynamic forces and moments due to the instantaneous distribution of the local angles of attack. Here the variables  $M_\infty$ ,  $\alpha$ ,  $\beta$ ,  $\delta_r$ ,  $\delta_e$ , and  $\delta_a$  characterize the forces and moments depending on the velocity, the angle of attack, the sideslip angle, and the control surface angles, while the variables  $\omega_x$ ,  $\omega_y$ , and  $\omega_z$  determine the forces and moments due to the change in the local angles of attack caused by rotation.

The time derivatives  $\dot{V}_\infty$ ,  $\dot{\alpha}$ ,  $\dot{\beta}$ ,  $\dot{\delta}_r$ ,  $\dot{\delta}_e$ ,  $\dot{\delta}_a$ ,  $\dot{\omega}_x$ ,  $\dot{\omega}_y$  and  $\dot{\omega}_z$  determine the additional forces of an inertial nature and appearing upon the accelerated motion of a body. This motion accelerates the air particles on the surface in the flow.

When investigating the motion of craft characterized by a small change in the dimensionless kinematic variables, the aerodynamic coefficients are written in the form of a Taylor series in which the second-order infinitesimals may be retained. Assuming the number  $Re_\infty$  to be fixed, we shall present, particularly, such a series for the

normal force coefficient:

$$\begin{aligned}
 c_y = & c_{y0} + c_y^M \Delta M_\infty + c_y^\alpha \Delta \alpha + c_y^\beta \Delta \beta + c_y^{\delta_r} \Delta \delta_r + c_y^{\delta_e} \Delta \delta_e + c_y^{\delta_a} \Delta \delta_a \\
 & + c_y^{o_x} \Delta \omega_x + c_y^{o_y} \Delta \omega_y + c_y^{o_z} \Delta \omega_z + c_y^{\dot{x}} \Delta \dot{V}_\infty + c_y^{\dot{\alpha}} \Delta \dot{\alpha} - c_y^{\dot{\beta}} \Delta \dot{\beta} \\
 & + c_y^{\dot{\delta}_r} \Delta \dot{\delta}_r + c_y^{\dot{\delta}_e} \Delta \dot{\delta}_e + c_y^{\dot{\delta}_a} \Delta \dot{\delta}_a + c_y^{o_x} \Delta \dot{\omega}_x + c_y^{o_y} \Delta \dot{\omega}_y + c_y^{o_z} \Delta \dot{\omega}_z \\
 & + \dots + \frac{1}{2} c_y^{\beta o_y} \Delta \beta \Delta \omega_x + \dots + \frac{1}{2} c_y^{o_x o_y} \Delta \omega_x \Delta \omega_y + \dots \quad (9.1.4)
 \end{aligned}$$

Here the coefficient  $c_{y0}$ , the derivatives  $c_y^M = \partial c_y / \partial M_\infty$ ,  $c_y^\alpha = \partial c_y / \partial \alpha$ ,  $c_y^\beta = \partial c_y / \partial \beta$  and others are calculated for certain initial values of the variables. If these values equal zero, one must assume that  $\Delta \alpha = \alpha$ ,  $\Delta \dot{\alpha} = \dot{\alpha}$ , etc.

The derivatives can be considered as the rates of change in a coefficient of any force or moment depending on the number  $M_\infty$ , the angle of attack or the sideslip angle, the control surface angles, the angular and linear velocities, and also on their time derivatives.

The derivatives being considered are aerodynamic characteristics used in the investigation of a flight and first of all in solving stability problems. This is why such characteristics are usually called **stability derivatives**.

The stability derivatives in (9.1.4) do not depend on the time and are determined by the values of the dimensionless kinematic variables at the point of a trajectory for which the aerodynamic coefficient being considered is expanded into a Taylor series. For unsteady motion, the values of these coefficients are not only determined by the values of the kinematic variables at a given instant, but are also dependent on the history of the motion, i.e. on how it occurred in the preceding period. In an appreciable number of problems of practical interest, we can determine the law of motion beforehand with a high authenticity and thereby substantially simplify the investigation of non-stationary aerodynamic characteristics. The calculations are simplified, particularly, if the kinematic variables determining the nature of motion change **harmonically**, i.e. the values of these parameters can be written in the form

$$q_i = q_i^* \cos p_i t \quad (9.1.5)$$

where  $q_i$  is the set of dimensionless kinematic variables,  $q_i^*$  is the amplitude, and  $p_i$  is the circular frequency of the oscillations.

In accordance with (9.1.5), the time derivative is

$$\dot{q}_i = dq_i/dt = -q_i^* p_i^* \sin p_i t \quad (9.1.6)$$

where we have introduced the **Strouhal number**

$$p_i^* = p_i l/V_\infty \quad (9.1.7)$$

For example, if  $q_i = \alpha$ ,  $q_i^* = \alpha_0$  (the amplitude of the oscillations with respect to the angle of attack),  $\dot{q}_i = (d\alpha/dt)$ ,  $\dot{l}/V_\infty = \dot{\alpha}$ ,  $p_i^* = p_\alpha^*$ , and  $p_i = p_\alpha$ , then

$$\alpha = \alpha_0 \cos p_\alpha t, \quad \dot{\alpha} = -\alpha_0 p_\alpha^* \sin p_\alpha t \quad (9.1.8)$$

Important solutions from a practical viewpoint have been obtained for the particular case of harmonic oscillations. They allow one to determine the basic aerodynamic characteristics for the unsteady motion of wings, bodies of revolution, and separate kinds of aircraft.

Expressions (9.1.3) and (9.1.4) for the aerodynamic coefficients relate to a craft with an undeformed (rigid) surface. It must be taken into account here that in real conditions such a surface may deform, for example, because of bending, which leads to an additional change in the non-stationary characteristics. Considered below are problems on the determination of such characteristics without account taken of deformation, i.e. for inelastic bodies in a flow. The results of investigating unsteady-flow aerodynamic characteristics for the more general case of deformed surfaces are given in [4, 19].

## 9.2. Analysis of Stability Derivatives and Aerodynamic Coefficients

The first seven terms in Eq. (9.1.4) determine the static, and the remaining ones, the dynamic components of the aerodynamic coefficients. The static components correspond to steady conditions of flow over a craft in which its velocity is constant, while the angle of attack, the sideslip angle, and also the control surface angles are fixed. The dynamic components appear in non-stationary motion attended by acceleration or deceleration of the flow over a craft, its rotation, and a change in time of the control surface angles.

In accordance with the above, the derivatives  $c_y^{M_\infty}$ ,  $c_y^\alpha$ ,  $c_y^\beta$ , and  $c_y^{\delta r}$  are called static stability derivatives, and the remaining ones, ( $c_y^{\omega_x}$ ,  $c_y^{\dot{V}_\infty}$ ,  $c_y^{\dot{\alpha}}$ ,  $c_y^{\dot{\beta}}$ ,  $c_y^{\dot{\delta}r}$ , etc.), the dynamic stability derivatives.

As can be seen from (9.1.4), the aerodynamic coefficients are determined by the corresponding first and second order stability derivatives.

The first order ones include the values of  $c_y^{M_\infty}$ ,  $c_y^\alpha$ ,  $c_y^{\dot{\alpha}}$ ,  $c_y^\beta$ ,  $c_y^{\dot{\beta}}$ , and the second order ones,  $c_y^{\alpha\beta} = \partial^2 c_y / \partial \alpha \partial \beta$ ,  $c_y^{\alpha\omega_x} = \partial^2 c_y / \partial \alpha \partial \omega_x$ , etc.

An analysis of (9.1.4) reveals that the aerodynamic coefficients are determined by two groups of derivatives, one of which depends on the control surface variables ( $c_y^{\delta r}$ ,  $c_y^{\dot{\delta}r}$ , . . .), while the other is not related to them ( $c_y^\alpha$ ,  $c_y^{\dot{\alpha}}$ , . . .). The magnitude of a coefficient depends on the action of these controls. This is due to the change

in the angle of attack and sideslip angle upon deflection of the control surfaces. The values of the angles  $\alpha$  and  $\beta$  correspond to the position of static equilibrium of a craft.

To retain the given flight conditions, the control surfaces must be fixed in place. Such a flight with "fixed" control surfaces becomes uncontrollable. Its conditions are determined completely by the stability derivatives that depend on the intrinsic aerodynamic properties of a craft if controls are absent or are fixed in place.

Derivatives such as  $c_y^\alpha$ ,  $c_y^\beta$ ,  $c_y^{\delta_r}$ , . . . , determined as a result of differentiation of the aerodynamic coefficients with respect to  $\alpha$ ,  $\beta$ ,  $\delta_r$  (static stability derivatives) relate to the first group of derivatives. The partial derivatives of the coefficients with respect to one of the variables  $\omega_x$ ,  $\omega_y$ ,  $\omega_z$  form the second group of what we call rotary derivatives (for example,  $c_y^{\omega_x}$ ,  $c_y^{\omega_y}$ ,  $m_z^{\omega_z}$ , . . . ). This group also includes derivatives similar to  $c_y^{\dot{\alpha}}$ ,  $c_y^{\dot{\beta}}$ ,  $c_y^{\dot{\delta}_r}$ , and also acceleration derivatives determined as the partial derivatives of the aerodynamic coefficients with respect to one of the parameters  $\dot{V}_\infty$ ,  $\dot{\omega}_x$ ,  $\dot{\omega}_y$ , or  $\dot{\omega}_z$ .

If the non-stationary disturbances are finite, non-linearity becomes a noticeable feature. It is reflected in expansion (9.1.4) where there are several second-order terms. The latter are determined by stability derivatives of the second order (for example,  $c_y^{\alpha\beta}$  and  $c_y^{\alpha\omega_x}$ ) that are in the fourth group.

Investigations show that the influence of the derivatives on the aerodynamic coefficients is not the same and that a practical significance is a feature of only a part of such derivatives, among which second order derivatives form a quite small fraction. This influence is analysed in each specific case depending on the aerodynamic configuration of a craft and the conditions of its motion. As a result, we find the derivatives which the aerodynamic coefficients (or the corresponding forces and moments) depend on and the influence of which of them may be ignored. For each coefficient, we can reveal the characteristic trend associated with such a relation. Let us consider, for example, the longitudinal (axial) force coefficient, the expression for which will be written in the form

$$c_x = c_{x0} + c_x^{\alpha^2} \alpha^2 + c_x^{\alpha\delta_e} \alpha\delta_e + c_x^{\delta_e^2} \delta_e^2 + c_x^{\beta^2} \beta^2 + c_x^{\beta\delta_r} \beta\delta_r - c_x^{\delta_r^2} \delta_r^2 \quad (9.2.1)$$

where  $c_{x0}$  is the value of  $c_x$  at  $\alpha = \beta = \delta_e = \delta_r = 0$ ,  $c_x^{\alpha^2}$ , . . . ,  $c_x^{\delta_r^2}$  are the second-order partial derivatives of the longitudinal force coefficient with respect to  $\alpha^2$ , . . . ,  $\alpha\delta_e$  (for example,  $c_x^{\alpha^2} = \partial^2 c_x / \partial \alpha^2$ ).

In accordance with expression (9.2.1), the longitudinal force coefficient is a quantity not depending on the rotary derivatives or the acceleration derivatives. This quantity is determined in the form

of a quadratic dependence on the angle of attack and the sideslip angle, as well as the elevator and rudder angles. Here the components of the coefficient  $c_x$  depending on the derivatives  $c_x^{\delta_e}$  and  $c_x^{\delta_r}$  are of significance when control surfaces are present in the form of movable wings or empennage whose deflection may lead to a substantial change in the longitudinal force.

The normal force coefficient can be written in the form of the linear relation

$$c_y = c_{y0} + c_y^\alpha \alpha + c_y^{\delta_e} \delta_e \quad (9.2.2)$$

where  $c_{y0}$  is the value of  $c_y$  at  $\alpha = \delta_e = 0$ .

Relation (9.2.2) is suitable for small values of  $\alpha$  and  $\delta_e$ . The larger these angles (beginning approximately from values of  $10^\circ$ ), the more does the non-linear nature of the dependence of the coefficient  $c_y$  on them manifest itself. The non-linear nature increases with a decrease in the aspect ratio of the lifting planes, and also with an increase in the Mach number ( $M_\infty > 3-4$ ). In accordance with (9.2.2), when determining the normal force coefficient, no account is taken of the influence of the sideslip, rudder, elevator, and aileron angles, and also of the rotation of the craft and its acceleration. At the same time, when a movable wing (empennage) is present, the quantity  $c_y^{\delta_e} \delta_e$  differs appreciably from that for conventional control surfaces. In the latter case, this quantity may be negligibly small.

The lateral force coefficient  $c_z$  (in body axes) can be calculated by analogy with the normal force coefficient  $c_y$ , i.e. by using formula (9.2.2) in which the angle of attack and the elevator angle must be replaced with the sideslip and rudder angles, respectively:

$$c_z = c_z^\beta \beta + c_z^{\delta_r} \delta_r \quad (9.2.3)$$

According to this expression, when  $\beta = \delta_r = 0$ , the lateral force coefficient equals zero, which corresponds to symmetry of a craft about the vertical plane  $xOy$ .

The pitching moment at a given number  $M_\infty$  for a flight depends mainly on parameters such as the angle of attack  $\alpha$  and the elevator angle  $\delta_e$ , the rate of change in these angles  $\dot{\alpha}$  and  $\dot{\delta}_e$ , and also the angular velocity  $\Omega_z$ . The influence of other parameters, in particular of the sideslip angle, the aileron angle, and the angular velocities  $\Omega_y$  or  $\Omega_x$ , is not great and is usually disregarded.

In accordance with the above, for the pitching moment coefficient we can obtain the following linear relation suitable for small values of the indicated variables (in a body axis coordinate system):

$$m_z = m_{z0} + m_z^\alpha \alpha + m_z^{\delta_e} \delta_e + m_z^{\omega_z} \omega_z + m_z^{\dot{\alpha}} \dot{\alpha} + m_z^{\dot{\delta}_e} \dot{\delta}_e \quad (9.2.4)$$

where  $m_{z0}$  is the moment coefficient when  $\alpha = \delta_e = \omega_z = \dot{\alpha} = \dot{\delta}_e = 0$ .

A glance at the above expression reveals that the pitching moment coefficient is determined by two static stability derivatives  $m_z^\alpha$ ,  $m_z^{\delta_e}$  and three rotary derivatives  $m_z^{\omega_z}$ ,  $m_z^{\dot{\alpha}}$ ,  $m_z^{\dot{\delta}_e}$ .

By analogy with the pitching moment, the yawing moment may be considered to depend mainly on the sideslip and rudder angles  $\beta$  and  $\delta_r$ , the rates of their change in time  $\dot{\beta}$ ,  $\dot{\delta}_r$ , and also on the angular velocity  $\Omega_z$ . Such a relation exists for axisymmetric craft. If symmetry is disturbed, however, account must also be taken of the influence of the angular velocity  $\Omega_x$ . This can be done, for example, with the presence of a non-symmetric vertical empennage when the upper panel upon rotation about its longitudinal axis creates a lateral (side) force that produces an additional moment about the vertical axis.

Deflection of the ailerons also produces a certain yawing moment, which is associated with the longitudinal forces differing in value on horizontal wings upon deflection of the ailerons (this is similar to the appearance of a small pitching moment upon the deflection of the ailerons on vertical wings). Investigations show that such an additional yawing moment is usually very small in modern aircraft. Accordingly, the yawing moment coefficient may be expressed by the following linear relation:

$$m_y = m_y^{\beta} \beta + m_y^{\delta_r} \delta_r + m_y^{\omega_x} \omega_x + m_y^{\omega_y} \omega_y + m_y^{\dot{\beta}} \dot{\beta} + m_y^{\dot{\delta}_r} \dot{\delta}_r \quad (9.2.5)$$

In accordance with this relation, the yawing moment at  $\beta = \delta_r = \dots = 0$  equals zero. This is always observed in aircraft symmetric about the plane  $xOy$ . By (9.2.5), the yawing moment coefficient is determined by two static derivatives  $m_y^\beta$ ,  $m_y^{\delta_r}$  and four rotational derivatives  $m_y^{\omega_x}$ ,  $m_y^{\omega_y}$ ,  $m_y^{\dot{\beta}}$ , and  $m_y^{\dot{\delta}_r}$ .

A rolling moment (a moment about the longitudinal axis  $Ox$ ) is due to the asymmetry of the flow caused by sideslip and control surface deflection angles or rotation of the craft. For a given craft design and a definite flight speed (number  $M_\infty$ ), this moment can be considered as a function of the angle of attack  $\alpha$ , the sideslip angle  $\beta$ , the elevator, rudder, and aileron angles  $\delta_e$ ,  $\delta_r$ ,  $\delta_a$ , and also of the rotational velocities  $\Omega_x$ ,  $\Omega_y$ ,  $\Omega_z$ . Accordingly, the rolling moment coefficient can be written as

$$\begin{aligned} m_x = & m_x^{\beta} \beta + m_x^{\delta_r} \delta_r + m_x^{\delta_a} \delta_a + m_x^{\alpha \beta} \alpha \beta + m_x^{\alpha \delta_r} \alpha \delta_r \\ & + m_x^{\beta \delta_e} \beta \delta_e + m_x^{\omega_x} \omega_x + m_x^{\omega_y} \omega_y + m_x^{\alpha \omega_y} \alpha \omega_y + m_x^{\beta \omega_z} \beta \omega_z \end{aligned} \quad (9.2.6)$$

According to this expression, the rolling moment at  $\beta = \delta_r = \delta_a = \dots = 0$  equals zero, which corresponds to an ideal design of the craft produced without any technological errors. When study-

ing the motion of a real craft, particularly rolling motion, account must be taken of the presence of such errors, especially of those associated with inaccurate wing installation, which has the maximum influence on the rolling moment.

Inspection of (9.2.6) reveals that the rolling moment is determined as the function of derivatives not only of the first, but also of the second order ( $m_x^\beta$ ,  $m_x^{\delta_r}$ , ...,  $m_x^{\alpha\beta}$ ,  $m_x^{\alpha\delta_r}$ , ...). Therefore, such a function is non-linear, which occurs even with small angular values of  $\alpha$ ,  $\beta$ ,  $\delta_e$ ,  $\delta_r$ ,  $\delta_a$ , and small velocities  $\omega_x$ ,  $\omega_y$ ,  $\omega_z$ . At the same time, the rolling moment coefficient when performing approximate calculations may be found without taking into account the influence of the rates of change in the angle of attack and the sideslip angle, and also of the acceleration, this influence being negligible.

All the derivatives determining the aerodynamic coefficients are functions depending mainly on the number  $M_\infty$ , and also on the geometric configuration and dimensions of the craft. In a more general case, these derivatives depend on the arguments determining the aerodynamic coefficients, particularly on the angle of attack and the sideslip angle, the angular velocities and the relevant accelerations, and also on the acceleration of the translational motion. Such a relation is found separately in each case for a given kind of motion of a craft.

A part of the considered stability derivatives characterize the aerodynamic properties of a craft regardless of the action of the control surfaces ( $c_y^\alpha$ ,  $m_z^\alpha$ ,  $m_x^{\omega_x}$ , ...), whereas the other part is associated with their deflection ( $c_y^{\delta_e}$ ,  $m_z^{\delta_e}$ ,  $m_x^{\delta_a}$ ,  $m_x^{\delta_r}$ , ...). Each of these derivatives has a physical meaning and may be helpful in studying the motion of a craft.

The static derivatives  $c_y^\alpha$  and  $c_z^\beta$  characterize the property of a craft to change the normal and lateral forces depending on the angle of attack and the sideslip angle, whereas the derivatives  $c_y^{\delta_e}$  and  $c_z^{\delta_r}$  characterize the same property, but associated with the deflection of the corresponding control surfaces. These derivatives are important for controlling the motion of the centre of mass of a craft in the longitudinal and lateral directions.

The static second-order derivatives  $c_x^{\alpha^2}$ ,  $c_x^{\beta^2}$ ,  $c_x^{\delta_e^2}$ , and  $c_x^{\delta_r^2}$  determine the additional increment of the longitudinal force due to deflection of a craft through the angles  $\alpha$  and  $\beta$ , and also to the controlling action of the control surfaces. The derivatives  $c_x^{\alpha\delta_e}$  and  $c_x^{\beta\delta_r}$  characterize the influence on the longitudinal force of the interaction of the angle of attack and the elevator angle, while  $c_x^{\delta_e\delta_r}$  characterizes the influence of the sideslip and rudder angles [in accordance with this, the quantities  $c_x^{\alpha\delta_e\alpha\delta_e}$  and  $c_x^{\beta\delta_r\beta\delta_r}$  in (9.2.1) are called interaction terms].

The static stability derivatives  $m_z^\alpha$ ,  $m_y^\beta$ , and  $m_x^\beta$  characterize an important property of a craft such as the stiffness of its longitudinal,

sideslipping, and lateral motions, while the derivatives  $m_z^{\delta_e}$ ,  $m_y^{\delta_r}$ , and  $m_x^{\delta_a}$  characterize the effectiveness of the corresponding control surface.

The rotational derivatives act on the motion like damping variables, and they are called, respectively, longitudinal damping coefficients ( $m_z^{\omega_z}$ ,  $m_z^{\dot{\alpha}}$ ,  $m_z^{\dot{\delta}_e}$ ), yawing damping coefficients ( $m_y^{\omega_y}$ ,  $m_y^{\dot{\beta}}$ ,  $m_y^{\dot{\delta}_r}$ ), and rolling damping coefficients ( $m_x^{\omega_x}$ ).

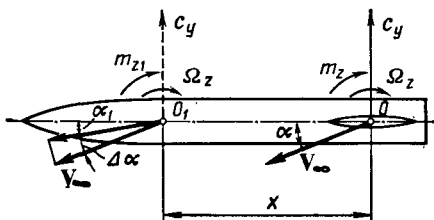
The components  $m_y^{\omega_x \omega_x}$  in (9.2.5) and  $m_x^{\omega_y \omega_y}$  in (9.2.6) are, respectively, the coefficients of the spiral yawing and rolling moments. These moments appear because a craft combines translational motion with rotation about the axes  $Ox$  and  $Oy$ , i.e. performs spiral motion. The investigation of this complicated motion is associated with the calculation of the rotary (spiral) derivatives  $m_y^{\omega_x}$  and  $m_x^{\omega_y}$ .

Formula (9.2.6) for the rolling moment coefficient includes interaction terms determined by second-order stability derivatives. For example, the derivative  $m_x^{\alpha\beta}$  is related to the change in the rolling moment caused by the additional angles of attack on the port and starboard wing panels during flight with side-slipping. A similar effect characterized by the derivative  $m_x^{\alpha\delta_r}$  is produced by deflection of the rudder. An additional rolling moment may also be caused by a change in the sideslip angle upon deflection of the elevators. The magnitude of the lateral moment depends on the second derivative  $m_x^{\beta\delta_e}$ . Rotation of a craft about the  $Oy$  or  $Oz$  axis may lead to an additional change in the angle of attack and the sideslip angle on opposite panels of lifting surfaces and to the relevant spiral rolling moments characterized by the derivatives  $m_x^{\alpha\omega_y}$  and  $m_x^{\beta\omega_z}$ .

From the more general expression (9.1.4) for the aerodynamic coefficient, we can see that it also depends on the other stability derivatives that were not taken into account in the considered expressions. In separate kinds of motion, the influence of such derivatives may be substantial.

One of these motions is associated with the rolling of a craft at a sufficiently high angular velocity  $\Omega_x$ . Such rotation produces the **Magnus effect** consisting in that with the presence of an angle of attack and a sideslip angle, forces and moments appear that are proportional to the products  $\alpha\Omega_x$  or  $\beta\Omega_x$ , the direction of the forces coinciding with a normal to the planes containing the angles  $\alpha$  and  $\beta$ . Accordingly, the increments of the lateral force coefficients are  $\Delta c_z = c_z^{\alpha\omega_x}\alpha\omega_x$ , and of the normal force ones are  $\Delta c_y = c_y^{\beta\omega_x}\beta\omega_x$ . The increments of the yawing and pitching moment coefficients are, respectively,  $\Delta m_y = m_y^{\alpha\omega_x}\alpha\omega_x$  and  $\Delta m_z = m_z^{\beta\omega_x}\beta\omega_x$ . In these expressions, the quantities  $c_z^{\alpha\omega_x}$  and  $m_y^{\alpha\omega_x}$  are called the **Magnus stability derivatives**.

The origin of still another group of forces and moments is associated with the simultaneous rotation of a craft about two axes and is of a gyroscopic nature. Gyroscopic forces and moments are pro-

**Fig. 9.3.1**

To the conversion of the aerodynamic coefficients and their stability derivatives from one reduction centre to another

portional to the product of two angular velocities. For example, upon the simultaneous rotation about the axes  $Ox$  and  $Oy$ , these additional forces and moments are proportional to the product  $\Omega_x \Omega_y$ , and the corresponding aerodynamic coefficients, to the product of the dimensionless variables  $\omega_x \omega_y$ . This is why the derivatives of a coefficient with respect to  $\omega_x \omega_y$  ( $c_y^{\omega_x \omega_y}$ ,  $m_z^{\omega_x \omega_y}$ , etc.) are known as the **gyroscopic stability derivatives**.

### 9.3. Conversion of Stability Derivatives upon a Change in the Position of the Force Reduction Centre

Let us consider the conversion of the pitching moment and normal force coefficients, and also of the relevant stability derivatives calculated with respect to a reduction centre at point  $O$  for a new position  $O_1$  of this centre at a distance of  $x$  from  $O$  (Fig. 9.3.1). A similar problem is solved, particularly, when determining the aerodynamic characteristics of an empennage relative to the centre of mass that is the centre of rotation of a craft in flight and coincides, consequently, with the centre of moments.

Assuming that the pitching moment coefficient at  $\alpha = \Omega_z = 0$  equals zero ( $m_{z0} = 0$ ) and that the airspeed is constant, let us form a general expression for this coefficient relative to the lateral axis passing through point  $O$ :

$$m_z = m_z^\alpha \alpha + m_z^{\dot{\alpha}} \dot{\alpha} + m_z^{\omega_z} \omega_z + m_z^{\dot{\omega}_z} \dot{\omega}_z \quad (9.3.1)$$

in which the derivatives  $m_z^\alpha$ ,  $m_z^{\dot{\alpha}}$ , . . . , are known.

We can obtain a similar expression for the new reduction centre:

$$m_{z1} = m_{z1}^\alpha \alpha_1 + m_{z1}^{\dot{\alpha}} \dot{\alpha}_1 + m_{z1}^{\omega_{z1}} \omega_{z1} + m_{z1}^{\dot{\omega}_{z1}} \dot{\omega}_{z1} \quad (9.3.2)$$

Here the derivatives  $m_{z1}^\alpha$ ,  $m_{z1}^{\dot{\alpha}}$ , . . . are to be found in terms of their corresponding values obtained for the reduction centre  $O$ .

For this purpose, let us first consider the relations between  $\alpha$ ,  $\dot{\alpha}$ ,  $\omega_z$ ,  $\dot{\omega}_z$ , and  $\alpha_1$ ,  $\dot{\alpha}_1$ ,  $\omega_{z1}$ ,  $\dot{\omega}_{z1}$ . A glance at Fig. 9.3.1 reveals that

$$\alpha_1 = \alpha + \Delta\alpha = \alpha - \omega_z \bar{x}$$

where  $\bar{x} = x/l$ ,  $\omega_z = \Omega_z l/V_\infty$ , and, consequently,  $\dot{\alpha}_1 = \dot{\alpha} - \dot{\omega}_z \bar{x}$ . The angular velocities and their derivatives do not change upon a change in the reduction centres, i.e.  $\omega_{z1} = \omega_z$ , and  $\dot{\omega}_{z1} = \dot{\omega}_z$ . Using these relations, let us reduce the formula for the moment coefficient:

$$m_z = m_z^{\alpha_1} \alpha_1 + m_z^{\dot{\alpha}_1} \dot{\alpha}_1 + m_z^{\omega_{z1}} \omega_{z1} + m_z^{\dot{\omega}_{z1}} \dot{\omega}_{z1} \quad (9.3.3)$$

expressed in terms of the new kinematic parameters (for point  $O_1$ ) to the form

$$m_z = m_z^\alpha \alpha + m_z^{\dot{\alpha}} \dot{\alpha} + (m_z^{\omega_{z1}} - m_z^{\alpha} \bar{x}) \omega_z + (m_z^{\dot{\omega}_{z1}} - m_z^{\dot{\alpha}} \bar{x}) \dot{\omega}_z \quad (9.3.4)$$

By comparing (9.3.1) and (9.3.4) we find

$$m_z^{\alpha_1} = m_z^\alpha, \quad m_z^{\dot{\alpha}_1} = m_z^{\dot{\alpha}}, \quad m_z^{\omega_{z1}} = m_z^{\omega_z} + m_z^{\alpha} \bar{x}, \quad m_z^{\dot{\omega}_{z1}} = m_z^{\dot{\omega}_z} + m_z^{\dot{\alpha}} \bar{x}$$

With this in view, expression (9.3.3) acquires the form

$$m_z = m_z^\alpha \alpha_1 + m_z^{\dot{\alpha}} \dot{\alpha}_1 + (m_z^{\omega_z} + m_z^{\alpha} \bar{x}) \omega_{z1} + (m_z^{\dot{\omega}_z} + m_z^{\dot{\alpha}} \bar{x}) \dot{\omega}_{z1} \quad (9.3.5)$$

The obtained moment coefficient can be expressed in terms of its value found for the new centre  $O_1$  by means of the formula  $m_z = m_{z1} + c_y \bar{x}$  (Fig. 9.3.1). Here formula (9.3.2) can be substituted for  $m_{z1}$ , and  $c_y$  written in the form of a relation similar to (9.3.5):

$$c_y = c_y^\alpha \alpha_1 + c_y^{\dot{\alpha}} \dot{\alpha}_1 + (c_y^{\omega_z} + c_y^{\alpha} \bar{x}) \omega_{z1} + (c_y^{\dot{\omega}_z} + c_y^{\dot{\alpha}} \bar{x}) \dot{\omega}_{z1} \quad (9.3.6)$$

By comparing the expression obtained for  $m_z = m_{z1} + c_y \bar{x}$  with the corresponding relation (9.3.6), we find formulas for the stability derivatives relative to point  $O_1$ :

$$\left. \begin{aligned} m_z^{\alpha_1} &= m_z^\alpha - c_y^{\alpha} \bar{x}, & m_z^{\omega_{z1}} &= m_z^{\omega_z} + (m_z^\alpha - c_y^{\omega_z}) \bar{x} - c_y^{\omega_z} \bar{x}^2 \\ m_z^{\dot{\alpha}_1} &= m_z^{\dot{\alpha}} - c_y^{\dot{\alpha}} \bar{x}, & m_z^{\dot{\omega}_{z1}} &= m_z^{\dot{\omega}_z} + (m_z^{\dot{\alpha}} - c_y^{\dot{\omega}_z}) \bar{x} - c_y^{\dot{\omega}_z} \bar{x}^2 \end{aligned} \right\} \quad (9.3.7)$$

The new stability derivatives of the normal force coefficient are obtained by comparing Eq. (9.3.6) and an equation similar to (9.3.2):

$$c_y_1 = c_y^\alpha \alpha_1 + c_y^{\dot{\alpha}} \dot{\alpha}_1 + c_y^{\omega_{z1}} \omega_{z1} + c_y^{\dot{\omega}_{z1}} \dot{\omega}_{z1}$$

in which we assume that  $c_{y1} = c_y$  (because upon a change in the reduction centre the aerodynamic force does not change). The comparison yields

$$\begin{aligned} c_{y1}^{\alpha_1} &= c_y, \quad \dot{c}_{y1}^{\dot{\alpha}_1} = \dot{c}_y^{\dot{\alpha}}, \quad c_{y1}^{\omega z_1} = c_y^{\omega z} + c_y^{\alpha -} \\ c_{y1}^{\dot{\omega} z_1} &= c_{y1}^{\dot{\omega} z} + c_y^{\dot{\alpha} -} \end{aligned} \quad (9.3.8)$$

Similarly, we can convert the aerodynamic characteristics for a rear arrangement of the new reduction centre.

## 9.4. Particular Cases of Motion

### Longitudinal and Lateral Motions

To simplify our investigation of the motion of a controllable craft and facilitate the finding of the required aerodynamic characteristics, including the stability derivatives, we shall use the method of resolving the total motion into individual components. The possibility of resolution into **longitudinal and lateral motions** in principle is due to the symmetry of a craft about its longitudinal axis. The longitudinal motion (pitching motion), in turn, consists of the translational displacement of the centre of mass *in the vertical flight plane* (the trajectory differs only slightly from a plane one) and rotation about the lateral axis  $Oz$ . In such motion, good stability in roll is ensured, and variables such as  $\beta$ ,  $\gamma$ ,  $\omega_x$ , and  $\omega_y$  may be considered negligibly small (the surfaces controlling rolling and yawing are virtually not deflected).

Upon lateral motion in the direction of the axis  $Oz$ , the centre of mass moves, and the craft experiences rotation about the axes  $Ox$  and  $Oy$  (here the control surfaces function that ensure yawing and rolling motion).

When investigating longitudinal motion, we usually consider the aerodynamic coefficients in the form of the following functions:

$$\left. \begin{aligned} c_x &= c_x(M_\infty, \alpha, \delta_e), \quad c_y = c_y(M_\infty, \alpha, \delta_e) \\ c_z &= 0, \quad m_x = 0, \quad m_y = 0, \quad m_z = m_z(M_\infty, \alpha, \delta_e, \dot{\alpha}, \dot{\delta}_e) \end{aligned} \right\} \quad (9.4.1)$$

To study lateral motion, we use the coefficients in the form of

$$\left. \begin{aligned} c_y &= c_y(M_\infty, \alpha, \delta_e), \quad c_z = c_z(M_\infty, \beta, \delta_r) \\ m_x &= m_x(M_\infty, \alpha, \beta, \delta_e, \delta_r, \dot{\alpha}, \omega_x, \omega_y, \omega_z) \\ m_y &= m_y(M_\infty, \beta, \delta_r, \omega_x, \omega_y, \dot{\beta}, \dot{\delta}_r) \end{aligned} \right\} \quad (9.4.2)$$

It must be had in view that longitudinal motion is studied independently of lateral motion, whereas the latter is considered with account taken of the parameters of longitudinal motion, which are determined beforehand. Particularly, the magnitude of the control normal force  $c_u$  is found.

## Motion of the Centre of Mass and Rotation about It

The division of the total motion of a craft into these two modes is possible if we assume that the control system functions perfectly and during the entire flight ensures the equality of the moments  $M_x$ ,  $M_y$ , and  $M_z$  to zero. Such a craft and its control system are considered as *inertiafree (fast-response)*. The assumption on the absence of inertia signifies that when control surfaces are deflected, the angle of attack and the sideslip angle instantaneously (or sufficiently rapidly) take on values corresponding to a statically stable position of the craft. In these conditions, the motion of its centre of mass in the plane of flight is investigated independently. When performing such investigation, we shall write the aerodynamic coefficients in the form

$$\left. \begin{array}{l} c_x = c_x(M_\infty, \alpha, \beta, \delta_e, \delta_r), \quad c_y = c_y(M_\infty, \alpha, \delta_e) \\ c_z = c_z(M_\infty, \beta, \delta_r) \\ m_y = m_y(M_\infty, \beta, \delta_r), \quad m_z = m_z(M_\infty, \alpha, \delta_e) \end{array} \right\} \quad (9.4.3)$$

Assuming that  $m_y = m_z = 0$ , we can find the elevator and rudder angles corresponding to the required angle of attack and sideslip angle, and to the given trajectory.

The possibility of using such a method of investigation of the trajectory is based on the low sensitivity of displacement of the centre of mass to the rotation of the craft about this centre up to the instant

Table 9.4.1

when the craft occupies a position of statically stable equilibrium. This motion due to deflection of the control surfaces or random disturbances can be studied independently of the longitudinal motion of the craft. Table 9.4.1 shows the different modes of these motions and the corresponding control surface angles  $\delta_e$ ,  $\delta_r$ ,  $\delta_a$ , the angle of attack  $\alpha$ , the sideslip angle  $\beta$ , and also the angular velocities  $\Omega_x$ ,  $\Omega_y$ ,  $\Omega_z$ .

The investigation of a particular mode of motion can be simplified by excluding the influence of accelerations. This is justified in practice when the motion develops sufficiently slowly. When it is necessary to take the acceleration into account, one can introduce a correction to the aerodynamic coefficient in the form of a term equal to the product of the first stability derivative with respect to the acceleration and the relevant dimensionless acceleration.

### Pitching Motion

Of special interest is pitching motion, which is called the principal mode of motion. Longitudinal oscillations that are described quite well by a harmonic function such as (9.1.6) usually appear in this motion. According to this law, the time derivatives of the angles of attack and trajectory inclination are

$$\dot{\alpha} = A \sin p_\alpha t, \quad \dot{\vartheta} = \Omega_z = B \sin p_\vartheta t \quad (9.4.4)$$

where  $A$ ,  $B$  are the amplitudes, and  $p_\alpha$ ,  $p_\vartheta$  are the frequencies of oscillations of the corresponding derivatives.

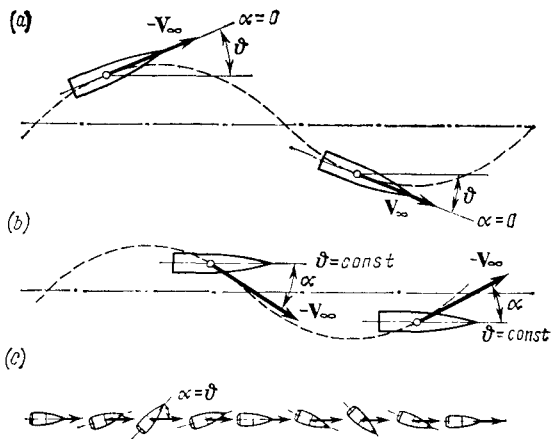
We can consider three modes of motion each of which is described by a harmonic function.

The first mode (Fig. 9.4.1a) corresponds to the condition  $\alpha = 0$ ,  $\dot{\vartheta} = \Omega_z = B \sin p_\vartheta t$ . In this mode, the axis of a body, coinciding with the direction of flight ( $\alpha = 0$ ), performs harmonic oscillations along the trajectory.

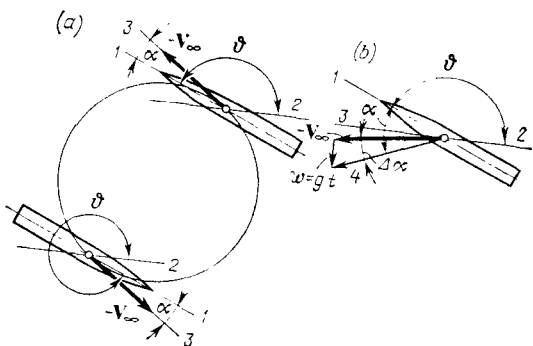
The second mode of motion (Fig. 9.4.1b) is characterized by the fact that the axis of the body retains its orientation along the trajectory so that  $\Omega_z = \dot{\vartheta} = 0$ . Here, however, the angle of attack changes to follow the harmonic change in its derivative  $\dot{\alpha}$ .

The third mode of motion (Fig. 9.4.1c) is characterized by a rectilinear trajectory with the angle between the axis of the craft and the trajectory changing sinusoidally. In this case, the angles  $\vartheta$  and  $\alpha$  are equal and coincide in phase so that  $\dot{\alpha} = \dot{\vartheta} = \Omega_z$ . Important derivatives in this motion are  $c_y^{\dot{\alpha}} + c_y^{\omega z}$  and  $m_z^{\dot{\alpha}} + m_z^{\omega z}$ .

All these three modes of motion, which are of a quite intricate nature, are encountered comparatively frequently. Two other modes

**Fig. 9.4.1**

Particular cases of motion of a craft:

a—at a zero angle of attack; b—with constant orientation of the craft ( $\theta = \text{const}$ ); c—along a straight trajectory**Fig. 9.4.2**

Modes of motion of a craft:

a—perfect loop; b—free fall

are simpler, but are encountered less frequently. Each of them allows one to understand the distinction between the modes of motion characterized by two conditions:  $\dot{\alpha} = 0$ ,  $\Omega_z \neq 0$  and  $\dot{\alpha} \neq 0$ ,  $\Omega_z = 0$ , and accordingly to gain an idea of the derivatives  $m_1^{\dot{\alpha}}$  and  $m_2^{\Omega_z}$ . The three modes of sinusoidal motions indicated above can be treated as combinations of these two modes.

The first of them (Fig. 9.4.2a) is characterized by the fact that the angle of attack between the instantaneous direction 3 of the vector

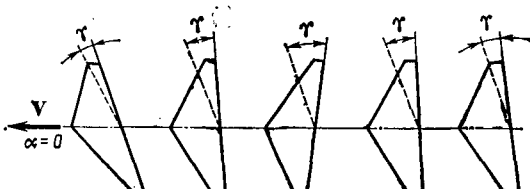


**Fig. 9.4.3**  
Banking of a craft

$-\bar{V}_\infty$  and body axis 1 does not change and, consequently, the derivative  $\dot{\alpha} = 0$ . In this motion, however, a varying angle  $\vartheta$  forms between fixed direction 2 and axis 1. Therefore  $\Omega_z = d\vartheta/dt \neq 0$ . In a particular case when  $\Omega_z = \text{const}$ , the trajectory in Fig. 9.4.2a characterizes the motion of a craft performing a perfect loop.

Figure 9.4.2b shows a second mode of motion corresponding to the conditions  $\dot{\alpha} \neq 0$  and  $\Omega_z = 0$ . This motion may occur if free fall with a velocity of  $w = gt$  (where  $g$  is the acceleration of free fall) is superposed on the longitudinal motion. Here the angle  $\vartheta$  between the fixed direction 2 and body axis 1 remains constant, while the angle  $\alpha$  changes (between the instantaneous flight direction 4 and axis 1). Consequently, the derivatives  $\dot{\vartheta} = \Omega_z = 0$  and  $\dot{\alpha} \neq 0$ ; in the given case the derivative  $\dot{\alpha} = \text{const}$ .

In a more general case (for example, in sinusoidal motions), it is necessary to use both derivatives  $\dot{m}_z^\alpha$  and  $\dot{m}_z^{\omega_z}$ . If one of the considered modes of motion dominates, only one derivative is significant, and it is exactly what should be used. Figure 9.4.3 shows a wing for which translational motion along its longitudinal axis, at a zero angle of attack, is supplemented with rotation about this axis at the angular velocity  $\Omega_x = d\gamma/dt$ . The non-zero variables  $\omega_x$  and  $\dot{\omega}_x$  correspond to this mode of motion. If the rotation about the axis  $Ox$  is steady, then  $\omega_x \neq 0$ , while the derivative  $\dot{\omega}_x = 0$ .

## 9.5. Dynamic Stability

### Definition

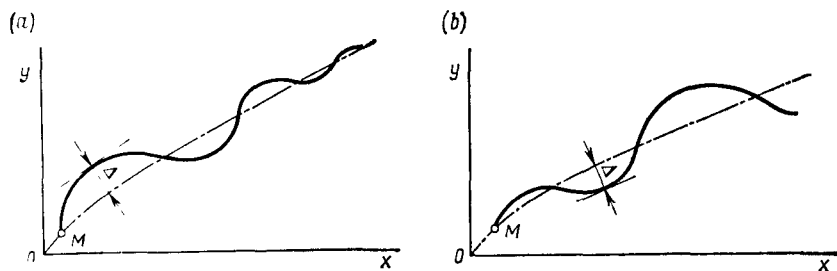
An analysis of the derivatives of the aerodynamic moments with respect to  $\alpha$  or  $\beta$  allows us to establish the kind of static stability. This analysis is not sufficient for estimating the flight performance of a moving body, however, because it does not allow one to establish the nature of the body's motion after the removal of a disturbance and to find the variables determining this motion.

Actually, if we know, for example, that the derivative  $m_z^\alpha$  is negative and that, consequently, the centre of pressure is behind the centre of mass, we can arrive at a conclusion only on longitudinal static stability. But we cannot establish, for example, the amplitude of oscillations of the angle of attack at a certain value of the initial disturbance and how it changes in time. These and other problems are studied by the theory of the **dynamic stability of a craft or of the stability of its motion**. This theory makes it possible, naturally, to study not only the oscillations of a craft, but also the general case of the motion of a craft along its trajectory and the stability of this motion. The theory of dynamic stability uses the results of aerodynamic investigations obtained in conditions of unsteady flow in which, unlike static conditions, a body experiences the action of additional time-dependent aerodynamic loads.

The concept of dynamic stability is associated with two modes of motion of a craft, namely, undisturbed (basic) and disturbed. Motion is said to be **undisturbed (basic)** if it occurs along a definite trajectory at a velocity varying according to a given law at standard parameters of the atmosphere and known initial parameters of this motion. This theoretical trajectory described by specific flight equations with nominal parameters of the craft and control system is also said to be undisturbed. Owing to random disturbing factors (gusts of wind, interference in the control system, failure of the initial conditions to correspond to the preset ones, deviation of the actual parameters of a craft and its control system from the nominal ones, deviation of the actual parameters of the atmosphere from the standard ones), and also because of disturbances due to deflection of the control surfaces, the basic motion may be violated. After removal of the random disturbances, a body moves during a certain time according to a law differing from the initial one. This motion is called **disturbed**.

If the forces or moments produced upon a deviation from undisturbed motion are such that they return the craft to its initial trajectory, the motion is **stable**, otherwise it is **unstable**. Figure 9.5.1a shows a stable flight in which a craft after leaving its trajectory at point  $M$  because of a disturbance continues its motion with a constantly diminishing deviation from the initial direction of flight; Fig. 9.5.1b shows an unstable flight characterized by an increasing deviation.

In the general case, the motion of a craft is determined by kinematic parameters that are functions of time such as the velocity  $V_\infty(t)$ , the angle of attack  $\alpha(t)$ , the sideslip angle  $\beta(t)$ , the components of the angular velocity [ $\Omega_x(t)$ ,  $\Omega_y(t)$ ,  $\Omega_z(t)$ ], and the pitching, yawing (course angle) and rolling angles [ $\vartheta(t)$ ,  $\psi(t)$ , and  $\gamma(t)$ ].

**Fig. 9.5.1**

Modes of motion of a craft:

1—stable; 2—unstable;  $\Delta$ —amplitude of oscillations

Let us assume that the values of the same variables  $V_\infty^0(t)$ ,  $\alpha^0(t)$  etc. correspond to a given *undisturbed motion*. If at sufficiently small initial deviations (at the initial disturbances)  $\Delta V_\infty^0$ ,  $\Delta \alpha^0$ , ... (here  $\Delta V_\infty^0 = V_\infty^0 - V_\infty^0$ ,  $\Delta \alpha^0 = \alpha^0 - \alpha^0$ , ...) the subsequent deviations  $\Delta V_\infty = V_\infty - V_\infty^0$ ,  $\Delta \alpha = \alpha - \alpha^0$  do not exceed certain preset values, the motion is **stable**. If these deviations increase unlimitedly, the motion is **unstable**. A flight may occur when the deviations neither attenuate nor increase: here **neutral stability** of motion is observed.

Such a definition of stability is associated with investigation of the response of a craft to disturbing actions provided that these actions impart initial deviations to the variables of the undisturbed flow, while the following motion is considered already without disturbances. In such motion, the control surfaces remain fixed. This mode of disturbed motion due to initial disturbances of the variables is called **proper or free**. The proper motion of a craft can conditionally be considered as a new undisturbed motion.

The stability of free motion of a craft can be investigated by analysing the differential equations describing this motion. If the lateral variables and the time derivatives of the longitudinal variables in the undisturbed flow are not great, we may consider longitudinal and lateral motions independently and, consequently, study the stability of each of them separately. When the nature of motion changes abruptly, for example, when a manoeuvre is executed, such a resolution of motion into its components is not justified, and the solution of the system of equations of longitudinal and lateral motion must be considered jointly. This solution makes it possible to establish the nature and influence of the aerodynamic coefficients on stability in the most general form.

If the intensity of action of random factors is not great, the disturbed trajectory differs only slightly from the undisturbed one. This allows one to use the method of small perturbations that is based on linearized equations.

### Stability Characteristics

Let us consider the characteristics of dynamic stability, and also the role and place of the aerodynamic coefficients (stability derivatives) in investigating the dynamics of a flight using the example of translational motion of a craft also performing rotation (oscillations) about the axis  $Oz$  (Fig. 9.4.1c).

We shall write the equation of such disturbed motion in the form

$$\ddot{\alpha} + (a_1 + a_2) \dot{\alpha} + a_3 \alpha = 0 \quad (9.5.1)$$

where

$$\left. \begin{aligned} a_1 &= -m_z^{\Omega z} q_{\infty} Sl/J_z, & a_2 &= -m_z^{\dot{\alpha}} q_{\infty} Sl/J_z \\ a_3 &= -m_z^{\alpha} q_{\infty} Sl/J_z \end{aligned} \right\} \quad (9.5.2)$$

Here  $J_z$  is the principal central moment of inertia of the craft about the axis  $Oz$  that is one of the principal central axes.

Taking into account that  $m_z^{\Omega z} = m_z^{\dot{\alpha}}$ , we obtain for the sum of the coefficients

$$a_1 + a_2 = -2m_z^{\dot{\alpha}} q_{\infty} Sl/J_z \quad (9.5.3)$$

With a view to the value of the coefficient  $a_3$  (9.5.1) can be written as

$$\ddot{\alpha} J_z / (q_{\infty} Sl) - 2\dot{\alpha} m_z^{\dot{\alpha}} - \alpha m_z^{\alpha} = 0 \quad (9.5.4)$$

Assuming that the coefficients  $a_i$  are constant, we find a solution of Eq. (9.5.4) in the following form:

$$\alpha = C_1 e^{p_1 t} + C_2 e^{p_2 t} \quad (9.5.5)$$

Here  $p_1$  and  $p_2$  are the roots of the characteristic equation  $p^2 + (a_1 + a_2)p + a_3 = 0$  determined by the formula

$$p_{1,2} = -0.5(a_1 + a_2) \pm \sqrt{0.25(a_1 + a_2)^2 - a_3} \quad (9.5.6)$$

We find the constants  $C_1$  and  $C_2$  from the conditions that can be determined by the derivative  $\dot{\alpha} = \dot{\alpha}_0$  and the zero disturbance  $\alpha = 0$  at the instant  $t = 0$ . For these conditions, the constants are

$$C_1 = C_2 = 0.5\dot{\alpha}_0 [0.25(a_1 + a_2)^2 - a_3]^{-1/2}$$

and the solution becomes

$$\alpha = 0.5\dot{\alpha}_0 b^{-1} e^{-\lambda_1 t} (e^{bt} - e^{-bt}) \quad (9.5.7)$$

where  $b = \sqrt{\lambda_1^2 - a_3}$ ,  $\lambda = 0.5(a_1 + a_2)$ .

Let us consider static stability when the derivative  $m_z^\alpha < 0$  and, consequently,  $a_3 > 0$ . If we have in view here that in real conditions the damping moment is considerably smaller than the stabilizing one and that therefore  $|a_3| > \lambda_1^2$ , we obtain the relation

$$\alpha = \dot{\alpha}_0 \bar{b}^{-1} e^{-\lambda_1 t} \sin \bar{b} t \quad (9.5.8)$$

in which  $\bar{b} = \sqrt{|a_3| - \lambda_1^2}$ .

Examination of (9.5.8) reveals that the change in the angle of attack has the nature of periodic oscillations. Since the quantity  $\lambda_1$  is always positive, these oscillations are damped ones; consequently, we have to do with **oscillatory stability**.

Let us consider the characteristics of this stability. The **period of the oscillations** is

$$T = 2\pi (|m_z^\alpha| q_\infty S l J_z^{-1} - \lambda_1^2)^{-1/2} \quad (9.5.9)$$

and their **frequency** is

$$\omega = 2\pi/T = (|m_z^\alpha| q_\infty S l J_z^{-1} - \lambda_1^2)^{1/2} \quad (9.5.10)$$

The oscillation frequency is influenced mainly by the degree of static stability, whereas the influence of damping is not great. The nature of action of these factors is different. An increase in the degree of static stability leads to a higher frequency, while an increase in damping, conversely, leads to its diminishing somewhat.

The **logarithmic decrement** is

$$\varepsilon = \lambda_1 T \quad (9.5.11)$$

where

$$\lambda_1 = |m_z^\alpha| q_\infty S l J_z^{-1} \quad (9.5.12)$$

The larger the coefficient  $m_z^\alpha$  (or  $m_z^{\alpha z}$ ), the greater is the logarithmic decrement and the more rapidly do the oscillations damp in time.

One of the important characteristics of oscillatory motion is the time to damp to half amplitude:

$$t_2 = \lambda_1^{-1} \ln 2 \quad (9.5.13)$$

When investigating oscillatory stability, the quantity  $\lambda_1$  can be considered as an independent characteristic of this stability called the **damping coefficient**. A glance at (9.5.12) and (9.5.13) reveals that its magnitude does not depend on the degree of static stability  $m_z^\alpha$ .

Let us consider the **wavelength of oscillations**

$$\lambda = TV_\infty = 2\pi V_\infty / \sqrt{|a_3| - \lambda_1^2} \quad (9.5.14)$$

In practice, it is expedient to ensure aerodynamic properties of a moving body such that the damping coefficient is sufficiently great because here the time  $t_2$  is short, although the wavelength grows somewhat, which is not desirable. Good practice dictates decreasing of this length. To do this, it is necessary to increase the stabilizing moment, which, in turn, leads to such a positive phenomenon as a decrease in the amplitude of oscillation.

In the case being considered, a body has static stability that also produces in it longitudinal oscillatory stability. A similar analysis can be performed for the case when such static stability is absent, i.e. when the derivative  $m_z^\alpha > 0$ . Solution of (9.5.4) yields a relation for  $\alpha$  indicating the undamping aperiodic nature of motion. Hence, static instability also gives rise to instability of motion.

In this case, agreement can be observed between static and dynamic stability or instability. Such agreement is not obligatory, however, for the general case of motion of a craft. One may have a statically stable craft that, however, does not have dynamic stability and in its tendency to the position of equilibrium will perform oscillations with an increasing amplitude. Such cases are observed in practice in some aircraft at low-speed flight, and also in flying wings with a small sweep of the leading edge.

It must be noted that the overwhelming majority of aircraft owing to special devices have static stability, i.e. the ability to respond to disturbances so as to reduce their magnitude at the initial instant. This property is of major practical significance regardless of how an aircraft behaves in the process of disturbed motion. Free development of the disturbances is usually attended by deflection of the control surfaces to return the craft to its preset flight conditions. The use of these control surfaces is a necessary condition for ensuring the preset motion of a statically unstable (with fixed control surfaces) aircraft.

The concept of stability presumes the existence not of two separate kinds of stability—static and dynamic, but of a single stability reflecting the real motion of a craft in time and its ability to retain the initial flight conditions. Since the dynamic coefficients of the equations depend on the parameters of the undisturbed flight, the same aircraft can have different dynamic properties along a trajectory, for example, its motion may be stable on some sections of the trajectory and unstable on others.

Unsteady motion is described by equations whose dynamic coefficients depend on the design of the craft. Unlike craft of the aeroplane type, such coefficients for bodies without an empennage, or with an only slightly developed empennage (fin assembly), correspond to unstable motion characterized by slow damping of the oscillations. This requires the use of means of stabilization that ensure greater damping.

## 9.6. Basic Relations for Unsteady Flow

### Aerodynamic Coefficients

Let us consider a flat lifting surface moving translationally at a constant velocity in the absence of sideslip ( $\beta = 0$ ) and of an angular velocity  $\Omega_y$ . The projection of the area of an aircraft or its separate elements (wings, fuselage) onto the plane  $xOz$  may be such a surface. The aerodynamic stability derivatives obtained for this surface are very close to those that would have been found for real bodies in an unsteady flow.

The normal aerodynamic force, and also the pitching and rolling moments are due to the pressure difference  $\Delta p = p_b - p_u$  on the bottom and upper sides of the lifting surface (Fig. 9.6.1) and are determined by the formulas

$$Y = \iint_{(S)} \Delta p \, dx \, dz, \quad M_z = \iint_{(S)} \Delta p x \, dx \, dz,$$

$$M_x = - \iint_{(S)} \Delta p z \, dx \, dz \quad (9.6.1)$$

in which integration is performed over the area  $S$  of the lifting surface.

Let us introduce the pressure coefficient  $\bar{p} = (p - p_\infty)/q_\infty = 2(p - p_\infty)/(\rho_\infty V_\infty^2)$  and the dimensionless coordinates

$$\xi = x/x_k \text{ and } \zeta = z/x_k \quad (9.6.2)$$

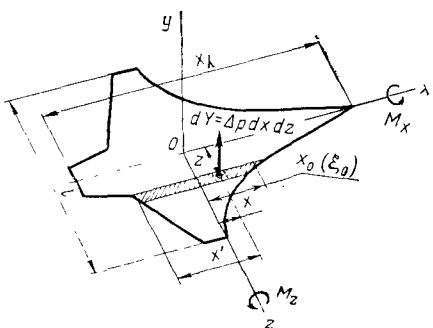
related to the length  $x_k$  of the lifting surface.

Now we obtain the following relations for the force and moment coefficients at any unsteady motion of a lifting surface with the dimensions  $l$ :

$$c_y = \frac{Y}{q_\infty S} = \frac{2x_k^2}{S} \left\{ \int_0^{l/(2x_k)} \int_{\xi_0}^{\xi_1} \Delta \bar{p} d\xi d\zeta \right\}$$

$$m_z = \frac{M_z}{q_\infty S x_k} = \frac{2x_k^2}{S} \left\{ \int_0^{l/(2x_k)} \int_{\xi_0}^{\xi_1} \Delta \bar{p} \xi d\xi d\zeta \right\}$$

$$m_x = \frac{M_x}{q_\infty S x_k} = - \frac{2x_k^2}{S} \left\{ \int_0^{l/(2x_k)} \int_{\xi_0}^{\xi_1} \Delta \bar{p} \zeta d\xi d\zeta \right\} \quad (9.6.3)$$

**Fig. 9.6.1**

To the determination of the aerodynamic coefficients for a lifting surface

Here  $\xi_0$  and  $\xi_1$  are the dimensionless coordinates of the leading and trailing edges of the lifting surface, respectively.

For a non-standard coordinate system in which the axis  $Ox$  is directed from the leading edge to the trailing one, the signs in formulas (9.6.3) should be reversed.

Let us find relations for the aerodynamic characteristics of the lifting surface cross sections. For the normal force, longitudinal moment, and rolling moment of a section, we have, respectively

$$\begin{aligned} dY &= \int_{x_0}^{x_1} \Delta p \, dx \, dz, \quad dM_z = \int_{x_0}^{x_1} \Delta p x \, dx \, dz, \\ dM_x &= - \int_{x_0}^{x_1} \Delta p z \, dx \, dz \end{aligned} \quad (9.6.4)$$

The corresponding coefficients are as follows:

$$\left. \begin{aligned} c_y' &= \frac{dY}{q_\infty x' dz} = \frac{x_h}{x'^2} \int_{\xi_0}^{\xi_1} \bar{\Delta p} \, d\xi \\ m_z' &= \frac{dM_z}{q_\infty x'^2 dz} = \frac{x^2 k}{x'^2} \int_{\xi_0}^{\xi_1} \bar{\Delta p} \xi \, d\xi \\ m_x' &= \frac{dM_x}{q_\infty x'^2 dz} = - \frac{x_h^2}{x'^2} \int_{\xi_0}^{\xi_1} \bar{\Delta p} \zeta \, d\xi \end{aligned} \right\} \quad (9.6.5)$$

where  $x'$  is a chord of a lifting surface element in the section  $z = \text{const}$  being considered.

We calculate the integral in (9.6.5) over a given section from the trailing ( $\xi_1 = x_1/x_h$ ) to the leading ( $\xi_0 = x_0/x_h$ ) edges. We can

represent the difference of the pressure coefficients in (9.6.3) and (9.6.5) on the basis of the Taylor formula [see (9.1.4)] in the form of a series expansion in terms of the kinematic variables:

$$\left. \begin{aligned} q_1 &= \alpha(\tau), \quad q_2 = \omega_x(\tau) = \Omega_x(t) l/V_\infty \\ q_3 &= \omega_z(\tau) = \Omega_z(t) l/V_\infty, \quad \dot{q}_1 = \dot{\alpha} = d\alpha/d\tau, \quad \dot{q}_2 = \dot{\omega}_x = d\omega_x/d\tau \\ \dot{q}_3 &= \dot{\omega}_z = d\omega_z/d\tau \quad \tau = V_\infty t/l \end{aligned} \right\} \quad (9.6.6)$$

(here  $l$  is the characteristic geometric dimension).

This expansion has the following form:

$$\Delta \bar{p} = \sum_{i=1}^3 (p^{q_i} q_i + p^{\dot{q}_i} \dot{q}_i) = p^\alpha \alpha + p^{\dot{\alpha}} \dot{\alpha} + p^{\omega_x} \omega_x + p^{\dot{\omega}_x} \dot{\omega}_x + p^{\omega_z} \omega_z + p^{\dot{\omega}_z} \dot{\omega}_z \quad (9.6.7)$$

where  $p^\alpha = \Delta p^\alpha$ ,  $p^{\dot{\alpha}} = \Delta p^{\dot{\alpha}}$ , etc. are the derivatives of the difference of the pressure coefficients.

By (9.6.7), the aerodynamic coefficients can be written as

$$\left. \begin{aligned} c_y &= \sum_{i=1}^3 (c_y^{q_i} q_i + c_y^{\dot{q}_i} \dot{q}_i) \\ m_z &= \sum_{i=1}^3 (m_z^{q_i} q_i + m_z^{\dot{q}_i} \dot{q}_i) \\ m_x &= \sum_{i=1}^3 (m_x^{q_i} q_i + m_x^{\dot{q}_i} \dot{q}_i) \end{aligned} \right\} \quad (9.6.8)$$

In formulas (9.6.8) for the non-stationary aerodynamic coefficients expressed in the form of series, the values of the stability derivatives that are coefficients of  $q_i$  and  $\dot{q}_i$  must correspond to expansion (9.6.7) for the quantity  $\Delta p$ . Accordingly, the relevant derivatives take on the following values:

$$\begin{aligned} c_y^{q_i} &= c_y^\alpha, \quad c_y^{\omega_x}, \quad c_y^{\omega_z}; & c_y^{\dot{q}_i} &= c_y^{\dot{\alpha}}, \quad c_y^{\dot{\omega}_x}, \quad c_y^{\dot{\omega}_z} \\ m_z^{q_i} &= m_z^\alpha, \quad m_z^{\omega_x}; \quad m_z^{\omega_z}; & m_z^{\dot{q}_i} &= m_z^{\dot{\alpha}}, \quad m_z^{\dot{\omega}_x}, \quad m_z^{\dot{\omega}_z} \\ m_x^{q_i} &= m_x^\alpha, \quad m_x^{\omega_x}; \quad m_x^{\omega_z}; & m_x^{\dot{q}_i} &= m_x^{\dot{\alpha}}, \quad m_x^{\dot{\omega}_x}, \quad m_x^{\dot{\omega}_z} \end{aligned}$$

Assuming that the craft length  $x_k$  has been adopted as the characteristic geometric dimension, we obtain from (9.6.3), (9.6.7) and (9.6.8) expressions for the derivatives of the aerodynamic coefficients in terms of the derivatives of the difference of the pressure coeffi-

cients:

$$\left. \begin{aligned} c_y^{q_i} &= \frac{2x_h^2}{S} \int_0^{l/(2x_h)} \int_{\xi_1}^{\xi_0} p^{q_i} d\xi d\zeta, \quad c_y^{\dot{q}_i} = \frac{2x_h^2}{S} \int_0^{l/(2x_h)} \int_{\xi_1}^{\xi_0} p^{\dot{q}_i} d\xi d\zeta \\ m_x^{q_i} &= -\frac{2x_h^2}{S} \int_0^{l/(2x_h)} \int_{\xi_1}^{\xi_0} p^{q_i} \xi d\xi d\zeta, \\ m_x^{\dot{q}_i} &= -\frac{2x_h^2}{S} \int_0^{l/(2x_h)} \int_{\xi_1}^{\xi_0} p^{\dot{q}_i} \xi d\xi d\zeta \\ m_z^{q_i} &= \frac{2x_h^2}{S} \int_0^{l/(2x_h)} \int_{\xi_1}^{\xi_0} p^{q_i} \xi d\xi d\zeta, \quad m_z^{\dot{q}_i} = \frac{2x_h^2}{S} \int_0^{l/(2x_h)} \int_{\xi_1}^{\xi_0} p^{\dot{q}_i} \xi d\xi d\zeta \end{aligned} \right\} \quad (9.6.9)$$

The above expressions are linear relations between the aerodynamic derivatives and the dimensionless kinematic variables  $q_i$  and  $\dot{q}_i$  that ensure quite reliable results provided that the values of these variables are small in comparison with unity.

In linearized problems on the unsteady flow over lifting surfaces, such relations are exact for a harmonic law of the change in the kinematic variables (see [4, 19]).

Let us consider some features of the stability derivatives. Since we are dealing with motion in the absence of sideslip and an angular velocity about the axis  $Oy$  ( $\beta = 0$ ,  $\Omega_y = 0$ ), here the derivatives of the aerodynamic coefficients with respect to the parameters  $\beta$  and  $\Omega_y$  evidently equal zero. In addition, we have excluded the coefficients of the longitudinal and lateral forces ( $c_x$ ,  $c_z$ ) and also the yawing moment coefficient  $m_y$  from our analysis because independent investigations are devoted to them. It must be had in view here that when analysing the stability of a craft, these quantities are of a smaller practical significance.

For a lifting surface that is symmetric about plane  $xOy$  and moves translationally in the absence of rotation ( $\Omega_x = 0$ ), the pressure is distributed symmetrically; therefore, the corresponding derivatives equal zero:  $m_x^{q_i} = 0$ ,  $m_x^{\dot{q}_i} = 0$  ( $i = 1, 3$ ).

With rotation about the axis  $Ox$ , the pressure is distributed asymmetrically about symmetry plane  $xOy$ , hence the aerodynamic loads produced by the angular velocity  $\omega_x$  are also asymmetric, and, consequently, the following stability derivatives equal zero in this case:

$$c_y^{\omega_x} = 0, \quad c_y^{\dot{\omega}_x} = 0, \quad m_z^{\omega_x} = 0, \quad m_z^{\dot{\omega}_x} = 0$$

**Cauchy-Lagrange Integral**

Let us consider the basic expression of the theory of unsteady flow relating the parameters of the disturbed flow (the velocity, pressure, density) and the potential function  $\Phi$ . For such a flow,  $\operatorname{curl} \mathbf{V} = 0$ , and, consequently, the local velocity vector can be written in terms of the potential function as  $\mathbf{V} = \operatorname{grad} \Phi$ . With this in view, the equation of motion (3.1.22'') can be given thus

$$\frac{\partial \operatorname{grad} \Phi}{\partial t} + \operatorname{grad} \frac{V^2}{2} = -\frac{1}{\rho} \operatorname{grad} p \quad (9.6.10)$$

Considering that the gas flowing over a body is a **barotropic fluid** whose density depends only on the pressure, i.e.  $\rho = \rho(p)$ , we can introduce a function  $P$ , assuming that

$$P = \int dp/\rho(p) \quad (9.6.11)$$

Accordingly,

$$(1/\rho) \operatorname{grad} p = \operatorname{grad} P \quad (9.6.12)$$

We can therefore write (9.6.10) as

$$\operatorname{grad} (\partial \Phi / \partial t + V^2/2 + P) = 0$$

Hence we obtain an equation suitable for the entire space of a disturbed flow near a lifting surface including the vortex wake:

$$\partial \Phi / \partial t + V^2/2 + P = F(t) \quad (9.6.13)$$

where  $F(t)$  is an arbitrary function of time determined with the aid of the undisturbed flow variables for which  $\partial \Phi / \partial t = 0$ .

Assuming that  $V^2 = V_\infty^2$  and  $P = P_\infty$ , we find

$$F(t) = V_\infty^2/2 + P_\infty$$

Consequently,

$$\partial \Phi / \partial t + V^2/2 + P = V_\infty^2/2 + P_\infty \quad (9.6.14)$$

This equation is known as the **Cauchy-Lagrange integral**. For an incompressible medium, we have  $\rho_\infty = \rho = \text{const}$ . Therefore,  $P = p/\rho_\infty$  and  $P_\infty = p_\infty/\rho_\infty$ . Hence,

$$\partial \Phi / \partial t + V^2/2 + p/\rho_\infty = V_\infty^2/2 + p_\infty/\rho_\infty \quad (9.6.15)$$

For an isentropic flow of a compressible gas in the region of a continuous change in the thermodynamic properties, we have  $p/\rho^k = p_\infty/\rho_\infty^k$  (where  $k = c_p/c_v = \text{const}$  is the adiabatic exponent). As a result, we obtain

$$P = \frac{k}{k-1} \cdot \frac{p}{\rho}, \quad P_\infty = \frac{k}{k-1} \cdot \frac{p_\infty}{\rho_\infty}$$

Therefore, the Cauchy-Lagrange integral will acquire the following form:

$$\frac{\partial \Phi}{\partial t} + \frac{V^2}{2} + \frac{k}{k-1} \cdot \frac{p}{\rho} = \frac{V_\infty^2}{2} + \frac{k}{k-1} \cdot \frac{p_\infty}{\rho_\infty} \quad (9.6.16)$$

Assuming that the flow over a body is nearly uniform, we linearize Eq. (9.6.16). The square of the velocity is

$$V^2 = V_x^2 + V_y^2 + V_z^2 = (V_\infty + u)^2 + v^2 + w^2$$

where  $u$ ,  $v$ , and  $w$  are infinitesimal components of the disturbed velocity ( $u \ll V_\infty$ ,  $v \ll V_\infty$ , and  $w \ll V_\infty$ ). Excluding the second-order infinitesimals, we obtain  $V^2 = V_\infty^2 + 2V_\infty u$ . In a nearly uniform flow, the excess pressure  $p - p_\infty = p'$  of the gas at any point in space is also small. With this in view, we find the linearized value of the difference of the functions  $P - P_\infty$ . For an isentropic flow, this difference is

$$P - P_\infty = [k/(k-1)] (p/\rho - p_\infty/\rho_\infty)$$

We determine the ratio  $p/\rho$  from the adiabat equation  $p/\rho^k = p_\infty/\rho_\infty^k$ , in accordance with which

$$p/\rho = (p_\infty/\rho_\infty) (p/p_\infty)^{(k-1)/k}$$

Introducing  $p = p_\infty + p'$  into this expression, we obtain

$$p/\rho = (p_\infty/\rho_\infty) (1 + p'/p_\infty)^{(k-1)/k}$$

Expanding this expression into a binomial series, we find with an accuracy within linear terms that

$$\frac{p}{\rho} = \frac{p_\infty}{\rho_\infty} \left( 1 + \frac{k-1}{k} \frac{p'}{p_\infty} \right)$$

Accordingly,

$$P - P_\infty = p'/\rho_\infty = (p - p_\infty)/\rho_\infty \quad (9.6.17)$$

Hence, a linearized expression of the Cauchy-Lagrange integral suitable for investigating nearly uniform unsteady flows has the form

$$p - p_\infty = -\rho_\infty (V_\infty \partial \varphi / \partial x + \partial \varphi / \partial t) \quad (9.6.18)$$

where  $\varphi = \Phi - \Phi_\infty$  is the additional disturbance potential ( $\Phi_\infty$  is the velocity potential of the undisturbed flow).

In the above form, the Cauchy-Lagrange integral holds both for a compressible and an incompressible fluid. Equation (9.6.18) has been obtained for a coordinate system whose axis  $Ox$  is oriented toward the trailing edge. If the axis  $Ox$  is oriented in the opposite direction, the sign of the derivative with respect to  $x$  has to be reversed:

$$p - p_\infty = \rho_\infty (V_\infty \partial \varphi / \partial x - \partial \varphi / \partial t) \quad (9.6.18')$$

Let us introduce the pressure coefficient  $\bar{p}$ , the difference of its values for the bottom and upper sides  $\Delta\bar{p}$ , the dimensionless potential  $\bar{\varphi}$ , and also the relative coordinates and time:

$$\left. \begin{aligned} \bar{p} &= (p - p_\infty)/q_\infty, \quad \Delta\bar{p} = \bar{p}_b - \bar{p}_u \\ \xi &= x/x_k, \quad \eta = y/x_k, \quad \zeta = z/x_k, \quad \tau = V_\infty t/x_k \\ \varphi(x, y, z, t) &= V_\infty x_k \bar{\varphi}(\xi, \eta, \zeta, \tau) \end{aligned} \right\} \quad (9.6.19)$$

When these dimensionless quantities are taken into account, the Cauchy-Lagrange integral becomes

$$\bar{p} = -2 (\partial\bar{\varphi}/\partial\xi + \partial\bar{\varphi}/\partial\tau) \quad (9.6.20)$$

Having in view that from considerations of symmetry, the velocity potentials on the upper and bottom sides are identical in magnitude, but opposite in sign, i.e.  $\varphi(x, y, z, t) = -\varphi(x, -y, z, t)$ , we obtain the following formula for  $\Delta p$ :

$$\Delta\bar{p} = \bar{p}_b - \bar{p}_u = -4 (\partial\bar{\varphi}/\partial\xi + \partial\bar{\varphi}/\partial\tau) \quad (9.6.21)$$

Let us represent the expressions for  $\dot{\bar{\varphi}}$  and  $\ddot{\bar{\varphi}}$  in the form of linear dependences on  $q_i$  and  $\dot{q}_i$ :

$$\dot{\bar{\varphi}} = \sum_{i=1}^3 (\bar{\varphi}^{q_i} q_i + \bar{\varphi}^{\dot{q}_i} \dot{q}_i); \quad \ddot{\bar{\varphi}} = \sum_{i=1}^3 (p^{q_i} q_i + p^{\dot{q}_i} \dot{q}_i) \quad (9.6.22)$$

We shall insert these relations into (9.6.21) with a view to the aerodynamic coefficients not depending on the time:

$$\begin{aligned} \sum_{i=1}^3 (p^{q_i} q_i + p^{\dot{q}_i} \dot{q}_i) &= -4 \left[ \sum_{i=1}^3 \left( \frac{\partial \bar{\varphi}^{q_i}}{\partial \xi} q_i + \frac{\partial \bar{\varphi}^{\dot{q}_i}}{\partial \xi} \dot{q}_i \right) \right. \\ &\quad \left. + \sum_i \left( \bar{\varphi}^{q_i} \dot{q}_i + \bar{\varphi}^{\dot{q}_i} \frac{\partial \dot{q}_i}{\partial \tau} \right) \right] \end{aligned} \quad (9.6.23)$$

For harmonic time dependences of the kinematic variables ( $q_i = q_i^* \cos p_i t$ ), the derivative

$$\partial \dot{q}_i / \partial \tau = \ddot{q}_i = -(p_i^*)^2 q_i$$

where  $p_i^* = p_i x_k / V_\infty$  is the Strouhal number ( $i = 1, 2, 3$ ).

With a view to the obtained value for  $\dot{q}_i$ , we find the following expressions for the derivatives of the difference of the pressure coefficients from (9.6.23):

$$p^{q_i} = -4 [\partial \bar{\varphi}^{q_i} / \partial \xi + (p_i^*)^2 \bar{\varphi}^{\dot{q}_i}]; \quad p^{\dot{q}_i} = -4 (\partial \bar{\varphi}^{\dot{q}_i} / \partial \xi + \bar{\varphi}^{q_i}) \quad (9.6.24)$$

In accordance with the above relations, the values of  $p^{qi}$  and  $p^{\dot{q}_i}$  are determined by the derivatives of the dimensionless potential function with respect to the relevant kinematic parameters.

### Wave Equation

Let us obtain an equation which the velocity potential  $\varphi$  satisfies. For this purpose, we shall transform the continuity equation (2.4.2) with account taken of the expressions

$$\begin{aligned}\frac{\partial \rho}{\partial x} &= \frac{1}{a^2} \cdot \frac{\partial p}{\partial x}; & \frac{\partial \rho}{\partial y} &= \frac{1}{a^2} \cdot \frac{\partial p}{\partial y}; & \frac{\partial \rho}{\partial z} &= \frac{1}{a^2} \cdot \frac{\partial p}{\partial z} \\ \frac{\partial \rho}{\partial t} &= \frac{1}{a^2} \cdot \frac{\partial p}{\partial t}\end{aligned}\quad (9.6.25)$$

These expressions relate to a barotropic fluid for which the density is a function of the pressure [ $\rho = \rho(p)$ ], and the square of the speed of sound  $a^2 = dp/d\rho$ . By (9.6.25), the continuity equation becomes

$$\begin{aligned}\frac{1}{\rho} \cdot \frac{\partial p}{\partial t} + a^2 \left( \frac{\partial V_x}{\partial x} + \frac{\partial V_y}{\partial y} + \frac{\partial V_z}{\partial z} \right) + \frac{V_x}{\rho} \cdot \frac{\partial p}{\partial x} \\ + \frac{V_y}{\rho} \cdot \frac{\partial p}{\partial y} + \frac{V_z}{\rho} \cdot \frac{\partial p}{\partial z} = 0\end{aligned}\quad (9.6.26)$$

Let us exclude the dynamic variables from this equation, retaining only the kinematic ones. To do this, we shall use the Cauchy-Lagrange integral (9.6.18') from which we shall find expressions for the pressure derivatives with respect to the corresponding coordinates  $x, y, z$ , and also the time  $t$  related to the density:

$$(1/\rho) \frac{\partial p}{\partial x}, \quad (1/\rho) \frac{\partial p}{\partial y}, \quad (1/\rho) \frac{\partial p}{\partial z}$$

For this purpose, we shall differentiate (9.6.18) consecutively with respect to  $x, y, z$ , and  $t$ :

$$\left. \begin{aligned}\frac{1}{\rho} \cdot \frac{\partial p}{\partial x} &= \frac{\rho_\infty}{\rho} \left[ V_\infty \frac{\partial^2 \varphi}{\partial x^2} - \frac{\partial^2 \varphi}{\partial x \partial t} \right] \\ \frac{1}{\rho} \cdot \frac{\partial p}{\partial y} &= \frac{\rho_\infty}{\rho} \left( V_\infty \frac{\partial^2 \varphi}{\partial x \partial y} - \frac{\partial^2 \varphi}{\partial y \partial t} \right) \\ \frac{1}{\rho} \cdot \frac{\partial p}{\partial z} &= \frac{\rho_\infty}{\rho} \left( V_\infty \frac{\partial \varphi}{\partial x \partial t} - \frac{\partial^2 \varphi}{\partial z \partial t} \right) \\ \frac{1}{\rho} \cdot \frac{\partial p}{\partial t} &= \frac{\rho_\infty}{\rho} \left( V_\infty \frac{\partial^2 \varphi}{\partial x \partial t} - \frac{\partial^2 \varphi}{\partial t^2} \right)\end{aligned}\right\} \quad (9.6.27)$$

We shall write the relation for the square of the speed of sound  $a^2$  in a linearized flow on the basis of the Cauchy-Lagrange integral. Since

$$P - P_\infty = \frac{k}{k-1} \left( \frac{p}{\rho} - \frac{p_\infty}{\rho_\infty} \right) = \frac{1}{k-1} (a^2 - a_\infty^2)$$

then with a view to (9.6.17) and (9.6.18'), we have

$$a^2 = a_\infty^2 + (k - 1) (V_\infty \partial\varphi/\partial x - \partial\varphi/\partial t) \quad (9.6.28)$$

We can represent the velocity components in (9.6.26) in the form

$$V_x = V_\infty + \partial\varphi/\partial x, \quad V_y = \partial\varphi/\partial y, \quad V_z = \partial\varphi/\partial z \quad (9.6.29)$$

Let us introduce (9.6.27)-(9.6.29) into continuity equation (9.6.26). Disregarding second-order infinitesimals and assuming that the density ratio  $\rho_\infty/\rho \approx 1$ , we obtain

$$(1 - M_\infty^2) \frac{\partial^2 \varphi}{\partial x^2} + \frac{\partial^2 \varphi}{\partial y^2} + \frac{\partial^2 \varphi}{\partial z^2} + \frac{2M_\infty}{a_\infty} \cdot \frac{\partial^2 \varphi}{\partial x \partial t} - \frac{1}{a_\infty^2} \cdot \frac{\partial^2 \varphi}{\partial t^2} = 0 \quad (9.6.30)$$

where  $M_\infty = V_\infty/a_\infty$  is the Mach number for an undisturbed flow. The obtained equation is called the wave one. It satisfies the velocity potential  $\varphi$  of an unsteady linearized flow. If in a body-axis system of coordinates, the longitudinal axis  $Ox$  is directed from the nose to the tail, the sign of the term  $(2M_\infty/a_\infty) \partial^2 \varphi / \partial x \partial t$  in (9.6.30) must be reversed.

With a view to the notation (9.6.19), the wave equation in the dimensionless form can be written as follows:

$$(1 - M_\infty^2) \frac{\partial^2 \bar{\varphi}}{\partial \xi^2} + \frac{\partial^2 \bar{\varphi}}{\partial \eta^2} + \frac{\partial^2 \bar{\varphi}}{\partial \zeta^2} + 2M_\infty^2 \frac{\partial^2 \bar{\varphi}}{\partial \xi \partial \tau} - M_\infty^2 \frac{\partial^2 \bar{\varphi}}{\partial \tau^2} = 0 \quad (9.6.31)$$

To determine the aerodynamic characteristics of a craft, it is sufficient to solve wave equation (9.6.31), finding the potential of the disturbed velocities  $\bar{\varphi}$ . The solution for the function  $\bar{\varphi}$  must satisfy the boundary conditions on the surface in the flow, the conditions on the vortex sheet, and also at infinity.

*The boundary condition on the surface of a craft* reflects the requirement of a flow without separation (a smooth flow), in accordance with which the normal component of the velocity on the wall is zero. This signifies that the velocity of the disturbed flow  $\partial\varphi/\partial y + \Omega_{xz} + \Omega_z x$  must cancel the corresponding component  $\alpha V_\infty$  of the velocity vector  $\bar{V}_\infty$  on the surface in the flow. Consequently,

$$\partial\varphi/\partial y + \Omega_x(t) z + \Omega_z(t) x + \alpha(t) V_\infty = 0 \quad (9.6.32)$$

or in the dimensionless form

$$\partial\bar{\varphi}/\partial\eta + \omega_x(\tau) \zeta + \omega_z(\tau) \xi + \alpha(\tau) = 0 \quad (9.6.32')$$

*The condition on the vortex sheet* formed behind a craft is stated as the requirement that there be no difference of disturbed pressures on its upper and bottom sides. According to this requirement, we obtain the following expression on the basis of the Cauchy-Lagrange equation:

$$\partial\varphi_b/\partial t - V_\infty \partial\varphi_b/\partial x = \partial\varphi_u/\partial t - V_\infty \partial\varphi_u/\partial x \quad (9.6.33)$$

or in the dimensionless form

$$\bar{\partial}\varphi_b/\partial\tau - \bar{\partial}\varphi_b/\partial\xi = \bar{\partial}\varphi_u/\partial\tau - \bar{\partial}\varphi_u/\partial\xi \quad (9.6.34)$$

In accordance with the *condition at infinity*, we assume that the fluid is undisturbed, i.e. all the disturbances produced by the craft vanish. Accordingly, the potential of the disturbance and its derivatives equal zero, i.e.

$$\varphi = \partial\varphi/\partial x = \partial\varphi/\partial y = \partial\varphi/\partial z = 0 \quad (9.6.35)$$

## 9.7. Basic Methods of Solving Non-Stationary Problems

### Method of Sources

This method is one of the most widespread ones in the theory of flow over craft or their isolated elements (wings, fin assembly, empennage, body). It establishes expressions relating in the general form the required potential function  $\varphi$  satisfying wave equation (9.6.31) to the geometric parameters of a lifting surface and to the values of the derivatives  $\partial\varphi/\partial y$  at points on it. The physical meaning of the method of sources was considered in detail in Chap. 8. We shall give a general scheme of the derivation of a formula for the potential  $\varphi$  as applied to the conditions of supersonic unsteady flow over a preset lifting surface.

The basic idea of the method of sources consists in replacing a flat surface with a system of continuously distributed sources of varying strength that induces the same field of velocities and pressures as in an unsteady flow over the given surface. This method is based on the expression for the retarded potential of a stationary fluctuating strength source at the instant  $t$  [see (2.9.14)]:

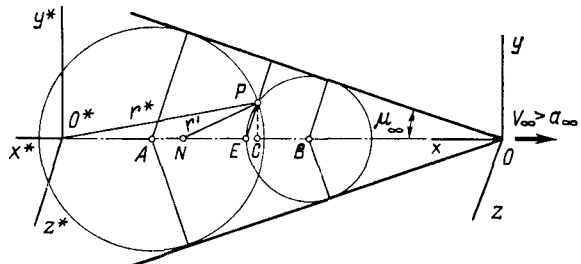
$$\left. \begin{aligned} \varphi^*(x^*, y^*, z^*, t) &= q/r^* \\ r^* &= \sqrt{x^{*2} + y^{*2} + z^{*2}} \end{aligned} \right\} \quad (9.7.1)$$

Here  $q(t)$  is the varying strength of the source determined at the instant  $t' = t - r^*/a_\infty$  (where  $a_\infty$  is the speed of sound).

Hence, this strength  $q(t - r^*/a_\infty)$  is taken for the instant when a sonic disturbance wave emerges from the source and reaches point  $P$  with the coordinates  $x^*, y^*, z^*$  at the considered instant  $t$  (Fig. 9.7.1).

When selecting any doubly differentiable function  $\varphi(t')$ , expression (9.7.1) satisfies wave equation (9.6.31).

Let us assume that beginning from the instant  $t = 0$ , point source  $O$  begins to move from point  $O^*$  at the velocity  $V_\infty$ . Hence, at any instant  $t$ , section  $OO^*$  is filled with sources changing according

**Fig. 9.7.1**

To the determination of the velocity potential of non-stationary sources

to the law  $q(t - t^*)$ , where  $t^*$  is the instant a source originates at a point  $N$  (Fig. 9.7.1). The retarded potential at point  $P(x^*, y^*, z^*)$  due to these sources can be written in the form

$$\varphi'(x^*, y^*, z^*, t) = \int_{t_1}^{t_2} \frac{1}{r'} q \left( t - t^* - \frac{r'}{a_\infty} \right) dt^* \quad (9.7.2)$$

where  $r' = \sqrt{(x^* + V_\infty t^*)^2 + y^{*2} + z^{*2}}$  is the distance between points  $P$  and  $N$ ,  $t'_1$  and  $t'_2$  are the integration limits taking into account the sources from which the disturbances arrive at point  $P$  at the instant  $t$ .

Let us consider a moving coordinate system for which  $x = x^* + V_\infty t$ ,  $y = y^*$ , and  $z = z^*$ . We shall assume below that  $r_2 = a_\infty(t - t^*) - r'$ . In this case for  $V_\infty > a_\infty$ , we can find the following expression for the potential:

$$\varphi'(x, y, z, t) = \frac{1}{a_\infty} \int_0^{r_2} \frac{1}{r_1} q_1 \left( \frac{r_2}{a_\infty} \right) dr_2 + \frac{1}{a_\infty} \int_0^{r_2} \frac{1}{r_1} q_2 \left( \frac{r_2}{a_\infty} \right) dr_2 \quad (9.7.3)$$

where

$$\left. \begin{aligned} r_1 &= \sqrt{(x - M_\infty r_2)^2 - \alpha'^2(y^2 + z^2)} \\ M_\infty &= V_\infty/a_\infty, \quad \alpha' = \sqrt{M_\infty^2 - 1} \end{aligned} \right\} \quad (9.7.4)$$

The upper limit of the integrals  $r'_2 = a_\infty(t - t_1^*) - r'$  is determined by the instant  $t_1^*$  at which point  $O$  moves to point  $E$  on normal  $PE$  to the Mach line. The first term in (9.7.3) takes into account the influence on point  $P$  of the sources on section  $AE$  (the leading front of the sound wave), and the second, on section  $BE$  the trailing front of the wave).

Let us consider the case when a source is located only at moving point  $O$ , and at the instant  $t$  point  $P$  is influenced by the disturbance

ces from the spherical waves occurring at the instants  $t'_1$  and  $t''_1$ . We shall find the potential at point  $P$  by formula (9.7.3) as a result of a limiting process, assuming  $r_2 \rightarrow 0$ . We shall presume that

$$q(t_1) = \frac{1}{a_\infty} \int_0^{r'_2} q_1 \left( \frac{r_2}{a_\infty} \right) dr_2, \quad q(t_2) = \frac{1}{a_\infty} \int_0^{r''_2} q_2 \left( \frac{r_2}{a_\infty} \right) dr_2 \quad (9.7.5)$$

where  $t_1 = t - \Delta t_1$ ;  $t_2 = t - \Delta t_2$ ;  $\Delta t_1$ ,  $\Delta t_2$  are intervals during which the signal is transmitted from the origin of coordinates to a point  $(x, y, z)$  with the wave front and its rear surface.

With a view to (9.7.5), we have the following expression for the velocity potential:

$$q(x, y, z, t) = q(t_1)/r + q(t_2)/r; \quad r = \sqrt{x^2 - \alpha'^2(y^2 + z^2)} \quad (9.7.6)$$

Here  $q(t_1)/r$  determines the potential due to the source at point  $A$  and  $q(t_2)/r$ , at point  $B$  (Fig. 9.7.1).

We consider that at the instant  $t = 0$  sources with a strength of  $q(x, z, t)$  appear simultaneously on the entire area occupied by the lifting surface. The potential produced by such sources at a point with the coordinates  $x_1, y_1, z_1$  can be written as

$$\varphi(x_1, y_1, z_1, t) = \iint_{\sigma_1} \frac{q(x, z, t_1) dx dy}{r} + \iint_{\sigma_2} \frac{q(x, z, t_2) dx dz}{r}$$

where  $r = \sqrt{(x_1 - x)^2 - \alpha'^2(y_1^2 - (z_1 - z)^2)}$  is a conditional distance between the points  $(x_1, y_1, z_1)$  and  $(x, 0, z)$ .

The integration regions  $\sigma_1(x_1, y_1, z_1)$  and  $\sigma_2(x_1, y_1, z_1)$  are the parts of plane  $xOz$  confined within the branch of the Mach (characteristic) cone issuing from the point  $(x_1, y_1, z_1)$ . This branch is determined by the equation

$$\alpha'^2 y_1^2 = (x_1 - x)^2 - \alpha'^2(z_1 - z)^2$$

As a result of differentiating (9.7.7) with respect to the coordinate  $y_1$ , we find an expression for the strength of a source:

$$q(x, z, t) = -\frac{1}{2\pi} \left[ \frac{\partial \varphi(x_1, y_1, z_1, t)}{\partial y_1} \right]_{y=0} \quad (9.7.8)$$

The instants  $t_1 = t - \Delta t_1$  and  $t_2 = t - \Delta t_2$  in (9.7.7) are determined according to the following values:

$$\left. \begin{aligned} \Delta t_1 &= \frac{M_\infty^2}{V_\infty \alpha'^2} \left( x_1 - x - \frac{r}{M_\infty} \right) \\ \Delta t_2 &= \frac{M_\infty^2}{V_\infty \alpha'^2} \left( x_1 - x + \frac{r}{M_\infty} \right) \\ r &= \sqrt{(x_1 - x)^2 - \alpha'^2(y_1^2 + (z_1 - z)^2)} \end{aligned} \right\} \quad (9.7.9)$$

Relations (9.7.8) and (9.7.9) are derived in [19].

When solving problems on the unsteady flow over flat lifting surfaces, we may assume that  $y_1 = 0$  because to determine the aerodynamic characteristics, we must find the values of the potential function on this surface.

The velocity potential  $\varphi$  [see (9.7.7)], in addition to the conditions on the surface of bodies, must satisfy the conditions on the vortex sheet and at infinity, and also the Chaplygin-Zhukovsky condition in accordance with which *a flow does not bend around a trailing subsonic edge, but is cast off it*. In accordance with this condition, disturbed velocities near such edges change continuously, therefore the derivatives  $\partial\varphi/\partial x$ ,  $\partial\varphi/\partial y$ , and  $\partial\varphi/\partial z$  are continuous. The Chaplygin-Zhukovsky condition for the supersonic flow over a lifting surface with subsonic trailing edges is used in the form

$$\left. \begin{aligned} \lim_{x \rightarrow x^*} \frac{\partial \varphi}{\partial y} &= \frac{\partial \varphi}{\partial y} \Big|_{x=x^*} \\ \lim_{x \rightarrow x^*} \varphi(x, 0, z, t) &= \varphi(x^*, 0, z, t) \end{aligned} \right\} \quad (9.7.10)$$

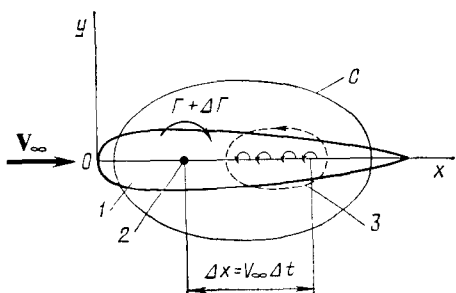
where  $x^*$  ( $z$ ) are the coordinates of points on the trailing edges, and  $\varphi(x^*, 0, z, t)$  is the value of the potential on these edges.

### Vortex Theory

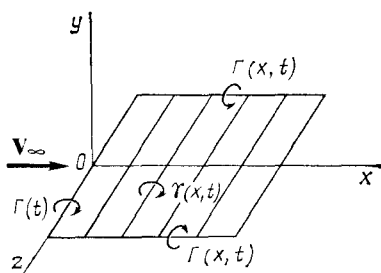
When solving problems on the unsteady incompressible or subsonic compressible flows over a body, it is good practice not to seek directly the velocity potential satisfying the wave equation (as in the method of sources for supersonic velocities), but to use what is known as the **vortex theory**, which does not require the finding of  $\varphi$ . According to this theory, the disturbed motion near a lifting surface can be studied with the aid of a vortex pattern including the bound and free vortices that produce the same distribution of the velocities and pressures as the given surface in the flow.

Let us consider a non-stationary vortex pattern using the example of a lifting surface with a rectangular planform (Fig. 9.7.2). The motion of such a surface is characterized by a constant velocity  $V_\infty$  and small velocity increments due to additional translational or rotational modes of motion. These velocities cause a change in the local angles of attack, and also in the angle of attack as a whole, which results in corresponding changes in time of the lift force of the sections and, consequently, according to Zhukovsky's formula, of the circulation  $\Gamma(t)$  as well [see formula (6.4.6)]. This circulation is due to the rectilinear bound vortex core used to model the lifting surface with a rectangular planform.

Assume that the circulation during the time  $\Delta t$  changes by the value  $\Delta\Gamma$ . In accordance with the Helmholtz theorem, in an ideal fluid the circulation of the velocity over closed contour  $C$  (Fig. 9.7.2)

**Fig. 9.7.2****Vortex system:**

1—lifting surface; 2—bound vortex with varying circulation; 3—sheet of non-stationary vortices

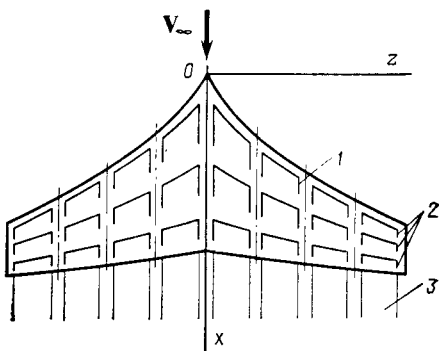
**Fig. 9.7.3****Vortex pattern of rectangular lifting surface**

passing through the same particles does not depend on the time. Consequently, when the circulation  $\Gamma(t)$  changes, a system of free vortices with the circulation  $-\Delta\Gamma$  appears behind the lifting surface that compensates the change in the circulation up to its initial value. Accordingly, a vortex sheet forms behind the lifting surface that consists both of longitudinal vortices parallel to the vector  $V_\infty$  and moving along with the flow, and of lateral (bound) vortices that are stationary relative to the lifting surface.

The intensity of vortex filament distribution in the sheet along the longitudinal axis \$Ox\$ is  $\gamma = -d\Gamma/dx = -(1/V_\infty) d\Gamma/dt$ . It follows from coupling equation (6.4.8) that the circulation is proportional to the lift force coefficient  $c_y$ . With a linear dependence of  $c_y$  on the angle of attack ( $c_y = c_y^\alpha \alpha$ ), the circulation is also a linear function of  $\alpha$ , i.e.  $\Gamma = \Gamma^\alpha \alpha$  (where  $\Gamma^\alpha = d\Gamma/d\alpha = \text{const}$ ). Therefore, the strength of the vortex sheet  $\gamma = -(\Gamma^\alpha/V_\infty) d\alpha/dt$  depends on the rate of change in the angle of attack.

Figure 9.7.3 shows a vortex pattern modelling a rectangular lifting surface. It consists of straight bound vortices with a vortex sheet cast off them.

For a lifting surface of an intricate planform, the vortex pattern consists of a number of bound vortex filaments each of which is replaced with several discrete bound vortices from which a pair

**Fig. 9.7.4**

Vortex model of intricate lifting surface:

1—discrete oblique horseshoe vortex; 2—vortex filaments consisting of discrete oblique vortices; 3—vortex sheet

of free vortex filaments is shed. Such vortex patterns are called **oblique horseshoe vortices** (Fig. 9.7.4).

Let us consider the Kutta-Zhukovsky theorem allowing us to determine the aerodynamic loads acting on a surface element in unsteady flow. This theorem relates to **circulation flow** that is attended by the appearance of a trailing vortex and circulation over the contour enveloping the lifting surface.

According to the Kutta-Zhukovsky theorem, the pressure difference on the bottom and upper sides of a surface element in a linearized flow is

$$\Delta p = p_b - p_u = \rho_\infty \gamma V_\infty \quad (9.7.11)$$

where  $\gamma = (1/V_\infty) \partial \Gamma / \partial t$  is the **linear strength of the bound vortices**, and  $V_\infty$  is the velocity of translational motion.

Formula (9.7.11) is an application of the Kutta-Zhukovsky theorem to an arbitrary unsteady flow over a thin lifting surface and indicates the absence of the influence of free vortices on the aerodynamic loads. From this theorem, particularly, there follows the absence of a pressure difference on a vortex sheet consisting of free vortices.

Let us write the strength of a vortex layer in the form of a series:

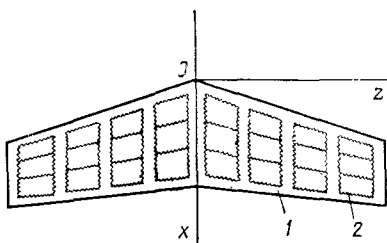
$$\gamma = V_\infty \sum_{i=1}^3 (\gamma^q q_i + \dot{\gamma}^q \dot{q}_i) \quad (9.7.12)$$

Introducing this quantity into the formula for calculating the difference of the pressure coefficients

$$\bar{\Delta p} = 2(p_b - p_u)/(\rho_\infty V_\infty^2) = 2\gamma/V_\infty \quad (9.7.13)$$

we obtain

$$\bar{\Delta p} = 2 \sum_{i=1}^3 (\gamma^q q_i + \dot{\gamma}^q \dot{q}_i) \quad (9.7.14)$$

**Fig. 9.7.5**

Vortex model for non-circulatory flow:

1—lifting surface; 2—discrete closed attached vortices

Comparing this expression with the second formula (9.6.22), we find expressions for the derivatives of the pressure coefficient difference in terms of the corresponding derivatives of the linear strength of the bound vortex layer:

$$p^q_i = 2\gamma^q t, \quad p^{\dot{q}}_i = 2\dot{\gamma}^q i \quad (i = 1, 2, 3) \quad (9.7.15)$$

The above relations are exact if the kinematic variables change harmonically.

For circulation problems, the Chaplygin-Zhukovsky condition on the passing off of the flow from the trailing edge of a surface and on the finiteness of the velocity at this edge is satisfied. According to this condition, the strength of the bound vortices on the trailing edges is zero, i.e.

$$\gamma(x, z, t) = 0 \quad (9.7.16)$$

When bodies move at very low speeds, or when oscillations occur in the absence of translational motion, a scheme of non-circulatory flow is realized. Here no wake forms behind a body, and the circulation over an arbitrary contour enveloping the lifting surface is zero.

Accordingly, a vortex layer equivalent to the lifting surface is represented as a system of closed vortex filaments of constant strength (Fig. 9.7.5). Some results of studying non-circulatory flow, in particular the derivation of Zhukovsky's theorem for such flow, are given in [4, 19].

## 9.8. Numerical Method of Calculating the Stability Derivatives for a Wing in an Incompressible Flow

### Velocity Field of an Oblique Horseshoe Vortex

The numerical method of calculating the stability derivatives for a wing in an unsteady flow is based on its replacement by a vortex lifting surface which, in turn, is represented by a system of oblique horseshoe discrete transient vortices.

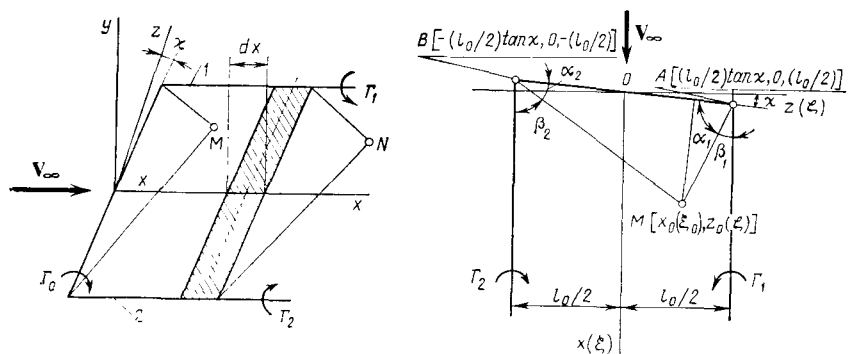


**Fig. 9.8.1**  
Oblique horseshoe vortex in an unsteady flow:  
1, 2—free vortices

Let us consider the velocities induced by such vortices. With non-stationary motion of a wing, the circulation (strength) of a bound vortex varies with time, i.e.  $\Gamma = \Gamma(t_0)$ . In accordance with the condition of constancy of the circulation over a closed contour, this change in the strength is attended by the casting off of free vortices carried away behind the wing together with the flow. The velocity of casting off the free vortices equals the free-stream velocity  $V_\infty$ , while all the vortices are in the wing plane  $xOz$ . The axes of the bound vortices and of the free ones cast off the wing are parallel, while the strength of each of these vortices 1 and 2 (Fig. 9.8.1) at the instant of shedding equals the strength of the bound vortex at this instant.

Let us determine the velocity induced by a bound vortex of strength  $\Gamma(t_0) = \Gamma V_\infty b$  (where  $\Gamma$  is the dimensionless magnitude of the circulation, and  $b$  is a characteristic linear dimension) at point  $M(x_0, 0, z_0)$ . According to the Biot-Savart relation, the magnitude of this velocity is

$$W' = \frac{\Gamma_0(t_0)}{4\pi h} (\cos \alpha_1 + \cos \alpha_2) = - \frac{V_\infty \Gamma}{4\pi} \cdot \frac{\cos \alpha_1 + \cos \alpha_2}{\xi_0 \cos \kappa - \zeta_0 \sin \kappa} \quad (9.8.1)$$

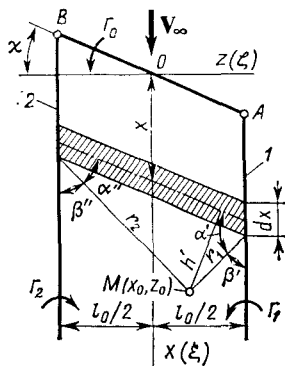
where  $\xi_0 = x_0/b$ ,  $\zeta_0 = z_0/b$ .

The relevant value of the velocity produced by the free vortices is determined by the formula

$$W'' = - \frac{V_\infty \Gamma}{4\pi} \left( \frac{1 + \cos \beta_1}{0.5\bar{l}_0 - \zeta_0} + \frac{1 + \cos \beta_2}{0.5\bar{l}_0 + \zeta_0} \right) \quad (9.8.2)$$

where  $\bar{l}_0 = l_0/b$ .

The total velocity induced by the bound and free vortices is  $W = W' + W''$ . It will be more convenient in the following to

**Fig. 9.8.2**

To the determination of the velocities induced by a vortex sheet and free vortex filaments of varying strength:

1, 2—free vortices

use the dimensionless value of the velocity:

$$w'(\xi_0, \zeta_0, \varkappa) = W'(4\pi/V_\infty \Gamma) = -\frac{\cos \alpha_1 + \cos \alpha_2}{\xi_0 \cos \varkappa - \zeta_0 \sin \varkappa} \quad (9.8.3)$$

$$w''(\xi_0, \zeta_0, \varkappa) = W''(4\pi/V_\infty \Gamma) = -\left(\frac{1 + \cos \beta_1}{\bar{l}_0 - \zeta_0} + \frac{1 + \cos \beta_2}{\bar{l}_0 + \zeta_0}\right) \quad (9.8.4)$$

The corresponding value of the total dimensionless velocity is

$$w(\xi_0, \zeta_0, \varkappa) = W(4\pi/V_\infty \Gamma) = w'(\xi_0, \zeta_0, \varkappa) + w''(\xi_0, \zeta_0, \varkappa) \quad (9.8.5)$$

The values of the geometric parameters determining the induced velocities (the cosines of the angles  $\alpha_1$ ,  $\alpha_2$ ,  $\beta_1$ ,  $\beta_2$ ) depend on the coordinates of point  $M[x_0(\xi_0), z_0(\xi_0)]$  and the angle of inclination  $\varkappa$  of an oblique vortex (Fig. 9.8.1). These values are given in [4].

Let us consider an elementary vortex layer of width  $dx$  at a distance of  $x$  from the bound vortex (Fig. 9.8.2). The linear strength of this layer at the instant  $t_0$  is determined by the magnitude of the derivative

$$\gamma(x, t_0) = -\frac{1}{V_\infty} \cdot \frac{d\Gamma_0(t_1)}{dt_1}; \quad t_1 = t_0 - \frac{x}{V_\infty} \quad (9.8.6)$$

We shall write the strengths of the free vortex filaments  $\Gamma_1(x, t_0)$  and  $\Gamma_2(x, t_0)$  in the section  $x = \text{const}$  as functions:

$$\left. \begin{aligned} \Gamma_1(x, t_0) &= \Gamma_0 \left( t_0 - \frac{x - 0.5l_0 \tan \varkappa}{V_\infty} \right) \\ \Gamma_2(x, t_0) &= \Gamma_0 \left( t_0 - \frac{x + 0.5l_0 \tan \varkappa}{V_\infty} \right) \end{aligned} \right\} \quad (9.8.7)$$

The elementary velocity  $dV'$  induced at point  $M(x_0, \zeta_0)$  by a vortex layer with a strength of  $d\Gamma_0 = \gamma(x, t_0) dx$  is determined

with the aid of the Biot-Savart formula (9.8.1):

$$dV' = -\frac{d\Gamma_0(x, t_0)}{4\pi h'} (\cos \alpha' + \cos \alpha'') = -\frac{\gamma(x, t_0) dx (\cos \alpha' + \cos \alpha'')}{4\pi [(x_0 - x) \cos \kappa - z_0 \sin \kappa]}$$

By integrating with respect to  $\xi$  from 0 to infinity and going over to dimensionless coordinates, we obtain

$$V' = -\frac{1}{4\pi} \int_0^\infty \frac{\gamma(x, t_0) (\cos \alpha' + \cos \alpha'')}{(\xi_0 - \xi) \cos \kappa - \zeta_0 \sin \kappa} d\xi \quad (9.8.8)$$

Here the cosines of the angles  $\alpha'$  and  $\alpha''$  are determined from Fig. 9.8.1 as a function of the dimensionless coordinates  $\xi_0$ ,  $\xi$ , the angle  $\kappa$ , and the relative span of a vortex  $\bar{l}_0 = l_0/b$ .

The velocities  $dV'_1$  and  $dV'_2$  induced by elements of the free vortex filaments 1 and 2 are determined by the Biot-Savart formulas (see Fig. 9.8.1) as follows:

$$dV'_1 = -\frac{\Gamma_1 \sin \beta' dx}{4\pi r_1^2}, \quad dV'_2 = -\frac{\Gamma_2 \sin \beta'' dx}{2\pi r_2^2}$$

The geometric variables in these expressions are determined with the aid of Fig. 9.8.2. For example,

$$\sin \beta' = (0.5l_0 - z_0)/r_1, \quad r_1 = \sqrt{(x_0 - x)^2 + (0.5l_0 - z_0)^2}$$

We find the values of  $\sin \beta''$  and  $r_2$  in a similar way. Integrating with respect to  $x$  from  $-0.5l_0 \tan \kappa$  and  $0.5l_0 \tan \kappa$  to  $\infty$  and passing over to dimensionless geometric variables, we obtain

$$\left. \begin{aligned} V'_1 &= -\frac{1}{4\pi b} \int_{0.5\bar{l}_0 \tan \kappa}^{\infty} \frac{\Gamma_1(x, t_0) (0.5\bar{l}_0 - \zeta_0) d\xi}{[(\xi_0 - \xi)^2 + (0.5\bar{l}_0 - \zeta_0)^2]^{3/2}} \\ V'_2 &= -\frac{1}{4\pi b} \int_{-0.5\bar{l}_0 \tan \kappa}^{\infty} \frac{\Gamma_2(x, t_0) (0.5\bar{l}_0 + \zeta_0) d\xi}{[(\xi_0 - \xi)^2 + (0.5\bar{l}_0 + \zeta_0)^2]^{3/2}} \end{aligned} \right\} \quad (9.8.9)$$

The total velocity induced by the bound vortex, the vortex sheet, and the free vortices is

$$V = W' + V' + V'_1 + V'_2 \quad (9.8.10)$$

Let us consider a harmonic change in the circulation

$$\Gamma_0(t) = V_\infty b \Gamma \sin pt \quad (9.8.11)$$

where  $p$  is the angular frequency and  $\Gamma$  is a dimensionless constant.

In accordance with this law, we shall write the circulation (9.8.6) in the form

$$\gamma(x, t_0) = -b \Gamma p \cos pt_1 = -V_\infty p * \Gamma \cos(pt_0 - p * \xi) \quad (9.8.12)$$

We shall represent formulas (9.8.7) for the circulations as follows:

$$\Gamma_1(x, t_0) = V_\infty b \Gamma \sin \left[ p \left( t_0 - \frac{x - 0.5l_0 \tan \alpha}{V_\infty} \right) \right]$$

$$\Gamma_2(x, t_0) = V_\infty b \Gamma \sin \left[ p \left( t_0 - \frac{x + 0.5l_0 \tan \alpha}{V_\infty} \right) \right]$$

Introducing the Strouhal number  $p^* = bp/V_\infty$  and the dimensionless quantities  $\xi = x/b$  and  $\bar{l}_0 = l_0/b$ , we obtain the generalized expression

$$\Gamma_{1(2)}(x, t_0) = V_\infty b \Gamma \sin [pt_0 - p^*(\xi \mp 0.5\bar{l}_0 \tan \alpha)] \quad (9.8.13)$$

where the minus sign corresponds to the quantity  $\Gamma_1$ , and the plus sign to  $\Gamma_2$ .

After inserting the obtained values of the strength  $\gamma(x, t_0)$  and of the circulations  $\Gamma_{1(2)}(x, t_0)$  into (9.8.8) and (9.8.9), respectively, we find expressions for the induced velocities  $W'$ ,  $V'$ ,  $V''_1$ , and  $V''_2$  in the integral form for a harmonic (sinusoidal) change in the circulation. It is not difficult to see that the total induced velocity  $V = W' + V' + V''_1 + V''_2$  can be represented in a general form in terms of the dimensionless velocity function  $v(\xi_0, \zeta_0, \alpha, p^*, t_0)$ :

$$V = \frac{V_\infty \Gamma}{4\pi} v(\xi_0, \zeta_0, \alpha, p^*, t_0) \quad (9.8.14)$$

where, in turn,

$$\begin{aligned} v &= v^{(1)}(\xi_0, \zeta_0, \alpha, p^*) \sin pt_0 + v^{(2)}(\xi_0, \zeta_0, \alpha, p^*) \cos pt_0 \\ v^{(1)} &= w'(\xi_0, \zeta_0, \alpha) + p^* v'_1(\xi_0, \zeta_0, \alpha, p^*) + v''_1(\xi_0, \zeta_0, \alpha, p^*) \\ v^{(2)} &= p^* v'_2(\xi_0, \zeta_0, \alpha, p^*) + v''_2(\xi_0, \zeta_0, \alpha, p^*) \end{aligned} \quad \left. \right\} \quad (9.8.15)$$

We determine the dimensionless velocity  $w'$  from (9.8.3), and we find the functions  $v'_1$ ,  $v''_1$ ,  $v'_2$ , and  $v''_2$  from an analysis of integrals (9.8.8) and (9.8.9) after introducing into them, respectively, the harmonically changing quantities  $\gamma(x, t_0)$  and  $\Gamma_{1(2)}(x, t_0)$ .

The above relations describe a sinusoidal change in the strength of a bound vortex. If this change is cosinusoidal, i.e.

$$\Gamma_0(t) = V_\infty b \Gamma \cos pt \quad (9.8.16)$$

then we have

$$\begin{aligned} \gamma(x, t_0) &= b \Gamma p \sin pt = V_\infty p^* \sin(pt - p^* \xi) \\ \Gamma_{1(2)}(x, t_0) &= V_\infty b \Gamma \cos [pt_0 - p^*(\xi \mp 0.5\bar{l}_0 \tan \alpha)] \end{aligned} \quad \left. \right\} \quad (9.8.17)$$

With a view to the above, instead of the first of expressions (9.8.15) we have the general relation

$$v = v^{(1)}(\xi_0, \zeta_0, \alpha, p^*) \cos pt_0 - v^{(2)}(\xi_0, \zeta_0, \alpha, p^*) \sin pt_0 \quad (9.8.18)$$

One of the important problems in unsteady aerodynamics is the one on the harmonic oscillations of craft with small Strouhal numbers ( $p^* \rightarrow 0$ ). For such numbers

$$v^{(1)}(\xi_0, \zeta_0, \alpha, 0) = w' + v'_1 \Big|_{p^* \rightarrow 0} \quad (9.8.19)$$

$$\frac{\partial v^{(2)}}{\partial p^*} \Big|_{p^* \rightarrow 0} = v'_2(\xi_0, \zeta_0, \alpha, 0) + \frac{\partial v'_2}{\partial p^*} \Big|_{p^* \rightarrow 0} \quad (9.8.20)$$

The last derivative is used directly for calculation of unsteady flow parameters. The finding of this derivative, and also of other functions determining the dimensionless induced velocities is described in [4].

### Vortex Model of a Wing

A vortex model of a wing in the form of a flat lifting surface in an unsteady circulatory flow is shown in Fig. 9.8.3. If a wing has curved edges, they are replaced approximately with a contour formed of segments of straight lines. Hence, in a most general case, a lifting surface has breaks.

Let us divide the entire area of a wing into zones by drawing sections parallel to the axis  $Ox$  through the breaks in the contour. Let us further divide each segment  $l_\delta$  between the breaks into  $N_\delta^*$  strips and number their boundaries from right to left (the boundary having the number  $p = 0$  coincides with the tip of the wing, and having  $p = N$  with the longitudinal axis). Usually the values of the width of a strip  $l_{p,p-1}$  differ only slightly from one another.

Let us consider the strip between the sections  $p$  and  $p - 1$  in any of the zones  $\delta$ . We shall denote the dimensionless coordinate of the leading edge in the section  $p$  by  $\xi_{0,p}$ , and of the trailing one by  $\xi_{*,p}$ .

The relative chord of the section is

$$\bar{b}_p = b_p/b_0 = \xi_{*,p} - \xi_{0,p}$$

Let us assume that a strip consists of  $n$  cells. For this purpose, we shall divide each chord in the relevant section into  $n$  parts by means of points with the coordinates

$$\left. \begin{aligned} \xi_{v,p} &= \xi_{0,p} + 0.5\bar{b}_p \left( 1 - \cos \frac{v\pi}{n} \right) \\ \xi_{v,p-1} &= \xi_{0,p-1} + 0.5\bar{b}_{p-1} \left( 1 - \cos \frac{v\pi}{n} \right) \end{aligned} \right\} \quad (9.8.21)$$

$$v = 0, 1, 2, \dots, n$$

The cells arranged along the line  $v$  separating them along the span of the wing form panels whose number is the same as that of the cells in a strip ( $n$ ). We shall designate the boundaries of the panels

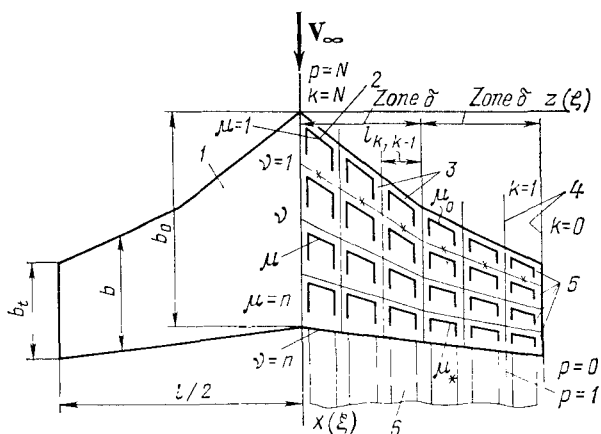


Fig. 9.8.3

Vortex model of a wing in an unsteady circulatory flow:

1—wing; 2—oblique horseshoe vortex; 3—cells; 4—strip; 5—panels; 6—vortex wake

by  $v$  (for the leading edge  $v = 0$ , for the trailing one  $v = v_*$ ). We shall designate the coordinates of points at the intersections of the lines  $v$  and  $p$  by the subscripts  $v$  and  $p$ .

Hydrodynamically, the plane of the wing is equivalent to a vortex surface that is approximately depicted by a system of bound discrete vortices. Each of such vortices evidently consists of **oblique horseshoe vortices** adjoining one another, while the total number of these vortices coincides with the number of cells in which they are accommodated.

We shall characterize the bound vortex filaments by a serial number  $\mu$  counted from the nose. Let us introduce for the sections dividing the plane of the wing along its span, in addition to the numbers  $p$ , the serial number  $k$  counted from a tip where we assume that  $k = 0$ . Accordingly,  $0 \leq k \leq N$ .

We shall denote the points of intersection of the lines  $\mu$  and  $k$  by the same subscripts. We consider here that the coordinates of points on the leading edge in section  $k$  and the magnitude of the chord in this section  $b_{k(p)}$  of each zone  $\delta$  are known.

We shall determine the position of discrete vortices as follows. We separate the chords in the sections  $\zeta_h$  and  $\zeta_{h-1}$  with points having the coordinates

$$\left. \begin{aligned} \xi_{\mu,h} &= \xi_{0,h} + 0.5 \bar{b}_h \left( 1 - \cos \frac{2\mu-1}{2n} \pi \right) \\ \xi_{\mu,h-1} &= \xi_{0,h-1} + 0.5 \bar{b}_{h-1} \left( 1 - \cos \frac{2\mu-1}{2n} \pi \right) \end{aligned} \right\} \quad (9.8.22)$$

$$\mu = 1, 2, \dots, n$$

Points with identical  $\mu$ 's coincide with the ends of discrete vortices. We have the following relations for the dimensionless coordinates of the middles of the oblique bound vortices, their span  $l_{k,k-1}$ , and sweep angles  $\tan \chi_{\mu, k-1}^{\mu, k}$ :

$$\left. \begin{aligned} \xi_{\mu, k-1}^{\mu, k} &= 0.5 (\xi_{\mu, k} + \xi_{\mu, k-1}) = 0.5 (\xi_{0, k} + \xi_{0, k-1}) \\ &+ 0.25 (\bar{b}_k + \bar{b}_{k-1}) \left( 1 - \cos \frac{2\mu-1}{2n} \pi \right) \\ \xi_{\mu, k-1}^{\mu, k} &= 0.5 (\zeta_{\mu, k} + \zeta_{\mu, k-1}), \quad \bar{l}_{k, k-1} = \frac{l_{k, k-1}}{b_0} = \zeta_{\mu, k-1} - \zeta_{\mu, k} \\ \tan \chi_{\mu, k-1}^{\mu, k} &= (\xi_{\mu, k-1} - \xi_{\mu, k}) / (\zeta_{\mu, k-1} - \zeta_{\mu, k}) \\ \mu &= 1, 2, \dots, n; \quad k = 1, 2, \dots, N \end{aligned} \right\} \quad (9.8.23)$$

The coordinates of the centre of another vortex symmetric about plane  $xOy$  on the port half of the craft and also the sweep angle are as follows:

$$\left. \begin{aligned} \sigma \xi_{\mu, k-1}^{\mu, k} &= \xi_{\mu, k-1}^{\mu, k}, \quad \sigma \zeta_{\mu, k-1}^{\mu, k} = -\zeta_{\mu, k-1}^{\mu, k} \\ \sigma \bar{l}_{k, k-1} &= \bar{l}_{k, k-1}, \quad \sigma \chi_{\mu, k-1}^{\mu, k} = -\chi_{\mu, k-1}^{\mu, k} \end{aligned} \right\} \quad (9.8.24)$$

where the variables for the port side of the wing are designated by the factor  $\sigma$ .

For a wing with rectangular edges, the sweep angles of the bound vortices are constant ( $\chi_{\mu} = \text{const}$ ), and each of them transforms into an ordinary straight **horseshoe vortex**. If a wing plane has breaks in its contour, then the corresponding breaks are present in the vortex filaments too.

The circulation of oblique and conventional (straight) horseshoe vortices along the span is constant, while free filaments parallel to the axis  $Ox$  are shed off the ends of the bound vortices. The free filaments propagate downstream, and when the flow is circulatory they pass away to infinity. In addition, when the circulation of the bound vortices changes with time, free vortices of the relevant strength are shed off them.

The vortex model being considered is very convenient for computerized calculations of a flow. This is due, first, to the sufficiently simple relations describing the disturbed flow near a wing, and, second, to a number of important properties of the system of algebraic equations which the solution of the problem is reduced to. One of these properties is that the diagonal terms in the matrix of the equation coefficients play a dominating role; the solutions themselves have a great stability relative to the initial conditions.

A significant feature of computerized calculations is also the fact that the use of oblique horseshoe vortices instead of the conventional ones leads to substantial simplification of the calculations and to more accurate results.

### Calculation of Circulatory Flow

**System of Equations.** Let us represent the dimensionless circulation of the oblique horseshoe vortex  $\Gamma_{\mu, h, k-1} = \Gamma'_{\mu, h, k-1} / (V_\infty b_0)$  in the following form:

$$\left. \begin{aligned} \Gamma_{\mu, h, k-1}(\tau) &= \sum_{i=1}^3 \left[ \Gamma_{\mu, h, k-1}^{q_i} q_i(\tau) + \Gamma_{\mu, h, k-1}^{q_i} \dot{q}_i(\tau) \right] \\ q_i &= \alpha, \omega_x, \omega_y; \quad \tau = V_\infty t / b_0, \end{aligned} \right\} \quad (9.8.25)$$

or in the expanded form

$$\left. \begin{aligned} \Gamma_{\mu, h, k-1}(\tau) &= \Gamma_{\mu, h, k-1}^\alpha \alpha + \Gamma_{\mu, h, k-1}^{\dot{\alpha}} \dot{\alpha} + \Gamma_{\mu, h, k-1}^{\omega_x} \omega_x \\ &+ \Gamma_{\mu, h, k-1}^{\dot{\omega}_x} \dot{\omega}_x + \Gamma_{\mu, h, k-1}^{\omega_z} \omega_z + \Gamma_{\mu, h, k-1}^{\dot{\omega}_z} \dot{\omega}_z \end{aligned} \right\} \quad (9.8.26)$$

where  $\Gamma_{\mu, h, k-1}^{q_i}$  are dimensionless functions not depending on the time; the only time-dependent variables are  $q_i$  and  $\dot{q}_i$ .

We shall assume that the kinematic variables change according to harmonic relations (9.1.5) and (9.1.6) which can be represented in terms of the dimensionless time  $\tau$  as follows:

$$q_i = q_i^* \cos p_i^* \tau, \quad \dot{q}_i = -q_i^* p_i^* \sin p_i^* \tau \quad (9.8.27)$$

where  $q_i^*$  are the amplitude values of the variables not depending on the time,  $p_i^* = p_i b_0 / V_\infty$  is the Strouhal number ( $p_i$  is the angular frequency), and  $\tau = t V_\infty / b_0$ .

With a view to (9.8.27), the circulation (9.8.25) is expressed as follows:

$$\Gamma_{\mu, h, k-1}(\tau) = \sum_{i=1}^3 q_i^* \left[ \Gamma_{\mu, h, k-1}^{q_i} \cos p_i^* \tau - \Gamma_{\mu, h, k-1}^{q_i} p_i^* \sin p_i^* \tau \right] \quad (9.8.28)$$

By (9.8.6)

$$\begin{aligned} \gamma(\xi_{\mu, h-1}, \tau) &= V_\infty \sum_{i=1}^3 q_i^* p_i^* \{ \Gamma_{\mu, h, k-1}^{q_i} \sin [p_i^* (\tau - \xi_{\mu, h-1}^{\mu, h-1})] \\ &+ p_i^* \Gamma_{\mu, h, k-1}^{q_i} \cos [p_i^* (\tau - \xi_{\mu, h-1}^{\mu, h-1})] \} \end{aligned} \quad (9.8.29)$$

where  $\xi_{\mu, h-1}^{\mu, h-1}$  is the longitudinal coordinate of the middle of an oblique bound vortex.

The expressions for the circulation of the free vortices (9.8.7) have the form

$$\begin{aligned} \Gamma_{1(2)}(\xi_{\mu, h-1}, \tau) &= V_\infty b_0 \sum_{i=1}^3 q_i^* [\Gamma_{\mu, h, k-1}^{q_i} \cos \{p_i^* [\tau - (\xi_{\mu, h-1}^{\mu, h-1} \right. \\ &\left. \mp 0.5 \bar{l}_{h, k-1} \tan \chi_{\mu, h-1}^{\mu, h-1})]\} - \Gamma_{\mu, h, k-1}^{q_i} p_i^* \sin \{p_i^* [\tau - (\xi_{\mu, h-1}^{\mu, h-1} \\ &\mp 0.5 \bar{l}_{h, k-1} \tan \chi_{\mu, h-1}^{\mu, h-1})]\}] \end{aligned} \quad (9.8.30)$$

Introducing (9.8.28), (9.8.29), and (9.8.30) into (9.8.1), (9.8.8), and (9.8.9), respectively, we obtain for a certain control point  $\xi_{v,p-1}^{v,p}$ ,  $\zeta_{v,p-1}^{v,p}$  of the wing the induced velocities  $W'$ ,  $V'$ ,  $V'_1$ , and  $V'_2$  expressed in terms of derivatives of the circulation. We shall assume that the control points are at the centre of the lines drawn through points with identical values of  $v$  (except for the forward and the rear points), i.e. at an identical distance between the free vortices. Hence the coordinates of the control points (indicated by crosses in Fig. 9.8.3) are determined by the relations

$$\left. \begin{aligned} \xi_{v,p-1}^{v,p} &= 0.5 (\xi_{v,p} + \xi_{v,p-1}) = 0.5 (\xi_{0,p} + \xi_{0,p-1}) \\ &+ 0.25 (\bar{b}_p + \bar{b}_{p-1}) \left( 1 - \cos \frac{v\pi}{n} \right) \\ \zeta_{v,p-1}^{v,p} &= 0.5 (\zeta_p + \zeta_{p-1}) \end{aligned} \right\} \quad (9.8.31)$$

$$v = 0, 1, 2, \dots, n-1; p = 0, 1, 2, \dots, N$$

The relative value of the total induced velocity at this point  $v = (W' + V' + V'_1 + V'_2)/V_\infty$  is determined by the dimensionless velocities  $v^{(1)}$  and  $v^{(2)}$  that are evaluated in accordance with general relations similar to (9.8.14) and (9.8.15).

Let us designate by  $\sigma v^{(1)}$  and  $\sigma v^{(2)}$  the additional velocities at the control point being considered produced by an oblique vortex located on the port half of the wing symmetrically about the plane  $xOy$ . The coordinates of the middle of such a vortex are  $\xi_{\mu,h-1}^{\mu,h}$  and  $-\zeta_{\mu,h-1}^{\mu,h}$ ! The values of  $\sigma v^{(1)}$  and  $\sigma v^{(2)}$  are determined with the aid of (9.8.1), (9.8.8) and (9.8.9), account being taken of the change in the direction of the coordinate axes and the transfer of their origin.

We shall add these values of the corresponding dimensionless velocities  $v^{(1)}$  and  $v^{(2)}$  for symmetric motion (for  $q_i = \alpha$ ,  $\omega_z$ , and even functions  $\Gamma_{\mu,h,k-1}^{q_i}$ ,  $\Gamma_{\mu,h,k-1}^{q_i}$ ) and subtract them for asymmetric motion (for  $q_i = \omega_x$  and odd derivatives of the dimensionless circulation). We shall determine the total velocity at a control point with account taken of the influence of all the other vortices, i.e. calculate it by double summation of the induced velocities over the number of strips  $N$  and panels  $n$ . This velocity is determined by the values of the derivatives of the dimensionless circulation  $\Gamma_{\mu,h,k-1}^{q_i}$  and  $\Gamma_{\mu,h,k-1}^{q_i}$ .

To find them, we must use the condition of flow without separation in accordance with which the total dimensionless velocity at a control point induced by the entire vortex pattern of the wing equals the undisturbed component determined by Eq. (9.6.32'):

$$\begin{aligned} v_{v,p,p-1} &= \frac{V_{v,p,p-1}}{V_\infty} = \frac{(W' + V' + V'_1 + V'_2)_{v,p,p-1}}{V_\infty} \\ &= -\omega_x \xi_{v,p-1}^{v,p} - \omega_z \zeta_{v,p-1}^{v,p} - \alpha \end{aligned} \quad (9.8.32)$$

The kinematic variables in this equation can be represented in the form of a harmonic relation:

$$q_i = q_i^* \cos p_i^* \tau_0 \quad (q_i = \alpha, \omega_x, \omega_z) \quad (9.8.33)$$

By satisfying Eq. (9.8.32) with a view to (9.8.33), we obtain the following three systems of linear algebraic equations for the required derivatives of the dimensionless circulation  $\Gamma_{\mu, h, k-1}^{q_i}$  and  $\dot{\Gamma}_{\mu, h, k-1}^{q_i}$ :

$$\left. \begin{aligned} & \frac{1}{4\pi} \sum_{h=1}^N \sum_{\mu=1}^n (v_v^{(1)\mu, h, k-1} \pm \sigma v_v^{(1)\mu, h, k-1}) \Gamma_{\mu, h, k-1}^{q_i} \\ & + \frac{p_i^*}{4\pi} \sum_{h=1}^N \sum_{\mu=1}^n (v_v^{(2)\mu, h, k-1} \pm \sigma v_v^{(2)\mu, h, k-1}) \\ & \times \dot{\Gamma}_{\mu, h, k-1}^{q_i} = v_{v, p, p-1}^{q_i} \\ & \sum_{h=1}^N \sum_{\mu=1}^n (v_v^{(2)\mu, h, k-1} \pm \sigma v_v^{(2)\mu, h, k-1}) \Gamma_{\mu, h, k-1}^{q_i} \\ & + p_i^* \sum_{h=1}^N \sum_{\mu=1}^n (v_v^{(1)\mu, h, k-1} \pm \sigma v_v^{(1)\mu, h, k-1}) \dot{\Gamma}_{\mu, h, k-1}^{q_i} = 0 \\ & p = 0, 1, 2, \dots, N; v = 0, 1, 2, \dots, n-1; \\ & k = 1, 2, 3, \dots, V \end{aligned} \right\} \quad (9.8.34)$$

The quantity  $v_{v, p, p-1}^{q_i}$  is determined in accordance with Eq. (9.8.32) as follows:

$$v_{v, p, p-1}^{\alpha} = -1; v_{v, p, p-1}^{\omega_v} = -\xi_{v, p-1}; v_{v, p, p-1}^{\omega_z} = -\xi_{v, p-1} \quad (9.8.35)$$

We find the dimensionless variables in (9.8.34) with a view to the relations

$$\left. \begin{aligned} v_{v, p, p-1}^{(1)\mu, h, k-1} &= v^{(1)}(\xi_{v, p, p-1}^{\mu, h, k-1}, \zeta_{v, p, p-1}^{\mu, h, k-1}, \tilde{l}_{h, k-1}, \chi_{\mu, h-1, p}^{\mu, h}), \\ v_{v, p, p-1}^{(2)\mu, h, k-1} &= v^{(2)}(\xi_{v, p, p-1}^{\mu, h, k-1}, \zeta_{v, p, p-1}^{\mu, h, k-1}, \tilde{l}_{h, k-1}, \chi_{\mu, h-1, p}^{\mu, h}), \\ \sigma v_{v, p, p-1}^{(1)\mu, h, k-1} &= v^{(1)}(\xi_{v, p, p-1}^{\mu, h, k-1}, \sigma \zeta_{v, p, p-1}^{\mu, h, k-1}, \tilde{l}_{h, k-1}, \\ & - \chi_{\mu, h-1, p}^{\mu, h}), \\ \sigma v_{v, p, p-1}^{(2)\mu, h, k-1} &= v^{(2)}(\xi_{v, p, p-1}^{\mu, h, k-1}, \sigma \zeta_{v, p, p-1}^{\mu, h, k-1}, \\ & \tilde{l}_{h, k-1}, -\chi_{\mu, h-1, p}^{\mu, h}) \end{aligned} \right\} \quad (9.8.36)$$

The dimensionless geometric parameters in these relations are determined in the form

$$\left. \begin{aligned} \xi_{v,p,p-1}^{\mu,h,h-1} &= \xi_{v,p-1}^v - \xi_{\mu,h-1}^{\mu,h}, \quad \xi_{v,p,p-1}^{\mu,h,h-1} = \xi_{v,p-1}^v - \xi_{\mu,h-1}^{\mu,h}; \\ l_{h,h-1} &= l_{h,h-1}/b_0 = \xi_{\mu,h-1} - \xi_{\mu,h}; \\ \tan \chi_{\mu,h-1}^{\mu,h} &= \frac{\xi_{\mu,h-1} - \xi_{\mu,h}}{\xi_{\mu,h-1} - \xi_{\mu,h}}; \quad \sigma \xi_{v,p,p-1}^{\mu,h,h-1} \\ &= \xi_{v,p-1}^v + \xi_{\mu,h-1}^{\mu,h} \end{aligned} \right\} \quad (9.8.37)$$

Each of the three systems of equations obtained includes  $(n-1)N$  linear algebraic equations, whereas the number of unknown derivatives  $\Gamma_{\mu,h,h-1}^{q_i}$  and  $\Gamma_{\mu,h,h-1}^{q_i}$  is  $nN$ . To close the system and obtain as many equations as there are unknowns, we must satisfy the Chaplygin-Zhukovsky condition by which the strength of the nearest bound vortex to the trailing edge in each section  $k, k-1$  must be zero. Hence, according to this condition, the derivatives can be taken equal to

$$\Gamma_{\mu,h,h-1}^{q_i}|_{\mu=\mu_*} = 0, \quad \dot{\Gamma}_{\mu,h,h-1}^{q_i}|_{\mu=\mu_*} = 0, \quad q_i = \alpha, \omega_x, \omega_z \quad (9.8.38)$$

Proceeding from (9.8.34) and (9.8.38), we shall compile three systems of equations for determining the derivatives of dimensionless circulation, taking into account the specific values of  $q_i$  and  $\dot{q}_i$ .

The first system is used for calculating the derivatives  $\Gamma_{\mu,h,h-1}^\alpha, \dot{\Gamma}_{\mu,h,h-1}^\alpha$ :

$$\left. \begin{aligned} &\frac{1}{4\pi} \sum_{h=1}^N \sum_{\mu=1}^n (v_{v,p,p-1}^{(1)\mu,h,h-1} + \sigma v_{v,p,p-1}^{(1)\mu,h,h-1}) \Gamma_{\mu,h,h-1}^\alpha \\ &- \frac{p^*}{4\pi} \sum_{h=1}^N \sum_{\mu=1}^n (v_{v,p,p-1}^{(2)\mu,h,h-1} + \sigma v_{v,p,p-1}^{(2)\mu,h,h-1}) \dot{\Gamma}_{\mu,h,h-1}^\alpha = 1 \\ &+ p^* \sum_{h=1}^N \sum_{\mu=1}^n (v_{v,p,p-1}^{(1)\mu,h,h-1} + \sigma v_{v,p,p-1}^{(1)\mu,h,h-1}) \dot{\Gamma}_{\mu,h,h-1}^\alpha = 0 \\ &\Gamma_{\mu,h,h-1}^\alpha|_{\mu=\mu_*} = 0, \quad \dot{\Gamma}_{\mu,h,h-1}^\alpha|_{\mu=\mu_*} = 0 \\ &p = 0, 1, 2, \dots, N; \quad v = 0, 1, 2, \dots, n-1; \\ &k = 1, 2, 3, \dots, N \end{aligned} \right\} \quad (9.8.39)$$

We find the derivatives  $\Gamma_{\mu, k, h-1}^{\omega_v}$  and  $\Gamma_{\mu, k, h-1}^{\omega_z}$  as a result of solving the second system:

$$\left. \begin{aligned} & \frac{1}{4\pi} \sum_{k=1}^N \sum_{\mu=1}^n (v_v^{(1)\mu, k, h-1} - \sigma v_v^{(1)\mu, k, h-1}) \Gamma_{\mu, k, h-1}^{\omega_v} \\ & - \frac{p^*}{4\pi} \sum_{k=1}^N \sum_{\mu=1}^n (v_v^{(2)\mu, k, h-1} + \sigma v_v^{(2)\mu, k, h-1}) \Gamma_{\mu, k, h-1}^{\omega_z} \\ & = -\xi_v^{v, p-1} \\ & \sum_{k=1}^N \sum_{\mu=1}^n (v_v^{(2)\mu, k, h-1} + \sigma v_v^{(2)\mu, k, h-1}) \Gamma_{\mu, k, h-1}^{\omega_z} \\ & + p^* \sum_{k=1}^N \sum_{\mu=1}^n (v_v^{(1)\mu, k, h-1} + \sigma v_v^{(1)\mu, k, h-1}) \Gamma_{\mu, k, h-1}^{\omega_z} = 0 \\ & \Gamma_{\mu, k, h-1}^{\omega_z} |_{\mu=\mu^*} = 0, \quad \Gamma_{\mu, k, h-1}^{\omega_z} |_{\mu=\mu^*} = 0 \\ & p = 0, 1, 2, \dots, N; \quad v = 0, 1, 2, \dots, n-1; \\ & k = 1, 2, 3, \dots, N \end{aligned} \right\} (9.8.40)$$

In Eqs. (9.8.39) and (9.8.40), we have chosen the plus sign in the parentheses because we are considering symmetric motions in which the distribution of the circulation over the span is also symmetric.

The third system of equations allows us to determine the derivatives  $\Gamma_{\mu, k, h-1}^{\omega_v}$  and  $\Gamma_{\mu, k, h-1}^{\omega_z}$  characterizing the asymmetric nature of motion of a craft. Choosing the minus sign in (9.8.34), we can write this system as

$$\left. \begin{aligned} & \frac{1}{4\pi} \sum_{k=1}^N \sum_{\mu=1}^n (v_v^{(1)\mu, k, h-1} - \sigma v_v^{(1)\mu, k, h-1}) \Gamma_{\mu, k, h-1}^{\omega_v} \\ & - \frac{p^*}{4\pi} \sum_{k=1}^N \sum_{\mu=1}^n (v_v^{(2)\mu, k, h-1} - \sigma v_v^{(2)\mu, k, h-1}) \Gamma_{\mu, k, h-1}^{\omega_z} \\ & = -\xi_v^{v, p-1} \\ & \sum_{k=1}^N \sum_{\mu=1}^n (v_v^{(2)\mu, k, h-1} - \sigma v_v^{(2)\mu, k, h-1}) \Gamma_{\mu, k, h-1}^{\omega_z} \\ & + p^* \sum_{k=1}^N \sum_{\mu=1}^n (v_v^{(1)\mu, k, h-1} - \sigma v_v^{(1)\mu, k, h-1}) \Gamma_{\mu, k, h-1}^{\omega_v} = 0 \\ & \Gamma_{\mu, k, h-1}^{\omega_v} |_{\mu=\mu^*} = 0, \quad \Gamma_{\mu, k, h-1}^{\omega_z} |_{\mu=\mu^*} = 0 \\ & p = 0, 1, 2, \dots, N; \quad v = 0, 1, 2, \dots, n-1; \\ & k = 1, 2, 3, \dots, N \end{aligned} \right\} (9.8.41)$$

We find the dimensionless geometric variables in Eqs. (9.8.39)–(9.8.41) from (9.8.37). The solution of these equations allows us to determine the derivatives of dimensionless circulation for an unsteady flow over a wing at arbitrary Strouhal numbers.

Let us consider the problem of motion at low Strouhal numbers ( $p_i^* \rightarrow 0$ ), which is of major theoretical and practical significance. In accordance with (9.8.19) and (9.8.20), we have

$$v_{\nu, p, p-1}^{(1) \mu, k, k-1} = v_{\nu, p, p-1}^{\mu, k, k-1}; \quad v_{\nu, p, p-1}^{(2) \mu, k, k-1} = p_i^* \partial v_{\nu, p, p-1}^{(2) \mu, k, k-1} / \partial p_i^* \quad (9.8.42)$$

Introducing these expressions into (9.8.34), we obtain the following systems of equations:

$$\frac{1}{4\pi} \sum_{k=1}^N \sum_{\mu=1}^n (v_{\nu, p, p-1}^{\mu, k, k-1} \pm \sigma v_{\nu, p, p-1}^{\mu, k, k-1}) \Gamma_{\mu, k, k-1}^{q_i} = v_{\nu, p, p-1}^{q_i} \quad (9.8.43)$$

$$\Gamma_{\mu, k, k-1}^{q_i} |_{\mu=\mu_*} = 0, \quad p = 1, 2, \dots, N;$$

$$v = 1, 2, \dots, n-1 \quad k = 1, 2, \dots, N$$

$$\sum_{k=1}^N \sum_{\mu=1}^n (v_{\nu, p, p-1}^{\mu, k, k-1} \pm \sigma v_{\nu, p, p-1}^{\mu, k, k-1}) \Gamma_{\mu, k, k-1}^{q_i}$$

$$= - \sum_{k=1}^N \sum_{\mu=1}^n (\partial v_{\nu, p, p-1}^{(2) \mu, k, k-1} / \partial p_i^*$$

$$\pm \sigma \partial v_{\nu, p, p-1}^{(2) \mu, k, k-1} / \partial p_i^*) \Gamma_{\mu, k, k-1}^{q_i} \quad (9.8.44)$$

$$\Gamma_{\mu, k, k-1}^{q_i} |_{\mu=\mu_*} = 0; \quad p = 1, 2, \dots, N;$$

$$v = 1, 2, \dots, n-1 \quad k = 1, 2, \dots, N$$

Consequently, the problem on the oscillations of a wing with low Strouhal numbers reduces to solving six (instead of three) systems of equations but simpler ones than for arbitrary values of  $p_i^*$ . The first system of equations (9.8.43) contains no derivatives

$\Gamma_{\mu, k, k-1}^{q_i}$  and is solved independently of system (9.8.44) for the derivative  $\Gamma_{\mu, k, k-1}^{q_i}$ . Its value is used to calculate the right-hand side of the equations of the second system (9.8.44), the solution

yielding the derivative  $\Gamma_{\mu, k, k-1}^{q_i}$ .

The dimensionless coefficients of equation (9.8.43) and (9.8.44) are determined from the relations

$$v_{\nu, p, p-1}^{\mu, k, k-1} = v(\xi_{\nu, p, p-1}^{\mu, k, k-1}, \zeta_{\nu, p, p-1}^{\mu, k, k-1}, \bar{l}_{k, k-1}, \chi_{\mu, k-1}^{\mu, k})$$

$$\sigma v_{\nu, p, p-1}^{\mu, k, k-1} = v(\xi_{\nu, p, p-1}^{\mu, k, k-1}, \sigma \zeta_{\nu, p, p-1}^{\mu, k, k-1}, \bar{l}_{k, k-1}, -\chi_{\mu, k-1}^{\mu, k})$$

$$\frac{\partial v_{\nu, p, p-1}^{(2) \mu, k, k-1}}{\partial p_i^*} = \frac{\partial v^{(2)}}{\partial p_i^*} \quad (9.8.45)$$

$$\times (\xi_v^{\mu, k, k-1}, \zeta_v^{\mu, k, k-1}, \bar{l}_{k, k-1}, x_{\mu, k-1}^{\mu, k}) \\ \sigma \frac{\partial v_v^{(2)\mu, k, k-1}}{\partial p_i^*} = \frac{\partial v^{(2)}}{\partial p_i^*} \\ \times (\xi_v^{\mu, k, k-1}, \sigma \zeta_v^{\mu, k, k-1}, \bar{l}_{k, k-1}, -x_{\mu, k-1}^{\mu, k})$$

Let us write Eqs. (9.8.43) and (9.8.44) with account taken of the specific values of  $q_i$  and  $\dot{q}_i$ , and also of the nature of motion, i.e. symmetric or asymmetric.

The system of equations for determining the derivatives  $\Gamma_{\mu, k, k-1}^{\alpha}$  has the following form:

$$\left. \begin{aligned} \frac{1}{4\pi} \sum_{h=1}^N \sum_{\mu=1}^n (v_v^{\mu, k, k-1} + \sigma v_v^{\mu, k, k-1}) \Gamma_{\mu, k, k-1}^{\alpha} &= -1 \\ \Gamma_{\mu, k, k-1}^{\alpha} \Big|_{\mu=\mu_*} &= 0; \quad p = 1, 2, \dots, N; \quad v = 1, 2, \dots, n-1; \\ k &= 1, 2, \dots, N \end{aligned} \right\} \quad (9.8.46)$$

We find the derivative  $\dot{\Gamma}_{\mu, k, k-1}^{\alpha}$  by solving a second system of equations:

$$\left. \begin{aligned} \sum_{h=1}^N \sum_{\mu=1}^n (v_v^{\mu, k, k-1} + \sigma v_v^{\mu, k, k-1}) \Gamma_{\mu, k, k-1}^{\alpha} \\ = - \sum_{h=1}^N \sum_{\mu=1}^n \left( \frac{\partial v_v^{(2)\mu, k, k-1}}{\partial p_i^*} + \sigma \frac{\partial v_v^{(2)\mu, k, k-1}}{\partial p_i^*} \right) \\ \times \dot{\Gamma}_{\mu, k, k-1}^{\alpha} \\ \dot{\Gamma}_{\mu, k, k-1}^{\alpha} \Big|_{\mu=\mu_*} &= 0; \quad p = 1, 2, \dots, N; \\ v &= 1, 2, \dots, n-1; \quad k = 1, 2, \dots, N \end{aligned} \right\} \quad (9.8.47)$$

We use a third system to find the derivative  $\Gamma_{\mu, k, k-1}^{\omega z}$ :

$$\left. \begin{aligned} \frac{1}{4\pi} \sum_{k=1}^N \sum_{\mu=1}^n (v_v^{\mu, k, k-1} + \sigma v_v^{\mu, k, k-1}) \Gamma_{\mu, k, k-1}^{\omega z} &= -\xi_v^{\nu, p, p-1} \\ \Gamma_{\mu, k, k-1}^{\omega z} \Big|_{\mu=\mu_*} &= 0; \\ p &= 1, 2, \dots, N; \quad v = 1, 2, \dots, n-1; \quad k = 1, 2, \dots, N \end{aligned} \right\} \quad (9.8.48)$$

A fourth system of equations is intended for calculating  $\Gamma_{\mu, h, h-1}^{\omega z}$ :

$$\left. \begin{aligned} & \sum_{k=1}^N \sum_{\mu=1}^n (v_{v, p, p-1}^{\mu, k, h-1} + \sigma v_{v, p, p-1}^{\mu, k, h-1}) \dot{\Gamma}_{\mu, h, k-1}^{\omega z} \\ & = - \sum_{k=1}^N \sum_{\mu=1}^n \left( \frac{\partial t_{v, p, p-1}^{(2)\mu, k, h-1}}{\partial p_i^*} + \sigma \frac{\partial v_{v, p, p-1}^{(2)\mu, k, h-1}}{\partial p_i^*} \right) \dot{\Gamma}_{\mu, h, k-1}^{\omega z} \\ & \dot{\Gamma}_{\mu, h, k-1}^{\omega z} \Big|_{\mu=\mu_*} = 0; \quad p=1, 2, \dots, N; \quad v=1, 2, \dots, n-1; \\ & \quad k=1, 2, \dots, N \end{aligned} \right\} \quad (9.8.49)$$

We compile a fifth system for determining the derivatives  $\Gamma_{\mu, h, k-1}^{\omega x}$ :

$$\left. \begin{aligned} & \frac{1}{4\pi} \sum_{k=1}^N \sum_{\mu=1}^n (v_{v, p, p-1}^{\mu, k, h-1} - \sigma v_{v, p, p-1}^{\mu, k, h-1}) \dot{\Gamma}_{\mu, h, k-1}^{\omega x} = - \xi_{v, p-1}^v \\ & \dot{\Gamma}_{\mu, h, k-1}^{\omega x} \Big|_{\mu=\mu_*} = 0; \quad p=1, 2, \dots, N; \quad v=1, 2, \dots, n-1; \\ & \quad k=1, 2, \dots, N \end{aligned} \right\} \quad (9.8.50)$$

A sixth system of equations, given below, allows us to find  $\dot{\Gamma}_{\mu, h, k-1}^{\omega x}$ :

$$\left. \begin{aligned} & \sum_{k=1}^N \sum_{\mu=1}^n (v_{v, p, p-1}^{\mu, k, h-1} - \sigma v_{v, p, p-1}^{\mu, k, h-1}) \dot{\Gamma}_{\mu, h, k-1}^{\omega x} \\ & = - \sum_{k=1}^N \sum_{\mu=1}^n \left( \frac{\partial v_{v, p, p-1}^{(2)\mu, k, h-1}}{\partial p_i^*} - \sigma \frac{\partial v_{v, p, p-1}^{(2)\mu, k, h-1}}{\partial p_i^*} \right) \dot{\Gamma}_{\mu, h, k-1}^{\omega x} \\ & \dot{\Gamma}_{\mu, h, k-1}^{\omega x} \Big|_{\mu=\mu_*} = 0; \quad p=1, 2, \dots, N; \quad v=1, 2, \dots, n-1; \\ & \quad k=1, 2, \dots, N \end{aligned} \right\} \quad (9.8.51)$$

### Aerodynamic Characteristics

The values of the circulation derivatives  $\Gamma_{\mu, h, h-1}^{qt}$  and  $\Gamma_{\mu, h, h-1}^{qi}$  can be used to calculate the distribution of the pressure coefficients, and according to them, the wing stability derivatives.

Here we calculate the difference of the pressure coefficients for the bottom and upper sides in the form of the series (9.6.22):

$$\Delta \bar{p} = p^\alpha \alpha + p^{\dot{\alpha}} \dot{\alpha} + p^{\omega x} \omega_x + p^{\dot{\omega x}} \dot{\omega}_x + p^{\omega z} \omega_z + p^{\dot{\omega z}} \dot{\omega}_z \quad (9.8.52)$$

In accordance with Zhukovsky's formula (9.7.15), we have

$$\begin{aligned} p^\alpha &= 2\gamma, \quad p^{\dot{\alpha}} = 2\gamma^{\dot{\alpha}}, \quad p^{\omega_x} = 2\gamma^{\omega_x}, \\ p^{\dot{\omega}_x} &= 2\gamma^{\dot{\omega}_x}; \quad p^{\omega_z} = 2\gamma^{\omega_z}, \quad p^{\dot{\omega}_z} = 2\gamma^{\dot{\omega}_z} \end{aligned} \quad (9.8.53)$$

Let us consider a cell containing a point with the coordinates  $\xi_{\mu, h-1}^{\mu, k}$ ,  $\zeta_{\mu, h-1}^{\mu, k}$  for which we shall calculate the pressure. We determine the strength of a bound vortex at this point by the appropriate value of the circulation related to the interval between the control points  $\Delta\xi_{\mu, h, h-1} = \xi_{v, p-1}^{v, p} - \xi_{v-1, p-1}^{v-1, p}$  in the section  $\xi_{\mu, h-1}^{\mu, k}$ :

$$\gamma(\xi_{\mu, h-1}^{\mu, k}, \zeta_{\mu, h-1}^{\mu, k}) = \Gamma(\xi_{\mu, h-1}^{\mu, k}, \zeta_{\mu, h-1}^{\mu, k}) / \Delta\xi_{\mu, h, h-1} \quad (9.8.54)$$

Let us write the strength of the vortex layer and the circulation of a discrete vortex in the form of the series (9.7.12) and (9.8.25):

$$\left. \begin{aligned} \gamma(\xi_{\mu, h-1}^{\mu, k}, \zeta_{\mu, h-1}^{\mu, k}) &= \sum_{i=1}^3 (\gamma_{\mu, h, h-1}^{q_i} q_i + \gamma_{\mu, h, h-1}^{\dot{q}_i} \dot{q}_i) \\ \Gamma(\xi_{\mu, h-1}^{\mu, k}, \zeta_{\mu, h-1}^{\mu, k}) &= \sum_{i=1}^3 (\Gamma_{\mu, h, h-1}^{q_i} q_i + \Gamma_{\mu, h, h-1}^{\dot{q}_i} \dot{q}_i) \end{aligned} \right\} \quad (9.8.55)$$

Introducing these expressions into (9.8.54), we obtain relations for the derivatives

$$\begin{aligned} \gamma_{\mu, h, h-1}^{q_i} &= \Gamma_{\mu, h, h-1}^{q_i} / \Delta\xi_{\mu, h, h-1}, \quad \gamma_{\mu, h, h-1}^{\dot{q}_i} \\ &= \Gamma_{\mu, h, h-1}^{\dot{q}_i} / \Delta\xi_{\mu, h, h-1} \end{aligned} \quad (9.8.56)$$

With account taken of these derivatives, the expressions for the strength of the vortices are determined by the quantities  $p_{\mu, h, h-1}^{q_i}$  and  $p_{\mu, h, h-1}^{\dot{q}_i}$  (9.8.53). Let us introduce them into formulas (9.6.5) in which  $\Delta p$  is replaced with series (9.8.52), the value of  $x_h$  is taken equal to  $b_0$  and  $x'$  to the local chord  $b_{h, h-1}$ :

$$\left. \begin{aligned} c'_y &= \frac{b_0}{b_{h, h-1}} \int_{\xi_0}^{\xi_1} \sum_{i=1}^3 (p^{q_i} q_i + p^{\dot{q}_i} \dot{q}_i) d\xi \\ m'_z &= \frac{b_0^2}{b_{h, h-1}^2} \int_{\xi_0}^{\xi_1} \sum_{i=1}^3 (p^{q_i} q_i + p^{\dot{q}_i} \dot{q}_i) \xi d\xi; \\ m'_x &= -\frac{b_0}{b_{h, h-1}} c'_y \zeta \end{aligned} \right\} \quad (9.8.57)$$

Let us replace the coefficients on the left-hand side of (3.8.57) with their expressions in the form of series similar to (9.6.8):

$$\left. \begin{aligned} c'_y &= \sum_{i=1}^3 (c'_y{}^{q_i} q_i + c'_y \dot{q}_i) \\ m'_z &= \sum_{i=1}^3 (m'_z{}^{q_i} q_i + m'_z \dot{q}_i) \\ m'_x &= \sum_{i=1}^3 (m'_x{}^{q_i} q_i + m'_x \dot{q}_i) \end{aligned} \right\} \quad (9.8.58)$$

As an example, let us write the right-hand side of (9.8.58) for the normal force coefficient in the expanded form:

$$c'_y = c'_y{}^\alpha \alpha + c' \dot{\bar{\alpha}} + c'_y \omega_x \omega_x + c'_y \dot{\omega}_x \dot{\omega}_x + c'_y \omega_z \omega_z + c'_y \dot{\omega}_z \dot{\omega}_z \quad (9.8.59)$$

Two other coefficients,  $m'_z$  and  $m'_x$ , are expressed similarly. As a result of the indicated replacement of the coefficients  $c'_y$ ,  $m'_z$ , and  $m'_x$  in (9.8.57) with series and of a transition from integrals to sums, we obtain the derivatives of the aerodynamic coefficients of the sections in the following form:

$$\left. \begin{aligned} c'{}^{q_i}_{y, k, k-1} &= \frac{2b_0}{b_{k, k-1}} \sum_{\substack{\mu=\mu_* \\ \mu=\mu_0 \\ \mu=\mu_*}}^{\mu=\mu_*} \Gamma_{\mu, k, k-1}^{q_i} \\ c'{}^{\dot{q}_i}_{y, k, k-1} &= \frac{2b_0}{b_{k, k-1}} \sum_{\mu=\mu_0}^{\mu=\mu_*} \Gamma_{\mu, k, k-1}^{\dot{q}_i} \end{aligned} \right\} \quad (9.8.60)$$

$$\left. \begin{aligned} m'{}^{q_i}_{z, k, k-1} &= \frac{2b_0^2}{b_{k, k-1}^2} \sum_{\substack{\mu=\mu_* \\ \mu=\mu_0}}^{\mu=\mu_*} \Gamma_{\mu, k, k-1}^{q_i} \xi_{\mu, k-1}^{\mu, k} \\ m'{}^{\dot{q}_i}_{z, k, k-1} &= \frac{2b_0^2}{b_{k, k-1}^2} \sum_{\mu=\mu_0}^{\mu=\mu_*} \Gamma_{\mu, k, k-1}^{\dot{q}_i} \dot{\xi}_{\mu, k-1}^{\mu, k} \end{aligned} \right\} \quad (9.8.61)$$

$$\left. \begin{aligned} m'{}^{q_i}_{x, k, k-1} &= -c'{}^{q_i}_{y, k, k-1} \xi_{\mu, k-1}^{\mu, k} \frac{b_0}{b_{k, k-1}} \\ m'{}^{\dot{q}_i}_{x, k, k-1} &= -c'{}^{\dot{q}_i}_{y, k, k-1} \xi_{\mu, k-1}^{\mu, k} \frac{b_0}{b_{k, k-1}} \end{aligned} \right\} \quad (9.8.62)$$

We obtain the stability derivatives for a wing as a whole by using the following relations for the total aerodynamic characteris-

ties of a wing:

$$\left. \begin{aligned} c_y &= \frac{2b_0}{S_w} \int_0^{l_0/(2b_0)} c'_y b(\zeta) d\zeta \\ m_z &= \frac{2}{S_w} \int_0^{l_0/(2b_0)} m'_z b^2(\zeta) d\zeta \\ m_x &= \frac{-2b_0}{S_w} \int_0^{l_0/(2b_0)} c'_y b(\zeta) d\zeta \end{aligned} \right\} \quad (9.8.63)$$

We can express the coefficients  $c_y$ ,  $m_z$ , and  $m_x$  for a wing in the form of series (9.6.8), and their corresponding values  $c'_y$ ,  $m'_z$ , and  $m'_x$  for the sections in the form of (9.8.58). After using the derivatives (9.8.60)-(9.8.62), we obtain the stability derivatives for a wing as a whole ( $c_y^{qi}$ ,  $c_y^{\dot{q}i}$ ,  $m_z^{qi}$ ,  $m_z^{\dot{q}i}$ ,  $m_x^{qi}$ , and  $m_x^{\dot{q}i}$ ).

Going over from integrals to sums, we obtain for symmetric motions ( $q_i = \alpha$ ,  $\omega_z$ ):

$$m_x^{qi} = m_x^{\dot{q}i} = 0 \quad (9.8.64)$$

$$\left. \begin{aligned} c_y^{qi} &= \frac{4b_0^2}{S_w} \sum_{k=1}^N \bar{l}_{k, k-1} \sum_{\mu=\mu_*}^{\mu=\mu_*} \Gamma_{\mu, k, k-1}^{qi} \\ c_y^{\dot{q}i} &= \frac{4b_0^2}{S_w} \sum_{k=1}^N \bar{l}_{k, k-1} \sum_{\mu=\mu_*}^{\mu=\mu_*} \Gamma_{\mu, k, k-1}^{\dot{q}i} \end{aligned} \right\} \quad (9.8.65)$$

$$\left. \begin{aligned} m_z^{qi} &= \frac{4b_0^2}{S_w} \sum_{k=1}^N \bar{l}_{k, k-1} \sum_{\mu=\mu_*}^{\mu=\mu_*} \Gamma_{\mu, k, k-1}^{qi} \xi_{\mu, k-1}^{\mu, k} \\ m_z^{\dot{q}i} &= \frac{4b_0^2}{S_w} \sum_{k=1}^N \bar{l}_{k, k-1} \sum_{\mu=\mu_*}^{\mu=\mu_*} \Gamma_{\mu, k, k-1}^{\dot{q}i} \xi_{\mu, k-1}^{\mu, k} \end{aligned} \right\} \quad (9.8.66)$$

For asymmetric motions ( $q_i = \omega_x$ ):

$$c_y^{qi} = c_y^{\dot{q}i} = 0 \quad (9.8.67)$$

$$m_z^{qi} = m_z^{\dot{q}i} = 0 \quad (9.8.68)$$

$$\left. \begin{aligned} m_x^{qi} &= \frac{4b_0^2}{S_w} \sum_{k=1}^N \bar{l}_{k, k-1} \sum_{\mu=\mu_*}^{\mu=\mu_*} \Gamma_{\mu, k, k-1}^{qi} \xi_{\mu, k-1}^{\mu, k} \\ m_x^{\dot{q}i} &= \frac{4b_0^2}{S_w} \sum_{k=1}^N \bar{l}_{k, k-1} \sum_{\mu=\mu_*}^{\mu=\mu_*} \Gamma_{\mu, k, k-1}^{\dot{q}i} \xi_{\mu, k-1}^{\mu, k} \end{aligned} \right\} \quad (9.8.69)$$

Let us write these expressions in the expanded form with account taken of the corresponding values of  $q_t$  and  $q_i$ , and also of the numbers of the bound vortices  $\mu_0 = 1$  and  $\mu_* = n$  closest to the leading and trailing edges.

For symmetric motions ( $q_i = \alpha$ ,  $\omega_z$ ):

$$m_x^\alpha = m_x^{\dot{\alpha}} = m_x^{\omega z} = m_x^{\dot{\omega z}} = 0 \quad (9.8.70)$$

$$\left. \begin{aligned} c_y^\alpha &= \frac{4b_0^2}{S_w} \sum_{k=1}^N \bar{l}_{k, k-1} \sum_{\mu=1}^n \Gamma_{\mu, k, k-1}^\alpha \\ c_y^{\dot{\alpha}} &= \frac{4b_0^2}{S_w} \sum_{k=1}^N \bar{l}_{k, k-1} \sum_{\mu=1}^n \Gamma_{\mu, k, k-1}^{\dot{\alpha}} \end{aligned} \right\} \quad (9.8.71)$$

$$\left. \begin{aligned} c_y^{\omega z} &= \frac{4b_0^2}{S_w} \sum_{k=1}^N \bar{l}_{k, k-1} \sum_{\mu=1}^n \Gamma_{\mu, k, k-1}^{\omega z} \\ c_y^{\dot{\omega z}} &= \frac{4b_0^2}{S_w} \sum_{k=1}^N \bar{l}_{k, k-1} \sum_{\mu=1}^n \Gamma_{\mu, k, k-1}^{\dot{\omega z}} \end{aligned} \right\} \quad (9.8.72)$$

$$\left. \begin{aligned} m_z^\alpha &= \frac{4b_0^2}{S_w} \sum_{k=1}^N \bar{l}_{k, k-1} \sum_{\mu=1}^n \Gamma_{\mu, k, k-1}^\alpha \xi_{\mu, k, k-1}^\mu \\ m_z^{\dot{\alpha}} &= \frac{4b_0^2}{S_w} \sum_{k=1}^N \bar{l}_{k, k-1} \sum_{\mu=1}^n \Gamma_{\mu, k, k-1}^{\dot{\alpha}} \dot{\xi}_{\mu, k, k-1}^\mu \end{aligned} \right\} \quad (9.8.73)$$

$$\left. \begin{aligned} m_z^{\omega z} &= \frac{4b_0^2}{S_w} \sum_{k=1}^N \bar{l}_{k, k-1} \sum_{\mu=1}^n \Gamma_{\mu, k, k-1}^{\omega z} \xi_{\mu, k, k-1}^\mu \\ m_z^{\dot{\omega z}} &= \frac{4b_0^2}{S_w} \sum_{k=1}^N \bar{l}_{k, k-1} \sum_{\mu=1}^n \Gamma_{\mu, k, k-1}^{\dot{\omega z}} \dot{\xi}_{\mu, k, k-1}^\mu \end{aligned} \right\} \quad (9.8.74)$$

For asymmetric motions ( $q_t = \omega_x$ )

$$c_y^{\omega x} = c_y^{\dot{\omega x}} = m_z^{\omega x} = m_z^{\dot{\omega x}} = 0 \quad (9.8.75)$$

$$\left. \begin{aligned} m_x^{\omega x} &= \frac{4b_0^2}{S_w} \sum_{k=1}^N \bar{l}_{k, k-1} \sum_{\mu=1}^n \Gamma_{\mu, k, k-1}^{\omega x} \xi_{\mu, k, k-1}^\mu \\ m_x^{\dot{\omega x}} &= \frac{4b_0^2}{S_w} \sum_{k=1}^N \bar{l}_{k, k-1} \sum_{\mu=1}^n \Gamma_{\mu, k, k-1}^{\dot{\omega x}} \dot{\xi}_{\mu, k, k-1}^\mu \end{aligned} \right\} \quad (9.8.76)$$

The total values of the aerodynamic coefficients can be determined according to the found stability derivatives, using (9.6.8).

### Deformation of a Wing Surface

The above numerical method of aerodynamic calculations related to a wing with an undeformed (rigid) surface. In real conditions, however, such a surface may deform because of bending or deflection of the control surfaces. The flow over a wing with account taken of its deformation is considered in [4, 19].

The magnitude of the deformation can be expressed in the form

$$\eta(\xi, \zeta, \tau) = f_\delta(\xi, \zeta) \delta(\tau) \quad (9.8.77)$$

where  $f_\delta(\xi, \zeta)$  is a time-independent function determining the changing form of the surface, and  $\delta(\tau)$  is a time-dependent kinematic variable characterizing the scale of the deformation.

In addition to  $q_1$  ( $q_1 = \alpha$ ,  $q_2 = \omega_x$ ,  $q_3 = \omega_z$ ), we can also adopt the dimensionless time function  $q_4 = \delta(\tau)$  as a variable determining the unsteady flow of a deformable wing.

The right-hand side of expression (9.8.26) determining the circulation will additionally include the sum  $\Gamma_{\mu, k, k-1}^{\delta} \delta + \Gamma_{\mu, k, k-1}^{\dot{\delta}} \dot{\delta}$  [where the derivative  $\dot{\delta} = (d\delta/dt) b_0/V_\infty$ ]. This will lead to a corresponding change in the aerodynamic coefficients, the general expression for which can be written in the form of a series

$$c = c^\alpha \alpha + c^{\dot{\alpha}} \dot{\alpha} + c^{\omega_x} \omega_x + c^{\dot{\omega}_x} \dot{\omega}_x + c^{\omega_z} \omega_z + c^{\dot{\omega}_z} \dot{\omega}_z + c^{\delta} \delta + c^{\dot{\delta}} \dot{\delta}; \quad c = \Delta \bar{p}, c_y, m_x, m_z \quad (9.8.78)$$

The deformation of a wing changes the boundary condition of flow which instead of (9.6.32') acquires the form

$$\frac{\partial \bar{\Phi}}{\partial \eta} = -\alpha(\tau) - \omega_x(\tau) \zeta - \omega_z(\tau) \xi + \frac{\partial f_\delta}{\partial \xi} \delta(\tau) + f_\delta(\xi, \zeta) \dot{\delta}(\tau) \quad (9.8.79)$$

where  $(\partial f_\delta / \partial \xi) \delta(\tau) + f_\delta(\xi, \zeta) \dot{\delta}(\tau) = v/V_\infty$  is the dimensionless vertical component of the velocity of an undisturbed flow due to deformation of the wing and damped in unsteady flow by the disturbed stream.

With a view to (9.8.79), we shall write a system of algebraic equations for determining the circulation derivatives  $\Gamma_{\mu, k, k-1}^{q_i}$  and  $\Gamma_{\mu, k, k-1}^{q_i}$  which are then used to find the derivatives of the aerodynamic coefficients, and their local and total values with a view to the deformation of the aircraft. The results of solving this problem are given in detail in [4, 19].

**Influence of Compressibility  
(the Number  $M_\infty$ )  
on Non-Stationary Flow**

In definite conditions, the evaluation of the influence of compressibility on non-stationary linearized flow can be considered by solving the problem of incompressible flow over a fictitious lifting surface. The solution of such a problem allows us to find expressions relating the corresponding aerodynamic characteristics of a wing in an incompressible and compressible flows and take into account the influence of the number  $M_\infty$ . To consider these conditions, let us use differential equation (9.6.31) for the additional velocity potential  $\bar{\varphi}$  of the disturbed non-stationary flow of a compressible fluid [the symbol  $\bar{\varphi}$  is given in (9.6.19), where it is assumed that  $x_k = b_0$ ].

We determine the dimensionless coordinates in (9.6.31) in the form  $\xi = x/b_0$ ,  $\eta = y/b_0$ , and  $\zeta = z/b_0$ .

Let us express the dimensionless velocity potential  $\bar{\varphi}$  equal to  $\varphi/(bV_\infty)$  in terms of its derivatives  $\varphi^{q_i} = \partial\varphi/\partial q_i$  and  $\dot{\varphi}^{q_i} = \partial\varphi/\partial \dot{q}_i$  in the following form (see [4, 19]):

$$\bar{\varphi} = \varphi_0 + \sum_{i=1}^3 [\varphi^{q_i} q_i(\tau) + \dot{\varphi}^{q_i} \dot{q}_i(\tau)] \quad (9.8.80)$$

where  $\varphi_0$  is the velocity potential of stationary flow over a wing with a finite airfoil thickness at a zero angle of attack.

Let us introduce the functions  $\psi$ ,  $\psi^{q_i}$ , and  $\dot{\psi}^{q_i}$  related to the velocity potential and its derivatives by the following expressions:

$$\left. \begin{aligned} \varphi^{q_i} &= \psi^{q_i} \cos \omega \xi + p_i^* k^{-2} \dot{\psi}^{q_i} \sin \omega \xi \\ \dot{\varphi}^{q_i} &= k^{-2} \dot{\psi}^{q_i} \cos \omega \xi - p_i^{*-1} \psi^{q_i} \sin \omega \xi \\ \varphi_0 &= \psi_0, \quad \omega = M_\infty^2 k^{-2} p_i^* \end{aligned} \right\} \quad (9.8.81)$$

where  $k = \sqrt{1 - M_\infty^2}$ .

After the corresponding substitution for the derivatives in (9.8.80) of their values from (9.8.81) and then introducing  $\bar{\varphi}$  into (9.6.31), we obtain the following three equations:

$$k^2 \frac{\partial^2 \psi_0}{\partial \xi^2} + \frac{\partial^2 \psi_0}{\partial \eta^2} + \frac{\partial^2 \psi_0}{\partial \zeta^2} = 0 \quad (9.8.82)$$

$$\left. \begin{aligned} k^2 \frac{\partial^2 \psi^{q_i}}{\partial \xi^2} + \frac{\partial^2 \psi^{q_i}}{\partial \eta^2} + \frac{\partial^2 \psi^{q_i}}{\partial \zeta^2} + (p_i^*)^2 M_\infty^2 k^{-2} \psi^{q_i} &= 0 \\ k^2 \frac{\partial^2 \dot{\psi}^{q_i}}{\partial \xi^2} + \frac{\partial^2 \dot{\psi}^{q_i}}{\partial \eta^2} + \frac{\partial^2 \dot{\psi}^{q_i}}{\partial \zeta^2} + (p_i^*)^2 M_\infty^2 k^{-2} \dot{\psi}^{q_i} &= 0 \end{aligned} \right\} \quad (9.8.83)$$

Considering one of the basic cases of flow that is characterized by low Strouhal numbers ( $p_i^* \rightarrow 0$ ), instead of Eq. (9.8.83) we obtain

$$\left. \begin{aligned} k^2 \frac{\partial^2 \psi^{q_i}}{\partial \xi^2} + \frac{\partial^2 \psi^{q_i}}{\partial \eta^2} + \frac{\partial^2 \psi^{q_i}}{\partial \zeta^2} &= 0 \\ k^2 \frac{\dot{\partial}^2 \psi^{q_i}}{\partial \xi^2} + \frac{\dot{\partial}^2 \psi^{q_i}}{\partial \eta^2} + \frac{\dot{\partial}^2 \psi^{q_i}}{\partial \zeta^2} &= 0 \end{aligned} \right\} \quad (9.8.84)$$

Let us consider a rigid lifting surface. Instead of the flow of a compressible fluid over it, we shall study the flow of an incompressible fluid over the transformed surface. The coordinates of points in the incompressible flow are related to the coordinates of the space of the compressible gas by the expressions

$$x_{1c} = x/k, \quad y_{1c} = y, \quad z_{1c} = z \quad (9.8.85)$$

or in the dimensionless form

$$\begin{aligned} \xi_{1c} &= x_{1c}/b_{0,1c} = \xi, & \eta_{1c} &= y_{1c}/b_{0,1c} = \eta k, \\ \zeta_{1c} &= z_{1c}/b_{0,1c} = \zeta k \end{aligned} \quad (9.8.86)$$

Let us change the planform of the given lifting surface, using the relations between the coordinates in the form of (9.8.86). In accordance with these relations, the dimensionless geometric variables of the transformed surface can be written as follows:

$$\xi_{0,1c} = \xi_0 k, \quad \xi_{0,1c} = \xi_0 \quad \bar{b}_{1c}(\zeta_{1c}) = \bar{b}(\zeta) \quad (9.8.87)$$

where  $\xi_0$  and  $\zeta_0$  are the dimensionless coordinates of the leading edge;

$$\bar{b}_{1c} = b_{1c}/b_{0,1c}, \quad \bar{b} = b/b_0, \quad b_{1c} = b/k$$

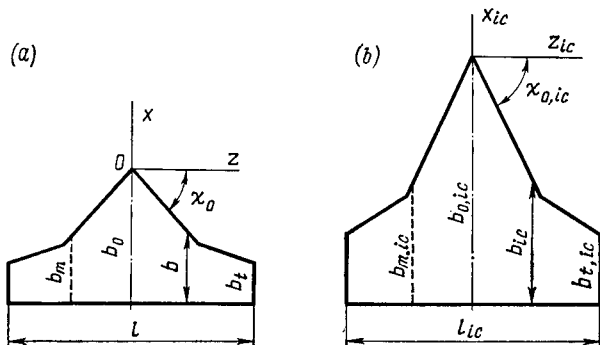
For the centre and running chords in (9.8.87), we have introduced the symbols  $b_0$  and  $b$ , respectively.

For wings with straight edges, the planform is usually set by dimensionless parameters, namely, the aspect ratio  $\lambda_w = l_0/b_m$ , the taper ratio  $\eta_w = b_0/b_t$ , and the sweep angle of the leading edge  $\chi_0$ . The corresponding dimensionless geometric variables of the transformed wing in an incompressible flow are:

$$\lambda_{1c,w} = k\lambda_w, \quad \eta_{1c,w} = \eta_w, \quad \lambda_{1c,w} \tan \chi_{0,1c} = \lambda_w \tan \chi_0 \quad (9.8.88)$$

where  $\lambda_{1c,w} = l_{1c}/b_{m,1c}$ ,  $\lambda_w = l/b_m$ ,  $\eta_{1c,w} = b_{0,1c}/b_{t,1c}$ , and  $\eta_w = b_0/b_t$ .

Figure 9.8.4 shows the given and transformed wing planes. The transformed plane retains its lateral dimensions and is extended in a longitudinal direction in accordance with the relation  $x_{1c} = x/\sqrt{1 - M_\infty^2}$ .

**Fig. 9.8.4**

Geometric dimensions of a wing:

a—given wing in a compressible flow; b—transformed wing in an incompressible flow

Let us go over in Eqs. (9.8.82) and the first equation (9.8.84) to the new variables  $\xi_{ic}$ ,  $\eta_{ic}$ , and  $\zeta_{ic}$  related to  $\xi$ ,  $\eta$ , and  $\zeta$  by expressions (9.8.86). As a result, we obtain

$$\frac{\partial^2 \psi_0}{\partial \xi_{ic}^2} + \frac{\partial^2 \psi_0}{\partial \eta_{ic}^2} + \frac{\partial^2 \psi_0}{\partial \zeta_{ic}^2} = 0 \quad (9.8.89)$$

$$\frac{\partial^2 \psi^{qi}}{\partial \xi_{ic}^2} + \frac{\partial^2 \psi^{qi}}{\partial \eta_{ic}^2} + \frac{\partial^2 \psi^{qi}}{\partial \zeta_{ic}^2} = 0; \quad \frac{\partial^2 \dot{\psi}^{qi}}{\partial \xi_{ic}^2} + \frac{\partial^2 \dot{\psi}^{qi}}{\partial \eta_{ic}^2} + \frac{\partial^2 \dot{\psi}^{qi}}{\partial \zeta_{ic}^2} = 0 \quad (9.8.90)$$

Let us now consider the motion of the transformed lifting surface in an incompressible fluid. Let us write the disturbing potential of the flow over the surface as follows:

$$\Phi_{ic} = k \left[ \Phi_0 + \sum_{i=1}^3 \left( \Phi_{ic}^{qi, ic} q_i, ic + \dot{\Phi}_{ic}^{qi, ic} \dot{q}_i, ic \right) \right] \quad (9.8.91)$$

where  $\Phi_{ic}$  is a dimensionless quantity equal to the potential related to the product  $b_{0,ic} V_\infty$ . Everywhere in the disturbed region of the flow over the surface, the potential must satisfy the continuity equation

$$\frac{\partial^2 \Phi_{ic}}{\partial \xi_{ic}^2} + \frac{\partial^2 \Phi_{ic}}{\partial \eta_{ic}^2} + \frac{\partial^2 \Phi_{ic}}{\partial \zeta_{ic}^2} = 0 \quad (9.8.92)$$

Introducing (9.8.91) into this equation, we obtain equations which the derivatives of the potential of the non-stationary incom-

pressible flow over the transformed wing must satisfy:

$$\left. \begin{aligned} \frac{\partial^2 \Phi_{ic}^{q_i, ic}}{\partial \xi_{ic}^2} + \frac{\partial^2 \Phi_{ic}^{q_i, ic}}{\partial \eta_{ic}^2} + \frac{\partial^2 \Phi_{ic}^{q_i, ic}}{\partial \zeta_{ic}^2} &= 0; \\ \frac{\dot{\partial}^2 \Phi_{ic}^{q_i, ic}}{\partial \xi_{ic}^2} + \frac{\dot{\partial}^2 \Phi_{ic}^{q_i, ic}}{\partial \eta_{ic}^2} + \frac{\dot{\partial}^2 \Phi_{ic}^{q_i, ic}}{\partial \zeta_{ic}^2} &= 0 \end{aligned} \right\} \quad (9.8.93)$$

By comparing Eqs. (9.8.89) and (9.8.92), and also (9.8.90) and (9.8.93), we find that the functions  $\psi_0$ ,  $\psi^{q_i}$ , and  $\dot{\psi}^{q_i}$  determining the velocity potential for a wing in a compressible flow, and the functions  $\Phi_0$ ,  $\Phi_{ic}^{q_i, ic}$ , and  $\dot{\Phi}_{ic}^{q_i, ic}$  determining the potential for a transformed wing in an incompressible flow satisfy the same differential equations. It is shown in [19] that the boundary conditions are identical. Accordingly, the values of these functions at the points related by conditions (9.8.86) are also identical, i.e.

$$\left. \begin{aligned} \psi^{q_i}(\xi, \eta, \zeta) &= \Phi_{ic}^{q_i, ic}(\xi_{ic}, \eta_{ic}, \zeta_{ic}) \\ \dot{\psi}^{q_i, ic}(\xi, \eta, \zeta) &= \dot{\Phi}_{ic}^{q_i, ic}(\xi_{ic}, \eta_{ic}, \zeta_{ic}) \end{aligned} \right\} \quad (9.8.94)$$

where

$$\xi = \xi_{ic}, \quad \eta = \eta_{ic}/k, \quad \zeta = \zeta_{ic}/k$$

Consequently, for finding the potential function and its derivatives for a compressible flow over a given lifting surface, we must solve the equivalent problem on the unsteady incompressible flow over a transformed surface with the corresponding boundary conditions. The formulas obtained allow us to directly calculate the relevant values for the given surface in a compressible fluid according to the found aerodynamic characteristics in an incompressible flow for the transformed surface. Particularly, the formulas relating the differences of the pressure coefficients and their derivatives have the following form:

$$\left. \begin{aligned} \bar{\Delta p}_0 &= \bar{\Delta p}_{0, ic}/k, \quad p^{q_i} = p_{ic}^{q_i, ic}/k \\ \dot{p}^{q_i} &= p_{ic}^{q_i, ic}/k - \xi_{ic} M_\infty^2 p_{ic}^{q_i, ic}/k^3 \end{aligned} \right\} \quad (9.8.95)$$

We use these data to find the difference of the pressure coefficients at the point of the surface being considered in a compressible flow:

$$\bar{\Delta p} = \bar{\Delta p}_0 + \sum_{i=1}^3 (p^{q_i} q_i + \dot{p}^{q_i} \dot{q}_i) \quad (9.8.96)$$

Taking (9.8.96) into account, we can obtain the aerodynamic coefficients of a wing in a compressible flow, while by using (9.8.84)

we can establish the relation between the stability derivatives of this wing and also of the transformed wing in an incompressible fluid:

$$\left. \begin{aligned} c_y^{q_i} &= c_{y, \text{ic}}^{q_i}/k, & c_y^{\dot{q}_i} &= (c_{y, \text{ic}}^{\dot{q}_i} - M_\infty^2 m_z^{q_i, \text{ic}})/k^3 \\ m_x^{q_i} &= m_{x, \text{ic}}^{q_i}/k^2, & m_x^{\dot{q}_i} &= (m_{x, \text{ic}}^{\dot{q}_i} + M_\infty^2 I_x)/k^4 \\ m_z^{q_i} &= m_{z, \text{ic}}^{q_i}/k, & m_z^{\dot{q}_i} &= (m_{z, \text{ic}}^{\dot{q}_i} - M_\infty^2 I_z)/k^3 \end{aligned} \right\} \quad (9.8.97)$$

where

$$\left. \begin{aligned} I_x &= \frac{2b_0^2, \text{ic}}{S_w, \text{ic}} \int \int p_{\text{ic}}^{q_i, \text{ic}} \xi_{\text{ic}} \zeta_{\text{ic}} d\xi_{\text{ic}} d\zeta_{\text{ic}} \\ I_z &= \frac{2b_0^2, \text{ic}}{S_w, \text{ic}} \int \int p_{\text{ic}}^{q_i, \text{ic}} \xi_{\text{ic}}^2 d\xi_{\text{ic}} d\zeta_{\text{ic}} \end{aligned} \right\} \quad (9.8.98)$$

The following formulas for the coefficients of the normal force and pitching moment for  $q_i = \dot{q}_i = 0$  correspond to the relation  $\Delta p_0 = \Delta p_{0, \text{ic}}/k$  between the values of the difference of the pressure coefficients in a compressible and incompressible flows:

$$c_{y0} = c_{y, \text{ic}}/k, \quad m_{z0} = m_{z, \text{ic}}/k \quad (9.8.99)$$

With a view to the stability derivatives (9.8.97) and the values (9.8.99), the total normal force and pitching moment coefficients of a wing in a compressible flow have the following form:

$$\left. \begin{aligned} c_y &= c_{y0} + \sum_{i=1}^3 (c_y^{q_i} q_i + c_y^{\dot{q}_i} \dot{q}_i) \\ m_z &= m_{z0} + \sum_{i=1}^3 (m_z^{q_i} q_i + m_z^{\dot{q}_i} \dot{q}_i) \end{aligned} \right\} \quad (9.8.100)$$

We can write the corresponding rolling moment coefficient  $m_x$  in the form of the third of expressions (9.6.8).

## 9.9. Unsteady Supersonic Flow over a Wing

Let us find the solution of the problem of an unsteady supersonic flow over a wing in the form of the velocity potential  $\varphi(x_1, y_1, z_1, t)$  of a transient (pulsating) source (9.7.7) satisfying the wave equation (9.6.30).

Let us consider the expression for such a potential for harmonic oscillations of a wing when the kinematic parameters vary in accord-

ance with the general relation

$$q_j = q_j^* \exp(ip t) \quad (j = \alpha, \omega_x, \omega_z) \quad (9.9.1)$$

It follows from (9.6.32) that the boundary conditions on a wing also vary harmonically. The derivative of the velocity potential on a wing (9.7.8) (let us call it the flow downwash) can be expressed by the harmonic function

$$\left| \frac{\partial \Phi}{\partial y} (x, y, z, t_{1(2)}) \right|_{y=0} = \frac{\partial \Phi}{\partial y} (x, y, z) \Big|_{y=0} e^{ip t_{1(2)}} \quad (9.9.2)$$

The required disturbance potential is related to the downwashes by formula (9.7.7). The quantities  $t_1$  and  $t_2$  are determined in accordance with formulas (9.7.9) as follows:

$$\begin{aligned} t_1 &= t - \Delta t_1 = t (x_1 - x) M_\infty / (a_\infty \alpha'^2) + M_\infty r / (a_\infty \alpha'^2) \\ t_2 &= t - \Delta t_2 = t (x_1 - x) M_\infty / (a_\infty \alpha'^2) - M_\infty r / (a_\infty \alpha'^2) \end{aligned} \quad \{ (9.9.3)$$

After introducing (9.9.2) and (9.9.3) into (9.7.7) for a wing (assuming that  $y = 0$ ), we obtain

$$\begin{aligned} \varphi(x_1, y_1, z_1, t) &= -\frac{1}{2\pi} \operatorname{Re} e^{ipt} \int \int_{\sigma(x_1, z_1)} \left[ \frac{\partial \Phi}{\partial y} (x, y, z) \right]_{y=0} \\ &\times e^{-ip \frac{(x_1 - x) M_\infty}{a_\infty \alpha'^2}} \left( e^{ip \frac{r}{a_\infty \alpha'^2}} + e^{-ip \frac{r}{a_\infty \alpha'^2}} \right) \frac{dx dz}{r} \end{aligned}$$

Taking into account that the sum in parentheses on the right-hand side equals  $2 \cos(pr/a_\infty \alpha'^2)$ , and the quantities

$$p^* = pb_0/V_\infty, \quad \omega = p^* M_\infty^2 / \alpha'^2 \quad (9.9.4)$$

we obtain the following expression for the velocity potential:

$$\begin{aligned} \varphi(x_1, y_1, z_1, t) &= -\frac{1}{\pi} \operatorname{Re} q^* e^{ipt} \\ &\times \int \int_{\sigma(x_1, z_1)} \left[ \frac{\partial \Phi}{\partial y} (x, y, z) \right]_{y=0} e^{-\frac{i\omega(x_1 - x)}{b_0}} \cos \left( \frac{\omega r}{b_0 M_\infty} \right) \frac{dx dz}{r} \end{aligned} \quad (9.9.5)$$

where  $r = \sqrt{(x_1 - x)^2 - \alpha'^2 [y_1^2 + (z_1 - z)^2]}$ .

With a view to the harmonic nature of motion of the wing, we can write the potential function as follows:

$$\begin{aligned} \varphi(x, y, z, t) &= V_\infty b_0 \sum_{j=1}^3 (\varphi^q j q_j + \dot{\varphi}^q j \dot{q}_j) \\ &= V_\infty b_0 \operatorname{Re} e^{ipt} \sum_{j=1}^3 q_j^* [\varphi^q j (x, y, z) + ip^* \dot{\varphi}^q j (x, y, z)] \end{aligned} \quad (9.9.6)$$

where

$$q_j = q_j^* e^{ipt}, \quad \dot{q}_j = dq_j/d\tau = (dq_j/dt) b_0/V_\infty = ip_j^* q_j^* e^{ipt} \quad (9.9.7)$$

In accordance with (9.9.6), the partial derivative of the potential function with respect to  $y$  is

$$\begin{aligned} \frac{\partial \Phi}{\partial y}(x, y, z, t) &= V_\infty b_0 \operatorname{Re} e^{ipt} \sum_{j=1}^3 q_j^* \left[ \frac{\partial \Phi^{q_j}}{\partial y}(x, y, z) \right. \\ &\quad \left. + ip^* \frac{\partial \dot{\Phi}^{q_j}}{\partial y}(x, y, z) \right] \end{aligned} \quad (9.9.8)$$

Inserting this derivative into the left-hand side of (9.9.2), we obtain the following relation for  $[\partial \Phi(x, y, z)/\partial y]_{y=0}$ :

$$\begin{aligned} \left[ \frac{\partial \Phi}{\partial y}(x, y, z) \right]_{y=0} &= V_\infty b_0 \sum_{j=1}^3 q_j^* \left[ \frac{\partial \Phi^{q_j}}{\partial y}(x, y, z) \right. \\ &\quad \left. + ip^* \frac{\partial \dot{\Phi}^{q_j}}{\partial y}(x, y, z) \right] \end{aligned} \quad (9.9.9)$$

Introducing this expression into (9.9.5), substituting (9.9.6) for the velocity potential on the left-hand side, and taking into account that

$$e^{\frac{-i\omega(x_1 - x)}{b_0}} = \cos \frac{\omega(x_1 - x)}{b_0} - i \sin \frac{\omega(x_1 - x)}{b_0}$$

we obtain relations for the derivatives of the potential function:

$$\left. \begin{aligned} \Phi^{q_j}(x, y, z) &= -\frac{1}{\pi} \iint_{\sigma(x_1, z_1)} \left\{ \left[ \frac{\partial \Phi^{q_j}}{\partial y}(x, y, z) \right]_{y=0} \right. \\ &\quad \times \cos \frac{\omega(x_1 - x)}{b_0} + p^* \left[ \frac{\partial \dot{\Phi}^{q_j}}{\partial y}(x, y, z) \right]_{y=0} \sin \frac{\omega(x_1 - x)}{b_0} \left. \right\} \\ &\quad \times \cos \left( \frac{\omega r}{b_0 M_\infty} \right) \frac{dx dy}{r} \\ \dot{\Phi}^{q_j}(x, y, z) &= -\frac{1}{\pi} \iint_{\sigma(x_1, z_1)} \left\{ \left[ \frac{\partial \dot{\Phi}^{q_j}}{\partial y}(x, y, z) \right]_{y=0} \right. \\ &\quad \times \cos \frac{\omega(x_1 - x)}{b_0} - \frac{1}{p^*} \left[ \frac{\partial \Phi^{q_j}}{\partial y}(x, y, z) \right]_{y=0} \sin \frac{\omega(x_1 - x)}{b_0} \left. \right\} \\ &\quad \times \cos \frac{\omega r}{b_0 M_\infty} \frac{dx dz}{r}. \end{aligned} \right\} \quad (9.9.10)$$

For unsteady motion with small Strouhal numbers ( $p^* \rightarrow 0$ ,  $\omega \rightarrow 0$ ), Eqs. (9.9.10) acquire the form

$$\left. \begin{aligned} \varphi^{q_j}(x, y, z) &= -\frac{1}{\pi} \int \int_{\sigma} \left[ \frac{\partial \varphi^{q_j}}{\partial y}(x, y, z) \right]_{y=0} \frac{dx dz}{r} \\ \dot{\varphi}^{q_j}(x, y, z) &= -\frac{1}{\pi} \int \int_{\sigma} \left\{ \left[ \frac{\partial \dot{\varphi}^{q_j}}{\partial y}(x, y, z) \right]_{y=0} \right. \\ &\quad \left. - \frac{M_{\infty}^2 (x_1 - x)}{\alpha'^2 b_0} \left[ \frac{\partial \varphi^{q_j}}{\partial y}(x, y, z) \right]_{y=0} \frac{dx dz}{r} \right\} \end{aligned} \right\} \quad (9.9.10')$$

Let us introduce the dimensionless coordinates (9.6.19), adopting the centre chord ( $x_k = b_0$ ) as the characteristic geometric dimension:

$$\xi = x/b_0, \quad \eta = y/b_0, \quad \zeta = z/b_0 \quad (9.9.11)$$

Considering that to determine the aerodynamic loads it is sufficient to find the value of the potential function on the wing ( $y = 0$ ), let us express (9.9.10') in terms of the dimensionless coordinates as follows:

$$\left. \begin{aligned} \varphi^{q_j}(\xi_1, 0, \zeta_1) &= -\frac{1}{\pi} \int \int_{\sigma} \left[ \frac{\partial \varphi^{q_j}}{\partial \eta} \right]_{\eta=0} \frac{d\xi d\zeta}{\bar{r}} \\ \dot{\varphi}^{q_j}(\xi_1, 0, \zeta_1) &= -\frac{1}{\pi} \int \int_{\sigma} \left\{ \left[ \frac{\partial \dot{\varphi}^{q_j}}{\partial \eta} \right]_{\eta=0} - \frac{M_{\infty}^2 (\xi_1 - \xi)}{\alpha'^2} \right. \\ &\quad \times \left. \left[ \frac{\partial \varphi^{q_j}}{\partial \eta} \right]_{\eta=0} \right\} \frac{d\xi d\zeta}{\bar{r}} \end{aligned} \right\} \quad (9.9.12)$$

where  $\bar{r} = \sqrt{(\xi_1 - \xi)^2 - \alpha'^2 (\zeta_1 - \zeta)^2}$ .

We can use the found derivatives  $\varphi^{q_j}$  and  $\dot{\varphi}^{q_j}$  to determine the dimensional value of the velocity potential:

$$\varphi(\xi_1, 0, \zeta_1) = V_{\infty} b_0 \sum_{j=1}^3 [\varphi^{q_j}(\xi_1, 0, \zeta_1) q_j + \dot{\varphi}^{q_j}(\xi_1, 0, \zeta_1) \dot{q}_j] \quad (9.9.13)$$

Equations (9.9.12) allow us to find the velocity potential at points on a wing plane if within the entire region of source influence (integration region  $\sigma$ ) we know the flow downwashes determined by the derivatives  $[\partial \varphi^{q_j} / \partial \eta]_{\eta=0}$  and  $[\partial \dot{\varphi}^{q_j} / \partial \eta]_{\eta=0}$ . The values of these downwashes must satisfy the boundary condition (9.6.32) on the wing ( $\eta = 0$ ) in accordance with which we have

$$\partial \varphi^{\alpha} / \partial \eta = -1, \quad \partial \dot{\varphi}^{\alpha} / \partial \eta = 0 \quad (j = 1) \quad (9.9.14)$$

$$\partial \varphi^{\omega_x} / \partial \eta = -\zeta_1, \quad \partial \dot{\varphi}^{\omega_x} / \partial \eta = 0 \quad (j = 2) \quad (9.9.15)$$

$$\partial \varphi^{\omega_z} / \partial \eta = -\xi_1, \quad \partial \dot{\varphi}^{\omega_z} / \partial \eta = 0 \quad (j = 3) \quad (9.9.16)$$

In addition, the values of the downwashes being sought must correspond to the value of the potential function on a vortex sheet (9.6.34). In theoretical investigations, (9.6.34) is replaced with the following condition on a vortex sheet:

$$\varphi(\xi, 0, \zeta, \tau) = \varphi(\xi^*, 0, \zeta^*, \tau^*); \quad \tau^* = \tau - (\xi^* - \xi) \quad (9.9.17)$$

that allows us to determine the velocity potential  $\varphi$  at a point of the vortex sheet  $(x, z)$  from its value directly behind the trailing edge of the wing (at a point with the coordinates  $x^*$  and  $z^* = z$ ), but at a different instant  $t^* < t$ . It is shown in [19] that condition (9.9.17) corresponds to the requirement of the absence of a pressure difference on the vortex sheet.

Let us expand the left-hand and right-hand sides of (9.9.17) into the series (9.9.6):

$$\begin{aligned} \sum_{j=1}^3 [\varphi^{q_j}(\xi, 0, \zeta) q_j(\tau) + \dot{\varphi}^{q_j}(\xi, 0, \zeta) \dot{q}_j(\tau)] \\ = \sum_{j=1}^3 [\varphi^{q_j}(\xi^*, 0, \zeta) q_j(\tau^*) + \dot{\varphi}^{q_j}(\xi^*, 0, \zeta) \dot{q}_j(\tau^*)] \end{aligned} \quad (9.9.18)$$

where by (9.9.1), we have

$$\begin{aligned} q_j(\tau) &= q_j^* e^{ipt}, \quad \dot{q}_j(\tau) = i q_j^* p e^{ipt} \\ q_j(\tau^*) &= q_j^* e^{ip[t-(x^*-x)/V_\infty]}, \quad \dot{q}_j(\tau^*) = i q_j^* p^* e^{ip[t-(x^*-x)/V_\infty]} \end{aligned}$$

After introducing the values of  $q_j$  and their derivatives into (9.9.18), we obtain (without the summation sign)

$$\begin{aligned} \varphi^{q_j}(\xi, 0, \zeta) + i p^* \dot{\varphi}^{q_j}(\xi, 0, \zeta) \\ = e^{-ip^*(\xi^*-\xi)} \varphi^{q_j}(\xi^*, 0, \zeta) + i p^* e^{-ip^*(\xi^*-\xi)} \dot{\varphi}^{q_j}(\xi^*, 0, \zeta) \end{aligned} \quad (9.9.19)$$

$$\text{Since } e^{-ip^*(\xi^*-\xi)} = \cos[p^*(\xi^* - \xi)] - i \sin[p^*(\xi^* - \xi)]$$

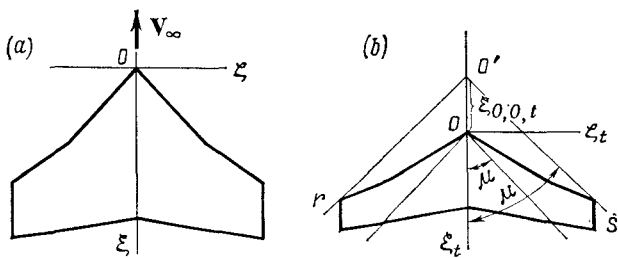
or at low Strouhal numbers ( $p^* \rightarrow 0$ )

$$e^{-ip^*(\xi^*-\xi)} = 1 - i p^* (\xi^* - \xi)$$

after introduction into (9.9.19) and separating the real and imaginary parts, we find the following expressions for the derivatives on the vortex sheet (excluding the term with  $p^{*2}$ ):

$$\begin{aligned} \varphi^{q_j}(\xi, 0, \zeta) &= \varphi^{q_j}(\xi^*, 0, \zeta) \\ \varphi^{\dot{q}_j}(\xi, 0, \zeta) &= \varphi^{\dot{q}_j}(\xi^*, 0, \zeta) - (\xi^* - \xi) \varphi^{q_j}(\xi^*, 0, \zeta) \end{aligned} \quad \} \quad (9.9.20)$$

Beyond the limits of the disturbance cones (a Mach cone or wave), the supersonic flow remains undisturbed, hence the potential function is constant. Therefore, the additional disturbance potential

**Fig. 9.9.1**

Adopted designations of the coordinate systems:

*a*—conventional ( $\xi, \eta, \zeta$ ); *b*—transformed ( $\xi_t, \eta_t, \zeta_t$ ); *r, r<sub>t</sub>*—characteristic coordinates

in this region, including the Mach wave, equals zero, i.e.

$$\varphi(\xi, \eta, \zeta, t) = 0 \quad (9.9.21)$$

Simultaneously everywhere in plane  $xOz$  except for the wing and the wake vortex behind it, the condition is satisfied that

$$\varphi(\xi, 0, \zeta, t) = 0 \quad (9.9.22)$$

according to which the function  $\varphi$  is continuous and odd relative to the coordinate  $y(\eta)$ .

Let us consider Eqs. (9.9.12). Their use for numerical calculations is hindered by that if the equality  $\xi_1 - \xi = \pm\alpha' (\zeta_1 - \zeta)$  holds, the integrands have a singularity of the order of  $r^{-1/2}$ . It is therefore necessary to transform Eqs. (9.9.12) to a form convenient for such calculations. To do this, we shall introduce a new system of coordinates (Fig. 9.9.1):

$$\xi_t = \xi/\alpha', \eta_t = \eta, \zeta_t = \zeta \quad (9.9.23)$$

The wing in the new system of coordinates is shown in Fig. 9.9.1 from which it can be seen that the lifting surface has been made shorter, while the transverse dimensions have been kept unchanged.

Equations (9.9.12) transformed to the coordinates  $\xi_t$ ,  $\eta_t$ , and  $\zeta_t$  have the following form:

$$\left. \begin{aligned} \varphi^{qJ}(\xi_1, t, 0, \zeta_1, t) &= -\frac{1}{\pi} \int \int_{\sigma_t} \left[ \frac{\partial \varphi^{qJ}}{\partial \eta_t} \right]_{\eta_t=0} \frac{d\xi_t d\zeta_t}{r_t} \\ \dot{\varphi}^{qJ}(\xi_1, t, 0, \zeta_1, t) &= -\frac{1}{\pi} \int \int_{\sigma_t} \left\{ \left[ \frac{\partial \dot{\varphi}^{qJ}}{\partial \eta_t} \right]_{\eta_t=0} \right. \\ &\quad \left. - \frac{M_\infty^2 (\xi_1, t - \xi_t)}{\alpha'} \left[ \frac{\partial \varphi^{qJ}}{\partial \eta_t} \right]_{\eta_t=0} \right\} \frac{d\xi_t d\zeta_t}{r_t} \end{aligned} \right\} \quad (9.9.24)$$

$$\bar{r}_t = \sqrt{(\xi_1, t - \xi_t)^2 - (\zeta_1, t - \zeta_t)^2}$$

To simplify the solution of Eqs. (9.9.24), we shall introduce the following relations for the derivatives of the function  $\varphi$  used for small Strouhal numbers ( $p^* \rightarrow 0$ ):

$$\left. \begin{aligned} \dot{\varphi}^{qj}(\xi_t, 0, \zeta_t) &= F^{qj}(\xi_t, 0, \zeta_t) \\ \dot{\varphi}^{qj}(\xi_t, 0, \zeta_t) &= \dot{F}^{qj}(\xi_t, 0, \zeta_t) - \frac{M_\infty^2 \xi_t}{\alpha'} F^{qj}(\xi_t, 0, \zeta_t) \end{aligned} \right\} \quad (9.9.25)$$

After inserting the value of  $\dot{\varphi}^{qj}$  (9.9.25) into the first of Eqs. (9.9.24), we obtain an integral equation for determining the derivative  $F^{qj}$ :

$$F^{qj}(\xi_1, t, 0, \zeta_1, t) = -\frac{1}{\pi} \int \int_{\sigma_t} \left[ \frac{\partial F^{qj}}{\partial \eta_t} \right]_{\eta_t=0} \frac{d\xi_t d\zeta_t}{r_t} \quad (9.9.26)$$

Let us introduce (9.9.25) into the second of Eqs. (9.9.24):

$$\begin{aligned} \dot{F}^{qj}(\xi_1, t, 0, \zeta_1, t) - \frac{M_\infty^2 \xi_1, t}{\alpha'} F^{qj}(\xi_1, t, 0, \zeta_1, t) \\ = -\frac{1}{\pi} \int \int_{\sigma_t} \left\{ \left[ \frac{\partial F^{qj}}{\partial \eta_t} \right]_{\eta_t=0} - \frac{M_\infty^2 \xi_t}{\alpha'} \left[ \frac{\partial F^{qj}}{\partial \eta_t} \right]_{\eta_t=0} \right. \\ \left. - \frac{M_\infty^2 (\xi_1, t - \xi_t)}{\alpha'} \left[ \frac{\partial \varphi^{qj}}{\partial \eta_t} \right]_{\eta_t=0} \right\} \frac{d\xi_t d\zeta_t}{r_t} \end{aligned}$$

Substituting for the derivative  $F^{qj}$  on the left-hand side of the equation its value from (9.9.26) and having in view that by (9.9.25)

$$\left[ \frac{\partial \varphi^{qj}}{\partial \eta_t} \right]_{\eta_t=0} = \left[ \frac{\partial F^{qj}}{\partial \eta_t} \right]_{\eta_t=0}$$

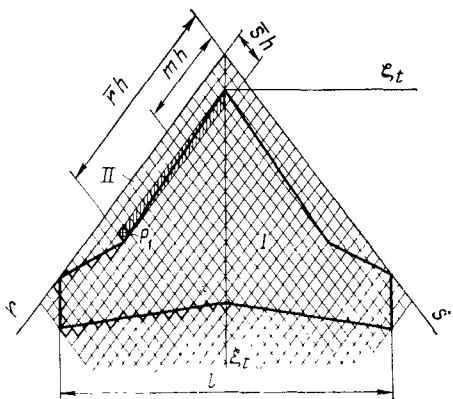
we obtain an expression for finding the derivative  $F^{qj}$ :

$$F^{qj}(\xi_1, t, 0, \zeta_1, t) = -\frac{1}{\pi} \int \int_{\sigma_t} \left[ \frac{\partial F^{qj}}{\partial \eta_t} \right]_{\eta_t=0} \frac{d\xi_t d\zeta_t}{r_t} \quad (9.9.27)$$

We perform our further transformations in characteristic coordinates (Fig. 9.9.1), namely,

$$r = (\xi_t - \xi_{0,0,t}) - \zeta_t, s = (\xi_t - \xi_{0,0,t}) + \zeta_t \quad (9.9.28)$$

selected so that only positive values of the variables will be used in the calculations. The value of  $\xi_{0,0,t}$  representing the displacement of the characteristic system of coordinates is determined as shown in Fig. 9.9.1 (the coordinate lines from the displaced apex  $O'$  pass through breaks of the wing at the tips).

**Fig. 9.9.2**

To the numerical calculation of a wing with combined leading and supersonic trailing edges in an unsteady flow:

I, II—regions for finding the downwash

Equations (9.9.26) and (9.9.27) acquire the following form in the characteristic coordinates:

$$\left. \begin{aligned} F^{qj}(r_1, 0, s_1) &= -\frac{1}{2\pi} \int_0^{r_1} \int_0^{s_1} \left[ \frac{\partial F^{qj}}{\partial \eta_t} \right]_{\eta_t=0} \frac{dr ds}{\sqrt{(r_1-r)(s_1-s)}} \\ F^{\dot{q}j}(r_1, 0, s_1) &= -\frac{1}{2\pi} \int_0^{r_1} \int_0^{s_1} \left[ \frac{\partial F^{\dot{q}j}}{\partial \eta_t} \right]_{\eta_t=0} \frac{dr ds}{\sqrt{(r_1-r)(s_1-s)}} \end{aligned} \right\} \quad (9.9.29)$$

For further transformations allowing us to eliminate the singularity in Eqs. (9.9.29), we shall introduce the variables

$$v = \sqrt{r_1 - r}, \quad u = \sqrt{s_1 - s} \quad (9.9.30)$$

Equations (9.9.29) acquire the following form in the variables (9.9.30)

$$\left. \begin{aligned} F^{qj}(r_1, 0, s_1) &= -\frac{2}{\pi} \int_0^{\sqrt{r_1}} \int_0^{\sqrt{s_1}} D_j dv du \\ F^{\dot{q}j}(r_1, 0, s_1) &= -\frac{2}{\pi} \int_0^{\sqrt{r_1}} \int_0^{\sqrt{s_1}} E_j dv du \end{aligned} \right\} \quad (9.9.31)$$

where

$$D_j = \left[ \frac{\partial F^{qj}}{\partial \eta_t} \right]_{\eta_t=0}, \quad E_j = \left[ \frac{\partial F^{\dot{q}j}}{\partial \eta_t} \right]_{\eta_t=0} \quad (9.9.32)$$

To perform numerical calculations, we shall divide the region occupied by the wing into separate cells as shown in Fig. 9.9.2.

Let  $h$  stand for the width of a cell in characteristic axes. This quantity is the dimensionless distance along the  $r$  (or  $s$ ) axis between the edges of a cell for points  $n$ ,  $n + 1$  (or  $i$ ,  $i + 1$ ), respectively. It is equal to

$$h = l/(2Nb_0) \quad (9.9.33)$$

where  $N$  is the number of parts into which the wing half-span  $l/2$  is divided.

Let  $\bar{r}$  and  $\bar{s}$  be the coordinates of a fixed point (point  $P_1$  in Fig. 9.9.2) at which we are finding the velocity potential (or its derivatives), and  $m$  and  $i$  be the coordinates of the running points used to perform numerical integration. Accordingly,

$$r_1 = \bar{r}h, s_1 = \bar{s}h, r = mh, s = ih \quad (9.9.34)$$

Assuming that the functions  $D_j$  and  $E_j$  [see (9.9.32)] within a cell are variable, let us write Eqs. (9.9.31) in terms of the sum of the integrals over all the cells:

$$\left. \begin{aligned} F^{qj}(r_1, 0, s_1) &= -\frac{2}{\pi} \sum_{m=0}^{\bar{r}-1} \sum_{i=0}^{\bar{s}-1} \int_{V^{mh}}^{\bar{r}} \int_{V^{ih}}^{\bar{s}} D_j dv du \\ F^{qj}(r_1, 0, s_1) &= -\frac{2}{\pi} \sum_{m=0}^{\bar{r}-1} \sum_{i=0}^{\bar{s}-1} \int_{V^{mh}}^{\bar{r}} \int_{V^{ih}}^{\bar{s}} E_j dv du \end{aligned} \right\} \quad (9.9.35)$$

The integration regions including the projection of the wing onto the plane  $\eta = 0$ , the vortex sheet, and also the sections of the disturbed flow outside the wing and vortex sheet are replaced with a sufficiently large number of whole cells producing a conditional wing with toothed edges (Fig. 9.9.2). A cell should be considered to belong to a section of the integration region if its centre is on this section.

Inside a cell with a sufficiently small area, the derivatives  $D_j$  and  $E_j$  can be assumed to be constant and equal to their values at the centre of a cell. Accordingly, Eqs. (9.9.35) can be written in a simpler form:

$$\left. \begin{aligned} F^{qj}(\bar{r}h, \bar{s}h) &= -\frac{2h}{\pi} \sum_{m=1}^{\bar{r}} \sum_{i=1}^{\bar{s}} D_{j,m,i} B_{\bar{r},m,\bar{s},i} \\ F^{qj}(\bar{r}h, \bar{s}h) &= -\frac{2h}{\pi} \sum_{m=1}^{\bar{r}} \sum_{i=1}^{\bar{s}} E_{j,m,i} B_{\bar{r},m,\bar{s},i} \end{aligned} \right\} \quad (9.9.36)$$

where

$$\left. \begin{aligned} D_{j,m,i} &= D_j [(m - 1/2) h, (i - 1/2) h] \\ E_{j,m,i} &= E_j [(m - 1/2) h, (i - 1/2) h] \\ B_{\bar{r},m,\bar{s},i} &= (\bar{V}_{\bar{r}-m+1} - \bar{V}_{\bar{r}-m}) (\bar{V}_{\bar{s}-i+1} - \bar{V}_{\bar{s}-i}) \end{aligned} \right\} \quad (9.9.37)$$

Formulas (9.9.36) allow us to determine the values of  $F^q_j$  and  $\dot{F}^q_j$  and, consequently, the derivatives of the velocity potential [see expressions (9.9.25)] if within the entire region of source influence (including the wing plane, vortex sheet, and the disturbed flow outside of them) we know the quantities  $D_{j,m,i}$  and  $E_{j,m,i}$  (the flow downwashes), and also the values of  $B_{\bar{r},m,\bar{s},i}$  (the kernel functions).

The downwashes are determined differently for the following three regions: (1) the wing, (2) the disturbed region confined by the leading edges, tips, and surface of the Mach cones issuing from the corresponding points of the wing (end regions), and (3) the vortex sheet.

Let us consider the downwashes in each of these regions, having in view the case of small Strouhal numbers ( $p^* \rightarrow 0$ ). For a wing with supersonic (or combined) leading and supersonic trailing edges, it is sufficient to know the downwashes on the lifting surface (section I in Fig. 9.9.2). They are determined by boundary conditions (9.9.14)-(9.9.16), in accordance with which

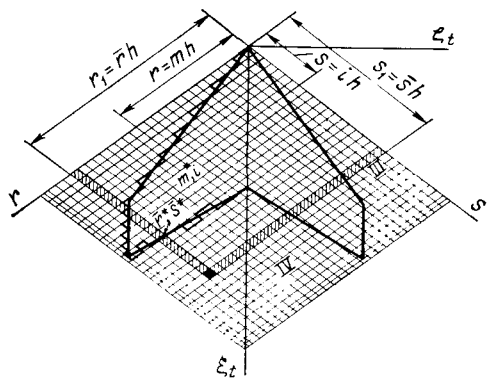
$$\left. \begin{aligned} D_{1mi}^{(1)} &= -1 \quad (j = 1); \quad D_{2mi}^{(1)} = h(m - i)/2 \quad (j = 2) \\ D_{3mi}^{(1)} &= -\alpha' h (m + i - 1)/2 - \alpha' \xi_{0,0,t} \quad (j = 3) \end{aligned} \right\} \quad (9.9.38)$$

$$\left. \begin{aligned} E_{1mi}^{(1)} &= M_\infty^2 [h(m + i - 1)/2 + \xi_{0,0,t}] / \alpha' \quad (j = 1) \\ E_{2mi}^{(1)} &= \{M_\infty^2 [h(m + i - 1)/2 + \xi_{0,0,t}] / (2\alpha')\} \\ &\quad \times h(m - 1) \quad (j = 2) \\ E_{3mi}^{(1)} &= -M_\infty^2 [h(m + i - 1)/2 + \xi_{0,0,t}]^2 \quad (j = 3) \end{aligned} \right\} \quad (9.9.39)$$

Section II (Fig. 9.9.2) between the characteristic axes, the leading edge and the Mach lines issuing from the vertex of the wing is occupied by an undisturbed flow region; hence, all the downwashes equal zero and, consequently,

$$D_{j,m,i}^{II} = E_{j,m,i}^{II} = 0 \quad (9.9.40)$$

Let us determine the flow downwashes in disturbed region III between the leading edge, the tip, and the Mach cone issuing from the points of a break in the wing contour (Fig. 9.9.3). The velocity potential in this region (outside of the wing and vortex wake behind

**Fig. 9.9.3**

To the numerical calculation of a wing with subsonic edges in an unsteady flow:

*III, IV*—regions for finding the downwash

it) in accordance with condition (9.9.22) is zero. Therefore, from (9.9.29), we obtain the conditions for region *III*:

$$\left. \begin{aligned} F^{q_j}(r_1, 0, s_1) &= -\frac{1}{2\pi} \int_0^{r_1} \int_0^{s_1} D_j \frac{dr ds}{V(r_1-r)(s_1-s)} = 0 \\ F^{\dot{q}_j}(r_1, 0, s_1) &= -\frac{1}{2\pi} \int_0^{r_1} \int_0^{s_1} F_j \frac{dr ds}{V(r_1-r)(s_1-s)} = 0 \end{aligned} \right\} \quad (9.9.41)$$

These integrals can be written in a somewhat different form:

$$\int_0^{s_1} \frac{ds}{V(s_1-s)} \int_0^{r_1} D_j \frac{dr}{V(r_1-r)} = 0; \quad \int_0^{s_1} \frac{ds}{V(s_1-s)} \int_0^{r_1} E_j \frac{dr}{V(r_1-r)} = 0 \quad (9.9.42)$$

or

$$\int_0^{r_1} \frac{dr}{V(r_1-r)} \int_0^{s_1} D_j \frac{ds}{V(s_1-s)} = 0; \quad \int_0^{r_1} \frac{dr}{V(r_1-r)} \int_0^{s_1} E_j \frac{ds}{V(s_1-s)} = 0 \quad (9.9.42')$$

The obtained equalities are Abel equations whose right-hand sides identically equal zero. Hence it follows that the inner integrals for  $s = s_1$  [Eqs. (9.9.42)] and for  $r = r_1$  [Eqs. (9.9.42')] equal zero. Accordingly, we obtain the following equations for determining the downwashes  $D_j^{(III)}$  in region *III* (Fig. 9.9.3):

$$\left. \begin{aligned} \int_{s_1-h}^{s_1} D_j^{(III)} \frac{ds}{V(s_1-s)} &= - \int_0^{s_1-h} D_j \frac{ds}{V(s_1-s)} \\ \int_{r_1-h}^{r_1} D_j^{(III)} \frac{dr}{V(r_1-r)} &= - \int_0^{r_1-h} D_j \frac{ds}{V(r_1-r)} \end{aligned} \right\} \quad (9.9.43)$$

The equations for the downwashes  $E_j^{(III)}$  have a similar form:

$$\left. \begin{aligned} \int_{s_1-h}^{s_1} E_j^{(III)} \frac{ds}{\sqrt{s_1-s}} &= - \int_0^{s_1-h} E_j \frac{ds}{\sqrt{s_1-s}} \\ \int_{r_1-h}^{r_1} E_j^{(III)} \frac{dr}{\sqrt{r_1-r}} &= - \int_0^{r_1-h} E_j \frac{dr}{\sqrt{r_1-r}} \end{aligned} \right\} \quad (9.9.44)$$

Assuming the values of the downwashes in the cells to be constant and going over from integrals to sums, we find in accordance with the variables (9.9.30) the following relations for determining the downwashes in a cell (point) with the coordinates  $r_1 = \bar{r}h$  and  $s_1 = \bar{s}h$ :

$$\left. \begin{aligned} D_j^{(III)}(\bar{r}h, \bar{s}h) &= - \sum_{m=1}^{\bar{r}-1} D_j [(m-0.5)h, (i-0.5)h] B_{\bar{r}, m} \\ E_j^{(III)}(\bar{r}h, \bar{s}h) &= - \sum_{m=1}^{\bar{r}-1} E_j [(m-0.5)h, (i-0.5)h] B_{\bar{r}, m} \end{aligned} \right\} \quad (9.9.45)$$

(for points to the left of the axis  $\xi_t$ );

$$\left. \begin{aligned} D_j^{(III)}(\bar{r}h, \bar{s}h) &= - \sum_{i=1}^{\bar{s}-1} D_j [(m-0.5)h, (i-0.5)h] B_{\bar{s}, i} \\ E_j^{(III)}(\bar{r}h, \bar{s}h) &= - \sum_{i=1}^{\bar{s}-1} E_j [(m-0.5)h, (i-0.5)h] B_{\bar{s}, i} \end{aligned} \right\} \quad (9.9.46)$$

(for points to the right of the axis  $\xi_t$ ).

In Eqs. (9.9.45) and (9.9.46), we have introduced the notation

$$B_{\bar{r}, m} = \sqrt{\bar{r}-m+1} - \sqrt{\bar{r}-m}, \quad B_{\bar{s}, i} = \sqrt{\bar{s}-m+1} - \sqrt{\bar{s}-i} \quad (9.9.47)$$

According to the above relations, the flow downwash at a point is determined by summation of the downwash values in all the cells in the corresponding strip  $m = \text{const}$  (or  $i = \text{const}$ ). The calculations are performed consecutively beginning from the cell at the vertex of the wing where the downwash is determined by formulas (9.9.38) and (9.9.39). Let us now calculate the downwashes on the vortex sheet behind the wing (region IV in Fig. 9.9.3). We shall find them from condition (9.9.20), which we shall write in the transformed coordinates

$$\left. \begin{aligned} \varphi^{q_J}(\xi_t, 0, \zeta_t) &= \varphi^{q_J}(\xi_t^*, 0, \zeta_t^*) \\ \dot{\varphi}^{q_J}(\xi_t, 0, \zeta_t) &= \dot{\varphi}^{q_J}(\xi_t^*, 0, \zeta_t^*) - \alpha' (\xi_t^* - \xi_t) \varphi^{q_J} \end{aligned} \right\} \quad (9.9.48)$$

where  $\xi_t^*$  and  $\zeta_t^* = \zeta$  are the transformed coordinates of points on the trailing edge.

Relations (9.9.48) can be represented with a view to (9.9.25) and the characteristic coordinates (9.9.28) as follows:

$$\left. \begin{aligned} \varphi^{q_J}(r_1, 0, s_1) &= F^{q_J}\left(\frac{r^*+s^*}{2}, \frac{s^*-r^*}{2}\right) \\ \dot{\varphi}^{q_J}(r_1, 0, s_1) &= \dot{F}^{q_J}\left(\frac{r^*+s^*}{2}, \frac{s^*-r^*}{2}\right) \\ -\frac{M_\infty^2}{2\alpha'}(r_1+s_1)F^{q_J}\left(\frac{r^*+s^*}{2}, \frac{s^*-r^*}{2}\right) \\ +\alpha'\left[\frac{r_1+s_1-(r^*+s^*)}{2}\right]F^{q_J}\left(\frac{r^*+s^*}{2}, \frac{s^*-r^*}{2}\right) \end{aligned} \right\} \quad (9.9.49)$$

These relations hold for the conditions

$$s_1 - r_1 = s^* - r^*, \quad r_1 > r^*, \quad s_1 > s^* \quad (9.9.50)$$

where  $s^*$  and  $r^*$  are characteristic coordinates of points on the trailing edge.

In addition to (9.9.49), we can use Eqs. (9.9.25) for the vortex sheet, which with account taken of (9.9.26) and (9.9.27) have the form

$$\left. \begin{aligned} \varphi^{q_J}(r_1, 0, s_1) &= -\frac{1}{2\pi} \int_0^{r_1} \int_0^{s_1} D_j \frac{dr ds}{V(r_1-r)(s_1-s)} \\ \dot{\varphi}^{q_J}(r_1, 0, s_1) &= -\frac{1}{2\pi} \int_0^{r_1} \int_0^{s_1} E_j \frac{dr ds}{V(r_1-r)(s_1-s)} \\ +\frac{M_\infty^2}{4\pi\alpha'}(r_1+s_1) \int_0^{r_1} \int_0^{s_1} D_j \frac{dr ds}{V(r_1-r)(s_1-s)} \end{aligned} \right\} \quad (9.9.51)$$

Replacing the derivatives  $\varphi^{q_J}$  and  $\dot{\varphi}^{q_J}$  in (9.9.51) with their relevant values from (9.9.49), we obtain integral equations for determining downwashes on a vortex sheet (region IV in Fig. 9.9.3):

$$\left. \begin{aligned} -\frac{1}{2\pi} \int_0^{r_1} \int_0^{s_1} D_j \frac{dr ds}{V(r_1-r)(s_1-s)} &= F^{q_J}\left(\frac{r^*+s^*}{2}, \frac{s^*-r^*}{2}\right) \\ -\frac{1}{2\pi} \int_0^{r_1} \int_0^{s_1} E_j \frac{dr ds}{V(r_1-r)(s_1-s)} &= \dot{F}^{q_J}\left(\frac{r^*+s^*}{2}, \frac{s^*-r^*}{2}\right) \\ +\frac{\alpha'[(r_1+s_1)-(r^*+s^*)]}{2}F^{q_J}\left(\frac{r^*+s^*}{2}, \frac{s^*-r^*}{2}\right) \end{aligned} \right\} \quad (9.9.52)$$

Both equations are solved in the same way. Let us consider as an example the first of Eqs. (9.9.52). We shall isolate on section *IV* a cell with the sides  $h$  and the characteristic coordinates  $s_1 = \bar{s}h$  and  $r_1 = \bar{r}h$ . We shall write the left-hand integral of the equation as the sum of four integrals:

$$\begin{aligned} & \int_0^{s_1} \int_0^{s_1} D_j \frac{dr ds}{\sqrt{(r_1 - r)(s_1 - s)}} = \int_0^{s_1-h} \frac{ds}{\sqrt{s_1 - s}} \int_0^{r_1-h} D_j \frac{dr}{\sqrt{r_1 - r}} \\ & + \int_{s_1-h}^{s_1} \frac{ds}{\sqrt{s_1 - s}} \int_0^{r_1-h} D_j \frac{dr}{\sqrt{r_1 - r}} + \int_0^{s_1-h} \frac{ds}{\sqrt{s_1 - s}} \int_{r_1-h}^{r_1} D_j \frac{dr}{\sqrt{r_1 - r}} \\ & + \int_{s_1-h}^{s_1} \frac{ds}{\sqrt{s_1 - s}} \int_{r_1-h}^{r_1} D_j \frac{dr}{\sqrt{r_1 - r}} \end{aligned} \quad (9.9.53)$$

As we have already indicated, the entire integration region should be divided into cells and the downwashes assumed to be constant in each of them. We determine the coordinates of the cells by means of the integers  $m$ ,  $i$ ,  $\bar{r}$  and  $\bar{s}$  (Fig. 9.9.3). Using (9.9.30), we go over to the variables  $v$  and  $u$ :

$$v^2 = (\bar{r} - m)h, \quad u^2 = (\bar{s} - i)h \quad (9.9.54)$$

The first of the integrals (9.9.53) has the following form:

$$\begin{aligned} & \int_0^{s_1-h} \frac{ds}{\sqrt{s_1 - s}} \int_0^{r_1-h} D_j \frac{dr}{\sqrt{r_1 - r}} = \int_{\bar{s}-1}^{\bar{s}} \frac{2du}{\sqrt{\bar{s}h}} \int_{\bar{r}-1}^{\bar{r}} \frac{2D_j dv}{\sqrt{\bar{r}h}} \\ & = 4 \sum_{i=1}^{\bar{s}-1} \int_{\bar{s}-m+1}^{\bar{s}} du \sum_{m=1}^{\bar{r}-1} \int_{\bar{r}-m+1}^{\bar{r}} D_j dv \\ & = 4h \sum_{i=1}^{\bar{s}-1} \sum_{m=1}^{\bar{r}-1} D_j(mh, ih) B_{\bar{r}, m, \bar{s}, i} \end{aligned} \quad (9.9.55)$$

where  $B_{\bar{r}, m, \bar{s}, i}$  is an influence function determined by the third formula (9.9.37).

For the second and third integrals on the right-hand side of (9.9.53), we obtain the relations:

$$\int_{s_1-h}^{s_1} \frac{ds}{\sqrt{s_1 - s}} \int_0^{r_1-h} D_j \frac{dr}{\sqrt{r_1 - r}} = 4h \sum_{m=1}^{\bar{r}-1} D_j(mh, \bar{s}h) B_{\bar{r}, m, \bar{s}, \bar{s}} \quad (9.9.56)$$

$$\int_0^{s_1-h} \frac{ds}{\sqrt{s_1 - s}} \int_{r_1-h}^{r_1} D_j \frac{dr}{\sqrt{r_1 - r}} = 4h \sum_{i=1}^{\bar{s}-1} D_j(\bar{r}h, ih) B_{\bar{r}, \bar{r}, \bar{s}, i} \quad (9.9.57)$$

where

$$\begin{aligned} B_{\bar{r}, m, \bar{s}, \bar{s}} &= \sqrt{\bar{r} - m + 1} - \sqrt{\bar{r} - m}; \quad B_{\bar{r}, \bar{r}, \bar{s}, i} \\ &= \sqrt{\bar{s} - 1 + 1} - \sqrt{\bar{s} - i} \end{aligned} \quad (9.9.58)$$

For the fourth integral (9.9.53), we have the formula

$$\int_{s_1-h}^{s_1} \frac{ds}{\sqrt{s_1-s}} \int_{r_1-h}^{r_1} D_j \frac{dr}{r_1-r} = 4h D_j (\bar{r}h, \bar{s}h) \quad (9.9.59)$$

By summing all the above values of the integrals, from (9.9.52) we obtain relations for numerical calculations of the downwashes in a cell with the coordinates  $\bar{r}$  and  $\bar{s}$  (Fig. 9.9.3):

$$D_j^{(IV)} (\bar{r}h, \bar{s}h) = -\frac{\pi}{2h} F^{q_j} (\bar{r}^*h, \bar{s}^*h) - \sum_{m=1}^{\bar{r}-1} \sum_{i=1}^{\bar{s}-1} D_j (mh, ih) B_{\bar{r}, m, \bar{s}, i} \quad (9.9.60)$$

$$\begin{aligned} E_j^{(IV)} (\bar{r}h, \bar{s}h) &= -\frac{\pi}{2h} \left[ F^{q_j} (\bar{r}^*h, \bar{s}^*h) \right. \\ &\quad \left. + \frac{\alpha' h}{2} (\bar{r} + \bar{s} - \bar{r}^* - \bar{s}^*) F^{q_j} (\bar{r}^*h, \bar{s}^*h) \right] - \sum_{m=1}^{\bar{r}} \sum_{i=1}^{\bar{s}} E_j (mh, ih) B_{\bar{r}, m, \bar{s}, i} \end{aligned} \quad (9.9.61)$$

We perform numerical integration by double summation over all the cells within the confines of an inverted Mach cone issuing from the point being considered  $(\bar{r}h, \bar{s}h)$  excluding the initial cell (at the vertex) at which the downwash is determined. Its magnitude is found consecutively beginning from the cell on the trailing edge with the smallest coordinate  $\bar{r}^*$  (for the starboard side) and  $\bar{s}^*$  (for the port side). The coordinates of points on the trailing edge are related to the coordinates  $\bar{r}, \bar{s}$  by the expressions

$$\bar{r}^* - \bar{s}^* = \bar{r} - \bar{s}, \quad \bar{r}^* < \bar{r}, \quad \bar{s}^* < \bar{s} \quad (9.9.62)$$

The calculations are performed as follows. The smallest values of the coordinates  $\bar{r}^*$  and  $\bar{s}^*$  are used to determine the derivatives  $F^{q_j} (\bar{r}^*h, \bar{s}^*h)$ ,  $F^{q_j} (\bar{r}^*h, \bar{s}^*h)$  for the first cell, next the above relations are used to calculate the downwashes and influence functions for the entire region within the Mach cone issuing from the adjacent cell (with the coordinates  $\bar{r}$  and  $\bar{s}$ ).

After this, double summation of the products of the downwashes and the influence functions is performed, and the required values of the downwashes at a point with the coordinates  $\bar{r}$  and  $\bar{s}$  are found by formulas (9.9.60) and (9.9.61). Passing along a strip  $\bar{r} = \text{const}$  ( $\bar{s} = \text{const}$ ) to the following cell with the coordinates  $[(s+1)h, \bar{r}]$ ,

we repeat the calculations and find the corresponding value of the downwash in this cell. By performing similar calculations, the downwashes can be found on the entire vortex sheet behind the wing.

The values of the downwashes are used to determine the derivatives  $F^{q_j}$  and  $F^{\dot{q}_j}$  at each point of the lifting surface. Next  $\varphi^{q_j}$ ,  $\varphi^{\dot{q}_j}$ , and the corresponding values of the velocity potential  $\varphi$  are found (9.9.13). This quantity directly determines the pressure coefficient and the difference between its values on the bottom and upper sides of the wing [see formulas (9.6.20) and (9.6.21)].

The difference of the pressure coefficients (9.6.21) can be written as the series (9.6.7). The derivatives  $p^{q_j}$  and  $p^{\dot{q}_j}$  in it are determined in terms of the values of  $F^{q_j}$  and  $F^{\dot{q}_j}$ ; by using (9.6.24) and (9.6.25), we obtain the following relations:

$$\left. \begin{aligned} p^{q_j}(\xi, \zeta) &= -\frac{4}{\alpha'} \frac{\partial F^{q_j}(\xi_t, \zeta_t)}{\partial \xi_t} \\ p^{\dot{q}_j}(\xi, \zeta) &= -\frac{4}{\alpha'^3} \left\{ -\alpha' F^{q_j}(\xi_t, \zeta_t) \right. \\ &\quad \left. + M_\infty^2 \alpha' \left[ \frac{\alpha'}{M_\infty^2} \frac{\partial F^{q_j}(\xi_t, \zeta_t)}{\partial \xi_t} - \xi_t \frac{\partial F^{q_j}(\xi_t, \zeta_t)}{\partial \zeta_t} \right] \right\} \end{aligned} \right\} \quad (9.9.63)$$

Hence, to find the derivatives of the difference of the pressure coefficients  $p^{q_j}$  and  $p^{\dot{q}_j}$  determining the value of  $\Delta \bar{p}$  [see (9.6.21)], it is necessary to calculate the derivatives  $\partial F^{q_j}/\partial \xi_t$  and  $\partial F^{\dot{q}_j}/\partial \xi_t$ . There are different ways of calculating these derivatives. In aerodynamic calculations, particularly, the method of differences is used, in accordance with which

$$\frac{\partial F^{q_j}}{\partial \xi_t} \approx \frac{\Delta F^{q_j}}{\Delta \xi_t} = \frac{1}{h} [F^{q_j}(\bar{r}+1, \bar{s}+1) - F^{q_j}(\bar{r}, \bar{s})] \quad (9.9.64)$$

The derivative  $\partial F^{q_j}/\partial \xi_t$  is calculated in a similar way. As a result, we can write the following relations for the values of  $p^{q_j}$  and  $p^{\dot{q}_j}$ :

$$\left. \begin{aligned} p^{q_j}(\xi, \zeta) &= \frac{4}{\alpha' h} [F^{q_j}(\bar{r}+1, \bar{s}+1) - F^{q_j}(\bar{r}, \bar{s})] \\ p^{\dot{q}_j}(\xi, \zeta) &= \frac{4}{\alpha'^3} \left\{ -\alpha' F^{q_j}(\bar{r}, \bar{s}) \right. \\ &\quad \left. + \frac{\alpha'^2}{h} [F^{q_j}(\bar{r}+1, \bar{s}+1) - F^{\dot{q}_j}(\bar{r}, \bar{s})] \right. \\ &\quad \left. - \frac{M_\infty^2 \alpha' (\bar{r}+\bar{s})}{2} [F^{q_j}(\bar{r}+1, \bar{s}+1) - F^{q_j}(\bar{r}, \bar{s})] \right\} \end{aligned} \right\} \quad (9.9.65)$$

To improve the accuracy of calculating the derivatives (9.9.65), it is necessary that the values of  $F^{qj}$  and  $F^{ij}$  be found in more cells than the number in which  $p^{qj}$  and  $p^{ij}$  are found. Hence, in this case the interval  $\Delta\xi_t$  can be increased  $m$  times (where  $m$  is an integer). Accordingly, the derivative

$$\frac{\partial F^{qj}}{\partial \xi_t} = \frac{1}{mh} [F^{qj}(\bar{r} + m, \bar{s} + m) - F^{qj}(\bar{r}, \bar{s})] \quad (9.9.66)$$

We determine the derivative  $\partial F^{qj}/\partial \xi_t$  in a similar way. With a view to the new values of  $\partial F^{qj}/\partial \xi_t$  and  $\partial F^{ij}/\partial \xi_t$ , we change formulas (9.9.65) for the derivatives  $p^{qj}$  and  $p^{ij}$ . We use these derivatives to find by means of (9.6.9) the derivatives of the lift force, rolling moment, and pitching moment coefficients. As a result of substitutions of (9.9.63) into (9.6.9), where we assume that  $x_k = b_0$ , we obtain relations for these derivatives that can be written as follows:

$$\left. \begin{aligned} \alpha' c_y^\alpha &= c_{y,t}^\alpha, & \alpha'^3 c_y^{\dot{\alpha}} &= \dot{c}_{y1,t}^\alpha + M_\infty^2 c_{y2,t}^{\dot{\alpha}} \\ \alpha' c_y^{\omega_z} &= c_{y,t}^{\omega_z}, & \alpha'^3 c_y^{\dot{\omega}_z} &= \dot{c}_{y1,t}^{\omega_z} + M_\infty^2 c_{y2,t}^{\dot{\omega}_z} \end{aligned} \right\} \quad (9.9.67)$$

$$\left. \begin{aligned} \alpha' m_z^\alpha &= m_{z,t}^\alpha, & \alpha'^3 m_z^{\dot{\alpha}} &= \dot{m}_{z1,t}^\alpha + M_\infty^2 m_{z2,t}^{\dot{\alpha}} \\ \alpha' m_z^{\omega_z} &= m_{z,t}^{\omega_z}, & \alpha'^3 m_z^{\dot{\omega}_z} &= \dot{m}_{z1,t}^{\omega_z} + M_\infty^2 m_{z2,t}^{\dot{\omega}_z} \end{aligned} \right\} \quad (9.9.68)$$

$$\alpha'^2 m_x^{\omega_x} = m_{x,t}^{\omega_x}, \quad \alpha'^4 m_x^{\dot{\omega}_x} = m_{x1,t}^{\dot{\omega}_x} + M_\infty^2 m_{x2,t}^{\dot{\omega}_x} \quad (9.9.69)$$

The following symbols have been used in these formulas

$$\left. \begin{aligned} c_{y,t}^\alpha &= \frac{4b_0^2 \alpha' \lambda_w}{l^2} \int_{-l/(2b_0)}^{l/(2b_0)} \int_{\xi_{0,t}}^{\xi_t^*} \frac{\partial F^{qj}(\xi_t, \zeta_t)}{\partial \xi_t} d\xi_t d\zeta_t, \quad d\xi_t \\ \dot{c}_{y1,t}^\alpha &= -\frac{4b_0^2 \alpha'^2 \lambda_w}{l^2} \int_{-l/(2b_0)}^{l/(2b_0)} \int_{\xi_{0,t}}^{\xi_t^*} F^\alpha(\xi_t, \zeta_t) d\xi_t d\zeta_t \\ \dot{c}_{y2,t}^\alpha &= \frac{4b_0^2 \alpha'^2 \lambda_w}{l^2} \left[ \frac{\alpha'}{M_\infty^2} \int_{-l/(2b_0)}^{l/(2b_0)} \int_{\xi_{0,t}}^{\xi_t^*} \frac{\partial F^\alpha(\xi_t, \zeta_t)}{\partial \xi_t} d\xi_t d\zeta_t \right. \\ &\quad \left. - \int_{-l/(2b_0)}^{l/(2b_0)} \int_{\xi_{0,t}}^{\xi_t^*} \frac{\partial F^\alpha(\xi_t, \zeta_t)}{\partial \xi_t} \xi_t d\xi_t d\zeta_t \right] \end{aligned} \right\} \quad (9.9.70)$$

$$\left. \begin{aligned} c_{y,t}^{\omega_z} &= \frac{4b_0^2\alpha'^2\lambda_w}{l^2} \int_{-l/(2b_0)}^{l/(2b_0)} \int_{\xi_0, t}^{\xi_t^*} \frac{\partial F^{\omega_z}(\xi_t, \zeta_t)}{\partial \xi_t} d\xi_t d\zeta_t \\ \dot{c}_{y,t}^{\omega_z} &= -\frac{4b_0^2\alpha'^2\lambda_w}{l^2} \int_{-l/(2b_0)}^{l/(2b_0)} \int_{\xi_0, t}^{\xi_t^*} F^{\omega_z}(\xi_t, \zeta_t) d\xi_t d\zeta_t \end{aligned} \right\} (9.9.71)$$

$$\left. \begin{aligned} \dot{c}_{y,t}^{\omega_z} &= \frac{4b_0^2\alpha'^2\lambda_w}{l^2} \left[ \frac{\alpha'}{M_\infty^2} \int_{-l/(2b_0)}^{l/(2b_0)} \int_{\xi_0, t}^{\xi_t^*} \frac{\partial F^{\omega_z}(\xi_t, \zeta_t)}{\partial \xi_t} d\xi_t d\zeta_t \right. \\ &\quad \left. - \int_{-l/(2b_0)}^{l/(2b_0)} \int_{\xi_0, t}^{\xi_t^*} \frac{\partial F^{\omega_z}(\xi, \zeta)}{\partial \xi} \xi d\xi d\zeta \right] \end{aligned} \right\}$$

$$m_{z,t}^x = \frac{4b_0^2\alpha'^2\lambda_w}{l^2} \int_{-l/(2b_0)}^{l/(2b_0)} \int_{\xi_0, t}^{\xi_t^*} \frac{\partial F^\alpha(\xi_t, \zeta_t)}{\partial \xi_t} \xi_t d\xi_t d\zeta_t$$

$$\dot{m}_{z,t}^x = -\frac{4b_0^2\alpha'^3\lambda_w}{l^2} \int_{-l/(2b_0)}^{l/(2b_0)} \int_{\xi_0, t}^{\xi_t^*} F^\alpha(\xi_t, \zeta_t) \xi_t d\xi_t d\zeta_t$$

$$\left. \begin{aligned} \dot{m}_{z,t}^x &= -\frac{4b_0^2\alpha'^3\lambda_w}{l^2} \left[ \frac{\alpha'}{M_\infty^2} \int_{-l/(2b_0)}^{l/(2b_0)} \int_{\xi_0, t}^{\xi_t^*} \frac{\partial F^\alpha(\xi_t, \zeta_t)}{\partial \xi_t} \xi_t d\xi_t d\zeta_t \right. \\ &\quad \left. - \int_{-l/(2b_0)}^{l/(2b_0)} \int_{\xi_0, t}^{\xi_t^*} \frac{\partial F^\alpha(\xi_t, \zeta_t)}{\partial \xi_t} \xi_t^2 d\xi_t d\zeta_t \right] \end{aligned} \right\} (9.9.72)$$

$$m_{z,t}^{\omega_z} = \frac{4b_0^2\alpha'^2\lambda_w}{l^2} \int_{-l/(2b_0)}^{l/(2b_0)} \int_{\xi_0, t}^{\xi_t^*} \frac{\partial F^{\omega_z}(\xi_t, \zeta_t)}{\partial \xi_t} \xi_t d\xi_t d\zeta_t$$

$$\dot{m}_{z,t}^{\omega_z} = -\frac{4b_0^2\alpha'^3\lambda_w}{l^2} \int_{-l/(2b_0)}^{l/(2b_0)} \int_{\xi_0, t}^{\xi_t^*} F^{\omega_z}(\xi_t, \zeta_t) \xi_t d\xi_t d\zeta_t$$

$$\left. \begin{aligned} \dot{m}_{z,t}^{\omega_z} &= -\frac{4b_0^2\alpha'^3\lambda_w}{l^2} \left[ \frac{\alpha'}{M_\infty^2} \int_{-l/(2b_0)}^{l/(2b_0)} \int_{\xi_0, t}^{\xi_t^*} \frac{\partial F^{\omega_z}(\xi_t, \zeta_t)}{\partial \xi_t} \xi_t d\xi_t d\zeta_t \right. \\ &\quad \left. - \int_{-l/(2b_0)}^{l/(2b_0)} \int_{\xi_0, t}^{\xi_t^*} \frac{\partial F^{\omega_z}(\xi_t, \zeta_t)}{\partial \xi_t} \xi_t^2 d\xi_t d\zeta_t \right] \end{aligned} \right\} (9.9.73)$$

$$m_{x,t}^{\omega} = - \frac{4b_0^2 \alpha' \lambda_w}{l^2} \left\{ \int_{-l/(2b_0)}^{l/(2b_0)} \int_{\xi_0,t}^{\xi_t^*} \frac{\partial F^{\omega,x}}{\partial \xi_t} (\xi_t, \zeta_t) \zeta_t d\xi_t d\zeta_t \right\} \quad (9.9.74)$$

$$m_{x_1}^{\dot{\omega}_x} = \frac{4b_0^2 \alpha'^3 \lambda_w}{l^2} \int_{-l/(2b_0)}^{l/(2b_0)} \int_{\xi_0, t}^{\xi_t^*} F^{\omega_x}(\xi_t, \zeta_t) \zeta_t d\xi_t d\zeta_t$$

$$m_{x2}^{(0)} = -\frac{4b_0^2 \alpha'^3 \lambda_w}{l^2} \left[ \frac{\alpha'}{M_\infty^2} \int_{-l/(2b_0)}^{l/(2b_0)} \int_{\xi_0, t}^{\xi_t^*} \frac{\partial F^{(0)x}(\xi_t, \xi_t)}{\partial \xi_t} \zeta_t d\xi_t d\xi_t \right. \\ \left. - \int_{-l/(2b_0)}^{l/(2b_0)} \int_{\xi_0, t}^{\xi_t^*} \frac{\partial F^{(0)x}(\xi_t, \xi_t)}{\partial \xi_t} \zeta_t \xi_t d\xi_t d\xi_t \right] \quad (9.9.75)$$

It must be taken into consideration that the velocity potential on the leading edge is zero. Consequently,

$$F^{q_j}(\xi_0, t, \xi_t) = F^{\dot{q}_j}(\xi_0, t, \xi_t) = 0 \quad (9.9.76)$$

Accordingly,

$$\int_{\xi_0, t}^{\xi_t^*} \frac{\partial F^{q_j}(\xi_t, \zeta_t)}{\partial \xi_t} d\xi_t = F^{q_j}(\xi_t^*, \zeta_t)$$

$$\int_{\xi_0}^{\xi_t^*} \frac{\partial F^{q_j}(\xi_t, \zeta_t)}{\partial \xi_t} \zeta_t d\xi_t = \zeta_t F^{q_j}(\xi_t^*, \zeta_t)$$

$$\int_{\xi_t^*, t}^{*} \frac{\partial F'^j(\xi_t, \zeta_t)}{\partial \xi_t} \xi_t \xi_t d\xi_t = \zeta_t \xi_t^* F'^j(\xi_t^*, \zeta_t)$$

$$-\int_{\xi_0, t}^{\xi_t^*} F^{q_j}(\xi_t, \zeta_t) \zeta_t d\xi_t$$

$$\int_{\xi_0, t}^{\xi_t^*} \frac{\partial F^{q_j}(\xi_t, \zeta_t)}{\partial \xi_t} \xi_t^2 d\xi_t = \xi_t^{*2} F^{q_j}(\xi_t^*, \zeta_t) \\ - \int_{\xi_0, t}^{\xi_t^*} \xi_t F^{q_j}(\xi_t, \zeta_t) d\xi_t$$

In a similar way, we shall write the relevant expressions related to the derivatives  $F^{q_j}$ . Let us go over in (9.9.70)-(9.9.75) to the characteristic coordinates  $s$  and  $r$  (9.9.28). Assuming that the velocity potential (or the function  $D$ ) is constant in the cells and replacing the integrals with sums, with a view to (9.9.77) we obtain relations for numerical calculations of the derivatives of the aerodynamic coefficients.

These relations, used for finding by (9.9.67) the corresponding derivatives of the aerodynamic coefficients of the lift force  $c_y^\alpha$ ,  $\dot{c}_y^\alpha$ ,  $c_y^{(0)z}$ ,  $\dot{c}_y^{(0)z}$ , and also for determining from (9.9.68) the derivatives of the pitching moment coefficients  $m_z^\alpha$ ,  $\dot{m}_z^\alpha$ ,  $m_z^{(0)z}$ ,  $\dot{m}_z^{(0)z}$  can be represented by the relations:

$$c_y^\alpha, t = \frac{4b_0^2 \alpha' \lambda_w}{l^2} h \sum_{\bar{r}^*} F^\alpha(\bar{r}^*, \bar{s}^*) \\ c_{y1, t}^\alpha = - \frac{4b_0^2 \alpha'^2 \lambda_w}{l^2} h^2 \sum_s \sum F^{\bar{\alpha}}(\bar{r}, \bar{s}) \\ c_{y, 2t}^{\dot{\alpha}} = \frac{4b_0^2 \alpha'^2 \lambda_w}{l^2} h \left\{ \frac{\alpha'}{M_\infty^2} \sum_{\bar{r}^*} F^{\dot{\alpha}}(\bar{r}^*, \bar{s}^*) \right\} \quad \} (9.9.78)$$

$$- \sum_{\bar{r}^*} [(\bar{r}^* + \bar{s}^*) h/2 + \xi_{0, 0, t}] F^\alpha(\bar{r}^*, \bar{s}^*) + h \sum_s \sum F^\alpha(\bar{r}, \bar{s}) \quad \}$$

$$c_y^{(0)z} = \frac{4b_0^2 \alpha' \lambda_w}{l^2} h \sum_{\bar{r}^*} F^{(0)z}(\bar{r}^*, \bar{s}^*) \\ c_{y1, t}^{(0)z} = - \frac{4b_0^2 \alpha'^2 \lambda_w}{l^2} h^2 \sum_s \sum F^{\bar{(0)z}}(\bar{r}, \bar{s}) \\ c_{y, 2t}^{\dot{(0)z}} = \frac{4b_0^2 \alpha'^2 \lambda_w}{l^2} h \left\{ \frac{\alpha'}{M_\infty^2} \sum_{\bar{r}^*} F^{\dot{(0)z}}(\bar{r}^*, \bar{s}^*) \right\} \quad \} (9.9.79)$$

$$\begin{aligned}
 & - \sum_{\bar{r}^*} [(\bar{r}^* + \bar{s}^*) h/2 + \xi_{0,0,t}] F^{0z}(\bar{r}^*, \bar{s}^*) \\
 & + h \sum_S \sum F^{0z}(\bar{r}, \bar{s}) \} \\
 m_{z,t}^\alpha = & \frac{4b_0^2 \alpha'^2 \lambda_w}{l^2} h \left\{ \sum_{\bar{r}^*} [(\bar{r}^* + \bar{s}^*) h/2 + \xi_{0,0,t}] F^\alpha(\bar{r}^*, \bar{s}^*) \right. \\
 & \left. - h \sum_S \sum F^\alpha(\bar{r}, \bar{s}) \right\} \\
 \dot{m}_{z1,t}^\alpha = & - \frac{4b_0^2 \alpha'^3 \lambda_w}{l^2} h^2 \sum_S \sum [(\bar{r} + \bar{s}) h/2 + \xi_{0,0,t}] F^\alpha(\bar{r}, \bar{s}) \\
 \dot{m}_{z2,t}^\alpha = & \frac{4b_0^2 \alpha'^3 \lambda_w}{l^2} h \left\{ + \frac{\alpha'}{M_\infty^2} \sum_{\bar{r}^*} [(\bar{r}^* + \bar{s}^*) h/2 \right. \\
 & + \xi_{0,0,t}] F^\alpha(\bar{r}^*, \bar{s}^*) + 2h \sum_S \sum [(\bar{r} + \bar{s}) h/2 \right. \\
 & \left. + \xi_{0,0,t}] F^\alpha(\bar{r}, \bar{s}) - \frac{\alpha' h}{M_\infty^2} \sum_S \sum \dot{F}^\alpha(\bar{r}, \bar{s}) \right. \\
 & \left. - \sum_{\bar{r}^*} [(\bar{r}^* + \bar{s}^*) h/2 + \xi_{0,0,t}]^2 F^\alpha(\bar{r}^*, \bar{s}^*) \right\} \quad (9.9.80)
 \end{aligned}$$

The aerodynamic derivatives of the rolling moment coefficient are calculated by the following formulas:

$$\begin{aligned}
 m_{x,t}^{\omega_x} = & - \frac{4b_0^2 \alpha'^2 \lambda_w}{l^2} h \sum_{\bar{r}^*} [(\bar{s}^* - \bar{r}^*) h/2] F^{\omega_x}(\bar{r}^*, \bar{s}^*) \\
 \dot{m}_{x1,t}^{\omega_x} = & \frac{4b_0^2 \alpha'^3 \lambda_w}{l^2} h^2 \sum_S \sum [(\bar{s} - \bar{r}) h/2] F^{\omega_x}(\bar{r}, \bar{s}) \\
 \dot{m}_{x2,t}^{\omega_x} = & - \frac{4b_0^2 \alpha'^3 \lambda_w}{l^2} h \left\{ \frac{\alpha'}{M_\infty^2} \sum_{\bar{r}^*} [(\bar{s}^* - \bar{r}^*) h/2] F^{\dot{\omega}_x}(\bar{r}^*, \bar{s}^*) \right. \\
 & - \sum_{\bar{r}^*} [(\bar{s}^* - \bar{r}^*) h/2] [(\bar{r}^* + \bar{s}^*) h/2 + \xi_{0,0,t}] F^{\omega_x}(\bar{r}^*, \bar{s}^*) \\
 & \left. + h \sum_S \sum [(\bar{s} - \bar{r}) h/2] F^{\omega_x}(\bar{r}^*, \bar{s}^*) \right\} \quad (9.9.81)
 \end{aligned}$$

If we take the wing span  $l$  as the characteristic dimension when calculating the rolling moment coefficient, and the half-span  $l/2$  when determining the kinematic parameter  $\omega_x$ , then the new values of the rolling moment coefficient and the corresponding derivatives are determined by the relations

$$m_{x1} = m_x b_0 / l, \quad m_{x1}^{\dot{\omega}_x} = 2m_x^{\dot{\omega}_x} (b_0/l)^2, \quad \dot{m}_{x1}^{\dot{\omega}_x} = 4m_x^{\dot{\omega}_x} (b_0/l)^3 \quad (9.9.82)$$

By analogy with (9.9.69), we shall give the following working formulas for the derivatives:

$$\alpha' m_{x1}^{\dot{\omega}_x} = m_{x1, t}^{\dot{\omega}_x}, \quad \alpha'^2 m_{x1}^{\dot{\omega}_x} = (m_{x1, t})_1 + M_\infty^2 (m_{x1, t})_2 \quad (9.9.83)$$

$$m_{x1, t}^{\dot{\omega}_x} = -8\alpha' \lambda_w (b_0/l)^4 h \sum_{\bar{r}^*} [(\bar{s}^* - \bar{r}^*) h/2] F^{\dot{\omega}_x} (\bar{r}^*, \bar{s}^*)$$

$$(m_{x1, t}^{\dot{\omega}_x})_1 = 16\alpha' \lambda_w (b_0/l)^5 h^2 \sum_S [(\bar{s} - \bar{r}) h/2] F^{\dot{\omega}_x} (\bar{r}, \bar{s})$$

$$(m_{x1, t}^{\dot{\omega}_x})_2 = -16\alpha' \lambda_w (b_0/l)^5 h \left\{ \frac{\alpha'}{M_\infty^2} \sum_{\bar{r}^*} [(\bar{s}^* - \bar{r}^*) h/2] \right. \quad (9.9.84)$$

$$\times F^{\dot{\omega}_x} (\bar{r}, \bar{s}) - \sum_{\bar{r}^*} [(\bar{s}^* - \bar{r}^*) h/2] [(\bar{r}^* + \bar{s}^*) h/2]$$

$$+ \xi_{0, 0, t} | F^{\dot{\omega}_x} (\bar{r}^*, \bar{s}^*) + h \sum_S [(\bar{s} - \bar{r}) h/2] F^{\dot{\omega}_x} (\bar{r}, \bar{s}) \}$$

In the above relations, the symbol  $\sum_{\bar{r}^*}$  signifies summation over the cells along the trailing edge, and the symbol  $\sum_S \sum$ , double summation over all the cells on the lifting surface.

When performing calculations of the total aerodynamic characteristics, one must have in view that these calculations are carried out in the system of coordinate axes depicted in Fig. 9.6.1 (with the rule of signs indicated in this figure). All the geometric quantities are measured and the pressure coefficients are found in the system of coordinates whose axis  $Oz$  passes through the vertex of the wing (see Fig. 9.11.1). When the mean aerodynamic chord  $b_0$  is taken as the characteristic dimension, the aerodynamic coefficients and derivatives are found by converting the values of  $c_y$ ,  $m_x$ ,  $m_z$ , and their derivatives by the following formulas:

$$\left. \begin{aligned} c_{y, A} &= c_y, & c_{y, A}^\alpha &= c_y^\alpha, & \dot{c}_{y, A}^\alpha &= \dot{c}_y^\alpha b_0/b_A \\ c_{y, A}^{\dot{\omega}_z} &= c_y^{\dot{\omega}_z} b_0/b_A, & \dot{c}_{y, A}^{\dot{\omega}_z} &= \dot{c}_y^{\dot{\omega}_z} (b_0/b_A)^2 \end{aligned} \right\} \quad (9.9.85)$$

$$\left. \begin{aligned} m_{z,A} &= m_z b_0 / b_A, & m_{z,A}^{\dot{\alpha}} &= m_z b_0 / b_A, & m_{z,A}^{\dot{\alpha}_A} &= \dot{m}_z^{\dot{\alpha}_A} (b_0 / b_A)^2 \\ m_{z,A}^{\dot{\omega}_z,A} &= m_z^{\dot{\omega}_z} (b_0 / b_A)^2, & m_{z,A}^{\dot{\omega}_z,A} &= \dot{m}_z^{\dot{\omega}_z} (b_0 / b_A) \end{aligned} \right\} \quad (9.9.86)$$

$$m_{x,A} = m_x b_0 / b_A, \quad m_{x,A}^{\dot{\omega}_x,A} = m_x (b_0 / b_A)^2, \quad m_{x,A}^{\dot{\omega}_x,A} = \dot{m}_x^{\dot{\omega}_x} (b_0 / b_A)^3 \quad (9.9.87)$$

In the above expressions, it is assumed that

$$\left. \begin{aligned} \dot{\alpha}_A &= (d\alpha/dt) b_A / V_\infty, & \omega_{z,A} &= \Omega_z b_A / V_\infty \\ \dot{\omega}_{z,A} &= (d\Omega_z/dt) b_A^2 / V_\infty^2, & \dot{\omega}_{x,A} &= (d\Omega_x/dt) b_0^2 / V_\infty^2 \end{aligned} \right\} \quad (9.9.88)$$

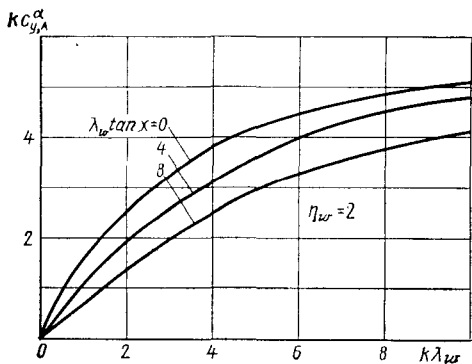
## 9.10. Properties of Aerodynamic Derivatives

Let us consider the general properties of the aerodynamic derivatives as applied to finite-span wings with a constant leading and trailing-edge sweep. Investigations show that at low Strouhal numbers ( $p^* \rightarrow 0$ ) the value of a derivative is a function of three arguments:  $k\lambda_w = \lambda_w \sqrt{1 - M_\infty^2}$ ,  $\tan \chi_0$ , and  $\eta_w$ . These arguments, called similarity criteria, are determined, as can be seen, by the aspect ratio  $\lambda_w$ , the leading-edge sweep angle  $\chi_0$ , the taper ratio  $\eta_w$ , and the Mach number  $M_\infty$ . For an incompressible fluid, there are two such arguments:  $\lambda_w \tan \chi_0$  and  $\eta_w$ . If a rectangular wing is being considered, it is necessary to assume that  $\lambda_w \tan \chi_0 = 0$  and  $\eta_w = 1$ ; for a triangular wing,  $\eta_w = \infty$ .

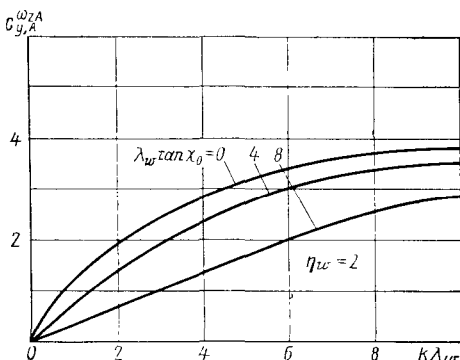
Diagrams characterizing the dependence of the stability derivatives on the similarity criteria for wings with a taper ratio of  $\eta_w = 2$  in a *subsonic flow* are shown in Figs. 9.10.1-9.10.10 as illustrations.

The mean aerodynamic chord  $b_A$  has been taken as the characteristic dimension when calculating the data in these figures (the kinematic variables  $\dot{\alpha}_A$ ,  $\omega_{z,A}$ ,  $\dot{\omega}_{z,A}$ , the coefficient  $m_{z,A}$ ). This makes the dependence of the aerodynamic derivatives on the geometric parameters of the wing more stable, the results approaching the relevant quantities for rectangular wings.

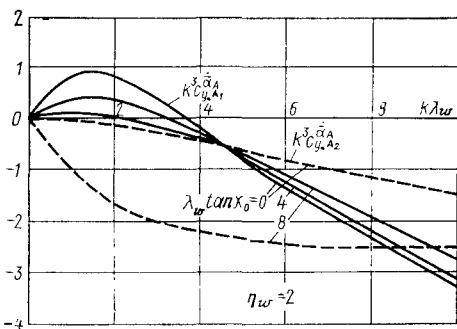
When calculating the rolling moment  $m_{x1}$ , we chose the wing span  $l$  as the characteristic geometric dimension, while for the kinematic variables  $\omega_{x1}$  and  $\dot{\omega}_{x1}$  we took the half-span  $l/2$ . The origin of coordinates is on the axis of symmetry, while the axis  $Oz$  passes through the beginning of the mean aerodynamic chord  $b_A$ . When necessary, we can convert the obtained derivatives to another characteristic dimension and to a new position of the axis  $Oz$ .

**Fig. 9.10.1**

Change in the quantity  $k c_{y,A}^\alpha$  used in calculating the stability derivative  $c_y^\alpha$  for a wing in a subsonic flow

**Fig. 9.10.2**

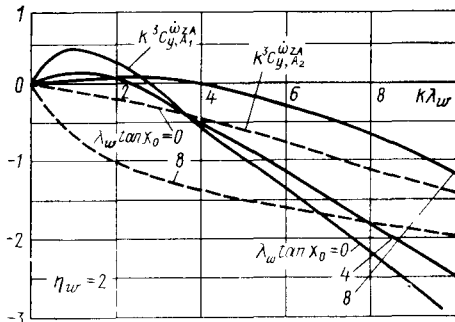
Change in the quantity  $k c_{y,A}^{\omega_z}$  determining the derivative  $c_{y,A}^{\omega_z}$  for a wing at subsonic velocities

**Fig. 9.10.3**

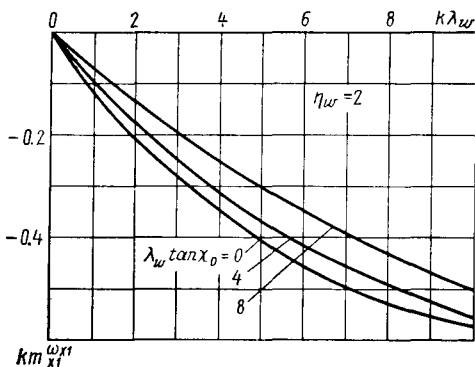
Values of  $k^3 c_{y,A}^{\dot{\alpha}_A 1}$  and  $k^3 c_{y,A}^{\dot{\alpha}_A 2}$  characterizing the change in the derivative of the coefficient  $c_y$  with respect to  $\dot{\alpha}_A$  for a lifting surface at  $M_\infty < 1$

**Fig. 9.10.4**

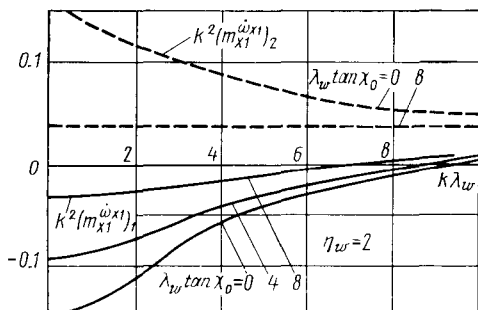
Values of  $k^3 c_y \dot{\omega}_z A_1$  and  $k^3 c_y \dot{\omega}_z A$  determining the derivative of  $c_y A$  with respect to  $\dot{\omega}_z A$  for a subsonic flow over a wing

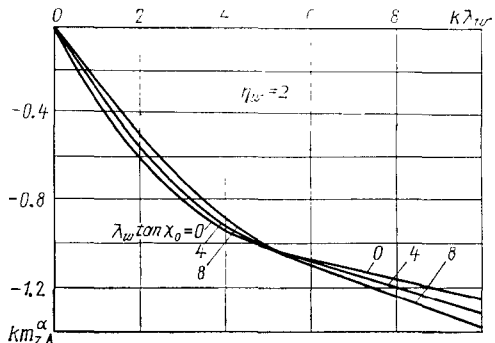
**Fig. 9.10.5**

Change in the variable  $km \dot{\omega}_{x1} x_1$  determining the derivative of the rolling moment coefficient with respect to  $\dot{\omega}_{x1}$  for a wing at  $M_\infty < 1$

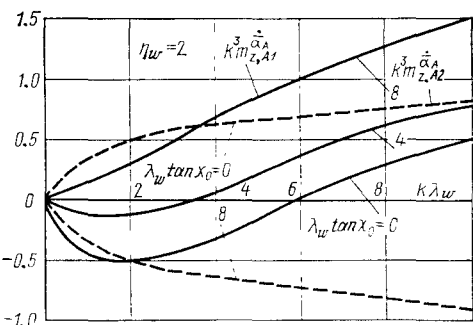
**Fig. 9.10.6**

Values of  $k^2(m_{x1} \dot{\omega}_{x1})_1$  and  $k^2(m_{x1} \dot{\omega}_{x1})_2$  characterizing the change in the rolling moment coefficient with respect to  $\dot{\omega}_{x1}$  for a wing in a subsonic flow

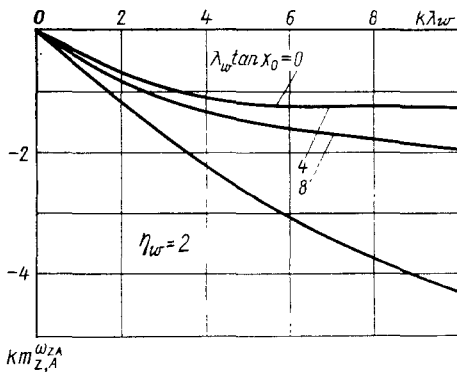


**Fig. 9.10.7**

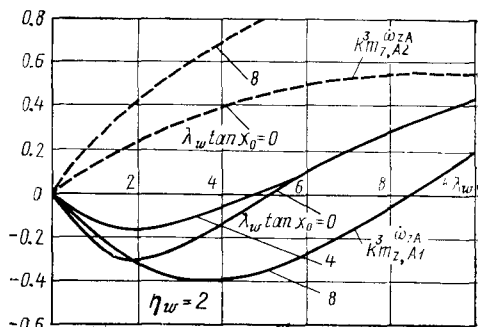
Function  $km_{z,A}^\alpha$  determining the derivative  $m_{z,A}^\alpha$  for a wing in a subsonic flow

**Fig. 9.10.8**

Values of  $k^3 \dot{m}_{z,A1}$  and  $k^3 \dot{m}_{z,A2}$  determining the derivative  $\dot{m}_{z,A}$  for a wing at subsonic velocities

**Fig. 9.10.9**

Values of  $km_{z,A}^{\omega_z,A}$  determining the derivative  $m_{z,A}^{\omega_z,A}$  for a wing at  $M_\infty < 1$

**Fig. 9.10.10**

Variables  $k^3 m_z^{\dot{\omega}_z, A_1}$  and  $k^3 m_z^{\dot{\omega}_z, A_2}$  characterizing the change in the derivative  $m_z^{\dot{\omega}_z, A}$  for a wing at  $M_\infty < 1$

According to the data shown in Figs. 9.10.1-9.10.10, the aerodynamic derivatives are determined as follows:

$$c_y^\alpha = (kc_y^\alpha)/k, \quad c_y^{\dot{\alpha}_A} = [(k^3 c_y^{\dot{\alpha}_A, A_1}) + M_\infty^2 (k^3 c_y^{\dot{\alpha}_A, A_2})]/k^3 \quad (9.10.1)$$

$$c_y^{\dot{\omega}_z, A} = (kc_y^{\dot{\omega}_z, A})/k, \quad c_y^{\dot{\omega}_z, A} = [(k^3 c_y^{\dot{\omega}_z, A_1}) + M_\infty^2 (k^3 c_y^{\dot{\omega}_z, A_2})]/k^3 \quad (9.10.2)$$

$$m_{x_1}^{\dot{\omega}_{x_1}} = (km_{x_1}^{\dot{\omega}_{x_1}})/k, \quad m_{x_1}^{\dot{\omega}_{x_1}} = [(k^2 m_{x_1}^{\dot{\omega}_{x_1}})_1 + M_\infty^2 (k^2 m_{x_1}^{\dot{\omega}_{x_1}})_2]/k^2 \quad (9.10.3)$$

$$m_z^\alpha = (km_z^\alpha, A)/k, \quad m_z^{\dot{\alpha}_A} = [(k^3 m_z^{\dot{\alpha}_A, A_1}) + M_\infty^2 (k^3 m_z^{\dot{\alpha}_A, A_2})]/k^3 \quad (9.10.4)$$

$$m_z^{\dot{\omega}_z, A} = (km_z^{\dot{\omega}_z, A})/k, \quad m_z^{\dot{\omega}_z, A} = [(k^3 m_z^{\dot{\omega}_z, A_1}) + M_\infty^2 (k^3 m_z^{\dot{\omega}_z, A_2})]/k^3 \quad (9.10.5)$$

We can use the graphs (Figs. 9.10.1-9.10.10) to find the stability derivatives for the entire range of subsonic numbers  $M_\infty$ , including an unsteady incompressible flow ( $M_\infty = 0, k = 1$ ). The data of these graphs point to the increase in the lifting capacity of the wings when going over from an incompressible ( $M_\infty = 0$ ) to a compressible fluid ( $M_\infty < 1$ ). Here the stability derivatives at  $M_\infty < 1$  can be calculated sufficiently accurately according to the Prandtl-Glauert compressibility rule  $c = c_{1e} (1 - M_\infty^2)^{-1/2}$ , where  $c$  and  $c_{1e}$  are aerodynamic variables in a compressible and incompressible fluid, respectively. The lower the aspect ratio, the smaller is the action of the compressibility, i.e. the smaller is the influence of the number  $M_\infty < 1$ . This is due to the fact that the disturbances introduced into a flow attenuate with a decrease in the cross-sectional dimensions of a wing, i.e. with a decrease in the aspect ratio.

Near the tips of a wing in a subsonic flow, the air flows from the bottom side where the pressure is higher to the upper one. This leads

to lowering of the lifting capacity of the wing. The intensity of such overflow grows with a decrease in the aspect ratio of a wing; consequently, an increase in this aspect ratio improves the lifting capacity.

An analysis of the influence of the leading-edge sweep angle  $\chi_0$  shows that its growth leads to an appreciable diminishing of the derivative  $c_y^z$  for a wing with a high aspect ratio. At small aspect ratios, the influence of the angle  $\chi_0$  is virtually absent because in this case even an insignificant change in  $\chi_0$  leaves the planform of the wing almost unchanged.

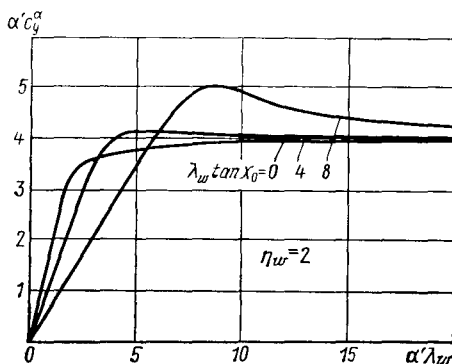
A change in the taper ratio  $\eta_w$  at given values of  $\lambda_w$  and  $\chi_0$  has a slight effect on the lifting capacities, especially for low aspect ratios of a wing. The explanation is that at  $M_\infty < 1$  most of the lift force is produced by the lifting surface near the leading edges, which is especially noticeable with low aspect ratios. A large value of the taper ratio  $\eta_w$  (at  $\chi_0 = \text{const}$ ) corresponds, as it were, to cutting off a part of the poorly lifting tail surface of the wing.

An analysis of the found values of the centre of pressure coefficient  $c_p = x_p b_0 = m_{z,A} c_{y,A}$  (where  $x_p$  is the distance to the centre of pressure from the front of the mean aerodynamic chord) allows us to conclude that the quantity  $c_p$  grows with an increase in the sweep angles (the centre of pressure is displaced more noticeably to the tail). The aspect ratio affects  $c_p$  in the same way as the angle  $\chi_0$ . At low values of  $\lambda_w$ , however (of the order of 0.5 and below), the position of the centre of pressure does not virtually change.

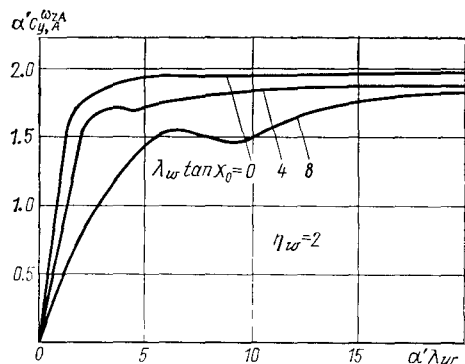
The derivatives  $m_{z,A}^{z,A}$  and  $m_{x1}^{x1}$  that characterize damping in oscillatory motion grow with an increase in the aspect ratio  $\lambda_w$ . This indicates an increase in the damping upon longitudinal unsteady motion and rolling of the wing. The above graphs allow us to conclude that the influence of the sweep angle and taper ratio on the damping of low-aspect-ratio wings is relatively small. The above-mentioned derivatives together with the quantity  $m_{z,A}^\alpha$  characterizing the longitudinal static stability grow with increasing subsonic numbers  $M_\infty$ .

Aerodynamic derivatives capped with dots depend greatly on the aspect ratio  $\lambda_w$  in the subsonic region. The values of the derivatives grow with an increasing number  $M_\infty$ . The change in the dotted derivatives, i.e. in the aerodynamic characteristics that are purely unsteady, is especially great at near-sonic velocities. At numbers  $M_\infty \rightarrow 1$ , the magnitudes of the derivatives with dots grow appreciably, and their signs change. A typical feature here is the growing influence of the wing planform on the aerodynamic variables for a non-stationary unsteady flow.

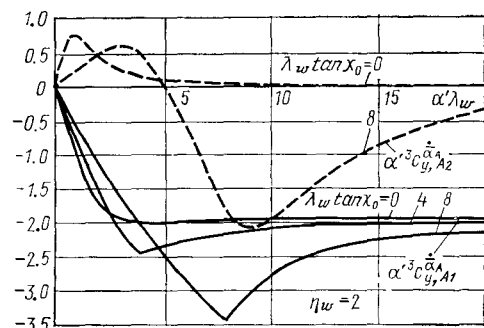
The data characterizing the change in the non-stationary derivatives for a wing at *supersonic velocities* are presented in Figs. 9.10.14-9.10.20. According to these data, the stability derivatives are deter-



**Fig. 9.10.11**  
Values of  $\alpha' c_y^\alpha$  determining the stability derivative  $c_y^\alpha$  for a wing in a supersonic flow



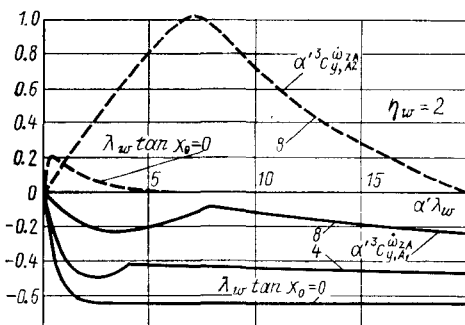
**Fig. 9.10.12**  
Change in the quantity  $\alpha' c_y^{\omega_z, A}$  determining the derivative  $c_y^{\omega_z, A}$  for a wing at supersonic velocities



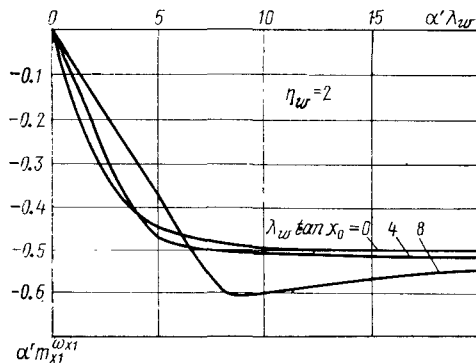
**Fig. 9.10.13**  
Relations for  $\alpha'^3 c_y^{\dot{\alpha}_A}$  and  $\alpha'^3 c_y^{\dot{\alpha}_A2}$  characterizing the change in the derivative of the coefficient  $c_y$  with respect to  $\dot{\alpha}_A$  for a wing at  $M_\infty > 1$

**Fig. 9.10.14**

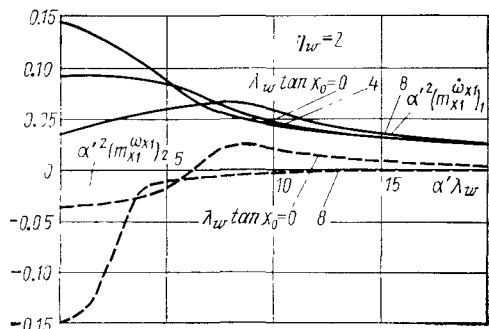
Values of  $\alpha'^3 c_y^{\omega_z, A_1}$  and  $\alpha'^3 c_y^{\omega_z, A_2}$  determining the derivative of  $c_y$  with respect to  $\omega_z, A$  in a supersonic flow over a wing

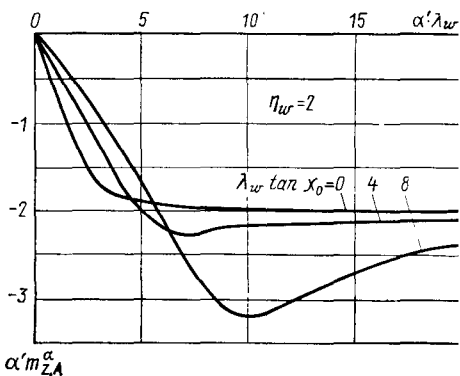
**Fig. 9.10.15**

Function  $\alpha'm_{x1}^{\omega_{x1}}$  characterizing the change in the derivative of the rolling moment coefficient with respect to  $\omega_{x1}$  for a wing at  $M_\infty > 1$

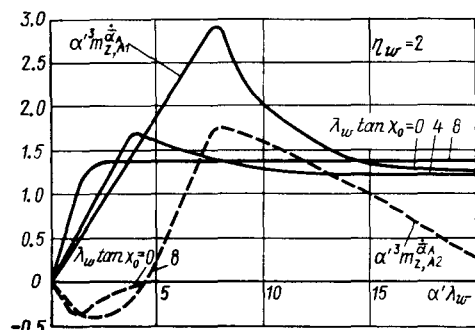
**Fig. 9.10.16**

Values of  $\alpha'^2(m_{x1}^{\omega_{x1}})_1$  and  $\alpha'^2(m_{x1}^{\omega_{x1}})_2$  characterizing the change in the derivative of the rolling moment coefficient with respect to  $\omega_{x1}$  for a wing in a supersonic flow

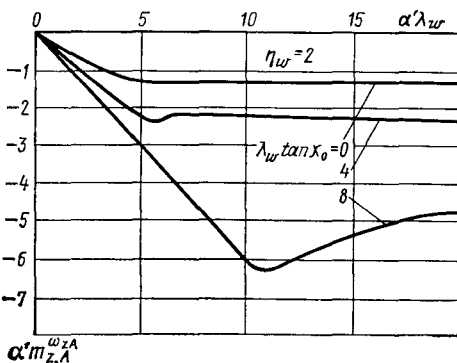


**Fig. 9.10.17**

Variable  $\alpha'm_{z,A}^\alpha$  determining the derivative  $m_{z,A}^\alpha$  for a wing at  $M_\infty > 1$

**Fig. 9.10.18**

Values of  $\alpha'^3 m_{z,A_1}^{\dot{\alpha}}$  and  $\alpha'^3 m_{z,A_2}^{\dot{\alpha}}$  determining the derivative  $m_{z,A}^{\dot{\alpha}}$  for a wing in a supersonic flow

**Fig. 9.10.19**

Function  $\alpha'm_{z,A}^\omega$  determining the derivative  $m_{z,A}^\omega$  for a wing at  $M_\infty > 1$

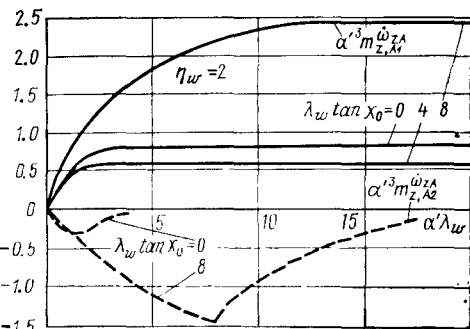


Fig. 9.10.20

Variables  $\alpha' m_z^{\omega_z, A}$  and  $\alpha'^3 m_z^{\omega_z, A^2}$  characterizing the change in the derivative  $m_z^{\omega_z, A}$  in a supersonic flow

mined with the aid of formulas (9.10.1)-(9.10.5) in which the quantity  $k = \sqrt{1 - M_\infty^2}$  is replaced with  $\alpha' = \sqrt{M_\infty^2 - 1}$ .

The graphs allow us to arrive at the conclusion that the lifting capacities of wings at  $M_\infty > 1$  grow with an increase in the aspect ratio, although to a smaller extent than at subsonic velocities. Particularly, for a rectangular wing ( $\chi_0 = 0$ ), the increase in  $c_y^\alpha$  when  $M_\infty > 1$  occurs only up to  $\lambda_w = 3-4$ , and then the derivative  $c_y^\alpha$  remains virtually constant. For triangular wings, the constancy of  $c_y^\alpha$  is observed beginning from  $\alpha' \lambda_w \geq 4$ , i.e. when the leading edges transform from subsonic into supersonic ones.

The derivatives of longitudinal and lateral damping ( $m_z^{\omega_z, A}$  and  $m_{x_1}^{\omega_x, 1}$ ), as with subsonic velocities, grow (in magnitude) with an increase in the aspect ratio. Their change for low-aspect-ratio wings is only slightly influenced by the sweep angle and the taper ratio. Unlike the case when  $M_\infty < 1$ , at supersonic velocities the derivatives  $m_z^{\omega_z, A}$  and  $m_{x_1}^{\omega_x, 1}$ , and also  $m_z^\alpha$  decrease when  $M_\infty$  increases.

The dotted aerodynamic derivatives change to a smaller extent under the influence of the wing aspect ratio at  $M_\infty > 1$ . But they grow in magnitude at supersonic flow near values of  $M_\infty > 1$ . For these velocities, as when  $M_\infty < 1$ , a sharp change in the magnitude of the non-stationary derivatives is also attended by a change in their signs.

At large numbers  $M_\infty$  ( $M_\infty \geq 2.5-3.0$ ), the aerodynamic derivatives with dots decrease, tending to zero at  $M_\infty \rightarrow \infty$ . The influence of the planform on their values is not so great at the usual velocities (sub- or supersonic), but becomes considerably greater in the transonic region where the number  $M_\infty$  equals unity or is somewhat larger than it.

### 9.11. Approximate Methods for Determining the Non-Stationary Aerodynamic Characteristics

#### Hypotheses of Harmonicity and Stationarity

The harmonicity of oscillations, which is the basis of the method of calculating non-stationary aerodynamic characteristics set out above, reflects only a partial, idealized scheme of unsteady flow over a craft. In the general form, such flow may be characterized by other time dependences of the kinematic parameters. At present, methods have been developed that can be used for unsteady flows described by any functions. But owing to their great intricacy, it is not always possible to use them in practice.

It is therefore necessary to have less strict and sufficiently simple methods of calculating the total and local non-stationary aerodynamic characteristics. One such method is based on what is called the hypothesis of harmonicity (see [19]). By this hypothesis, an aerodynamic coefficient for unsteady flow is represented by series (9.6.8) in which the stability derivatives  $c_{\alpha}^q$ ,  $c_{\dot{\alpha}}^q$ , and others are functions of the mean angle of attack  $\alpha_0$ , the Mach, Reynolds, and Strouhal numbers for a given wing.

In the linear theory of flow of an ideal fluid, such a relation is limited to the Mach and Strouhal numbers. According to this theory, the aerodynamic derivatives depend very slightly on the Strouhal number for low-aspect-ratio wings of any planform at all numbers  $M_\infty$  when the latter are large. We can assume that in a first approximation this is also true for any other time dependence of the kinematic variables. But now with any function describing wing motion, the stability derivatives can be taken from the results of calculations or experiments obtained for a harmonic change in the kinematic variables, and the values of these variables can be determined on the basis of their true time dependences for the given mode of motion.

This is the essence of the harmonicity hypothesis. It allows us to obtain more accurate results when the stability derivatives depend less on the Strouhal number. When solving problems on the flight stability of craft, the Strouhal numbers  $p^*$  quite rarely exceed values of 0.05-0.07. Consequently, in practice, we may use the non-stationary characteristics for  $p^* \rightarrow 0$  with sufficient accuracy and, therefore, proceed in our calculations from the harmonicity hypothesis.

The harmonicity hypothesis allows us to obtain more accurate results if the change in the kinematic variables can be represented by a smaller number of terms in the Fourier series corresponding to a narrower spectrum of frequencies characterizing this change.

When studying non-stationary flow over craft, researchers use rather widely what is known as the **steadiness hypothesis**. The content of this hypothesis consists in that all the aerodynamic characteristics are determined only by instantaneous values of the angle of attack.

The local values of the pressure coefficients are the same as in stationary flow at an angle of attack equal to its true value at the given instant. According to this hypothesis used in the linear theory, the aerodynamic coefficient is

$$c_y(t) = c_y^\alpha \alpha(t) \quad (9.11.1)$$

where  $\alpha(t)$  is the true angle of attack at the given instant, and  $c_y^\alpha$  is the stability derivative in steady flow.

If a craft rotates about its lateral axis at the angular velocity  $\Omega_z$ , the **expanded hypothesis of steadiness** is used according to which

$$c_y(t) = c_y^\alpha \alpha(t) + c_y^{\omega_z} \omega_z(t) \quad (9.11.2)$$

Experimental investigations show that the hypothesis of harmonicity yields more correct results than that of steadiness. This is especially noticeable for wings with low aspect ratios. An increase in the aspect ratios is attended by larger errors because at large values of  $\lambda_w$  the dependence of the aerodynamic derivatives on the Strouhal number becomes more appreciable. This is not taken into account in the approximate methods.

#### Tangent-Wedge Method

According to this method, in a stationary supersonic linearized flow over a thin sharp-nosed airfoil, the pressure coefficient at a certain point is determined according to the local angle of inclination of a tangent to the airfoil contour  $\alpha - \beta_N$  (for the upper side), and  $\alpha - \beta_L$  (for the bottom side), i.e. the corresponding value of this coefficient is the same as that of a local tangent surface of a wedge. By formulas (7.5.20) and (7.5.20'), in which we assume that  $\beta_N = \beta$  on the bottom and  $\beta_L = -\beta$  on the upper side of the airfoil, at the corresponding points we have

$$\bar{p}_b = 2(\alpha + \beta)/\sqrt{M_\infty^2 - 1}, \quad \bar{p}_u = -2(\alpha - \beta)/\sqrt{M_\infty^2 - 1} \quad (9.11.3)$$

where  $\beta$  is the local angle of inclination of the contour calculated with a view to the sign for the upper side of the airfoil.

With account taken of these data, the difference of the pressure coefficients on the bottom and upper sides is

$$\Delta \bar{p} = \bar{p}_b - \bar{p}_u = 4\alpha/\alpha' \quad (9.11.4)$$

where  $\alpha' = \sqrt{M_\infty^2 - 1}$ .

It is presumed that formula (9.11.4) for  $\Delta\bar{p}$  can also be applied to non-stationary flow if instead of  $\alpha$  we adopt the value of the local summary angle of attack determined from boundary condition (9.6.32) in the form

$$\alpha_{\Sigma} = -v/V_{\infty} = \alpha + \omega_{x1}\bar{z} - \omega_z\bar{x} \quad (9.11.5)$$

where  $\bar{x} = x/b_0$ ,  $\bar{z} = 2z/l$ , and  $\omega_{x1} = \Omega_x l/(2V_{\infty})$  [with a view to the chosen coordinate system, the sign of  $\omega_z x$  has been changed in comparison with (9.6.32)].

Let us write  $\Delta\bar{p}$  in the form of a series:

$$\Delta\bar{p} = p^{\alpha}\alpha + p^{\omega_{x1}}\omega_{x1} + p^{\omega_z}\omega_z \quad (9.11.6)$$

Substituting for  $\Delta\bar{p}$  in (9.11.6) its value from (9.11.4), but using  $\alpha_{\Sigma}$  from (9.11.5) instead of  $\alpha$ , we find the aerodynamic derivatives:

$$p^{\alpha} = 4/\alpha', \quad p^{\omega_{x1}} = 4\bar{z}/\alpha', \quad p^{\omega_z} = -4\bar{x}/\alpha' \quad (9.11.7)$$

According to the tangent-wedge method, for all wings we have

$$c_y^{\dot{\alpha}} = c_y^{\dot{\omega}_z} = m_z^{\dot{\alpha}} = m_z^{\dot{\omega}_z} = m_{x1}^{\dot{\omega}_{x1}} = 0 \quad (9.11.8)$$

Knowing the quantity (9.11.7), we can find the stability derivatives:

$$\left. \begin{aligned} c_y^{\alpha} &= \frac{\lambda_w b_0}{l} \int_0^1 \int_{\bar{x}_0}^{\bar{x}_1} p^{\alpha} d\bar{x} d\bar{z}; \quad c_y^{\omega_z} = \frac{\lambda_w b_0}{l} \int_{\bar{x}_0}^1 \int_{\bar{z}}^{\bar{z}_1} p^{\omega_z} d\bar{x} d\bar{z} \\ m_{x1}^{\omega_{x1}} &= -\frac{\lambda_w}{2} \int_0^1 \int_{\bar{x}_0}^{\bar{x}_1} p^{\omega_{x1}} \bar{z} d\bar{x} d\bar{z} \\ m_z^{\alpha} &= \frac{\lambda_w b_0}{l} \int_0^1 \int_{\bar{x}_0}^{\bar{x}_1} p^{\alpha} \bar{x} d\bar{x} d\bar{z}; \quad m_z^{\omega_z} = \frac{\lambda_w b_0}{l} \int_0^1 \int_{\bar{x}_0}^{\bar{x}_1} p^{\omega_z} \bar{x} d\bar{x} d\bar{z} \end{aligned} \right\} \quad (9.11.9)$$

We locate the origin of the coordinates at the nose of the centre chord of a wing (Fig. 9.11.1). We adopt the centre chord  $b_0$  as the characteristic dimension for  $m_z$  and  $\omega_z$ , and the span  $l$  and half-span  $l/2$ , respectively, for  $m_{x1}$  and  $\omega_{x1}$ . For such a wing, the equations of the leading and trailing edges in the dimensionless form are as follows:

$$\left. \begin{aligned} \bar{x}_0 &= \frac{x_0}{b_0} = -\frac{(\eta_w + 1) \eta_w \tan \gamma_0}{4\eta_w} \bar{z} \\ \bar{x}_1 &= \frac{x_1}{b_0} = -1 + \left( \frac{\eta_w - 1}{\eta_w} - \frac{\eta_w + 1}{\eta_w} \frac{\lambda_w \tan \chi_0}{4} \right) \bar{z} \end{aligned} \right\} \quad (9.11.10)$$

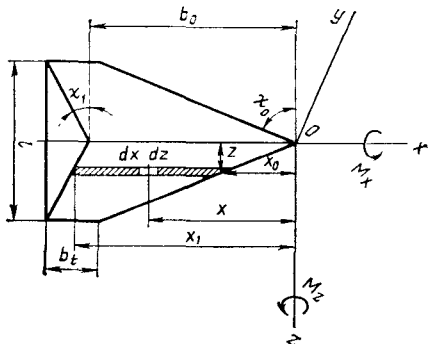
**Fig. 9.11.1**

Diagram of a wing in the calculation of stability derivatives according to the method of local wedges

Let us write the ratio of the centre chord to the span and the aspect ratio of a wing:

$$b_0/l = 2\eta_w/[\lambda_w(\eta_w + 1)], \quad \lambda_w = l^2/S = 2\eta_w l/[(\eta_w + 1)b_0] \quad (9.11.11)$$

The tangent of the sweep angle along the trailing edge is

$$\tan \chi_1 = \tan \chi_0 - (2b_0/l)(1 - 1/\eta_w) \quad (9.11.12)$$

Introducing (9.11.10) and (9.11.7) into (9.11.9), we obtain the stability derivatives of a wing:

$$c_y^\alpha = \frac{4}{\alpha'}, \quad c_y^{\omega_z} = \frac{4}{\alpha'} \left[ \frac{\eta_w^2 + \eta_w + 1}{3\eta_w(\eta_w + 1)} + \frac{\eta_w + 2}{3\eta_w} \cdot \frac{\lambda_w \tan \chi_0}{4} \right] \quad (9.11.13)$$

$$m_{x1}^{\omega_x1} = -\frac{1}{3\alpha'} \frac{\eta_w + 3}{\eta_w + 1} \quad (9.11.14)$$

$$m_z^\alpha = -c_y^{\omega_z}, \quad m_z^{\omega_z} = -\frac{2}{3\alpha'} \left[ \frac{\eta_w^2 + 1}{\eta_w^2} + \frac{\eta_w^2 + 2\eta_w + 3}{\eta_w^2} \cdot \frac{\lambda_w \tan \chi_0}{4} \right. \\ \left. + \frac{\eta_w^2 + 4\eta_w + 3}{\eta_w^2} \left( \frac{\lambda_w \tan \chi_0}{4} \right)^2 \right] \quad (9.11.15)$$

In the particular case of rectangular wings for which  $\tan \chi_0 = 0$  and  $\eta_w = 1$ , we have

$$c_y^\alpha = 4/\alpha', \quad c_y^{\omega_z} = 2/\alpha' \quad (9.11.16)$$

$$m_{x1}^{\omega_x1} = -2/(3\alpha') \quad (9.11.17)$$

$$m_z^\alpha = -2/\alpha', \quad m_z^{\omega_z} = -4/(3\alpha') \quad (9.11.18)$$

For triangular wings ( $\eta_w = \infty$  and  $\lambda_w \tan \chi_0 = 4$ ), we have

$$c_y^\alpha = 4/\alpha', \quad c_y^{\omega z} = 8/(3\alpha') \quad (9.11.19)$$

$$m_{x1}^{\omega x1} = -1/(3\alpha') \quad (9.11.20)$$

$$m_z^\alpha = -8/(3\alpha'), \quad m_z^{\omega z} = -2/\alpha' \quad (9.11.21)$$

It must be noted that the tangent-wedge method makes it possible to determine only the aerodynamic derivatives without dots. The results obtained coincide with the accurate solutions according to the linear theory for infinite-span rectangular wings, and also for triangular wings with supersonic leading edges, at small Strouhal numbers ( $p^* \rightarrow 0$ ). For finite-aspect-ratio wings, the tangent-wedge method yields more accurate solutions when the numbers  $M_\infty$  and the aspect ratios  $\lambda_w$  are larger.

## References

1. Sedov, L.I. *Similarity and Dimensional Methods in Mechanics*, trans. by Kisin, Mir Publishers, Moscow (1982).
2. Sedov, L.I. *A Course of Continuum Mechanics*, Vols. I-IV. Groningen, Wolters-Noorthoff (1971-1972).
3. Khristianovich, S.A. *Obtekание tel gazom pri bol'sikh skorostyakh* (High-Speed Flow of a Gas over a Body), Nauch. trudy TsAGI, vyp. 481 (1940).
4. Belotserkovsky, S.M. and Skripach, B.K. *Aerodinamicheskie proizvodnye letatel'nogo apparata i kryla pri dozvukovykh skorostyakh* (Aerodynamic Derivatives of a Craft and a Wing at Subsonic Velocities), Nauka, Moscow (1975).
5. Loitsyansky, L.G. *Mekhanika zhidkosti i gaza* (Fluid Mechanics), Nauka, Moscow (1970).
6. Predvoditelev, A.S., Stupochenko, E.V., Ionov, V.P., Pleshakov, A.S., Rozhdestvensky, I.B., and Samuilov, E.V. *Termodinamicheskie funktsii vozdukh dlya temperatur ot 1000 do 12 000 K i davlenii ot 0.001 do 1000 atm—grafiki funktsii* (Thermodynamic Functions of Air for Temperatures from 1000 to 12 000 K and Pressures from 0.001 to 1000 atm—Graphs of Functions), Izd. AN SSSR, Moscow (1960).
7. Predvoditelev, A.S., Stupochenko, E.V., Samuilov, E.V., Stakhanov, I.P., Pleshakov, A.S., and Rozhdestvensky, I.B. *Tablitsy termodinamicheskikh funktsii vozdukh (dlya temperatur ot 6000 do 12 000 K i давлений от 0.001 до 1000 atm)* [Tables of Thermodynamic Functions of Air (for Temperatures from 6000 to 12 000 K and Pressures from 0.001 to 1000 atm)], Izd. AN SSSR, Moscow (1957).
8. Kibardin, Yu.A., Kuznetsov, S.I., Lyubimov, A.N., and Shumyatsky, B.Ya. *Atlas gazodinamicheskikh funktsii pri bol'sikh skorostyakh i vysokikh temperaturakh vozduchnogo potoka* (Atlas of Gas-Dynamic Functions at High Velocities and High Temperatures of an Air Stream), Gosenergoizdat, Moscow (1961).
9. Kochin, N.E., Kibel, I.A., and Roze, N.V. *Teoreticheskaya gidromekhanika* (Theoretical Hydromechanics), Parts I, II, Fizmatgiz, Moscow (1963).
10. Fabrikant, I.Ya. *Aerodinamika* (Aerodynamics), Nauka, Moscow (1964).
11. Arzhnikov, N.S. and Sadekova, G.S. *Aerodinamika bol'sikh skorostei* (High-Speed Aerodynamics), Vysshaya shkola, Moscow (1965).
12. Irov, Yu.D., Keil, E.V., Pavlukhin, B.N., Porodenko, V.V., and Stepanov, E.A. *Gazodinamicheskie funktsii* (Gas-Dynamic Functions), Mashinostroenie, Moscow (1965).
13. Mkhitaryan, A.M. *Aerodinamika* (Aerodynamics), Mashinostroenie, Moscow (1976).

14. Krasnov, N.F., Koshevoi, V.N., Danilov, A.N., and Zakharchenko, V.F. *Aerodinamika raket* (Rocket Aerodynamics), Vysshaya shkola, Moscow (1968).
15. Rakhmatulin, Kh.A., Sagomonyan, A.Ya., Bunimovich, A.I., and Zverev, I.N. *Gazovaya dinamika* (Gas Dynamics), Vysshaya shkola, Moscow (1965).
16. Arzhanikov, N.S. and Maltsev, V.N. *Aerodinamika* (Aerodynamics), Oborongiz, Moscow (1956).
17. Krasilshchikova, E.A. *Krylo konechnogo razmaka v szhimaemom potoke* (A Finite-Span Wing in a Compressible Flow), Gostekhizdat, Moscow (1962).
18. Lebedev, A.A. and Chernobrovkin, L.S. *Dinamika poleta* (Flight Dynamics), Mashinostroenie, Moscow (1973).
19. Belotserkovsky, S.M., Skripach, B.K., and Tabachnikov, V.G., *Krylo v nestatsionarnom potoke gaza* (A Wing in an Unsteady Gas Flow), Nauka, Moscow (1971).

### **Supplementary Reading**

- Courant, R. and Friedrichs, K.O. *Supersonic Flow and Shock Waves*. New York, Interscience (1948).
- Ginzburg, I.P. *Aerodinamika* (Aerodynamics). Moscow, Vysshaya shkola (1966).
- Hayes, W.D. and Probstein, R.F. *Hypersonic Flow Theory*. New York, Academic Press (1959).
- Krasnov, N.F. (Ed.). *Prikladnaya aerodinamika* (Applied Aerodynamics). Moscow, Vysshaya shkola (1974).
- Kuethe, S. *Foundations of Aerodynamics*, 3rd ed. New York, Wiley (1976).
- Landau, L.D. and Lifshits, E.M. *Mekhanika sploshnykh sred* (Continuum Mechanics). Moscow, Gostekhizdat (1968).
- Liepmann, H.W. and Puckett, A.E. *Introduction to Aerodynamics of a Compressible Fluid*. New York, Wiley; London, Chapman & Hall (1948).
- Liepmann, H.W. and Roshko, A. *Elements of Gasdynamics*. New York, Wiley (1957).
- Milne-Thomson, L.M. *Theoretical Aerodynamics*. London, MacMillan (1958).
- Mironov, A. *Engineering Fluid Mechanics*. New York, McGraw-Hill (1979).
- Oswatitsch, K. *Gas Dynamics* (English version by G. Kuerti). New York, Academic Press (1956).
- Schlichting, H. *Boundary Layer Theory*, 6th ed. New York, McGraw-Hill (1968).
- Sedov, L. *Two-Dimensional Problems in Hydrodynamics and Aerodynamics*. New York, Wiley (1965).

## Name Index

Arzhanikov, N. S., 111, 238, 255, 256, 275, 276, 493, 494

Babenko, K. I., 2

Belotserkovsky, O. M., 23

Belotserkovsky, S. M., 22, 23, 398, 419, 427, 431, 433, 436, 451, 452, 455, 460, 488, 493, 494

Bernoulli, D., 13

Bunimovich, A. I., 209, 494

Burago, G. F., 275

Chaplygin, S. A., 15, 21, 22, 250, 269

Chernobrovkin, L. S., 384, 494

Cherny, G. G., 2

Copal, Z., 22

Courant, R., 494

Danilov, A. N., 193, 494

Dorodnitsyn, A. A., 19, 21, 23

Euler, L., 13, 11

Fabrikant, I. Ya., 95, 493

Falkovich, S. V., 22

Frankl, F. I., 21, 22, 206, 394

Friedrichs, K. O., 494

Garabedian, P., 23

Ginzburg, I. P., 494

Glauert, H., 21

Golubev, V. V., 21

Gromeka, I. S., 134, 136

Hayes, W. D., 494  
Helmholtz, H. L. F., 251

Ionov, V. P., 61, 62, 66, 165, 188, 493

Irov, Yu. D., 153, 157, 493

Iyelev, V. M., 19

Joukowski, *see* Zhukovsky

Kalikhman, L. E., 19

Karman, T. von, 19

Karpovich, E. I., 22

Keil, E. V., 153, 157, 493

Keldysh, M. V., 21, 22

Khristianovich, S. A., 21, 269, 270, 271, 273, 493

Kibardin, Yu. A., 62, 63, 67, 188, 493

Kibel, I. A., 19, 22, 82, 111, 493

Kochin, N. E., 19, 82, 111, 493

Koshevoi, V. N., 193, 494

Krasilshchikova, E. A., 22, 269, 381, 494

Krasnov, N. F., 193, 494

Kuethe, S., 494

Kuznetsov, S. I., 62, 63, 67, 188, 493

Landau, L. D., 494

Lavrentyev, M. A., 21, 22

Lebedev, A. A., 384, 494

Lenin, V. I., 15

Liepmann, H. W., 494

Lifshits, E. M., 494

Lighthill, M., 23

Loitsyansky, L. G., 19, 30, 493

Lyubimov, A. N., 62, 63, 67, 188, 493

- Mal'tsev, V. N., 238, 255, 256, 275,  
276, 494
- Melnikov, A. P., 19
- Meyer, T., 279
- Milne-Thomson, L. M., 494
- Mironer, A., 494
- Mkhitarian, A. M., 165, 255, 256,  
493
- Navier, A., 19
- Nekrasov, A. I., 22
- Newton, I., 32
- Oswatitsch, K., 494
- Pavlukhin, B. N., 153, 157, 493
- Petrov, G. I., 19
- Pleshanov, A. S., 61, 62, 66, 67, 165,  
188, 493
- Porodenko, V. V., 153, 157, 493
- Prandtl, L., 19, 21, 32, 279
- Predvoditelev, A. S., 61, 62, 66,  
67, 165, 188, 493
- Probstein, R. F., 494
- Puckett, A. E., 494
- Rakhmatulin, Kh. A., 209, 494
- Reynolds, O., 19
- Roshko, A., 494
- Roze, N. V., 82, 111, 493
- Rozhdestvensky, I. B., 61, 62, 63,  
67, 165, 188, 493
- Sadekova, G. S., 111, 493
- Sagomonyan, A. Ya., 209, 494
- Samuilov, E. V., 61, 62, 66, 67, 165,  
188, 493
- Schlichting, H., 494
- Sedov, L. I., 17, 20, 21, 22, 493, 494
- Shumyatsky, B. Ya., 62, 63, 67, 188,  
493
- Skripach, B. K., 23, 398, 419, 427,  
431, 433, 436, 451, 452, 455, 460,  
488, 493, 494
- Stakhanov, I. P., 61, 62, 66, 67, 165,  
188, 493
- Stepanov, E. A., 153, 157, 493
- Stokes, G. G., 19
- Struminsky, V. V., 19
- Stupochenko, E. V., 61, 62, 66, 165,  
188, 493
- Tabachnikov, V. G., 398, 419, 427,  
431, 451, 452, 455, 460, 488, 494
- Taylor, G. I., 32
- Voskresensky, G. P., 22
- Zakharchenko, V. F., 193, 494
- Zhukovsky, N. E., 15, 21, 250
- Zverev, I. N., 209, 494

## Subject Index

- Ablation, 15  
Acceleration,  
  resultant, 72f  
  vector, 72, 113  
Adiabat, shock, 172, 184  
Aerodynamic coefficients,  
  airfoil, 294  
  conversion from one aspect ratio  
    to another, 258ff  
  dynamic components, 398  
  and similarity method, 139ff  
  static components, 398  
  unsteady flow, 416ff  
Aerodynamics,  
  ablating surfaces, 23  
  blunt-nosed bodies, 23  
  bodies of revolution, 22  
  boundary layer, 19  
  classification, 17  
  continuum, 19f  
  controls, 22  
  definition, 13  
  development, 13  
  experimental, 15  
  force, 17f  
  high-speed, 14f, 18, 59  
  hulls, 22  
  hypersonic, 18  
  ideal fluid, 18  
  incompressible fluid, 18  
  interference, 23  
  low-speed, 14  
  optimal shapes, 24  
  radiating gas, 131  
  rarefied gases, 20  
  steady-state, 20  
  subsonic, 18  
  supersonic, 18, 59  
  transonic, 18
- Aerodynamics,  
  unsteady, 20, 436  
  wing, 21f  
Aerohydrodynamics, 14  
Aerotermodynamics, 18  
Air, *see also* Flow(s), Gas  
  diatomic model, 67, 69  
  dissociating, equation of state, 65  
  dissociation and ionization, 192f  
  motion at high speeds, 14  
  structure in dissociation, 67  
Aircraft, 20, *see also* Craft  
Airfoil,  
  aerodynamic forces, 293f  
  arbitrary configuration, 285ff  
  in compressible flow, 264ff  
  drag, 278  
  fictitious, 270f  
  in hypersonic flow, 291f, 297  
  longitudinal force, 293  
  in mid-span section, 337  
  polar, 296  
  sharp-nosed, 285f  
    curved, 290f  
  sideslipping wing, 299ff  
  in supersonic flow, 285ff  
  symmetric, 297ff, 317ff, 321ff  
  thin,  
    in incompressible flow, 234ff  
    in nearly uniform flow, 293  
    in subsonic flow, 264ff,  
      total drag, 275  
  wedge-shaped, 297f  
Angle(s).  
  attack, 38f  
    balance, 52  
    in normal section, 301f  
    optimal, 47  
    true, 252

- Angle(s),  
 balance rudder, 58  
 banking, 39  
 control surface, 407f  
 course, 39  
 downwash, 251f  
     span-averaged, 252f, 255, 257  
     total, 253  
 elevator, 407  
 flow deflection, 220f  
     behind shock, 166, 176f, 189  
     critical, 176f, 182  
     hypersonic velocities, 221  
     and shock angle, 182f  
 flow deviation, *see* Angle, flow deflection  
 Mach, 161, 212  
 pitching, 39f  
 rolling, 39f  
 rudder, 407  
 setting, 252, 260f  
 shock, 167f  
     oblique, 176ff  
     and velocity, 189  
 sideslip, 38f, 52  
 sweep, 299f, 363  
 ultimate flow, 221f  
 yawing, 39f  
 zero lift, 240
- Approach,  
 Eulerian, 72  
 Lagrangian, 71f
- Axis,  
 doublet, 102  
 flight path, 37  
 lateral, 37  
 lateral body, 38  
 lift, 37  
 longitudinal body, 38  
 normal, 38
- Backpressure, 155f
- Balancing, longitudinal, 56f
- Boundary conditions, 132ff, 424  
 dimensionless equations, 145  
 linearized flow, 310ff  
 unsteady flow, 451  
 on vortex sheet, 312, 424  
 and wall temperature, 145
- Boundary layer, 34ff  
 thickness, 36  
 turbulent core, 36
- Centering, 55  
 central, 55
- Centering,  
 neutral, 56
- Centre,  
 aerodynamic, 50f, 55  
     angle-of-attack, 51  
     coordinate, 240  
     elevator deflection, 51  
     sideslip angle, 58  
 force reduction, 404  
 moments, 36f  
 pressure, 48  
     and aerodynamic centre, 51  
     conical flow, 363
- Centre-of-pressure coefficient, 49, 295, 297, 389, 483
- compressible flow, 274  
 nearly uniform flow, 240  
 pentagonal wing, 371  
 sideslipping wing, 302  
 symmetric airfoil, 297ff  
 tetragonal wing, 365  
 wedge-shaped airfoil, 298
- Characteristics, 208ff
- aerodynamic,  
     rectangular wing, 385ff  
     triangular wing, 349  
     unsteady motion, 394ff
- conjugate, 210, 212  
 determination, 209f  
     in hodograph, 214, 282
- first family, 210ff, 216, 219, 222f
- kind, 209f
- nodal point, 227
- orthogonality, 213f
- in physical plane, 210f
- second family, 210ff, 216, 219, 222f
- stability, 413ff
- Chord,  
 local, wing, 259  
 mean aerodynamic, 45, 262  
 mean geometric, 45  
 wing, 45  
     in wing section with optimal plan-form, 258
- Circulation,  
 flow, 103f, 243, 430  
 intensity, of vortex, 236f  
 velocity, 91ff, 236, 311, 428f, 434  
     in vortex-free flow 92  
 vortex, 439, 447
- Coefficient(s),  
 aerodynamic, *see* Aerodynamic coefficients  
 centre-of-pressure, *see* Centre-of-pressure coefficient  
 correlation, 30  
     one-point, 31  
     two-point, 30

- Coefficient(s),**  
 damping, 414f  
     longitudinal, 403  
     rolling, 403  
     yawing, 403  
 drag, *see* Drag coefficient  
 Lame's, 82f, 85, 87  
 lateral-force, 44, 400  
 lateral linear deformation, 109  
 lateral motion, 406  
 lift, *see* Lift coefficient  
 longitudinal-force, 44, 296, 399  
 longitudinal moment, 297  
     compressible flow, 303  
 longitudinal motion, 406  
 moment, *see* Moment coefficient  
 normal-force, 44, 51, 56f, 296, 397,  
     448f, 456  
     compressible flow, 303  
     and stability derivatives, 400,  
     405f  
 pitching-moment, 43, 49, 51, 363,  
     401, 404f, 416ff, 448f, 456  
     body axis, 44  
 pressure, *see* Pressure coefficient  
 pressure-drop, 284  
 rolling-moment, 43, 401, 416ff,  
     448f  
     body axis, 44  
     spiral, 403  
 side-force, 43  
 stagnation pressure, behind shock,  
     175  
 static lateral stability, 57  
 static longitudinal stability, 54f  
 suction force, 306f, 383f  
 vortex drag, 315  
 wave drag, 277f, 283, 350, 387  
     induced, 315  
 wing drag, 315  
 yawing-moment, 43, 401  
     body axis, 44  
     spiral, 403  
 Compressibility, gas, 14, 16, 58f  
 influence on non-stationary flow,  
     452ff  
 Conditions,  
     boundary, *see* Boundary conditions  
     Chaplygin-Zhukovsky, 428, 431  
     compatibility, 209  
     at infinity, 425  
     initial, 132  
         Cauchy's, 206  
 Conductivity, thermal, 63f  
     and pressure, 63  
     and temperature, 63f  
 Cone,  
     disturbance, 160, 315, 319  
 Cone,  
     Mach, 160, 315, 319  
     inverted, 319  
     tip, 371  
 Contour,  
     multiply connected, 94  
     simply connected, 94  
 Controllability, craft, 395  
 Controls,  
     fast-response, 407  
     inertiafree, 407  
 Coordinate systems,  
     body axis, 37  
     curvilinear, 82ff  
     cylindrical, 82f  
     fixed, 37  
     flight path, 37  
     local geographic, 39  
     normal earth-fixed, 39  
     spherical, 82f  
     wind, 38  
 Core(s),  
     turbulent, 36  
     vortex, 256  
         semi-infinite, 253  
 Correction, Prandtl-Glauert, 268  
 Cosines, direction, 40  
 Craft,  
     banking, 410  
     controllability, 395  
     fast-response, 407  
     inertiafree, 407  
     manoeuvrability, 395  
     thermal protection, 23  
 Criterion(a), similarity, 17, 140ff, 187  
     hypersonic, 284f  
 Curl, velocity, 78  
 Curves,  
     characteristic, *see* Characteristics  
     equipotential, 90  
 Decrement, logarithmic, 414  
 Deformation, *see also* Strain  
     relative linear, 108f  
     relative volume, 109  
     wing surface, 451  
 Degree(s),  
     dissociation, 60  
         equilibrium, 69  
         and pressure, 60  
         and temperature, 60  
     freedom, inert, 194  
     ionization, 60f  
     static lateral stability, 57  
     static longitudinal stability, 54f  
 Density(ies),  
     characteristic, for dissociation, 69

- Density(ies),  
   critical, 152, 154  
   in jet, 153  
   ratio, 165, 172f, 184, 188, 189ff  
     limiting, 186  
   reduced mass, 157  
   source distribution, 316f  
   stagnation, 151, 153, 192
- Derivatives,  
   aerodynamic,  
     and aspect ratio, 483  
     properties, 478ff  
   circulation, 466  
   stability, *see* Stability derivatives  
   time, 396f
- Diagram,  
   enthalpy-entropy, 66f  
   phase, caloric, 67
- Diffusion, gas, 121
- Diffusivity, thermal, 128
- Dimensions, characteristic, 44f
- Dissociation, 60, 189ff
- Disturbance(s), 159  
   cone, 160  
   propagation, 159f  
   source, 159  
   in subsonic flow, 160  
   supersonic, 319  
   in supersonic flow, 160
- Divergence, velocity, 86
- Doublet, 102f  
   axis, 102  
   distribution function, 354, 358, 360  
     incompressible flow, 360f  
     supersonic linearized flow, 360
- moment, 102, 354
- potential function, 354f
- power, 354  
   in supersonic flow, 353ff  
   velocity potential, 103
- Downwash(es), 250ff, 465f  
   disturbed region, 465ff  
   semi-rate, 77  
   on vortex sheet, 467ff  
   wing, 468
- Drag, 38, 42  
   friction, 44  
   induced, 252  
   nose, 44  
   overall, 44  
   pressure, 44  
   profile, 275  
   total, 275, 314, 384  
   wave, 276f, 283  
   wing, 381ff  
     total, 384
- Drag coefficient, 42, 140, 296  
   airfoil, 333f
- Drag coefficient,  
   dimensionless, 145  
   distribution over wing span, 341  
   friction, 350  
   induced, 252f, 256f, 261, 384  
   and lift coefficient, 296  
   minimum, 47  
   overall, 44, 339, 341, 350  
   sideslipping wing, 302, 304  
   symmetric airfoil, 298f  
   tetragonal wing, 337ff, 345ff  
   thin wing, 381  
   wedge-shaped airfoil, 298
- Edge(s),  
   combined, 463  
   leading, *see* Leading edge(s)  
   side, *see* Tip(s)  
   trailing, *see* Trailing edge(s)
- Effect,  
   Magnus, 403  
   mid-span, 301  
   sideslip, 300  
   tip, 301
- Energy,  
   dissipation, 127  
   equation, 124ff  
   particle, 124ff  
     supplied by conduction, 125  
     supplied by diffusion, 125f  
     supplied by radiation, 126
- Enthalpy, 65  
   stagnation, 151, 185
- Entropy,  
   gradient, 216  
   non-dissociating perfect gas, 170  
   at stagnation point, 191
- Epicycloids, 219f
- Equation(s), *see also* Formula  
   Abel, 468  
   adiabat, shock, 172, 184  
   Bernoulli, 137f  
   Cauchy-Riemann, 97  
   Chaplygin, 269  
     characteristic, 208, 218  
       in hodograph, 219ff  
       non-isentropic flow, 219  
       roots, 209f  
       vortex-free flow, 219  
   continuity, 80ff, 164, 200f, 423f  
     in Cartesian coordinate system, 81f  
   in dimensionless variables, 142f  
   flow along curved surface, 88  
   incompressible flow, 81  
   linearized flow, 309  
   for potential motion, 81, 85f

- Equation(s),  
continuity,  
  steady flow, 81, 85, 88f  
  two-dimensional flow, 81, 88  
  unsteady flow, 81  
coupling, 254, 257  
diffusion, 121  
  in Cartesian coordinate system,  
    123  
  in cylindrical coordinate system,  
    122f  
dimensionless, 142f  
  and boundary conditions, 145  
energy, 124ff, 175  
  conservation, 165  
  in dimensionless variables, 143  
  two-dimensional plane motion,  
    127  
Euler, 113, 136  
flow rate, 89  
gas dynamics,  
  fundamental, 129, 201, 309  
  system, 129ff, 144  
Gromeka's, 134, 36  
 hodograph, 180  
Hugoniot, 172f  
integro-differential, 254  
kinematics, fundamental, 201  
Lagrange, 135  
Laplace, 81f, 266  
mass flow rate, 156ff  
momentum conservation, 164  
motion,  
  axisymmetric form, 117  
  curvilinear coordinates, 144f  
  cylindrical coordinates, 116f  
  in dimensionless variables, 142  
  disturbed, 413  
  ideal gas, 134  
  inviscid fluid, 113, 200f  
  linearized flow, 308  
  particle, 106  
  potential, 81, 85f  
  spherical coordinates, 118ff  
  steady flow, 117  
    two-dimensional, 119, 200f  
  vector form, 113f  
  viscous fluid, 113  
Navier-Stokes, 112f  
oblique shock, 163ff, 169f  
  basic, 171  
pathline, 71  
potential function, 367ff  
speed of sound, 264  
state,  
  diatomic gas mixture, 69  
  dissociating gas, 65  
  perfect gas, 65
- Equation(s),  
steady flow, 136  
stream function, differential, 205  
two-dimensional flow, near curved  
surface, 120f  
velocity potential, 201f, 264, 309f,  
  372ff  
  linearization, 264f  
vortex, 203f  
vortex lines, 91  
wave, 423ff
- Equilibrium,  
stable, 52  
static, 52f  
trim, of craft, 52  
unstable, 52
- Exponent, adiabatic, 26, 61f
- Factor, local friction, 42
- Fall, free, 409f
- Fan, Prandtl-Meyer (expansion), 280,  
  285f
- Field,  
  pressure, 326, 330  
  velocity, 71
- Filament,  
  stream, 74  
  vortex, 429  
  strength, 433f
- Fineness, 284. *see also* Ratio, lift-to-drag
- Flow(s), *see also* Motion(s)  
at angle of attack, 243ff, 354ff  
axisymmetric, 117, 200f, 222  
basic kinds, 17  
boundary condition, 451  
in boundary layer, 17, 19  
circulation (circulatory), 103f, 243,  
  430  
  calculations, 439ff  
compressible, 264ff, 274, 302f, 306  
  over circular cylinder, 241  
conical, 355ff, 386  
cross, 359  
along curved surface, 88  
disturbed, 420  
  from supersonic source, 319f
- downwash, 457, *see also* Downwash
- equilibrium, 194ff
- expanding radial, 231
- expansion, 220
- fictitious incompressible, 270f
- forward, 391f  
  plane-parallel, 98f
- free, 17  
  external, 35  
  streamline, 132

- Flow(s),**
- over hexagonal wing, 366ff
  - hypersonic, over thin airfoil, 291f
  - incompressible, 90, 240ff, 249ff, 360f
    - cross, 359
    - over flat plate, 243ff
    - velocity potential, 105
  - inviscid, 17, 35, 200f
  - isentropic, 138, 149ff, 222, 290f, 420f
  - isotropic, 31
  - laminar, 28
  - lateral, 299
  - linearized, 264f, 297, 308ff, 360
  - longitudinal, 299
  - nearly uniform, 235, 282, 293
    - at angle of attack, 351ff
    - linearized, 264
    - pressure, 235
    - velocity, 235
  - non-circulatory, 242f, 431
  - non-equilibrium, 193ff
    - behind shock, 197f
  - non-isentropic, 219, 222
  - one-dimensional, 158
  - parallel, 98, 249f
    - stream function, 98
    - streamlines, 98
    - velocity potential, 98
  - plane, 123, 222
  - over plate, 241ff
  - potential, 79, 104, 201f, 356
  - Prandtl-Meyer, 279, 285
    - at hypersonic velocities, 281f
    - limiting case, 286
  - purely subsonic, 275
  - from reservoir, 154ff
  - reverse, 391f
  - without separation, 132f, 145
    - two-dimensional, plane, 133
    - velocity ratio, 133
  - behind shock, 174f
  - steady, 73, 117, 122f, 200f
    - non-potential, 136f
    - potential, 136f
  - subcritical, 176
  - subsonic, 302f
    - stability derivatives, 478ff
    - over thin airfoil, 264f
  - supercritical, 177, 274ff
  - supersonic, 211, 282, 308ff, 353ff
    - over airfoil, 285ff
    - disturbed, 222ff
    - over finite-span wing, 308ff, 385
    - over rectangular wing, 385
    - over sharp-nosed airfoil, 285f, 290f
- Flow(s),**
- stability derivatives, 483ff
  - over tetragonal wing, 344
  - over thin plate, 269ff
  - over thin wing, 315f, 385
  - unsteady, 425, 456ff
  - over wings, 315f
  - over symmetric airfoil wing, 312
  - tetragonal, 331ff, 343ff
  - over tetragonal wing, 331ff, 343ff
  - over thin plate, 243
  - three-dimensional,
    - disturbed, 308
    - steady, 309
  - transverse, 359
    - over thin plate, 240ff
  - over triangular wing, 355ff
  - two-dimensional, 89f
    - axisymmetric, 200f
    - near curved surface, 120f
  - isentropic, 222
  - non-isentropic, 222
  - plane, 200f, 211, 264
  - spatial, 119, 211
  - supersonic, 211
  - vortex, 202
  - vortex-free, 219
  - turbulent, 28ff
  - quasi-steady, 31
  - unsteady, 73, 146, 394, 416ff, 425, 456ff
    - deformable wing, 451
    - nearly uniform, 421
  - velocity, in jet, 150f
  - viscous; 17, 19
    - in boundary layer, 134
    - pressure, 110
  - vortex, 78, 202, 309
    - steady, 89
  - vortex-free, 79ff, 92, 219, 309
- Fluid,**
- barotropic, 420, 423
  - ideal,
    - integrals of motion, 134ff
    - pressure, 26ff
  - incompressible, 158
  - inviscid, *see* Fluid, ideal
  - viscous, 127
- Fluid mechanics, 14, 18**
- Force(s),**
- aerodynamic, airfoil, 293f
  - body, 27
  - complex, 246f
  - conversion to another coordinate system, 40f
  - dissipative, 127
  - drag, 38, 42, *see also* Drag
  - gyroscopic, 403f

- Force(s),**  
 lateral, 38  
 lift, 38, 42, 250f, 254  
 flat plate, 248, 393  
 maximum, 47  
 nearly uniform flow, 236  
 rectangular wing, 386  
 total, 315  
 triangular wing, 362  
**longitudinal,** 38, 44, 293  
**mass,** 27  
 external, work, 124  
 on moving body, 25ff  
**normal,** 38, 416f  
 produced by pressure, 293  
**ponderomotive,** 27  
**side,** 38, 42  
**suction,** 249, 382ff  
 correction factor, 383f  
 sideslipping wing, 305ff  
 triangular wing, 362  
**surface,** 25f, 107f  
 work, 124f  
**viscous,** 146  
**Formula,** *see also* Equation(s)  
 Biot-Savart, 95  
 conversion, coordinate systems, 82ff  
 Euler, 97  
 Karman-Tsien, 268  
 Prandtl-Glauert, 268, 302, 306  
 Reynolds generalized, 33f  
 Sutherland's, 63  
 Zhukovsky, 248  
 Zhukovsky-Chaplygin, 247  
**Frequency,** oscillations, 414  
**Friction,** *see also* Viscosity  
 in turbulent flow, 32ff  
**Function,**  
 conformal, 240f  
 dissipative, 127  
 doublet distribution, 354, 358, 360f  
 potential, 79, 243, 354f, 367ff, 457,  
*see also* Velocity potential  
 derivatives, 458  
 doublet, 354f  
 gradient, 80  
 stream, 89f, 98, 202  
  
**Gas,** *see also* Air, Flow(s), Fluid  
 compressibility, 14, 16, 58f, 452ff  
 conduction of electricity, 19  
 diatomic, mean molar mass, 70  
 diffusion, 121  
 dissociation, 60, 189ff  
 dynamics, 14f, *see also* Aerodynamics, high-speed  
**Gas,**  
 equations, 129ff, 144  
 flow from reservoir, 154ff  
 heating, 59ff  
 ideal, 134, 149, *see also* Gas, perfect  
 interaction with body, 15f, 18  
 ionization, 189f  
 jet, configuration, 149f  
 kinetic coefficients, 63f  
 mixture, 67  
 mean molar mass, 70  
 parameters, at stagnation point, 191  
 perfect, *see also* Gas, ideal  
 calorically, 65  
 equation of state, 65  
 thermally, 65  
 recombination, 60  
 stream, configuration, 149f  
 viscous, flow in boundary layer, 134  
**Gradient,**  
 entropy, 216  
 normal velocity, 32  
 potential function, 80  
 pressure, 107  
 velocity, 34  
  
**Half-wing,** infinite triangular, 321  
**Heat,** specific, 61f  
**Heating,** aerodynamic, 15, 18, 23  
**Hodograph,** 179ff  
**Hypothesis,**  
 absence of reverse influence, 17  
 continuum, 16, 20  
 harmonicity, 488f  
 Khristianovich's, 273  
 Newton's, 32  
 plane sections, 253f  
 Prandtl's, 32f  
 steadiness, 17, 489  
 expanded, 489  
 stress-strain proportionality, 108  
 Zhukovsky-Chaplygin, 244  
  
**Instability,**  
 dynamic, 394  
 static, 53, 415  
 directional, 57f  
 lateral, 57  
 longitudinal, 54f  
**Integral(s),**  
 Bernoulli, 138  
 Couchy-Lagrange, 420ff  
 linearized expression, 421

- Integral(s)  
   Lagrange, 135  
   motion, 134ff
- Intensity,  
   source distribution, 318  
   turbulence, 29  
   vortex circulation, 236f
- Interaction,  
   body-plasma, 19  
   chemical, 15, 18  
   force, 15  
   mechanical, 15  
   terms, 402  
   thermal, 15, 18
- Interference, aerodynamic, 20f
- Ionization, 60, 189f  
   thermal, 60
- Isobars, 66f
- Isochors, 66f
- Isotherms, 66f
- 
- Law,  
   Dalton's, 69  
   elliptic, circulation distribution, 258f  
   energy conservation, 124, 165  
   Fourier, 125  
   mass conservation, 80  
   momentum conservation, 164  
   Newton's friction, 32  
   thermodynamics, second, 181
- Layer, boundary, *see* Boundary layer
- Leading edge(s), 367  
   sonic, 316, 363, 365, 384  
   subsonic, 303ff, 316, 326f, 331ff, 351ff, 355ff, 366ff, 381ff  
   supersonic, 303f, 316, 330f, 351f, 372ff, 385  
   sweep parameter, 316f
- Length,  
   mixing, 34  
   relaxation, 198
- Level, turbulence, 29
- Lift, 38, 42, *see also* Force, lift
- Lift coefficient, 43, 253ff, 296, 315  
   compressible flow, 274  
   and drag coefficient, 296  
   nearly uniform flow, 236, 238  
   pentagonal wing, 371  
   sideslipping wing, 302, 304  
   symmetric airfoil, 298f  
   tetragonal wing, 364f  
   total, 387  
   triangular wing, 362ff  
   wedge-shaped airfoil, 298f  
   wing tips, 387
- Line(s),  
   disturbance, 160  
   Mach, 160, 211  
   maximum thickness, 348f  
   vortex, 90f  
   weak disturbances, 161, 182, 211
- Loop, perfect, 409f
- 
- Magnetogasdynamics, 19
- Manoeuvrability, craft, 395
- Margin, static stability, 55
- Method,  
   Burago's, 275ff  
   characteristics, 22, 200ff  
   calculation of supersonic flow parameters, 285ff  
   and wind tunnel nozzle shaping, 230ff  
   conformal transformations, 240ff  
   doublet distribution, 353ff  
   Glauert-Trefftz, 255  
   Khristianovich, 269ff  
   mapping, 240  
   reverse-flow, 391ff  
   similarity, 139  
   small perturbations, 412  
   sources, 317ff, 425ff  
   field of application, 351ff  
   tangent wedges, 292, 489ff  
   stability derivatives, 490f
- Model, vortex,  
   intricate lifting surface, 430  
   non-circulatory flow, 431
- Modulus,  
   longitudinal elasticity, 108  
   shear, 109
- Moment(s),  
   conversion to another coordinate system, 40f  
   destabilizing, 53f  
   doublet, 102  
   gyroscopic, 403f  
   pitching, 38, 400f, 404f, 416f  
   positive, 38  
   rolling, 38, 401f, 416f  
   stabilizing, 52  
   tilting, 53  
   yawing, 38, 401
- Moment coefficient, 284, 295, 388  
   *see also* Coefficient(s): longitudinal moment, pitching-moment, rolling-moment, yawing-moment  
   compressible flow, 274  
   nearly uniform flow, 236, 239  
   pentagonal wing, 371  
   sideslipping wing, 302, 304  
   symmetric airfoil, 298f

Monent coefficient,  
tetragonal wing, 364f  
wedge-shaped airfoil, 298

Motion(s), *see also* Flow(s)  
air, at high speeds, 14  
asymmetric, 449f  
basic, 411  
centre of mass, 407  
disturbed, 411  
equations, 114ff  
fluid,  
inviscid compressible, 113f  
viscous incompressible, 113  
free, 412  
stability, 412  
integrals, ideal fluid, 134ff  
irrotational, 79  
lateral, 406f  
longitudinal, 406f  
at low Strouhal numbers, 444  
oscillatory, 414f, *see also* Oscillations  
damping, 483  
particle, 106  
fluid, 75ff  
pitching, 406, 408ff  
modes, 408ff  
proper, 412  
sinusoidal, 410  
spiral, 403  
stable, 411f  
symmetric, 449f  
undisturbed, 411  
unstable, 411f  
unsteady, 415, 459  
aerodynamic characteristics, 394ff  
vortex-free, 79ff

Neutrality, 55, 57f

Nose, blunted, 23

Nozzle,

critical section area, 231  
two-dimensional supersonic, 231ff  
shaped, 232f  
unshaped, 231  
wind tunnel, for supersonic flow, 230f

Number(s),

dimensionless, 17  
Froude, 142, 146f  
Mach, 47, 141f, 147, 395  
critical, 303  
initial value, 271, 273f  
limiting value, 186f  
behind normal shock, 184, 186f

Number(s),  
Prandtl, 143, 146f  
Reynolds, 47, 141f, 146f, 395  
Strouhal, 142, 146, 397f

Operator, Laplacian, 111, 117, 119  
Oscillations,  
damped, 414  
frequency, 414  
harmonic, 398  
longitudinal, 408  
period, 414  
periodic, 414  
wavelength, 414

Paradox, Euler-D'Alembert, 248

Parameter(s), *see also* Characteristics, Variables

averaged, 31  
disturbed supersonic flow, 222ff  
stagnation, 191  
behind normal shock, 184f  
supersonic flow, calculation by method of characteristics, 285ff  
sweep, leading edge, 316f  
Particle, fluid,  
angular strain, 76, 78  
energy, 125f  
internal, 124  
kinetic, 124  
linear strain, 76, 78  
motion, 75ff  
relative volume deformation, 109  
Pathline, particle, 71, 74  
equation, 71

Pattern, wing,

Chaplygin's horseshoe, 250  
vortex, *see also* Model, vortex

non-stationary, 428f

Period, oscillations, 414

Plane,

independent variables, 205  
physical, 205

Plate, 241ff, *see also* Wing(s)

fineness, 284

potential, 243

rhombiform, 364

thin, 240ff

at angle of attack, 243ff

Point,

nodal, characteristics, 227

stagnation, 185f, 191f, 268

Polar,

airfoil, 296

- Polar,**  
 craft, 46ff  
 first kind, 46  
 second kind, 47  
 shock, 180, 182
- Potential,**  
 additional, 310f, 313, 321  
 complex, 97, 104  
 circulatory-forward flow, 243  
 cylinder, 244f  
 flow over circular cylinder, 241  
 flow over plate, 241f  
 non-circulatory flow, 243  
 parallel flow, 98  
 disturbance, 457  
 disturbed velocities, 424  
 doublet region, 356  
 elementary source, 318ff  
 retarded, 425  
 total, 313f  
 velocity, *see* Velocity potential
- Pressure(s),**  
 absolute, 272  
 critical, 152, 154f  
 dimensionless, 145  
 excess, 235, 265  
 gradient, 107  
 in ideal fluid, 26ff  
 in jet, 152f  
 linearized flow, 265  
 nearly uniform flow, 235  
 ratio, 166, 172f, 189f,  
     behind shock, 175  
     normal shock, 184  
 stagnation, 151, 153, 191f, 224  
     flow behind shock, 174f
- Pressure coefficient,** 42, 172, 187f,  
 281f, 390, 416  
 compressible flow, 268, 306  
 conical flow, 362  
 conversion to various Mach numbers, 271f  
 hexagonal wing, 370, 372  
 hypersonic flow, 292, 297  
 limiting value, 186  
 nearly uniform flow, 235, 293  
 ratio, 166, 172f, 186  
 rectangular wing, 385f  
 behind shock, 291  
 sideslipping wing, 302, 304  
 at stagnation point, 185f, 191, 268  
 tetragonal wing, 337, 339, 345f  
 triangular wing, 325ff, 363
- Principle,**  
 flow superposition, 105  
 freezing, 196  
 inverted flow, 16
- Problem,** Cauchy, 206ff
- Rate,** mass flow, 156ff  
 specific, 156f
- Ratio,**  
 aspect,  
     influence on aerodynamic derivatives, 483  
     and wing lifting capacity, 482f, 487  
 density, 165, 172f, 184, 188  
     dissociation and ionization, 189ff  
     limiting, 186  
 lift-to-drag, 46f, *see also* Fineness maximum, 47  
 mass velocity, 156f  
 pressure, 166, 172f, 186  
     dissociation and ionization, 189f  
     normal shock, 184  
     behind shock, 175  
 pressure coefficient, 186  
 pressure recovery, across shock, 174  
 taper, and wing lifting capacity, 483  
 temperature, 166, 172f, 184, 189ff  
     dissociation and ionization, 189ff  
 velocity (speed), 152, 156, 271  
     flow without separation, 133  
     and Mach number, 152
- Recombination,** 60
- Region,**  
 doublet,  
     influence, 356f  
     potential, 356  
 integration, 320  
 multiply connected, 94  
 simply connected, 94  
 source influence, 319f
- Relaxation,** 194  
 dissociative, 194f  
 length, 198  
 in shock waves, 196ff  
 time, 194, 199  
     dissociative, 194f  
     vibrational, 194f  
     vibrational, 194f
- Resistance,** *see* Drag
- Rotation,** about centre of mass, 407
- Rule,** Prandtl-Glauert compressibility, 482
- Scale,** turbulence, 30f
- Sheet, vortex, *see* Vortex sheet**
- Shock (s),** 156, 159, *see also* Wave(s),  
 shock

- Shock(s)**  
 adiabat, 172, 184  
 angle, 159  
 attached, 183f, 187  
 curved, 159f  
 straight, 159f  
 curved, 159f, 178f  
 density ratio, 165, 172f  
 detached,  
 curved, 159f  
 flow over sharp-nosed cone, 177  
 expansion, 181, 211, 281  
 at hypersonic velocities, 186ff  
 lambda-shaped, 275  
 local, 275  
 normal, 159, 168f, 184ff  
 in dissociated and ionized gas, 189ff  
 oblique, 159, 163ff, 171  
 in dissociated and ionized gas, 189  
 formation, 161f  
 polar, 180, 182  
 possibility, 182  
 pressure ratio, 166, 172f  
 strength, 172  
 temperature behind, 170, 172  
 temperature ratio, 166, 172f  
 thickness, 163  
 and Mach number, 163  
 velocity behind, 166, 171
- Similarity,**  
 aerodynamic, 138ff  
 dynamic, 139, 144f  
 full-scale and model flows, 146f  
 complete, 147  
 partial, 146  
 geometric, 139
- Sink,**  
 point,  
 three-dimensional, 100  
 two-dimensional, 100  
 strength, 100
- Sound,** speed, 67f, 142f, 151f, 155, 264  
 critical, 151f, 155  
 local, 152  
 and pressure, 67f  
 stagnation conditions, 151  
 and temperature, 67f  
 in undisturbed flow, 142f
- Source,**  
 distribution density, 318f  
 disturbances, 159  
 elementary, potential, 318ff  
 point,  
 three-dimensional, 100
- Source,**  
 two-dimensional, 99  
 region of influence, 319f  
 strength, 100, 427  
 varying, 425f  
 vortex, two-dimensional, 103
- Span,** characteristic dimension, 262
- Specific heats,**  
 and pressure, 61f  
 and temperature, 61f
- Speed,** *see also Velocity*  
 fluctuation, 29  
 sound, *see Sound, speed*
- Stability,**  
 dynamic, 394f, 410ff  
 free motion, 412  
 motion, 411  
 neutral, 412  
 longitudinal, oscillatory, 415  
 oscillatory, 414  
 static, 52ff, 415  
 axisymmetric craft, 54  
 lateral, 53, 57f  
 directional, 57f  
 rolling, 57  
 longitudinal, 53ff  
 and elevator deflection, 56  
 margin, 55
- Stability derivatives,** 397f, 418f  
 acceleration, 399  
 and aerodynamic coefficients, 399  
 and control surfaces, 402f  
 conversion, 404ff  
 dynamic, 398  
 first order, 398  
 groups, 399  
 gyroscopic, 404  
 Magnus, 403  
 potential function, 458  
 rotary, 399  
 second order, 398  
 static, 398, 402f  
 in subsonic flow, 478ff  
 in supersonic flow, 483ff  
 wing, 449
- Strain,** *see also Deformation*  
 angular 76, 78  
 linear, 76, 78  
 specific volume, rate, 78
- Stream,**  
 filament, 74  
 free, 25  
 function, 89f, 98, 202
- Streamlines,** 73f, 98, 104f  
 family, 74, 104  
 zero, 104f
- Strength,**  
 bound vortex, 435

- Strength,**  
 free vortex filaments, 433f  
 shock, 172  
 sink, 100  
 source, 100, 425ff  
 vortex, 430, 433, 435, 447  
 vortex layer, 430, 433, 447  
 vortex sheet, 429f  
 vortex tube, 91
- Stress,**  
 friction, *see Stress, shear*  
 normal, 107ff  
 shear, 31ff, 107f  
     in laminar flow, 31f  
     in turbulent flow, 32ff
- Strophoid,** 180f
- Sublayer,**  
 laminar, 35  
 viscous, 35
- Surface(s),**  
 control, 402f  
     angles, 407f  
 discontinuity, 156, *see also Shock(s)*  
 lifting,  
     flat, 428  
     intricate planform, 429f  
     rectangular, 428f  
 wave, 211  
 wing, deformation, 451
- System(s),**  
 coordinate, *see Coordinate systems*  
 disturbed sources, 320  
 vortex, 429
- Theorem,**  
 equivalence, 209  
 Helmholtz, 78, 91  
 Kutta-Zhukovsky, 430  
 Stokes, 93f
- Theory,**  
 aerodynamic, of wing, 21  
 boundary layer, 19  
 finite-span wing, 21  
 heat transfer, gas-dynamic, 19  
 infinite-span wing, 21  
 linearized, supersonic flow over  
     finite-span wing, 308ff  
 "loaded line", 253  
 second-order aerodynamic, 293, 296,  
     298
- Theory,**  
 shock wave, 159ff  
 vortex, 428ff
- Time,**  
 relaxation, 194, 199  
     dissociative, 194f  
     vibrational, 194f
- Tip(s),**  
 influence on flow over wing, 342f  
 rounding, 260  
 sonic, 317  
 subsonic, 317, 385  
 supersonic, 317, 364
- Trailing edge(s),**  
 sonic, 317, 365  
 subsonic, 317, 428  
 supersonic, 317, 364, 366ff, 372ff
- Trajectory, particle, *see Pathline***
- Triangle, definiteness,** 232
- Trim, lateral,** 58
- Trimming,** 55
- Tube,**  
 stream, 74  
 vortex, 91  
     strength, 91
- Tunnels, wind,** 15  
 aerodynamic, 29
- Turbulence,**  
 homogeneous, 31  
 initial, 29f  
 intensity, 29  
 isotropic, 31  
 scale, 30f
- Variables,**  
 dimensionless, 141f, *see also Criteria, similarity*  
 Eulerian, 72  
 kinematic, 395f, 441
- Vector,**  
 acceleration, 72  
     total, 113  
 aerodynamic forces, resultant, 36f,  
     252  
 moment of aerodynamic forces, re-  
     sultant, 36f
- principal, hydrodynamic pressure**  
 forces, 246
- velocity,** 72  
     divergence, 78, 86
- Velocity(ies),**  
 actual, 28  
 additional, 323, 325f, 328ff, 355  
 average, 28  
 calculation, 226ff  
     at characteristic-shock intersec-  
     tion, 227ff

- Velocity,  
 at characteristic-surface intersection, 227ff  
 circulation, 91ff  
 complex, 97, 245, 247  
 curl, 78  
 dimensionless, 433, 435  
 divergence, 78, 86  
 fictitious, 266  
 fluctuation, 28  
     component, 28  
 free-stream, 25  
 in gas jet, 150f  
 induced, 251, 440  
     by bound vortex, 432, 434  
     compound due to doublets, 362  
     by free vortices, 432, 434  
     by vortex sheet, 434  
 local, 154  
 nearly uniform flow, 235  
 potential, *see* Velocity potential  
 ratio, 152, 156, 271  
     fictitious, 266  
     flow without separation, 133  
     and Mach number, 152  
 relative, 152, *see also* Velocity, ratio  
 behind shock, 166, 171  
 supersonic, 275, 303f  
 total, 245  
 vector, 72  
 vortex flow, 89  
 vortex-induced, 94ff  
 Velocity potential, 79, 98, 103, 105,  
     201f, 264f, 372ff, 457  
     dimensionless, 452  
 doublet, 103  
 elementary source, 318ff  
 hexagonal wing, 366, 368f  
 incompressible flow, 266  
 induced by doublets, 360  
 linearized flow, 264f  
 non-stationary sources, 426f  
 on plate, 243  
 rectangular wing, 385f, 389  
 supersonic unsteady flow, 425  
 two-dimensional flow, 264  
 on vortex sheet, 460  
 Viscosity,  
     dynamic, 32, 63  
     and pressure, 63  
     and temperature, 63f  
     and fluid flow, 28ff  
 Volume, relative rate of change, 78  
 Vortex(ices), 103  
     bound, 250, 311, 429  
     strength, 435  
     linear, 430  
     velocity induced by, 432, 434  
 Vortex(ices),  
     circulation, 439, 447  
     intensity, 236f  
     components, 78  
     core(s), 256  
         semi-infinite, 253  
         strength, 253  
     curvilinear, 95  
     equivalent, 250  
     filament, distribution, 429  
     free, 250, 429  
         strength, 433f  
         velocity induced by, 432, 434  
     horseshoe, 256, 438  
         oblique, 430ff, 437  
     infinite, 95f  
     interaction, 96  
     layer, strength, 430, 433, 447  
     line, 95f  
     model (pattern), 428ff  
     point, 104  
     semi-infinite, 96  
     sheet, *see* Vortex sheet  
     source, two-dimensional, 103  
     strength, 430, 433, 435, 447  
     system, 429  
     theory, 428ff  
     tube, 91  
         strength, 91  
 Vortex sheet, 251, 256, 312, 429  
     boundary conditions, 424  
     strength, 429f  
     velocity induced by, 312, 434  
     velocity potential, 460  
 Vorticity, 91, 93  
 Warp, geometric, 259  
 Wave(s),  
     Mach, 161  
         three-dimensional, 211  
     shock, 159, *see also* Shock(s)  
         formation, 159ff  
         infinitesimal, 182  
         weak, 161  
     simple pressure, 161  
     spherical, 427  
     stationary, 159  
     surface, 211  
 Wavelet, *see* Line(s), weak disturbances  
 Wing(s),  
     conditional, with toothed edges, 464  
     downwashes, 465  
     finite-span, 249ff, 254, 258ff, 300f,  
     308ff  
         in incompressible flow, 249ff

- Wing(s),  
finite-span, 301  
in supersonic flow, 308ff  
hexagonal, 364, 366ff, 372ff  
with dovetail, 370  
infinite-span,  
in plane parallel flow, 249f  
swept, 299  
lift force, 21, 362, 386  
lifting capacity,  
and aspect ratio, 482f, 487  
and taper ratio, 483  
in linearized flow, 310ff  
non-elliptical planform, 260  
optimal planform, 258ff  
pentagonal, 364, 370  
rectangular, 260, 385ff  
aerodynamic characteristics,  
385ff  
in linearized flow, 386  
in supersonic flow, 386  
**semi-infinite**, 328ff  
sideslipping, 299f, 302, 304ff  
in subsonic compressible flow, 302f  
in supersonic flow, 308ff, 315, 344  
surface deformation, 451  
swept, 300, 341  
symmetric airfoil, 312, 317ff  
idealized, 313, 317
- Wing(s),  
taper ratio, 263  
tetragonal, 364f  
with dovetail, 364f  
in supersonic flow, 344  
symmetric airfoil, 331ff  
with vee-shaped appendage, 364f  
thin, 315f  
at angle of attack, 351ff  
in nearly uniform flow, 351ff  
symmetric airfoil, 317ff  
trapezoidal, 260, 262  
aerodynamic characteristics, 349  
lift force, 362f  
pressure field, 326, 330  
semi-infinite, 328ff  
suction force, 362  
symmetric about  $x$ -axis, 326f,  
330f  
vortex model, 436ff  
**zero-thickness**, 312f
- Work**,  
external mass forces, 124  
surface forces, 124f
- Zone**, non-equilibrium, 197

## TO THE READER

Mir Publishers would be grateful for your comments on the content, translation and design of this book.

We would also be pleased to receive any other suggestions you may wish to make.

Our address is:

Mir Publishers  
2 Pervy Rizhsky Pereulok  
I-110, GSP, Moscow, 129820, USSR

*Printed in the Union of Soviet Socialist Republics*

ALSO FROM MIR PUBLISHERS

**Similarity and Dimensional Methods  
in Mechanics**

L. I. SEDOV

The book presents the general theory of dimensions of physical quantities, the theory of mechanical and physical scaling, and the theory of modelling.

Typical examples of applications of the similarity and dimensions theory are given, illustrating how the fundamental mechanical relationships are obtained in ship hydrodynamics, aviation, explosion technology, astrophysics, and some other fields. The book presents the general theory of self-similar motions of continuum, the theory of shock wave propagation through gases, the theory of one-dimensional unsteady motions in a gas, the fundamentals of the gas dynamics theory of atomic explosion in the atmosphere, the theory of averaging gas flow characteristics in ducts, the modelling and dimensionless characteristics of compressors, the theory of thrust of jet engines, and the theory of efficiency of the ideal propeller both at subsonic and supersonic flight velocities.